SERIES OF BOOKS

ON

ELECTRONIC VALVES

PHILIPS' TECHNICAL LIBRARY

The series of books on electronic valves include:

Book I: Fundamentals of Radio Valve technique
547 pages 6″ × 9″ — 384 illustrations, cloth bound.

Book II: Data and Circuits of Radio Receiver- and Amplifier Valves 1933/39, 424 pages, 531 illustrations

Book III: idem 1940/41, 220 „ , 267 illustrations

Book III A: idem 1945/50 (in preparation)

Book IV: Application of the Electronic Valve in Radio Receivers and Amplifiers.
1. R.F. and I.F. Amplification, 2. Frequency changing,
3. Determination of the padding curve, 4. Interference and distortion due to bend in characteristics of the receiving valves, 5. Detection.
467 pages 6″ × 9″ — 256 illustr.

Book V: Application of the Electronic Valve in Radio Receivers and Amplifiers.
6. A.F. Amplification, 7. Power amplification, 8. Inverse feedback, 9. Power supply, (in preparation).

BOOK VI: Application of the Electronic Valve in Radio Receivers and Amplifiers.
10. Control devices - 11. Stability and Instability of Circuits,
12. Parasitical Feedback, 13. Interference phenomena, 14. Calculations of Receivers and Amplifiers (in preparation).

BOOK VII: Transmitting Valves (in preparation)

BOOK IV

APPLICATION OF THE ELECTRONIC VALVE IN RADIO RECEIVERS AND AMPLIFIERS

APPLICATION OF THE ELECTRONIC VALVE IN RADIO RECEIVERS AND AMPLIFIERS

621.383.1; 621.396.621; 621.396.694

R. F. and I. F. Amplification – Frequency changing – Determining the tracking curve – Parasitic effects and distortion due to curvature of valve characteristics – Detection

BY

DR. B. G. DAMMERS, J. HAANTJES,
J. OTTE AND H. VAN SUCHTELEN

BOOK IV

1950

PUBLISHED BY

N.V. PHILIPS' GLOEILAMPENFABRIEKEN - EINDHOVEN (NETHERLANDS)
TECHNICAL AND SCIENTIFIC LITERATURE DEPARTMENT

Translated by
S. H. ALEXANDER
London

Publishers' note. This work has been published
in Dutch, English and German. A French edition
is in preparation

PRINTED IN THE NETHERLANDS

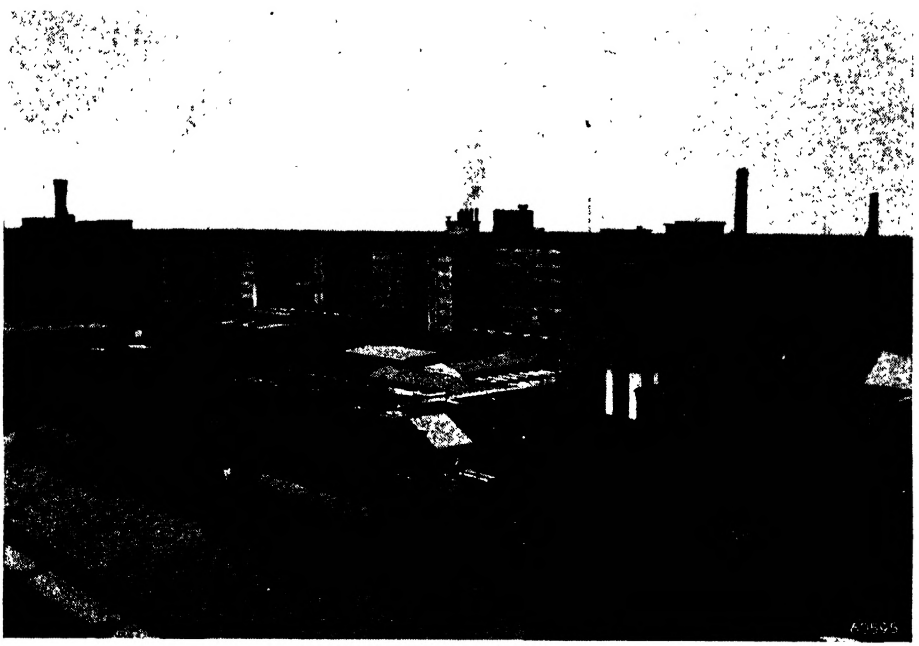

Part of the Philips' Works at Eindhoven

FOREWORD

to the English edition

Scientific books dealing with radio engineering applications are always welcome, particularly when the applications are concerned with the use of thermionic valves. Such books invariably stimulate interest among a wide circle of scientists and engineers, while at the same time providing the essential data for those who are engaged on problems of design in radio and allied fields.

The appearance of the English edition of "Application of the Electronic Valve in Radio Receivers and Power Amplifiers" is most timely, for it fills a gap in current literature on the subject of thermionic valve applications and meets a long-felt need. The illustration of fundamental theory with figures based on current valve types has produced a publication of wide interest which will appeal especially to designers and engineering students; judicious selection and preparation of material has resulted in a carefully condensed standard work of reference containing all necessary engineering information ably supplemented with mathematical explanations.

The bibliography which appears at the end of each chapter is invaluable to the designer and student alike in providing an easy reference to other published work.

In congratulating the authors on their book reference must be made to the many valuable contributions from the scientific staff of N.V. Philips' Gloeilampenfabrieken which regularly appear all over the world. This volume amply maintains the high technical standard for which Philips have earned an international reputation.

T. E. GOLDUP, M.I.E.E.
Technical Director
The Mullard Radio Valve Co. Ltd.

PREFACE

It is the intention of the authors to present in this book all the information necessary to give the maximum assistance to those engaged in the application of electronic valves for receiving and amplifying equipment. A start was made with a series of articles already published in Philips Setmakers' Bulletin, a publication devoted solely to the applications of electronic valves. In order to maintain the correct sequence, however, most of these articles have been completely re-written and in several cases the subject matter has been treated in greater detail.

For a good understanding of all the basic principles of electronic valve technique a sound fundamental knowledge is required — see Volume I of this series, "Fundamentals of Radio Valve Technique" — but in this book the various problems involved have been dealt with in the most practical manner, keeping the mathematical treatment as simple as possible.

As implied by its title, this book deals only with the electronic valve and those components immediately associated with it. Obviously it is difficult to draw a line as to the exact function of any component relative to the appropriate valve, since a great deal depends upon individual opinion. It will be seen that circuits, bandpass filters, transformers etc. have been dealt with, whilst aerials, coils, capacitors, loudspeakers, etc. have been omitted.

At the end of each chapter a list is given of the relevant literature. Only publications have been mentioned which, in our opinion, give different interpretations or are of primary interest on the subject in question.

The authors are grateful for the permission to use articles written by Mr. A. J. Heins van der Ven and Mr. J. M. van Hofweegen, and for the knowledge placed at their disposal by the Philips Research Laboratory at Eindhoven, Netherlands. Furthermore they are indebted to Dr. E. Oosterhuis for his constructive criticism and inspiring hints, which have been of great assistance in the compilation of this book. Finally thanks are due to Mr. S. H. Alexander for his invaluable aid in preparing the English translation.

The authors.

INDEX

INTRODUCTION

For the transmission of music or speech by means of wireless use is made of modulated electro-magnetic waves; those currently employed vary in wavelength from a few centimetres to some thousands of metres, though for broadcasting the range is rather less, from about 15 to 2000 metres. Up to the present time, variation of amplitude has been the type of modulation principally employed, and in this book only that method will be considered.

A carrier wave, amplitude-modulated by a tone of pure sine form, can be represented by the equation:

$$v = V_m(1 + m \cos pt) \sin \omega t.$$

Here ω is the angular frequency of the transmitted carrier, p that of the modulation, and m the depth of modulation. By simple trigonometric operations this formula can be converted into:

$$v = V_m \sin \omega t + {}^1/_2 m\ V_m \sin (\omega + p)\, t + {}^1/_2\ V_m \sin (\omega - p)\, t.$$

In this form the modulated oscillation is seen as a carrier wave, with two sidebands separated therefrom by a frequency difference of $+p$ and $-p$ respectively. The result of the appearance of these sidebands is that for every transmitter a certain band of frequencies must be reserved, the breadth of which is determined by the highest modulation frequency to be radiated; no frequencies from the sidebands of other stations must be permitted to fall in this band. Carrier frequencies are therefore distributed evenly over the available broadcast bands and, by international agreement, each station is normally allotted sidebands of 4.5 kc/s; the mutual separation between carrier waves thus amounts to 9 kc/s. An ideal receiver ought therefore to be able to select any desired band of 9 kc breadth throughout the broadcast bands; its sensitivity, should be constant within such a band, falling rapidly outside it, so that even a strong signal next to a desired weak transmission is adequately suppressed. In practice a compromise is unavoidable, and the extremities of the sidebands may be attenuated ten times, for example, when the response to an adjacent carrier is about one hundred

times down. The various means by which this selection can be attained are dealt with in Chapter I. It will at once be apparent that the properties of the components available make it impossible to reach a satisfactory compromise at the higher-frequency end of the radio spectrum, without using a very great number of tuned circuits; such a course would be far too costly and would give rise to many difficulties. In consequence the almost invariable current practice is to change the frequency of the incoming wave to a new frequency, at which the requisite selectivity can be obtained by practicable means; such a process is referred to as superheterodyne reception, in contradistinction to the original "straight" reception. Frequency-changing is dealt with in Chapter II.

The received signal V_i of frequency ω_i is applied together with an auxiliary voltage V_h of frequency ω_h to a system of which the characteristic $I = f(V_i, V_h)$ is intentionally non-linear. The system is called a modulator. If now $f(V_i, V_h)$ is written as a power series, products of V_i and V_h appear, which by means of a trigonometric operation result, among others, in signals with frequency $\omega_0 = \omega_h - \omega_i$. "Radio frequency" (R.F.) is the customary term for ω_i, and "intermediate frequency" (I.F.) the usual connotation for ω_0, while oscillations within the aural range are termed "audio frequency" (A.F.). The heterodyne voltage V_h is generated in an oscillator; this subject will be dealt with in chapter II, in rather greater detail than in the average textbook. Generally the oscillator valve and the modulator are combined in one envelope, forming a so-called mixer. In the vast majority of cases the heterodyne frequency ω_h is so adjusted in relation to the frequency to be received, ω_i, that a constant intermediate frequency ω_0 appears; thereby good selectivity is attainable by simple means. Usually preselection, with one or two tuned R.F. circuits, precedes the frequency changer. The tuning curve of the oscillator must therefore run parallel, throughout the wave band, with the tuning curve of the input circuit or circuits, in order to obtain a constant frequency-difference between them. This is very difficult to attain; one of the methods of approaching the ideal is discussed in Chapter III.

A receiver is not only required to select the desired signal from all those reaching the aerial; it must also change the form of the signal and increase its power, so that it may be reproduced acoustically by the loudspeaker. The metamorphosis, involving the process of demodulation and also, in most cases, a change of frequency, is achieved by making use of the non-linear properties of radio valves; thereby, unfortunately, distortion occurs as well as the effect desired. To raise the power level use is made of the

relay action of valves, the signal controlling the energy drawn from a battery or supply-unit; in the power amplifier further distortion inevitably creeps in, for valves with perfectly straight characteristics are unrealizable in practice, and in any case are not always desirable. The various types of distortion introduced by curvature of characteristics are considered in Chapter IV.

Of the successive changes in its form to which the signal is subjected, frequency-conversion has already been mentioned; the process whereby the modulated R.F. or I.F. oscillation becomes a pure A.F. oscillation is known as demodulation or detection. It operates in the same manner as frequency-changing. For demodulation the carrier wave and the sidebands are fed to a non-linear system; thereby, among others, the difference-frequency between the carrier and its sidebands, which is the required audio frequency, is made to appear. The incidental modulation products of much higher frequency are easily separated from the desired signal and rendered harmless. Owing to the similarity in operation between a detector and a mixer, the latter is also called a first detector. If the characteristic of a non-linear system is approximately square-law, then in calculating the result the given expression for carrier wave and sidebands must be squared. It can easily be demonstrated that, besides the audio frequency p, a frequency $2p$ also appears, which is particularly unwelcome; being of the same order as p, it cannot be separated therefrom. Although rectifiers with a square-law characteristic — leaky-grid and anode-bend detectors — are still used, it is clearly preferable to employ a demodulator which does not generate the frequencies $2p$, $3p$, etc. The required performance can be obtained from a device of which the characteristic consists of a straight line with a knee in it. Provided that the input is kept above a certain level a diode realizes linear detection. Detailed consideration of this method of detection is given in Chapter V. Although this type of rectification does not, strictly speaking, deal with the signal in linear fashion, the accepted term "linear detection" is in general justified. In contrast with square-law rectification, linear detection produces a DC voltage which is proportional to the amplitude of the unmodulated carrier. The output voltage delivered by a linear detector is nearly equal to the peak value of the applied A.C. voltage; such a detector may therefore be regarded as an unloaded rectifier.

In most cases the A.F. voltages obtained will be amplified before they are applied to the output stage. The next book in this series will begin with a description of this process and will also deal with power amplification and the supply of the receiver.

EXPLANATION OF THE SYMBOLS EMPLOYED

Before giving a list of the symbols and signs employed it is necessary to explain the guiding principles that have been followed for the most important symbols.
Voltages and currents are denoted respectively by the letters V and I, both for alternating and for direct voltages and currents.
The letters v and i are used for strictly momentary values of voltages and currents respectively. The currents to and the voltages at the electrodes of the electronic valves are characterized by indices representing the respective electrodes.

Examples:

V_a	= anode voltage
V_{g1}	= voltage at the first grid reckoned from the cathode
$V_{(g2+g4)}$	= voltage at the grids 2 and 4
I_a	= anode current
I_{g2}	= current flowing to the second grid

Resistances, capacitances, self-inductances and impedances are signified respectively by the symbols R, C, L and Z. In many cases the indices added indicate where the element in question is placed in the circuit.

Examples:

R_{g2}	= resistance in the screen-grid line
R_k	= cathode resistance
C_{ag1}	= capacitance between anode and grid 1 of an electronic valve
C_{gk}	= capacitance between grid and cathode

In some cases the meaning of the indices has to be found from the respective illustration or the text.

SYMBOLS

A = voltage gain of a high-frequency circuit, or of an aerial circuit
A_c = conversion gain
C = capacitance; constant
C_a = aerial capacitance
C_i = input capacitance
C_{ind} = apparent capacitance due to induction effect
C_k = coupling capacitance
C_o = output capacitance; zero capacitance of a tuning circuit
C_p = parallel capacitance; padding capacitance
C_r = grid capacitor
C_{tot} = total capacitance
C_v = tuning capacitance
d_2 = A.F. distortion due to second harmonic
d_3 = A.F. distortion due to third harmonic
D_2 = modulation distortion due to second harmonic
D_3 = modulation distortion due to third harmonic
f = frequency
f_h = oscillator frequency
f_i = R.F. input frequency
f_o = intermediate frequency
f_s = interference frequency
$g = \frac{V_o}{V_i}$ = gain per stage
I = current im amperes
I_a = anode current; current in the aerial circuit
I_{ao} = anode current when $V_g = 0$
$I_{a\,med}$ = mean anode current
I_{g1} = current flowing to the first grid
$j = \sqrt{-1}$
k = coupling factor
K = corrected coupling factor; cross-modulation factor
L = self-inductance
L_k = coupling self-inductance
ln = natural logarithm to base $\varepsilon = 2.72$
log = common logarithm to base 10
M = mutual inductance; percentual depth of modulation
m = modulation depth factor
m_b = hum-modulation depth factor

m_k = cross-modulation depth factor
O = area in cm^2
P = energy
Q = quality factor of coil; charge
r = loss resistance of tuning coil
R = resistance
R_a = external anode resistance
R_d = internal resistance of diode
R_g = grid-leak resistance; D.C. load resistance in diode circuit; grid current damping
R_{g2} = resistance in screen grid line
R_{HF} = equivalent damping resistance
R_i = internal resistance of an electronic valve
R_w = A.C. load resistance in diode circuit
S = slope, or mutual conductance
S_{13} = slope of the first grid with respect to the third
S_c = conversion conductance of frequency converter
S_{eff} = effective oscillator slope
S_o = static slope of oscillator triode
t = voltage ratio; time in seconds
T = oscillation time
v = momentary value of alternative voltage; velocity
V = voltage in volts
$V_{=}$ = direct voltage
V_a = anode voltage
V_{ant} = aerial alternating voltage
V_b = supply voltage
V_g = grid voltage
V_{g2} = voltage at the second grid
V_{go} = grid voltage with $I_a = 0$ (cut- off voltage)
V_h = auxiliary voltage or oscillator voltage
V_i = input voltage
V_o = output voltage
V_{osc} = oscillator voltage
V_r = direct voltage across diode load resistance in the absence of a signal
V_s = interfering alternating voltage
V_T = temperature voltage
W_a = anode dissipation
X = reactance
Y = admittance

Z = impedance

$\beta = \frac{\omega}{\omega_0} - \frac{\omega_0}{\omega}$ = relative detuning; factor in power series

δ = loss angle

$\varepsilon = \delta_1 - \delta = \delta - \delta_2$; base of natural logarithm = 2.72

η = efficiency

λ = wavelength

μ = amplification factor

π = 3.14

ϱ = radius of curvature

σ = relative selectivity

φ = phase angle

$\omega = 2\pi f$ = angular velocity

$=$ = equal to

$\approx$ = approximately equal to

$\neq$ = not equal to

$//$ = parallel to

$<$ = less than

$\ll$ = much less than

$>$ = greater than

$\gg$ = much greater than

∞ = infinitely great

$+$ = approximately proportional to

I. R.F. AND I.F. AMPLIFICATION

Introduction

The design of a radio receiver calls for the solution, among many others, of such problems as selectivity, quality of reproduction, and amplification. In recent years the ever-higher standard of reproduction demanded from receivers has conflicted sharply with requirements in the matter of selectivity.

To obtain good quality, transmission of a wide band of frequencies by the R.F. and I.F. stages of the receiver is necessary, for example not less than 2×10 kc/s; the A.F. section must also pass frequencies up to say 10,000 cycles per second without attenuation. A set of such performance will provide very good reproduction of a powerful transmission such as the local station, provided that the transmitters using the adjacent channels are too weakly received to cause appreciable interference. On the other hand, should such a receiver be required to pick up a weak station any stronger transmission of which the carrier or sideband falls partly within the pass-band of the R.F. and I.F. stages will cause severe interference. Higher selectivity must in this case be given preference over a wide frequency-response; admittedly the reproduction of the upper frequencies will then suffer, but as the interference is lessened at the same time the net result is more satisfactory.

By means of tuned circuits, used either alone or in conjunction with valves, the designer is enabled to give selective amplification to A.C. voltages. The properties of these circuits, and their arrangements, determine the magnification obtained and control the compromise between quality and selectivity. The very important part thus played by the tuned circuit may be explained as follows. The simplest circuit-coupling element is a pure resistance, which transmits all frequencies uniformly. In order to select a particular band of frequencies, the resistance may be paralleled by an inductance, which will reduce the impedance of the coupling at low frequencies, and by a capacitance, which will reduce the impedance at high frequencies. In this way a parallel resonant circuit containing L, C, and the parallel damping R is obtained.

To estimate the response of such a coupling it is necessary to calculate its impedance and its dependance of frequency.
Similar behaviour is to be expected from an alternative form of tuned circuit in which a resistance is connected in series with the other two elements. A further possibility is to connect several circuits one after another. We shall in the first place consider the properties of simple tuned circuits and then enquire how, by optimum choice of circuit combinations and methods of coupling, varying requirements may be satisfied.

A. Single tuned circuit

§ 1. Capacitance, inductance and parallel resistance

The impedance of this circuit (fig. 1) can be calculated from:

$$\frac{1}{Z} = \frac{1}{R} + \frac{1}{j\omega L} + j\omega C \quad \ldots\ldots\ldots\ldots \quad (\text{I A } 1)$$

therefore from:

$$\frac{1}{Z} = \left| \frac{1}{R} + j\left(\omega C - \frac{1}{\omega L}\right) \right| \quad \ldots\ldots\ldots \quad (\text{I A } 2)$$

$$\frac{1}{Z} = \sqrt{\frac{1}{R^2} + \left(\omega C - \frac{1}{\omega L}\right)^2} \quad \ldots\ldots\ldots \quad (\text{I A } 3)$$

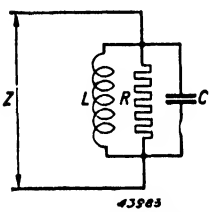

Fig. 1. Simple oscillatory circuit with parallel resistance.

The absolute value of Z is a maximum (and $\frac{1}{Z}$ a minimum) when the term within brackets in equation (I A 3) is equal to 0*.

This is the case for frequency ω_0:

$$\omega_0 C - \frac{1}{\omega_0 L} = 0,$$

or:

$$\omega_0^2 = \frac{1}{LC} \quad \ldots\ldots\ldots\ldots \quad (\text{I A } 4)$$

This makes $\frac{1}{Z_0} = \frac{1}{R}$,

or:

$$Z_0 = R \quad \ldots\ldots\ldots\ldots \quad (\text{I A } 5)$$

In this case the circuit resonates: ω_0 is the resonant frequency. At this frequency Z has its maximum value and is real; at all other frequencies Z is smaller and complex. When the tuned circuit is connected to a circuit in

* Absolute values of a complex term will be indicated by placing the term between vertical strokes. Should this value be indicated by a letter, this will bear no special sign.

which equal alternating currents of frequency ω and ω_0 are flowing, the voltages developed across the tuned circuit are proportional to the impedance at each frequency; the voltage at frequency ω is thus attenuated by comparison with that at frequency ω_0. For this attenuation, which is equal to the relation between the respective impedances, we can write:

$$a = \left|\frac{Z_0}{Z}\right| = R\left|\frac{1}{R} + j\left(\omega C - \frac{1}{\omega L}\right)\right|,$$

or:

$$a = \left|1 + jR\left(\omega C - \frac{1}{\omega L}\right)\right|.$$

Introducing ω_0 from equation (I A 4) we get:

$$a = \left|1 + jR\omega_0 C\left(\frac{\omega}{\omega_0} - \frac{\omega_0}{\omega}\right)\right| \quad \ldots\ldots\ldots \quad \text{(I A 6)}$$

We now write:

$$R\omega_0 C = Q = \frac{1}{tan\ \delta} \quad \ldots\ldots\ldots\ldots \quad \text{(I A 7)}$$

The quantity Q is the so-called quality factor. We will introduce further the term

$$\beta = \frac{\omega}{\omega_0} - \frac{\omega_0}{\omega} \quad \ldots\ldots\ldots\ldots\ldots \quad \text{(I A 8)}$$

Equation (I A 6) can now be simplified to:

$$a = \left|1 + j\,\beta Q\right| \quad \ldots\ldots\ldots\ldots\ldots \quad \text{(I A 9)}$$

The absolute value of this relation becomes:

$$a = \left|\frac{Z_0}{Z}\right| = \sqrt{1 + (\beta Q)^2}. \quad \ldots\ldots\ldots \quad \text{(I A 10)}$$

This gives us an equation of general form for the resonance curve of a tuned circuit with parallel damping, β being a measure of the mistuning of ω in relation to the resonant frequency ω_0; this is clearer when we write:

$$\beta = \frac{\omega}{\omega_0} - \frac{\omega_0}{\omega} = \frac{\omega^2 - \omega_0^2}{\omega_0\omega} = \frac{(\omega - \omega_0)(\omega + \omega_0)}{\omega_0\omega}.$$

If the difference between ω and ω_0 is small, we can put instead of β:

$$\beta = 2\frac{\omega - \omega_0}{\omega_0} = \frac{2\,\Delta\,\omega}{\omega_0} \quad \ldots\ldots\ldots \quad \text{(I A 11)}$$

The expression $\Delta\omega$ in the foregoing represents the difference between the frequency ω under consideration and the resonant frequency ω_0. Thus the factor β is approximately equal to twice the relative detuning. From (I A 10) we now easily derive:

$$a = \sqrt{1 + (2\ RC\ \Delta\omega)^2}. \quad \ldots\ldots\ldots\ldots \quad \text{(I A 12)}$$

This is a more practical equation for the resonance curve, and it shows the attenuation $a = \left|\frac{Z_0}{Z}\right|$ as a function of $\Delta\omega$. It gives a clearer picture of selectivity, for with even spacing of carrier frequencies over the radio spectrum the attenuation obtained for a specific amount of detuning $\Delta\omega$ is a useful criterion (see also § 5). Every circuit has of course its own curve. The circuit constants R and C are parameters.

With the help of equation (I A 10) it is possible to delineate the same resonance curves for tuned circuits having the most diverse constants, being considered $\left|\frac{Z_0}{Z}\right|$ as a function of βQ, i.e. as a function of $(2\ RC\ \Delta\omega)$ in equation (I A 12). This resonance curve is shown in fig. 2; see also fig. 17 *.

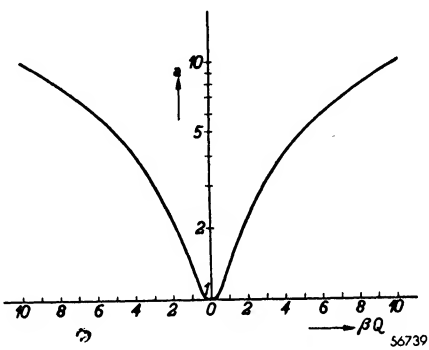

Fig. 2. Typical resonance curve of an oscillatory circuit.

§ 2. Capacitance, inductance and series resistance

A tuned circuit with parallel damping only does not exist in practice. Every inductor has a certain ohmic resistance, which is regarded as being in series with the inductance. The circuit shown in fig. 1 must therefore be considered hypothetical. We shall now ascertain what constants a tuned circuit possesses in which only series resistance is present, as in fig. 3. Its impedance will be:

$$\frac{1}{Z} = \frac{1}{r + j\omega L} + j\omega C \quad \ldots\ldots\ldots\ldots \quad \text{(I A 13)}$$

or:

$$\frac{1}{Z} = \frac{r - j\omega L}{r^2 + \omega^2 L^2} + jC\omega.$$

* The term "resonance curve" is also used to denote a curve which shows $1/a$ as a function of $\Delta\omega$ or β. Such a curve is an inversion of fig. 2. The two sorts of curve are so closely allied that the use of the same expression really causes no difficulty.

Generally r^2 is negligible by comparison with $\omega^2 L^2$, so that we may write:

$$\frac{1}{Z} = \frac{r}{\omega^2 L^2} + j\left(\omega C - \frac{1}{\omega L}\right) \quad \ldots\ldots\ldots \quad \text{(I A 14)}$$

This equation is very similar to (I A 2), $\frac{1}{R}$ being replaced by $\frac{r}{\omega^2 L^2}$. Since,

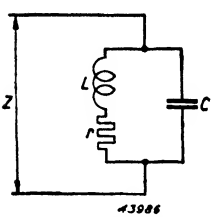

Fig. 3. Oscillatory circuit with series resistance.

in equation (IA 14), the latter term contains the frequency ω, the maximum value of Z does not lie exactly at the resonant frequency ω_0 [as in equation (I A 4)], but at a somewhat higher frequency; however, the difference is slight, and there is no objection to saying that resonance occurs when:

$$\omega_0^2 = \frac{1}{LC} \quad \ldots\ldots\ldots\ldots\ldots\ldots \quad \text{(I A 4)}$$

At this frequency the impedance is nearly a real quantity and amounts to:

$$Z_0 = \frac{\omega_0^2 L^2}{r} = \frac{L}{rC} \quad \ldots\ldots\ldots\ldots \quad \text{(I A 15)}$$

For the attenuation factor we deduce:

$$a = \left|\frac{Z_0}{Z}\right| = \frac{\omega_0^2 L^2}{r} \times \left|\frac{r}{\omega^2 L^2} + j\left(\omega C - \frac{1}{\omega L}\right)\right| = \left|\frac{\omega_0^2}{\omega^2} + j\frac{\omega_0^2 L^2}{r}\omega_0 C\beta\right|.$$

At this point also, the equation can be considerably simplified by introducing and substituting Q:

$$\frac{\omega_0 L}{r} = Q. \quad \ldots\ldots\ldots\ldots\ldots\ldots \quad \text{(I A 16)}$$

As in the case of equation (I A 7), Q here represents the quality factor. For the attenuation we may now write:

$$a = \left|\left(\frac{\omega_0}{\omega}\right)^2 + j\frac{\omega_0 L}{r}\beta\right| = \left|\left(\frac{\omega_0}{\omega}\right)^2 + j\beta Q\right| \quad \ldots \quad \text{(I A 17)}$$

This equation is seen to be nearly the same as (I A 9).

In most cases we are concerned only with a small part of the resonance curve on each side of the peak, i.e. with a frequency band in which ω differs little from ω_0, and in which therefore it is practically true that:

$$\frac{\omega_0}{\omega} = 1.$$

For this part of the curve the same attenuation factor is applicable for series as for parallel damping, viz:

$$a = \left| \frac{Z_0}{Z} \right| = \sqrt{1 + (\beta Q)^2} \quad \ldots\ldots\ldots \quad \text{(I A 10)}$$

Substituting (I A 11) and (I A 16) in equation (I A 10) we get:

$$a = \sqrt{1 + (2 \frac{L}{r} \Delta\omega)^2} \quad \ldots\ldots\ldots\ldots \quad \text{(I A 18)}$$

The ratio $\frac{L}{r} = \frac{1}{r/L}$ of the coil is thus a measure of the selectivity of a circuit with series damping. It is clear that a tuned circuit with series damping, just as one with parallel damping, may be used for the selective transfer of R.F. voltages.

§ 3. Tuned circuit with mixed damping

In practice a tuned circuit inevitably contains series resistance, and in most cases also the parallel damping present is too heavy to be neglected. It is therefore of interest to examine a circuit with mixed damping (fig. 4). On considering equations (I A 14) and (I A 2) together, we discover a simple way of calculating the selectivity of such a circuit. It is evident that an $L - r - C$ circuit, with series resistance r, can be replaced by a circuit containing the same values of L and C, shunted by a resistance R', when:

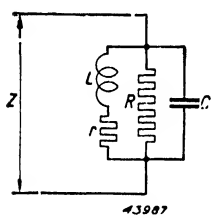

Fig. 4. Oscillatory circuit with mixed damping.

$$\frac{1}{R'} = \frac{r}{\omega^2 L^2} = \left(\frac{\omega_0}{\omega}\right)^2 \frac{rC}{L} \quad \ldots\ldots\ldots \quad \text{(I A 19)}$$

The circuit of fig. 4 is thus entirely equivalent to a circuit in which the inductor possesses no resistance and in which a resistance R' is connected additionally in parallel with R. At resonance the admittance is then:

$$\frac{1}{Z_0} = \frac{1}{R} + \frac{1}{R'}, \text{ therefore } \frac{1}{Z_0} = \frac{1}{R} + \frac{rC}{L}\left(\frac{\omega_0}{\omega}\right)^2.$$

For the section of the resonance curve under consideration it is almost always permissible to put:

$$\frac{\omega}{\omega_0} = 1.$$

The selectivity now agrees with that of a circuit with shunt resistance R_p when:

$$\frac{1}{R_p} = \frac{1}{R} + \frac{1}{R'} = \frac{1}{R} + \frac{rC}{L} \quad \ldots\ldots\ldots \quad \text{(I A 20)}$$

Having thus calculated R_p, we then find the total value of RC in order to estimate the selectivity from (I A 12):

$$\frac{1}{R_p C} = \frac{1}{RC} + \frac{r}{L} \quad \ldots\ldots\ldots\ldots \quad \text{(I A 21)}$$

It is already clear from equations (I A 18) and (I A 12) that in the estimation of selectivity RC and L/r are equivalent; and in the case of a circuit with mixed damping the relation between RC and L/r is evident from equation (I A 21). Since in practice series resistance is always present, it is customary to regard any parallel damping as an augmentation thereof and it follows from (I A 21) that:

$$\Delta \frac{r}{L} = \frac{1}{RC} \quad \ldots\ldots\ldots\ldots\ldots \quad \text{(I A 22)}$$

The simplest result is obtained, however, by calculating the attenuation from equation (I A 10). Dividing equation (I A 21) by ω_0, we find in this way the quality of the equivalent circuit:

$$\frac{1}{R_p \omega_0 C} = \frac{1}{R\omega_0 C} + \frac{r}{\omega_0 L},$$

or:

$$\frac{1}{Q_{\text{total}}} = \frac{1}{Q_{\text{par}}} + \frac{1}{Q_{\text{series}}} \quad \ldots\ldots\ldots \quad \text{(I A 23)}$$

The attenuation factor $\frac{Z_0}{Z}$ is, according to equation (I A 12), equal to $\sqrt{2}$ when:

$$2\,RC\,\Delta\omega = 1,$$

or when

$$\frac{1}{R_p C} = 2\,\Delta\omega = \frac{1}{RC} + \frac{r}{L}.$$

This relation is utilised when the damping of a circuit is to be measured. The circuit under examination is loosely coupled to a signal source and the voltage developed across it is then measured at resonance. Next the two frequencies are ascertained at which the voltage falls to $\frac{1}{\sqrt{2}}$ of the

figure at resonance; the difference between these two frequencies corresponds to $2\,\Delta\,\omega$, and therefore directly indicates the damping in the expression:

$$\frac{1}{RC} + \frac{r}{L}.$$

§ 4. Series connection of C and R in parallel to a tuned circuit

This circuit (fig. 5) also occurs frequently in practice. To facilitate study and calculation of its behaviour, it is recommended to transform the layout of fig. 5*a* to the form shown in fig. 5*b*. The capacity C_2 is then simply added to C_1, while with the help of equation (I A 22):

$$\Delta \frac{r}{L} = \frac{1}{R_2(C + C_2)}$$

the resistance R_2 can be converted to a series resistance.

On closer consideration it will be obvious that an interchange of $C_1 - R_1$ and $C_2 - R_2$ can be effected only at a single frequency; at other frequencies the circuits 5*a* and 5*b* no longer behave alike.

As is well-known, with a series-connection of C_1 and R_1 the current flowing between points 1 and 2 in fig. 5*a* leads the voltage. The same is true of the

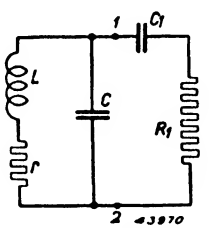

Fig. 5a. Capacitance and resistance in series, shunted across an oscillatory circuit.

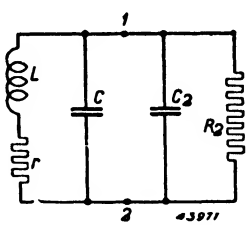

Fig. 5b. Equivalent curcuit of 5a, the series combination C_1R_1 being replaced by the parallel combination C_2R_2.

circuit in fig. 5*b*. For specific values of C_1 and R_1 and for a stated frequency such values of C_2 and R_2 must be chosen that the same resulting impedance is obtained, and the same phase shift. For the circuit to the left of 1 and 2 it then makes no difference which of the two combinations is connected between those points, because the current which passes through point 1 is the only factor which influences the tuned circuit.

If, however, the frequency is altered, being raised for instance, then the impedance of the right-hand part of fig. 5*a* becomes a resistance. That of the right part of fig. 5b however beçomes a capacitance.

If the frequency is lowered naturally the converse takes place. It follows from this that the two circuits are equivalent only at a single frequency. In practice, however, we have to work with the equivalent circuit over the whole frequency band passed by the tuned circuits; this band, however, is in most cases comparatively narrow.
From the foregoing considerations, therefore, we conclude that the series- and the parallel-circuit are equivalent only when the two impedances have the same absolute value and when they give rise to the same phase difference between current and voltage.

For the right-hand section of fig. 5*a* we have:

$$Z^2 = R_1^2 + \frac{1}{\omega^2 C_1^2} \quad \ldots\ldots\ldots\ldots \quad \text{(I A 24)}$$

and

$$tan\ \varphi = -\frac{1}{R_1 \omega C_1} \quad \ldots\ldots\ldots\ldots \quad \text{(I A 25)}$$

For fig. 5b we have:

$$Z^2 = \frac{R_2^2}{1 + R_2^2\ \omega^2\ C_2^2} \quad \ldots\ldots\ldots\ldots \quad \text{(I A 26)}$$

and

$$tan\ \varphi = -\ R_2 \omega\ C_2 \quad \ldots\ldots\ldots\ldots \quad \text{(I A 27)}$$

If in these equations the corresponding parts are put equal to one another, the following results may easily be derived; i.e. the RC combinations of fig. 5 are equivalent when:

$$R_2 = R_1\left(1 + \frac{1}{R_1^2\ \omega^2\ C_1^2}\right) \quad \ldots\ldots\ldots \quad \text{(I A 28)}$$

and

$$C_2 = \frac{C_1}{1 + R_1^2\ \omega^2\ C_1^2} \quad \ldots\ldots\ldots\ldots \quad \text{(I A 29)}$$

or conversely when:

$$R_1 = \frac{R_2}{1 + R_2^2\ \omega^2\ C_2^2} \quad \ldots\ldots\ldots\ldots \quad \text{(I A 30)}$$

and

$$C_1 = C_2\left(1 + \frac{1}{R_2^2\ \omega^2\ C_2^2}\right) \quad \ldots\ldots\ldots \quad \text{(I A 31)}$$

These equations are for normal use somewhat impractical, but in most cases they can be applied in a very simple way.

In all four equations the term $R\omega C$ occurs, which is the ratio of the impedance of R and C. If for example $R\omega C = 5$, this means that R is 5 times as great as the impedance $\frac{1}{\omega C}$.

When making a transformation as in fig. 5 we first ascertain the magnitude of $R_1\ \omega\ C_1$. If it is large in relation to unity, for instance more than three, then it follows from equation (I A 28) that R_2 is practically equal to R_1. Or we can say: if the series circuit is mainly resistive in character then the equivalent resistance in the substituted circuit will have the same value.

From equation (I A 29) it further follows that the equivalent capacitance is roughly equal to the original capacitance divided by the square of $R_1\ \omega\ C_1$. This approximation is about 10% out when $R_1\ \omega\ C_1 = 3$; for lower values precise calculations should be made with the aid of equations (I A 28) and (I A 29), if an error exceeding 10% must be considered inadmissible.

On the other hand, from equation (I A 29) we observe that C_2 is roughly equal to C_1 if $R_1\ \omega\ C_1$ is considerably less than unity. Furthermore, from equations (I A 28) and (I A 29) it follows: if $R_1\ \omega\ C_1$ is appreciably smaller than unity, i.e. if the series circuit is essentially capacitive, then the equivalent capacitance is equal to the original capacitance, while the new resistance is about $\left(\frac{1}{R_1\ \omega\ C_1}\right)^2$ times the old one.

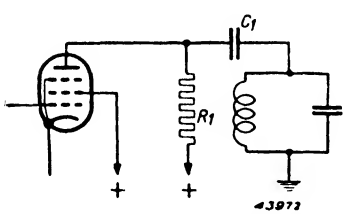

Fig. 6. IF amplifying valve with parallel feed.

A practical case of the foregoing will now be considered, in which a circuit tuned to 125 kc/s is parallel-fed from an amplifying valve, as in fig. 6. It is desired to know the magnitude of the damping and of the detuning caused by the combination R_1C_1 shunted across the tuned circuit. It is assumed that R_1 is 200,000 Ω and that $C_1 = 25$ pF. At 125 kc/s the reactance of C_1 is 50,000 Ω.

The character of the series circuit comprised by R_1 and C_1 is, clearly, mainly resistive, for R_1 is four times as large as $\frac{1}{\omega\ C_1}$.

In the equivalent circuit R_2 will therefore also be 200,000 Ω and the tuned circuit will be damped to that extent. The equivalent shunt capacitance, however, is about $\frac{1}{16}$ of the original figure, that is 1.5 pF. With parallel

feed the resonant frequency of the tuned circuit is shifted by this equivalent capacitance.

Now consider a coupling with other values of R_1 and C_1 — e.g. with $R_1 =$ 50,000 Ω and $C_1 = 5$ pF. The reactance of a capacitance of 5 pF amounts to 250,000 Ω at 125 kc/s. In this case the series circuit has a more capacitive nature, and the equivalent shunt capacitance remains equal to C_1. Accordingly a capacitance of 5 pF is added in parallel with the tuned circuit; as its reactance is five times as great as the resistance in the equivalent circuit the resistance becomes five times as great as the reactance, viz. $5 \times 250{,}000$ Ω. The tuned circuit is thus damped by a resistance 1.25 MΩ.

From equations (I A 30) and (I A 31) it is easy to deduce that the same arguments may be used to derive a series circuit from a parallel circuit.

Once more, however, it should be emphasised that this transformation is valid for only *one* frequency; consequently the calculated equivalent resistance, for instance, could not be used to compute the contour of a resonance curve over a large frequency band.

§ 5. The resonance curve and selectivity

The concept of selectivity has already been introduced in I A § 1. We mean by this term the property of suppressing a signal whose frequency differs from that of the desired signal, as exemplified by a tuned circuit which, when resonant at the required frequency, offers a lower impedance at all other frequencies. The formulae (I A 10), (I A 12) and (I A 18), and especially the resonance curve in fig. 2, indicate how the impedance diminishes on detuning of the signal and enable us to quote selectivity in numerical terms.

One of the most common cases is the separation of two transmitters working on frequencies close together and producing signals of about equal strength at the receiving aerial. By international agreement the frequency-separation between adjacent broadcasting stations is theoretically 9 kc/s. The problem is, therefore, to suppress the beat frequencies and other interferences from the two transmitters whose carrier frequencies differ 9 kc/s or more from that of the desired station.

The suppression of the adjacent transmissions is accompanied, however, by an undesirable attenuation of side-bands, corresponding to the higher modulation frequencies, which are separated from one another by less than 9 kc/s.

Since it is in every case necessary to suppress almost completely all frequencies removed from the required carrier by more than 9 kc/s a satisfactory compromise is to reduce the response to frequencies separated by 5 kc/s

from the carrier in the ratio 1 : 10 or 1 : 7; by such figures the selectivity can be fixed.

That such a compromise can never be reached by means of a single tuned circuit is evident from figure 2. If, for attenuation of $a = 10$, βQ corresponds to 5 kc/s, then at βQ corresponding to 9 kc/s (i.e. 1.8 times as much) the attenuation amounts to about 18 times. Such a ratio is far too small for good suppression of interference: to reach a satisfactory compromise it is necessary to use several tuned circuits in cascade.

A further requirement is the adequate suppression of a local station whose signal is, for example, 100 times stronger than that of a desired transmitter; this demands an attenuation of the order of 1000 to 10,000 times. The requisite selectivity for such a case is therefore to be specified by two figures, namely a combination of $a = 10{,}000$ for a specified amount of $\Delta\omega$.

If the modulation side bands are not to be lost, attenuation of such a degree can be obtained only if the frequency difference is at least 27 kc/s, and even then only by using several tuned circuits. Transmitters whose carrier frequencies differ from that of the local station by less than 27 kc/s are in practice unreceivable; four transmitters working at 9 and 18 kc/s below and 9 and 18 kc/s above the interfering station are thus ruled out.

By the selectivity of a circuit we mean also the coefficient $\frac{\omega_0}{\Delta\omega}$ relating to a specified attenuation, for example $a = 10$. This we should refer to as relative selectivity (since it is based on the relative detuning), in contradistinction to absolute selectivity, already defined.

Starting with $a = 10$, so that, approximately, $\beta Q = 10$ (see fig. 2) we therefore have for the relative selectivity σ:

$$\beta = \frac{2\Delta\omega}{\omega_0} = \frac{10}{Q}, \quad Q = \frac{\omega_0 L}{r};$$

thus

$$\sigma = \frac{\omega_0}{\Delta\omega} = 0.2\,\frac{\omega_0 L}{r} = 0.2\,\frac{1}{r}\sqrt{\frac{L}{C}} \quad \ldots\ldots \quad \text{(I A 32)}$$

The relation $\frac{\omega_0 L}{r}$, which has so far been called the quality factor, here assumes a special significance: it determines the relative selectivity; equation (I A 32) may therefore also be written:

$$\sigma = 0.2\,Q \quad \ldots\ldots\ldots\ldots\ldots\ldots \quad \text{(I A 33)}$$

Now it appears that the Q of most inductors changes little over a large range of frequencies such as the medium or the long-wave band. It is therefore characteristic of the tuned circuit without parallel damping that its relative selectivity is fairly constant.

It follows from the foregoing that the absolute selectivity, i.e. the detuning $\Delta\omega$, is only of interest for a specified attenuation. This selectivity, however, is not constant over the waveband, for the relation $\frac{r}{L}$ of an inductor is nearly proportional to frequency. Moreover the almost invariable practice is to bring an R.F. tuned circuit into resonance by means of a variable capacitor connected in parallel with a fixed coil; the shunt damping then increases with frequency, as is evident from equation (I A 22), while C decreases. In order to obtain constant selectivity over all the wave bands used for broadcasting the superheterodyne principle is adopted; the frequency of the received signal is first changed to a fixed intermediate frequency and is then tuned by selective circuits. While, in the case of R.F. coils, values for r/L from about 30,000 at 2,000 m to about 500,000 at 15 m can be attained, I.F. coils can readily be manufactured with an r/L value of 15,000 at 125 kc/s and 20,000 at 475 kc/s (these figures are obtained with r measured in ohms and L in henrys).

§ 6. Tuned circuits in cascade

As was observed in the preceding section, a resonance curve of the shape delineated in fig. 2, that of a single circuit, is unsuitable for radio purposes even if the quality of this circuit is made very high. Ideally, a resonance curve should have a flat top and steep sides.

One way to secure better performance is to arrange several circuits one after the other. For tuned circuits with identical Q factor, the relation βQ for a specific detuning of $\Delta\omega$, and therefore also the attenuation factor, will then be the same; if such circuits are connected in cascade the total attenuation then becomes:

$$a = \sqrt{1 + (\beta Q)^2}^{\,n} \quad \ldots\ldots\ldots\ldots \quad \text{(I A 34)}$$

Fig. 7 shows the result for one, two and three circuits. Especially when three tuned circuits are employed a really useful improvement is obtained. If at 5 kc/s an attenuation of ten times is permissible, so that $\beta Q = 2$, then at 9 kc/s, βQ being 3.6, the attenuation exceeds 50.

Although these curves fall far short of the requirements specified in § 5, for a long time nothing better was available. In order that the relation Q may equal 2 at a detuning of 5 kc/s, r/L must equal 30,000 (see fig. 20). Indeed

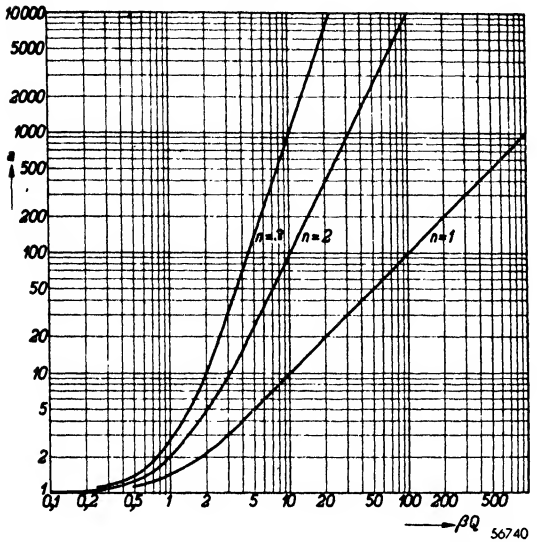

Fig. 7. Resonance curves for a single tuned circuit ($n = 1$), a combination of two circuits ($n = 2$), and of three circuits ($n = 3$), the quality of the circuits being the same.

straight sets were built with three such circuits; however, the performance mentioned was not obtained over the whole of the wavebands; at some wavelengths the selectivity was still lower.

A second possible method of securing a better-shaped resonance curve is a cascade arrangement of tuned circuits having different quality factors. In such a case the attenuation, for example for two circuits, would be:

$$a = \sqrt{[1+(\beta Q_1)^2][1+(\beta Q_2)^2]} \qquad \text{(I A 35)}$$

If Q_2 is made equal to $\frac{1}{2} Q_1$ we obtain the dotted curve which in fig. 8 is compared with the full-line curve for two similar circuits for which $Q_1 = Q_2$; it is plain that the dotted curve is inferior.

Finally it is possible, Q being made equal (if in this case Q_1 and Q_2 differ asymmetrical resonance curves would be obtained), to vary the resonant frequency ω_0 of each circuit, i.e. ω_1, ω_2, etc. At a specified frequency ω, each circuit then has, from equation (I A 8), its own value of β. Furthermore $\beta_1 = 0$ when $\omega = \omega_1$, $\beta_2 = 0$ when $\omega = \omega_2$, etc. For two circuits we can write this approximation:

$$a = \sqrt{[1+(\beta_1 Q)^2][1+(\beta_2 Q)^2]} \qquad \text{(I A 36)}$$

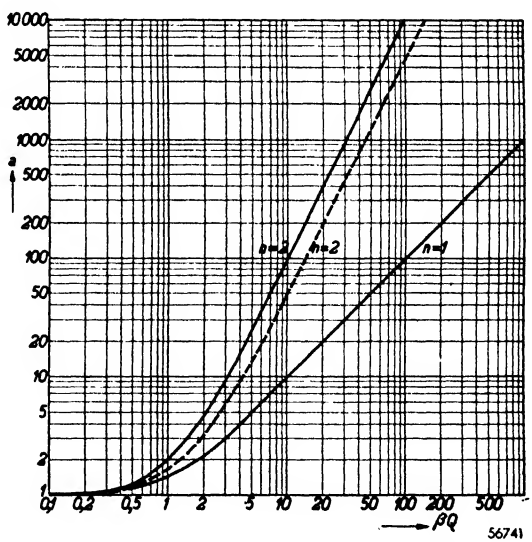

Fig. 8. Resonance curves of a single circuit ($n = 1$) and for a combination of two circuits ($n = 2$). The full-line curve refers to the case of identical quality factors; the dotted curve relates to circuits of differing quality factors, viz. $Q_2 = \frac{1}{2} Q_1$.

In this case a represents the attenuation in relation to the magnification which would be obtained if the two circuits resonated at the same frequency. In the band between the frequencies ω_1 and ω_2, β_1^2 increases, while β_2^2 decreases, and at its limits either β_2 or β_1 is zero. The overall response of the two circuits reaches maximum between ω_1 and ω_2, and a must be calculated by relation to this peak.

Between ω_1 and ω_2, β_1 and β_2 are varying in opposite sense, and the response is fairly constant, while outside this band β_1 and β_2 vary in the same sense and the response falls sharply. Superficial consideration suggests, therefore, that this arrangement presents advantages compared with a pair of tuned circuits in cascade with the same value of β.

To facilitate further analysis we shall use ω_0 to denote the mid-frequency between ω_1 and ω_2 and relate detuning to that frequency. Thus:

$$\beta \approx 2\frac{\omega-\omega_0}{\omega_0},$$

$$\beta_1 \approx 2\frac{\omega-\omega_1}{\omega_1} \approx 2\frac{\omega-\omega_0+\omega_0-\omega_1}{\omega_0},$$

$$\beta_2 \approx 2\frac{\omega-\omega_2}{\omega_2} \approx 2\frac{\omega-\omega_0+\omega_0-\omega_2}{\omega_0}.$$

As ω_0 represents the mean of ω_1 and ω_2, $\omega_0-\omega_1 = \omega_2-\omega_0$, and we can therefore write:

$$2\frac{\omega_0-\omega_1}{\omega_0} = 2\frac{\omega_2-\omega_0}{\omega_0} = \beta_v.$$

The foregoing equations simplify to:

$$\beta_1 = \beta + \beta_v \text{ and } \beta_2 = \beta-\beta_v. \quad \ldots\ldots\ldots \quad \text{(I A 37)}$$

For the frequency $\omega = \omega_0$ the detuning of the first circuit is:

$$\beta_1 = 2\frac{\omega_0-\omega_1}{\omega_0} = \beta_v,$$

and of the second circuit:

$$\beta_2 = 2\frac{\omega_0-\omega_2}{\omega_0} = -\beta_v.$$

The attenuation of the first circuit against the frequency ω_0 is now:

$$a_1 = \frac{\sqrt{1+(\beta_1 Q)^2}}{\sqrt{1+(\beta_v Q)^2}}.$$

The overall attenuation is accordingly:

$$a = \frac{\sqrt{[1+(\beta_1 Q)^2]\,[1+(\beta_2 Q)^2]}}{1+(\beta_v Q)^2} \quad \ldots\ldots\ldots \quad \text{(I A 38)}$$

Substituting from equation (I A 37) gives us:

$$a = \frac{\sqrt{[1+(\beta+\beta_v)^2\,Q^2]\,[1+(\beta-\beta_v)^2\,Q^2]}}{1+\beta_v^2\,Q^2} \quad \text{(I A 39)}$$

Rearranging we find:

$$a = \frac{\sqrt{(1+\beta_v^2\,Q^2)^2+2\,(1-\beta_v^2\,Q^2)\,\beta^2\,Q^2+\beta^4 Q^4}}{1+\beta_v^2\,Q^2} \quad \text{(I A 40)}$$

If $1 - \beta_v^2\,Q^2$ is positive, a increases as soon as β becomes greater or less than 0 (fig. 9*a*). But if $1-\beta_v^2\,Q^2$ is negative the attenuation first decreases as the value of β increases, and increases again as soon as $\beta^4\,Q^4$ exceeds $2\,(1-\beta_v^2 Q_2)\beta^2$ (fig. 9, curve *b*).

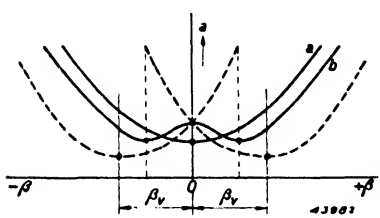

Fig. 9. Resonance curves of a combination of two circuits with different resonant frequencies:
a. for small frequency-difference;
b. for a fairly large frequency-difference.

If the resonant frequencies of the tuned circuits are so widely separated that $\beta_v > 1/Q$, curves as in fig. 9*b* are obtained, which are a considerable improvement over those of fig. 7.

From equation (I A 40) it is easy to deduce that the attenuation a reaches minimum when:

$$\beta^2 = \beta_v^2 - \frac{1}{Q^2} \quad \ldots\ldots\ldots\ldots\ldots \quad \text{(I A 41)}$$

It will be realised that $+\beta_v$ and $-\beta_v$ correspond with the natural frequencies of the two circuits.

The flat part of the resonance curve, the existence of which is evident from equation (I A 41), can advantageously be utilised to pass the whole modulation-frequency band at the same level. The cascade connection of tuned circuits with staggered resonant frequencies resulted in greatly improved receivers, but the development of the superheterodyne resulted in the gradual disappearance of the straight set.

The greatest difficulty with such an arrangement was to keep the inter-

circuit frequency-differences constant throughout each waveband, and this same problem arose in another form when the superheterodyne was developed. Detailed reference to this matter will be found in Chapter III.

In a case where there are three tuned circuits the third is tuned to the frequency ω_0, thus to the mid-point between ω_1 and ω_2, in order to preserve the overall symmetry. The resultant resonance curve appears if the curves of figs 2 and 9 are multiplied, any difference of Q being taken into account. With straight sets in which the selecting circuits are tuned over a whole band by means of variable capacitors, the number of circuits is limited to a maximum of four. When only one carrier frequency requires to be amplified, four circuits, or more, may be employed without any difficulty. However, the number of circuits may then exceed the total number of valves necessary; the possibility then presents itself of coupling some of the tuned circuits, not by valves, but by such elements as capacitance, inductance or mutual inductance. The overall response is then no longer a simple multiplication of the responses of the individual circuits, for the coupled circuits influence one another, giving rise to so-called band-pass filters.

B. Band-pass filters

Introduction

The discussion which follows is limited to two-circuit filters of types used in the R.F. and I.F. stages of receiving apparatus.

Although we normally endeavour to make the natural frequencies of the two tuned circuits alike, we shall begin by deriving the equations for a band-pass filter whose circuits resonate on different frequencies, keeping the results as general as possible. By this means the formulae can be used directly for section E (Variable-Selectivity), in which are described band-pass filters consisting of circuits with different natural frequencies.

It is appropriate first of all to derive formulae for an inductively coupled band-pass filter, for this type may be regarded as typical; the formulae can then be modified in conformity with the differing characteristics of alternative forms of coupling*.

We shall use the following symbols:

ω_1 = the angular frequency to which the primary circuit is tuned.

ω_2 = the angular frequency to which the secondary circuit is tuned.

These definitions of ω_1 and ω_2 allow of varying interpretation when two tuned circuits are involved. In the course of the discussion ω_1 and ω_2, referring to the resonant frequencies in specified circumstances of the primary and secondary circuits respectively, will be expressed in terms of various circuit constants.

In the case of an inductive coupling, for instance, the secondary circuit is ignored in determining ω_1, for otherwise the stray capacitance of the secondary winding too would enter into the calculation; with top-capacitance coupling the secondary circuit is regarded as short-circuited, and so on.

$\omega_0 = \sqrt{\omega_1 \omega_2}$. As we are considering only the case in which ω_1 and ω_2 differ by a small amount, we can make an approximation and say

$$\omega_0 = \frac{\omega_1 + \omega_2}{2}.$$

ω_0 is thus the frequency which lies midway between ω_1 and ω_2.

$\omega = 2\pi f$ for the frequency of the signal.

---

* We here follow the idea put forward by B. D. H. Tellegen, "Coupled Circuits", Philips Research Reports, Vol 2. No. 1, Febr. 1947.

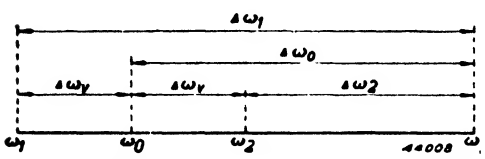

Fig. 10. Relation of various angular frequencies:
ω_1 = angular frequency of the primary circuit;
ω_2 = angular frequency of the secondary circuit;
ω_0 = angular frequency lying midway between ω_1 and ω_2;
ω = angular frequency of the signal.

$\Delta\omega_1 = \omega - \omega_1$ = detuning of the primary circuit from the signal.
$\Delta\omega_2 = \omega - \omega_2$ = detuning of the secondary circuit from the signal.
$\Delta\omega_0 = \omega - \omega_0$ detuning of ω_0 from the signal.
$\Delta\omega_v = \omega_0 - \omega_1 = \omega_2 - \omega_0$ = detuning of the circuits from ω_0.

The relative magnitude of these frequencies is indicated in fig. 10.

We now introduce:

$$\beta_1 = \frac{\omega}{\omega_1} - \frac{\omega_1}{\omega},$$

$$\beta_2 = \frac{\omega}{\omega_2} - \frac{\omega_2}{\omega},$$

$$\beta = \frac{\omega}{\omega_0} - \frac{\omega_0}{\omega},$$

$$\beta_v = \frac{\omega_2}{\omega_0} - \frac{\omega_0}{\omega_2} = \frac{\omega_0}{\omega_1} - \frac{\omega_1}{\omega_0}.$$

If we are considering only frequencies close to ω_0 we can write approximately:

$$\beta_1 = 2\frac{\Delta\omega_1}{\omega_0},$$

$$\beta_2 = 2\frac{\Delta\omega_2}{\omega_0},$$

$$\beta = 2\frac{\Delta\omega_0}{\omega_0},$$

$$\beta_v = 2\frac{\Delta\omega_v}{\omega_0}.$$

§ 1. General formulae for the inductively-coupled band- pass filter

The filters used in practice may be divided into two classes:

a. R.F. band-pass filters with variable tuning;

b. I.F. band-pass filters with fixed tuning.

Filters of the first type are used in the aerial circuit, or in the anode circuit of the R.F. valve, while those of the second type are found only in the anode circuit of a frequency converter or I.F. amplifying valve.

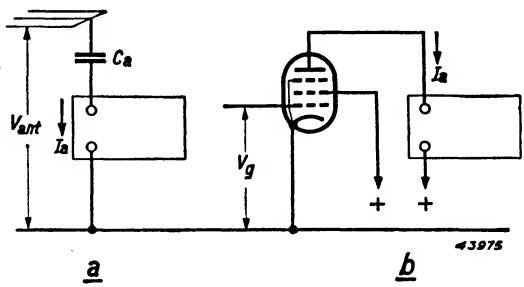

Fig. 11a. Block diagram of a band-pass filter in the aerial circuit.
b. Block diagram of a band-pass filter in the anode circuit of an R.F. or I.F. amplifying valve.

We assume in both cases that a certain alternating current is supplied to the input side, and that from the output side it is desired to take off an AC voltage. The alternating current may be supplied, for example, by an aerial (see fig. 11a) in accordance with the formula:

$$I_a = V_{ant}\, \omega\, C_a,$$

C_a being regarded as in parallel with the input and included in the band-pass filter circuit. Or it may be supplied by a valve (see fig. 11b) in accordance with the formula:

$$I_a = S\, V_g,$$

R_i being in parallel with the input.

By a simple calculation this reasoning may be applied also to the case of inductive aerial-coupling. In fig. 12 we have a generalised circuit of an inductively-coupled band-pass filter. All values are numbered to indicate to which circuit they belong. We begin with the assumption that the current through the right-hand branch of the primary circuit has a magnitude I_1. In the left-hand branch, therefore, a current of magni-

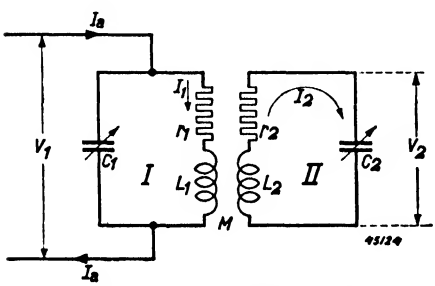

Fig. 12. Inductively-coupled band-pass filter.

tude $I_1 - I_a$ flows. The current through the secondary circuit, which is assumed to be non-loaded, is I_2. We can now state in a simple manner the voltage equilibrium for each individual tuned circuit.

For circuit I we have:

$$I_1 (r_1 + j\omega L_1) + (I_1 - I_a) \frac{1}{j\omega C_1} + I_2 j\omega M = 0 \quad . \quad \text{(I B 1)}$$

and circuit II:

$$I_2 \left(r_2 + j\omega L_2 + \frac{1}{j\omega C_2}\right) + I_1 j\omega M = 0 \quad . \quad . \quad . \quad . \quad \text{(I B 2)}$$

The equation for the first circuit can also be written:

$$I_1 \left(r_1 + j\omega L_1 + \frac{1}{j\omega C_1}\right) + I_2 j\omega M = \frac{I_a}{j\omega C_1} \quad . \quad . \quad \text{(I B 3)}$$

From the last two equations the relation between the currents I_2 and I_a must now be determined; I_1 has therefore to be eliminated so that V_2 may be calculated from I_2.

For $j\omega L_1 + \frac{1}{j\omega C_1}$ can be written:

$$j\omega L_1 + \frac{1}{j\omega C_1} = j\omega_1 L_1 \left(\frac{\omega}{\omega_1} - \frac{1}{\omega\, \omega_1\, L_1\, C_1}\right) = j\omega_1 L_1 \left(\frac{\omega}{\omega_1} - \frac{\omega_1}{\omega}\right),$$

or:

$$j\omega L_1 + \frac{1}{j\omega C_1} = j\omega_1 L_1 \beta_1 \quad . \quad . \quad . \quad . \quad . \quad . \quad . \quad . \quad . \quad \text{(I B 4)}$$

Similarly for $j\omega L_2 + \frac{1}{j\omega C_2}$ we may write:

$$j\omega L_2 + \frac{1}{j\omega C_2} = j\omega_2 L_2 \beta_2 \quad . \quad . \quad . \quad . \quad . \quad . \quad . \quad . \quad . \quad \text{(I B 5)}$$

Substituting from equations (I B 4) and (I B 5) in (I B 2) and (I B 3) and eliminating I_1, we get:

$$I_2 = - I_a \frac{M/C_1}{(r_1 + j\omega_1 L_1 \beta_1)(r_2 + j\omega_2 L_2 \beta_2) + \omega^2 M^2}$$

From this it follows that the voltage across the secondary circuit is:

$$V_2 = I_2 \frac{1}{j\omega C_2} = -I_a \frac{1}{j\omega C_2} \frac{M/C_1}{(r_1 + j\omega_1 L_1 \beta_1)(r_2 + j\omega_2 L_2 \beta_2) + \omega^2 M^2}.$$

Putting Q_1 for $\frac{\omega_1 L_1}{r_1}$ and Q_2 for $\frac{\omega_2 L_2}{r_2}$, we get:

$$V_2 = -I_a \frac{1}{j\omega C_2 C_1 (1 + j\beta_1 Q_1)(1 + j\beta_2 Q_2) + \omega^2 \frac{M^2}{r_1 r_2}} \frac{M/r_1 r_2}{} \quad \ldots\ldots \text{(I B 6)}$$

Now M may be written:

$$M = k\sqrt{L_1 L_2} \quad \ldots\ldots\ldots\ldots\ldots \text{(I B 7)}$$

in which k is the coupling factor between the two coils $L_1 L_2$. Furthermore $\frac{1}{C_1}$ may be substituted by $\omega_1^2 L_1$ and $\frac{1}{C_2}$ by $\omega_2^2 L_2$, yielding:

$$V_2 = -I_a \frac{\omega_1\omega_2}{j\omega} \frac{Q_1 Q_2 k \sqrt{L_1 L_2}}{(1 + j\beta_1 Q_1)(1 + j\beta_2 Q_2) + \frac{\omega^2}{\omega_1\omega_2} Q_1 Q_2 k^2} \quad \ldots \text{(I B 8)}$$

When making use of the definition $\omega_0^2 = \omega_1\omega_2$ the combination $\frac{\omega^2}{\omega_0^2} k^2$ appears in the denominator, a combination that will be met again in the formulae for other types of band-pass filters; it may be expressed by:

$$K^2 = \left(\frac{\omega}{\omega_0}\right)^2 k^2 = \left(\frac{\omega}{\omega_0}\right)^2 \frac{M^2}{L_1 L_2} \quad \ldots\ldots\ldots \text{(I B 9)}$$

Equation (I B 8) now becomes:

$$V_2 = j I_a \frac{\omega_0^3}{\omega^2} \frac{Q_1 Q_2 K \sqrt{L_1 L_2}}{(1 + j\beta_1 Q_1)(1 + j\beta_2 Q_2) + Q_1 Q_2 K^2} \quad \ldots\ldots \text{(I B 10)}$$

This equation gives V_2 for any case of two coupled circuits.
There are four particular cases to be distinguished, namely:
a. Two identically tuned circuits, but with (i) the same Q; (ii) differing Q.
b. Two unequally tuned circuits, with (i) the same Q; (ii) differing Q.
The two cases mentioned under *a* occur most frequently, the first as a simplification for convenience of the second case. Both are dealt with in §§ 2—9 inclusive. Band-pass filters with mutually-detuned circuits are less often encountered; they are considered in § 10.

In the simplest case the two tuned circuits are identical, and therefore $Q = Q_1 = Q_2$ and $\beta = \beta_1 = \beta_2$. Equation (I B 10) then becomes:

$$V_2 = jI_a \frac{\omega_0^3}{\omega^2} \frac{Q^2 K \sqrt{L_1 L_2}}{(1 + j\beta Q)^2 + Q^2 K^2} \quad \ldots\ldots\ldots \text{(I B 11)}$$

The resonance curve gives us the relation a between the voltage V_{2res} at resonance and the voltage V_2.

$$a = \left| \frac{V_{2res}}{V_2} \right| = \left| \frac{\omega^2}{\omega_0^2} \frac{(1 + j\beta Q)^2 + Q^2 K^2}{1 + Q^2 K^2} \right| \quad \ldots \text{(I B 12)}$$

If once more we put $\omega/\omega_0 = 1$ we can write:

$$a = \left| \frac{(QK - j + \beta Q)(QK + j - \beta Q)}{1 + Q^2 K^2} \right|,$$

$$a = \left| -\frac{[(\beta + K) Q - j][(\beta - K) Q - j]}{1 + Q^2 K^2} \right|$$

or:

$$a = \sqrt{\frac{[1 + (\beta + K)^2 Q^2][1 + (\beta - K)^2 Q^2]}{1 + Q^2 K^2}} \quad \ldots \text{(I B 13)}$$

Comparing now equations (I B 13) and (I A 39) — the latter refers to the case of two mutually-detuned circuits in cascade — we note that they are identical if β_v is replaced by K.

It is thus possible to obtain with a band-pass filter the same results as are given by two separate tuned circuits in cascade.

In place of the detuning term in the equation for cascade circuits, the band-pass filter equation includes a term for the inter-circuit coupling. This similarity of behaviour was mentioned at the end of A § 5.

§ 2. Filter with identically-tuned circuits; properties at resonance

In the case of circuits with the same resonant frequency we can write: $\omega_1 = \omega_2 = \omega_0$. The general equation (I B 10) then becomes:

$$V_2 = jI_a \frac{\omega_0^3}{\omega^2} \frac{Q_1 Q_2 K \sqrt{L_1 L_2}}{(1 + j\beta Q_1)(1 + j\beta Q_2) + Q_1 Q_2 K^2} \quad \text{(I B 14)}$$

It is proposed first of all to deduce the behaviour of a band-pass filter with regard to an A.C. voltage to which it is tuned; in radio parlance, with regard to the signal to be received. For the moment we need not consider whether the signal is at its original frequency or has been converted to the intermediate frequency.

The applied frequency ω being equal to ω_0, the factor β is 0. Equation (I B 14) then simplifies considerably:

$$V_2 = j I_a \frac{\omega_0 Q_1 Q_2 K \sqrt{L_1 L_2}}{1 + Q_1 Q_2 K^2}$$

or:

$$V_2 = j I_a \frac{K \sqrt{Q_1 Q_2}}{1 + Q_1 Q_2 K^2} \times \omega_0 \sqrt{L_1 L_2} \sqrt{Q_1 Q_2}.$$

If we substitute for $\sqrt{Q_1 Q_2}$ the mean factor Q we can write:

$$V_2 = j I_a \frac{Q K}{1 + Q^2 K^2} \frac{\omega_0 \sqrt{L_1 L_2} \times \sqrt{\omega_1 \omega_2 L_1 L_2}}{\sqrt{r_1 r_2}},$$

$$V_2 = j I_a \frac{Q K}{1 + Q^2 K^2} \sqrt{\frac{L_1}{r_1 C_1} \frac{L_2}{r_2 C_2}},$$

or:

$$V_2 = j I a \frac{Q K}{1 + Q^2 K^2} \sqrt{Z_1 Z_2} \quad \ldots\ldots\ldots \quad \text{(I B 16)}$$

The result appears very simple. The expression $\sqrt{Z_1 Z_2} = Z$ might be described as "average dynamic resistance". If a single tuned circuit were used instead of the band-pass filter, the output voltage would be given by:

$$V_2 = -I_a \cdot Z.$$

In equation (I B 16) a new fraction will be observed, the magnitude of which for various values of $Q K$ may be ascertained from fig. 13. The relation $\frac{V_2}{I_a}$, the transmission of the filter, is a maximum when $Q K = 1$. The fraction in question then attains a value of 0.5 and the transmission of the filter is then half that of a single circuit with the same impedance. The coupling $K = \frac{1}{Q}$ at which this maximum occurs is known as "critical coupling", and equation (I B 16) then becomes:

$$V_2 = \tfrac{1}{2} j I_a \cdot Z \quad \ldots\ldots\ldots\ldots\ldots \quad \text{(I B 17)}$$

If the coupling is greater or less than critical the exact value of the factor $\frac{Q K}{1 + Q^2 K^2}$ is given directly by fig. 13; in this expression Q again represents the mean of the original Q-factors.

Clearly it is advantageous for the coupling in I.F. transformers to correspond to the critical amount; such degree of coupling is arrived at by adjusting for maximum transmission. It is apparent from fig. 13, however, that the coupling may be varied a good deal without appreciably altering the transmission of the filter, and for that reason the simplified equation is of considerable practical value.

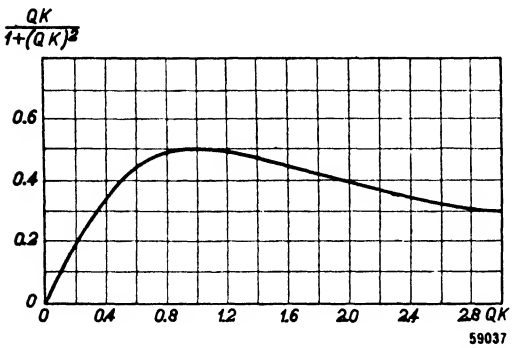

Fig. 13. The term $\frac{QK}{1+Q^2K^2}$ from equation (I B 16), as a function of QK.

The precise value of the relation KQ will rarely be known accurately. The coupling factor K, however, is easily determined by measurement. In this connection it should be noted that we are dealing with the resonance condition, so that K will be equal to the actual coupling factor k.

Similarly the factors Q_1 and Q_2 may be ascertained by direct measurements. In the case of I.F. transformers no large error will arise if $Q = \frac{\omega L}{r}$ is calculated, taking for r the DC resistance of the winding.

It is necessary to bear in mind, however, when determining both Z and Q that the damping imposed by the valves has to be allowed for. In calculating Z this is a simple matter, for Z_{tot} is given by:

$$\frac{1}{Z_{tot}} = \frac{rC}{L} + \frac{1}{R_p} \quad \ldots\ldots\ldots\ldots \quad \text{(I B 18)}$$

where R_p represents the anode A.C.-resistance, the grid-cathode impedance, or the diode damping. From the value of Z thus ascertained we then find the total value of Q. For a circuit at resonance we can write:

$$Z = \frac{L}{rC} \text{ and } \omega_0 Z = \frac{\omega_0 L}{r} \cdot \frac{1}{C}$$

therefore:

$$Q = \frac{\omega_0 L}{r} = \omega_0 ZC \quad \ldots\ldots\ldots\ldots \quad \text{(I B 19)}$$

With the help of this last equation we can deduce Q_1 from Z_1, and Q_2 from Z_2. This is considered in detail in § 9.

We shall now take a practical example: an I.F. transformer working at 125 kc/s, preceded by an EF 22 pentode and followed by a diode detector. For both primary and secondary circuits of the band-pass filter with a Q of 60:

$$L = 17{,}000\ \mu\text{H},\ r = 220\ \Omega,\ C = 95\ \text{pF and}\ \omega_0 = 785{,}000.$$

From these values $\frac{L}{rC}$ is thus 810,000 Ω for each circuit. But the primary is shunted by the A.C.-resistance of the preceding valve, 1.2 MΩ, and the resultant dynamic resistance therefore amounts to 480,000 Ω. On the secondary side the diode damping, which we may estimate at 250,000 Ω, is in parallel with the tuned circuit (see chapter V, Detection). Allowing for this damping, the dynamic resistance of the secondary is 190,000 Ω. The amplification of this I.F. stage, with critical coupling, may now be ascertained very simply from equation (I B 17); by amplification we mean the relation between the voltage V_2 applied to the diode and the voltage V_1 fed to the grid of the I.F. valve. In equation (I B 17) I_a is therefore $S.\ V_g$ and $S =$ 0.0022 A/V. Thus we have:

$$V_2 = V_g \times 0.0022 \times \tfrac{1}{2} \sqrt{480{,}000 \times 190{,}000} = 330\ V_g \quad \ldots \quad \text{(I B 20)}$$

Such high gain nearly always leads to difficulties owing to feed-back. In most cases a larger tuning capacitor is accordingly chosen, and the dynamic resistance of the circuit is then lower. If the primary circuit also feeds an AVC diode, its effective dynamic resistance is of course computed in exactly the same way as that of the secondary; the amplification is in this case smaller.

It is appropriate at this point to examine the behaviour of a band-pass filter designed to be lightly loaded, when it is damped by a diode; we shall assume that the band-pass filter considered in the foregoing example is just critically coupled when both sides have a load of 1.2 MΩ. Then:

$$K \sqrt{Q_1 Q_2} = 1 \text{ and } Z_1 = Z_2 = 480{,}000\ \Omega.$$

Connection of the diode reduces Z_2 to 190,000 Ω, i.e. it is 2.5 times smaller than before. It follows from equation (I B 19) that Q_2 then becomes 2.5 times smaller too, and if the coupling between the coils remains unchanged

the amount $K\sqrt{Q_1Q_2}$ is than $\sqrt{2.5}$ times smaller. The coupling has become sub-critical. QK now has a value of:

$$\frac{1}{\sqrt{2.5}} = 0.63$$

From fig. 13 it is apparent that in equation (I B 20) the factor 0.5 must be replaced by 0.45; the transmission of the filter is then only a little lower.
In the case of an R.F. band-pass filter it is necessary to take into consideration the fact that the Q-factor can have different values as the tuning is varied. Consequently a filter which is, for instance, critically coupled at the lower end of the wave-band may be over or under-coupled at the upper end.

§ 3. Primary voltage

Sometimes it is important to know the voltage at the terminals of the primary circuit, for example in the case of the AVC circuit already mentioned, in which the control diode is fed from the primary (see Book III, Chapter X).
A quite simple equation gives V_1 with sufficient accuracy.

Referring to fig. 12, we assume that only the current I_1 flows through C_1, and neglect I_a. For V_2 we have:

$$V_2 = I_2 \frac{1}{j\omega C_2}.$$

Similarly

$$V_1 = \frac{I_1}{j\omega C_1}.$$

Therefore:

$$\frac{V_1}{V_2} = \frac{I_1}{I_2}\frac{C_2}{C_1}.$$

The relation I_1/I_2 may be determined with the help of equations (I B 2) and (I B 5), which yield the following:

$$\frac{I_1}{I_2} = -\frac{r_2 + j\omega L_2 + \frac{1}{j\omega C_2}}{j\omega M} = -\frac{r_2 + j\omega_2 L_2 \beta}{j\omega M} = \left(\frac{j}{Q_2} - \beta\right)\frac{\omega_2}{\omega}\frac{L_2}{M} \quad \text{(I B 21)}$$

At resonance β equals 0, and using identical tuned circuits $\omega_2/\omega = \omega_0/\omega = 1$.

So we get:

$$\frac{V_1}{V_2} = \frac{C_2}{C_1}\,\frac{jL_2}{Q_2 M} = j\,\frac{C_2}{C_1}\sqrt{\frac{L_2}{L_1}}\sqrt{\frac{Q_1}{Q_2}}\,\frac{\sqrt{L_1}\sqrt{L_2}}{\sqrt{Q_1}\sqrt{Q_2}},$$

$$\frac{V_1}{V_2} = j\sqrt{\frac{C_2}{C_1}}\sqrt{\frac{Q_1}{Q_2}}\,\frac{\sqrt{L_1 L_2}}{M}\,\frac{1}{\sqrt{Q_1 Q_2}},$$

$$\frac{V_1}{V_2} = j\sqrt{\frac{C_2}{C_1}}\sqrt{\frac{Q_1}{Q_2}} \times \frac{1}{Qk} \quad \ldots\ldots\ldots \quad \text{(I B 22)}$$

As the phase-shift usually does not interest us, the factor $j = \sqrt{-1}$ is unimportant. Furthermore, in the case of two identical tuned circuits the factors $\sqrt{\frac{C_2}{C_1}}$ and $\sqrt{\frac{Q_1}{Q_2}}$ both become equal to unity; consequently the relation V_1/V_2 then depends only on the coupling. It is now apparent that with critical coupling ($Q\,K = 1$) the voltages across primary and secondary are equal; in the case of sub-critical coupling V_1 is proportionally greater, and with over-critical coupling proportionally less. When the circuits are not identical the ratios C_2/C_1 and Q_1/Q_2 must be taken into account.

The first I.F. transformer in a receiver generally has identical primary and secondary circuits, so that when the coupling is critical the voltages across the two windings may be assumed equal.

For the example on page 27 (concerning the second I.F. transformer) the expression $\sqrt{\frac{C_2}{C_1}}$ drops out because the two capacitors of the I.F. transformer are equal. However, it has already been stated that $Q_1/Q_2 = 2.5$, so that $\sqrt{Q_1/Q_2} = 1.58$.

It therefore follows that if in such a case the coupling is critical, V_1 is about 1.6 times as large as V_2. Taking into consideration that the coupling is less than critical in the example quoted, $\frac{1}{Qk}$ in equation (I B 22) is $\sqrt{2.5} = 1.58$ and therefore $V_1/V_2 = 1.58 \times 1.58 = 2.5$.

§ 4. Methods of coupling

So far we have dealt only with inductive coupling between the two tuned circuits of the band-pass filter. However there are various other methods of coupling, and in fig. 14 a filter is shown with a common coupling-capacitance C_k; this arrangement is sometimes called capacitive current-coupling.

Drawing up once again the equations for the voltage-equilibrium in the two circuits, we get for circuit I:

$$I_1 (r_1 + j\omega L_1 + \frac{1}{j\omega C_k}) + (I_1 - I_a) \frac{1}{j\omega C_1} + I_2 \frac{1}{j\omega C_k} = 0 \quad . \quad . \quad \text{(I B 23)}$$

and for circuit II:

$$I_2 (r_2 + j\omega L_2 + \frac{1}{j\omega C_2} + \frac{1}{j\omega C_k}) + I_1 \frac{1}{j\omega C_k} = 0 \quad . \quad . \quad . \quad . \quad . \quad . \quad \text{(I B 24)}$$

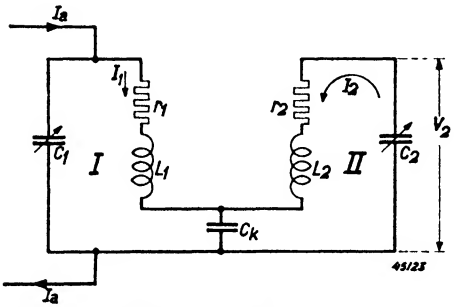

Fig. 14. Band-pass filter with capacitive current-coupling.

The term $\frac{1}{j\omega C_k}$ occurring in both equations indicates that the circuit capacitances are reduced somewhat by the coupling capacitance. This is taken into account in the definition of ω_0 (vide page 19). The calculation follows the same lines as that of the inductively-coupled band-pass filter.

It is evident from equations (I B 23) and (I B 24) that the term $I_2 j\omega M$ in equation (I B 1) is replaced by $I_2 \frac{1}{j\omega C_k}$, and the term $I_1 j\omega M$ in equation (I B 2) by $I_1 \frac{1}{j\omega C_k}$. In the formulae of the preceding section we can substitute $\frac{1}{\omega^2 C_k}$ for M throughout.

The expression $K^2 = \frac{\omega^2}{\omega_0^2} \frac{M^2}{L_1 L_2}$ therefore becomes:

$$K^2 = \frac{\omega^2}{\omega_0^2} \frac{1}{L_1 L_2} \frac{1}{\omega^4 C_k^2},$$

or:

$$K^2 = \frac{\omega_0^2}{\omega^2} \frac{C_1 C_2}{C_k^2} \quad . \quad . \quad . \quad . \quad . \quad . \quad . \quad . \quad . \quad . \quad . \quad . \quad \text{(I B 25)}$$

The important band-pass filter equations, such as (I B 14, 16, 17, 22), keep

their original form, the value of K being replaced, however, by the figure obtained from equation (I B 25).

It follows from this that the coupling in the filter of fig. 14 may be calculated simply and accurately. In the inductively-coupled filter, however, M must be ascertained by measurement.

It is of interest to calculate the coupling capacitance needed for critical coupling of the two circuits in the example on page 27, § 2. The value of the factor K must, from equation (I B 25), satisfy:

$$K^2 = \frac{1}{Q_1 Q_2}.$$

The Q-factors are most easily calculated with the help of equation (I B 19). As we are considering the case of resonance, $\omega_0/\omega = 1$ and the equation (I B 25) may therefore be further simplified.

We now get:

$$K^2 = \frac{C_1 C_2}{C_k^2} = \frac{1}{\omega_0 Z_1 C_1} \times \frac{1}{\omega_t Z_2 C_2},$$

or:

$$C_k^2 = C_1^2 C_2^2 Z_1 Z_2 \omega_0^2.$$

In our example $C_1 = C_2 = 95$ pF, and $\omega_0 = 785{,}000$.

We therefore find:

$C_k = (95.10^{-12})^2 \times 785{,}000 \times \sqrt{480{,}000 \times 190{,}000} = 2100$ pF.

It is immediately evident from equation (I B 25) that when capacitive coupling is used in R.F. band-pass filters the coupling factor is dependent on the capacitance of the tuning capacitors C_1 and C_2; in other words $Q\,K$, which determines the transmission of the filters, varies considerably. As C_1 and C_2 increase towards the upper end of the waveband, the relation $Q\,K$ becomes greater. Thus if the circuits are less than critically coupled at the lower end of the band, the coupling may, neglecting a possible variation of Q, be critical at the top of the waveband; the transmission of the filter accordingly increases with wavelength, as shown in fig. 13. On the other hand, as is well known, the dynamic resistance of the circuits falls with increasing wavelength; the result is that the gain calculated from equation (I B 16) obtainable with this type of filter remains sensibly constant over the whole waveband. If the magnitude of Q is known over the band, the response may be accurately computed with the aid of equation (I B 16).

A third well-known method of coupling is by top capacitance, as seen in fig. 15; this is sometimes called capacitive voltage-coupling. To ascertain the behaviour of such a coupling it is necessary to modify equations (I B 1) and (I B 2) somewhat.

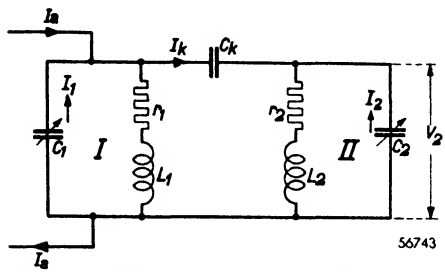

Fig. 15. Band-pass filter with capacitive voltage-coupling.

In circuit I the current through the capacitance C_1 is equal to $I_1 - I_a + I_k$, the last term representing the current through the coupling capacitance. In circuit II the current through the capacitance C_2 equals $I_2 - I_k$. The current I_k may be calculated from the voltage equilibrium in the circuit $C_1 - C_k - C_2$, accepting as a first approximation that C_1 is traversed by a current I_1, and C_2 by I_2. The balance is then:

$$\frac{I_1}{j\omega C_1} + \frac{I_k}{j\omega C_k} - \frac{I_2}{j\omega C_2} = 0,$$

or:

$$I_k = I_2 \frac{C_k}{C_2} - I_1 \frac{C_k}{C_1}.$$

For the voltage equilibrium in circuit I we therefore have:

$$I_1 (r_1 + j\omega L_1) + (I_1 - I_a + I_k) \frac{1}{j\omega C_1} = 0,$$

or:

$$I_1 (r_1 + j\omega L_1) + (I_1 - I_a - I_1 \frac{C_k}{C_1}) \frac{1}{j\omega C_1} + I_2 \frac{C_k}{C_2} \frac{1}{j\omega C_1} = 0. \quad \text{(I B 26)}$$

In the second term we note an increased circuit capacitance, as the value of the whole term has become smaller; this increased capacitance we allow for when defining ω_0, that is to say: $\omega_0 L (C_1 + C_k) = 1$. In the last term the original expression $j \omega M$ in equation (I B 1) is replaced by $\frac{C_k}{j\omega C_1 C_2}$.

In the same way the voltage equilibrium in circuit II may be drawn up. So, in further calculation M must in all equations be replaced by $\frac{C_k}{\omega^2 C_1 C_2}$;

if we introduce this substitution the original equation becomes:

$$K^2 = \frac{\omega^2}{\omega_0^2} \frac{1}{L_1 L_2} \frac{C_k^2}{\omega^4 C_1^2 C_2^2},$$

or:

$$K^2 = \frac{\omega_0^2}{\omega^2} \frac{C_k^2}{C_1 C_2} \quad \ldots\ldots\ldots\ldots\ldots \quad \text{(I B 27)}$$

In the case of inductively-coupled filters the stray capacitance between the high-potential ends of the two circuits often leads to difficulties, as it may cause tighter coupling even than the intended inductive linking. In order to elucidate this, we shall calculate what capacitance will give critical coupling in the example already discussed several times (§ 2, page 27).

We assume once again that $K^2 = \frac{1}{Q_1 Q_2}$; consequently at resonance:

$$K^2 = \frac{C_k^2}{C_1 C_2} = \frac{1}{\omega_0 Z_1 C_1} \times \frac{1}{\omega_0 Z_2 C_2} \quad \text{(see equation I B 19)}$$

$$C_k^2 = \frac{1}{\omega_0^2 Z_1 Z_2} \quad \ldots\ldots\ldots\ldots\ldots \quad \text{(I B 28)}$$

$$C_k = \frac{10^{12}}{785{,}000 \sqrt{480{,}000 \times 190{,}000}} = 4.2 \text{ pF}.$$

Such a very small capacitance will very often appear as a stray between the windings, and it is doubtful whether many I.F. transformers are purely inductively coupled.

The values of Z_1 and Z_2 are usually determined by the amplification desired. It is apparent from the last equation that stray capacitance has a greater influence at a high intermediate frequency than at a low one. When using 475 kc/s I.F. transformers there is certainly some risk of excessive coupling.

Finally we may consider a coupling by means of resistance.

If the coupling capacitance C_k in fig. 14 is replaced by a resistance the terms $I_2 j\omega M$ and $I_1 j\omega M$ in equations (I B 1) and (I B 2) become $-I_2 R_k$ and $-I_1 R_k$ respectively. In the latter equations $j \frac{R_k}{\omega}$ then takes the place of M, and for the coupling factor K we find:

$$K = j \frac{R_k}{\omega_0 \sqrt{L_1 L_2}} \quad \ldots\ldots\ldots\ldots\ldots \quad \text{(I B 29)}$$

or:

$$K^2 = -\frac{1}{\omega_0^2} \frac{R_k^2}{L_1 L_2} \quad \ldots\ldots\ldots\ldots\ldots \quad \text{(I B 30)}$$

In this case the coupling factor K is thus imaginary, and with mixed coupling complex values of K are to be expected. Such couplings are however rarely used in practice; but they are liable to occur fortuitously, and it is therefore necessary to include them in our considerations.

§ 5. Off-resonance transmission of the band-pass filter

So far we have investigated the properties of the band-pass filter at resonance only. If we draw graphs of the transmission or gain as a function of frequency, we obtain so-called resonance curves; these are influenced markedly by the relation $Q\ K$ (see fig. 16).

In I B § 2 page 25 the relationship between amplification and $Q\ K$ was discussed, but we were then considering only the resonance frequency ω_0 of the band-pass filter.

It is clear from fig. 13 that the gain at resonance falls gradually when the critical value $Q\ K = 1$ is exceeded. In consequence a depression occurs in the middle of the resonance curve and at certain off-tune frequencies gain reaches the maximum figure obtained at critical coupling; the resonance curve thus shows two peaks, each as high as the single peak which occurs when the coupling is critical.

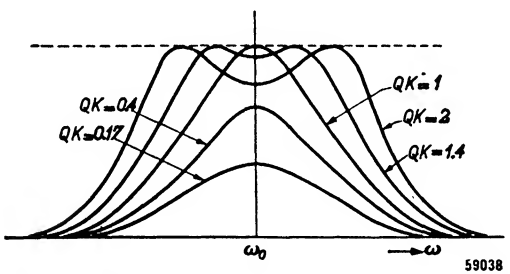

Fig. 16. Resonance curves for a band-pass filter, with various values of QK.

In fig. 16 resonance curves are drawn for various values of $Q\ K$. It is clear from the figure that when $Q\ K$ is less than unity the curve has the well-known shape with a maximum at ω_0, the amplification at that frequency being greatest for $Q\ K = 1$. As $Q\ K$ is increased beyond unity the gain at ω_0 declines, as we saw in fig. 13. Simultaneously another phenomenon occurs: in the neighbourhood of maximum response the curve opens out sideways, and on each side of the resonant frequency a peak appears, of the same height as the single peak at critical coupling. As the coupling is tightened, the resonance curve broadens and the trough in the middle deepens. In practical calculations it may be assumed, however, that with over-critical coupling the response between the two peaks is constant.

By differentiating the general band-pass filter equation and putting it equal to 0, it can be shown that the maximum gain attained when $Q\ K = 1$ is not exceeded at the two peaks of the resonance curves when $Q\ K > 1$.

If we ascertain, for a particular value of $Q\,K$ — for instance 2, the frequencies at which the response is greatest and then calculate the amplification with the help of equation (I B 14), we get the same figure as for the gain at ω_0 when $Q\,K = 1$.

§ 6. Resonance curves of symmetrical band-pass filters

In the preceding sections it was deduced that the same equation could be used for filters coupled by any means if K is appropriately defined in each case. The following is a recapitulation of the equations from which K may be calculated for each type of filter:

Inductive coupling: $$K^2 = \frac{\omega^2}{\omega_0^2}\,\frac{M^2}{L_1 L_2} \quad \text{(I B 9)}$$

Capacitive current coupling: $$K^2 = \frac{\omega_0^2}{\omega^2}\,\frac{C_1 C_2}{C_k^2} \quad \text{(I B 25)}$$

Capacitive voltage coupling: $$K^2 = \frac{\omega_0^2}{\omega^2}\,\frac{C_k^2}{C_1 C_2} \quad \text{(I B 27)}$$

Resistive current coupling: $$K^2 = \frac{-1}{\omega_0^2}\,\frac{R_k^2}{L_1 L_2} \quad \text{(I B 30)}$$

The general band-pass filter equation when the circuits are tuned to the same frequency is for all four cases:

$$V_2 = j\,I_a \left(\frac{\omega_0}{\omega}\right)^2 \frac{\omega_0\,Q_1\,Q_2\,K\,\sqrt{L_1 L_2}}{(1 + j\beta\,Q_1)\,(1 + j\beta Q_2) + Q_1 Q_2 K^2} \quad \text{(I B 14)}$$

Whilst the frequency response for different forms of coupling has already been considered in § 5, for the estimation of selectivity it is important to know the relation between the gain on tune and that at neighbouring frequencies. Essentially this means that the absolute gain is ignored, and in fig. 16 only the ratio $\frac{V_{2res}}{V_2}$ is considered. We thus obtain resonance curves entirely similar to that of fig. 2 for the single circuit. This relation, which we shall again call a, is best calculated as a function of βQ. In the simplest case the natural frequencies of the two circuits, ω_1 and ω_2, are both equal to ω_0; the Q-factors also are equal, and therefore $Q_1 = Q_2 = Q$. Such a filter may be called completely symmetrical; its attenuation has already been calculated in B § 1 in the form:

$$a = \sqrt{\frac{[1 + (\beta + K)^2 Q^2]\,[1 + (\beta - K)^2 Q^2]}{1 + Q^2 K^2}} \quad \text{(I B 13)}$$

the relation $\frac{\omega}{\omega_0}$ having been assumed equal to unity. Multiplying we get:

$$a = \frac{\sqrt{(Q^2K^2+1)^2 - 2\beta^2 Q^2 (Q^2K^2-1) + \beta^4 Q^4}}{1+Q^2K^2} \quad \ldots\ldots \text{(I B 31)}$$

Here a is a function of the quantity βQ, not of the detuning or of β alone. In fig. 17 the equation is shown graphically, with the product $Q\,K$ as para-

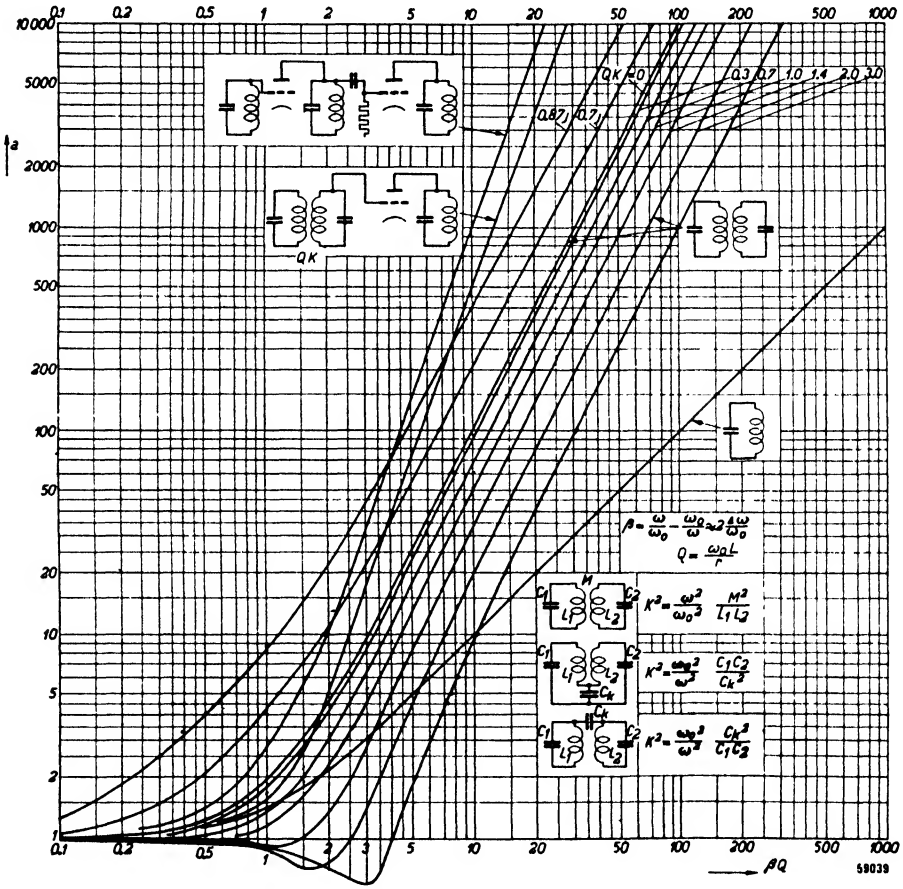

Fig. 17. Resonance curves for a single circuit and for various combinations of circuits, with QK as parameter; detuning is expressed in terms of $\beta\ Q$.

meter. This simplified form holds good for all symmetrical band- pass filters; such an advantage is not outweighed by the drawback that the detuning $\Delta\omega$ must first be converted to $\beta\ Q = \frac{2\,\Delta\,\omega}{r/L}$ (see also fig. 20).

It will be observed that so long as QK is less than 1 the curves have only one minimum; accordingly there is only one peak in the curve (fig. 16). If $Q\,K$ becomes greater than 1, that is if the coupling is tighter than critical, the two peaks already mentioned make their appearance, one each side of the resonant frequency.

We shall now consider a practical application of fig. 17: the determination of the selectivity of the I.F. transformer which has already been used several times as an example. It is desired to ascertain the degree of suppression of an interfering signal whose frequency differs 10 kc/s from that to which the transformer is tuned.

The transformer will be assumed connected between the mixer and I.F. amplifier valves, with $Z_1 = Z_2 = 480{,}000\ \Omega$ (see pag. 27); and the coupling is critical.

First we determine the magnitude of β:

$$\beta = \frac{\omega}{\omega_0} - \frac{\omega_0}{\omega} = \frac{135}{125} - \frac{125}{135} = 0.15.$$

In the present case $Q_1 = Q_2 = Q$. With the help of equation (I B 19) we then find that:

$$Q = \frac{785{,}000 \times 480{,}000 \times 95}{10^{12}} = 35.7$$

The relation $\beta\,Q$ thus becomes $0.15 \times 35.7 = 5.35$.

From the curve for critical coupling ($Q\,K = 1$) we now find that $a = 15$. If the required signal and the interfering signal reach the frequency changer at equal strength, at the grid of the I.F. valve the undesired signal will be 15 times weaker than the wanted one. In the case of the second I.F. transformer Q_1 is again 35.7, but owing to damping imposed by the following diode (see page 27):

$$Q_2 = \frac{785{,}000 \times 190{,}000 \times 95}{10^{12}} = 14.2.$$

For the sake of simplicity we now use the curves for a symmetrical band-pass filter and introduce for this purpose the mean quality factor $Q = \sqrt{Q_1 Q_2}$. In § 7 we shall return to this approximation. So:

$$Q = \sqrt{Q_1 Q_2} = \sqrt{35.7 \times 14.2} = 22.5.$$

Accordingly $\beta\,Q = 3.4$ and, for critical coupling, $a = 6$. At the diode the

interfering signal is $15 \times 6 = 90$ times down compared with the required signal. The influence of the coupling will be obvious from the foregoing example. If the attenuation obtained is thought too small, the coupling in both transformers might be loosened: for example, until $Q\,K = 0.7$. It is apparent from fig. 13 that the amplification would then fall only a little; but for a we now get values of 20 and 8.2 respectively in the first and second transformers.

The overall attenuation thus becomes 164 times, which is a considerable improvement over the previous figure of 90 times. It must not be forgotten, however, that the side-bands of the wanted signal will also suffer greater attenuation and reproduction will worsen due to the weakening of the higher audio frequencies. If irreproachable response to the upper frequencies is required, we can ascertain from the curves in fig. 17 how much $Q\,K$ can be increased by making the coupling tighter. With $\beta\,Q$ about 3.0 for the first transformer and 1.9 for the second, a side-band of 5 kc/s is passed without attenuation. In the case of the second transformer the result of tightening the coupling is very obvious: whereas with critical coupling ($\beta\,Q = 1.9$) a 5 kc/s side-band is attenuated 2 times, when $Q\,K = 1.5$ the attenuation amounts to only 1.1 times. The discrimination against an interfering signal 10 kc/s removed from the resonant frequency is at the same time reduced from 6 to 3.4. It can be seen from fig. 13 that the transmission has remained practically constant. Moreover it follows from fig. 17 that it is even possible, by tightening the coupling still further, to emphasize certain side-bands; by this means a loss of the higher frequencies in the A.F. stage may be compensated.

§ 7. Using band-pass filter curves for staggered circuits

It was demonstrated in § 1 of section B that the resonance curve of a band-pass filter with identical tuned circuits may be represented by the same formulae as the overall curve for two mutually detuned circuits in cascade [cf. equations (I B 13) and (I A 39)]. The curves in fig. 17 may thus also be used for two tuned circuits in cascade.

In this case the resonant frequency difference β_v^2 is substituted for K^2; that is, $Q\,K$ becomes $\beta_v\,Q$. With the help of equation (I A 37) we can elaborate this relationship as follows:

$$Q\,K = \beta_v\,Q = \frac{\omega_2 - \omega_1}{\omega_0}\,Q = \frac{L}{r}\,(\omega_2 - \omega_1) = (\omega_2 - \omega_1)\,RC \quad . \quad . \quad . \quad \text{(I B 32)}$$

The significance of the band-pass filter curve for $Q\,K = 0$ is now apparent: the filter with $K = 0$, that is without coupling, gives no transmission and

is therefore absurd. $K = 0$ is however equivalent to $\beta_v = 0$, so that the curve $Q\,K = 0$ is the curve of two identically tuned circuits in cascade.

§ 8. The band-pass filter with dissimilar dampings

In deriving the formula (I B 31) $Q_1 = Q_2 = Q$ was presupposed, in order to obtain a simpler form of equation for the resonance curve. This equation and the curves of fig. 17 are therefore exact only when the two circuits are equally damped. Cases are often met, however, in which the circuits, although tuned to the same frequency, are unequally damped; use of these curves in fact leads to error, as happened with the second band-pass filter in § 6.

We shall now first of all enquire whether the error is considerable, and then make a more exact calculation for a filter with unequal dampings.

Using equation (I B 14) as a starting point we arrive at:

$$a = \frac{\omega^2}{\omega_0^2} \frac{(1 + j\beta Q_1)(1 + j\beta Q_2) + Q_1 Q_2 K^2}{1 + Q_1 Q_2 K^2}.$$

If we assume $\omega^2/\omega_0^2 = 1$ we then have:

$$a = \left| \frac{1 - Q_1 Q_2 \beta^2 + Q_1 Q_2 K^2 + j\beta (Q_1 + Q_2)}{1 + Q_1 Q_2 K^2} \right| . \quad \text{(I B 33)}$$

Writing $Q_1 Q_2 = Q^2$, we then get:

$$a = \frac{\sqrt{(1 - Q^2\beta^2 + Q^2K^2)^2 + \beta^2 (Q_1 + Q_2)^2}}{1 + Q^2 K^2} . \quad \text{(I B 34)}$$

If we now consider, instead of the filter discussed above, a fictitious one with similar damping of both circuits, $Q = \sqrt{Q_1 Q_2}$, we should still arrive at equation (I B 34), except that in the numerator of the fraction we should write: $\beta^2 (2Q)^2$ or $4\,\beta^2 Q^2$ instead of $\beta^2 (Q_1 + Q_2)^2$

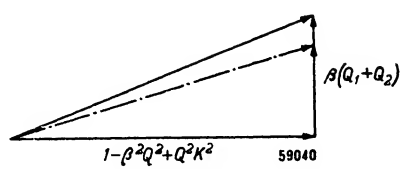

Fig. 18. Vectorial representation of the effect of error on the absolute value of the numerator in equation (I B 34), when $Q_1 = Q_2 = Q$.

The numerator of (I B 34), the root of the sum of two squares, may be regarded as the hypotenuse of a right-angled triangle (see fig. 18), and it is easy to observe the effect of the error made in the second term.

The factor $4\,Q^2$ should strictly be:

$$(Q_1 + Q_2)^2 = Q_1^2 + Q_2^2 + 2\,Q_1 Q_2 = \left[\frac{Q_1}{Q_2} + \frac{Q_2}{Q_1} + 2\right] Q^2.$$

When $Q_1 = Q_2 = Q$ the factor between brackets is indeed equal to 4, but in an extreme case, for instance if $Q_1 = 5\,Q_2$, its value becomes $5 + 1/5 + 2 = 7.2$. Thus the perpendicular vector in fig. 18 must be equal to $\beta Q \sqrt{7.2}$ instead of $\beta Q \sqrt{4}$, or $2.65\ \beta Q$ in place of $2\ \beta Q$. The influence of this error depends very much on the magnitude of the horizontal vector, and this, in turn, on KQ and βQ.

The table below indicates the error for several cases, Q_2 being equal to $5\ Q_1$.

TABLE

KQ	βQ	Approximated value of the numerator	Actual value of the numerator	Error
0	1	$\sqrt{0 + 2^2} = 2$	$\sqrt{0 + 2.65^2} = 2.65$	25%
0	2	$\sqrt{3^2 + 4^2} = 5$	$\sqrt{3^2 + 5.3^2} = 6$	16%
0	5	$\sqrt{24^2 + 10^2} = 26$	$\sqrt{24^2 + 13^2} = 27.5$	5.5%
1	1	$\sqrt{1^2 + 2^2} = 2.2$	$\sqrt{1^2 + 2.65^2} = 2.8$	21%
1	2	$\sqrt{2^2 + 4^2} = 4.5$	$\sqrt{2^2 + 5.3^2} = 5.7$	21%
1	5	$\sqrt{23^2 + 10^2} = 25$	$\sqrt{23^2 + 13^2} = 26.25$	5%
2	1	$\sqrt{4^2 + 2^2} = 4.5$	$\sqrt{4^2 + 2.65^2} = 4.8$	6%
2	2	$\sqrt{1^2 + 4^2} = 4.1$	$\sqrt{1^2 + 5{,}3^2} = 5.4$	24%
2	5	$\sqrt{20^2 + 10^2} = 22$	$\sqrt{20^2 + 13^2} = 24$	7.5%

It is clear from the table that the error becomes smaller as the detuning β becomes greater; if βQ exceeds 5 the errors are fairly small. We conclude from fig. 17 that only at such values of βQ does a become appreciable.

In the practical example on page 37 the attenuation of the second transformer was calculated for $\beta Q = 3.4$. Certainly this is less than 5, but on the other hand Q_1/Q_2 in the example was only 2.6. It may therefore be expected that the error in this case will not be very large.

The greatest error occurs, of course, when the horizontal vector in fig. 18 is very small or zero; then the overall error equals the error in the vertical vector. If once more we consider the practical case of $Q_1/Q_2 = 2.6$, then $Q_1/Q_2 + Q_2/Q_1 + 2 = 5.0$ instead of 4, the factor used. The maximum error in this example therefore amounts to $\frac{1.0}{5.0} = 20\%$ when

$$1 - Q^2\beta^2 + Q^2K^2 = 0.$$

When $Q_1 \neq Q_2$ the resonance curve can be calculated in the following way. Contrary to the foregoing we introduce in place of the quality factor the damping:

$$\delta = 1/Q = r/\omega L.$$

Now we write for the mean damping

$$\delta = \frac{\delta_1 + \delta_2}{2},$$

or: $$\delta_1 = \delta + \varepsilon \text{ and } \delta_2 = \delta - \varepsilon \quad \ldots\ldots\ldots\ldots \text{(I B 35)}$$

If we first divide the numerator and denominator of (I B 14) by $Q_1 Q_2$, putting δ_1 for $1/Q_1$ and δ_2 for $1/Q_2$, and then substitute (I B 35) we get:

$$a = \left| \frac{\omega^2}{\omega_0^2} \frac{[\delta + j\beta + \varepsilon][\delta + j\beta - \varepsilon] + K^2}{[\delta + \varepsilon)(\delta - \varepsilon) + K^2} \right|,$$

or:

$$a = \left| \frac{\omega^2}{\omega_0^2} \frac{(\delta + j\beta)^2 - \varepsilon^2 + K^2}{\delta^2 - \varepsilon^2 + K^2} \right|,$$

or:

$$a = \left| \frac{\omega^2}{\omega_0^2} \frac{(1 + j\,Q\,\beta)^2 + Q^2(K^2 - \varepsilon^2)}{1 + Q^2(K^2 - \varepsilon^2)} \right| \quad \ldots\ldots \text{(I B 36)}$$

Comparison of this equation with (I B 12) reveals that the resonance curve is the same as that of a band-pass filter with both circuits similarly damped and with a coupling of:

$$K'^2 = K^2 - \varepsilon^2 \quad \ldots\ldots\ldots\ldots\ldots\ldots \text{(I B 37)}$$

where

$$\varepsilon = \delta_1 - \delta = \delta - \delta_2. \quad \ldots\ldots\ldots\ldots\ldots \text{(I B 38)}$$

This result may now be applied to the second example on page 37.
We calculate the average damping of the second band-pass filter from:

$$\delta = \frac{1/35.7 + 1/14.2}{2} = 0.048 \text{ or } Q = 20.8,$$

and

$$\varepsilon = 0.048 - 1/35.7 = 0.021.$$

In the case concerned $QK = 1$ and $Q = 23.2$; therefore $K = 0.043$.
Unless the relative positions of the coils are altered, this value of K must be used in further calculations. We therefore get:

$$K'^2 = 0.043^2 - 0.021^2$$

or:

$$K' = 0.037.$$

The relative coupling in the equivalent band-pass filter becomes:

$$QK' = 20.8 \times 0.037 = \text{approx. } 0.8.$$

The resonance curve to be expected in practice is therefore that of a filter with just under-critical coupling.
At 10 kc/s the proportionate detuning is no longer $\beta Q = 3.5$, but as a result of the new value of Q:

$$\beta Q = 3.5 \times \frac{20.8}{23.2} = 3.1$$

The value of a must now be estimated from fig. 17, as the curve for $QK = 0.8$ is lacking. From the curve for $QK = 0.7$ we get a value for a of about 6.5 when $\beta Q = 3.1$. When all the figures in this example are compared, it is plain that the results of precise calculation differ from those obtained on page 37 to a degree not worth mentioning. At small values of βQ, when considerably larger errors are to be expected, precise calculation is always preferable, despite the greater complication.

In certain circumstances $K'^2 = K^2 - \varepsilon^2$ can be negative; in that case resonance curves are obtained like those in fig. 17 to the left of the curve for $Q K = 0$. These are less favourable than the curve for the tuned circuits in cascade. If K'^2 is negative, K' is imaginary; for these last curves, therefore, the parameter QK' is indicated by $0.7j$ etc.

§ 9. Band-pass filter with parallel damping

In deriving formulae for the various types of band-pass filter it was assumed that in each tuned circuit series resistance was present. The quality in each case was designated by:

$$Q_1 = \frac{\omega_1 L_1}{r_1} \text{ and } Q_2 = \frac{\omega_2 L_2}{r_2} \text{ respectively.}$$

Generally, however, the circuits are damped by shunt resistance as well, and following the reasoning in A § 1 we may expect that in this case [see also equation (I A 23)]

$$\Delta \frac{1}{Q_1} = \frac{1}{R_1 \omega_1 C_1} \text{ and } \Delta \frac{1}{Q_2} = \frac{1}{R_2 \omega_2 C_2} \quad \ldots . \quad \text{(I A 7)}$$

For complete certainty we ought to examine the correctness of this deduc-

tion. If we combine the circuit capacitance and the parallel resistance in a single circuit element, then the second term in equation (I B 1) and the first in (I B 2) have to be modified: instead of $\frac{1}{j\omega C}$ we now have the impedance of the parallel combination RC. This impedance, as we saw in A § 4, is equal to the reactance of C plus a series resistance:

$$\Delta r = \frac{R}{1 + R^2\omega^2C^2} \approx \frac{1}{R\omega^2C^2} \quad \ldots\ldots\ldots \quad \text{(I A 30)}$$

Accordingly a further term $-\frac{I_1}{R_1\omega^2C_1^2}$ comes into equation (I B 1), and into (I B 2) $\frac{I_2}{R_2\omega^2C_2^2}$.

If we put these terms into the equations it is apparent that the series resistance in each circuit is increased by an amount:

$$\left.\begin{aligned} \Delta r_1 &= \frac{1}{R_1\omega^2C_1^2} = \left(\frac{\omega_1}{\omega}\right)^2 \frac{1}{R_1\omega_1^2C_1^2} \\ \Delta r_2 &= \frac{1}{R_2\omega^2C_2^2} = \left(\frac{\omega_2}{\omega}\right)^2 \frac{1}{R_2\omega_2^2C_2^2} \end{aligned}\right\} \quad \ldots\ldots \quad \text{(I B 39)}$$

The Q we find decreased by parallel damping as follows:

$$\left.\begin{aligned} \frac{1}{Q_1} &= \frac{r_1 + \Delta r_1}{\omega_1 L_1} = \frac{r_1}{\omega_1 L_1} + \left(\frac{\omega_1}{\omega}\right)^2 \frac{1}{R_1\omega_1 L_1\omega_1^2C_1^2} = \\ &= \frac{r_1}{\omega_1 L_1} + \left(\frac{\omega_1}{\omega}\right)^2 \frac{1}{R_1\omega_1 C_1} \\ \text{and} \qquad \frac{1}{Q_2} &= \frac{r_2}{\omega_2 L_2} + \left(\frac{\omega_2}{\omega}\right)^2 \frac{1}{R_2\omega_2 C_2} \end{aligned}\right\} \quad \ldots\ldots\ldots \quad \text{(I B 40)}$$

The final conclusion is that Q_1 and Q_2 have been decreased by parallel damping, following the rule of (I A 23), the Q of the shunt being found within close limits by (I A 7). The new values of Q_1 and Q_2 derived at the beginning of this section are thus accurate as long as the frequency does not differ very much from ω_1 and ω_2 respectively; that is to say, when we are considering only a narrow band each side of the resonant frequency. This is nearly always the case, but see also section C, § 11.

The second term of equation (I B 1) includes not only I_1 but also I_a. These must also of course be multiplied by the amended impedance. However it is simpler to regard the impedance as unchanged, and I_a as somewhat modified; since this change is relatively small, the effect on the final result is unimportant.

§ 10. Band-pass filter with mutually-detuned circuits

In order not to make the calculation too complicated we shall limit our consideration to the case of a filter in which the two circuits are equally damped; thus $Q_1 = Q_2 = Q$.

As a basis for the calculation we shall make use of equation (I B 10), in which, however, values for β_1 and β_2 must first be substituted from (I A 37). If follows from (I B 10):

$$V_2 = jI_a \frac{\omega_0^3}{\omega^2} \frac{Q^2 K \sqrt{L_1 L_2}}{[1 + jQ(\beta + \beta_v)][1 + jQ(\beta - \beta_v)] + Q^2 K^2},$$

or:

$$V_2 = jI_a \frac{\omega_0^3}{\omega^2} \frac{Q^2 K \sqrt{L_1 L_2}}{(1 + j\beta Q)^2 + Q^2(\beta_v^2 + K^2)} \quad \text{(I B 41)}$$

This is the same equation as (I B 11) for filters with two indentically tuned circuits, save that K^2 in the denominator is increased to $K^2 + \beta_v^2$. So we may now write:

$$K'^2 = K^2 + \beta_v^2 \quad \text{(I B 42)}$$

We again calculate the attenuation in relation to V_{2res}

$$V_{2res} = jI_a \frac{\omega_0 Q^2 K \sqrt{L_1 L_2}}{1 + Q^2(K^2 + \beta_v^2)} \quad \text{(I B 43)}$$

Hence we find:

$$a = \left| \left(\frac{\omega}{\omega_0}\right)^2 \frac{(1 + j\beta Q)^2 + Q^2 K'^2}{1 + Q^2 K'^2} \right| \quad \text{(I B 44)}$$

This is once more the equation (I B 12) used for the curves of fig. 17. Thus for filters with mutually detuned circuits we may use these general curves if we first calculate the apparent increased coupling K' according to equation (I B 42). In order to calculate the gain, i.e. V_{2res}, it is necessary to know the value of K as well as that of K'. It will be evident from equation (I B 43) that the detuning β_v reduces gain.

Detuned band-pass filters are used only rarely. An example will be found in E § 2 (Band-pass filters with variable band-width).

§ 11. Band-pass filter with complex coupling

In § 4 of this section we found that with resistance coupling K^2 had a negative value. Although such coupling is scarcely used in practice, we should consider it briefly as it is liable to occur incidentally.

For pure resistance-coupling and, therefore, a negative value for K^2, and with identical tuned circuits, we find from equation (I B 14):

$$a = \left| \left(\frac{\omega}{\omega_0}\right)^2 \frac{(1 + j\beta Q)^2 - Q^2K^2}{1 - Q^2K^2} \right| \quad \ldots\ldots \quad \text{(I B 45)}$$

In this the absolute value of K has to be inserted. The last equation can be factorised thus:

$$a = \left| \left(\frac{\omega}{\omega_0}\right)^2 \frac{(1 + QK + j\beta Q)\,(1 - QK + j\beta Q)}{(1 + QK)\,(1 - QK)} \right|,$$

or:

$$a = \left| \left(\frac{\omega}{\omega_0}\right)^2 \left(1 + \frac{j\beta Q}{1 + QK}\right)\left(1 + \frac{j\beta Q}{1 - QK}\right) \right| \quad \ldots \text{(I B 46)}$$

We now clearly recognise the attenuation of two circuits in cascade with quality $\frac{Q}{1 + QK}$ and $\frac{Q}{1 - QK}$ respectively.

Apart from the ratio $\frac{\omega}{\omega_0}$, it is evident from equation (I B 45) that the resonance curve is always symmetrical. This becomes obvious when we represent the absolute value of a in the following way:

$$a = \left(\frac{\omega}{\omega_0}\right)^2 \frac{\sqrt{(1 - \beta^2Q^2 - Q^2K^2)^2 + 4\,\beta^2Q^2}}{1 - Q^2K^2} \quad \ldots \quad \text{(I B 47)}$$

Here β occurs only as a squared quantity.

When incidental resistance coupling is present in a filter coupled by inductance or capacitance $Q^2K'^2$ has a complex value, for example $l + jm$; equation (I B 44) is then written:

$$a = \left| \left(\frac{\omega}{\omega_0}\right)^2 \frac{(1 + j\beta Q)^2 + (l + jm)}{1 + (l + jm)} \right| \quad \ldots\ldots \quad \text{(I B 48)}$$

If for the sake of simplicity we consider only that part which varies with β,

namely the numerator, the absolute value of a becomes:

$$\sqrt{(1 - \beta^2 Q^2 + l)^2 + (2\beta Q + m)^2}$$

Since the term $4\,\beta Qm$ occurs under the root sign, the numerator — and therefore a — is not symmetrical in relation to β. We thus arrive at the important result that two identical tuned circuits, when partly resistance-coupled, yield an asymmetrical resonance curve.

§ 12. Approximations and corrections

In the foregoing calculations we have of necessity made frequent use of approximations and simplifications in order to obtain simpler formulae; we shall now look at these short cuts more closely, so that we may be able to judge whether in certain cases corrections will be necessary.

(a) The detuning β

It was clear from equation (I A 11) that for β it is a good enough approximation to put double the relative detuning. In the case of band-pass filters at resonance, $\beta = 0$ and accordingly there is no error. It can, however, be of interest when calculating selectivity. The accompanying table shows the error which results from using the approximation in question.

$\frac{\omega}{\omega_0}$	$2\frac{\Delta\omega}{\omega_0}$	β
1.01	0.02	0.02
1.05	0.10	0.10
1.10	0.20	0.19
1.25	0.50	0.45
1.50	1.00	0.83
2.0	2.00	1.50

In fig. 19 the two functions in the table are depicted graphically. The last two cases listed in the table will rarely be of any practical value, but the fourth line down is of interest, as it covers the case of a 125 kc/s filter at detuning of 31 kc/s — i.e. at three channels off-tune; the error here is already appreciable, and it is accordingly preferable, when high accuracy is required, to calculate β from the definition.

(b) The various coupling factors K.

In the preceding discussion the coupling factor occurred always in conjunc-

tion with a factor ω/ω_0 or ω_0/ω, save in the case of resistance coupling. This gives rise to difficulties in using the curves of fig. 17. If it is desired to ascertain the selectivity at different frequencies several curves (corresponding to various values of QK) have to be referred to.

The foregoing table indicates the magnitude of ω/ω_0 for a given value of β (see also fig. 19), so that it is possible to check beforehand whether approximation of these factors produces a big error. Furthermore it is clear at once from the curves in fig. 17 than an error in QK results in almost as large an error in the average attenuation.

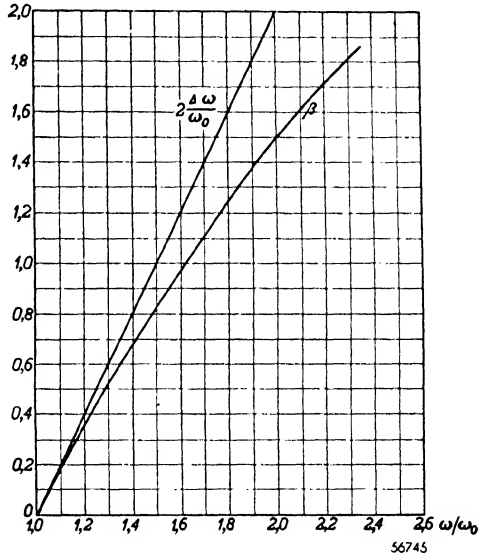

Fig. 19. The double percentage-detuning $2\Delta\omega/\omega_0$, and β, as a function of ω/ω_0.

(*c*) *Errors in the curves of fig. 17.*

For equation (I B 14), used to determine the curves in fig. 17, the factor ω/ω_0 was made equal to unity. As already observed, we can correct this error afterwards by taking the values of ω/ω_0 from the table on page 46 (see also fig. 19). We notice, however, that with inductive coupling this error compensates somewhat the discrepancy indicated under b. In this case, therefore, it is advantageous to make use of the contrary effects of these two simplifications. If $\omega/\omega_0 = 1.25$ the approximation makes K too small, and the figure we get for the attenuation is 25 % high. Approximating $(\omega/\omega_0)^2$ in equation (I B 14), however, causes the figure ascertained for attenuation to be 55 % low; thus the first error partly compensates for the second. Naturally this partial compensation is not obtained in the case of capacitive coupling, for then the approximated factor is ω/ω_0. On the contrary, if we neglect both items the error will be approximately $(\omega/\omega_0)^3$.

(*d*) *Influence of the coupling factor on the adjustment of a band-pass filter.*

In most of our calculations we assumed that the two circuits, L_1C_1 and L_2C_2, were tuned to the same frequency ω_0, which is what is required in practice. When a filter is set up maladjustment is likely to occur if the coupling is over-critical, since maximum gain is obtained not at the resonant

frequency but at two frequencies, one higher and one lower than resonance (see fig. 16). In this case the filter should not be trimmed for maximum gain without certain precautions, or asymetry of the resonance curve will result. Correct adjustment may be effected by temporarily shunting one of the tuned circuits with a resistor of such value that QK is reduced below unity.

§ 13. The abscissa scale for the resonance curves

The various resonance curves in fig. 17 have a relative abscissa scale. This leads to the advantage that the curves are of general application and are not limited to circuits of any particular quality. The abscissa can no longer, however, be read off directly in kc/s. But if we represent the quality of a given circuit by the relation $r/L = \frac{\omega_0}{Q}$ between its resistance and inductance, as is sometimes done, there then exists a very simple relationship between the detuning in kilocycles and the abscissa of the resonance curve. For small degrees of detuning we can write for β:

$$\beta = \frac{2\Delta\omega}{\omega_0} \quad \ldots\ldots\ldots\ldots\ldots\ldots \quad \text{(I A 11)}$$

As now $Q = \frac{\omega_0 L}{r}$, βQ can be replaced by:

$$\beta Q = \frac{2\Delta\omega}{r/L} = \frac{2 \times 2\pi\, \Delta f}{r/L} = \frac{12.5\, \Delta f}{r/L} \quad \ldots \quad \text{(I B 49)}$$

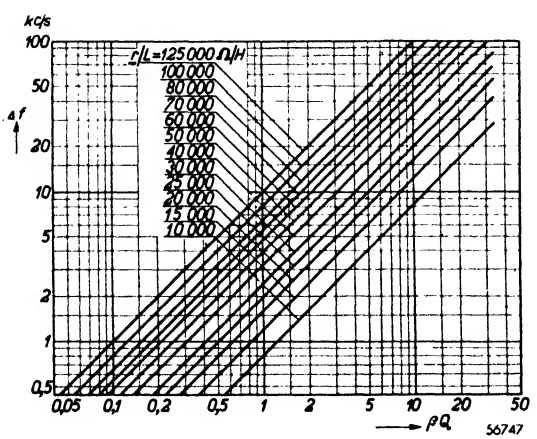

Fig. 20. The detuning Δf in kc/s as a function of the relation βQ with r/L as parameter.

In this formula Δf is measured in cycles per second, and r/L in ohms per henry.

Fig. 20, showing Δf in kc/s as a function of βQ for various values of r/L, will be found of help when putting the various resonance curves to practical use. If we represent the quality of the circuits by Q, it is necessary only to deduce $\beta = \frac{2\Delta f}{f}$ from the detuning Δf.

C. Circuits for the reduction of shunt damping

Introduction

A simple numerical example demonstrates that parallel damping often markedly affects circuit quality. If we have an I.F. circuit with, say, $Q = 150$ at 475 kc/s and a tuning capacitance C of 100 pF, we find from equation (I A 23) for a shunt R of 250,000 Ω (for instance a diode — see Chapter V on Detection):

$$Q_{par} = \omega_0 RC = 2\pi \times 475{,}000 \times 250{,}000 \times 100 \times 10^{-12} = 75.$$

$$\frac{1}{Q_{\text{total}}} = \frac{1}{150} + \frac{1}{75} = 0.02; \text{ and } Q_{\text{total}} = 50.$$

Thus Q is decreased threefold by the addition of the shunt.
As both magnification and selectivity are directly proportional to Q, it is well to investigate the possibility of minimising the effect of parallel resistance.

§ 1. Increasing C and reducing L

Equation (I A 22) shows that $1/Q_{\text{par}}$ becomes smaller as we choose a higher value for C. Whether $1/Q_{\text{series}} + 1/Q_{\text{par}}$ will also diminish is not immediately obvious, for in order te keep the tuning unaltered we must reduce L as C is increased. We distinguish two cases:

(a) Lowering of inductance by reducing the number of turns on the coil, the wire diameter being unchanged.

(b) Lowering of inductance by reducing the number of turns on the coil, the size of the coil being maintained.

(a) *Reduction of the number of turns; wire diameter unchanged*

If we reduce the number of turns n times, the inductance decreases n^2 times; to regain the original resonant frequency the tuning capacitance must therefore be increased n^2 times. As the number of turns is reduced the resistance of the coil falls in like ratio. The factor Q thus becomes $\frac{n^2}{n} = n$ times as small.

If we indicate Q after the n-fold reduction in the number of turns by Q_n, then:

$$\frac{1}{Q_n} = \frac{n}{Q} + \frac{1}{n^2 R \omega_0 C},$$

or:

$$\frac{Q}{Q_n} = n + \frac{L}{n^2 RC r} \quad \ldots\ldots\ldots\ldots \quad \text{(I C 1)}$$

This expression is a minimum when:

$$n = \sqrt[3]{\frac{2L}{RCr}} \quad \ldots\ldots\ldots\ldots\ldots\ldots \quad \text{(I C 2)}$$

This formula accordingly tells us by how many times we should reduce the number of turns to obtain the highest factor Q_n and therefore the highest selectivity. If the result of the calculation is $n < 1$, it means that to get the maximum value for Q_n we must increase the number of turns and reduce the tuning capacitance.

Equation (I C 2) may also be written as follows:

$$\frac{1}{n^2 C} \cdot \frac{\frac{1}{n^2} L}{\frac{1}{n} r} = \tfrac{1}{2} R \quad \ldots\ldots\ldots\ldots \quad \text{(1 C 3)}$$

The left-hand side of this equation is now the dynamic resistance of the circuit at resonance, ignoring the parallel resistance. Thus we arrive at the following conclusion:

If the capacitance and inductance of a tuned circuit shunted by a resistance R are varied, without altering the wire diameter of the coil, and keeping the resonant frequency unchanged, the highest Q factor is reached when the dynamic resistance of the circuit, undamped by parallel resistance, equals $\frac{1}{2} R$.

The dynamic resistance of the circuit at resonance is given by:

$$Z = \frac{1}{n^3 \frac{rC}{L} + \frac{1}{R}} \quad \ldots\ldots\ldots\ldots\ldots \quad \text{(I C 4)}$$

Thus it will depend on the value of R whether the dynamic resistance of

the tuned circuit remains satisfactory from the point of view of amplification or whether it will be necessary to compromise between gain and selectivity.

(*b*) *Reduction of the number of turns; size of winding maintained with thicker wire.*

If we use n times fewer turns in the same winding space, the wire diameter increases n times and the resistance per turn falls in the same ratio. The total resistance, like the inductance, is thus reduced by a factor n^2 and the relation r/L remains unchanged; for simplicity we are ignoring the skin effect at the moment. We now have:

$$\frac{1}{Q_n} = \frac{1}{Q} + \frac{1}{n^2 R\omega_0 C} \quad \ldots\ldots\ldots\ldots \quad \text{(I C 5)}$$

or:

$$\frac{Q}{Q_n} = 1 + \frac{1}{n^2}\frac{L}{RCr} \quad \ldots\ldots\ldots\ldots \quad \text{(I C 6)}$$

As n increases Q increases; for maximum selectivity the inductance must be as small as possible. To obtain a measure of the amplification we calculate Z, the dynamic resistance, once more:

$$Z = \frac{1}{n^2 \frac{rC}{L} + \frac{1}{R}} \quad \ldots\ldots\ldots\ldots \quad \text{(I C 7)}$$

In this case also, Z falls as n rises, though not as rapidly as in (a). Improvement in selectivity is at the expense of amplification.

§ 2. Tapping the damped coil

A second method often used to lessen the damping imposed by a shunt resistance is to make a tapping (see fig. 21). If the number of turns across which R lies is $\frac{1}{n}$ of the total, the effect of R is that of a resistance n^2R in parallel with the whole coil, as the latter acts as an auto-transformer. The quotient $1/Q$ of the entire circuit is now:

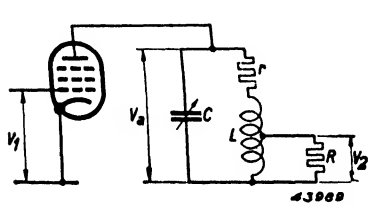

Fig. 21. Amplifying valve with tuned anode circuit, the resistive load R being connected to a tapping on the coil.

$$\frac{1}{Q_n} = \frac{1}{Q} + \frac{1}{n^2 R\omega_0 C} \quad \ldots\ldots \quad \text{(I C 8)}$$

This is the same result as equation (I C 5). Here again by making n larger a higher Q and a better selectivity is obtained. Making n bigger means in this case that the damping resistance affects a smaller part of the coil. (Neither in this instance nor in that dealt with in § 1 can we assert that the higher value of Q will necessarily result in higher gain. It was assumed in fig. 21 that R forms part of the load to which the voltage developed across the tuned circuit is applied, e.g. a diode detector, or the grid leak of a following valve.) Certainly the ratio $\left|\frac{V_a}{V_1}\right|$ increases as Q is made higher, but of the higher voltage only a fraction $\frac{1}{n}$ is used, for at the tapping the voltage is n times smaller than at the top of the coil.

The realised amplification is thus:

$$\left|\frac{V_2}{V_1}\right| = \frac{1}{n}\left|\frac{V_a}{V_1}\right| = \frac{1}{n} S Z = \frac{1}{n} S \frac{L_n}{r_n C}\left(= \frac{1}{n} S \frac{Qn}{\omega_0 C}\right)$$

$$= S \frac{1}{n\left(\frac{r}{L} + \frac{1}{n^2 RC}\right) C} = S \frac{1}{n\frac{rC}{L} + \frac{1}{nR}} \quad \ldots \quad \text{(I C 9)}$$

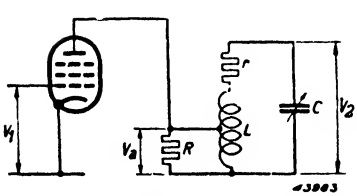

Fig. 22. Amplifying stage in which the anode is joined to a tapping on the tuning coil in order to reduce the damping imposed by the A.C. resistance of the valve.

It will be noted that the gain is determined not by the dynamic resistance Z but by $\frac{1}{n} \times Z$. This also holds for the case shown in fig. 22, where the resistance damping the circuit belongs to the preceding stage, e.g. the A.C. resistance of the previous valve (see also D § 10). The impedance inserted in the anode circuit of the valve is here not the dynamic resistance of the tuned circuit, Z, but by reason of the step-down transformation $\frac{1}{n^2} \cdot Z$. The A.C. voltage at the anode of the valve is stepped up, the alternating potential across the whole tuned circuit being n times greater ; so in this case the overall gain is:

$$\left|\frac{V_2}{V_1}\right| = n\left|\frac{V_a}{V_1}\right| = nS\frac{1}{n^2} Z = S\frac{1}{n} Z = S \frac{1}{n\frac{rC}{L} + \frac{1}{nR}}.$$

The gain is thus the same as we found in equation (I C 9); the latter is a maximum when:

$$n = \sqrt{\frac{L}{RCr}} \quad \ldots\ldots\ldots\ldots\ldots\ldots \quad \text{(I C 10)}$$

From this we obtain the fraction of the total number of turns which should lie between the tap and the low-potential end of the coil in order that amplification may be the highest possible. If the equation gives for n a figure below unity the coil must not be tapped but must have further turns added; the load is then applied across the whole of the coil thus lengthened. In practice, however, this course is rarely followed.
Equation (I C 10) may also be written:

$$\frac{L}{rC} = n^2R,$$

or in plain language:

If, in order to reduce its damping effect on a tuned circuit, a shunt impedance is connected to a tap on the coil, the highest gain will occur when the dynamic resistance of the unloaded circuit equals that resistance which, applied across the whole circuit, would cause the same damping as that of the load actually connected to the tap.

The general conclusion to be drawn is that the use of a tapped inductor always leads to better selectivity, and often to greater amplification, whenever $\frac{L}{rC}$ is larger than R.

§ 3. Inductive coupling

Instead of using a tapped coil, the load may be coupled inductively to the tuning inductor by means of a separate winding (see fig. 23a and b). When the coupling between the two coils is extremely tight, as it would be if the

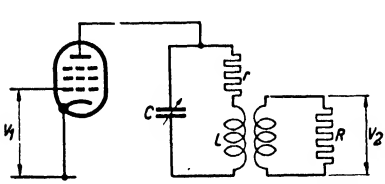

Fig. 23a. Tuned-anode amplifying stage, in which the resistive load is inductively coupled to the tuned circuit (inductive tapping).

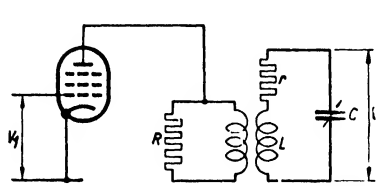

Fig. 23b. Amplifying stage in which the valve is inductively coupled to the tuned circuit in order to reduce the damping due to its A.C.-resistance.

windings were interlaced, the behaviour of the circuit to AC voltages is identical to that with a coil tapped at $\frac{1}{n}$, n being the turns ratio in the case of the inductive coupling. Accordingly the formulae evolved in § 2 apply. The use of a separate winding is advantageous when it is necessary to keep the tuned circuit isolated, from the DC point of view, from the preceding or the following circuit. Thus in fig. 23b the tuned circuit is safeguarded against the anode voltage of the valve to which it is coupled.

§ 4. Capacitive tapping

If, parallel to the tuned circuit, capacitors C_1 and C_2 are arranged in series and the load is connected across one of them, as in fig. 24, it can be shown that the damping imposed by the resistance R is precisely as great when it is joined to a tap at $\frac{1}{n}$ on the coil, where

$$n = \frac{C_1 + C_2}{C_1} \quad \ldots\ldots\ldots\ldots\ldots\ldots \quad \text{(I C 11)}$$

provided that the reactance of C_2 is small in relation to R.

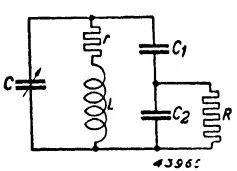

Fig. 24. Capacitive coupling of a damping resistance R to a tuned circuit.

The equations of C § 2 are valid here if for n we use the figure given by (I C 11). By this method it is often possible to lessen the damping with the use of only one capacitor C_1, the inter-wiring capacitance, the input-capacitance of the following valve, etc., taking the place of the second capacitor C_2. As these stray capacitances are generally quite small — 10 pF for instance — it is necessary to make C_1 small if any notable reduction of damping is to be brought about.

§ 5. Band-pass filters

The measures already discussed are applicable to band-pass filters also, and the results are in general similar; possible divergences will now be considered.

(*a*) *Increasing C and reducing L*

If we make the coupling in a band-pass filter critical the selectivity is determined by:

$$Q = \sqrt{Q_1 Q_2}$$

(in which the numerals 1 and 2 refer to the first and second tuned circuits

respectively). When one of the circuits of a band-pass filter is damped by a resistance the quality of that circuit is the same as with the case of a single circuit, but the effect on the filter as a whole is less, since in the last expression both Q_1 and Q_2 appear under a root sign. Similarly the effect on gain must be calculated with $\sqrt{Z}$ instead of Z, since the amplification with a critically-coupled filter is proportional to $\sqrt{Z_1 Z_2}$. It follows at once that, with a band-pass filter also, highest selectivity is reached when minimum inductance and maximum capacitance form the tuned circuits, whereas highest gain demands the converse. Variation of inductance and capacitance influences selectivity and gain less than in the case of a single circuit, however; this is to be expected because only one of the two circuits is affected. It should be remembered that with an inductive band-pass filter the coupling factor does not change when the inductance of one or both circuits is reduced if the physical dimensions of the coils remain unaltered. In a filter coupled by common capacitance the coupling becomes tighter as inductance falls, for the tuning capacitances necessarily become larger; with top-capacitance coupling, on the other hand, reducing the inductance loosens the coupling, and to restore the latter to its original value the top-capacitance must be made larger.

(b) Tapping the damped coil

As with the single circuit, selectivity is improved in the case of a band-pass filter if the damped circuit is tapped, since the Q factor for the tapped coil becomes higher. There is this difference, however, that the Q-factor appeared as $\sqrt{Q}$ in the equation for selectivity. It is otherwise with amplification; with a single circuit it is possible (see D § 2) to improve gain and selectivity simultaneously when $\frac{L}{rC}$ exceeds R, but with a bandpass-filter it is not possible. From fig. 25 the amplification is:

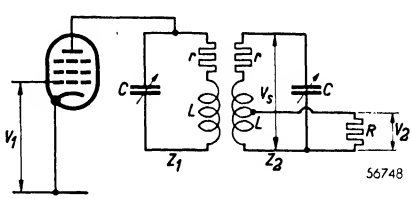

Fig. 25. Band-pass filter in the anode circuit of an amplifying valve, with the resistive load R tapped across the secondary tuned circuit.

$$\left|\frac{V_2}{V_1}\right| = \frac{1}{n}\left|\frac{Vs}{V_1}\right| = \frac{1}{n}\,{}^1/_2\,S\,\sqrt{Z_1 Z_2} \quad . \quad . \quad . \quad . \quad . \quad \text{(I C 12)}$$

The equation also holds good if the first circuit, and not the second, is tapped. Amplification is determined by $\frac{1}{n}\sqrt{Z}$.

Now:

$$\frac{1}{n}\sqrt{Z} = \sqrt{\frac{1}{n^2}\frac{1}{\left(\frac{rC}{L}+\frac{1}{n^2R}\right)}} = \frac{1}{\sqrt{n^2\frac{rC}{L}+\frac{1}{R}}} \quad \ldots\ldots \text{(I C 13)}$$

It is clear that gain falls progressively as n increases; with a band-pass filter, therefore, improved selectivity is always at the expense of amplification.

§ 6. Final remarks

A value for n smaller than 1 (in §§ 2 and 3) means that, instead of a tap, an extension of the winding is called for. This, however, raises the self-capacitance of the coil, so that, as in § 1, there is a lower limit for n; thus a very small value has no practical meaning. With the capacitive tapping dealt with in § 4, n clearly cannot be less than 1. A further limitation in the case of a band-pass filter is that at small values of n it becomes impossible to maintain critical coupling. As n is reduced a point is reached at which K must equal 1 if coupling is to be critical; any further reduction means that the coupling is bound to be sub-critical. Then, however, Q would have to equal 1, a very low value, so that this limitation is of no practical significance.

For clarity the various results are summarised in a table, in which Q_n (circuit quality) and dynamic resistance (important for judging gain) are calculated as a function of the tapping ratio; from this we can quickly locate the optimum ratio for selectivity and amplification.

TABLE

Summary of the results obtained by increasing C and reducing L, and by using a tapping or inductive or capacitive coupling, when a tuned circuit or band-pass filter is damped by parallel resistance.

	Device	Circuit	Selectivity	Gain
Single circuit	Increase of C and reduction of L; Q_n decreases proportionately to n.	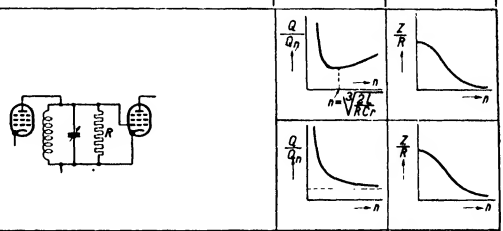		
	Increase of C and reduction of L; Q_n remains constant.			
Band-pass filter	Increase of C and reduction of L; Q_n decreases proportionately to n.	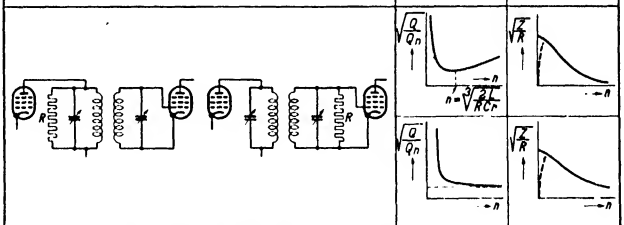		
	Increase of C and reduction of L; Q_n remains constant.			
Single circuit	Tapping on the coil.	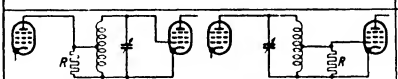	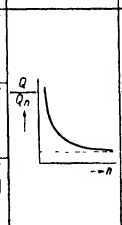	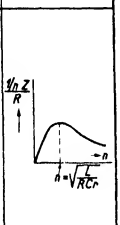
	Inductive coupling.	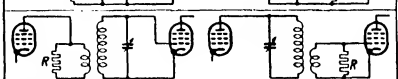		
	Capacitive coupling.			
Band-pass filter	Tapping on the coil.		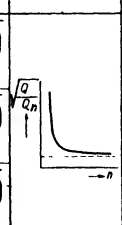	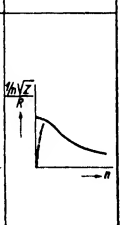
	Inductive coupling.			
	Capacitive coupling.			

56766

D. R.F. Amplification

Introduction

By R.F. amplification we mean amplification of the signal received by the aerial, before it is applied to the frequency-changer or detector. It is to be noted that such amplification may be effected at frequencies lower than those encountered in I.F. amplifiers; this is the case, for example, when a signal in the long-wave band (300—150 kc/s) undergoes amplification in a superheterodyne with a 475 kc/s intermediate frequency.

An important difference, however, is that the R.F. amplifying stage operates over an extensive range of frequencies, whereas the I.F. part of the receiver handles only a single frequency band. In its effect on the selectivity of the receiver and on the strengthening of the input signal the aerial stage is of as much importance as the anode tuned circuit of an R.F. valve; for this reason, as was mentioned in the introduction to this book, the input circuit and its coupling to the aerial are also discussed in the present chapter.

It will first be shown that the aerial circuit with its coupling can always be replaced by an equivalent circuit to which a certain current is supplied. The voltage developed across the tuned circuit, whether simple or band-pass, is dependent, like the dynamic resistance, on frequency.

The attenuation of the signal off resonance is thus equal to a, the factor calculated in sections A and B, allowing of course for the capacitance of the aerial and for the damping the latter imposes; this subject will be regarded as having been by now sufficiently explained.

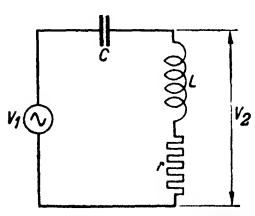

Fig. 26. Tuned circuit with a voltage V_1 induced therein, and a voltage V_2 across the coil.

The raising of the voltage induced in the aerial to that which is fed to the grid of the first valve is often referred to as magnification. This process is most easily explained with the aid of fig. 26, in which V_1 represents the voltage induced in the tuned circuit. If the resistance r of the coil is small in relation to its reactance ωL, the relation between the voltages V_2 and V_1 at resonance is given by:

$$\frac{V_2}{V_1} = \frac{j\omega_0 L}{r} = j\,Q. \quad \ldots\ldots\ldots\ldots \quad \text{(I D 1)}$$

Since at resonance $j\omega_0 L + \frac{1}{j\omega_0 C} = 0$, $I = \frac{V_1}{r}$. Therefore $V_2 = \frac{V_1}{r}(r + j\omega_0 L)$,

and as $r \ll j\omega_0 L$, $V_2 = \frac{V_1}{r} j\omega_0 L$ or $\frac{V_2}{V_1} = \frac{j\omega_0 L}{r}$.

V_2 can accordingly be many times greater than V_1. The equivalent circuit of an aerial input stage is in fact never as simple as that shown in fig. 26; but inasmuch as, at the received frequency, part of the circuit acts as inductance and part as capacitance, the circumstances are fairly similar to those of the figure.

We shall consider this matter in more detail. With a band-pass filter, as with a single circuit, we can speak of magnification and our further consideration will therefore be in two parts, dealing first with single circuits and afterwards with filters.

§ 1. Coupling the aerial to a tuned circuit

The simplest equivalent circuit for an aerial is a voltage source with a voltage V_{ant} (namely the voltage induced in the aerial by the received signal) and with an internal impedance consisting of the aerial capacitance C_a (see fig. 27*a*).

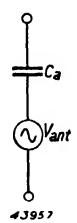

Fig. 27a. Equivalent circuit of an aerial.

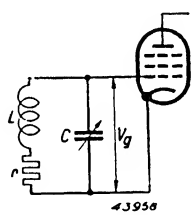

Fig. 27b. Tuned circuit connected to the grid of an amplifying valve.

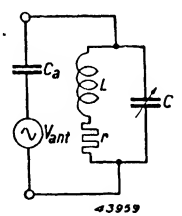

Fig. 27c. Equivalent circuit of an aerial in parallel with the tuned circuit.

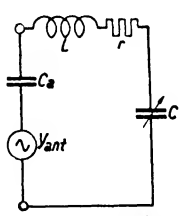

Fig. 27d. Equivalent circuit of an aerial in series with the inductor and capacitor comprising the tuned circuit.

This aerial must now be so connected to the circuit given in fig. 27b that the tuning of this circuit is affected to the minimum degree by the aerial capacitance. (Otherwise the accuracy of the wavelength scale will depend on the aerial employed, while in receivers with several tuned circuits the accuracy of the ganging will be much impaired.)

There are, basically, two ways of linking the aerial of fig. 27a with the tuned circuit of fig. 27b. The first method is to connect it across the top and bottom of the circuit, as in fig. 27c, and the second is to join the aerial to

the inductance and the tuning capacitance C in series, as in fig. 27d. Bearing in mind the need for minimum disturbance of tuning by the aerial, it is clear that the circuit of fig. 27c is practicable only when, in relation to C, the aerial has but very small capacitance. As normal aerials have a capacitance of about 200 pF, a further impedance in series is essential. By making this impedance large enough, the influence of C_a on the tuning of the circuit may be made as small as desired; either a small capacitance C_{k1} or a large inductance L_{k1} serves the purpose. We thus come to the practical arrangements shown in figs 28a and b.

In fig. 27d, C_a must be large in proportion to C for minimum disturbance of the tuning. As, for this arrangement, the capacitance of a normal aerial is

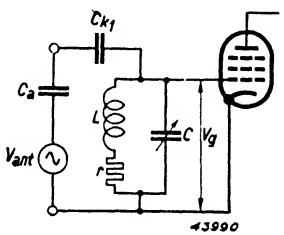

Fig. 28a. Aerial coupled to the top of the tuned circuit by means of a capacitor C_{k_1} (capacitive top-coupling).

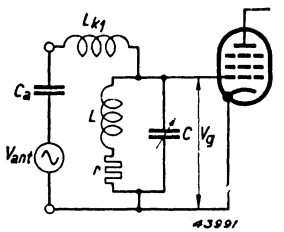

Fig. 28b. Aerial coupled to the top of the tuned circuit by means of an inductor L_{k_1} (inductive top-coupling).

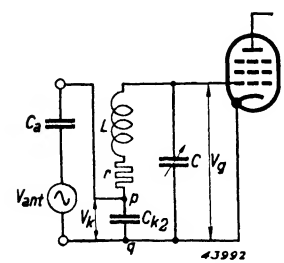

Fig. 28c. Aerial coupled to the bottom of the tuned circuit by means of a capacitor C_{k_2} (capacitive bottom-coupling).

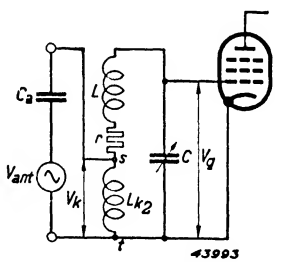

Fig. 28d. Aerial coupled to the bottom of the tuned circuit by means of an inductor L_{k_2} (inductive bottom-coupling).

too small, it is necessary to connect a low impedance in parallel with the aerial; a capacitance C_{k2} large in relation to C, or an inductance L_{k2} small in relation to L, may be used (figs 28c and d).

Fig. 28 sets out the four basic types of aerial coupling. Circuits *a* and *b*, in which the aerial is connected to the top of the tuned circuit through a capacitance or inductance, we shall call "aerial coupling to the top of the tuned

circuit" or, shortly, "top coupling". In circuits *c* and *d*, owing to the small impedance represented by C_{k_2} and L_{k_2}, the aerial is connected practically to the bottom of the tuned circuit; these methods we shall term "aerial coupling to the bottom of the tuned circuit" or, shortly, "bottom coupling". Our next task is to calculate the magnification of the circuits in fig. 28.

§ 2. Coupling to the top of the tuned circuit

(*a*) *Capacitive top coupling* (*see fig.* 28*a*)

If the series combination C_a — C_{k_1} is replaced by a capacitance C_{k_1}' the circuit of fig. 29a is obtained. In this the magnification may be most simply calculated by using the following argument: a voltage source with voltage V

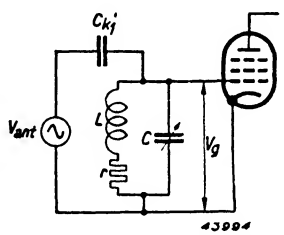

Fig. 29a. Aerial coupled to the top of the tuned circuit by means of a capacitor; the series capacitances C_a (aerial capacitance) and C_{k_1} (coupling capacitance) are here replaced by a capacitance C_{k_1}'.

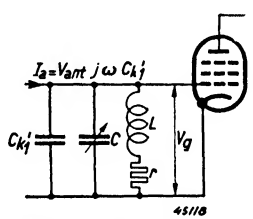

Fig. 29b. Equivalent circuit of fig. 29a.

and impedance Z can be replaced by a current source delivering a constant current, of magnitude $I = \frac{V}{Z}$ (the short-circuit current), to the impedance Z connected in parallel with the current source. If we now regard the aerial as a voltage source with voltage V_{ant} and impedance $\frac{1}{j\omega C'_{k_1}}$ we can replace fig. 29a by fig. 29b, and if in the latter we assume the tuned circuit to be resonant at the frequency to be received its dynamic resistance amounts to:

$$Z_0 = \frac{L}{r\,(C + C'_{k_1})} \quad \ldots\ldots\ldots\ldots \quad \text{(I D 2)}$$

The AC voltage at the grid will therefore be:

$$V_g = I_a \frac{L}{r\,(C + C'_{k_1})} = V_{ant}\, j\omega C'_{k_1} \frac{L}{r\,(C + C'_{k_1})} \quad \ldots\ldots \quad \text{(I D 3)}$$

As we are interested only in the magnitude of V_g, and not in the phase shift, we refer to the relation between the moduli of V_g and V_{ant} as the "magnification". Therefore:

$$A = \left| \frac{V_g}{V_{ant}} \right| = \frac{C'_{k1}}{C + C'_{k1}} \frac{\omega L}{r} = \frac{C'_{k1}}{C + C'_{k1}} Q \quad . \quad . \quad \text{(I D 4)}$$

It is clear from this equation that the magnification is proportional to the Q of the tuned circuit; the better the quality of the circuit, the higher the magnification. A further deduction to be drawn from equation (I D 4) is that the magnification is dependent on the capacitance of the variable capacitor C. Over any particular waveband Q may be considered roughly constant. As the value of C is greater at longer wavelengths, at the upper end of the waveband the magnification will be less than at the lower. Consequently the sensitivity of the receiver will vary with wavelength; often this is not permissible, and measures have to be taken to compensate for the variation. If for the circuit $Q = 100$, the capacitance of the aerial coupling capacitor $C_{k1} = 20$ pF ($C_{k1} \ll C_a$, so that $C'_{k1} \cong C_{k1}$) and the capacitance of the tuning capacitor is variable from 30 to 500 pF, then for the magnification at the bottom of the waveband we find:

$$A = \frac{20}{30 + 20} 100 = 40$$

and at the top of the band

$$A = \frac{20}{500 + 20} 100 = 3.8.$$

This variation must generally be regarded as a drawback of the circuit of fig. 28*a*.

(b) *Inductive top coupling (see fig.* 28b)

The magnification in this case is most easily calculated with the help of an equivalent circuit. First we shall replace the impedance

$$j\omega L_{k1} + \frac{1}{j\omega C_a}$$

by

$$j\omega L'_{k1} = j\omega L_{k1} \left(1 - \frac{\omega_k^2}{\omega^2}\right) \quad . \quad . \quad . \quad . \quad . \quad . \quad . \quad . \quad \text{(I D 5)}$$

in which

$$\omega_k^2 = \frac{1}{L_{k1}\, C_a} \quad \ldots\ldots\ldots\ldots\ldots\ldots \quad \text{(I D 6)}$$

In this way, by putting L'_{k1} in place of L_{k1}, the aerial capacitance is taken into account (fig. 30a).

If now we substitute a current source for the aerial, the circuit seen in fig. 30b is obtained.

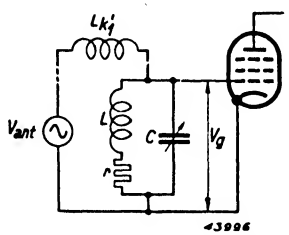

Fig. 30a. Aerial coupled to the top of the tuned circuit by means of an inductor; the series combination C_a-L_{k1} is here replaced by an inductance L_{k1}'.

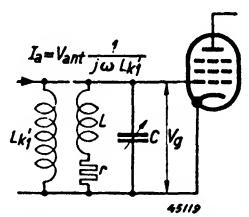

Fig. 30b. Equivalent circuit of fig. 30a.

As disturbance of the tuning by the aerial should be very small, L'_{k1} must in practice be large in relation to L.

The dynamic resistance of the circuit in fig. 30b is therefore about equal to $\frac{L}{rC}$, and the AC voltage at the grid is:

$$V_g = \frac{V_{ant}}{j\omega L_{k1}'} \frac{L}{rC} \quad \ldots\ldots\ldots\ldots\ldots\ldots \quad \text{(I D 7)}$$

For the magnification we find:

$$A = \left| \frac{V_g}{V_{ant}} \right| = \frac{1}{\omega L_{k1}'} \frac{L}{rC} = \frac{L}{L_{k1}'} \frac{1}{\omega C r}. \quad \ldots\ldots \quad \text{(I D 8)}$$

or, since at the resonant frequency $\omega_0 L = \frac{1}{\omega_0 C}$,

$$A = \frac{L}{L_{k1}'} \frac{\omega_0 L}{r} = \frac{L}{L_{k1}} Q \frac{\omega_0^2}{\omega_0^2 - \omega_k^2} \quad \ldots\ldots\ldots \quad \text{(I D 9)}$$

As a result of the large value of L_{k1}, ω_k is always in practice several times

smaller than ω_0, so that as an approximation of equation (I D 9) we may write:

$$A = \frac{L}{L_{k1}} Q \quad \ldots\ldots\ldots\ldots\ldots \quad \text{(I D 10)}$$

If Q is assumed to be a constant quantity, the magnification is thus independent of the resonant frequency. Only at the upper end of the waveband will the magnification calculated from equation (I D 9) increase somewhat, for in that region the difference between ω_0 and ω_k becomes smaller. Should ω_0 equal ω_k, the magnification is then not, as might be expected from equation (I D 9), infinitely large, for precise calculation shows that in such a case the resistance of L_{k1}, and other factors we have neglected, keep magnification finite. By suitable choice of ω_k we can influence the variation of magnification and in this way attain the desired course of sensitivity in a receiver. In order to reach a specific value for ω_k it is possible to connect a capacitance in series or in parallel witk L_{k1}; ω_k is then less affected by C_a and sensitivity changes less with the use of different aerials.

§ 3. Coupling to the bottom of the tuned circuit

(a) *Capacitive bottom coupling (see fig. 28c)*

Here we shall deal only with the most important practical case, that in which C_{k2} is so large by comparison with C and C_a that the impedance between points p and q is about equal to $\frac{1}{j\omega C_{k2}}$.

The voltage between these two points is then:

$$V_k = V_{ant} \frac{C_a}{C_{k2} + C_a} \quad \ldots\ldots\ldots\ldots \quad \text{(I D 11)}$$

For the frequency to which the circuit is tuned we find that the relation between V_g and V_k is equal to $j\,Q$ (see fig. 26).
The AC voltage at the grid therefore amounts to:

$$V_g = j\, V_{ant} \frac{C_a}{C_a + C_{k2}} Q \quad \ldots\ldots\ldots\ldots \quad \text{(I D 12)}$$

and for the magnification we find:

$$A = \left| \frac{V_g}{V_{ant}} \right| = \frac{C_a}{C_a + C_{k2}} Q \quad \ldots\ldots\ldots\ldots \quad \text{(I D 13)}$$

With this circuit, therefore, magnification is nearly independent of wave-

length; for example if $C_a = 200$ pF, $C_{k_2} = 5000$ pF and $Q = 100$, then for the entire waveband:

$$A = \frac{200}{200 + 5000} \times 100 = 3.8.$$

In this respect the circuit of fig. 28c is better than that of fig. 28a. A disadvantage, however, is that, in order to maintain accurate ganging, capacitors of the same capacitance as C_{k_2} must be included in the other tuned circuits. With the arrangement of fig. 28a, on the other hand, the influence of C_{k_1} can be balanced in the other circuits by means of the trimmers.

(*b*) *Inductive bottom coupling* (*see fig. 28d*)

We shall consider only one case: that in which L_{k_2} is small in relation to L, and the impedance between points s and t therefore practically equal to $j\omega L_{k_2}$. The voltage between these points is then:

$$V_k = V_{ant} \frac{j\omega L_{k_2}}{j\omega L_{k_2} + \frac{1}{j\omega C_a}} = V_{ant} \frac{1}{1 - \frac{\omega_k^2}{\omega^2}} = -V_{ant} \frac{\omega^2}{\omega_k^2 - \omega^2}. \quad \text{(I D 14)}$$

where

$$\omega_k^2 = \frac{1}{L_{k_2} C_a}.$$

Here again, at the resonant frequency ($\omega = \omega_0$) of the circuit, $V_g / V_k = j\,Q$ and the AC voltage at the grid is:

$$V_g = -j\,V_{ant} \frac{\omega_0^2}{\omega_k^2 - \omega_0^2} Q. \quad \text{(I D 15)}$$

while the magnification is:

$$A = \left| \frac{V_g}{V_{ant}} \right| = \frac{\omega_0^2}{\omega_k^2 - \omega_0^2} Q \quad \text{(I D 16)}$$

Owing to the small value of L_{k_2}, ω_k is in practice always large in comparison with ω_0, so that for equation (I D 16) we can write:

$$A = \frac{\omega_0^2}{\omega_k^2} Q = \frac{1}{\omega_k^2 L C} Q \quad \text{(I D 17)}$$

In this case, as in that of fig. 28a, magnification varies with the capacitance of the tuning capacitor and is smaller at the top of the waveband than at

the bottom. By suitable choice of ω_k it is possible to modify the magnification, but this is not of great practical value.
The circuits described are not the only methods of connecting the aerial to the first tuned circuit of a receiver. With capacitances and inductances, arrangements can be devised with very diverse magnification frequency characteristics, and different coupling methods may be combined so that a combination of their properties is obtained.
As it is the intention, however, to give only a short survey of these aerial circuits, the more complicated kinds will not be further discussed. There remains one commonly used circuit to be dealt with; the mutual-inductance aerial coupling.

§ 4. Mutual-inductance coupling

In fig. 31a the aerial is inductively coupled to the tuning coil by means of a coupling coil. The induced voltage V_{ant} and the aerial capacitance C_a are

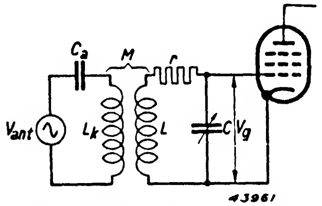

Fig. 31a. Basic circuit of an inductive aerial coupling.

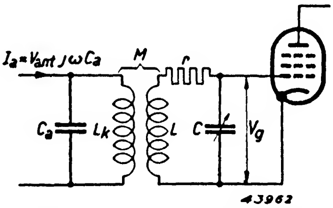

Fig. 31b. Equivalent circuit of fig. 31a.

indicated in the diagram. Using the same argument as before, we replace the circuit of fig. 31a by that of 31b; instead of the induced voltage we now have a current source, with C_a shunted across it:

$$I_a = V_{ant}\, j\omega C_a \quad \text{(I D 18)}$$

This type of aerial coupling really amounts to a band-pass filter in which the second circuit is tuned to the desired signal; the first circuit consists of the aerial capacitance C_a and the undetermined inductance L_k. To calculate the performance of this circuit we therefore go back to the general band-pass filter equation (I B 10), which in this case we write:

$$V_g = -V_{ant}\, \omega C_a \, \frac{\omega_0^3}{\omega^2} \, \frac{Q_2 K \sqrt{L_k L}}{j\beta_1 (1 + j\beta_2 Q_2) + K^2 Q_2} \quad \text{(I D 19)}$$

Here I_a has been replaced by substitution from equation (I D 18) and, as in fig. 31, resistance in the primary circuit is neglected ($Q_1 = \infty$).

From equation (I D 19) we now get for the absolute value of the output voltage V_g:

$$V_g = V_{ant}\, C_a \frac{\omega_0^3}{\omega} \frac{Q_2\, K \sqrt{L_k L}}{\sqrt{(K^2 - \beta_1\beta_2)^2\, Q_2^2 + \beta_1^2}} \quad . \quad \text{(I D 20)}$$

In this, β_1 represents the detuning of the fixed circuit $C_a L_k$ from the signal frequency ω, and β_2 the detuning therefrom of the secondary circuit.
It is desirable to make V_g as large as possible, and it might be expected that the maximum would be reached when $\beta_2 = 0$.
Closer consideration of equation (I D 20), however, shows that this is not so. With a fixed primary circuit, that is to say when β_1 is fixed, V_g attains its maximum if

$$K^2 - \beta_1\beta_2 = 0 \quad . \quad . \quad . \quad . \quad . \quad . \quad . \quad . \quad . \quad . \quad . \quad . \quad . \quad \text{(I D 21)}$$

Only when K^2 is very small is it right to say that β_2 must equal 0. In general, the highest magnification is attained when, as equation (I D 21) indicates, the circuit LC is detuned a little. The equation then becomes:

$$A = \left|\frac{V_g}{V_{ant}}\right| = C_a \frac{\omega_0^3}{\omega} \frac{Q_2\, K \sqrt{L_k L}}{\beta_1} \quad . \quad . \quad . \quad . \quad . \quad \text{(I D 22)}$$

If in equation (I D 22) we substitute:

$$K \sqrt{L_k L} = \frac{\omega}{\omega_0} M \text{ [from equation (I B 9)]},$$

$$\frac{1}{\beta_1} = \frac{1}{\omega/\omega_1 - \omega_1/\omega} = \frac{\omega\,\omega_1}{\omega^2 - \omega_1^2},$$

$$\omega_0^2 = \omega_1\omega_2 \text{ and } \omega_1 C_a = \frac{1}{\omega_1 L_k},$$

we can write for the magnification:

$$A = C_a \frac{\omega_0^3}{\omega} \frac{\omega}{\omega_0} M\, Q_2 \frac{\omega\omega_1}{\omega^2 - \omega_1^2} = \frac{M}{L_k} Q_2 \frac{\omega^2}{\omega^2 - \omega_1^2} \frac{\omega_2}{\omega} \quad . \quad . \quad . \quad . \quad \text{(I D 23)}$$

It will later be shown that ω and ω_2 are about equal; this was to be expected. The tuning is determined almost entirely by the second circuit, so we may put the fourth term in equation (I D 23) equal to unity; the formula then simplifies to:

$$A = \frac{M}{L_k} Q_2 \frac{\omega^2}{\omega^2 - \omega_1^2} \quad . \quad . \quad . \quad . \quad . \quad . \quad . \quad . \quad . \quad . \quad \text{(I D 24)}$$

Over the whole waveband Q remains, as already noted, sensibly constant, and the magnification will also vary little if we take care that the last fraction is constant, i.e. if we make ω_1 small in relation to ω. Otherwise the variation of equation (I D 24) with frequency is in all respects the same as in the case of an inductive coupling to the top of the circuit [see equation (I D 9)].
Usually we make ω_1 much lower than the lowest value of ω in the waveband; if it is only just lower, the magnification will rise towards the upper end of the band.
The primary resonant frequency ω_1 may also be made higher than the highest value of ω, and in that case the variation of magnification with frequency is the same as in equation (I D 16). Such a coupling is therefore equivalent to that of fig. 28d. It is not often used.
The commonest arrangement is to make ω_1 fairly low, by giving a relatively large value to L_k; this is known as a "large-primary" aerial coupling. It is of interest to know how the secondary tuning should be determined in this case, for the simple relationship $\omega^2 LC = 1$ is clearly not valid. L and C may then be calculated from the equation (I D 21).
In the latter we substitute for β_1, β_2, and K^2 in accordance with the definitions on page 20 and equation (I B 9) respectively:

$$(\omega/\omega_1 - \omega_1/\omega)\,(\omega/\omega_2 - \omega_2/\omega) - \frac{\omega^2}{\omega_1\omega_2}k^2 = 0 \quad . \quad . \quad \text{(I D 25)}$$

hence

$$\omega_2{}^2\left(1 - \frac{\omega_1{}^2}{\omega^2}\right) + \omega_1{}^2 - \omega^2\,(1 - k^2) = 0. \quad . \quad . \quad . \quad \text{(I D 26)}$$

or

$$\omega_2{}^2 = \frac{\omega^2\,(1 - k^2) - \omega_1{}^2}{\omega^2 - \omega_1{}^2}\,\omega^2 . \quad . \quad . \quad . \quad . \quad . \quad . \quad . \quad . \quad \text{(I D 27)}$$

For a given primary resonant frequency ω_1 and a given angular frequency ω, the required figure ω_2 and the consequent product LC are easily calculated with the help of equation (I D 27).
Treating the circuit as a band-pass filter is logical; the formulae for a filter have already been derived and equations (I D 24) and (I D 27) are in practice quite satisfactory for the present case.
However, it might be claimed, in view of the considerable detuning of the primary, that the circuit could better be regarded as a transformer-coupled single circuit. The equivalent circuit would then need modification, and the

requirement for resonance might be expected to take the form:

$$\omega^2 L'C' = 1 \text{ or } \omega^2 = \frac{1}{L'C'},$$

where L' and C' represent the corrected values of L and C.

Equation (I D 26) can also be brought to this form. We then write:

$$\omega^2 (1 - k^2) = \omega_2^2 + \omega_1^2 (1 - \omega_2^2/\omega^2) \quad . \quad . \quad . \quad . \quad \text{(I D 28)}$$

Multiplying equation (I D 25) by $\frac{\omega_1 \omega_2}{\omega^2}$, we get:

$$(1 - \omega_2^2/\omega^2)(1 - \omega_1^2/\omega^2) = k^2 \quad . \quad . \quad . \quad . \quad . \quad . \quad . \quad \text{(I D 29)}$$

Substitution from equation (I D 29) in (I D 28) gives us:

$$\omega^2 (1 - k^2) = \omega_2^2 + \omega_1^2 \frac{k^2}{1 - \omega_1^2/\omega^2} \quad . \quad . \quad . \quad . \quad \text{(I D 30)}$$

or:

$$\omega^2 = \frac{1}{L(1 - k^2)} \left[\frac{1}{C} + k^2 \frac{L}{L_k} \frac{1}{C_a (1 - \omega_1^2/\omega^2)} \right] \quad . \quad . \quad . \quad . \quad . \quad . \quad \text{(I D 31)}$$

Here $L(1 - k^2)$ is the inductance of the secondary when the primary winding is short-circuited, and its value may be denoted by L'. Within the square brackets we notice the series connection C' of two capacitances, viz. the tuning capacitor C with:

$$C_a \frac{1}{\frac{L}{L_k} k^2} (1 - \omega_1^2/\omega^2) = \frac{C_a}{u^2} (1 - \omega_1^2/\omega^2) \quad . \quad . \quad . \quad \text{(I D 32)}$$

$\sqrt{\frac{L}{L_k}} k^2$ represents, of course, the transformer ratio u. The correction to C is therefore the insertion in series of a capacitance equivalent to the reflected capacitance C_a multiplied by $(1 - \omega_1^2/\omega^2)$. The equivalent circuit is given in fig. 32.

This result is important in connection with the alignment of circuit 31 with another single circuit. In the latter, therefore, it is necessary to insert a capacitance in series with C, of a value determined by L' and C'. Fig. 32 makes it clear, however, that accurate ganging over the whole waveband is possible only if $(1 - \omega_1^2/\omega^2)$ is tolerably constant, i.e. if ω_1^2/ω^2 remains very small.

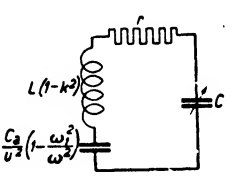

Fig. 32. Equivalent circuit of the inductive aerial coupling of fig. 31.

As the resonant frequency ω_2 is now fixed, we can correct equation (I D 24). The unknown quantity $\frac{\omega_2^2}{\omega^2}$ can be calculated from equation (I D 30):

$$\omega_2^2/\omega^2 = 1 - k^2 - k^2 \frac{\omega_1^2}{\omega^2 - \omega_1^2} \quad \ldots\ldots\ldots \quad \text{(I D 33)}$$

and can then be inserted in equation (I D 23).

The selectivity of the circuit can be deduced from the basic equation (I D 19). It is clear that the resonance curve is neither that of a single circuit nor that of a band-pass filter, though it seems logical to expect resemblance to a single circuit. Accordingly, equation (I D 19) should be rearranged as follows: if we put in the numerator $\frac{\omega}{\omega_0} k$ for K, the equation becomes:

or:

$$\left.\begin{aligned} V_g &= - V_{ant}\, C_a \frac{\omega_0^2}{j\beta_1} \frac{Q_2\, k \sqrt{L_k L}}{(1 + j\beta_2\, Q_2) - j \frac{K^2 Q_2}{\beta_1}} \\ V_g &= j\, V_{ant}\, C_a \frac{\omega_0^2}{\beta_1} \frac{Q_2\, k \sqrt{L_k L}}{1 + j\beta_2'\, Q_2} \end{aligned}\right\} \quad \text{(I D 34)}$$

As in most cases β_1 is here fairly large, its variation on detuning from resonance will be relatively small, and the dependence of V_g on frequency will be mainly determined by $1 + j\beta_2' Q_2$. For the attenuation factor we now find:

$$a = \left| 1 + j\beta_2' Q_2 \right| \text{ or } a = \sqrt{1 + (\beta_2' Q_2)^2}$$

With this we may compare equation (I A 10), relating to a single circuit. Indeed the circuit may be regarded, roughly speaking, as a single circuit if we take into consideration that:

$$\beta_2' = \beta_2 - \frac{K^2}{\beta_1} \quad \ldots\ldots\ldots\ldots\ldots \quad \text{(I D 35)}$$

It can be shown that this correction of the detuning factor agrees with the revised circuit elements of fig. 32, i.e. it should also be possible to calculate the selectivity from:

$$Q_2' = \frac{\omega_2 L'}{r} = \frac{\omega_2 L (1 - k^2)}{r}$$

We conclude from this equation that the quality of the coil must be measured with the primary winding short-circuited.

§ 5. Coupling the aerial to a band-pass filter

A band-pass filter may also be coupled to the aerial by any of the foregoing methods. In fig. 33a capacitive coupling to the top of the circuit is shown.

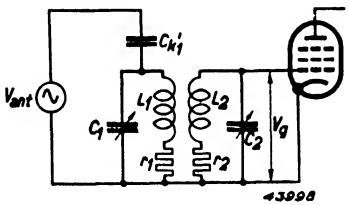

Fig. 33a. Capacitive aerial coupling to a band-pass filter.

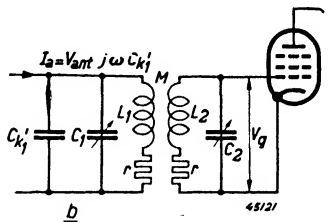

Fig. 33b. Equivalent circuit of fig. 33a.

If once more we substitute a current-source I_a for the voltage-source V_{ant} we get circuit *b*. Equation (I B 16) now gives, for the voltage V_g:

$$V_g = \mp j I_a \frac{Q K}{1 + Q^2K^2} \sqrt{Z_1 \times Z_2} =$$

$$= - V_{ant}\, \omega\, C_{k1}' \frac{Q K}{1 + Q^2K^2} \sqrt{Z_1 \times Z_2} \quad . \; . \; . \quad \text{(I D 36)}$$

Z_1 and Z_2 here stand for the dynamic resistance of the primary and secondary circuits respectively.

The magnification is therefore:

$$A = \left| \frac{V_g}{V_{ant}} \right| = \omega C_{k1}' \frac{Q K}{1 + Q^2K^2} \sqrt{Z_1 \times Z_2} \; . \quad \text{(I D 37)}$$

If the circuits are identical (namely $L_1 = L_2 = L$, $r_1 = r_2 = r$, $C_1 + C_{k1} = C_2 = C$) and if the coupling is critical ($KQ = 1$) we find:

$$A = \omega C_{k1} \tfrac{1}{2} \frac{L}{rC} = \tfrac{1}{2} \frac{C_{k1}}{C_1 + C_{k1}} Q \; . \; . \; . \; . \; . \; . \; . \quad \text{(I D 38)}$$

We can therefore say that a critically-coupled filter yields half the magnification which would be given by one of its circuits used alone as a single tuned circuit. This holds not only for the coupling shown in fig. 33, but also for the other coupling methods dealt with in section B. If the coupling is not critical, or if the two circuits are dissimilar, the magnification must be computed with the help of equation (I D 37). As fig. 13 on page 26 proves, the highest magnification occurs with critical coupling.

Magnification is a voltage gain requiring no valves. We therefore endeavour to make it as high as possible, first in order to increase the sensitivity of the receiver inexpensively, and secondly in order to obtain a favourable ratio of signal-to-valve noise. Since the increased gain occurs before the first valve, less amplification is needed in later stages and noise is therefore less troublesome.

To secure high magnification it is important to use circuits of good quality, i.e. circuits for which Q is large.

Besides circuit quality there are other quantities which affect magnification. Thus, for example, the capacitance C_{k1} in fig. 28a should, from equation (I D 4), be large; and in fig. 31 M/L_k must be large, in accordance with equation (I D 24), and so on. It is important, therefore, to couple the aerial to the tuned circuit as tightly as possible. The choice of circuit quality and coupling factor is however narrowed for various reasons, one of the most important being the detuning and damping caused by a tightly-coupled aerial; these effects will be considered in § 6.

§ 6. Influence of the aerial on the tuning of the first circuit

If we connect a receiver having more than one tuned circuit to an aerial whose capacitance differs from that used in aligning the circuits and calibrating the scale, detuning of the input circuit occurs and becomes greater as aerial coupling is tightened; to compensate for this detuning it is necessary to readjust the aerial-circuit trimmer. However, it is usually desirable to be able to connect a receiver to any aerial without the need for adjustment, and accordingly the coupling must be so chosen that any likely detuning will fall within acceptable limits. Whether a given degree of detuning is tolerable may be judged by its effect in reducing magnification and in distorting the set's overall resonance curve. The latter is less important in superheterodynes, as the I.F. circuits predominate; indeed, in such receivers signal-frequency selectivity is mainly concerned with preventing cross-modulation (see chapter IV). Here we shall deal only with the reduction of magnification.

By means of equation (I A 10) we can calculate the permissible detuning for a circuit of given quality. According to this equation:

$$a^2 = 1 + \beta^2 Q^2 \quad \text{(I A 10)}$$

or we can write

$$\left(\frac{2\Delta\omega}{\omega}\right)^2 = \frac{a^2 - 1}{Q^2}$$

The permissible relative detuning is therefore:

$$\frac{\Delta\omega}{\omega} = \pm \tfrac{1}{2} \frac{\sqrt{a^2 - 1}}{Q} \quad \text{(I D 39)}$$

The detuning effect of the aerial may be regarded as a modification of the capacitance and inductance of the tuned circuit. The effective values of capacitance and inductance may therefore differ from C and L, and in the following calculations the effective values will be indicated by C' and L'. In fig. 29, for instance, $C' = C + C'_{k_1}$.

A change in the aerial capacitance may cause a variation of either C' or L'. It is therefore useful to state, instead of the permissible detuning, the permissible deviation of C' or L', which we can calculate as follows:

$$\omega = \frac{1}{\sqrt{L'C'}};$$

$$\Delta\omega = -\tfrac{1}{2} \frac{1}{\sqrt{L'C'}} \frac{\Delta C'}{C'} = -\tfrac{1}{2}\omega \frac{\Delta C'}{C'}.$$

$$\left.\begin{aligned} \text{Therefore } \frac{\Delta C'}{C'} &= -2\frac{\Delta\omega}{\omega} = \pm\sqrt{a^2 - 1} \cdot \frac{1}{Q} \\ \text{Similarly: } \frac{\Delta L'}{L'} &= \pm\sqrt{a^2 - 1} \cdot \frac{1}{Q} \end{aligned}\right\} \quad \text{(I D 40)}$$

The capacitance of receiving aerials varies within wide limits; that of a small indoor aerial may be 50 pF, while a large outdoor aerial with screened down-lead may reach 1500 pF. Thus it must be possible for the aerial impedance to vary greatly, without detuning the first circuit too much. From this point of view we shall now examine more closely the two most important types of aerial coupling.

(*a*) *Top-capacitance coupling* (see fig. 28a)

In this case we may first consider a change of aerial capacitance from nil to infinity, corresponding on the one hand to a free aerial terminal and on the other to an aerial terminal short-circuited to earth. If the receiver is connected to an aerial whose capacitance equals that with which the tuned circuits were aligned, then:

$$C' = C + C_{k_1}'.$$

With the aerial terminal disconnected:

$$C' = C;$$

and with the aerial and earth terminals short-circuited

$$C' = C + C_{k1}.$$

Since normal aerials have a capacitance which in relation to C_{k1} is so large that $C'_{k1} \approx C_{k1}$, the greatest detuning occurs when the aerial terminal is disconnected; the change of C' is then:

$$\Delta C' = C_{k1}' \quad \ldots\ldots\ldots\ldots\ldots \quad \text{(I D 41)}$$

Equation (I D 40) now becomes:

$$\frac{C_{k1}'}{C'} = \frac{C_{k1}'}{C + C_{k1}'} = \sqrt{a^2 - 1} \cdot \frac{1}{Q} \quad \ldots\ldots \quad \text{(I D 42)}$$

From this we obtain for the maximum value of C_{k1}':

$$\frac{C_{k1}'_{max}}{C_{min} + C_{k1}'_{max}} = \sqrt{a^2 - 1} \cdot \frac{1}{Q} \quad \ldots\ldots \quad \text{(I D 43)}$$

This maximum value for C_{k1}' must be calculated at the lowest occurring value of C (C_{min} = capacitance at the bottom of the waveband). As $C_{k1}' \approx C_{k1} \ll C_{min}$, the maximum permissible value of C_{k1} can be approximately stated as follows:

$$C_{k1max} = C_{min} \sqrt{a^2 - 1} \cdot \frac{1}{Q} \quad \ldots\ldots\ldots \quad \text{(I D 44)}$$

With such a coupling capacitance the highest attainable magnification would, from equations (I D 4) and (I D 43), be:

$$A_{max} = \frac{C_{k1}'}{C_{min} + C_{k1}'} Q = \sqrt{a^2 - 1} \quad \ldots\ldots \quad \text{(I D 45)}$$

If, for example, it is considered that a reduction of magnification of $a = \sqrt{2}$ is admissible, then at the bottom of the waveband the magnification will, according to equation (I D 45), be no more than unity. At the top of the waveband the magnification is obviously still smaller.

When $Q = 100$ and $C_{min} = 50$ pF, equation (I D 44) shows that the above-mentioned magnification is obtained with a capacitance of

$$C_{k1max} = 50 \times 1 \times \frac{1}{100} = 0.5 \text{ pF}.$$

This capacitance is thus the maximum variation of the tuning capacitance that can be tolerated.

The magnification obtainable is therefore very small, but if we provide for a smaller variation of aerial capacitance than from nil to infinity we can allow C_{k1} to be larger, thereby obtaining greater magnification. If we consider

only aerials with a capacitance of from 50 to 1500 pF, C_{k1} may then be made 6 pF. In that case C_{k1}' has the following values:

when $C_a = 50$ pF:

$$C_{k1}' = \frac{C_a C_{k1}}{C_a + C_{k1}} = \frac{50 \times 6}{50 + 6} = 5.36 \text{ pF};$$

when $C_a = 200$ pF:

$$C_{k1}' = \frac{200 \times 6}{200 + 6} = 5.83 \text{ pF};$$

when $C_a = 1500$ pF:

$$C_{k1}' = \frac{1500 \times 6}{1500 + 6} = 5.98 \text{ pF}.$$

If the tuned circuit is accurately adjusted with an aerial capacitance of 200 pF, the maximum deviation will be

$$C' = 5.83 - 5.36 = 0.47 \text{ pF}.$$

This amount is just within the figure of $\frac{1}{2}$ pF calculated above.
With an aerial of 200 pF the magnification at the bottom of the waveband is:

$$A = \frac{C_{k1}'}{C + C_{k1}'} \cdot Q = \frac{5.83}{55.83} \; 100 = 10.4.$$

In order that still larger values of C_{k1} may be used, it is common practice to connect a capacitor C_b between the aerial and earth terminals (see fig. 34). Variation of C_a then has less influence on C_{k1}'. If we make $C_b = 100$ pF for instance, and $C_{k1} = 12$ pF, then:

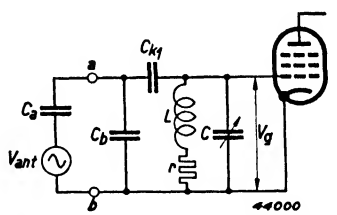

Fig. 34. Capacitive aerial coupling with ballast capacitor C_b.

when $C_a = 50$ pF:

$$C_{k1}' = \frac{(50 + 100)\,12}{50 + 100 + 12} = 11.11 \text{ pF};$$

when $C_a = 200$ pF:

$$C_{k1}' = \frac{(200 + 100)\,12}{200 + 100 + 12} = 11.53 \text{ pF};$$

when $C_a = 1500$ pF:

$$C_{k1}' = \frac{(1500 + 100)\,12}{1500 + 100 + 12} = 11.91 \text{ pF}.$$

The receiver being aligned with $C_a = 200$ pF, the greatest capacitance change that can occur in the aerial circuit is

$$\Delta C = 11.53 - 11.11 = 0.42 \text{ pF}.$$

The magnification is in this case:

$$A = \frac{C_a}{C_a + C_b} \cdot \frac{C_{k_1}'}{C + C_{k_1}'} \cdot Q. \quad \ldots\ldots\ldots \quad \text{(I D 46)}$$

Consequently at the lower end of the waveband ($C_{min} = 50$ pF)

$$A = \frac{200}{200 + 100} \cdot \frac{11.53}{50 + 11.53} \cdot 100 = 12.5.$$

(b) *Inductive coupling* (fig. 31)

With this method of coupling, too, we may first distinguish the two limiting cases: that in which the aerial terminal is free and that in which it is earthed. If we represent the circuit by a tuning capacitance C, with an inductance L in one case and $L\,(1 - k^2)$ in the other, equation (I D 40) obviously takes the form:

$$\frac{\Delta L'}{L} = \frac{1 - (1 - k^2)}{1 - k^2} = \frac{k^2}{1 - k^2} = \sqrt{a^2 - 1} \cdot \frac{1}{Q} \quad \ldots\ldots\ldots \quad \text{(I D 47)}$$

From this we ascertain the quality of coil which is required for a given coupling k and a given permissible attenuation a.

Equation (I D 24) then indicates the magnification obtainable:

$$A = \frac{M}{L_k}\left(\frac{1}{1 - \omega_1^2/\omega^2}\right) Q \approx \frac{M}{L_k} \frac{1 - k^2}{k^2} \sqrt{a^2 - 1},$$

and as $M = k\sqrt{L_k L}$:

$$A \approx \frac{1}{k} \sqrt{\frac{L}{L_k}} \sqrt{a^2 - 1} \quad \ldots\ldots\ldots\ldots \quad \text{(I D 48)}$$

Suitable choice of k thus makes it possible to increase the permissible magnification to any degree, assuming we are in a position to provide a coil of the quality required by equation (I D 47).

It is useful to compare the inductive coupling with the circuit of fig. 34, in which the detuning effect of the aerial may be made as small as desired by suitable choice of C_b; in this case, too, the required magnification may be secured by correct choice of coil quality, though there are limits to the quality attainable in practice, and consequently to the magnifi-

cation also. Accordingly it is necessary also with inductive coupling to allow for the aerial capacitance varying over only a limited range, the required coupling factor k being fixed in relation to the attainable coil quality. As with the calculation of C' in the case of the capacitive coupling, the simplest course is to make use of the equivalent circuit of fig. 32. With a provisional value of u^2, i.e. of $k^2 L/L_k'$, C' alters by $\Delta C'$ when the aerial capacitance is, for example, increased from 200 to 1500 pF; that this change $\Delta C'$ is permissible must then be confirmed by calculation from equation (I D 40). As was indicated at the beginning of D § 4 (page 68), magnification is practically independent of wavelength when $\omega_1 \ll \omega$. In modern receivers uniform sensitivity is desirable, and the inductive circuit is preferable. Since ω_1 is easily affected by the aerial capacitance, it is important to ensure that it remains less than ω even when the receiver is connected to a very small aerial. Generally this is achieved by making the coil L_k resonant just at the upper end of the medium waveband, say between 600 and 700 metres. In most cases a capacitor must be shunted across the coil L_k. The addition of this capacitance C_b gives us the circuit of fig. 35.

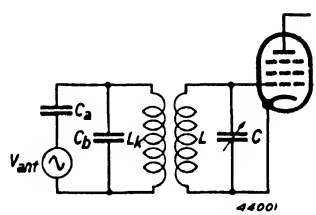

Fig. 35. Inductive aerial coupling with a capacitor C_b shunting the primary coil of the R.F.transformer, in order to lower the resonant frequency of the aerial circuit.

The primary resonance is then given by:

$$\omega_1^2 L_k (C_a + C_b) = 1,$$

and when making the calculation of detuning a primary capacitance of $(C_a + C_b)$ must be brought in.

The use of a large aerial with the circuit of fig. 35 results in the resonance frequency ω being low; when the receiver is working on medium waves it may fall within the long waveband; should ω coincide with the carrier frequency of a LW transmitter interference will occur. To avoid this trouble the tuned circuit formed by L_k and $(C_a + C_b)$ should be so heavily damped that its resonance curve is flat. Or the circuit may be modified so that the primary resonance is never shifted too far into the long waveband; this may be achieved by using a capacitor C_1 in series with the aerial, as well as a shunt capacitor C_2 across the coupling coil (see fig. 36).

To take a practical example, if with this circuit L_k is 800 μH, and C_1 and C_2 are respectively 200 and 125 pF, then L_k and C_2 resonate at about 600 metres. Short-circuiting aerial and earth terminals puts C_1 in parallel with C_2, and the resonance of L_k with $(C_1 + C_2)$ then falls at about 1000 metres. Thus no variation of the aerial capacitance can shift the resonance

frequency beyond these limits. If ω_1 lies close to the upper end of the waveband, magnification rises as this point is approached.

In order to obtain more uniform magnification, a combination of inductive and top-capacitance coupling is often employed (see fig. 37). As the capacitive coupling yields the greatest magnification at the lower end of the wave-

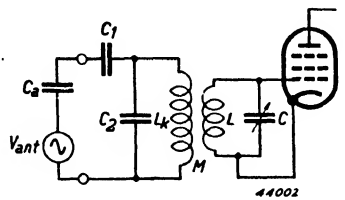

Fig. 36. Inductive aerial coupling, with a series capacitor C_1 to prevent the resonant frequency of the primary circuit falling within the long waveband if a large aerial is used.

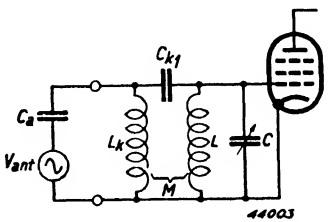

Fig. 37. Combined inductive and capacitive aerial coupling, designed to maintain uniform magnification over the waveband.

band, it is possible by judicious choice of L_k, M and C_{k1} to make the magnification very even.

Finally it is worth noting that when a band-pass filter precedes the first valve the aerial coupling may be tighter than when there is a single circuit, for the aerial detunes only the first circuit and detuning of one circuit of a filter has a less serious effect than detuning of a single circuit.

§ 7. Damping of the input circuit by the aerial

As has already been mentioned, the degree of coupling between aerial and tuned circuit is also limited on account of the damping imposed by the aerial. Apart from its capacitance, the aerial has also a certain resistance, which, if the coupling were too tight, would unduly impair the quality of the circuit. Under the heading of aerial resistance must be included not only the resistance of the copper conductor but also that of the receiver's earth lead and, especially, the resistance introduced by defective insulation of the aerial; furthermore the radiation-resistance must be taken into account. The resistance of an aerial can vary from about 20 Ω for a good installation with suitable earthing to about 300 Ω for a relatively poor specimen. This resistance must be regarded as being in series with the aerial capacitance C_a. In consequence of this damping, the magnification varies with the degree of aerial coupling not strictly according to the foregoing calculations, in which a constant value of Q was assumed. If it is desired to take aerial resistance into account it is best to adopt a figure of 25 ohms, the value customary in artificial aerials (see also fig. 38). In the capacitive coupling of fig. 28a in D § 2 the aerial resistance in series with C_a is first

converted to a resistance in parallel with C_a, using equation (I A 28). In fig. 29*b* this resistance, like the capacitance C_{k1}', shunts the tuned circuit, and by means of equation (I A 23) its effects may be computed in the form of a decrease of Q.

With inductive aerial coupling it is logical first to combine the aerial resistance and the coupling coil resistance to form a single resistance r_1. The primary Q, which has so far been neglected, then becomes:

$$Q_1 = \frac{\omega_1 L_k}{r_1} .$$

Equation (I B 10) is now written:

$$V_g = -V_{ant}\, C_a \omega_0^2 \frac{Q_1 Q_2 K \sqrt{L_k L}}{(1 + j\beta_1 Q_1)(1 + j\beta_2 Q_2) + Q_1 Q_2 K^2} \quad \ldots \quad \text{(I D 49)}$$

The frequency-dependent part of this equation is the denominator of the fraction, namely:

$$(1 + j\beta_1 Q_1)(1 + j\beta_2 Q_2) + Q_1 Q_2 K^2$$

Near resonance β_1 is large compared with β_2, and its variation with frequency will be relatively small. This leaves β_2 as the only variable. For the calculations of the selectivity, therefore, we may again, following the argument on page 69, regard the circuit as approximating to a single tuned circuit. This means that we should be able to recognise the form:

$$1 + j\,\beta\,Q$$

of (I A 9).

Division by the constant factor $(1 + j\beta_1 Q_1)$ yields:

$$1 + j\,\beta_2 Q_2 + \frac{K^2 Q_1 Q_2}{1 + j\beta_1 Q_1}$$

or approximately:

$$1 + j\,\beta_2 Q_2 + \frac{K^2 Q_1 Q_2 - j\,K^2 Q_1 Q_2 \beta_1 Q_1}{\beta_1^2 Q_1^2} =$$

$$= 1 + \frac{K^2 Q_2}{\beta_1^2 Q_1} + j\left(\beta_2 - \frac{K^2}{\beta_1}\right) Q_2$$

By a further division we rearrange the expression in the required form:

$$1 + j\left(\beta_2 - \frac{K^2}{\beta_1}\right) \frac{Q_2}{1 + \frac{K^2 Q_2}{\beta_1^2 Q_1}} .$$

It now appears that the coupling of the aerial circuit to the secondary cir-

cuit results in a variation of the detuning β_2 by an amount $\frac{K^2}{\beta_1}$ and in a decrease of the factor Q_2. The analogy may be continued further by imagining an equivalent increase Δr of the resistance in the secondary circuit. We then write:

$$\frac{1}{Q_{2tot}} = \frac{1 + \frac{K^2 Q_2}{\beta_1^2 Q_1}}{Q_2} = \frac{1}{Q_2} + \frac{K^2}{\beta_1^2}\frac{1}{Q_1} \quad \ldots \quad \text{(I D 50)}$$

or:

$$\frac{r_{tot}}{\omega_2 L} = \frac{r}{\omega_2 L} + \frac{K^2}{\beta_1^2}\frac{r_1}{\omega_1 L_k}.$$

As r_{tot} is composed of r and Δr:

$$\frac{\Delta r}{\omega_2 L} = \frac{K^2}{\beta_1^2}\frac{r_1}{\omega_1 L_k} = K^2 \frac{1}{(\omega/\omega_1 - \omega_1/\omega)^2}\frac{r_1}{\omega_1 L_k};$$

thus:

$$\Delta r = K^2 \frac{L}{L_k}\frac{\omega_2}{\omega}\frac{1}{(1 - \omega_1^2/\omega^2)} r_1.$$

As approximately $\omega = \omega_2$:

$$\Delta r = k^2 \frac{L}{L_k}\frac{1}{1 - \omega_1^2/\omega^2} r_1 \quad \ldots \quad \text{(I D 51)}$$

The series resistance r_1 is consequently transferred to the secondary circuit in the ratio $u^2 = k^2 L/L_k$. Furthermore the detuning factor already mentioned must be taken into account. Although calculation of the aerial damping may be required in special cases, it is clear that in most instances the aerial coupling needs to be so loose, for the reasons discussed in D § 6, that damping by the aerial ceases to be of much importance.

§ 8. Inductance of the aerial

In addition to capacitance and resistance, an aerial possesses a certain inductance; this is so small however that its effect becomes noticeable only at high frequencies. In the medium waveband it may cause an apparent increase of the aerial capacitance around 200 metres. On short waves, on the other hand, the inductance and capacitance of the aerial are likely to

lead to resonances at various frequencies, with the result that, depending on the wavelength of the received signal, the aerial has either a capacitive or an inductive impedance.

As aerial impedance is not a fixed quantity, it is customary when aligning receivers to use an impedance known as an artificial aerial. Formerly this consisted, for medium and long wavebands, of 200 pF, 20 μH and 25 Ω in series; on short waves a simple 400 Ω resistor satisfactorily represented the average impedance of the aerial at various frequencies. At present a combination of both is used, so that the required impedance for various wavebands is obtained without switching (see fig. 38).

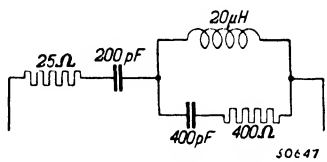

Fig. 38. Dummy aerial, suitable for use on short, medium and long wavebands.

§ 9. Influence of aerial coupling on the suppression of image frequencies in superheterodynes

We shall now consider what effect a particular method of aerial coupling has in suppressing frequencies differing widely from the resonant frequency.

This is of especial interest in the case of superheterodynes, for it is well known that a transmitter whose frequency differs from that of the received signal by twice the intermediate frequency can cause strong whistles (see also Chapter IV D § 4). The equations and curves which are generally used in calculating selectivity are all concerned with a narrow band each side of the resonant frequency and cannot, therefore, serve for ascertaining the measure in which image frequencies are suppressed. Although the requisite corrections are given in section A, it is usually possible, by inspection of the circuit diagram, to determine at once how much image suppression there will be. For frequencies much higher than the resonant frequency the reactance of the tuning coil L is considerably greater than that of the tuning capacitor C. It is immediately apparent on looking at fig. 29a that, in the case of top-capacitance coupling, very high frequencies are attenuated in the ratio $\frac{C_{k_1}'}{C + C_{k_1}'}$. As the magnification at the frequency of the desired transmission, given by equation (I D 4), is

$$A = \frac{C_{k_1}'}{C + C_{k_1}'} Q \quad \ldots\ldots\ldots\ldots\ldots \quad \text{(I D 4)}$$

the image frequency is suppressed in the ratio of about Q.

Low frequencies are suppressed much more strongly, since the reactance of L is very small compared with the reactance of C and C_{k_1}'. The resonance curve of this type of aerial coupling over a broad frequency band accordingly takes the form seen in fig. 39a. Capacitive coupling to the bottom of the tuned circuit, however, presents an entirely different resonance curve. As fig. 28c shows, with this circuit very low frequencies are attenuated only in the ratio $\frac{C_a}{C_a + C_{k_2} + C}$. The higher frequencies are suppressed much more strongly, as the reactance of C is so much smaller than that of L. The curve of this circuit therefore has the form indicated in fig. 39b.

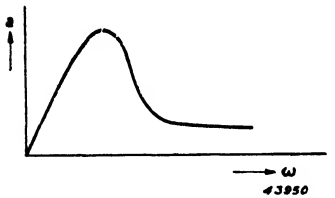

Fig. 39a. Resonance curve of the capacitive aerial top-coupling of fig. 28a.

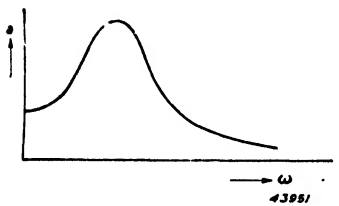

Fig. 39b. Resonance curve of the capacitive aerial bottom-coupling of fig. 28c.

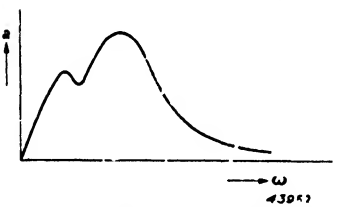

Fig. 39c. Resonance curve of the inductive aerial coupling of figs 28b, 28d and 31a.

For a band-pass filter coupling, and therefore also, following D § 4, for an inductive coupling, the exact equation (I B 8) shows that when $\omega = 0$ or when $\omega = \infty$ the output voltage approaches zero, since in both cases β_1 and β_2 are infinitely great. In the case of the "large-primary" coupling the resonance curve is in the form seen in fig. 39c, the smaller peak corresponding to the resonant frequency of the primary circuit. The circuits of figs 28b and 28d yield a curve similar to that of fig 39c, but with only one peak.

Compared with capacitive couplings, inductive aerial couplings thus have the notable advantage of giving more effective suppression of interfering frequencies on each side of the resonant frequency.

Although capacitive bottom-coupling is found on close examination to provide better suppression of higher frequencies, that is to say of image frequencies, this type of coupling is not often used, for, as was noted in D § 3, it is necessary also to insert a series condenser in other signal-frequency tuned circuits. A further drawback of this circuit is that low frequencies, such as a hum voltage induced in the aerial circuit by the mains, can easily reach the grid of the first valve and give rise to modulation hum (see chapter IV, page 309).

§ 10. Amplification in the R.F. valve

The simplest circuit for an R.F. valve is shown in fig. 40a. The valve can be regarded as a current-source $I_a = S.Vg$, shunted by R_i, the A.C.-resistance of the valve. Fig. 40a is thus equivalent to fig. 40b. The blocking capacitor

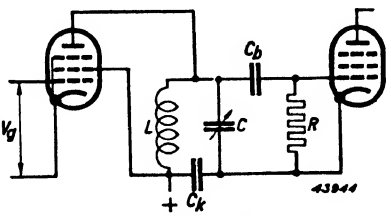

Fig. 40a. R.F. amplifying valve with a tuned anode circuit.

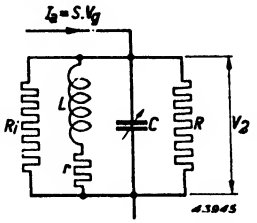

Fig. 40b. Equivalent circuit of fig. 40a.

C_b has been omitted for simplicity: this is quite permissible in view of its size. Similarly the capacitor C_k bridging the H.T. supply has been ignored. It is now apparent that in judging the gain and selectivity we have to reckon with the tuned circuit $L - r - C$, shunted by R_i and R. The calculation of the dynamic resistance Z_0 and the selectivity has been exhaustively treated in A § 3. For the dynamic resistance at resonance we may write:

$$Z_0 = \frac{L}{rC} /\!/ R_i /\!/ R.$$

The amplified voltage is then:

$$V_2 = S\ V_g\ Z_0 = S\ V_g \left(\frac{L}{rC} /\!/ R_i /\!/ R \right).$$

A practical disadvantage of the circuit of fig. 40a is that the H.T. voltage is applied across the variable capacitor, and the blocking capacitor C_b is therefore sometimes inserted in the tuned circuit in front of C. More often, however, the inductor L is double-wound and coupled to the anode inductively; the winding in the anode circuit can be of quite thin wire.
The blocking circuit consisting of C_b and R then becomes redundant and the second valve is connected directly across the secondary of the coil (fig. 23b).

Another solution is to supply the anode of the R.F. valve through a choke, with a capacitive coupling to the top of the tuned circuit. Neither of these modifications differs radically from the basic circuit of fig. 40b. In each of

the three cases the gain is determined chiefly by the impedance L/rC; as the latter varies strongly with C, amplification is smallest at the top of the waveband. This drawback has led to a search for a coupling equivalent to the aerial coupling of D § 4; that circuit differs from the arrangement seen in fig. 23b only in having a primary winding of higher inductance than the secondary, and additional capacitance shunting the primary. This capacitance generally consists, in the case of an R.F. coupling, of the valve and primary winding capacitances and is indicated in fig. 41 by C_p. The circuit is equivalent to that of fig. 31b, but instead of equation (I D 18) we have $I_a = S.V_g$. The further calculation need not be repeated; the final result, however, corresponding to equation (I D 24), is:

$$A = \left|\frac{V_2}{V_g}\right| = \frac{S.M}{\omega C_p L_k} Q \frac{\omega^2}{\omega^2 - \omega_1^2},$$

or:

$$A = \frac{S}{\omega C_p}. k \sqrt{\frac{L}{L_k}}. Q \frac{\omega^2}{\omega^2 - \omega_1^2} \quad \ldots\ldots\ldots \quad \text{(I D 52)}$$

If ω_1 has a sufficiently small value the last fraction is again fairly constant. As was observed earlier, Q is also fairly constant, and amplification thus varies in inverse proportion to ω.

For the circuit of fig. 40 the gain is approximately:

$$A = S \,.\, Z_0 = S \frac{L}{rC} = S\, Q\, \omega L \quad \ldots\ldots\ldots \quad \text{(I D 53)}$$

Here we have the factor ω as well as Q and consequently the amplification in this case is roughly proportional to ω. Neither of the two circuits, therefore, provides the desired constant gain.

The large-primary coupling of fig. 41 can, however, be advantageously combined with top-capacitance coupling as used in aerial circuits, since the trend of amplification with frequency is opposite in the two forms of coupling. A very small capacitance between the high-potential ends of the two inductors provides adequate compensation. The direction of the respective windings must be such that the two couplings assist one another. The coupling capacitance is often obtained by connecting a single open-circuited turn to the top of the secondary coil, the correct spacing being ascertained experimentally.

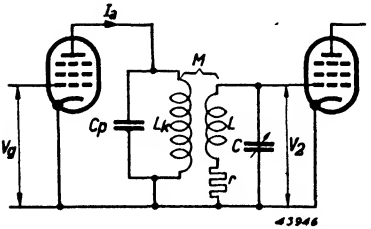

Fig. 41. R.F. amplifying valve with a high-inductance coupling to the following tuned circuit (the so-called "large-primary" coupling).

The choice of coupling coil depends on the following considerations:
In order to keep the last fraction in equation (I D 52) reasonably constant, the natural frequency ω_1 of the coupling coil should not be too high; on the other hand it must not be too low, otherwise the dependent product $C_p \cdot L_k$ results in reduced amplification. The frequency ω_1 may be about half the lowest value of ω.

The product $C_p \,.\, L_k$ being fixed, it remains to ascertain the coupling.
If we write:

$$M = k \sqrt{L_k L},$$

then to secure high gain it is important to make the coupling factor k as large as possible; the coils should therefore be wound very close together. Further, L_k can be made large by keeping the parallel capacitance as low as possible; a limit is set, however, by the necessity to ensure that possible variations of wiring and valve capacitances do not have too much effect on C_p.
High R.F. amplification is less important in modern superheterodynes than in the straight receivers formerly used; it is in most cases limited by the occurrence of distortion in the mixing valve. Accordingly, in a superheterodyne the primary capacitance may be made large, the required amplification being obtained by appropriate choice of coupling.
The influence of the primary circuit on the tuning of the secondary may be calculated as in D § 6 for the inductive aerial coupling, since the circuits are analogous. The anode capacitance now replaces the aerial capacitance. It is also of interest to know how far the A.C. resistance of the valve, R_i, affects the total damping. In this case the primary damping, hitherto ignored, must be taken into consideration, in accordance with equation (IB40).

$$\frac{1}{Q_1} = \frac{1}{R_i\, \omega_1\, C_p} \left(\frac{\omega_1}{\omega}\right)^2,$$

as was calculated in B § 9.

Equation (I D 50) relating to the inductive aerial coupling holds also for this comparable case:

$$\Delta \frac{1}{Q_2} = \frac{K^2}{\beta_1^2} \frac{1}{Q_1};$$

therefore

$$\Delta r = \omega_2 L \frac{\omega^2}{\omega_1 \omega_2} k^2 \frac{1}{(\omega/\omega_1 - \omega_1/\omega)^2} \frac{1}{R_i\, \omega_1\, C_p} \frac{\omega_1^2}{\omega^2}.$$

As $\omega_1^2 L_k C_p = 1$, we get:

$$\Delta r = k^2 \frac{L}{L_k} \frac{1}{(1 - \omega_1^2/\omega^2)^2} \cdot \frac{1}{R_i \omega_1^2 C_p^2} \quad . \quad . \quad . \quad . \quad \text{(I D 54)}$$

The R.F. gain required is not usually large, and the ratio $k^2 L/L_k$ may therefore be made fairly small; consequently the increase of resistance Δr is not great. The quantity $(1 - \omega_1^2/\omega^2)$ should not become too small at the end of the waveband, and it is therefore important to make the natural frequency ω_1 sufficiently low.

E. I.F. Amplification

Introduction

The essential advantage of the superheterodyne receiver is that the selective amplification takes place at only one frequency; by simple means, namely fixed tuned band-pass filters, it therefore becomes possible to achieve very satisfactory resonance characteristics. Single-circuit couplings are not often employed in I.F. amplifiers; occasionally they are used in small cheap superhets, with reaction to counteract damping. General practice is to have two band-pass filters each of two tuned circuits, i.e. four circuits in all. The inductively-coupled filter is most commonly employed, because it calls for no additional components.

When the intermediate frequency is about 125 kc/s the coil quality Q amounts to between 40 and 50, with average materials; at a frequency around 475 kc/s Q is approximately 150—200. With such coil quality, resonance curves can be obtained which satisfy most requirements. Data for calculating the response curves and magnification of band-pass filters will be found in section B of this chapter.

For high-grade receivers costing more than the minimum, two ways of improving the I.F. stages are open: to employ more than four circuits and thus obtain a better overall resonance curve, and to introduce variable-selectivity band-pass filters so that the response may be adjusted in accordance with the circumstances.

These possibilities will be examined in the following paragraphs.

§ 1. Superheterodyne receivers with more than four I.F. circuits

In practice a satisfactory compromise between output quality and selectivity is obtained with a fixed-bandwidth receiver when the R.F. and I.F. stages pass a level band of about 6—8 kc/s and strongly suppress frequencies lying outside that band. We attempt to achieve such a performance by using band-pass filters, though we obtain, of course, only an approximation to the ideal.

The commonest type of receiver is a superheterodyne with two I.F. band-pass filters separated by a pentode amplifying valve.

Fig. 42 shows the resonance curve for such a combination of two filters,

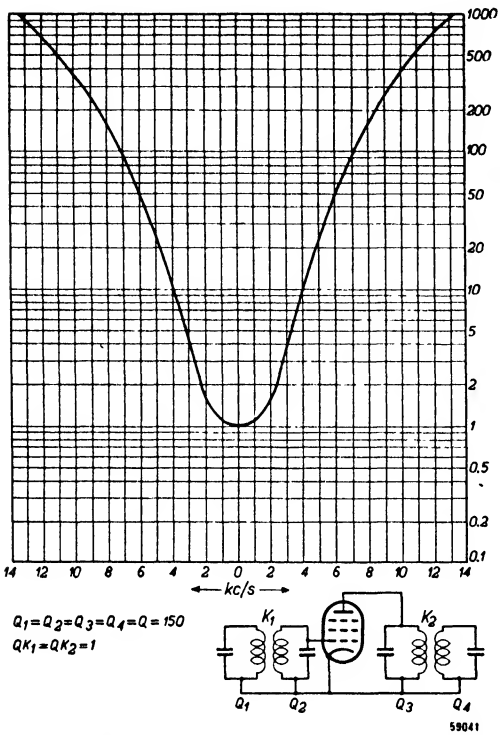

Fig. 42. Resonance curve for a pair of band-pass filters coupled by a valve; Q = 150.

the effect of the signal-frequency circuits on the overall response being ignored. It is assumed that all the circuits have the same factor $Q = 150$, that the intermediate frequency is 475 kc/s and that the coupling in both filters is critical. As the diagram reveals, the response over the pass-band is not uniform, while the suppression of frequencies outside the band is far from complete. A more uniform response over the desired frequency band can be obtained by making the coupling in one or both band-pass filters more than critical, but the discrimination against frequencies lying outside the required band is then not so good.

Conversely, looser coupling in the filters improves the suppression of neighbouring frequencies, but results in less uniform transmission of the desired band.

Thus although the use of four I.F. circuits represents an important step towards the attainment of the ideal rectangular resonance curve, their performance is still not good enough for a really high-grade receiver. Two courses are now open:

The first method by which the ideal may be more closely approached is to increase the number of tuned circuits; this naturally requires more material.

The second method is to limit the I.F. circuits to four, varying the coupling to meet prevailing conditions. Thus when good reproduction is desired, and interference is absent, the coupling is tightened, and when interfering transmitters necessitate increased selectivity, even at the cost of poorer reproduction, the coupling is loosened. This method calls for little extra material but has the drawback of demanding greater care in the handling of the receiver.

We shall first consider the use of more than four I.F. circuits.

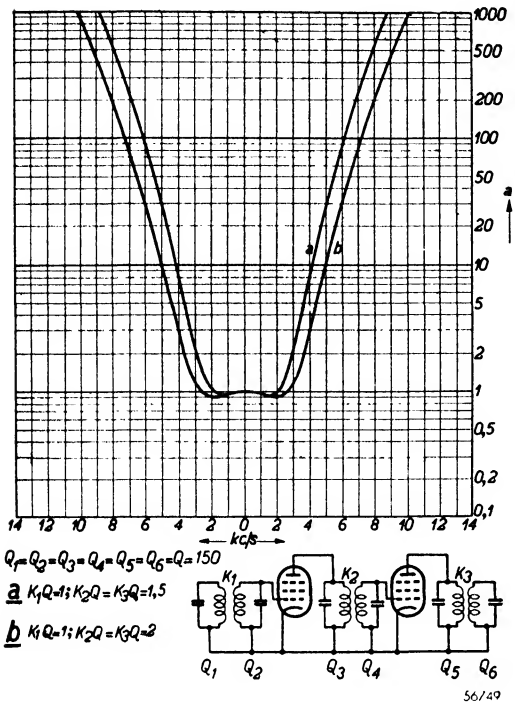

Fig. 43. Resonance curves for a combination of three two-circuit band-pass filters; Q = 150.
(a) $QK_1 = 1$; $QK_2 = QK_3 = 1.5$;
(b) $QK_1 = 1$; $QK_2 = QK_3 = 2$.

It is important to know how best to include the additional tuned circuits in the receiver. If six circuits are to be used, for example, they may be arranged as three I.F. transformers, each containing two tuned circuits; the three transformers have to be coupled by valves, and this arrangement consequently requires an additional I.F. amplifying valve. Another solution is to employ only two band-pass filters, each of three tuned circuits; in that case no additional valve is needed. The respective properties of these alternative arrangements will now be compared.

In fig. 43 two resonance curves, obtainable with a combination of three two-circuit I.F. band-pass filters, are reproduced; they refer to an intermediate frequency of 475 kc/s, and a factor $Q = 150$ for all the I.F. circuits. One filter was critically coupled, and in the two others the coupling was over-critical; curve *a* relates to a coupling of $QK = 1.5$ in the second and third filters, curve *b* to a coupling of $QK = 2$. These curves were drawn with the aid of the band-pass filter equations derived in section B. Comparison of figs 42 and 43 shows that in the second case the response obtained meets the requirements of selectivity and high-note reproduction much more satisfactorily.

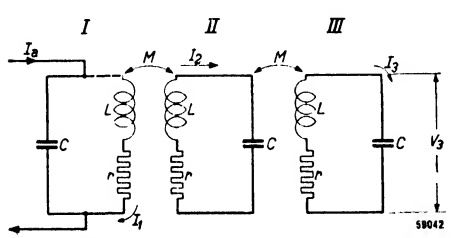

Fig. 44. Basic arrangement of three-circuit band-pass filter.

The equation for the resonance curve of a three-circuit band-pass filter may be derived as follows: It is assumed that the first circuit is coupled to the second, and the

second to the third, but that no coupling exists between the first and third circuits; this is roughly true when the coil of the second circuit is mounted between those of the other circuits. In the first tuned circuit an alternating current I_a flows (see fig. 44). If the three circuits are identical, and if the coupling between circuits I and II is as tight as that between II and III, it follows from the voltage equilibrium that:

$$\left.\begin{aligned} I_1\left(r + j\omega L + \frac{1}{j\omega C}\right) + I_2 j\omega M &= I_a \frac{1}{j\omega C} \\ I_2\left(r + j\omega L + \frac{1}{j\omega C}\right) + I_1 j\omega M + I_3 j\omega M &= 0 \\ I_3\left(r + j\omega L + \frac{1}{j\omega C}\right) + I_2 j\omega M &= 0 \end{aligned}\right\} . \quad \text{(I E 1)}$$

Eliminating I_1 and I_2, we get:

$$I_3 = \frac{\omega^2 M^2 \frac{1}{j\omega C}}{\left(r + j\omega L + \frac{1}{j\omega C}\right)\left\{2\omega^2 M^2 + \left(r + j\omega L + \frac{1}{j\omega C}\right)^2\right\}} I_a . \quad \text{(I E 2)}$$

The voltage across the last circuit is:

$$V_3 = I_3 \frac{1}{j\omega C} =$$

$$= \frac{M^2/C^2}{\left(r + j\omega L + \frac{1}{j\omega C}\right)\left\{2\omega^2 M^2 + \left(r + j\omega L + \frac{1}{j\omega C}\right)^2\right\}} I_a \quad \text{(I E 3)}$$

Substituting

$$\omega_0 = \frac{1}{\sqrt{L\,C}},$$

$$\beta = \frac{\omega}{\omega_0} - \frac{\omega_0}{\omega},$$

$$Q = \frac{\omega_0 L}{r},$$

$$K = \frac{\omega}{\omega_0}\frac{M}{L},$$

we get:

$$V_3 = \frac{M^2/C^2}{r^3(1 + j\beta Q)\{(1 + j\beta Q)^2 + 2Q^2K^2\}} I_a . \quad \text{(I E 4)}$$

The modulus of this voltage is:

$$V_3 = \frac{M^2/C^2}{r^3 \sqrt{(2\,Q^2K^2 - \beta^2Q^2 + 3)^2\,\beta^2Q^2 + (1 + 2\,Q^2K^2 - 3\,\beta^2Q^2)^2}}\,I_a \quad \ldots\ldots \text{(I E 5)}$$

At resonance ($\beta = 0$) this becomes:

$$V_{30} = \frac{M^2/C^2}{r^3\,(1 + 2\,Q^2K^2)}\,I_a \quad \ldots\ldots\ldots\ldots \text{(I E 6)}$$

Off resonance the attenuation in relation to the voltage V_{30} is therefore:

$$a = \left|\frac{V_{30}}{V_3}\right| = \frac{\sqrt{(2\,Q^2K^2 - \beta^2Q^2 + 3)^2\beta^2Q^2 + (1 + 2\,Q^2K^2 - 3\,\beta^2Q^2)^2}}{1 + 2\,Q^2K^2} \quad \ldots\ldots \text{(I E 7)}$$

With the help of this last equation the curves of fig. 45 may now be drawn. They refer to a combination of two three-circuit band-pass filters, separated by a pentode, the intermediate frequency being again 475 kc/s and the factor $Q = 150$. The inter-circuit coupling is assumed to be the same in both filters; in the case of curve *a*, $QK = 1$. The resonance curve obtained certainly has steep sides, but there is no flat top; tightening the coupling so that, for example, $QK = 2$, yields curve *b*: again the top is not flat *.

Comparison of figs 43 and 45 makes clear the great advantage of using three two-circuit band-pass filters and an additional I.F. amplifying

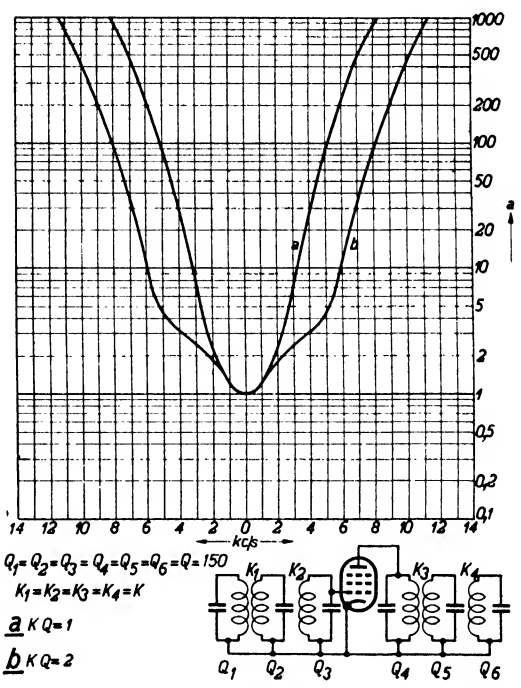

Fig. 45. Resonance curves for a combination of two three-circuit band-pass filters coupled by a pentode; the quality Q = 150, and the inter-circuit coupling in both filters is (a) QK = 1 and (b) QK = 2.

* It can be shown mathematically that a resonance curve with three peaks of even height would be obtained if the damping of the second circuit in each filter were zero ($Q_2 = Q_4 = \infty$). Of course this is unrealisable in practice. The desired form of curve may be obtained, however, by detuning the first and third circuits symmetrically in relation to the second tuned circuit; trimming then becomes very tricky.

valve: much better transmission of the sidebands, combined with strong suppression of adjacent-channel interference.

A further advantage of the circuit of fig. 43 is that the gain per stage may be much smaller; consequently the three I.F. transformers can be of lower dynamic resistance (with small inductance and large capacitance). Thus the damping effect of resistance shunting the tuned circuits is greatly reduced, and it is easier to obtain good circuit quality, while the use of a larger tuning capacitance in the I.F. transformers lessens the effect of small capacitance variations, due for instance to replacing valves, on the tuning of the circuits. If the amplification in a superheterodyne with a single I.F. valve is A in both the mixer and I.F. stages, then in a receiver with two I.F. valves the stage-gain need be only $A' = \sqrt[3]{A^2}$ for the same overall amplification.

For example if $A = 100$, then $A' = 22$. The dynamic resistance of the I.F. circuits in the second case can therefore be more than four times smaller; keeping the factor Q unchanged, this means a fourfold reduction of inductance and a fourfold increase of capacitance.

Naturally when using an additional I.F. valve it is not necessary to reduce the stage-gain so drastically that the overall amplification is no greater than without the extra valve. An incidental benefit of the arrangement is then that the receiver has higher sensitivity.

By comparison with that obtained with a two-circuit band-pass filter the gain with a three-circuit filter is less *; to avoid reducing the sensitivity of the receiver it is therefore necessary to raise the dynamic resistance of the I.F. circuits. Parallel resistances in that case exert a larger influence on selectivity.

§ 2. Band-pass filters with variable coupling

As has already been remarked in the introduction to this chapter, when receiving a weak transmission it is often essential that the bandwidth be quite small, in order to prevent interference by stronger neighbouring stations. When receiving a strong local transmission, on the other hand, greater bandwidth in the R.F. and I.F. stages is allowable, and good reproduction can then be obtained. Further, a moderately strong transmission may be subject to little interference during daylight, so that wide-band reception is practicable, whereas during darkness, when distant stations come in more strongly, it may be essential to reduce the bandwidth in order to suppress interference.

* The IF gain with an IF valve of slope S and with circuit dynamic resistance of Z is, for the case of curve 45a ($QK = 1$), equal to $1/3\ SZ$; for a critically-coupled two-circuit band-pass filter it is equal to $1/2\ SZ$.

Consequently if the best possible quality of reproduction is to be obtained in varying circumstances with a single receiver, it is essential to provide means of suiting the accepted frequency-band to the prevailing conditions; the bandwidth ought therefore to be adjustable, and for preference continuously variable.

A special case which may be considered in conclusion is that of a transmission varying in strength within wide limits, on account of fading. Interference from a nearby station with the desired signal will then vary a good deal over a period, and it is accordingly desirable that the bandwidth should be automatically regulated by the strength of the wanted carrier.

Both manual adjustment according to the whim of the listener and control by automatic means will be considered exhaustively.

In practice the bandwidth is varied by only one method: alteration of the resonance curve of one or more band-pass filters. The first requirement is that such alteration shall not affect amplification unduly, though the permissible variation of I.F. gain is not as limited as might be thought on superficial consideration.

The operation of the AVC (see chapter X) largely compensates for any change in the I.F. amplification, and in most receivers a twofold variation of gain is quite permissible. Next we shall examine various ways of modifying the resonance curve and ascertain the extent to which amplification is affected.

There are, in the case of a band-pass filter, three basic methods:

(*a*) by altering the coupling between the circuits;

(b) by altering the Q of the circuits;

(c) by altering the tuning of the circuits.

Each of these methods will be considered in detail. First we shall deal with a single band-pass filter and later with the I.F. amplifier as a whole.

§ 3. Variation of the inter-circuit coupling of a band-pass filter

If the Q and the tuning of both circuits are kept constant, then the variation of gain and bandwidth with change of coupling factor K can be read from fig. 17. Taking as bandwidth the band lying between the frequencies at which $a \leqslant 10$, then it is clear from fig. 17 that a change in the product QK from 0.7 to 2 alters the width of the I.F. band in the ratio of 1 : 2. The greatest variation of the I.F. amplification which occurs is seen from fig. 13 to be $0.5 : 0.4 = 1.25 : 1$; this is almost always admissible. Alteration of the inter-circuit coupling is the most usual method of controlling the bandwidth. Generally the two I.F. tuned circuits are coupled inductively and the coupling is varied by altering the distance between the inductors. This

method lends itself well to continuous adjustment; it has the further advantage of not affecting the tuning, and in consequence the circuit remains simple. Other methods of adjusting the coupling often have the drawback that incidental detuning of the circuits must be compensated and are therefore unsuitable for a continuously-variable band-pass filter. Fig. 46 shows, for example, the basic circuit of a filter coupled by a combination of top- and bottom-capacitance. Were the circuits coupled only by bottom capacitance, and the coupling varied by altering C_{k_2}, the tuning of the circuits would be disturbed, for the tuning capacitances consist respectively of C_1 and C_{k_2} in series, and C_2 and C_{k_2} in series.

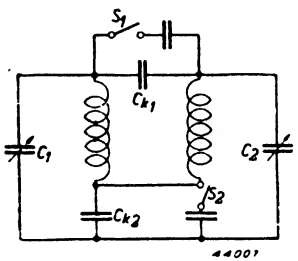

Fig. 46. Band-pass filter with combined top- and bottom-capacitive coupling.

To compensate for this detuning, top-capacitance coupling may be included as well and arranged so that when C_{k_2} is increased (by closing S_2) C_{k_1} is simultaneously reduced (by opening S_1). Both circuit changes result in looser coupling. Clearly this method is suitable only for varying the bandwidth in a single step.

As the inter-circuit coupling is over-critical when the filter is adjusted to pass a wide band, the resonance curve shows double humps; the effect of these peaks is however not great, since the high modulation frequencies, although accentuated by the filter, usually become weakened elsewhere in the receiver.

But if it is desired to make the overall resonance curve of the set as nearly flat-topped as possible, the twin humps of the band-pass filter curve may in large degree be compensated by giving the curve of other tuned circuits a complementary shape. This point will be dealt with further when the design of the I.F. amplifier as a whole is discussed.

§ 4. Variation of the Q-factor of band-pass filter circuits

Increasing the losses in a single circuit results, as is well-known, in a reduction of selectivity and thus also in an increase of the bandwidth accepted; at the same time the amplification obtainable declines. This method is less suitable for bandwidth control: instead of the top of the resonance curve broadening, as in fig. 17, and the steepness of the sides remaining nearly the same at all adjustments, the resonance curve as a whole takes on a flatter shape. Discrimination against frequencies several channels away from the wanted transmission thus deteriorates, whereas the object of adjustable bandwidth is only to broaden the top of the resonance curve, leaving the suppression of remote frequencies unimpaired.

A band-pass filter behaves rather differently. If the Q of one or both tuned circuits is lowered, the coupling remaining constant, the product QK diminishes. Fig. 17 then no longer shows clearly how the resonance curve alters with change of Q, for Q affects not only the parameter but also the scale of the abscissa. If now the curve is drawn with a constant abscissa scale (as in the following example) it becomes apparent that, in spite of Q_1 or Q_2 having a lower value, the peak of the curve is narrower. Simultaneously, however, the sides become less steep. Thus the suppression of stations on remote frequencies is not as good with the narrow-band adjustment (corresponding to a low value of Q_1 or Q_2) as with the wide-band adjustment: suppression of an adjacent-channel transmission is obtained at the cost of lower selectivity with regard to signals far from resonance. This last feature does not necessarily make the system valueless, however.

We shall now show what results are obtained by damping one of the tuned circuits of a band-pass filter.

Let the quality factor of both circuits of a filter be Q_0, so that $Q_1 = Q_2 = Q_0$. The quality of one circuit, for example Q_1, is kept constant and that of the other circuit is decreased n times. In order to prevent the resonance curve being too sharp at a small value of QK, the coupling is made appreciably over-critical for the original Q, i.e. when $n = 1$. In this example we take $Q_0^2K^2 = 10$. With the help of equation (I B 34) it is now easy to construct the curve corresponding to $n = 1$. (In fig. 17 this curve is lacking.) The detuning is expressed as βQ_0 (see fig. 46, $n = 1$).
As, at full damping, Q_1 and Q_2 are intentionally made very different, it is logical to use the reasoning of B § 8 once again. The average damping is accordingly:

$$\delta = \frac{\delta_1 + \delta_2}{2} = \frac{\delta_0 + n\,\delta_0}{2} = \delta_0 \frac{n+1}{2}$$

or:

$$Q = Q_0 \frac{2}{n+1} \quad \ldots\ldots\ldots\ldots\ldots\ldots \quad \text{(I E 8)}$$

Simultaneously with the increase of damping an apparent reduction of coupling takes place, as indicated by equation (I B 37):

$$K'^2 = K^2 - \varepsilon^2, \quad \ldots\ldots\ldots\ldots\ldots \quad \text{(I B 37)}$$

in which, from equation (I B 38):

$$\varepsilon = \frac{\delta_2 - \delta_1}{2} = \frac{n-1}{2}\,\delta_0 = \frac{n-1}{2}\,\frac{1}{Q_0} \quad \ldots\ldots \quad \text{(I E 9)}$$

As an example the resonance curve for $n = 4$ may be calculated. First it is necessary to know the new relative coupling QK'. This is derived from equations (I B 37) and (I E 9):

$$Q_0^2K'^2 = Q_0^2K^2 - \varepsilon^2Q_0^2 = Q_0^2K^2 - \frac{(n-1)^2}{4} .$$

Substituting from (I E 8) gives:

$$Q^2K'^2 = Q_0^2K'^2\frac{4}{(n+1)^2} = Q_0^2K^2\frac{4}{(n+1)^2} - \frac{(n-1)^2}{(n+1)^2} \quad . \quad . \quad . \quad . \quad \text{(I E 10)}$$

With $Q_0^2K^2 = 10$ we find for $n = 4$:

$$Q^2K'^2 = 10 \times \frac{4}{25} - \frac{9}{25} = \frac{31}{25},$$

or

$$QK' = 1.1.$$

With this degree of damping the band-pass filter is thus about critically coupled, and the appropriate curve may be read from fig. 17. If, however, it is desired to compare this curve with the original resonance curve it has to be remembered that the measure of detuning βQ must be changed to βQ_0. Should it be found in fig. 17 that $a = 10$ when $\beta Q = 4.5$, then in fig. 47 this value of a holds when $\beta Q_0 = 11$, as the average Q is decreased 2.5 times, for equation (I E 8) shows that, when $n = 4$:

$$Q = Q_0\frac{2}{4+1} = \frac{Q_0}{2.5}.$$

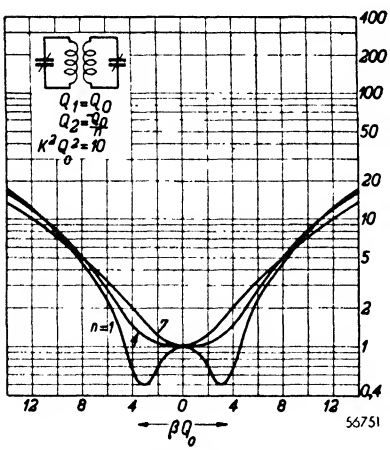

Fig. 47. Resonance curves for a band-pass filter in which the coupling is varied by altering the quality of one of the circuits.

Fig. 47 makes it plain that the curve has become narrower near the top, though at frequencies far removed from resonance the selectivity is much worse. When n is about 7 the relative coupling QK' becomes zero. The curve may again be derived from fig. 17. As drawn in fig. 47 however, with βQ_0 as abscissa, its sides appear still less steep than those of the curve for $n = 4$.

When using this method we have to ensure that the selectivity for frequencies remote from resonance still remains satisfactory when the filter is

adjusted for narrow-band working (i.e. small value of Q_2). This will usually require a greater number of signal-frequency circuits.

The effect of bandwidth adjustment on amplification remains to be considered. For the calculation of the gain we can use equation (I B 16) as a starting-point, notwithstanding the large variation of damping.
In this case therefore:

$$Q = \sqrt{Q_1 Q_2} = \sqrt{Q_0 \cdot Q_0/n} = \frac{Q_0}{\sqrt{n}}.$$

If now we denote the dynamic resistance of the two circuits at resonance and with adjustment to maximum bandwidth ($n = 1$) by Z_0, then $Z_1 = Z_0$, and, with adjustment to minimum bandwidth, $Z_2 = Z_0/n$. The gain is then, from equation (I B 16):

$$A = \left| \frac{V_2}{V_g} \right| = S \frac{\dfrac{Q_0 K}{\sqrt{n}}}{1 + \dfrac{Q_0^2 K^2}{n}} \frac{Z_0}{\sqrt{n}},$$

or

$$A = S \frac{Q_0 K}{n + Q_0^2 K^2} Z_0 \quad \ldots \quad \text{(I E 12)}$$

In our example $Q_0^2 K^2$ was equal to 10, so that equation (I E 12) becomes:

$$A = S \frac{\sqrt{10}}{n + 10} Z_0 \quad \ldots \quad \text{(I E 13)}$$

The term $\dfrac{\sqrt{10}}{n + 10}$ which appears in this equation is in fig. 48 shown as a function of n; this graph indicates the relative amplification obtainable with either a band-pass filter, or a single circuit of which the dynamic resistance at resonance is Z_0. When n varies from 1 to 10, gain declines in the ratio of about 1 : 2; this result is thus less favourable than that obtained with variable coupling.
Closer consideration of the equation concerned shows that fig. 47 holds

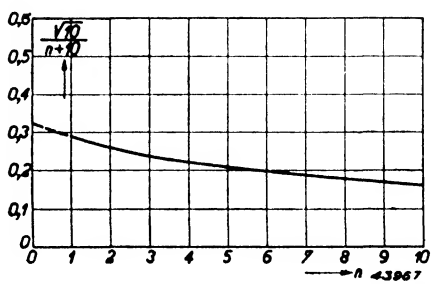

Fig. 48. The term $\dfrac{\sqrt{10}}{n + 10}$ from equation (I E 13), as a function of n.

good not only for the case of a constant Q_1 and a decreasing Q_2, but also for the case in which Q_1 is lowered, Q_2 remaining fixed. Another possibility of course is to vary the quality of both tuned circuits simultaneously. The variations of bandwidth and amplification would with such an arrangement be roughly similar to those indicated in fig. 47 and there is consequently no point in considering it further.

The great advantage of bandwidth-control by variation of the quality is that it can easily be achieved without mechanical devices. One method of varying Q_1 and Q_2, for example, is to arrange for the circuit concerned to be damped by the AC-resistance of a parallel-connected valve, and to control this A.C. resistance by adjusting the working voltages of the valve. An additional valve for damping-control only may be connected across one or more I.F. circuits, but it is also possible to alter the A.C. resistance of the I.F. amplifying valve by varying the voltage applied to the suppressor grid. As an example, the A.C. resistance of the EF 22 pentode may be varied from 1.2 to 0.2 MΩ by increasing the negative bias on the third grid from 0 to -33 V, the slope nevertheless remaining almost constant (see fig. 49). This purely electrical method is clearly exceptionally suitable for automatic bandwidth control. A further discussion of automatic controls will be found in § 13.

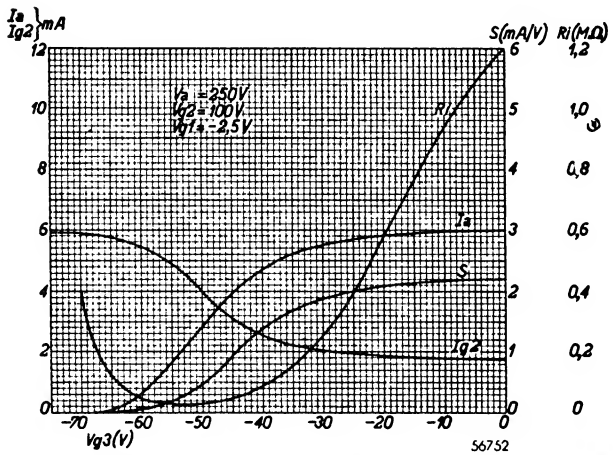

Fig. 49. Anode current, screen-grid current, slope and AC resistance as a function of suppressor-grid voltage, for the EF 22 pentode.

§ 5. Variation of the tuning of band-pass filter circuits

If the two circuits of a band-pass filter are slightly detuned in opposite directions a broadening of the resonance curve takes place. As is shown by the calculation in B § 10, the curve then acquires the same shape as that of a filter with the same damping but tighter coupling:

$$K'^2 = K^2 + \beta_v^2 \quad \ldots\ldots\ldots\ldots \quad (I,B\ 42)$$

in which β_v represents half the difference between the relative detunings of the two circuits, namely:

$$\beta_v = \frac{\beta_1 - \beta_2}{2} \quad \ldots\ldots\ldots \text{[see equation (I A 37)]}$$

For the determination of the form of the resonance curve a symmetrical detuning of the circuits may therefore be converted directly into an increase of K, but in ascertaining the trend of amplification such a conversion is not possible, as will be realised on closer examination of equation (I B 41). When the alternating current I_a is supplied by an I.F. pentode of slope S with a grid AC input of V_g, then $I_a = S \times V_g$, and from equation (I B 41) it follows that I.F. gain is:

$$A = \left|\frac{V_{2res}}{Vg}\right| = S\frac{\omega_0 Q^2 K \sqrt{L_1 L_2}}{1 + Q^2 K'^2} = S\frac{QK}{1 + Q^2K'^2}Z \quad \text{(I E 14)}$$

For this equation there has been substituted:

$$Z = \sqrt{Z_1 Z_2} = \sqrt{\frac{L_1}{r_1 C_1}\frac{L_2}{r_2 C_2}}.$$

Seeing that K' occurs only in the denominator of equation (I E 14), the detuning of the circuits (increase of K') has a greater influence on amplification than an increase of coupling (increase of K). This is made clear by the following example. We start with a critically-coupled filter in which both circuits have the same quality. The bandwidth is enlarged by symmetrical detuning of the circuits. The resonance curves which then arise are exactly the same as those reproduced in fig. 17 for an adjustable coupling. For clarity these are given once more in fig. 50. If we begin with a critically-coupled band-pass filter it is obviously impossible to obtain, by detuning, curves corresponding to $QK' < 1$; such curves have therefore been omitted from fig. 50.

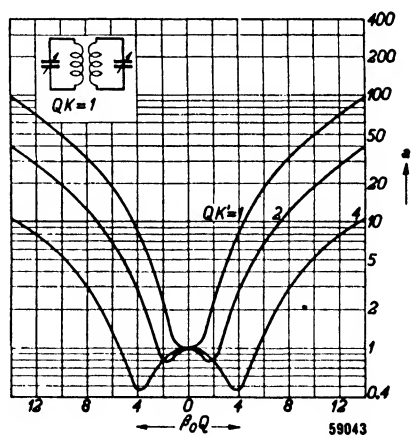

Fig. 50. Resonance curves for a band-pass filter in which the band-width is controlled by detuning the circuits.

In order to illustrate the trend of amplification with detuning fig. 51 shows the expression occurring in equation (I E 14):

$\frac{QK}{1 + Q^2 K'^2}$ as a function of QK'.

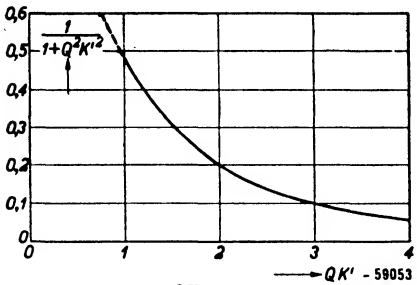

Fig. 51. The term $\frac{QK}{1+Q^2K'^2}$ from equation (I E 14) as a function of QK', for the case in which QK = 1.

As a critically-coupled filter is presupposed, $QK = 1$, and the expression represented in fig. 51 is accordingly:

$$\frac{1}{1 + Q^2K'^2}$$

It is now plain that altering QK' in the ratio 1 : 2 causes amplification to vary by a factor of 2.5, which is rather more than if the bandwidth were increased to the same extent by adjusting the coupling. Detuning of the circuits is of course achieved most simply by altering the tuning capacitors in opposite sense. The tuning of a circuit may, however, also be influenced by means of a valve; such a purely electrical method lends itself especially to automatic bandwidth control and will therefore be examined further in § 13.

§ 6. Combination of a fixed band-pass filter and a filter with variable coupling

It has already been observed, on page 94, that when the coupling in a variable band-pass filter is made over-critical, for wideband transmission, the resonance curve presents two humps. We endeavour, of course, to ensure, when the bandwidth is increased, that the top of the overall response curve of the receiver has as flat a form as possible, for then the modulation frequencies will be uniformly reproduced. This aim may be attained by giving the resonance curve of the remainder of the set such a shape that the trough in the band-pass filter curve is as nearly as possible filled in. One method is to combine an adjustable filter with a single circuit having half the Q of the filter-tuned circuits; the curves of such a combination are given in fig. 52.

The quality in both the circuits of the band-pass filter is denoted by Q_0, so that the quality of the single tuned circuit is $\frac{1}{2}\ Q_0$. The resonance curve of this single circuit is, consequent on equation (I A 10), given by:

$$a = \sqrt{1 + \tfrac{1}{4}\beta^2 Q_0^2} \quad \ldots\ldots\ldots\ldots \quad \text{(I E 15)}$$

Thus the total attenuation a_t in fig. 52 is the product of the respective values of a derived from equations (I B 34) and (I E 15). The figure shows that the resonance curves for $Q_0K > 1$ have a nearly flat top, and the double-hump effect which accompanies over-critical coupling is thus satisfactorily compensated.

In this respect the arrangement is ideal for adjustable-bandwidth receivers, but a drawback is that with only three I.F. tuned circuits, including one of rather poor quality, it is impossible to obtain sufficient selectivity. In general, two I.F. band-pass filters, each with tuned circuits of the highest quality, are essential. The next thing to be investigated, therefore, is the influence on the overall resonance curve of a variable-coupling band-pass filter when the latter is used in combination with a filter having fixed coupling.

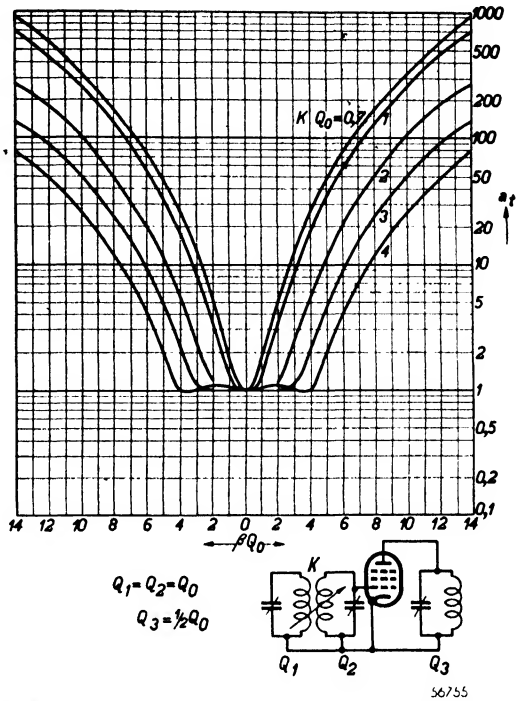

Fig. 52. Resonance curves for a combination of a variable band-pass filter and a single circuit, the quality of the latter being half that of the filter circuits.

In fig. 53 overall resonance curves are drawn for two band-pass filters of the same circuit quality, the coupling in one being critical and fixed, that in the other being variable. It is seen that at the wide-band adjustment the top of the curve has by no means the flatness found in fig. 52. The resonance curve of the fixed band-pass filter has much steeper sides than the single circuit employed in the preceding example, and in consequence the attenuation caused by the fixed filter far outweighs the effect of the humps in the curve of the variable-coupling band-pass filter.

Now it has been assumed that all the tuned circuits in the two filters had the same quality; in practice this is not so. The circuits of the final band-pass filter are almost always so loaded by the detector and AVC diodes that the Q of both tuned circuits is appreciably smaller than that of the circuits in the preceding filter. In fig. 54 we have the overall resonance curves of a combination of two band-pass filters, the first with adjustable coupling and the second with fixed, critical coupling and tuned circuits of half the Q-factor. (The question of whether the first or the second filter should be made variable will be gone into later.) We find that here a flat top is approached much more closely than in fig. 53.

Seeing that the curves of fig. 54 agree much better with the response ob-

tained in practice than those of fig. 53, we may conclude that varying the coupling between the circuits of the first filter is a satisfactory method of controlling bandwidth. If once more we regard the points at which $a_t = 10$ as marking the edges of the frequency-band passed, we find in fig. 54 that a bandwidth-variation of 1 : 2 occurs when the coupling in the first band-pass filter is altered from $Q_0K_1 = 0.7$ to $Q_0K_1 = 3$. The consequent change in amplification is of course the same as is indicated in fig. 13. The maximum variation of gain, when the coupling is altered within the above-mentioned limits, is in the ratio 0.5 : 0.3 = 1.67 : 1. Such a variation is usually permissible and is normally accommodated by the AVC.

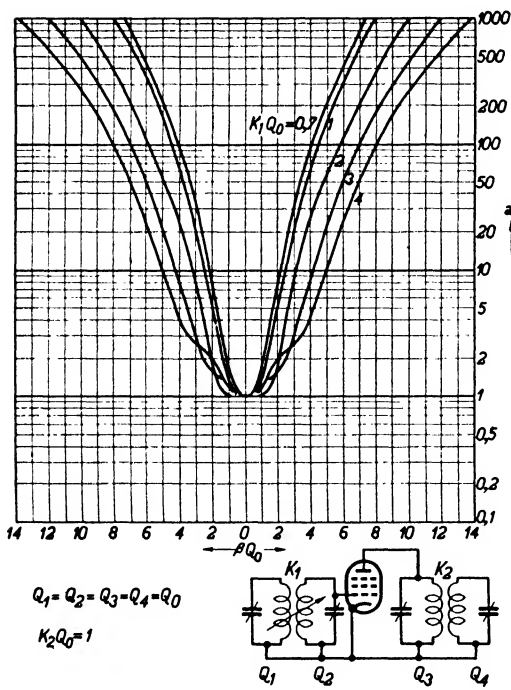

Fig. 53. Resonance curves for a pair of IF band-pass filters of the same circuit quality, one critically coupled and the other variable.

When, in special cases, the circuits of the second I.F. transformer are not damped by diodes, and a close approach to the ideal flat top of fig. 54 is nevertheless desired, the coupling in the fixed band-pass filter may be made over-critical. Fig. 55 illustrates the resonance curves yielded by a pair of I.F. band-pass filters, all the tuned circuits of which are of the same quality; one filter has variable coupling and the other fixed coupling of $Q_0K_2 = 2$. Admittedly the top of the curve is not as flat as in fig. 54, but it is a better shape than in fig. 53, when the fixed band-pass filter was critically coupled. It is obvious that tighter coupling of the circuits in the second filter must lead to lower selectivity, and comparison of figs 53 and 55 confirms this; the overcritical coupling in the second band-pass filter should, therefore, not be carried further than is absolutely necessary.

§ 7. Position of the variable I.F. band-pass filter

When a receiver includes two I.F. filters, one of which is to be adjustable, the question naturally arises as to which band-pass filter should be made

variable. It is now apparent that control of the first I.F. filter has considerable advantages over control of the second.

(1) As already noted, the Q values of the circuits of the second I.F. band-pass filter, being damped by the detector- and AVC-diodes, are appreciably lower than those of the tuned circuits comprising the first I.F. filter. Furthermore, owing to the lower quality of its circuits, the second band-pass filter has less influence on the overall resonance curve of the receiver than the first. A given variation of coupling in the second I.F. transformer thus has less effect on the overall response, and for a specified variation of bandwidth the change of coupling needs to be greater in the second filter than in the first. Minimum variation of coupling being desirable, control of bandwidth is generally effected at the first I.F. band-pass filter.

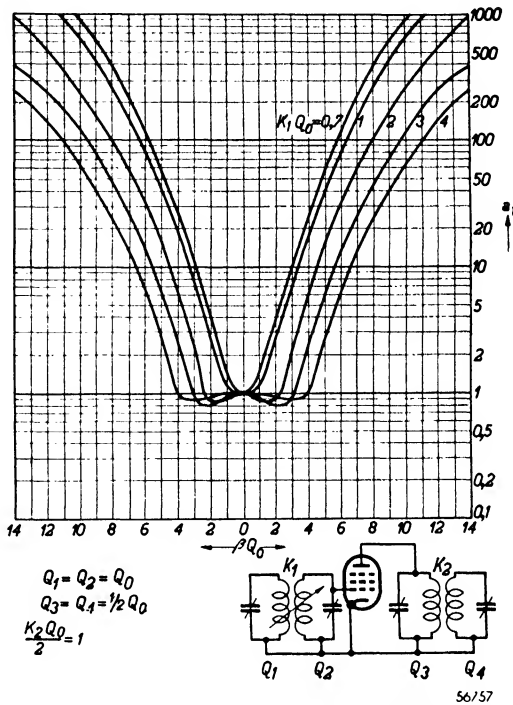

Fig. 54. Resonance curves for a pair of I.F. band-pass filters, the first variable and the second critically coupled; the quality of the circuits comprising the second filter is half that of the circuits in the first.

(2) In most present-day receivers the AF section is of low sensitivity. (For the advantages of low A.F. gain see Chapter V, Detection.) Either the output valve immediately follows the detector-diode or negative feedback is applied to the intermediate A.F. stage. Consequently the I.F. amplifying valve must be able to deliver a high signal-voltage to the detector-diode. The problems involved are dealt with exhaustively in Chapter XIII. It is there demonstrated that a specific impedance is required in the anode circuit of the I.F. amplifier for maximum input to the detector-diode. Now the magnitude of this anode-circuit impedance is closely dependent on the coupling between the tuned circuits comprising the I.F. transformer. If the dynamic

resistance of the primary circuit alone is denoted by Z_1, then the filter as a whole presents a dynamic resistance on the primary side of:

$$Z_p = Z_1 \frac{1}{1 + Q^2K^2} \quad \ldots\ldots\ldots\ldots \quad \text{(I E 16)}$$

This formula is derived from equation (I B 22) by substituting for V_2 the value given in (I B 16) and by assuming Q_1 equal to Q_2. Z_p is then the ratio V_1/I_a.

We see from this that Z_p becomes less as QK increases, i.e. as the coupling becomes tighter and the bandwidth greater. Since, in general, wide-band working is resorted to when the signal is strong, and when, as a result, overloading of the I.F. valve is likely to occur, it is essential in designing a receiver to allow for considerable variation of the load in the I.F. amplifier anode circuit. Experience has shown that serious difficulties can arise which are not encountered if, instead, the first I.F. transformer is made adjustable. In the mixer stage the I.F. voltages are much smaller and overloading of the frequency changer is less to be feared.

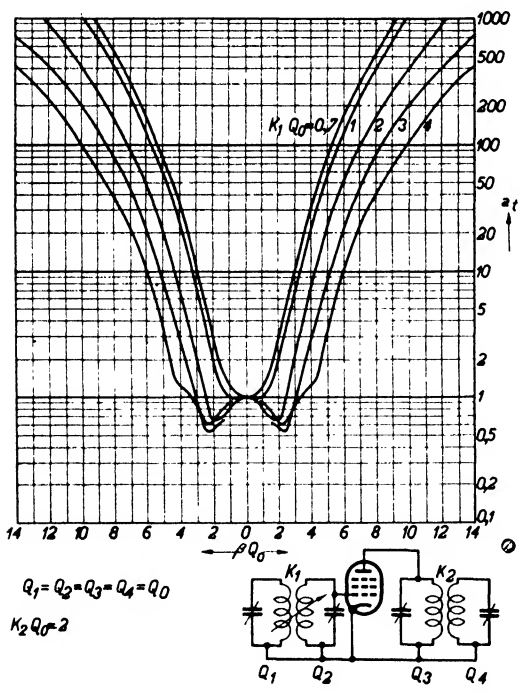

Fig. 55. Resonance curves for a pair of I.F. band-pass filters with the same circuit-quality; the first has adjustable coupling, while that of the second is fixed at $Q_0K_2 = 2$.

(3) The diode for automatic volume control, in present-day practice, is usually fed from the primary of the last I.F. transformer (see Chapter X). In consequence, variation of the coupling between the circuits of this transformer affects the form of the receiver's AVC regulation curve. Since the relation between the A.C. voltages across primary and secondary circuits respectively is proportional to QK, the level of input voltage to the signal-diode at which AVC comes into operation will also vary directly with this factor.

The sensitivity of the receiver is proportional to: $\frac{QK}{1 + Q^2K^2}$.

In fig. 56 some control curves are given for various values of QK, relating to a set requiring a detector input of 0.5 V at 30% modulation for standard output of 50 mW and having an aerial sensitivity of 10 μV; to load the output stage fully a detector input of 5 V is necessary.

If the AVC delay voltage is adjusted so that, with critical coupling of the band-pass filter, control begins when a signal modulated to a depth of 30% just loads the output valve, and if the control voltage is applied to both the ECH 21 triode-heptode and the EF 22 I.F. pentode, the regulation obtained is similar to that indicated by the curves of fig. 56a.

It is clear that with signal inputs of some millivolts the rectified voltage is nearly proportional to QK. Increasing the bandwidth by varying the coupling in the second band-pass filter causes the detector output, and therefore the volume level, to rise.

If, however, the coupling is varied in the first band-pass filter the change of detector output is much smaller, for the AVC comes into operation always at the same detector voltage. Fig. 56b shows regulation curves for the same receiver, this time, however, with variable coupling in the first I.F. band-pass filter. We see that the detector output, and consequently also the volume level, is practically independent of the bandwidth adjustment once the AVC begins to function. Constancy of volume level when the band-width is varied is an important advantage of effecting control at the first I.F. transformer.

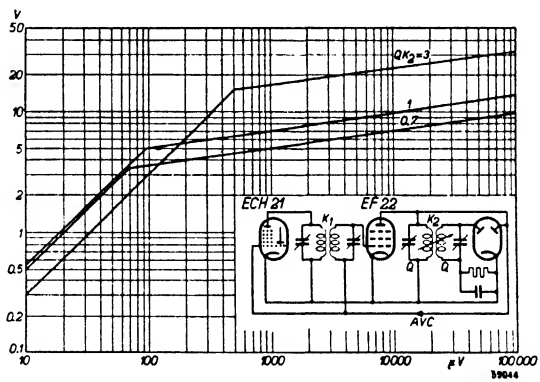

Fig. 56. Control curves for a receiver requiring a detector input of 0.5 V at 30% modulation for standard output of 50 mW and having an aerial sensitivity of 10 μV; a detector input of 5 V is needed to load the output stage fully. The delay voltage is so adjusted that, with critical coupling in the variable band-pass filter and a modulation-depth of 30%, control begins when the output valve is just fully loaded.
a. The inter-circuit coupling in the second I.F. filter is adjustable.

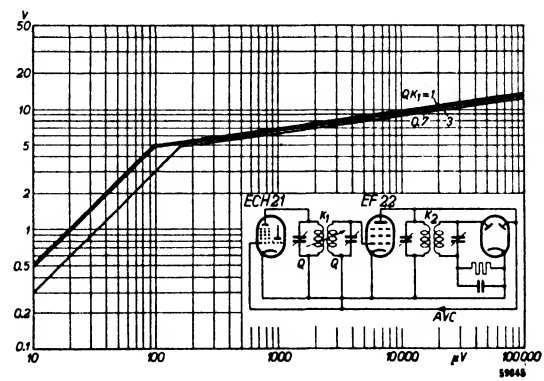

b. The inter-circuit coupling in the first I.F. filter is adjustable.

If the AVC diode is connected to the secondary circuit regulation curves like those in fig. 56b can also be obtained with coupling-variation in the second I.F. transformer. Such an arrangement, however, has various drawbacks, for example flatter tuning and greater distortion, and these will be found dealt with at length in the third volume, Chapter X. We conclude, therefore, that in general it is best to join the AVC diode to the primary circuit and to control bandwidth at the first I.F. transformer.

§ 8. Influence of the signal-frequency circuits

The resonance curves considered so far have all referred only to the I.F. part of the receiver. It must not be overlooked, however, that the frequency-changer is preceded by one or more R.F. circuits which contribute to the receiver overall response. If the R.F. section of the apparatus is designed to pass only a narrow band it is clearly pointless to give the I.F. amplifier a wider resonance curve, for the sidebands will already have been suppressed in the R.F. part of the set. Now the breadth of the resonance curve of the R.F. tuned circuits depends on the frequency to which the receiver is tuned, and accordingly the overall response curve of the receiver is narrower at lower frequencies *. As a result, the functioning of the bandwidth control is affected mainly at the upper end of the long waveband. To illustrate the influence of R.F. tuned circuits, fig. 57 gives the overall resonance curves of a receiver. In producing these curves it was assumed that the I.F. amplifier was the

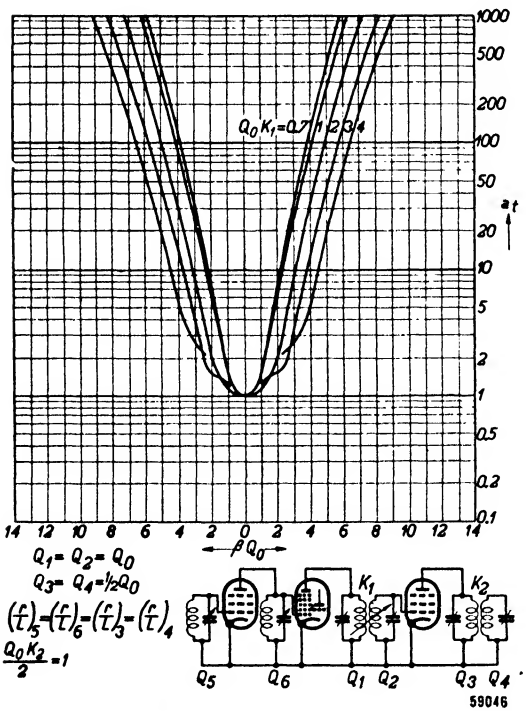

Fig. 57. Overall resonance curves for a receiver with two signal-frequency tuned circuits separated by a valve. The I.F. amplifier is the same as that shown in fig. 54, and the r/L ratio is the same for the R.F. circuits as for the second I.F. band-pass filter.

* The ratio r/L falls with decreasing frequency; it determines the absolute value of the detuning for a specified attenuation. See B § 13 of this chapter.

same as that in fig. 54. The Q of the tuned circuits comprising the second, critically-coupled, band-pass filter was thus taken as half that of the circuits in the first I.F. transformer; the coupling in this first filter is adjustable. It was further assumed that before the frequency-changer there were two signal-frequency circuits separated by a valve. The ratio r/L of these tuned circuits is put at the same figure as for the circuits of the second I.F. transformer — which is often the case at the top of the long wave-band. The respective Q-factors of these R.F. and I.F. tuned circuits are however not the same, owing to the different frequencies to which they are tuned. But when comparing their influence on the receiver's resonance curve the R.F. circuits and the circuits of the second I.F. transformer may be considered as being tuned to the same frequency and as having identical quality, for the attenuation a is determined by βQ, which can be converted to:

$$\frac{2\,\Delta\,\omega}{\omega_0} \cdot \frac{\omega_0 L}{r} = \frac{2\,\Delta\,\omega}{r/L} .$$

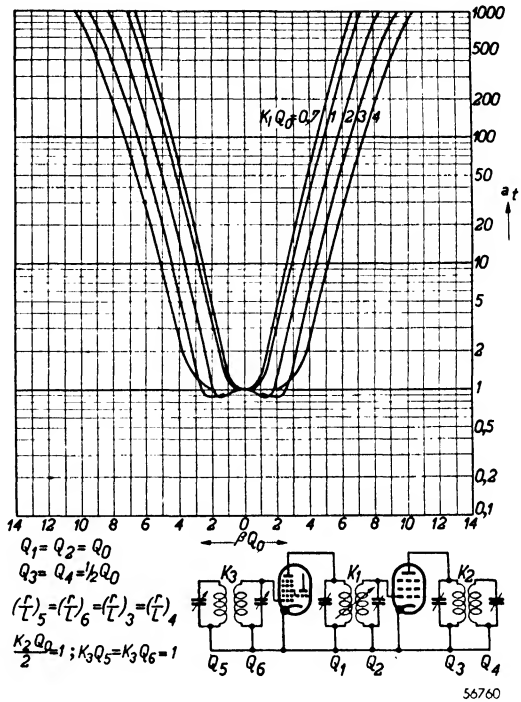

Fig. 58. Overall resonance curves for a receiver with the same tuned circuits as that of fig. 57; in this case, however, the R.F. circuits are combined to form a band-pass filter with critical coupling.

In this last expression neither ω_0 nor the quality factor Q occur.

All these points have been taken into consideration in drawing the curves of fig. 57. The figure shows that the desired flat response, which was approached fairly well in the I.F. amplifier, has been practically lost on adding the R.F. tuned circuits. In a receiver built to the design discussed above the inclusion of bandwidth control would therefore have little point. Better results are to be obtained by omitting the R.F. valve and coupling the two tuned circuits so that they form a band-pass filter. The top of the resonance curve of a band-pass filter is flatter than that of two single circuits in cascade, and the flat top of the overall resonance curve is therefore better

preserved. Fig. 58 reproduces the curves of a receiver with tuned circuits similar to those of fig. 57, except that the signal-frequency circuits are arranged as an inductively coupled band-pass filter. Comparing figs 57 and 58 we find that the circuit of the latter is much more suitable for bandwidth control. Should it be desired to employ the circuit of fig. 57 in a receiver embodying variable bandwidth, it is necessary to ensure that when the I.F. amplifier is adjusted to the low-selectivity position the required band of frequencies is also passed by the R.F. circuits satisfactorily. This may be done by damping the signal-frequency circuits or detuning them in opposite directions when the resonance curve of the I.F. circuits is broadened, but obviously this method makes the receiver much more complicated. This drawback of two cascade R.F. circuits is most noticeable on the long waves. At shorter wavelengths the signal-frequency tuned circuits have a larger r/L ratio and their influence on the overall resonance curve is therefore less.

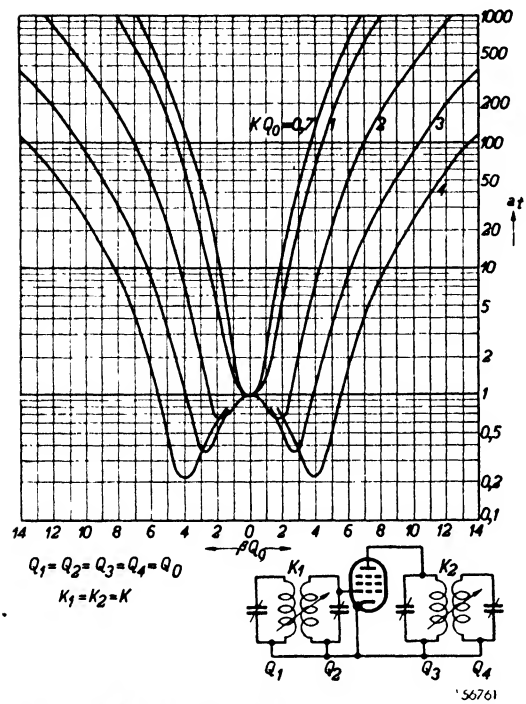

Fig. 59. Resonance curves for a pair of variable band-pass filters with circuits of the same quality. The coupling is the same in both filters.

In drawing the curves of figs 57 and 58 it was assumed that both R.F. circuits were tuned precisely to the incoming signal. But inasmuch as the tracking of R.F. and oscillator circuits is achieved by means of a padding capacitor, the frequency difference is accurate only at three points in the waveband; between these points the R.F. circuits are off-tune from the incoming signal. The asymmetry of the resonance curve thereby caused will however not be considered further at this junction; the distortion which results is discussed in Chapter V.

§ 9. Variation of coupling in two I.F. band-pass filters

In a receiver with two I.F. transformers it is of course also possible to vary

the inter-circuit coupling in both filters. The behaviour of such an arrangement will now be examined. Fig. 59 shows resonance curves for a combination of two band-pass filters containing tuned circuits of the same quality, the coupling being at all times the same in both filters. Double humps are of course even more in evidence than when only one transformer is adjustable. It is therefore better practice, when two band-pass filters of the same circuit quality are to be variable, to alter the respective couplings at different rates. (Apart from the difficulty caused by a marked double peak in the resonance curve, the objections to coupling variation in the second I.F. transformer mentioned on page 104 under (2) and (3) are also present.)

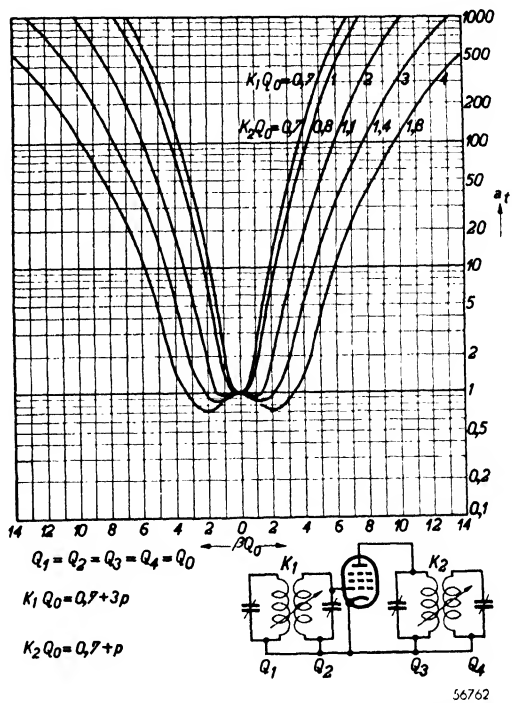

Fig. 60. Resonance curves for a pair of variable band-pass filters with circuits of the same quality. At high selectivity the coupling in the two filters is adjusted so that $Q_0K_1 = Q_0K_2 = 0.7$, while Q_0K_1 is made to increase three times as fast as Q_0K_2.

It is possible, by varying the coupling in one transformer less than in the other, to prevent the peaks in the responses of the two filters from coinciding, so making the humps in the overall resonance curve less marked. The coupling will normally be varied less in the second I.F. transformer. Fig. 60 illustrates resonance curves obtained with a combination of two transformers of the same circuit quality; in the most selective condition the coupling in the filters is such that $Q_0K_1 = Q_0K_2 = 0.7$, and Q_0K_1 is made to increase three times as fast as Q_0K_2. Clearly the desired flat top is now much more closely approached than in fig. 59. By increasing Q_0K_1 from 0.7 to 2.5 the width of the pass-band is doubled, an increase from 0.7 to 1.3 being sufficient for Q_0K_2. Comparison of figs 60 and 53 shows at once the remarkable improvement obtained by varying the coupling in the second I.F. band-pass filter as well. Of course the disadvantages of an adjustable second transformer, referred to in E § 7, remain, but since the variation required in this

transformer is small, these drawbacks are in most cases not of great account. We shall now consider, as we did when dealing with variable coupling in only one I.F. transformer, the extent to which the selectivity curve is affected by the normally poorer quality of the tuned circuits forming the second I.F. transformer. For this purpose we again assume that the quality factors of the circuits in this transformer are half those of the circuits comprising the first. It is advisable to arrange the variation of coupling in the second I.F. transformer such that at maximum bandwidth critical coupling is not greatly exceeded. The aim should be to give the resonance curve of the second I.F. filter such a form that the peaks, which appear in the curve of the first band-pass filter at the wide-band adjustment, are compensated as well as possible. Fig. 54 showed that critical coupling in the second I.F. transformer provides very satisfactory compensation: with tighter coupling, therefore, the top of the overall curve will not be so flat. The coupling in the second band-pass filter should be neither too tight in the wide-band position, nor too loose in the narrow-band position (or sensitivity will fall unduly); consequently when the circuits of the second I.F. transformer are of poor quality control of bandwidth must be mainly effected at the first I.F. transformer. In the example given in fig. 61 the filters are so adjusted that at high selectivity $Q_0K_1 = \frac{1}{2} Q_0K_2 = 0.7$, while the variation of Q_0K_1 is six times as large as that of Q_0K_2.

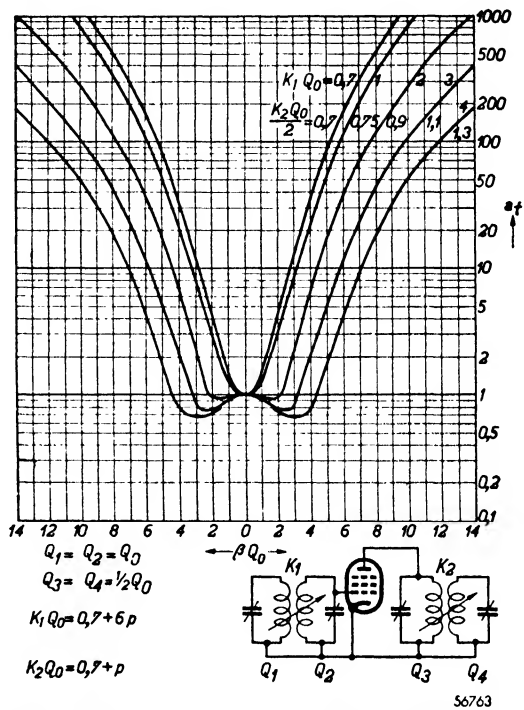

Fig. 61. Resonance curves for a pair of variable band-pass filters, the quality of the circuits in the second being half that of the circuits in the first filter. At high selectivity the coupling in the two filters is adjusted so that $Q_0K_1 = \frac{1}{2}Q_0K_2 = 0.7$ while Q_0K_1 is made to increase x times as fast as Q_0K_2.

Comparison of figs 54 and 61 makes it plain that variation of the coupling in the second I.F. transformer has little influence on the width of the band passed. The conclusion may therefore be drawn that simultaneous adjust-

ment of both transformers is worth while only when the tuned circuits of the second filter are of high quality. To ensure good quality it is necessary to connect the signal- and AVC-diodes to tappings on the I.F. coils, while the diode load-resistances must be chosen with an eye to minimising damping.

§ 10. Design details for variable I.F. band-pass filters

We shall next consider how the coupling between the tuned circuits of a band-pass filter may be varied. As was mentioned in E § 3, variable mutual-inductance coupling is most commonly used, for this method does not cause detuning. Before going into details, it is necessary to distinguish two classes of intermediate frequency: the low (about 125 kc/s) and the high (about 470 kc/s).

With a low intermediate frequency the distance between the coils is fairly small, perhaps 10 mm, and can readily be varied to provide adequate change of mutual inductance. Obviously, neither the inductance nor the capacitance of the tuned circuit, of which the movable coil forms part, must alter. Such undesired changes might occur, for example, if the moving coil came too close to the wall of the screening can at some point in its travel; the resultant detuning would then cause asymmetry in the overall resonance curve. It is therefore important to ascertain that the overall response remains symmetrical when the bandwidth is varied; the resonance curves of experimental types may conveniently be examined on a cathode-ray tube. It is not possible to quote exact figures for the required travel of the movable coil, inasmuch as the separation of the inductors depends on the circuit quality, the diameter of the screen, etc. In order, however, to give a rough idea of the movement needed, it may be mentioned that, using a low intermediate frequency and a transformer tuned by 100 pF, the distance between the I.F. coils must be variable from about 6 to 12 mm. If the coupling in the second I.F. transformer is also varied, the movement required in the first is naturally less. At high intermediate frequencies the coupling between the coils must be looser than at low I.F. *. The large separation consequently needed often leads to mechanical difficulties. A possible method is to hinge one of the coils, so that their axes may be made perpendicular when minimum coupling is required; such an arrangement is not ideal, however, for altering the axis of the movable coil inside the screening can is apt to cause changes of inductance and self-capacitance.

* For the same selectivity, the same r/L ratio is needed at high as at low intermediate frequencies. With a high IF the quality $Q = \omega L/r$ is higher than with a low IF. Seeing that the coupling factor K for critical coupling is equal to $1/Q$ of the tuned circuits, it needs to be smaller at high intermediate frequencies.

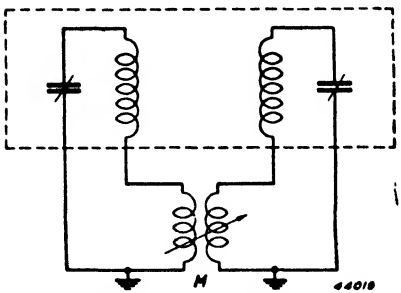

Fig. 62. Variable I.F. band-pass filter with fixed loose coupling between the main inductors: in each tuned circuit a small auxiliary coil is included, and the coupling between these small coils is adjustable.

Another method capable of very good results s to provide a fixed, very loose coupling between the I.F. inductors and to include in each tuned circuit a small auxiliary coil. The coupling between these auxiliary coils is adjustable. If they are connected on the earth side of the circuit the I.F. voltage present will be so low that they may be mounted outside the screening can without risk of instability (see fig. 62). The small coils may consist of some 40 turns of stranded wire, wave-wound on a core of 15 mm diameter.

§ 11. Selectivity control combined with tone control

When the accepted frequency-band can be varied within wide limits it is of course possible to employ the bandwidth regulator also as a tone-control. For strong suppression of high notes the frequency-band passed at maximum selectivity has to be so narrow that I.F. circuits of the requisite quality are unattainable in practice.

Accordingly, a separate tone-control is usually provided in the A.F. section. To simplify operation of the receiver the two controls may be ganged in such a manner that rotation of the knob in a given direction first reduces the bandwidth to minimum and then brings the A.F. tone-control into play. If the two adjustments merge smoothly, the uninitiated listener will find the combined control as simple to use as a conventional tone-control. The great advantage, compared with a separate tone-control and fixed bandwidth, is that under favourable conditions better reproduction of high notes can be obtained; another advantage of the combined control is that it is effective when the receiver is used for reproducing gramophone records, whereas variable bandwidth alone would clearly not be so.

§ 12. Inter-circuit coupling by means of valves

Variation of the coupling between the circuits of a band-pass filter by physical movement of a coil is not a method which lends itself to automatic control. For such a purpose a non-mechanical system is preferable. It has been found that two tuned circuits may be joined by valves so that they behave as if the coupling were inductive or capacitive. The coupling can then be varied by altering the slope of these valves.

There are very many methods of using valves to couple a pair of tuned

circuits, so that band-pass filter characteristics appear. The coupling of two circuits by means of an amplifying valve, as in an R.F. stage, naturally does not come into consideration, for in such a case, ignoring parasitic effects, the coupling is in one direction only, namely from the first circuit to the second.

The overall resonance curve is then the product of the curves of the individual circuits. For band-pass characteristics to appear, a coupling from the second to the first circuit must also be present and both the forward and backward couplings must satisfy certain requirements in order that the transferred voltages shall be correct in magnitude and phase. The backward coupling can be supplied, for example, by a valve of the same type as is used for the forward coupling. Such a circuit, which is the first we shall discuss, is shown in fig. 63. Here the mutual coupling of the tuned circuits is provided by a pair of resistance-capacitance-coupled pentodes, of slope S; the correct phase relationship is obtained automatically.

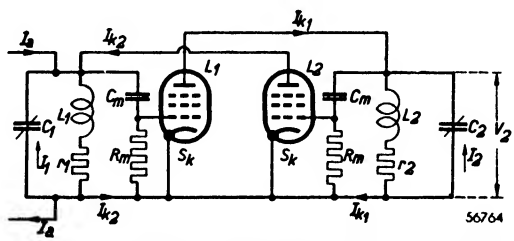

Fig. 63. I.F. transformer with mutual coupling provided by two pentodes of slope S and two RC coupling-elements.

The impedance of $(C_m + R_m)$ is assumed to be so high that the current through it is negligible compared with that flowing in the tuned circuit.

The equation for the voltage V_2 across the secondary circuit will now be derived. An alternating current I_a is fed to the input side, and from the voltage balance in the primary circuit we get:

$$I_1 \frac{1}{j\omega C_1} + (I_1 + I_a + I_{k2})(r_1 + j\omega L_1) = 0,$$

or:

$$I_1 (r_1 + j\omega L_1 + \frac{1}{j\omega C_1}) + I_{k2} (r_1 + j\omega L_1) = -I_a (r_1 + j\omega L_1),$$

or, since $r_1 \ll \omega L_1$:

$$I_1 (r_1 + j\omega L_1 + \frac{1}{j\omega C_1}) + I_{k2} j\omega L_1 = -I_a j\omega L_1 \quad \ldots\ldots\ldots \quad \text{(I E 17)}$$

Similarly, for the secondary circuit:

$$I_2 (r_2 + j\omega L_2 + \frac{1}{j\omega C_2}) + I_{k1} j\omega L_2 = 0 \quad \ldots\ldots\ldots\ldots \quad \text{(I E 18)}$$

Assuming now that the reactance of the capacitances C_m is large in relation to the resistances R_m, and that the A.C. resistance of the pentode is large compared with the dynamic resistance of the tuned circuits, we can write for I_{k1} and I_{k2}:

$$I_{k1} = I_1 \frac{1}{j\omega C_1} j\omega C_m R_m S = I_1 \frac{C_m R_m S}{C_1} \quad \ldots \quad \text{(I E 19)}$$

$$I_{k2} = I_2 \frac{1}{j\omega C_2} j\omega C_m R_m S = I_2 \frac{C_m R_m S}{C_2} \quad \ldots \quad \text{(I E 20)}$$

Substituting equations (I E 19) and (I E 20) in (I E 17) and (I E 18) we get:

$$I_1 (r_1 + j\omega L_1 + \frac{1}{j\omega C_1}) + I_2 j\omega L_1 \frac{C_m R_m S}{C_2} = -I_a j\omega L_1. \quad \ldots \quad \text{(I E 21)}$$

$$I_2 (r_2 + j\omega L_2 + \frac{1}{j\omega C_2}) + I_1 j\omega L_2 \frac{C_m R_m S}{C_1} = 0 \quad \ldots \ldots \quad \text{(I E 22)}$$

Now if both circuits are tuned to the same frequency

$(\omega_0 = \frac{1}{\sqrt{L_1 C_1}} = \frac{1}{\sqrt{L_2 C_2}})$, we deduce from equations (I E 21) and (I E 22) that for frequencies differing little from the resonant frequency ($\omega/\omega_0 \approx 1$) — see also pages 22 and 23:

$$I_2 = -I_a \frac{Q_1 Q_2 \frac{C_m R_m S}{C_1}}{(1 + j\beta Q_1)(1 + j\beta Q_2) + \frac{C_m^2 R_m^2 S^2}{C_1 C_2} Q_1 Q_2} \quad \ldots \quad \text{(I E 23)}$$

The voltage across the secondary circuit is then:

$$V_2 = I_2 \frac{1}{j\omega C_2} = -I_a \frac{Q_1 Q_2 \frac{C_m R_m S}{j\omega C_1 C_2}}{(1 + j\beta Q_1)(1 + j\beta Q_2) + \left(\frac{C_m R_m S}{\sqrt{C_1 C_2}}\right)^2 Q_1 Q_2}$$

or:

$$V_2 = I_a \frac{j\omega_0 Q_1 Q_2 \frac{C_m R_m S}{\sqrt{C_1 C_2}} \sqrt{L_1 L_2}}{(1 + j\beta Q_1)(1 + j\beta Q_2) + \left(\frac{C_m R_m S}{\sqrt{C_1 C_2}}\right)^2 Q_1 Q_2} \quad \ldots \quad \text{(I E 24)}$$

Comparison of this equation with (I B 14) reveals that they are the same if

$$K = \frac{C_m R_m S}{\sqrt{C_1 C_2}} \quad \ldots \ldots \ldots \ldots \ldots \quad \text{(I E 25)}$$

For top-capacitance coupling

$$K = \frac{C_{k1}}{\sqrt{C_1 C_2}}.$$

It follows that the circuit of fig. 63 [compare equation (I B 27)] will yield the same resonance curve as a band-pass filter coupled by a top-capacitance of

$$C_{k1} = R_m C_m S \quad \ldots \ldots \ldots \ldots \ldots \quad \text{(I E 26)}$$

Accordingly the coupling-factor can be controlled by varying the slope S. In order to gain an idea of the size of the coupling elements required we shall compute the values of R_m, C_m and S necessary for critical coupling of two similar tuned circuits. If, for example, $C_1 = C_2 = 100$ pF and $Q_1 = Q_2 = 100$, then for critical coupling ($K\sqrt{Q_1 Q_2} = 1$)

$$R_m C_m S = K\sqrt{C_1 C_2} = \frac{1}{100} \cdot 100.10^{-12} = 10^{-12}.$$

This equation may be satisfied, for instance, with

$$\begin{aligned} R_m &= 250\ \Omega, \\ C_m &= 4\ \text{pF}, \\ S &= 1\ \text{mA/V}; \end{aligned}$$

and these values may well be used in practice. The damping imposed on the tuned circuits by R_m is slight. If we substitute for $C_m R_m$ an equivalent parallel circuit, as described in A § 4, we find that the equivalent resistance is equal to $R_m \left(\frac{1}{\omega C_m R_m}\right)^2$, which for a high intermediate frequency (470 kc/s) is:

$$250 \left(\frac{1}{2\pi \,.\, 470{,}000.4.10^{-12} \,.\, 250}\right)^2 \Omega = 28.3\ \text{M}\Omega.$$

This calculation demonstrates that the influence of R_m on the I.F. circuits is negligible.

The arrangement of fig. 63 will rarely be used in practice, owing to the need for two additional valves. However, it is possible to vary the inter-

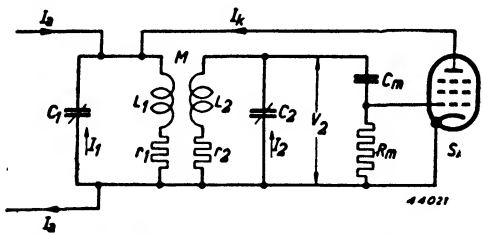

Fig. 64. I.F. transformer with inter-circuit coupling by mutual inductance and by means of a pentode.

circuit coupling, using only one extra valve; the tuned circuits are in that case coupled in the normal way as well, and their behaviour is a little different. If, for instance, in fig. 63 we substitute an inductive coupling between the coils L_1 and L_2 for valve I then we get the circuit of fig. 64. We shall calculate the voltage V_2 across the secondary tuned circuit of such an arrangement when an alternating current I_a is fed to the primary circuit.

From the voltage equilibrium in the primary circuit we have:

$$I_1 \frac{1}{j\omega C_1} + (I_1 + I_k + I_a)(r_1 + j\omega L_1) + I_2 j\omega M = 0,$$

or:

$$I_1 (r_1 + j\omega L_1 + \frac{1}{j\omega C_1}) + I_2 j\omega M + I_k (r_1 + j\omega L_1) = -I_a (r_1 + j\omega L_1),$$

or, since $r_1 \ll \omega L_1$:

$$I_1 (r_1 + j\omega L_1 + \frac{1}{j\omega C_1}) + I_2 j\omega M + I_k j\omega L_1 = -I_a j\omega L_1 \quad \ldots \quad \text{(I E 27)}$$

In the same way we find for the secondary circuit:

$$I_2 (r_2 + j\omega L_2 + \frac{1}{j\omega C_2}) + I_1 j\omega M = 0 \ldots \quad \text{(I E 28)}$$

For the current I_k can be written:

$$I_k = I_2 \frac{1}{j\omega C_2} j\omega C_m R_m S = I_2 \frac{C_m R_m S}{C_2} \quad \ldots \quad \text{(I E 29)}$$

Substituting this equation in (I E 27) gives:

$$I_1 (r_1 + j\omega L_1 + \frac{1}{j\omega C_1}) + I_2 (j\omega M + j\omega L_1 \frac{C_m R_m S}{C_2}) = -I_a j\omega L_1 \quad \text{(I E 30)}$$

In the case of the two circuits being tuned to the same frequency, $\omega_0 = \frac{1}{\sqrt{L_1 C_1}} = \frac{1}{\sqrt{L_2 C_2}}$, we deduce from equations (I E 28) and (I E 30) that for frequencies only slightly off resonance ($\omega/\omega_0 \approx 1$)

$$I_2 = -I_a \frac{Q_1 Q_2 M/L_2}{(1 + j\beta Q_1)(1 + j\beta Q_2) + \left(\frac{M^2}{L_1 L_2} + \omega_0^2 M C_m R_m S\right) Q_1 Q_2} \quad \text{(I E 31)}$$

The voltage across the secondary circuit is:

$$V_2 = I_2 \frac{1}{j\omega C_2} = I_a \frac{j \frac{M}{\omega L_2 C_2} Q_1 Q_2}{(1 + j\beta Q_1)(1 + j\beta Q_2) + \left(\frac{M^2}{L_1 L_2} + \omega_0^2 M C_m R_m S \right) Q_1 Q_2} \quad \text{(I E 32)}$$

Leaving out of consideration the coupling provided by the valve, the coupling-factor between the two circuits is $M/\sqrt{L_1 L_2}$.

If we put:

$$K = \frac{M}{\sqrt{L_1 L_2}},$$

and

$$K'^2 = K^2 + \omega_0^2 M C_m R_m S \quad \text{(I E 33)}$$

equation (I E 32) then becomes:

$$V_2 = I_a \frac{j\omega_0 Q_1 Q_2 K \sqrt{L_1 L_2}}{(1 + j\beta Q_1)(1 + j\beta Q_2) + Q_1 Q_2 K'^2} \quad \text{(I E 34)}$$

It appears from equations (I E 33) and (I E 34) that the additional coupling through the pentode alters the coupling factor in the numerator of equation (I E 34); the denominator is unaffected. This corresponds to what was deduced in B § 10 regarding the detuning of two circuits in opposite directions [see equation (I B 41)].

Consequently coupling by a single valve has the same effect as such detuning; that is to say, a tight coupling will make the resonance curve broaden out in the same way as if the mutual inductance M were increased. The accompanying change in amplification however is greater than if M were varied. Further, it is evident from equation (I E 33) that reducing the slope S can result in either an increase or a decrease of K'^2, according to the sign of M. Using the circuit of fig. 63 there are thus alternative methods of regulating the bandwidth:

(a) The inductive coupling between the circuits may be made loose enough to give the minimum bandwidth required, the direction of the mutual inductance being so chosen that raising the slope S of the coupling valve causes an increase of K'. Maximum bandwidth then corresponds to normal grid bias, and the frequency-band becomes narrower as the negative bias is increased.

(b) The inductive coupling may be made tight enough to provide the maximum bandwidth required, the direction of the mutual inductance being so chosen that increasing the slope S results in a reduction of K'. Normal bias then corresponds to minimum bandwidth, and the frequency-band widens as the grid is made more negative.

Circuits *a* and *b* differ not only in the contrary variation of bandwidth for a given change of coupling-valve bias. It follows from equation (I E 34) that, at a frequency to which both circuits are tuned, the voltage across the secondary circuit is:

$$V_{2\,(\omega = \omega_0)} = jI_a \frac{\omega_0 Q_1 Q_2 K \sqrt{L_1 L_2}}{1 + Q_1 Q_2 K'^2}$$

or:

$$V_{2\,(\omega = \omega_0)} = j I_a \sqrt{Z_1 Z_2} \frac{K \sqrt{Q_1 Q_2}}{1 + Q_1 Q_2 K'^2} \quad . \quad . \quad . \quad \text{(I E 35)}$$

Z_1 and Z_2 here represent the dynamic resistance at resonance of the primary and secondary circuits respectively, so that $Z_1 = L_1/r_1C_1$ and $Z_2 = L_2/r_2C_2$. Inasmuch as a specific value of K' corresponds to a smaller value of K with method *a* than with method *b*, we can conclude from equation (I E 35) that, for a given input and bandwidth, system *a* yields a smaller voltage across the secondary circuit than system *b*. Consequently when the circuit of fig. 63 is used in the anode circuit of the mixer or I.F. valve higher gain will be obtained with method *b*.

Another noteworthy fact which follows from equations (I E 33) and (I E 35) is that with a negative value of M (system *b*) increasing S causes K'^2 to fall [see (I E 33)]. When S is so large that

$$\left| \omega_0^2 M C_m R_m S \right| > K^2,$$

K'^2 becomes negative. For $K'^2 = -\frac{1}{Q_1 Q_2}$ the numerator in equation (I E 35) is nil, and in that case the voltage across the secondary circuit becomes infinitely great for a specific value of I_a, while a finite voltage appears even with $I_a = 0$. In other words the circuit oscillates. When employing system *b* we are therefore obliged to ensure that the above-mentioned limit is not overstepped at the highest value of S. With method *a* there is no danger of oscillation, as K'^2 is always greater than K^2 and thus can only be positive. Several variations of the circuits in figs 62 and 63 are possible, but all

involve this same principle: the feeding of a current to the primary or secondary circuit via a valve, the current being proportional to the voltage across the secondary or primary circuit and in correct phase-relation thereto.

§ 13. Automatic bandwidth control

As was mentioned in the introduction, the use of valves for inter-circuit coupling in band-pass filters is of special importance for automatic control of selectivity.

The ideal circuit would be one which always adjusted the bandwidth to the optimum value. But this value is not just a physical quantity: it depends on the taste of the listener. It is therefore obvious that a system which will give complete satisfaction in all circumstances is technically unattainable. Even if we concern ourselves only with the physics of the problem it will be difficult, and perhaps technically impossible, to devise a system which will at all times regulate the frequency band to the most favourable width. This optimum bandwidth, by which we mean the maximum bandwidth permitted by reception conditions, depends not only on the strength of the desired signal but also on the strength of the interfering transmission, the noise level and the modulation depth of the highest audio frequencies emitted by the interfering station. For instance, when the interfering station is radiating speech the required transmission may be received with a wider-band adjustment than if a musical program were going out on the interfering channel. A system which took account of all these circumstances would be so complicated as to be quite unsuited to present-day methods of receiver manufacture; further consideration will therefore be limited to a system in which the bandwidth is controlled only by the strength of the required transmission and in which, consequently, the pass-band is always narrow when a weak signal is being received. A quite simple circuit usually suffices for this purpose.

In a receiver with AVC, currents and voltages are present whose magnitude depends on the strength of the incoming signal; these may be used to operate the bandwidth control.

There are three basic methods of obtaining automatic regulation of bandwidth:

(a) variation of the inter-circuit coupling;
(b) variation of the quality of the circuits;
(c) variation of the tuning of the circuits.

As in the case of manual control, adjustment by variation of coupling is the most satisfactory system. Altering the quality has, compared with other methods, the great drawback that discrimination against frequencies

remote from resonance is poorer when the receiver is in the narrow-band condition. An advantage of this method, however, is that it offers the possibility of providing a limited variation of bandwidth without the use of additional valves: the damping imposed by a diode-detector falls off with increasing signal strength and the quality of the secondary circuit of the last I.F. transformer is thereby improved. Furthermore it is possible to vary the A.C. resistance of the I.F. valve within wide limits by applying a control voltage to its suppressor grid, the slope being scarcely affected (see fig. 49). By such means the quality of the tuned circuits comprising the last I.F. band-pass filter may be modified. There is however one difficulty: the AVC voltage cannot be used directly to regulate the suppressor-grid potential. The damping of the tuned circuits has to be reduced when the received signal is strong, and to achieve this the suppressor grid must be made less negative, while with a weak signal it requires to be made more negative. But seeing that the system is not very effective it is not proposed to deal further with its attendant problems.

Mutual detuning of band-pass filter circuits can also be carried out without the need for mechanical aids, by employing additional valves. One extra valve is needed for each tuned circuit. We have already seen, however, that the arrangement of fig. 64 gives results identical with those which are obtained by detuning filter circuits in opposite directions, and as it calls for only one additional valve per band-pass filter it is obviously preferable to a system needing an extra valve for each tuned circuit. The arrangement shown in fig. 64 will therefore be considered further.

As already noted, there are two ways of making use of this method.

System *b* has, however, the great advantage that maximum selectivity requires maximum slope, consequently the AVC voltage can be used to control the coupling valve as well.

We now introduce, by way of example, some practical values:

$$Q_1 = Q_2 = 100,$$
$$C_1 = C_2 = 100 \text{ pF},$$
$$C_m = 4 \text{ pF},$$
$$R_m = 500 \ \Omega.$$

Using an EF 22 as coupling valve, with its slope regulated to 1.4 mA/V ($V_{g2} = 75$ V), and the mutual inductance between the tuned circuits so adjusted that

$$K = \frac{M}{\sqrt{L_1 L_2}} = \frac{3}{100},$$

we get:

$$K' = \sqrt{K^2 - \omega_0^2 M\, C_m R_m S} = \sqrt{K^2 - \frac{M\, C_m R_m S}{L_1 C_1}} =$$

$$= \sqrt{9.10^{-4} - \frac{3}{100} \cdot \frac{4}{100} \cdot 500 \cdot 1.4 \cdot 10^{-3}} = \frac{0.77}{100}.$$

Therefore:

$$K' \sqrt{Q_1 Q_2} = 0.77.$$

The coupling between the circuits is thus under-critical. If now a control voltage of say -8 V is applied to the first grid of the EF 22 its mutual conductance is reduced about ten times, so that:

$$K' = \sqrt{9.10^{-4} - \frac{3}{100} \cdot \frac{4}{100} \cdot 500 \cdot 0.14.10^{-3}} = \frac{2.85}{100}.$$

Therefore:

$$K' \sqrt{Q_1 Q_2} = 2.85.$$

In the majority of receivers a control voltage of this magnitude is available from the AVC diode when a strong signal is received.
The signal voltage across the secondary circuit, at resonance ($\beta = 0$), will, in accordance with equation (I E 35), be:

$$V_2 = j\, I_a \cdot \tfrac{1}{2} \sqrt{Z_1 Z_2} \cdot 2\, \frac{K \sqrt{Q_1 Q_2}}{1 + Q_1 Q_2 K'^2} \quad \ldots \quad \text{(I E 35)}$$

With a normal critically-coupled band-pass filter this signal voltage would, from equation (I B 17), be:

$$V_2 = I_a \cdot \tfrac{1}{2} \sqrt{Z_1 Z_2} \quad \ldots \quad \text{(I E 36)}$$

The factor $2\, \frac{K \sqrt{Q_1 Q_2}}{1 + Q_1 Q_2 K'^2}$ thus represents the ratio of the I.F. gain, obtained with -8 V applied to the coupling-valve control grid, to the gain secured with a normal critically-coupled band-pass filter.

In our example $K \sqrt{Q_1 Q_2} = 3$, while with a weak signal $K' \sqrt{Q_1 Q_2} = 0.77$.

The factor mentioned above therefore amounts to $2 \times \frac{3}{1 + 0.77^2} = 3.76$.

For a weak signal the I.F. amplification in such a receiver and, therefore, also its sensitivity rises four times as high as in a set with an ordinary critically-coupled band-pass filter. With a large input $K' \sqrt{Q_1 Q_2}$ was found to be 2.85, and the factor is then reduced to $2 \times \frac{3}{1 + 2.85^2} = 0.66$. The IF gain will therefore drop more rapidly when a controlled coupling-pentode is employed than with AVC alone; in other words the introduction of automatic bandwidth-control leads to a flatter regulation curve.

At the close of § 12, page 118, it was mentioned that the circuit oscillates when $K'^2 = -\frac{1}{Q_1 Q_2}$. In our example this would occur if the slope of the coupling-pentode reached 1.66 mA/V. It is accordingly important to ensure that this danger point is not approached too closely with low inputs, and allowance must be made for the possibility of replacement valves possessing slightly higher mutual conductance. On the other hand the slope of the coupling valve must not be too low, or the frequency-band will not become narrow enough on weak signals. This small permissible tolerance represents the main drawback of the system and to counter the difficulty it is advisable to use negative feedback, so that the actual slope is less dependent on the characteristics of the individual valve.

Suitable feedback may be obtained by using an un-bypassed cathode resistor, but it is then of course necessary to provide a higher control voltage. The principle of feedback is discussed in Chapter VIII.

Method (*a*) of regulating bandwidth (page 117) does not require a critical value of mutual conductance, but compared with (*b*) it has several disadvantages:

(1) On account of the smaller value of M the influence of S on K' is less. A greater variation of S is accordingly needed and a larger control voltage. Furthermore C_m or R_m must usually be greater. If, using the tuned circuits of the previous example, we make the inductive coupling so weak that $K = M/\sqrt{L_1 L_2} = 0.006$, and if $C_m = 4$ pF and $R_m = 2000\ \Omega$, then with $S = 1.8$ mA/V

$$K' = \sqrt{0.6^2.10^{-4} + \frac{0.6}{100} \cdot \frac{4}{100} \cdot 2000 \cdot 1.8 \cdot 10^{-3}} = 0.03.$$

Thus $K' \sqrt{Q_1 Q_2} = 3$. If now we make the slope of the coupling valve 10 times smaller K' becomes 0.011, and $K' \sqrt{Q_1 Q_2} = 1.1$; the coupling is still over-critical. In order to make the coupling under-critical the

slope must be reduced still further. With $S = 0.018$ mA/V, K' drops to 0.0067 and $K'\sqrt{Q_1Q_2} = 0.67$.

For the same variation of coupling as with the alternative arrangement the change of slope of the coupling valve thus needs to be ten times as great; thus a higher control voltage is necessary, with an EF 22 about –19 V.

(2) It has already been shown above that system (*a*) gives a smaller I.F. gain, owing to K being less. With the tightest coupling corresponding to a powerful signal the ratio of the amplification obtained to that which is possible with a critically-coupled filter is equal to:

$$2\,\frac{K\sqrt{Q_1Q_2}}{1+Q_1Q_2K'^2} = 2\times\frac{0.6}{1+9} = 0.12,$$

and with the loosest coupling (corresponding to a weak signal):

$$2\times\frac{0{,}6}{1+0.67^2} = 0.82.$$

Thus the I.F. gain remains considerably lower than that obtained with system (*b*). In this case too the trend of amplification in relation to signal strength is such that the AVC regulation curve is made flatter.

(3) In system (*a*) the AVC voltage cannot be utilised directly, since with a weak signal the coupling valve requires a large negative bias. There are several ways of obtaining such a bias; one is to make use of the fact that the screen voltage of a valve in the AVC chain rises as the signal strength increases.

If an EF 22 I.F. valve is fed from a resistance network with the values indicated in fig. 65, its screen grid voltage will amount to about 100 V

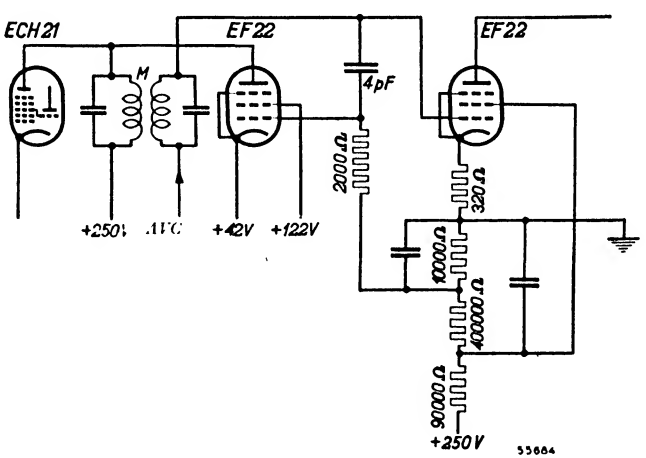

Fig. 65. Practical circuit developed from fig. 64. The inductive coupling is such as to give minimum bandwidth, and the EF 22 coupling-valve is so connected that increasing its slope S increases the coupling factor K'. The control voltage applied to the grid of the EF 22 is derived from a potentiometer and is most negative when the incoming signal is weakest.

when the incoming signal is too weak to bring the AVC into operation. When a strong signal arrives AVC reduces the screen grid current to a very low level and the potential at the electrode rises to about 200 V. With the control grid of the coupling valve connected as shown there is a variation of its potential from +20 to +40 V approximately, so that if the cathode is maintained at +42 V a grid bias varying from —22 to —2 V can be obtained and highest bias will occur with weakest signals.

When aligning band-pass filter circuits which are coupled in the manner illustrated by fig. 64 it is essential to make the coupling as loose as possible. A weak test signal should therefore be used for trimming the receiver, and it may be necessary to apply a fixed high negative bias to the coupling valve while alignment is in progress.

The question still remains whether it is possible to achieve automatic control of inter-circuit coupling without using additional valves. It may be said at once that such an effect does occur fortuitously in many receivers, owing to bad positioning of the components. A slight capacitive coupling between the anode of the I.F. valve and the high-potential side of the primary circuit in the preceding band-pass filter gives rise to an extra inter-circuit coupling in this filter; its characteristics are thereby rendered similar to those of the circuit shown in fig. 63. Depending on the direction of the inductive coupling, the I.F. gain can thus either be increased or reduced, the bandwidth at the same time becoming smaller or larger.

Control of the I.F. valve results in modifying the coupling through the valve, and the bandwidth therefore becomes altered. If this effect is intentionally made so marked that a sufficient variation of bandwidth is obtained, only system (*b*) comes into consideration.

The negative grid bias of the I.F. valve rises with increasing signal strength. Certainly we shall then get very high amplification, but the drawback of system (*b*) is present also in this case: the I.F. valve goes into oscillation as soon as the slope slightly exceeds the figure needed for satisfactorily loose coupling of the preceding band-pass filter.

In ill-adjusted receivers this phenomenon can easily appear. It is a difficulty which will always occur when valves are employed for coupling-variation and simultaneously for other purposes. We can therefore conclude that obtaining automatic variation of coupling without using additional valves may lead to many difficulties.

BIBLIOGRAPHY

1. *Amos, S. W.* Aerial coupling circuits. Electronic Engineering Vol. XVIII, Febr. 1945.
2. *Austin, C. & Oliver, A. L.* Some notes on iron-dust cored coils at radio frequencies. Marconi Review 1938, Nr 70.
3. *Butterworth, S.* Effective resistance of inductance coils at radio frequency. Experimental Wireless & Wireless Engineer 1926, p. 203.
4. *Hermanspann, P.* Die Vorausberechnung der Selektionskurven von H.F. Verstärkern. Telefunken Zeitung 12, 1931, p. 53.
5. *Mesny, R.* Représentation nouvelle des propriétés de deux circuits couplés. L'onde électrique 13, 1934, p. 289.
6. *Mezey, M.* Etude du circuit d'entrée d'un poste récepteur radiophonique. L'onde électrique 12, 1933 p. 149.
7. *Tellegen, B. D. H.* Coupled circuits. Philips Resarch Reports, Vol. 2, No 1, Febr. 1947.
8. *Wheeler, H. A.* Image suppression in superheterodyne receivers. Proceedings I.R.E. 23. 1935, p. 569.
9. *Wheeler, H. A. & Kelly Johnson, J.* High fidelity receivers with expanding selectors. Proceedings I.R.E. 23, 1935, p. 594.

II. FREQUENCY-CHANGING

A. Mixing

The advantages of the superheterodyne circuit have already come to our notice repeatedly in Chapter I. With this type of circuit all carrier frequencies received are changed to a fixed frequency known as the intermediate frequency; using this device it becomes possible to produce comparatively simple receivers possessing a fair degree of selectivity.

Moreover, the tuned circuits used at this single frequency, which is usually lower than that of the signals to be received, have generally a higher dynamic resistance than signal-frequency circuits; greater amplification can therefore be obtained. For these reasons practically all present-day receivers are superheterodynes, and only very small local-station sets still rely on signal-frequency amplification (straight sets).

In superheterodyne receivers the intermediate frequency is obtained by mixing the received signal with an oscillator voltage the frequency of which is so adjusted that the frequency-difference arising has always the same value: the chosen intermediate frequency. Every mixer stage must therefore include, in addition to the mixing valve, an oscillator to generate the heterodyne voltage *. Generally, however, the two valves are combined in a single bulb, the combination valve fulfilling both functions.

In the first part of this chapter the problems peculiar to the mixing process will be dealt with; in the second part the various oscillator circuits will be considered, and in the other sections the parasitic effects which are liable to occur will be discussed.

§ 1. The mixing process

Basically, the R.F. input voltage $V_i \sin \omega_i t$, together with a heterodyne voltage $V_h \cos \omega_h t$, is applied to one or two electrodes of a valve of which the characteristic $i_a = f(v_g, v_g')$ is not linear, and in which the grid voltages v_g and v_g' are dependent on the R.F. input v_i and the heterodyne voltage v_h.

---

* Also referred to as oscillator voltage.

Finally we can say, therefore, that:

$$i_a = f(v_h, v_i)$$

If in this case we write i_a as a power series, the following product occurs, among others:

$$V_i \sin \omega_i t.\ V_h \cos \omega_h t = \tfrac{1}{2}\ V_i\ V_h \sin(\omega_i + \omega_h)\ t - \tfrac{1}{2}\ V_i V_h \sin(\omega_h - \omega_i)\ t \qquad \text{(II A 1)}$$

The origin of this product will be evident from (II A 5). Consequently there arise in the anode circuit of the mixing valve, among others, an alternating voltage with the intermediate frequency

$$\omega_o = \omega_h - \omega_i, \quad \ldots\ldots\ldots\ldots\ldots \qquad \text{(II A 2)}$$

which is subjected to further amplification.

The current of frequency ω_o which flows in the anode circuit is dependent on V_i and V_h, and also on the anode voltage, which varies with the I.F. voltage V_o. Now in practice V_i and V_o are small in relation to V_h, and consequently it is possible to write the anode current as a Taylor series, the first terms of which are:

$$i_a = f(v_h, 0{,}0) + v_i \frac{\partial f}{\partial v_i} + v_o \frac{\partial f}{\partial v_o} + \ldots\ldots \qquad \text{(II A 3)}$$

The first term in the series, $f(v_h, 0{,}0)$, represents the anode current controlled by the heterodyne voltage V_h, if the R.F. input voltage V_i and the I.F. voltage V_o are zero. The currents represented by the other terms are superimposed on this current.

The second term is the product of the instantaneous value of the R.F. input signal V_i and the instantaneous value of the slope of the characteristic $i_a = f(v_i)$. This characteristic refers to the anode and to the grid to which the R.F. input voltage is applied. The slope fluctuates at the frequency of the heterodyne voltage V_h, and accordingly we may write:

$$\frac{\partial f}{\partial v_i} = s_i = S_o + S_1 \cos \omega_h t + S_2 \cos 2\ \omega_h t\ \ldots \qquad \text{(II A 4)}^*$$

in which S_o, S_1 etc. are dependent on the magnitude of V_h.

The product $v_i \dfrac{\partial f}{\partial v_i}$ then becomes:

$$v_i \frac{\partial f}{\partial v_i} = S_o\ V_i \sin \omega_i t + V_i \sin \omega_i t.\ S_1 \cos \omega_h t +$$
$$+ V_i \sin \omega_i t\ .\ S_2 \cos 2\ \omega_h t\ \ .\ .$$

* In this equation the cosine function is used in preference to the sine function, as this simplifies the calculation which follows.

For the amplification of the I.F. voltage the only terms of importance in the above are those which include a frequency ω_0; the only one is:

$$V_i \sin \omega_i t \cdot S_1 \cos \omega_h t = {}^1/_2 S_1 V_i [-\sin(\omega_h - \omega_i) t + \sin(\omega_h + \omega_i) t] = -{}^1/_2 S_1 V_i \sin \omega_0 t + \ldots \quad \text{(II A 5)}$$

As a result of the modulation of the slope S_i by the frequency ω_h, there appears in the anode circuit an I.F. current:

$$I_{o1} \sin \omega_o t = {}^1/_2 S_1 V_i \sin \omega_o t$$

or:

$$I_{o1} = \tfrac{1}{2} S_1 V_i = S_c V_i \ldots \quad \text{(II A 6)}$$

the expression conversion-conductance, S_c, being introduced in place of ${}^1/_2 S_1$. As I_{o1} arises by reason of modulation of the slope, the mixer is also known as modulator valve.

In the third term of equation (II A 3), $\frac{\partial f}{\partial v_o}$ stands for the reciprocal of the anode A.C. resistance. This admittance, Y, is also modulated by the frequency ω_h, so that:

$$Y = Y_o + Y_1 \cos \omega_h t + Y_2 \cos 2\omega_h t + Y_3 \cos 3\omega_h t + \ldots\ldots$$

On multiplying by $V_o \sin \omega_o t$, the frequency ω_o occurs only in the first term; thus:

$$I_{o2} \sin \omega_o t = Y_o V_o \sin \omega_o t$$

or:

$$I_{o2} = Y_o V_o \ldots \quad \text{(II A 7)}$$

The first term of the Fourier series Y_o is the mean value of Y when it is modulated by the frequency ω_h.

For the total I.F. current in equation (II A 3) may now be written:

$$I_o = I_{o1} - I_{o2} = {}^1/_2 S_1 V_i - Y_o V_o \ldots \quad \text{(II A 8)}$$

The minus sign appears because V_o and I_{o1} are in opposite phase and the equation is concerned with amplitudes.

It is clear from the foregoing that a mixing valve behaves in the same way as an R.F. amplifier if the conversion conductance is put in place of the slope and if instead of the normal A.C. resistance the A.C. resistance as mixer $R_i = \frac{1}{Y_o}$ is introduced.

If these quantities are known the conversion gain can be obtained from the equation:

$$A_c = S_c \frac{R_i \,.\, Z_o}{R_i + Z_o}, \quad \ldots\ldots\ldots\ldots\ldots \quad \text{(II A 9)}$$

where S_c is the conversion conductance, R_i the A.C. resistance as mixer, and Z_o the dynamic resistance of the tuned circuit.

In order to obtain high amplification, the A.C. resistance R_i must be large in comparison with the circuit dynamic resistance. In modern broadcast receivers the I.F. band-pass filter has a dynamic resistance of about 160,000—200,000 Ω and the A.C. resistance of the valve should therefore be of the order of 1 MΩ.

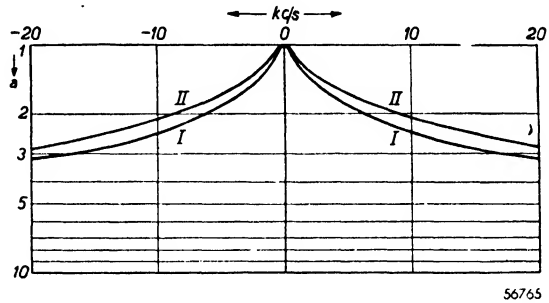

Fig. 66. Influence of the A.C. resistance of the mixing valve on the selectivity of a tuned circuit. I is the selectivity-curve of the circuit, $Q = 50$; II is the curve obtained with a mixer, having $R_i = 1$ Megohm, in parallel with the tuned circuit.

Selectivity is affected by the A.C. resistance in the same way as amplification. This is determined by the quality factor $Q = \frac{\omega L}{r}$ (see chapter I A § 3).

Resistance shunting the tuned circuit may be considered as decreasing Q, that is:

$$\Delta Q = \omega R_i C,$$

where C is the total capacitance of the circuit.

With $C = 100$ pF an A.C. resistance of 1 MΩ decreases the quality factor for an I.F. frequency of 475 kc/s as follows:

$$\Delta Q = 10^6 \times 10^{-10} \times 3 \times 10^5 = 300.$$

The effect of such damping on a tuned circuit with $Q = 50$ is seen in fig. 66, where the attenuation α is shown as a function of the detuning; curve I represents the case in which the valve has an infinite A.C. resistance, curve II that in which the A.C. resistance amounts to 1 MΩ.

§ 2. Calculation of the conversion conductance

If the s_i/v_h characteristic of the valve is known to follow a mathematical law (e.g. a logarithmic characteristic), then with a cosinusoidal oscillator

voltage V_h we can also write s_i as a function of $x = \omega_h t$. It is then possible to calculate S_1 exactly:

$$S_1 = \frac{1}{\pi} \int_0^{2\pi} s_i \cos x \, dx \quad \ldots\ldots\ldots\ldots \quad \text{(II A 10)}$$

In most cases, however, the curve connecting s_i and v_h has no definite mathematical form, and it is therefore necessary to determine the aforementioned coefficient of the Fourier series by graphical means, or to ascertain S_1 by measurement.

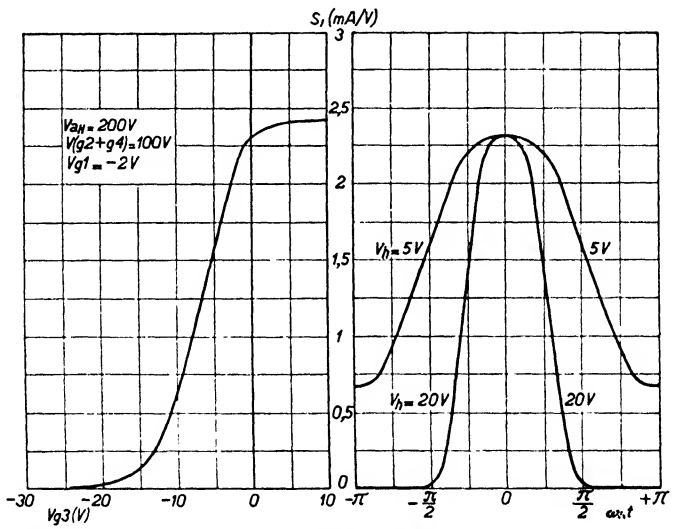

Fig. 67. Left: S_i as a function of the voltage on the third grid, for the UCH 21. Right: S_i as a function of time, for heterodyne voltages of 5 V and 20 V respectively.

Fig. 67 shows the slope s_i of the first grid of the Philips type UCH 21 as a function of the negative voltage v_{g3} on the third grid; the remaining electrodes are at the potentials indicated in the diagram. On the right of the figure, slope is shown against time for two values of the oscillator voltage V_h added to the standing bias *; these curves are deduced from the s_i/v_h characteristic. In order to ascertain the conversion conductance from these time curves, which clearly are not of sine form, we shall divide one cycle of the heterodyne voltage V_h into 4N equal parts.

* The standing negative bias is obtained by using a grid capacitor and grid leak; for every value of V_h there is thus a corresponding standing bias V_{g_s} (see Chapter II, B § 9).

From the s_i/v_h characteristic the slope is now read off for the following values of modulator voltage:

$$V_o = -V_{g3} + V_h;\ V_1 = -V_{g3} + V_h \cos\frac{\pi}{2N} \text{ etc.};$$

$$V_{2N} = -V_{g3} + V_h \cos\frac{2N\pi}{2N}.$$

V_{g3} is the standing negative bias already mentioned, and V_h is the alternating voltage from the oscillator.
The slope corresponding to these voltages will be indicated by:

$$S_o, S_I, S_{II}, S_{III} \ldots\ldots\ldots\ldots S_{2N}.$$

The integral, which determines the amplitude of the fundamental of the Fourier series, approximates to the sum of $4N$ terms.

The amplitudes S_I, S_{II} . S_{III} etc. are multiplied by the corresponding cosines, and for the element dx we take $\frac{1}{4N}$ of the whole cycle 2π .

Furthermore the sum of the first $2N$ terms is equal to that of the last $2N$ terms, so that we can write:

$$S_1 = \frac{2}{\pi}\sum_{o}^{2N} p\ S_p \frac{\pi}{2N} \cos\frac{p\pi}{2N},$$

or:

$$S_1 = \frac{1}{N}\sum_{o}^{2N} p\ S_p \cos\frac{p\pi}{2N} \quad \ldots\ldots\ldots\ldots \text{(II A 11)}$$

As the conversion conductance S_c amounts to half S_1:

$$S_c = \frac{1}{2N}\left\{\frac{S_o}{2} + S_I \cos\frac{\pi}{2N} + S_{II}\cos\frac{2\pi}{2N} + S_{III}\cos\frac{3\pi}{2N} + \ldots\frac{S_{2N}}{2}\right\}\ldots \quad \text{(II A 12)}$$

(In this sum the first and last terms are halved, because if we regard each term dx or $\frac{\pi}{2N}$ as symmetrical in relation to the corresponding x, only half a term remains for the first and last.)

The general term in this series is represented by $S_p \cos\frac{p\pi}{2N}$; here p will have

the values 0–16 inclusive, if we make N equal to 16. We then obtain the following values for $\cos \frac{p\pi}{2N}$:

p	$\cos \frac{p\pi}{32}$	p	$\cos \frac{p\pi}{32}$	p	$\cos \frac{p\pi}{32}$	p	$\cos \frac{p\pi}{32}$
0	1.000	5	0.882	9	0.634	13	0.295
1	0.995	6	0.832	10	0.557	14	0.195
2	0.981	7	0.773	11	0.471	15	0.098
3	0.957	8	0.707	12	0.382	16	0
4	0.925						

If we assume that the grid bias amounts to –19.3 V and the peak oscillator voltage to 20 V, we then find for $S_p \cos \frac{p\pi}{2N}$:

p	V_{g1}	S_p	$S_p \cos \frac{p\pi}{32}$	p	V_{g1}	S_p	$S_p \cos \frac{p\pi}{32}$
0	+ 0.7	2.34	1.17	17	—21.3	—	—
1	+ 0.6	2.33	2.32	18	—23.2	—	—
2	+ 0.3	2.31	2.26	19	—25.1	—	—
3	— 0.2	2.29	2.19	20	—27.0	—	—
4	— 0.8	2.25	2.08	21	—28.7	—	—
5	— 1.7	2.15	1.89	22	—30.4	—	—
6	— 2.7	2.00	1.66	23	—31.9	—	—
7	— 3.9	1.75	1.36	24	—33.5	—	—
8	— 5.1	1.55	1.10	25	—34.7	—	—
9	— 6.7	1.25	0.79	26	—35.9	—	—
10	— 8.2	0.95	0.53	27	—36.9	—	—
11	— 9.9	0.65	0.31	28	—37.8	—	—
12	—11.6	0.45	0.17	29	—38.5	—	—
13	—13.5	0.20	0.08	30	—39.0	—	—
14	—15.4	0.10	0.03	31	—39.3	—	—
15	—17.3	0.05	0.01	32	—39.4	—	—
16	—19.3	—	—				

It follows from this table that:

$$S_c = \frac{1}{32} 17.95 = 0.56 \text{ mA/V}.$$

The conversion conductance for heterodyne voltages of 15, 10, 5 and 2.5 V

is calculated in exactly the same way, and the figures obtained are 0.605, 0.630, 0.425 and 0.190 mA/V. A curve connecting conversion conductance with oscillator voltage (see fig. 68) shows at once that at small values of the

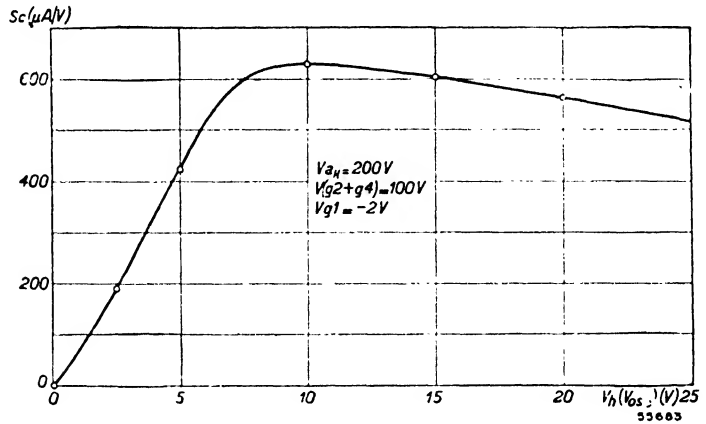

Fig. 68. Conversion conductance of the UCH 21, as a function of the oscillator voltage.

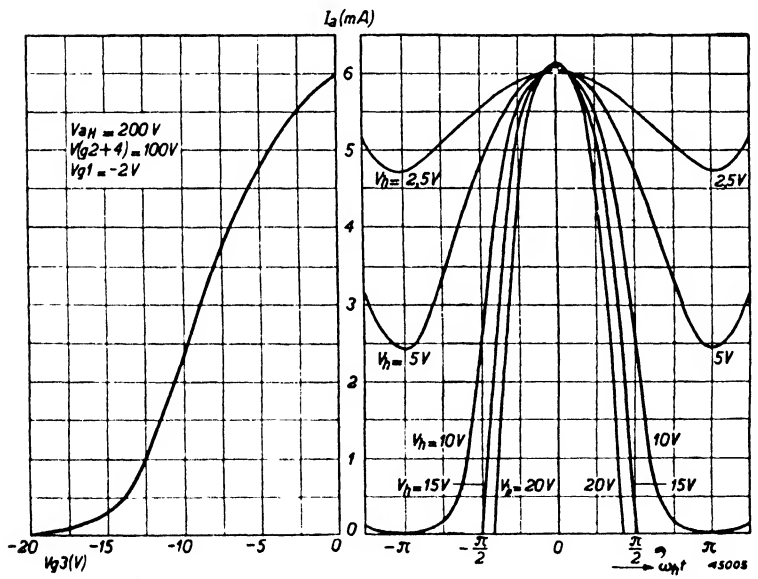

Fig. 69. Left: anode current of the UCH 21, as a function of the voltage on the third grid. Right: anode current of the UCH 21, as a function of time, for heterodyne voltages of 2.5, 5, 10, 15 and 20 V.

latter the conductance rises rapidly until a maximum is reached; thereafter the slope slowly falls as the heterodyne voltage is further increased, owing to the modulator grid becoming much more negative.

In fig. 69 anode current is shown as a function of the voltage on the third grid, and as a function of time, in the same way that slope was depicted in fig. 67. It is clear from this diagram that a greater direct anode current flows with small oscillator voltages than with large ones. The peaks of current seen in the current/time curves become narrower with increasing oscillator voltage, and the direct anode current therefore drops. In Chapter XIII this fact will be seen to have an important bearing on valve noise.

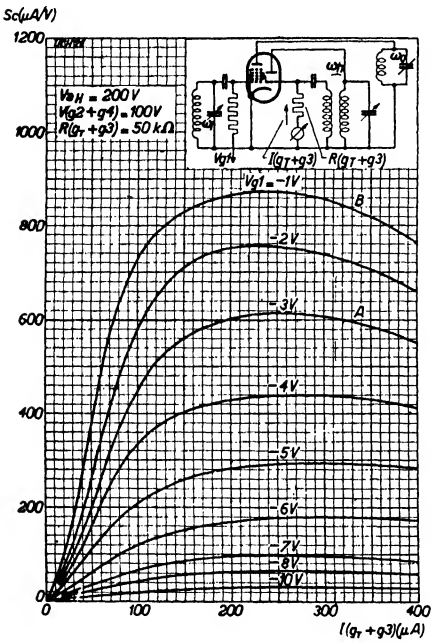

Fig. 70. Conversion conductance of the UCH 21 as a function of the oscillator grid current, for various values of control grid bias.

The foregoing calculation can of course be repeated for other values of standing bias on the R.F.-input grid. In fig. 70 curves connecting S_c and V_{osc} are given for various negative grid potentials, the heterodyne voltage being indicated here by the current $I_{(gT+g3)}$ through the grid leak; this current is easily measured.

The figure shows immediately in what operating conditions the highest conversion conductance is obtainable. The curves are also of interest in that over a given waveband the oscillator voltage is usually not constant but may vary considerably. For two reasons a value of 190 μA is therefore recommended for the current through the resistance $R_{(gT+g3)}$ in the case of the UCH 21:

1) conversion conductance is then a maximum;
2) around this point conversion conductance is fairly independent of the magnitude of the heterodyne voltage.

Finally, the curves of fig. 70 are of value for AVC calculations and in investigating distortion introduced by the valve.

§ 3. Measuring conversion conductance and AC resistance

Calculation of the conversion conductance from the s_i/v_h characteristic is, as we saw above, a rather cumbersome method; furthermore it is not very accurate, and in practice it is therefore usual to resort to measurements. In fig. 71 the set-up for measuring the conversion conductance of a triode-

heptode is given. To the first grid a voltage $V_i \cos \omega_i t$ is applied, say of 0.1 V; the grid bias may be adjusted with the aid of the battery B. To the third grid a heterodyne voltage $V_h \cos \omega_h t$ is fed, negative bias being obtained by means of the grid leak and capacitor connected to the triode section. In the anode lead of the heptode a tuned circuit is connected; this is resonant at the intermediate frequency $\omega_o = \omega_h - \omega_i$, and its dynamic resistance is accurately known. By suitable choice of V_i and Z_o the output

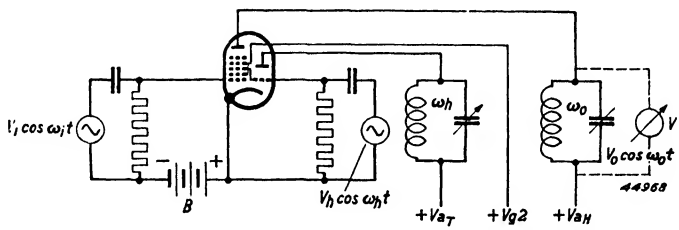

Fig. 71. Circuit for measuring the conversion-conductance and AC resistance of a mixing valve.

voltage V_o appearing in the anode circuit is kept low, in order that its influence on I_o may be negligible. The voltage across the tuned circuit can then be measured directly and the magnitude of the anode current I_o then follows from $I_o = \frac{V_o}{Z_o}$. The conversion conductance is $\frac{I_o}{V_i}$. With some frequency-changers, for instance the pentagrid and the octode, it is essential to take the oscillator section into consideration when making measurements, as the oscillator anode current affects the modulator operating conditions. To measure the A.C. resistance the valve is fed with the same supply voltages as before, and with the requisite oscillator voltage; the anode voltage is then altered by an amount $\triangle V_a$, causing the anode current to change by ΔI_a. The A.C. resistance is then $R_i = \frac{\Delta V_a}{\Delta I_a}$.

§ 4. Mixing circuits

The circuits used in radio receivers may be divided into two classes:

1. those in which the heterodyne and signal voltages are applied to the same electrode of the mixer valve (additive mixing);
2. those in which the heterodyne and signal voltages are applied to different electrodes of the mixer valve (multiplicative mixing).

a. Diode

The simplest circuit in the first group is that which uses a diode as mixing

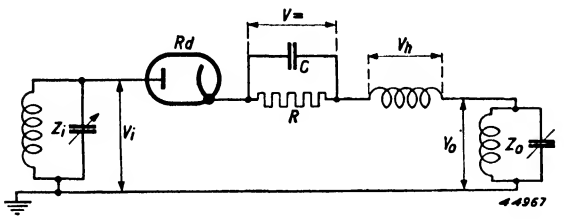

Fig. 72. The diode as mixing valve.

valve. As in this case there is only one current circuit, V_i, V_h and V_o are connected in series, as in fig. 72. If the heterodyne voltage V_h is not made too small, say about 2V, the characteristic of the diode may be represented by a straight line (fig. 73), and the conversion conductance and the amplification are fairly easy to calculate. As will be shown later, it is advisable to apply a standing bias $V_{\overline{\overline{\ }}}$ to the diode; this is achieved simply by including a resistor R in the circuit, across which the rectified current due to V_h causes a potential drop. If R is high in relation to R_d, the A.C. resistance of the diode, then $V_{\overline{\overline{\ }}}$ will approximate to V_h (see Chapter V). In these circumstances a current flows through the diode for part of each cycle, indicated in fig. 73 by $2a$. During this time the slope equals $\frac{1}{R_d}$ but is zero for the remainder of the cycle.

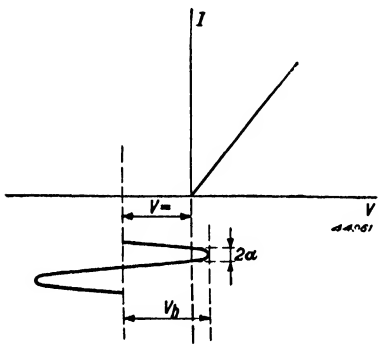

Fig. 73. Current/voltage characteristic of a diode.

In order to calculate the conversion conductance we shall again ascertain the fundamental of the slope from the Fourier series:

$$S_1 = \frac{1}{\pi} \int_0^{2\pi} S \cos x \, dx \quad \ldots\ldots\ldots\ldots \quad \text{(II A 10)}$$

As S is other than nil only between the time points $x = -a$ and $x = +a$, we can also write:

$$S_1 = \frac{1}{\pi} \int_{-a}^{+a} \frac{1}{R_d} \cos x \, dx \quad \ldots\ldots\ldots\ldots \quad \text{(II A 13)}$$

or:

$$S_1 = \frac{1}{\pi} \cdot \frac{1}{R_d} \sin x \Big|_{-a}^{+a} = \frac{2 \sin a}{\pi R_d} \quad \ldots\ldots\ldots \quad \text{(II A 14)}$$

The conversion conductance is thus: $S_c = \frac{\sin a}{\pi R_d}$.

Now in order to ascertain the delivered I.F. voltage V_o it is first necessary to know the I.F. current. This depends not only on the conversion conductance, but, since R_d has a fairly low value, the second term of equation (II A 8) becomes important too. Therefore we must also determine the mean A.C. resistance of the diode.
During the cycle 2π the A.C. resistance is equal to R_d only for th cbrief period $2a$. From this it follows that

$$\frac{1}{Y_o} = R_d \frac{2\pi}{2a} = \frac{\pi R_d}{a} \quad \ldots\ldots\ldots\ldots \quad \text{(II A 15)}$$

The I.F. voltage V_o in equation (II A 8) appears as a potential difference across the I.F. tuned circuit Z_o, and for (II A 8) we may therefore write:

$$I_o = {}^1/_2 S_1 Vi - Z_o Y_o I_o. \quad \ldots\ldots\ldots \quad \text{(II A 16)}$$

or:

$$I_o = V_i \frac{\frac{1}{2} S_1}{1 + Z_o Y_o} \quad \ldots\ldots\ldots\ldots \quad \text{(II A 17)}$$

The conversion gain is thus:

$$A_c = \frac{V_o}{V_i} = \frac{I_o Z_o}{V_i} = \frac{\frac{1}{2} S_1 Z_o}{1 + Z_o Y_o} \quad \ldots\ldots \quad \text{(II A 18)}$$

Gain is greatest when $Z_o Y_o$ is much larger than unity; the quantity 1 in the denominator can then be ignored and the amplification becomes:

$$A_c = \tfrac{1}{2} \frac{S_1}{Y_o},$$

or, after substituting from equations (II A 14) and (II A 15):

$$A_c = \tfrac{1}{2} \frac{2 \sin a}{a} = \frac{\sin a}{a} \quad \ldots\ldots\ldots\ldots \quad \text{(II A 19)}$$

Thus the conversion gain increases as the current angle a diminishes and

approaches $A_c = 1$ when $a = 0$. The advantage of high bias is obvious; without bias a would be $\frac{\pi}{2}$ and A_c would be equal to $\frac{2}{\pi}$.

In order to make the product $Z_o Y_o$ large in relation to unity, Z_o must be so chosen that:

$$Z_o \gg \frac{1}{Y_o} \text{ or } Z_o \gg \frac{\pi}{a} R_d \quad \ldots\ldots\ldots\ldots \quad \text{(II A 20)}$$

The current angle a is determined exclusively by the ratio $\frac{R}{R_d}$ (see II B § 9), and for a small current angle $\frac{R}{R_d}$ must be large; in such a case equation (II B 56) holds good (see page 191) and

$$tan\ a - a = \pi \frac{R_d}{R}.$$

As the input and output circuits are traversed by the diode current, they are both fairly heavily damped. Regarding the damping of the I.F. tuned circuit, it might at first sight be expected that this would amount to Y_o, and this would be the case if the input circuit were a current-source without internal resistance. However, this is not so. To determine the damping R_o of the output circuit we imagine an I.F. voltage V_o in place of the I.F. circuit, and enquire what I.F. current I_o flows in the diode circuit as a result of V_o. The damping is then:

$$R_o = \frac{V_o}{I_o} \quad \ldots\ldots\ldots\ldots\ldots\ldots \quad \text{(II A 21)}$$

Now the voltage V_o causes not only an I.F. current, determined by the admittance Y_o, but also, through mixing, a current of signal frequency which traverses the input circuit. As the arrangement is symmetrical, we can write for this extra current:

$$\Delta I_i = V_o \frac{\frac{1}{2} S_1}{1 + Z_i Y_o} \quad \ldots\ldots\ldots\ldots \quad \text{(II A 22)}$$

Across the input circuit there is then a voltage drop, once again of signal frequency, which through mixing gives rise to a further I.F. current. It is apparent that the input circuit affects the damping of the output circuit.

Taking this voltage drop $V_i = -A\, I_i Z_i$ into account, we get from equation (II A 8):

$$I_o = V_o \left(Y_o - \tfrac{1}{2} S_1 Z_i \frac{\tfrac{1}{2} S_1}{1 + Z_i Y_o} \right);$$

$$\frac{1}{R_o} = \frac{I_o}{V_o} = Y_o - \frac{Z_i S_1^2}{4 (1 + Z_i Y_o)}.$$

By substituting for S_1 and Y_o from equations (II A 14) and (II A 15) we then obtain:

$$\frac{1}{R_o} = \frac{1}{\pi R_d} \left(a - \frac{sin^2 a}{\pi R_d / Z_i + a} \right) \quad \ldots\ldots\ldots \quad \text{(II A 23)}$$

To calculate the damping of the input circuit we need only replace Z_i by Z_o, thus:

$$\frac{1}{R_i} = \frac{1}{\pi R_d} \left(a - \frac{sin^2 a}{\pi R_d / Z_o + a} \right) \quad \ldots\ldots\ldots \quad \text{(II A 24)}$$

The AC resistance R_d of the diode is of the order of 5000 Ω. From equations (II A 23) and (II A 24) it is clear that in order to minimise damping it is important to keep a small. Various factors set a limit however. If a is to be small, the ratio R/R_d must be made large. But as a becomes smaller, less of the diode characteristic is traversed, so that the AC resistance R_d (which varies owing to curvature of the characteristic) increases. For this reason it becomes progressively more difficult to reduce a further, unless impractically large values of V_h are used.

Moreover the reduction of a and the simultaneous increase of R_d lead to difficulty in satisfying equation (II A 20), and amplification declines. The situation in practice is that with likely values of a the damping resistances R_i and R_o are so low that diode-mixing can find no place in domestic receivers. Another drawback, in conclusion, is the fairly tight coupling between the input and oscillator circuits, which results in the receiver radiating on a frequency of ω_h.

An advantage of diode-mixing is the low degree of noise introduced (see chapter XIII).

b. Triode, tetrode and pentode

If instead of a diode a triode or multi-grid valve is employed, considerable reduction of circuit damping becomes possible. With a triode the AC resistance $\frac{1}{Y_o}$ is still rather low, and this type of valve is therefore not much

used as a mixer in broadcast receivers. The tetrode and the pentode were however commonly used in early superheterodynes. Since with these screen-grid valves the back-coupling from the anode circuit to the input circuit is almost completely eliminated, damping of the output circuit is determined by the value of $\frac{1}{Y_o}$, which is generally of the order of 1 MΩ.

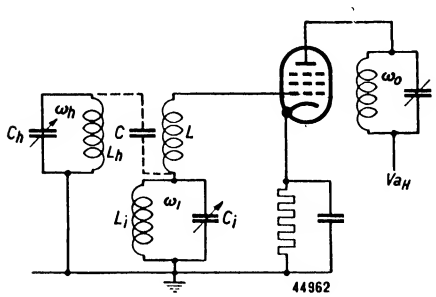

Fig. 74. The pentode as frequency convertor.

In the grid circuit, where V_i and V_h are in series, flow of grid current can be prevented by applying sufficient negative bias; consequently the input circuit also is onlyslightly damped. When calculating the conversion conductance by the method described in § 1, we need therefore to take into account only the first harmonic of the slope, S_1.

An example of the circuit used with this type of valve is given in fig. 74. In the grid circuit the signal-frequency-tuned circuit L_iC_i is joined in series with a coil to which the oscillator circuit L_hC_h is coupled. There exists, however, a certain capacitance C between the inductors L_h and L and thus also between the circuits L_hC_h and L_iC_i. This coupling between the two tuned circuits causes pulling, and also results in radiation from the aerial on a frequency of ω_h. If the coil L and the tuned circuit L_iC_i are interchanged the coupling between the tuned circuits certainly becomes weaker, but a drawback of this arrangement is that neither side of the capacitor C_i may then be earthed directly. Another possibility is the circuit of fig. 75. The two voltages V_i and V_h are now earthed. Although this arrangement avoids the capacitive coupling between the coils, a coupling is now present through the grid-to-cathode capacitance of the valve; this, however, is weaker than in the previous circuit. The voltage of frequency ω_h which appears across the input circuit may be readily calculated with the aid of the equation derived in Chapter ID for a circuit with capacitive coupling.

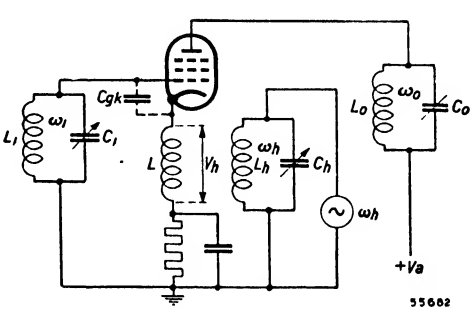

Fig. 75. Another mixing circuit using a pentode.

If the heterodyne voltage V_h were to have the same frequency as the natural resonance of the input circuit, the unwanted voltage V_s transferred to the signal-frequency-tuned circuit would, from equation (I D 4), be:

$$V_s = V_h \frac{C_{gk}}{C_i + C_{gk}} \cdot \frac{\omega_i L_i}{r} \quad \text{(II A 25)}$$

V_h is however considerably off-tune in relation to V_i, so that in reality V_s is smaller. From equation (I A 9) the attenuation a is:

$$a = |1 + j\beta Q| \approx \beta Q.$$

The interference voltage V_s developed across the input circuit is therefore:

$$V_s = \frac{C_{gk}}{C_i + C_{gk}} \cdot \frac{\omega_i L}{r} \frac{1}{\beta Q} V_h = \frac{C_{gk}}{C_i + C_{gk}} \frac{1}{\beta} V_h \quad \text{(II A 26)}$$

where:

$$\beta = \frac{\omega_h}{\omega_i} - \frac{\omega_i}{\omega_h}.$$

V_s is greatest at the bottom of the waveband, for then C_i and β are smallest. Further, the induced voltage is larger on medium than on long waves for a given size of variable capacitor, for β is smaller in the medium than in the long waveband. This we shall illustrate with an example.

Let us suppose that the intermediate frequency is 475 kc/s; at 200 metres ($\omega_i = 9.4 \times 10^6$) $\omega_h = 12.4 \times 10^6$. From this it follows that $1/\beta = 1.8$.

If the grid-to-cathode capacitance of the mixer valve is 5 pF and the tuning capacitance at 200 metres is 80 pF, then the interference voltage amounts to:

$$V_s = \frac{5}{85} \cdot 1.8\ V_h = \text{approx. } 0.1\ V_h.$$

If the oscillator voltage is 10 V, an interfering voltage of 1 V could be developed across the input circuit, enough to cause considerable radiation from the aerial.

As the frequency ω_h is greater than ω_i, the impedance of the input circuit is mainly capacitive on medium and long waves. The voltage V_h is consequently divided over two capacitances, 0.9 V_h appearing between grid and cathode.

At a wavelength of 15 metres β becomes 0.0475, and the interference voltage is then:

$$V_s = \frac{5}{85} \times \frac{1}{0.0475} V_h = 1.24\ V_h.$$

This result seems somewhat strange at first sight. The very high interference voltage is manifestly due to magnification, and the input circuit

thus has, despite what might have been expected, an inductive character. It should not be forgotten, however, that the tuned circuit, including the parallel capacitance C_{gk}, is tuned to ω_i. The circuit itself can therefore easily be resonant at a frequency even higher than ω_h.

Such a value of interference voltage is obviously inadmissible, and for this reason the circuit is quite unsuitable for use on short waves.

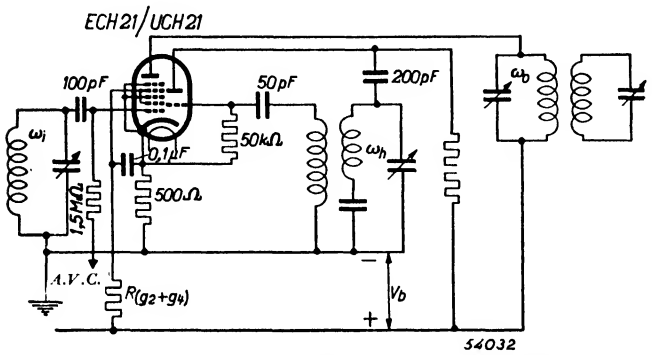

Fig. 76. Circuit diagram of a triode-heptode frequency changer as additive mixer.

A variation of this circuit in which the Philips triode-heptode mixers ECH 21 and UCH 21 are employed is represented in fig. 76. In this circuit the oscillator voltage of the triode part of the valves is induced in the cathode lead by means of a nonshunted resistor of about 500 ohms. The amplitude of this voltage must not, on the one hand, be so great as to give rise to grid current, as otherwise diode mixing would occur at the same time, the effect of which is diametrically opposed to the effect of the desired mixing. On the other hand the oscillator voltage induced has to be of as large an amplitude as possible so as to get sufficient conversion conductance. In this connection it is essential that the working point of the oscillator triode should be in the straight part of the curve (class A adjustment). Unless special precautions are taken, however, there will arise in the aerial circuit induction voltages amounting to about 0.1 V at 1500 kc/s and about 0.5 V at 20 Mc/s. This induction voltage would give rise to excessive radiation in the aerial. The radiation voltage can, however, be easily compensated by coupling the wiring leading to the triode-anode to that leading to the input circuit of the heptode part, this coupling being done behind the waveband switch. Owing to this compensation the induction voltage in the aerial circuit is reduced to about 1-2 mV in the medium and long-wave ranges and to about 5-10 mV in the short-wave range.

Since the cathode is connected to the bottom screening and the latter also carries the radiation voltage, it is necessary to place a screening can round the valve. Finally it is essential that the screen-grid decoupling capacitor should be connected to the cathode and not to the chassis.

Although the conversion conductance of the ECH 21 and the UCH 21 is

lower (about 550 μA/V) in this form of circuit than in the classical circuit (fig. 78), this method of circuiting has the advantage of a lower noise level, the equivalent noise resistance being 15,000 Ohms as compared to 55,000 Ohms in the circuit of fig. 78.

The simplest circuit in which V_i and V_h are applied to separate electrodes employs a triode with the input voltage fed to the grid and the oscillator voltage to the anode. This arrangement has been used in the past, but it has the serious drawback of requiring a high heterodyne voltage, while the circuits are still coupled to some extent through the capacitance C_{ag}.

It is more satisfactory to use valves possessing separate negatively-biased control grids, so that the slope of one grid may be modulated by the heterodyne voltage applied to another grid. Two possibilities then exist:

1. to modulate the electron stream first by the R.F. voltage andthen by the oscillator voltage;
2. to modulate the electron stream first by the oscillator voltage and then by the R.F. voltage.

c. *Hexode and heptode*

In the first of the above-mentioned groups we may include hexodes and heptodes which have an independent built-in oscillator section, and also the Philips self-oscillating hexode E 448.

To the second category belong self-oscillating mixers such as the pentagrid, the octode, and valves like the American type 6SA7.

Fig. 77 shows the basic circuit for a heptode. The R.F. input is applied to the first grid, and the oscillator voltage to the third grid. The electron stream is drawn through the first (control) grid by the positive voltage at the second (screen) grid, and this voltage imparts such velocity to the electrons that they rush through the meshes of this electrode and reach the neighbourhood of the third (modulator) grid. A space-charge or virtual cathode appears before the negatively-biased third grid, its density being determined by the quantity of electrons permitted to pass through the first grid. From this space-charge cloud, pulsating in tune with the signal voltage on the first grid, the strongly-positive fourth grid sucks electrons, and these fly through the meshes of the third and fourth grids to the anode. The electrons in the space-charge cloud have varying speeds. Some aim straight for the third

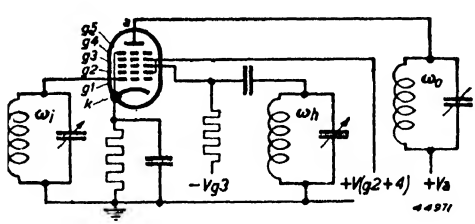

Fig. 77. The heptode as mixing valve.

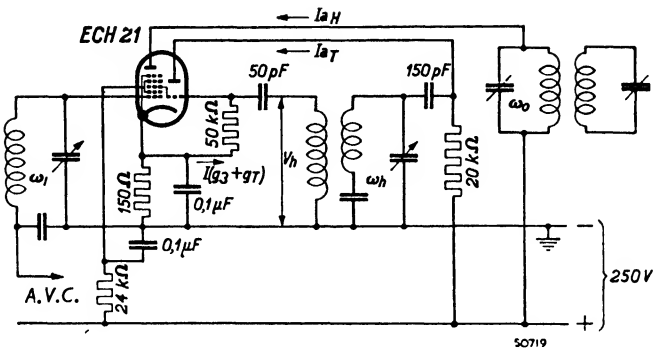

Fig. 78. Complete mixing circuit for the triode-heptode ECH 21.

grid and nearly reach it, others go off at a tangent. A slightly increased potential at the third grid is enough to draw the former electrons right through and on towards the fourth electrode, while the obliquely-moving electrons require a higher third-grid voltage if they are to be pulled through. The fraction of the space-charge which reaches the anode is thus roughly proportional to the voltage rise at the third grid. First the electron stream was modulated by the voltage on the first grid, and then by that on the third. The screen grid between the first and third electrodes serves to reduce the capacitance between these grids, and so to minimise interaction between the signal-frequency and oscillator circuits. The fourth grid fulfils the same function as the screen grid in a pentode and results in the A.C. resistance being high; the fifth grid, like the suppressor grid in a pentode, prevents harmful secondary-emission effects.

The slope of the control-grid/anode characteristic depends on the voltage at the third grid. If the last-named electrode has a large negative potential, few electrons reach the anode and the slope is therefore low. By applying the oscillator voltage through a grid capacitor and leak, the potential on the third grid is made to vary between zero and a certain maximum negative value. The conversion conductance can be deduced from the S_{g1a}/V_h characteristic by the Fourier method described in II A § 2.

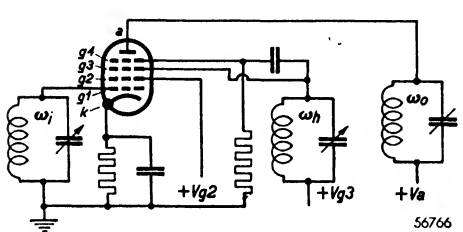

Fig. 79. Mixing circuit using the self-oscillating hexode E 448.

Fig. 78 shows the basic circuit for the combination valve ECH 21, which comprises a heptode and an oscillator-triode in one bulb.

The working of the self-oscillating hexode (fig. 79) is best understood by thinking of it as two valves put together:

1. a tetrode: cathode, control grid g_1, screen-grid g_2 and anode g_3;
2. a triode: virtual cathode between g_3 and g_4, control grid g_4 and anode a.

The R.F. circuit is shielded from the oscillator circuit by the screen grid g_2. The first grid/anode slope S_{g1a} depends on the oscillator voltage on the fourth grid. Anode current is practically nil when the fourth grid is strongly negative, all electrons then going to the third grid. As the fourth electrode becomes less negative, more electrons reach the anode and the electron stream to the third grid diminishes. Thus the fourth grid possesses a negative slope in relation to the third grid, and this property may be utilised for the generation of oscillation by connecting a tuned circuit in the lead to the third grid and coupling it capacitively to the fourth grid.

The greatest drawback of the self-oscillating hexode is that its gain cannot be controlled by variation of the bias on the control grid, for when the voltage on this electrode becomes more negative the electron stream is reduced; the negative slope S_{g1g3} then declines and may cause the valve to cease oscillating. In modern receivers this type of valve is no longer employed.

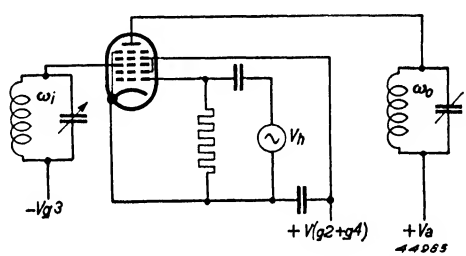

Fig. 80a. The 6SA7 as mixing valve, with a separate oscillator.

d. Pentagrid and octode

As first representative of the second group, i.e. multi-grid valves in which the modulator grid comes before the control grid, we cite the American type 6SA7 (fig. 80a). The first screen grid of this valve lies between the modulator grid and the input grid. This screen grid attracts electrons from the cathode and these form a space-charge in front of the negatively-biased third grid. The modulated space-charge now serves as cathode for the pentode, the slope of which is controlled by the signal voltage. The screen grid also prevents coupling between the modulator grid and the input grid.

In fig. 80a the heterodyne voltage V_h is supplied externally, but the 6SA7 is also much used as a self-oscillating valve in the circuit of fig. 80b. Here we have a Hartley oscillator, the cathode being connected to a tap on the coil (see Chapter II, B § 8). In addition to the voltage of frequency ω_h between the cathode and the first grid, a similar voltage is present between the third grid and the cathode, and both voltages contribute to the mixing

process. They work in opposition, however, and the conversion conductance is in consequence only about half that obtained when a separate oscillator is used. Furthermore there exists a danger, which is present in any circuit where there is an alternating voltage between heater and cathode, of crackling and other disturbing noises, due to the inconstancy of the heater/cathode insulation.

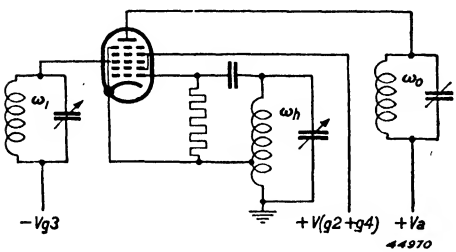

Fig. 80b. The 6SA7 as self-oscillating mixer.

Another disadvantage of circuits which include an impedance in the cathode lead is that the I.F. current causes a potential drop across the impedance; a feedback voltage is consequently applied to the third grid and the original I.F. current is reduced.

The 6SA7 possesses five grids and consequently is called a pentagrid; its working is however entirely different from that of the ordinary American pentagrid, which resembles the European octode. Neither the ordinary American pentagrid nor the octode suffers from the drawbacks mentioned above.

Both have an additional electrode, called the oscillator anode, mounted between the modulator grid and the first screen grid. This oscillator anode is small and absorbs only a fraction of the emission from the cathode; the voltage at this anode scarcely affects the mixing process. With the cathode, the first grid and the oscillator anode form a complete oscillator triode; next comes a screen grid, and after that there is a tetrode (in the pentagrid) or a pentode (in the octode).

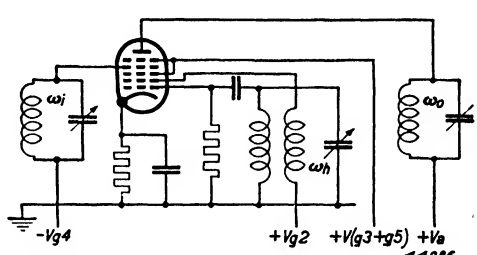

Fig. 81. The pentagrid mixing valve.

The pentagrid has a somewhat low working A.C. resistance, equal to the mean static A.C. resistance [equation (II A 7)]; but secondary emission from the anode to the screen grid affects the effective A.C. resistance unfavourably. The difficulty is overcome in the octode by introducing a suppressor grid between the screen grid and the anode. Thus the octode has six grids altogether, the first of which is the modulator grid, the second the oscillator anode, the third a screen grid, the fourth the control grid, the fifth a screen grid and the sixth the suppressor grid. In the DK 21 battery-octode the construction is somewhat

different, for the first screen grid is omitted and its function performed by the oscillator anode. This electrode consists in the DK 21 of four small rods, so placed that most of the electrons become bunched in passing between them to the control grid. A few of the electrons, however, go straight to the oscillator anode. By beaming the electrons in this way it is possible to obtain a better conversion conductance than with the normal type of octode. In place of the third grid in the ordinary octode, the DK 21 has two small rods which are bonded to the first grid; these serve to compensate for the coupling which exists between the R.F. input grid and the oscillator section. The basic circuit for the DK 21 is given in fig. 82 *.

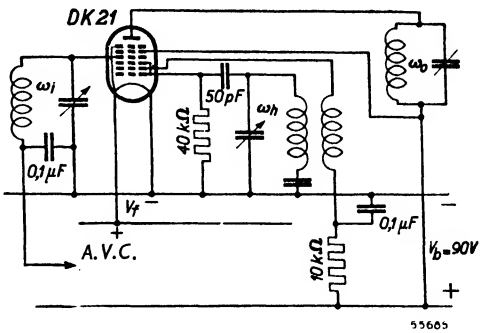

Fig. 82. The DK 21 battery octode as mixing valve.

* An exact description of this valve is published in: Data and circuits of modern receiver and amplifier valves (Supplement) Book III.

B. Properties of oscillator circuits

§ 1. Introduction

The published data usually quote an optimum value of heterodyne voltage for the mixer valve in question, but methods of obtaining the necessary voltage are not normally indicated. When it comes to using the valve in a practical circuit, opposing requirements are encountered. In the first place, it is necessary to cover a whole band of frequencies, yet the oscillator voltage should not at any point diverge from the recommended optimum value. This, as will be seen, is almost impossible to achieve. The problem, then, is to find means of influencing the oscillator voltage so that the ideal constancy is approached as closely as possible. Further questions are the value of mutual conductance needed for the generation of the required oscillator voltage, and the current consumption which is demanded. There are many types of oscillator circuit; in order to choose the most satisfactory type we shall consider some of the arrangements most often used, noting especially the factors which determine the magnitude of the heterodyne voltage. We begin with the basic circuit of a reaction-back-coupled valve (fig. 83).

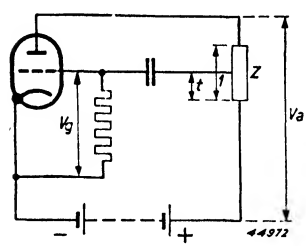

Fig. 83. Basic circuit of a back-coupled valve.

In this, as in all other oscillator circuits, there is an impedance Z in the anode circuit. Oscillation appears in this impedance, giving rise to an alternating anode voltage V_a. By one means or another a proportion $V_g = t \, . \, V_a$ of this anode voltage is tapped off and applied to the grid. Ignoring, for the moment, the existence of the grid capacitor and leak, an alternating anode current occurs of:

$$I_a = S \, V_g = S \, t \, V_a \, . \, . \, . \, . \, . \, . \, . \, . \, . \, . \, . \, . \quad \text{(II B 1)}$$

and oscillation is thereby maintained. In this expression the effect of the anode load Z on the anode voltage is neglected, but correction is made by regarding the effective A.C. resistance as a shunt across Z.

A voltage is developed across the anode impedance:

$$V_a = -S \, V_g \, Z = -S \, t \, V_a \, Z \, . \, . \, . \, . \, . \, . \, . \quad \text{(II B 2)}$$

For the maintenance of oscillation, the ratio of the alternating voltages at grid and anode, and S and Z must have such values that the resultant voltage V_a at the anode at least equals the figure assumed to begin with. Thus:

$$-S\,t\,V_a\,Z = V_a,$$

or:

$$t\,S\,Z = -1 \quad \text{(II B 3)}$$

This equation applies to all oscillator circuits and may be regarded as expressing the condition for oscillation. If we take S as the slope at the moment when oscillation begins, this is the minimum, at corresponding values of t and Z, for starting oscillation, but if S is the effective slope * for a given amplitude this is the condition for maintaining oscillation.

With normal positive values of S and Z the voltage division t is found to be negative, i.e. the grid voltage must be in opposite phase to the anode voltage.

It is necessary to ensure that equation (II B 3) is more than satisfied at the moment when oscillation begins. As amplitude grows, the grid generally becomes more negative due to grid-rectification (see Chapter V), and the effective slope diminishes. This decline goes on until the equilibrium represented by equation (II B 3) is reached; oscillation then remains constant.

The alternating voltage V_a obtained in the anode circuit must be identical both in phase and amplitude to the anode alternating voltage assumed to begin with. To conclude that the phase is bound to be correct is not justifiable, for generally Z is a tuned circuit, in which in certain circumstances marked phase-shift can occur. Moreover, the device employed to tap the anode voltage, consisting of some combination of L, C and R, may introduce shift varying with frequency.

In such a case the circuit would adjust itself to such a frequency of oscillation that the phase-shift in Z would be compensated by that in the tapping t, thereby again bringing I_a and V_g into phase.

This automatic phase adjustment will not, on the wavelengths used for broadcasting, be hindered by phase-shift due to electron transit-time, as the latter effect is then negligible. How the frequency adjusts itself until phase-equilibrium is reached is not easy to explain by pure physics. The most we can say is that a stable condition is unimaginable without balanced phase. By mathematics it is however fairly easy to demonstrate that phase-equilibrium must eventually supervene; this may be done by solving the

* The exact definition of S_{eff} is given on page 151.

differential equation of the system. Such an equation really sets out the building-up process, though it is not particularly easy to understand. This mathematical treatment is not of great importance here, but it will be encountered in general form in Chapter XI with reference to instability and stability of electronic circuits.

We may also say that in equation (II B 3) S is real, whereas t and Z may be complex. The equation can be satisfied only when $t.Z$ is real; as in most cases t is real, Z must be too.

Normal back-coupled circuits all contain a tuned circuit, from which the grid voltage is tapped off in such a way that t is real and the correct phase is obtained. Since S and Z are positive quantities, the coupling ratio t must be negative; this means, as already mentioned, that reversal of phase must be provided. One of the common methods of tapping off the grid voltage is the inductive coupling, with which phase-reversal is very simply accomplished.

We shall now consider a practical case in which Z is a tuned anode circuit. Usually part of the voltage across this impedance is taken off by means of an inductive coupling and applied to the grid; the coupling ratio t is less than 1 because for practical reasons the coupling coil has fewer turns than the tuning inductor. It is also possible, however, to put the coupling coil in the anode lead; Z then represents the impedance of the tuned circuit as reflected into the anode circuit. Z being low, the voltage developed across it is also low and has to be transformed up; the feedback ratio is thus greater than 1.

Equation (II B 3) makes plain that the requisite slope will usually vary over a waveband, mainly because the impedance Z alters with frequency; in many circuits, too, the voltage-division t is also dependent on frequency.

§ 2. Effective slope and anode current in oscillator valves having a straight characteristic

To simplify our investigation we shall assume for the present that the i_a/v_g characteristic of the oscillator valve is straight and that a sine-wave voltage is fed to the grid. Further, we shall suppose that the grid capacitor and leak give a bias voltage equal to the peak amplitude of the applied alternating voltage.

The situation is shown diagrammatically in fig. 84. With a small grid swing, which does not result in the cut-off point V_{go} being overstepped, a sinusoidal anode current (I) appears. With larger grid inputs the anode current consists of a series of separated pulses (II). In the first case the slope does not need further explanation, but in the second, where the anode

current is distorted, we must regard the oscillation as being maintained by that component of the anode alternating current which is of oscillator frequency. In order to determine the magnitude of this component, we have to ascertain what fundamental is contained in curve II of fig. 84; *the effective slope is then the ratio of this current component and the alternating grid voltage.*

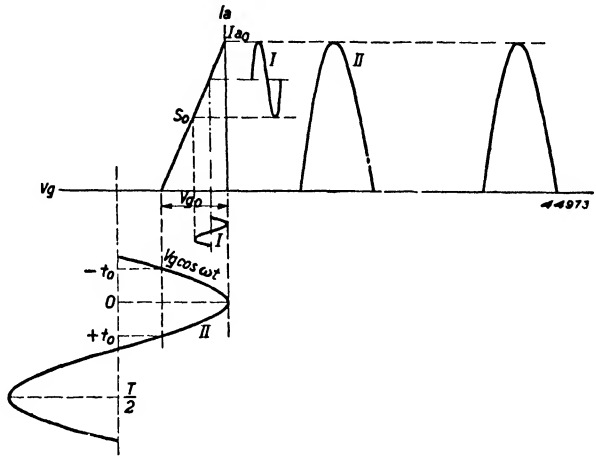

Fig. 84. Idealised straight characteristic of an oscillator valve. In case I the alternating voltage at the grid is so small that the cut-off point V_{go} is not overstepped. In case II the grid alternating voltage is greater than V_{go} and the anode current accordingly consists of pulses.

If the alternating voltage applied to the grid is of amplitude V_g, the fundamental appearing in the anode current will have an amplitude of:

$$I_{a1} = V_g S_{eff} \quad \ldots\ldots\ldots\ldots\ldots \quad \text{(II B 4)}$$

When $I_a \geqslant 0$, the equation for curve II of fig. 84 is:

$$i_a = S_o \{ V_g \cos \omega t - (V_g - V_{go}) \}. \quad \ldots\ldots \quad \text{(II B 5)}$$

The amplitude of the fundamental is now found by Fourier's method from the equation:

$$I_{a1} = \frac{2}{T} \int_o^T i_a \cos \omega t \, dt.$$

Here we must substitute i_a from equation (II B 5). Since a contribution to the integral occurs only while i_a has a value other than nil, we finally integrate between the points $-t_o$ and $+t_o$ at which the current begins and ceases, and obtain the following result:

$$S_{eff} = \frac{I_{a1}}{V_g} = 2 \frac{S_o t_o}{T} - \frac{S_o}{2\pi} \sin 2 \omega t_o,$$

or:

$$\frac{S_{eff}}{S_o} = \frac{\omega t_o}{\pi} - \frac{\sin 2 \omega t_o}{2 \pi} \quad \ldots\ldots\ldots\ldots \quad \text{(II B 6)}$$

in which:

$$\omega t_0 = arc\cos\frac{V_g - V_{go}}{V_g}.$$

It follows, as was to be expected, that the effective slope is proportional to the normal slope, and otherwise depends only on the ratio $\frac{V_g}{V_{go}}$.

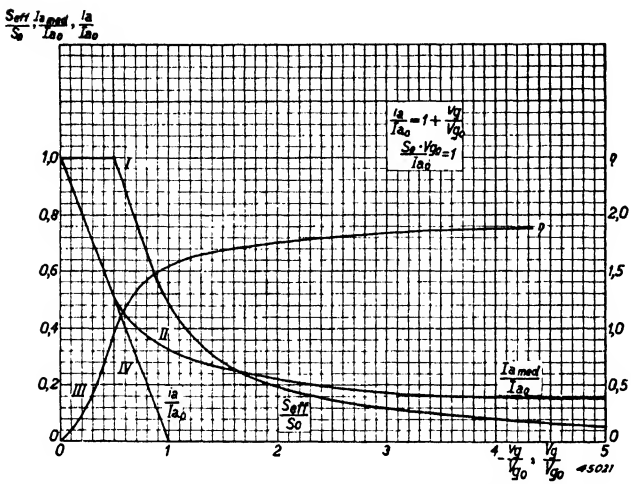

Fig. 85. $\frac{S_{eff}}{S_o}$, $\frac{I_{a\,med}}{I_{ao}}$ and η as functions of $\frac{V_g}{V_{go}}$, when $\frac{S_o \cdot V_{go}}{I_{ao}} = 1$ (straight characteristic). Curve IV represents the relative i_a/v_g characteristic.

Using a table of sines we can now easily calculate from equation (II B 6) the magnitude of S_{eff}/S_o for various values of V_g/V_{go} and plot a curve connecting these quantities (fig. 85, curve I). As long as V_g is less than $^1/_2 V_{go}$ the effective slope is of course constant and equal to S_o. The curve being drawn to a universal scale, it is applicable to all valves with a straight characteristic.

Similarly the i_a/v_g curve may be expressed in universal form; the equation

$$i_a = I_{ao} + S_o v_g$$

is then written as

$$\frac{i_a}{I_{ao}} = 1 + \frac{S_o \cdot v_g}{I_{ao}} = 1 + \frac{v_g}{V_{go}} \quad \ldots\ldots\ldots \quad (II\ B\ 7)$$

This equation is represented by curve IV of fig. 85; the horizontal axis is in terms of $-v_g/V_{go}$.

If we consider one particular valve, so that V_{go} and S_o are fixed, we see from curve I that the alternating grid voltage, roughly speaking, is inversely proportional to the effective slope; and it is this grid voltage V_g which in almost all circuits is employed as the heterodyne voltage for the mixer valve. If in a given circuit the required slope increases over a waveband

in the ratio 1 : 3, the oscillator voltage will decrease in about the same ratio, at any rate as long as V_g remains greater than $\frac{1}{2}\ V_{go}$. This holds for every valve with a straight characteristic. The choice of V_{go} and S_o will not affect the variation, because only the scale of the curve in fig. 85 is thereby modified; the inverse proportion between V_g and S_{eff} remains unchanged. The slope S_o and the cut-off voltage V_{go} are important in other respects too. There are limits to Z and t, and a certain minimum slope is therefore needed if equation (II B 3) is to be satisfied.

To make this clear, let us consider an oscillator in the short wave band of 15—50m with a tuned anode circuit; Z will then be not much more than 5000 Ω. Experience shows that the absolute value of the feedback ratio t should not, if possible, exceed 1 if tuning difficulties are to be avoided. It follows that for a coupling ratio of say —0.5 the minimum value of S_{eff} *is*:

$$S_{eff} = \frac{-1}{t.\,Z} = \frac{-1}{-0{,}5 \times 5000} = 0{,}4\ \text{mA/V}.$$

There is, therefore, a certain minimum effective slope which must be provided. For this given effective slope and various values of the normal slope S_o we find the corresponding V_g/V_{go} ratio from curve I of fig. 85. Remembering that there is for every mixer valve an optimum heterodyne voltage, which the alternating grid voltage of the oscillator must equal, it is clear that the relation V_g/V_{go} fixes the cut-off voltage V_{go} for the chosen value of S_o. The characteristic is thus determined by S_o and V_{go}.

The required slope S_{eff} and the oscillator voltage V_g can therefore be obtained with various ratios S_{eff}/S_o and V_g/V_{go}; the question is, what values is it desirable for these ratios to have. If we make S_o smaller, curve I of fig. 85 shows that the ratio V_g/V_{go} also decreases. Fig. 84 shows what this means; we go from case II to case I, and get a quite small alternating current superimposed on an unwanted and wasteful direct current. Clearly it is well to relate the choice of S_o to the current consumption of the valve. In order that the required oscillator voltage V_g may be available at the tapping tZ, a certain A.C. component is necessary in the anode current; usually we try to ensure that the mean anode current is as small as possible in relation to this alternating current, by appropriate choice of V_g/V_{go} and S_{eff}/S_o.

For small amplitudes of V_g, I_a is always greater than nil and consequently the mean current Ia_{med} is determined by the mean grid voltage, which is equal to $-v_g$ (fig. 84). In this case, therefore:

$$Ia_{med} = I_{ao} - S_o\ V_g = I_{ao} - \frac{I_{ao}}{V_{go}}\ Vg = I_{ao}\left(1 - \frac{V_g}{V_{go}}\right) \ldots \quad \text{(II B 8)}$$

V_g here denotes the amplitude of the grid swing and is therefore a positive figure, in contradistinction to v_g in equation (II B 7).
With amplitudes greater than $\frac{1}{2}\ V_{go}$ the current is intermittent and the mean value Ia_{med} must be ascertained from equation (II B 5), thus:

$$Ia_{med} = \frac{1}{T} \int_o^T i_a \, dt.$$

The value of i_a is derived from equation (II B 5). We may in this instance confine our attention to the period from $-t_o$ to $+t_o$, where t_o is given by:

$$\omega t_o = arc\ cos \frac{V_g - V_{go}}{V_g}.$$

Integrating we obtain:

$$Ia_{med} = S_o \left| (V_{go} - V_g) \frac{\omega t_o}{\pi} + \frac{V_g}{\pi} \sin \omega t_o \right|.$$

If we substitute $\frac{Ia_o}{V_{go}}$ for S_o we can write:

$$\frac{Ia_{med}}{I_{ao}} = \left(1 - \frac{V_g}{V_{go}}\right) \frac{\omega t_o}{\pi} + \frac{1}{\pi} \frac{V_g}{V_{go}} \sin \omega t_o \quad . \quad . \quad \text{(II B 9)}$$

This relation between $\frac{Ia_{med}}{I_{ao}}$ and $\frac{V_g}{V_{go}}$ is indicated in curve II of fig. 85. The first part of the curve is determined by equation (II B 8), and coincides therefore with the static characteristic (curve IV).
For the amplitude of the AC component we can write:

$$I_{a1} = S_{eff}\, V_g = \frac{S_{eff}}{S_o} V_g\, S_o,$$

and for the average anode current:

$$Ia_{med} = \frac{Ia_{med}}{I_{ao}} I_{ao} = \frac{Ia_{med}}{I_{ao}} S_o\, V_{go}.$$

Consequently the current efficiency is:

$$\eta = \frac{I_{a1}}{Ia_{med}} = \frac{\frac{S_{eff}}{S_o}}{\frac{Ia_{med}}{I_{ao}}} \frac{V_g}{V_{go}} \quad . \quad . \quad . \quad . \quad . \quad . \quad . \quad . \quad . \quad \text{(II B 10)}$$

The efficiency figure is therefore found by dividing the values from curve I by the corresponding values from curve II and multiplying this quotient by the corresponding values of $\frac{V_g}{V_{go}}$. Thereby we obtain curve III of fig. 85. It is apparent that efficiency remains fairly constant over a considerable range but falls off rapidly when $\frac{V_g}{V_{go}}$ becomes less than 1; accordingly S_o may be reduced without greatly affecting current consumption if care is taken to keep $\frac{V_g}{V_{go}}$ above unity. If we choose for S_{eff} the minimum value of 0.4 mA/V, which was the figure calculated on page 153, we then find from fig. 85 that, for $\frac{V_g}{V_{go}} = 1$, the slope of a hypothetical valve with a straight characteristic is $S_o = \frac{0.4}{0.5} = 0.8$ mA/V.

§ 3. Effective slope and anode current in oscillator valves having a quadratic characteristic

In order to bring the foregoing discussion more into line with reality, without sacrificing accuracy of calculation, we shall now regard the valve characteristic as approximating to a quadratic curve.

Thus:

$$i_a = I_{ao} + \alpha v_g + \beta v_g^2 . . . . . \text{(II B 11)}$$

In order to make this equation more convenient for practical use, we shall replace the parameters α and β by values which can be taken directly from the characteristic. In the case of a straight characteristic these would be I_{ao} and S_o or, after conversion, I_{ao} and V_{go}. We shall use these values again here and express the parameters for a quadratic characteristic in I_{ao}, S_o and V_{go}.

At $V_g = 0$ we find that $i_a = I_{ao}$, and the slope S will then be:

$$\frac{di_a}{dv_g} = \alpha + 2\beta v_g = S$$

Therefore, when $v_g = 0$, $S = S_o = \alpha$.

When $v_g = -V_{go}$, i_a must be zero, so that:

$$0 = I_{ao} - \alpha V_{go} + \beta V_{go}^2.$$

Substituting $\alpha = S_o$, we get:

$$\beta = \frac{S_o V_{go} - I_{ao}}{V_{go}^2}.$$

A quadratic equation may therefore be written:

$$i_a = I_{ao} + S_o v_g + \left(\frac{S_o V_{go} - I_{ao}}{V_{go}^2} \right) v_g^2 \quad . \quad . \quad . \quad \text{(II B 12)}$$

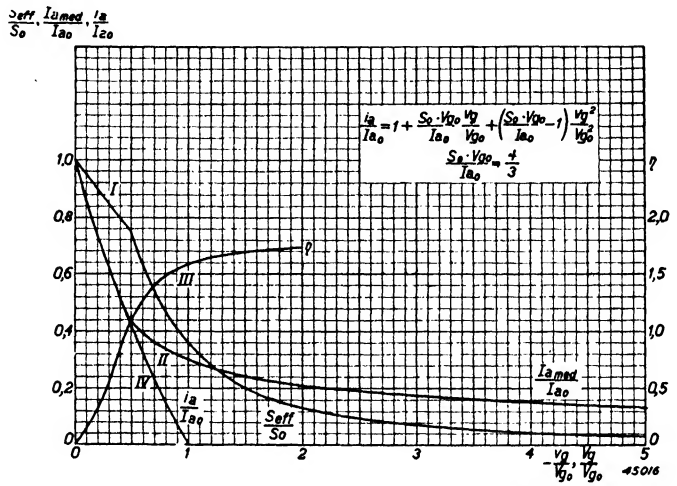

Fig. 86. $\frac{S_{eff}}{S_o}$, $\frac{I_{a\,med}}{I_{ao}}$ and η as functions of $\frac{V_g}{V_{go}}$, when $\frac{S_o V_{go}}{I_{ao}} = \frac{4}{3}$ (quadratic characteristic). Curve IV represents the relative i_a/v_g characteristic.

If we wish to use the universal scale as in equation (II B 7) we may write (II B 12) as follows:

$$\frac{i_a}{I_{ao}} = 1 + \frac{S_o V_{go}}{I_{ao}} \frac{v_g}{V_{go}} + \left(\frac{S_o V_{go}}{I_{ao}} - 1 \right) \frac{v_g^2}{V_{go}^2} \quad \text{(II B 13)}$$

The form of this universal characteristic is determined by the value of the parameter $\frac{S_o V_{go}}{I_{ao}}$; if we make this equal to unity, the characteristic becomes straight. A slightly curved line results when the parameter equals $\frac{4}{3}$ (see curve IV of fig. 86), and with a value of 2 there is marked curvature (see curve IV of fig. 87). The v_g axis is a tangent of this last curve.

By means of these curves we can, in the same way as on page 154, calculate

the effective slope, the mean anode current, and the current-efficiency * of the fundamental. Here again it is assumed that the negative bias is equal to the amplitude of the A.C. voltage at the grid. We then obtain the curves of figs 86 and 87, which are seen not to differ greatly from those of fig. 85; the similarity indicates that the conclusions derived from the calculations for a straight characteristic are of value also in the case of quadratic valve-characteristics.

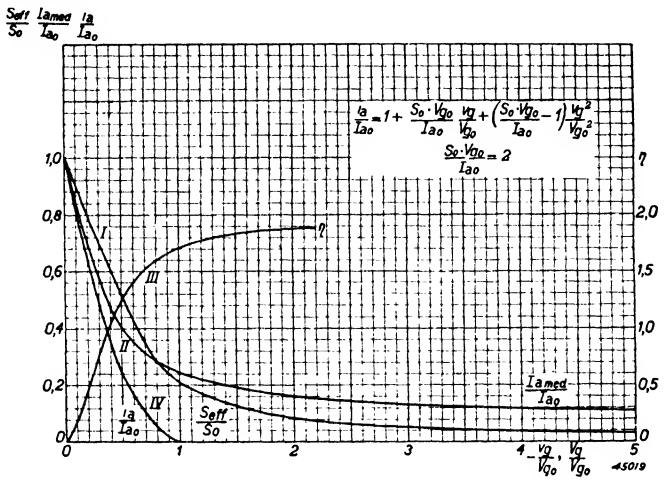

Fig. 87. $\frac{S_{eff}}{S_o}$, $\frac{I_{a\,med}}{I_a}$ and η as functions of $\frac{V_g}{V_{go}}$, when $\frac{S_o \cdot V_{go}}{I_{ao}} = 2$ (quadratic characteristic). Curve IV represents the relative i_a/v_g characteristic.

Referring to curve IV of fig. 87, which most nearly resembles an actual characteristic, we find that with $\frac{V_g}{V_{go}} = 1$ the current efficiency is about the same as for a straight characteristic.

$\frac{S_{eff}}{S_o}$, however, is a good deal smaller than in the previous case: about 0.2, against 0.5. An effective slope of 0.4 mA/V therefore necessitates a normal

* This follows from the first two curves. We can again write:

$$I_{a_1} = S_{eff} V_g = \frac{S_{eff}}{S_o} V_g S_o = \frac{S_{eff}}{S_o} \frac{V_g}{V_{go}} S_o V_{go}; \quad I_{amed} = \frac{I_{amed}}{I_{ao}} I_{ao};$$

$$\eta = \frac{I_{a_1}}{I_{amed}} = \frac{\frac{S_{eff}}{S_o}}{\frac{I_{amed}}{I_{ao}}} \frac{V_g}{V_{go}} \frac{S_o V_{go}}{I_{ao}}.$$

This time, however, we must insert a value of 4/3 for $\frac{S_o V_{go}}{I_{ao}}$ in the case of the characteristic in fig. 86, and 2 in the case of the fig. 87 characteristic. For a straight characteristic (fig. 85) $\frac{S_o V_{go}}{I_{ao}}$ was equal to unity.

slope of:

$$S_o = \frac{0.4}{0.2} = 2 \text{ mA/V}.$$

This agrees with what we find in practice.
If the oscillator voltage $V_g = 12$ V (say 8 V_{RMS}), then it follows from $S_{eff} = 0.4$ mA/V that:

$$I_{a1} = 0.4 \times 12 = 4.8 \text{ mA}.$$

Further, at $\frac{V_g}{V_{go}} = 1$ we find that the efficiency $\eta = 1.72$, and accordingly the mean anode current will be:

$$Ia_{med} = \frac{I_{a1}}{\eta} = 2.8 \text{ mA}.$$

§ 4. Measurement of effective slope and anode current

In order to find out how well the suppositions in the preceding discussion agree with conditions in practice, a number of test measurements were made using the circuit of fig. 88, and the relation between oscillator voltage

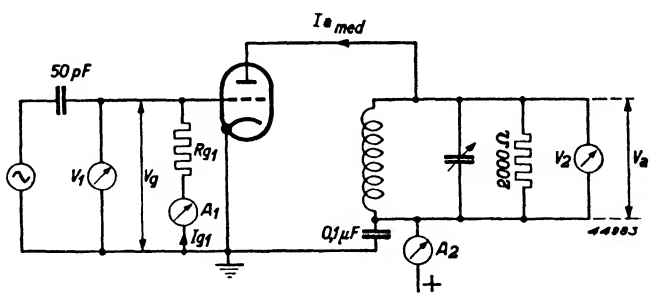

Fig. 88. Circuit for determining the relation between the oscillator voltage V_g (peak), S_{eff} and the mean anode current Ia_{med}.

$V_{g(peak)}$, S_{eff} and the mean anode current Ia_{med} thereby ascertained. The value of the grid leak is that normally specified for the oscillator valve in question, and is chosen with a view to minimising a tendency towards squegging oscillation, which manifests itself when working at large amplitudes on wavelengths around 15 metres (see Chapter IIE). The measurements show, however, that there are also other factors which have an important bearing on the choice of R_{g1}.
This is understandable: in the foregoing discussion it was assumed that the

grid never became positive, whereas the value of R_{g1} determines whether this is in fact the case.

An alternating voltage with a frequency of about 500 kc/s is fed to the grid of the valve under test, via the normal grid capacitor.

If the grid current is then measured by means of the micro-ammeter A_1, the mean negative grid bias can be found at once; and a valve voltmeter V_1 serves to indicate the alternating voltage V_g at the grid. For the measurement of the amplitude I_{a1} of the fundamental component in the anode current, a resonant circuit tuned to 500 kc/s is included in the anode circuit. This tuned circuit is heavily damped by a shunt of 2000 ohms, so that its dynamic resistance is low: about 2000 ohms to the fundamental frequency; and to harmonics, negligible. Due to this small anode load, the anode voltage remains fairly constant, and in the following discussion we shall assume that the anode has a fixed potential. In practical oscillator circuits, however, the anode circuit impedance is usually considerable and variations of anode voltage can then no longer be neglected.

The value of the fundamental component in the anode current is determined by measuring the voltage across the tuned circuit by means of the valve-voltmeter V_2. The effective slope is then given by:

$$I_{a1} = \frac{V_a}{2000} = S_{eff}\, V_g;$$

so that:

$$S_{eff} = \frac{V_a}{V_g\, 2000}.$$

Finally, the current-consumption Ia_{med} is ascertained from the milliammeter A_2.

Measured curves for an ECH 21 triode-heptode are given in fig. 89 *.

The variation of effective slope agrees with calculation. Here also the curve for η shows a fairly constant value for oscillator voltages exceeding the cut-off voltage and reaches a limiting value of 1.8. Further, the curve for $\frac{Ia_{med}}{I_{ao}}$ shows a tendency to become horizontal. This agreement with calculation confirms the correctness of the assumptions which were made.

The battery octode DK 21, for which curves are given in fig. 90, behaves quite differently. The ratio $\frac{Ia_{med}}{I_{ao}}$ is seen to rise rapidly when V_g exceeds

* In the case of octodes and triode-heptodes, Ia_{med} refers of course to the anode current of the oscillator section only.

a certain value, thus departing notably from the trend observed in the previous case. Moreover, the magnitudes of $\frac{S_{eff}}{S_o}$ are rather high.

The increase in Ia_{med} suggests that the grid becomes more positive than we originally supposed. Grid current measurements show, in fact, that at the peaks of the oscillation the grid is strongly positive. Whereas with A.C. valves the grid may become about 2.5 V positive, with battery types positive potentials of 7.5 V are found at large amplitudes ($V_{g\ max} = 15$ V).

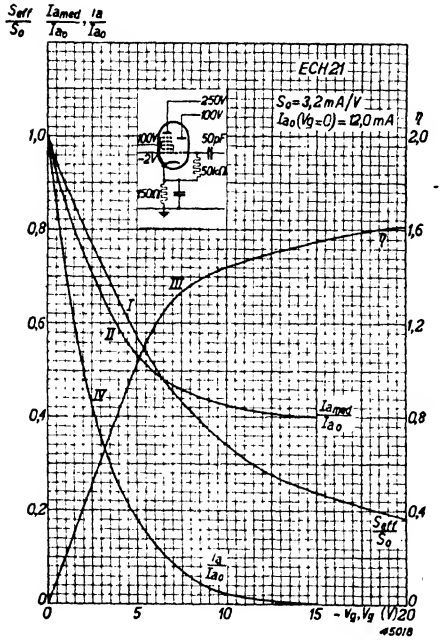

Fig. 89. $\frac{S_{eff}}{S_o}$, $\frac{Ia_{med}}{Ia_o}$ and η as functions of oscillator voltage (peak) for the triode section of the ECH 21. Curve IV represents the relative i_a/v_g characteristic.

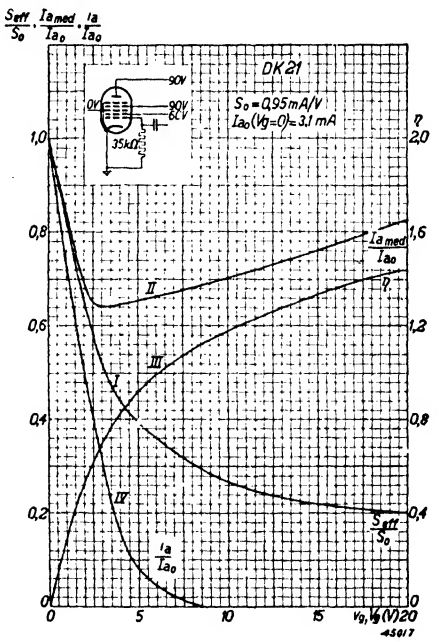

Fig. 90. $\frac{S_{eff}}{S_o}$, $\frac{Ia_{med}}{Ia_o}$ and η as functions of oscillator voltage (peak), for the DK 21 with a grid leak of 35000 ohms. Curve IV represents the relative i_a/v_g characteristic.

Now it is known that in battery valves the grid current characteristic is fairly flat, and better agreement with the conditions calculated will therefore be obtained if the positive grid voltage peaks are limited by increasing R_{g1}.

This is confirmed by measurement. Fig. 91 illustrates the result of raising the resistance of the grid leak from 35,000 to 100,000 ohms; these curves more resemble those of A.C. valves. Conversely, A.C. valves used with a grid leak of abnormally low resistance display battery valve characteristics.

These discrepancies can be avoided by modifying somewhat the definitions of the quantities I_{ao}, V_{go} and S_o, as indicated in fig. 92. Here I_{ao} is the maximum current which occurs, and S_o the maximum slope; I_{ao}, S_o and V_{go} then depend on the magnitude of the oscillator voltage. In this way the quantities are again made to agree with the theoretical deductions. In practice the values are easily ascertained from the static characteristic if in each instance the mean grid bias is calculated from the grid current and the resistance of the leak. In §§ 9 and 11 of this section the relation between grid current and oscillator voltage is calculated. Therefrom we may fix the positive value of the grid potential for every value of oscillator voltage, and the effective slope and the mean anode current may then be deduced.

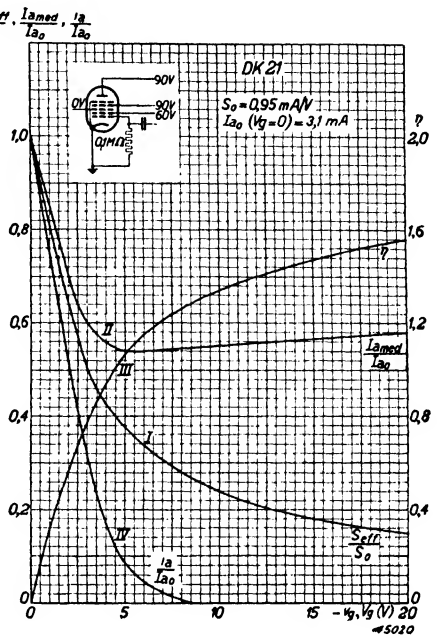

Fig. 91. $\frac{S_{eff}}{S_o}$, $\frac{I_{amed}}{I_{ao}}$ and η as functions of oscillator voltage (peak) for the DK 21 with a grid leak of 100,000 ohms. Curve IV represents the relative ia/vg characteristic.

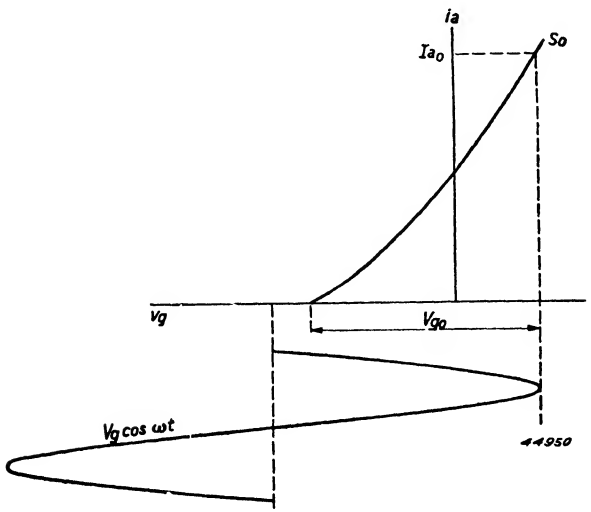

Fig. 92. Definition of V_{go} and S_o, if Ia_0 denotes the maximum value of the anode current.

If I_{ao} is also determined in this way, the curve for the reduced current $\frac{Ia_{med}}{I_{ao}}$ will be as shown in fig. 93. Since this curve agrees with the expected results, it may be assumed that no disturbing effects are present. We have considered the $\frac{Ia_{med}}{I_{ao}}$ curve of fig. 90 in some detail, because important prac-

tical conclusions are to be drawn from it. First it is evident that, given the same current efficiency as in A.C. valves, a very favourable $\frac{S_{eff}}{S_o}$ ratio is obtainable; in other words a specific value of S_{eff} may be reached with a comparatively low normal slope S_o. We have already noticed to what factor this advantage is due. Whereas, in fig. 90, S_o was considered to be the slope when $v_g = 0$, in practice higher values of S_o occur when the grid is positive. It should also be mentioned that the low grid current permits using the valve at maximum current and maximum slope: this would not otherwise be possible. Closer investigation reveals a rather important drawback, however. In the foregoing discussions we have always taken as a basis the minimum value of S_{eff} which is required in conjunction with the least favourable value of $t.Z$ in equation (II B 3). In nearly all circuits this quantity varies over the waveband. As $t.Z$ increases a smaller S_{eff} is needed, and the amplitude of the oscillation grows in accordance with curve I of fig. 90. Simultaneously mean anode current rises rather rapidly, a particularly unwelcome result in the case of battery valves; with AC valves, on the other hand, anode consumption falls in these circumstances.

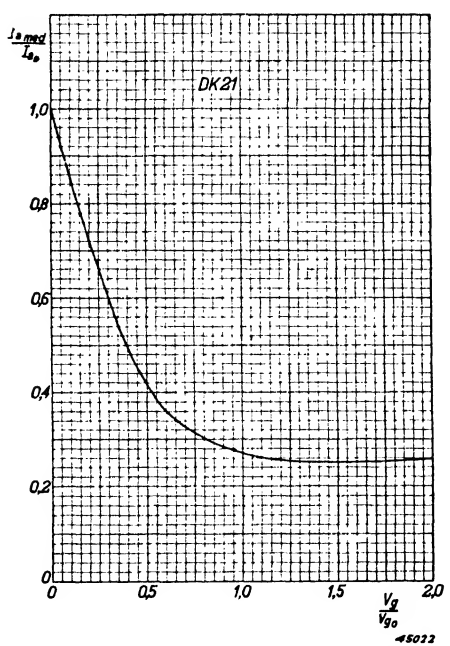

Fig. 93. $\frac{Ia_{med}}{Ia_o}$ as a function of $\frac{Vg}{Vg_o}$, Ia_o being defined as in fig. 92; for the case of curve II of fig. 90.

It is therefore advisable to limit the positive grid swing, by making the resistance of the grid leak as high as is practicable without running the risk of squegging oscillation. Only a small grid current is then needed to ensure that the grid remains sufficiently negative. The characteristic given in fig. 91 shows the effectiveness of increasing the value of the grid leak.

Another fairly obvious method of limiting the rise in current consumption is to feed the anode through a high series resistance; thereby anode voltage will fall as the mean current increases, resulting in the characteristic of the oscillator triode being shifted to the right, i.e. in the same direction as the

peaks of the increasing oscillator voltage. In consequence the oscillator voltage adjusts itself in about the same manner as with A.C. valves. Unfortunately it is generally impossible to feed battery valves through a high series resistance because of the low voltage available.

There remains a third course: to use an oscillator circuit which requires a value of S_{eff} as nearly constant over the waveband as possible. The behaviour of different circuits in this connection is discussed in section C.

§ 5. Requirements for oscillation and their variation with frequency

In order to investigate how, in various circuits, the conditions for oscillation vary with frequency, we shall begin from the basic equation:

$$S_{eff} \cdot t.Z = -1 \quad \text{(II B 3)}$$

For some circuits it is not necessary to start from this fundamental equation, simpler methods of calculation sufficing. But as the method used here has important advantages when complex circuits are to be investigated, it will be followed in every case.

a. Condition for oscillation in a tuned-anode circuit damped by series and parallel resistance

The phase shift which may occur owing to the presence of the grid capacitor and leak will for the present be ignored (but see Chapter III B).

The basic circuit is shown in fig. 94a and the equivalent circuit in 94b. C_v here represents the combined capacitance of the tuning, padding and trimming capacitors *. By means of the equivalent circuit the quantities t and Z may be determined at once. For t we get:

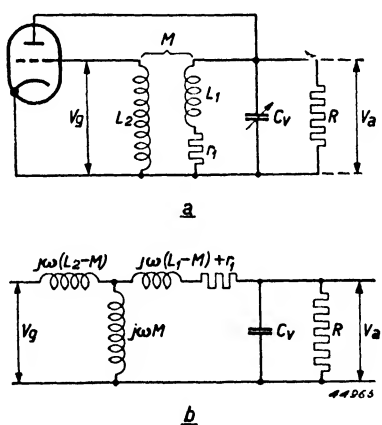

Fig. 94a. Basic circuit of an oscillator with tuned-anode circuit containing series- and parallel-resistance.
Fig. 94b. Equivalent circuit.

$$t = \frac{V_g}{V_a} = \frac{j\omega M}{j\omega L_1 + r_1} \text{ **}.$$

Z consists of $(j\omega L_1 + r_1)$, R and $\frac{1}{j\omega C_v}$ in parallel, and is equal to:

$$Z = \frac{(j\omega L_1 + r_1)\, R}{(j\omega L_1 + r_1)\,(1 + jR\omega C_v) + R}.$$

* The need for the padder and the trimmer is explained in detail in Chapter III.
** As at this stage only the oscillator frequency is being considered, the indication h will be omitted.

The product $t.Z$ is therefore:

$$t\,Z = \frac{j\omega M}{j\omega L_1 + r_1} \frac{(j\omega L_1 + r_1)\ R}{(j\omega L_1 + r_1)\ (1 + jR\omega C_v) + R},$$

$$t\,Z = \frac{j\omega MR}{(j\omega L_1 + r_1)\ (1 + jR\omega C_v) + R} \quad \ldots \quad \text{(II B 14)}$$

This equation falls into two parts, one supplying the condition for oscillation and the other the oscillator frequency.

As it has been assumed that no phase-shift occurs in the valve, the product $t.Z = -\frac{1}{S_{eff}}$ is real, and the numerator in equation (II B 14) must be imaginary; thus:

$$r_1 + R - \omega^2 L_1 C_v R = 0$$

or:

$$\omega^2 L_1 C_v = 1 + \frac{r_1}{R} \quad \ldots \quad \text{(II B 15)}$$

For $t.Z$ may now be written:

$$t\,Z = \frac{MR}{L_1 + r_1 R C_v}.$$

The condition for oscillation therefore becomes:

$$\frac{S_{eff} MR}{L_1 + r_1 R C_v} = -1 \quad \ldots \quad \text{(II B 16)}$$

It follows from this equation that M must be a negative quantity.

This agrees exactly with the observation made in II B § 1, that phase reversal of the tapped-off voltage is essential.

If $r_1 = 0$, equation (II B 16) becomes:

$$\frac{S_{eff} M R}{L_1} = -1. \quad \ldots \quad \text{(II B 17)}$$

which means that S_{eff}, and therefore the oscillator voltage also, remains constant whatever the position of the tuning capacitor. For the case that $R = \infty$, that is when only series resistance is present, equation (II B 16) becomes:

$$\frac{S_{eff} M}{r_1 C_v} = -1 \quad \ldots \quad \text{(II B 18)}$$

In this case we may insert $\frac{r_1}{R} = 0$ in equation (II B 15); furthermore, by introducing the quality factor $Q = \omega L_1/r_1$, equation (II B 18) may be written:

$$S_{eff}\, M\, Q\, \omega = -1 \quad \ldots\ldots\ldots\ldots \quad \text{(II B 19)}$$

The quality factor Q may be considered to be fairly constant over a waveband, and it therefore follows that the effective slope requires to be smallest at high frequencies. Inasmuch as the oscillator voltage is roughly inversely proportional to the effective slope, it is clear that the voltage will increase in about direct proportion to frequency. Moreover we see from equation (II B 15) that with mixed damping the frequency of oscillation is affected by the relation between the series resistance and the parallel resistance of the tuned circuit. The influence of these resistances on the tracking curve will be dealt with in Chapter III.

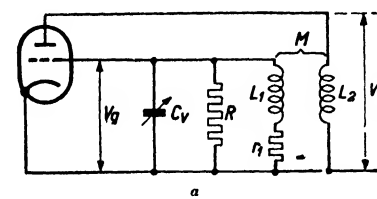

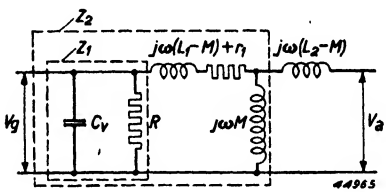

Fig. 95a. Basic circuit of an oscillator with tuned-grid circuit containing series- and parallel-resistance.
Fig. 95b. Equivalent circuit.

b. Condition for oscillation in a tuned-grid circuit damped by series and parallel resistance

The basic circuit is reproduced in fig. 95a, and the equivalent circuit in 95b. In the latter two separate impedances Z_1 and Z_2 will be noted; the purpose of this treatment will become obvious in the calculations which follow.

The quantities t and Z are obtained directly from fig. 95b;

$$t = \frac{V_g}{V_a} = \frac{Z_2}{Z_2 + j\omega\,(L_2 - M)} \cdot \frac{Z_1}{Z_1 + j\omega\,(L_1 - M) + r_1}$$

and:

$$Z = Z_2 + i\omega\,(L_2 - M)$$

If these values of t and Z are substituted in equation (II B 3) we get, after inserting the values of Z_1 and Z_2:

$$S_{eff}\, t\, Z = \frac{S_{eff}\, R\, j\omega\, M}{(j\omega\, L_1 + r_1)\,(1 + jR\,\omega C_v) + R} = -1 \quad \text{(II B 20)}$$

As S_{eff} must be real, the numerator of this expression must be imaginary,

and therefore:

$$-\omega^2 L_1 R C_v + r_1 + R = 0$$

or:

$$\omega^2 L_1 C_v = 1 + \frac{r_1}{R},$$

which agrees with equation (II B 15).

For the condition for oscillation we once more obtain equation (II B 16). From the value of S_{eff} and the measured relation between S_{eff} and the oscillator voltage, the magnitude of this voltage can be calculated. It is a matter of indifference, as far as oscillator frequency and voltage are concerned, whether the tuned circuit be connected in the grid or in the anode circuit.

By means of the foregoing equations and the valve characteristics in § 4 it is now possible to determine the oscillator voltage as a function of the capacitance of the tuning capacitor; an example will be given later.

Certain deductions may already be made. First, with either type of circuit it is apparent that the oscillator voltage can be held more nearly constant over the waveband if a tuned circuit of small series resistance is used; this calls for a coil of good quality and fairly high parallel damping. Practice confirms this conclusion.

There are, however, limits to the coil quality obtainable and it is generally necessary to increase the shunt damping and, for a given slope, to tighten the coupling correspondingly. There are disadvantages in this course; more risk of phase shift owing to the greater overall damping (see III B, § 2), and enhanced effects of inter-electrode capacitance variations by reason of the tighter coupling (see II H, § 1).

In order to ascertain what value of damping is required in a typical case, we shall consider an oscillator circuit for use on the medium wave-band (intermediate frequency of 470 kc/s) tunable from 1970 to 1006 kc/s; the total tuning capacitance will vary from 90 to 340 pF (see III A, § 6). Over this frequency band an endeavour must be made to keep the amount $(L_1 + r_1 R C_v)$ from equation (II B 16) as constant as possible.

So we can write:

$$1 + \frac{r_1}{L_1} R C_v = \text{constant, or } 1 + \frac{\omega R C_v}{Q} = \text{constant.}$$

We shall assume that Q is equal to 60; the change of C_v is partly compensated by the variation in frequency from 1970 to 1006 kc/s. Nevertheless

we must still try to make the second term in the equation small compared with unity, even with C_v at its maximum.
Thus:

$$\frac{\omega RC_v}{Q} < 1$$

or:

$$\frac{2\pi \times 1006 \times 10^3 R \times 340 \times 10^{-12}}{60} < 1$$

To reduce this amount to 0.34 parallel resistance of about 10,000 is required. At a frequency of 1970 kc/s we then find:

$$1 + \frac{\omega RC_v}{Q} = 1 + \frac{2\pi \times 1970 \times 10^3 \times 10^4 \times 90 \times 10^{-12}}{60}$$
$$= 1.18 \text{ instead of } 1.34.$$

In this way a fairly constant oscillator voltage is obtained.
The shunt is formed partly by the anode or grid damping, which may amount to about 15,000 ohms, though it varies with the type of oscillator valve and the choice of grid leak. Additional parallel resistance of 30,000 ohms serves to bring the total damping to 10,000 ohms.

c. Condition for oscillation in a circuit with the padding capacitor connected in series with the tuning capacitor

At the beginning of this section it was assumed that C_v represented the combined capacitance of the tuning, padding and trimming capacitors. This is correct only if the padder C_p (fig. 96) is joined in series with the variable tuning capacitor (the strays may safely be regarded as lying parallel to C_v). This circuit is thus equivalent to that of fig. 94a, the capacitance C_v in equations (II B 15) and (II B 16) being replaced by C_{tot}, the capacitance of C_v and C_p in series. In this case equations (II B 15) and (II B 16) therefore become:

$$\omega^2 L_1 C_{tot} = 1 + \frac{r_1}{R} \quad \ldots\ldots\ldots\ldots \quad \text{(II B 21)}$$

and

$$\frac{S_{eff} M R}{L_1 + r_1 C_{tot} R} = -1 \text{ or } S_{eff} = -\frac{L_1}{MR} - \frac{r_1 C_{tot}}{M} \quad \ldots\ldots\ldots \quad \text{(II B 22)}$$

if:

$$C_{tot} = \frac{C_v C_p}{C_v + C_p} \quad \ldots\ldots\ldots\ldots\ldots \quad \text{(II B 23}$$

d. Condition for oscillation in a circuit with the padding capacitor connected in series with the tuning coil

In very many cases the padding capacitor is joined in series with the tuning coil; the basic arrangement is shown in fig. 97.

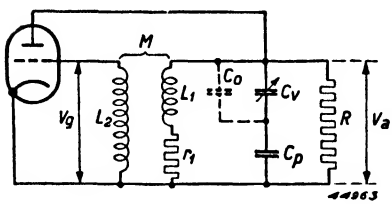

Fig. 96. Tuned-anode oscillator, with the padding capacitor connected in series with the tuning capacitor.

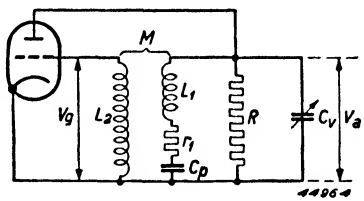

Fig. 97. Tuned-anode oscillator, with the padding capacitor connected in series with the tuning coil.

For t and Z we can now write:

$$t = \frac{V_g}{V_a} = \frac{j\omega M}{j\omega L_1 + r_1 + \frac{1}{j\omega C_p}};$$

$$Z = \frac{\left(j\omega L_1 + r_1 + \frac{1}{j\omega C_p}\right) R}{\left(j\omega L_1 + r_1 + \frac{1}{j\omega C_p}\right)(jR\omega C_v + 1) + R}.$$

For t Z we therefore find:

$$t Z = \frac{j\omega MR}{\left(j\omega L_1 + r_1 + \frac{1}{j\omega C_p}\right)(jR\omega C_v + 1) + R} \qquad \text{(II B 24)}$$

Since the product $tZ = -\frac{1}{S_{eff}}$ is real, the numerator on the right-hand side must be imaginary. For the oscillator frequency we accordingly get:

$$r_1 + R - \omega^2 L_1 RC_v + \frac{R C_v}{C_p} = 0,$$

or:

$$\omega^2 L_1 \frac{C_v C_p}{C_v + C_p} = 1 + \frac{r_1}{R} \frac{C_p}{C_v + C_p} \quad . \quad . \quad . \quad . \quad . \qquad \text{(II B 25)}$$

The product tZ now becomes:

$$t\,Z = \frac{MR}{L_1 + r_1 RC_v - \dfrac{1}{\omega^2 C_p}}$$

and the condition for oscillation is:

$$S_{eff}\,\frac{MR}{L_1 + r_1 RC_v - \dfrac{1}{\omega^2 C_p}} = -1 \quad . \quad . \quad . \quad . \quad . \quad \text{(II B 26)}$$

Therefore:

$$S_{eff} = -\frac{r_1 C_v}{M} - \frac{L_1}{MR}\left(1 - \frac{1}{\omega^2 L_1 C_p}\right).$$

This can be amended, using equation (II B 25), to

$$S_{eff} = -\left(\frac{r_1 C_v}{M} + \frac{L_1}{MR}\,\frac{C_p}{C_p + C_v}\right) \quad . \quad . \quad . \quad . \quad \text{(II B 27)}$$

(The value of $\frac{r_1}{R}$ is here regarded as negligible in relation to 1.)

§ 6. Comparison of the cases c and d

We shall now compare the respective conditions for oscillation in the two circuits of § 5c and d, and also consider the extreme cases in which:

(1) the shunt resistance is infinite ($R = \infty$), and

(2) the series resistance is nil ($r_1 = 0$).

In the first we put $R = \infty$, equations (II B 22) and (II B 27) becoming respectively:

$$S_{eff} = -\frac{r_1 C_{tot}}{M} \quad . \quad . \quad . \quad \text{(II B 28)}$$

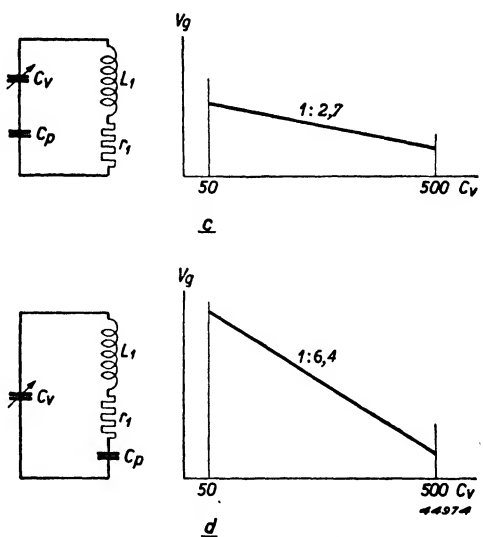

Fig. 98c. Variation of oscillator voltage as a function of tuning capacitance, for the circuit of fig. 96, if the parallel resistance is infinitely great ($R = \infty$)
d. Variation of oscillator voltage as a function of tuning capacitance, for the circuit of fig. 97, if the parallel resistance is infinitely great ($R = \infty$)

and

$$S_{eff} = -\frac{r_1 C_v}{M} \quad \ldots\ldots\ldots\ldots\ldots \quad \text{(II B 29)}$$

The resistance r_1 can be considered constant if a resistor of say 30 ohms is joined in series with the tuning coil. Assuming $C_p = 200$ pF *, $C_{v\,min} = 50$ pF and $C_{v\,max} = 500$ pF, we get $C_{tot\,min} = 40$ pF and $C_{tot\,max} = 140$ pF. In case *c*, therefore, S_{eff} varies by a factor of 3.5, and in case *d* by a factor of 10.

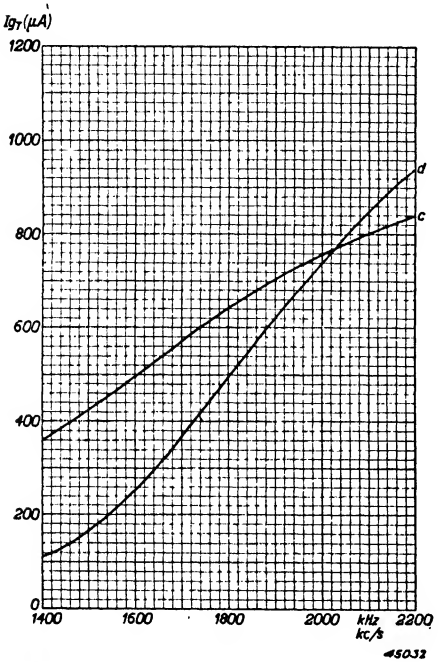

Fig. 99. Variation of oscillator grid current (proportional to oscillator voltage) as a function of frequency, measured with an EF 6 in a tuned-anode circuit: $C_p = 200$ pF, $r_1 = 32$ ohms, $R = \infty$.
c. with the padder C_p joined in series with the tuning capacitor,
d. with the padder C_p joined in series with the tuning coil.

Taking fig. 87 as an example of a curve relating $\frac{S_{eff}}{S_o}$ and $\frac{V_g}{V_{go}}$, and assuming that at the highest frequency $\frac{S_{eff}}{S_o} = 0.04$, it follows that in case *c* the oscillator voltage varies by a factor of about 2.7 ($\frac{V_g}{V_{go}}$ varies from 3.8 to 1.4) and in case *d* by a factor of about 6.4 ($\frac{V_g}{V_{go}}$ varies from 3.8 to 0.6).

The respective variation of oscillator voltage in the two cases is shown diagrammatically in fig. 98. In order to discover how far this calculation agreed with practice, the two circuits were investigated experimentally, using the EF 6 pentode as ocillator valve. The reasons for using a pentode are that it is not otherwise possible to approach $R = \infty$, owing to the comparatively low A.C. resistance of other types of valve, and that with triodes an additional phenomenon occurs (described in II B § 10) which affects the variation of oscillator voltage. The outcome of these measurements is shown in fig. 99 **. Clearly there is much greater variation of oscillator voltage in case *d* than in *c*; the actual ratios are 1 : 8.5 and 1 : 2.3 respectively.

* To demonstrate the effect, the padding capacitor had a value lower than normal.

** Both this diagram and fig. 101 show, instead of the oscillator voltage, the current through the grid leak; the relationship of these two quantities is dealt with in II B §11.

For the purpose of examining the second of the extreme cases mentioned above we shall assume that the oscillator circuit is so heavily damped by parallel resistance that the series resistance r_1 is negligible by comparison ($r_1 = 0$). The equations (II B 22) and (II B 27) then become respectively:

$$S_{eff} = -\frac{L_1}{MR} \quad \text{(II B 30)}$$

and:

$$S_{eff} = -\frac{L_1}{MR}\,\frac{C_p}{C_p + C_v} \quad \text{(II B 31)}$$

If $C_p = 200$ pF, we get:

$$\text{for } C_{v\,min} = 50\text{ pF}: \frac{C_p}{C_p + C_v} = 0.8, \text{ and}$$

$$\text{for } C_{v\,max} = 500\text{ pF}: \frac{C_p}{C_p + C_v} = 0.3$$

Consequently, in case *c* S_{eff} will be constant, whereas in case *d* the slope will vary in the ratio 0.8 : 0.3, namely 2.7 : 1. Oscillator voltage is thus constant in case *c* but, as will be noted from fig. 87, decreases by a factor of about 2.1 between top and bottom of the waveband in case *d*. The performance in the two cases is represented graphically in fig. 100. It should be possible, by a suitable choice of the damping resistances, to keep the oscillator voltage constant. In the circuit where C_v and C_p are in series (case *c*) all damping should be parallel to the tuned circuit; this condition is however unattainable, for some series resistance is always present, and it is not possible to do more than approach the constancy depicted in fig. 100c. The ultimate curve will resemble slightly that illustrated in fig. 98. With larger C_v, oscillator voltage will therefore decline. Curve *c* of fig. 101 indicates what can be achieved in practice; it was obtained by using an EF 6 as oscillator and with the tuned anode circuit shunted by 6400 ohms.

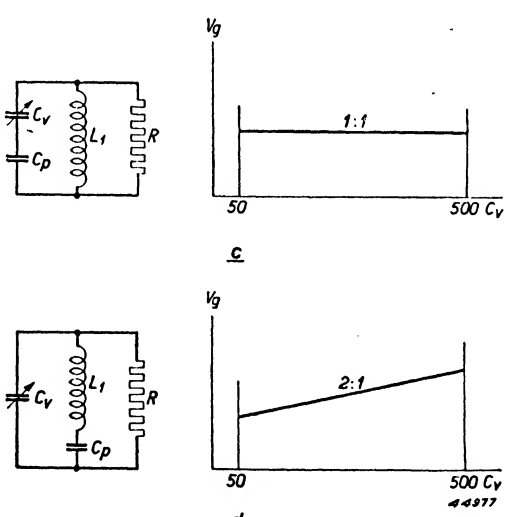

Fig. 100c. Variation of oscillator voltage as a function of tuning capacitance, for the circuit of fig. 96, if the series resistance is nil ($r_1 = 0$ Ohm).
d. The same, for the circuit of fig. 97.

In circuits which have C_p and L in series, and where a combination of series and parallel damping is present, the phenomenon mentioned above also occurs. In equation (II B 27) there is one term which increases with C_v and another which decreases, and their sum may thus be roughly constant. Curves *d* in fig.98 and 100 confirm this. The ultimate curve for this case, with normal series damping and shunt damping of 6400 Ohms, is reproduced in fig. 101 dand is fairly flat. Despite the fact that the parallel resistance has the same value, 6400 Ω, in this case the series resistance cannot be neglected.

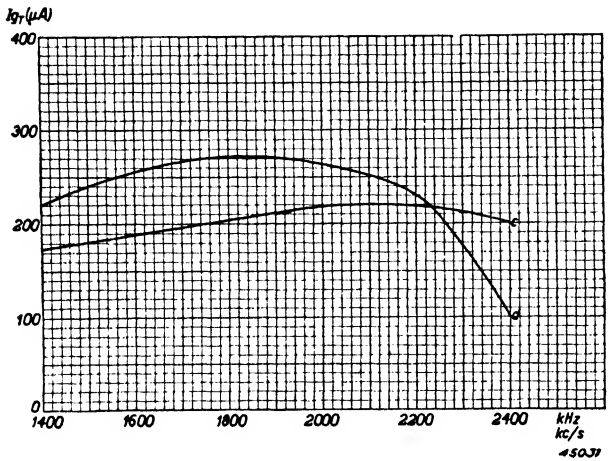

Fig. 101. Variation of oscillator grid current as a function of frequency, measured with an EF 6 in a tuned-anode circuit. C_p = 200 pF, R = 6400 Ohms.
c. with the padder C_p in series with the tuning capacitor.
d. with the padder C_p in series with the tuning coil.

The reason for this is that in equation (II B 27) r_1 is found in conjunction with C_v, and in (II B 22) with C_{tot}. Over a waveband C_v varies in the ratio of 1 : 6, C_{tot} in the ratio of 1 : 2.

With the aid of curve *d* in fig. 101, which relates to a practical circuit, we shall now consider the dimensioning of the oscillator circuit. For this purpose equation (II B 27) will be rewritten as follows:

$$S_{eff} = -\frac{L_1}{M}\left(\frac{r_1}{L_1}C_v + \frac{1}{R}\frac{C_p}{C_p + C_v}\right)$$

$$\text{or } S_{eff} = -\frac{L_1}{M}\left(\frac{\omega C_v}{Q} + \frac{1}{R}\frac{C_p}{C_p + C_v}\right) \quad \ldots \quad \text{(II B 32)}$$

The slope of the curve is fixed by the term between brackets.

The oscillator circuit will be assumed to have the undermentioned constants:

f (kc/s)	Q	C_v (pF)	C_p (pF)	$\frac{C_p}{C_p+C_v}$	$\frac{\omega Cv}{Q} + \frac{1}{R}\frac{C_p}{C_p+C_v}$
1006	60	90	600	0.9	$9.10^{-6} + 140.10^{-6}$
1970	60	570	600	0.5	$114.10^{-6} + 78.10^{-6}$

The effective slope required at 1006 kc/s is to that required at 1970 kc/s as 149 : 192. The respective oscillator voltages are in about inverse ratio; this agrees fairly well with the trend of curve *d* in fig. 101. If we regard the latter as satisfactory, it is simple to calculate the coupling ratio needed for any particular valve. With the ECH 21, for example, an oscillator voltage of 7.5 V_{RMS} is recommended, and fig. 89 shows that an effective slope $S_{eff} = 1$ mA/V is therefore required. If an oscillator voltage of 7.5 V_{RMS} is desired at a frequency of 1006 kc/s we find from equation (II B 32):

$$1 \times 10^{-3} = \frac{L_1}{M} \times 149 \times 10^{-6}$$

therefore:

$$\frac{M}{L_1} = 0.15.$$

This is a rather loose coupling, the figure being generally about 0.2. It should be noted, however, that this example relates to a circuit in which the padding capacitor is connected in series with the tuning coil; hence the practical feedback ratio is higher than $\frac{M}{L_1}$.

§ 7. The Colpitts circuit

A fairly well-known oscillator circuit is that in which the normal inductive reaction coupling is supplemented by a coupling through the padding capacitor, which is common to grid and anode circuits. The object of this circuit is to keep the oscillator voltage as constant as possible over the waveband.

For simplicity the coupling coil may also be omitted, only the reaction coupling through the padding capacitor then remaining. The resulting circuit then exemplifies in principle the classic Colpitts circuit, as is made clear in figs 102a and 102b. In fig. 102b C_2 is the padding capacitor, and C_1 the variable tuning capacitor; however the circuit is not basically altered if these capacitors are interchanged.

The circuit of fig. 102b has latterly found

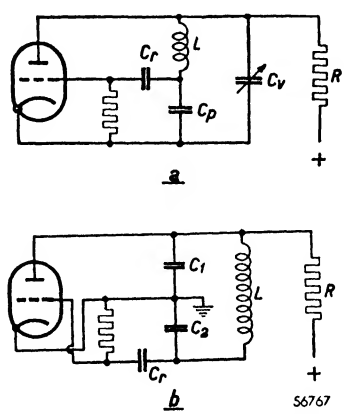

Fig. 102a. Oscillator circuit in which back-coupling takes place via the padding capacitor.
b. An alternative form of the circuit of fig. 102a, which shows more clearly its similarity to the classic Colpitts circuit.

application in simple receivers. Generally the tuning capacitor takes the place of C_2 and the padding capacitor that of C_1. As the circuit requires a mixing valve with a high oscillator slope, only newer types such as the ECH 42, ECH 21, ECH 35, etc. can be used.

On short waves a padding capacitor is seldom used, and even when one is employed its capacitance is much too large to provide adequate coupling; it is consequently impossible to utilise the Colpitts circuit. However, there is no reason why the Colpitts arrangement should not be used for the medium and long wavebands, in combination with an inductive reaction-coupled circuit on the short waveband. When considering the Colpitts circuit it is necessary to regard the damping as being composed of:

1. the series resistance of the coil L;
2. the anode damping, due to the AC-resistance of the oscillator valve and also, in most cases, to a parallel-feed resistance (R in figs 102a and b);
3. the grid damping, primarily due to grid current and the grid leak. This is equal to about one-third of the resistance of the grid leak (see Chapter II B § 9). Often the feed resistor is connected to the grid side of C_2, and in such a case R also forms part of the grid damping.

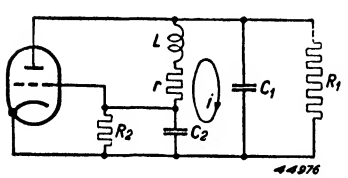

Fig. 103. Simplified Colpitts circuit, showing the various dampings:
r = coil damping
R_1 = anode damping
R_2 = grid damping

These dampings are shown in the simplified circuit of fig. 103.

For the moment C_v and C_p will be left out of consideration; later, when the behaviour of the basic circuit has been calculated, the question of how best to connect these capacitors can be examined.

To calculate the condition for oscillation in the Colpitts circuit we return to the basic equation (II B 3):

$$S_{eff} \,.\, t \,.\, Z = -1 \text{ or } S_{eff} = -\frac{1}{tZ}.$$

With the help of this equation the effective slope necessary for oscillation can be ascertained. Since the oscillator voltage is about inversely proportional to the effective slope (see II B § 2), this voltage will be small when the slope required is large. The latter may indeed be so high that the circuit fails to oscillate

The value of t may be calculated by using fig. 103 as a guide; if the tank current indicated by the arrow is regarded as flowing mainly in L-r -C_2-C_1 (the currents through R_1, R_2 and the valve are comparatively small), then the voltage ratio t is the inverse of the ratio of the capacitances C_2 and C_1.

Thus:

$$t = \frac{V_g}{V_a} = -\frac{C_1}{C_2} \quad \ldots\ldots\ldots\ldots\ldots \quad \text{(II B 33)}$$

Z is the total impedance between anode and cathode; it may be considered as a combination of three parallel links, namely the tuned circuit L-r-C_2-C_1, the resistance R_1, and the resistance R_2 lying between the tapping and cathode.

The impedance of a tuned circuit in the form given in fig. 103 is not usually known, and moreover it cannot be expressed in a simple formula. For the impedance of the circuit containing the inductance and resistance in one arm, and the series capacitances C_1 and C_2 in the other arm, we find:

$$Z_o = \frac{L}{r\, C_{tot}},$$

C_{tot} representing the series combination $C_1 C_2$. Now C_1 may be regarded as a tapping on C_{tot}. The impedance measured at such a tapping is given by a formula analogous to that relating to a transformer:

$$Z_1 = Z_o \frac{C_{tot}^2}{C_1^2} = \frac{L\, C_{tot}}{r\, C_1^2} \quad \ldots\ldots\ldots \quad \text{(II B 34)}$$

If $\frac{C_1\, C_2}{C_1 + C_2}$ is substituted for C_{tot} we get:

$$Z_1 = \frac{L\, C_2}{r\, C_1 (C_1 + C_2)} \quad \ldots\ldots\ldots\ldots \quad \text{(II B 35)}$$

R_1 is in parallel with this impedance, and R_2 with part of it.

This latter resistance, being connected across C_2, is equivalent to a resistance in parallel with C_1 of value $R_2 (C_2/C_1)^2$.

The overall impedance of the three paths is accordingly:

$$\frac{1}{Z} = \frac{1}{Z_1} + \frac{1}{R_1} + \frac{C_1^2}{C_2^2 R_2} = \frac{r\, C_1 (C_1 + C_2)}{L C_2} + \frac{1}{R_1} + \frac{C_1^2}{C_2^2\, R_2} \quad \ldots \quad \text{(II B 36)}$$

and the effective slope required is therefore:

$$S_{eff} = -\frac{1}{tZ} = \frac{r (C_1 + C_2)}{L} + \frac{C_2}{C_1 R_1} + \frac{C_1}{C_2 R_2} \quad \ldots\ldots\ldots \quad \text{(II B 37)}$$

How S_{eff} varies depends on whether the variable capacitor is C_1 or C_2, and on the presence or absence of the three kinds of damping. The various cases will now be dealt with in turn.

a. Colpitts circuit without parallel dampings

In practice this condition is unattainable, as damping by grid current is always present, and with triodes the damping due to the AC-resistance of the valve usually cannot be ignored. But this case is not of theoretical interest alone, for in equation (II B 37) S_{eff} consists of three components, each determined by only one of the three dampings.

If in the first place we put:

$$R_1 = R_2 = \infty$$

then equation (II B 37) becomes:

$$S_{eff} = \frac{r\,(C_1 + C_2)}{L} \quad \ldots\ldots\ldots\ldots \quad \text{(II B 38)}$$

In this equation C_1 and C_2 appear symmetrically; the influence of the damping due to coil resistance is therefore the same, whichever way C_p and C_v are connected. Only when parallel damping is also present does the manner of connecting these capacitors make any difference.

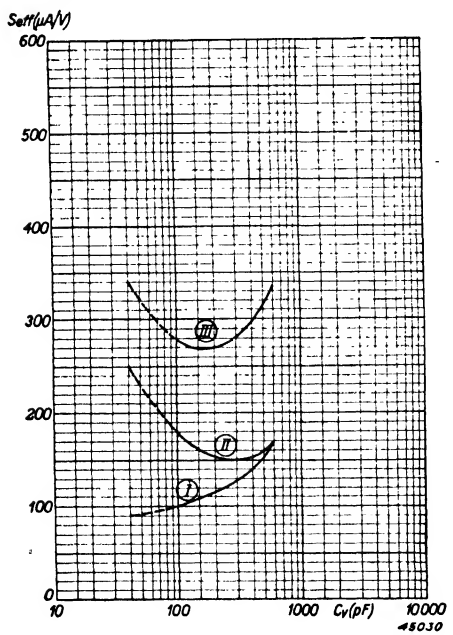

Fig. 104. S_{eff} as a function of C_v for the medium-wave band, taking only the coil resistance into consideration.
Curve I $r = 10$ Ohms
Curve II $Q = 50$
Curve III Curves I and II added

If the series resistance of the inductor were independent of frequency, the required effective slope would, from equation (II B 38), increase in proportion to C_v, while the oscillator voltage at the grid would decrease in about inverse proportion to the slope. Over the medium waveband, with a padding capacitor of 600 pF and a tuning capacitor (including trimmer) of 100—600 pF, a variation of oscillator voltage approximately as 1200 : 700 or say 2 : 1 may be expected. On long waves the padder has a capacitance of the order of 200 pF. The variation of oscillator voltage will therefore be greater, namely as 800 : 300 or about 2.7 : 1. Curve I of fig. 104 indicates the variation of S_{eff} over the medium waveband when $r = 10$ ohms. In reality the R.F. resistance of the coil varies with frequency,

but the quality factor Q is approximately constant over the waveband. We therefore write:

$$r = \frac{\omega L}{Q}.$$

Substituting this value for r in equation (II B 38) we get:

$$S_{eff} = \frac{\omega L}{Q} \frac{C_1 + C_2}{L} = \frac{\omega (C_1 + C_2)}{Q} \quad \ldots\ldots \quad \text{(II B 39)}$$

Over the medium waveband the variation of $C_1 + C_2$ is just about compensated by that of ω, as the oscillator frequency ranges from about 2000 to 1000 kc/s. The oscillator frequency/voltage curve is likely, therefore, to be fairly flat. If a specific figure is taken for Q the variation of the required slope is easily calculated.
Curve II of fig. 104 shows the variation when $Q = 50$, and curve III is the sum of curves I and II. As the frequency range in the long waveband is considerably smaller than that in the medium waveband the variation of effective slope is still rather great.

b. Colpitts circuit with preponderant anode damping

In this case we assume $r = 0$ and $R_2 = \infty$. The condition for oscillation now becomes:

$$S_{eff} = \frac{C_2}{C_1} \frac{1}{R_1} \quad \ldots\ldots\ldots\ldots\ldots \quad \text{(II B 40)}$$

The variation of S_{eff} is determined by the varying capacitance of the tuning capacitor C_v, whether the latter is in the place of C_1 or of C_2. If the tuning capacitor is connected to the anode end of the coil ($C_v = C_1$) then S_{eff} decreases with increasing C_v and when the tuning capacitor is joined to the grid end ($C_v = C_2$) S_{eff} increases with increasing C_v. The relative change of C_v alone is clearly greater than that of $C_v + C_p$, and in consequence a greater variation of slope is to be expected than in case (a) with constant series resistance.
Since it is only the direction and not the magnitude of the variation which is affected by the respective position of C_v and C_p, other factors than those hitherto mentioned will govern their placing.
The first consideration is the maximum value of the required S_{eff}.
It is assumed that on the medium waveband $C_p = 600$ pF and that C_v (including trimmer) varies from about 100 to 600 pF. If C_v is connected in the place of C_2 the highest value of C_2/C_1 is 600/600 = 1.

With C_v joined to the anode side, the maximum value of C_2/C_1 is 600/100 = 6. Greater effective slope is thus required if the tuning capacitor is connected to the anode side.

If we assume that the anode damping R_1 (including the feed resistance) amounts to 10,000 ohms, then an effective slope $S_{eff} = \frac{6.10^3}{10,000} = 0.6$ mA/V will be required — not an unduly high value. It must be remembered, however, that coil resistance and grid damping have also to be reckoned with; consequently it is in every case preferable to have C_v connected to the grid side.

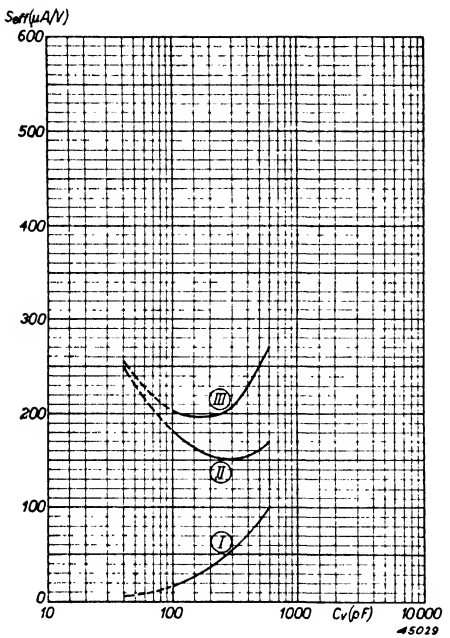

Fig. 105. S_{eff} as a function of C_v for the medium-wave band, taking also the anode damping into consideration.
Curve I $R_1 = 10000$ Ohms, $C_2 = C_v$, $r = 0$ Ohm
Curve II Curve II from fig. 104
Curve III Curves I and II added.

If, with the latter circuit, the required slope is plotted as a function of C_v, curve I of fig. 105 is obtained.

As has already been noted, the coil damping can be taken into account very simply by adding the S_{eff} curves in figs 104 and 105 respectively. If we consider a normal inductor, with a constant quality factor Q, curve II of fig. 104 may serve as example. This is reproduced once more in fig. 105. By adding curves I and II, curve III is obtained.

The variation of slope is now less and the required effective slope averages about 0.25 mA/V. Such a value is easily attained. Consequently if only anode damping and coil damping are present the circuit in which C_v is joined to the grid side is of practical value.

c. Influence of grid damping

The grid damping is determined, in equation (II B 37), by the term:

$$S_{eff} = \frac{C_1}{C_2 R_2} \quad \text{(II B 41)}$$

In this equation C_1 and C_2 appear in inverse relation compared with (IIB40) and by similar reasoning we conclude that C_v should in this case be connected to the anode side. If both grid damping and anode damping are

present it is necessary, when considering where to put the tuning capacitor, to ascertain which kind of damping predominates. Usually the anode damping is the heavier. In very simple receivers not covering the short waveband it is possible to reduce grid damping to a large degree by using a grid leak of higher value than the customary 50,000 ohms. It should then be possible to approach curve II of fig. 104. Using the normal leak of 50,000 ohms, however, results in grid damping of about 17000 ohms. Even this is a higher figure than that represented by the anode damping. The variable capacitor is therefore best connected to the grid side.

If we now calculate from equation (II B 41) the required slope for this circuit, taking $R_2 = 17000$ ohms, we obtain curve I of fig. 106.

By adding curve III of fig. 105, reproduced in fig. 106 as curve II, and curve I, we arrive at the effective slope necessary in the general case where anode, grid and coil dampings are all present.

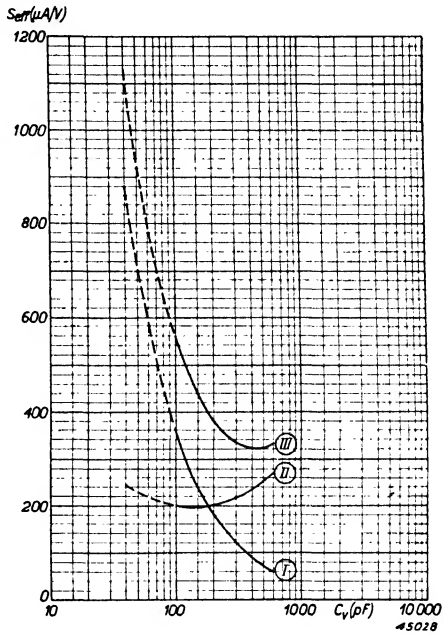

Fig. 106. S_{eff} as a function of C_v for the medium-wave band, taking also the grid damping into consideration.
Curve I $R_2 = 17000$ ohms, $C_2 = C_v$
Curve II Curve III from fig. 105
Curve III Curves I and II added. This curve shows therefore, the variation of effective slope in the normal case, where anode-, grid- and coil-dampings are present.

It will be seen that the variation of the effective slope is not very large; the value required is however about 0.5 mA/V.

d. Measured results

In order to ascertain how far practical results substantiate theory, some measurements were made with the EF 6 pentode. Owing to the high A.C. resistance of this valve, and to the fact that its anode was choke-fed, anode damping could be neglected, and by the use of a leak of 0.32 megohm the grid damping was greatly reduced.

The variable capacitor was connected to the grid side.

In the absence of grid damping a fairly flat oscillator-voltage curve might be expected. The equation indicates at once that with the smallest value of C_v the grid damping (0.1 megohm) requires as much slope as the coil

damping (Q = 50). Measurement yields curve I of fig. 107 *. At 2000 kc/s (C_v = approx. 100 pF) the grid current is about half that at 1000 kc/s (C_v = approx. 600 pF).

Connecting resistors of 10, 20 and 30 ohms respectively in series with the coil results in curves II, III and IV being obtained. The series resistance r will exert the greatest influence at the maximum value of C_v, not only because of the part played by C_v in equation (II B 38), but also because the effect of the parallel damping is then slight. This is immediately evident from the curve. Quantitatively also, the measured results confirm expectation. An inductor with a quality factor Q = 50 has at 1000 kc/s an RF resistance of about 9 ohms. By adding additional resistance of 10 ohms the required effective slope is about doubled, and the measured reduction of grid current agrees with this increased value of series resistance. If no extra coil damping is introduced, but anode damping is made heavier — a more likely condition in practice — the curves of fig. 108 are obtained; in these the anode damping was assumed to be infinite, 16,000 and 5,000 ohms respectively. The additional damping will have most influence when C_v is large, since the slope necessitated by this damping is:

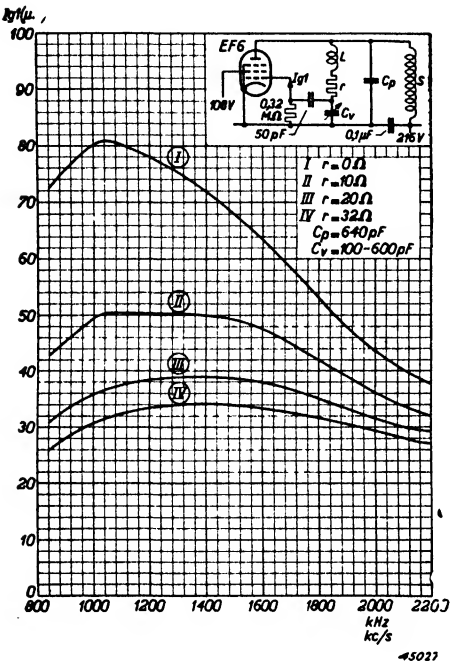

Fig. 107. Grid current as a function of frequency in the medium-wave band, measured with an EF 6 connected as oscillator.
$C_2 = C_v$, R_2 = 0.1 Megohm, Q = 50.

Curve I r = 0 ohm
Curve II r = 10 ohms
Curve III r = 20 ohms
Curve IV r = 32 ohms

$$S_{eff} = \frac{C_v}{C_p}\frac{1}{R_1} \quad \ldots\ldots\ldots \quad \text{[see equation (II B 40)]}$$

The effect was in fact most noticeable at 1000 kc/s. When C_v is small (2000 kc/s) the anode damping apparently diminishes by comparison with

* In practical tests the grid current was measured instead of the required slope. It would of course be possible from the corresponding oscillator voltage to calculate the slope necessary, but we have preferred to reproduce the actual measured current values as a function of frequency.

the other dampings. If instead of anode damping grid damping is applied, the curves of fig. 109 are obtained. The required slope then amounts to:

$$S_{eff} = \frac{C_p}{C_v}\,\frac{1}{R_2}.$$

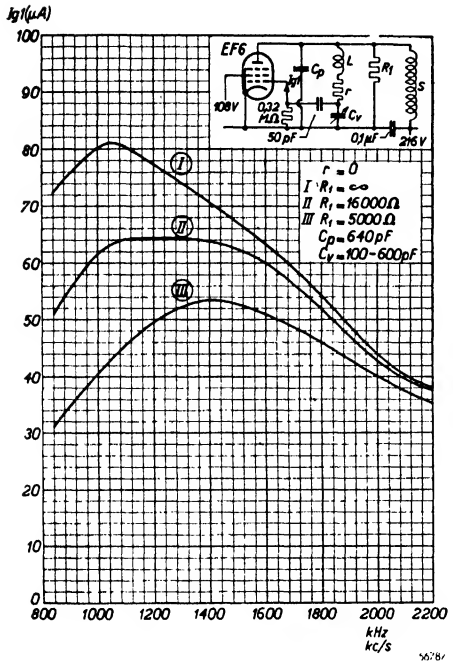

Fig. 108. Grid current as a function of frequency in the medium-wave band, measured with an EF 6 connected as oscillator.
$C_2 = C_v$, $r = 0$ ohm, $R_2 = 0.1$ megohm, $Q = 50$.
Curve I $R_1 = \infty$
Curve II $R_1 = 16{,}000$ ohms
Curve III $R_1 = 5{,}000$ ohms

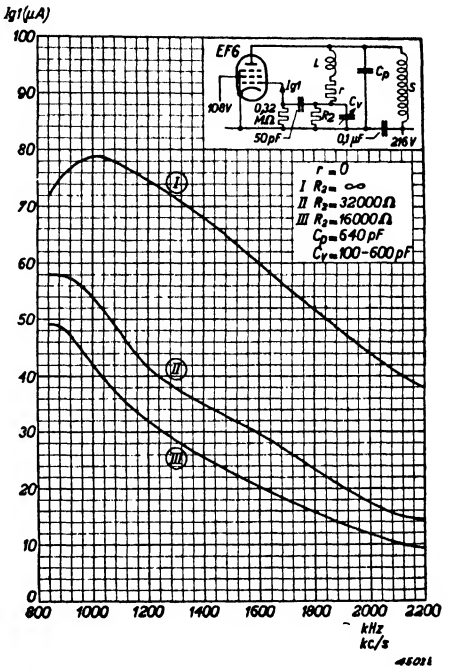

Fig. 109. Grid current as a function of frequency in the medium-wave band, measured with an EF 6 connected as oscillator.
$C_2 = C_v$, $R_1 = \infty$, $r = 0$ ohm, $Q = 50$.
Curve I $R_2 = \infty$
Curve II $R_2 = 32{,}000$ ohms
Curve III $R_2 = 16{,}000$ ohms

In this case the slope requires to be greatest when C_v is small, and it is therefore at that point that the oscillator voltage is most affected. Although the two cases may be regarded as more or less similar, it is worth noting that the influence of increased damping is here greater at maximum C_v than it was in the previous case at small values of C_v. In both cases the ratio of the capacitances is a minimum, but in the present instance this is $600/600 = 1$, whereas in the previous case of anode damping it was $100/600 = 1/6$.

For all measurements C_v was connected to the grid side. It would be logical to repeat them with C_v joined to the anode side, but rather greater

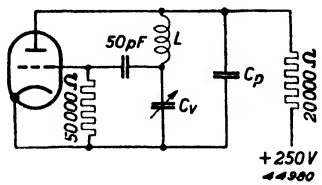

Fig. 110. Colpitts circuit for the triode section of the ECH 21 mixer.

divergences from calculated results will then be found. These discrepancies are to be attributed largely to the often very high anode A.C. voltage, which causes the mean anode current to be small and therefore reduces the potential-drop across the resistor. We shall in consequence not concern ourselves with the results of such tests, but turn to practical measurements with the ECH 21 mixer valve, for which the oscillator circuit is given in fig. 110. The grid capacitor and leak have the values specified in the published data, namely 50 pF and 50,000 ohms respectively.

The grid current, measured under normal conditions, is shown in fig. 111 curve I as a function of oscillator frequency for the medium waveband. This curve agrees fairly well with the calculated result indicated by curve III of fig. 106.

In order to find out what effect the parallel resistance R_1 had on performance, a choke S was substituted and the supply voltage reduced to 108 V; in these conditions curve II of fig. 111 was obtained. Therefrom it may be concluded that the parallel damping of the anode circuit is only slightly influenced by R_1 and that the AC resistance of the triode section is the chief factor. A variation of this circuit has the parallel resistor R_1 connected not directly to the anode but to the junction of L and C_v (C_2). The result of such a modification is, as might be expected, increased damping of the grid circuit, most evident when C_v is small (2000 kc/s); see curve III. Further measurements were made using this type of feed, but

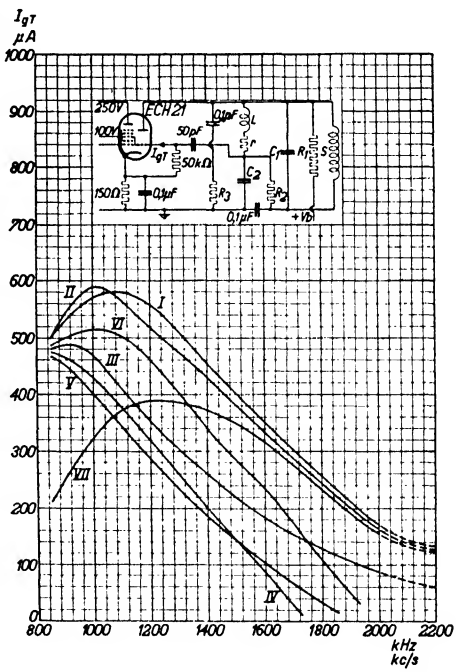

Fig. 111. Grid current as a function of frequency in the medium-wave band, for the triode section of the ECH 21 mixer.

Curve	C_1	C_2	R_1	R_2	R_3	S	Vb
I	Cp	Cv	20kΩ	∞	∞	∞	250 V
II	Cp	Cv	∞	∞	∞	20 mH	108 V
III	Cp	Cv	∞	20kΩ	∞	∞	250 V
IV	Cv	Cp	20kΩ	∞	∞	∞	250 V
V	Cv	Cp	∞	∞	∞	20 mH	108 V
VI	Cv	Cp	∞	20kΩ	∞	∞	250 V
VII	Cp	Cv	20kΩ	∞	5kΩ	∞	250 V

with C_v and C_p transposed; curves IV, V and VI were then obtained. It has already been observed that this circuit demands a high effective slope, and it will be seen from these last-mentioned curves that, owing to the oscillator cutting out, the end of the waveband cannot be reached. The most suitable circuit is accordingly that of fig. 110, the performance of which is indicated by curve I.

Around 1000 kc/s the oscillation is excessively strong. In simple sets this is not of great importance, for it will be remembered that the conversion-conductance of the ECH 21 is not much effected by above-optimum oscillator voltage. In better-class receivers too strong an oscillation is to be avoided, since noise and distortion are thereby increased.

One method of limiting this tendency to excessive oscillation at low frequencies (e.g. 1000 kc/s) would seem, from the foregoing, to be the provision of heavier anode damping. Such cannot be attained merely by reducing R_1, for the anode voltage would thereby be raised. It is, however, possible to connect a resistor R_3 across C_p (C_1) from which direct current is excluded.

With additional damping of 5000 ohms parallel to C_p curve VII of fig. 111 was obtained; the effect of the increased damping is very evident. Disadvantages of this course are that it requires an extra resistor and that it influences the tracking curve unfavourably (see Chapter III B).

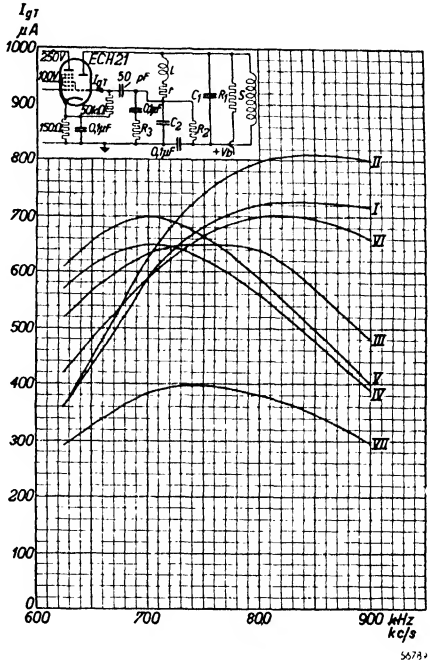

Fig. 112. Grid current as a function of frequency in the long-wave band, for the triode section of the ECH 21 mixer

Curve	C_1	C_2	R_1	R_2	R_3	S	Vb
I	Cp	Cv	20 kΩ	∞	∞	∞	250 V
II	Cp	Cv	∞	∞	∞	20 mH	108 V
III	Cp	Cv	∞	20 kΩ	∞	∞	250 V
IV	Cv	Cp	20 kΩ	∞	∞	∞	250 V
V	Cv	Cp	∞	∞	∞	20 mH	108 V
VI	Cv	Cp	∞	20 kΩ	∞	∞	250 V
VII	Cp	Cv	20 kΩ	∞	16 kΩ	∞	250 V

When the circuit of fig. 110 is employed on the long-wave band the frequency varies within narrower limits, namely from about 600 to 900 kc/s. As a consequence C_p has a different value. The influence of the coil-damping on the required slope now becomes quite small.

The grid current/frequency curves of fig. 112 indicate the performance. It will be noticed that the shape of curve I in fig. 112 is the reverse of that for the medium waveband; this must be attributed to the circuit elements being different. In addition the A.C. resistance R_i of the triode section is high at 900 kc/s, when oscillator voltage is large; confirmation is provided by the fact that the substitution of choke feeding, with which anode damping is removed almost entirely, has a marked effect (curve II). On the other hand, the application of the supply voltage to the lower end of L, resulting in increased grid-circuit damping, causes the amplitude of oscillation to decrease with small C_v (900 kc/s) and to increase with large C_v owing to the reduced anode damping (see curve III). Interchanging C_v and C_p again gives rise to the phenomena observed earlier; oscillation ceases, though in this case the decline is not so rapid. It is worth noting that on the long waveband the general level of oscillator voltage is higher, and since the relation of C_v to C_p also determines the back-coupling ratio with this circuit the only way to lower it is to introduce further damping. Starting with the circuit of fig. 110, and therefore with curve I, we may attempt a solution by adding R_3, suitably isolated in order to avoid the flow of direct current, so as to increase the grid damping. With $R_3 = 16{,}000$ ohms curve VII is obtained; naturally with still heavier damping the current diminishes further.

The following conclusions may be drawn from the foregoing.

From the general form of the condition for oscillation with the Colpitts circuit it is evident that the circuit is suitable for use with the oscillator of converter valves; but it is essential that the oscillator has a reasonably high slope. The tuning capacitor should preferably be connected to the grid side, and the padding capacitor to the anode side.

With an ECH 21 in this circuit (fig. 110) sufficiently high oscillator voltages are obtained; indeed at some frequencies the amplitude is excessive. However it is possible to reach a lower level of oscillation by introducing extra damping. But the values of resistance required on medium and long wavebands respectively are different, and the point of connection is not the same for the two bands; consequently this solution entails the use of rather much material. In general, therefore, the rather large rise of oscillator voltage in one direction or the other has to be tolerated.

Detailed consideration will not be given to the influence of valve capacitances on this circuit, but it may be expected that, owing to the tight coupling of the tuned circuit to the grid, inter-electrode capacitance variations will cause frequency shift. For these reasons the Colpitts circuit is suitable only for the cheaper type of receiver.

§ 8. The Hartley circuit

If in the Colpitts circuit the capacitances comprising the resonant circuit are replaced by inductances, and the inductance by capacitance, the Hartley circuit (fig. 113) is obtained.

Another version of this circuit is shown in fig. 114, the tapping on the

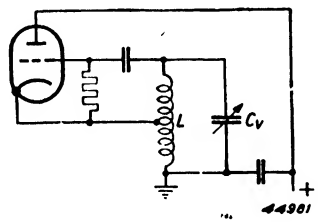

Fig. 113. Basic Hartley circuit.

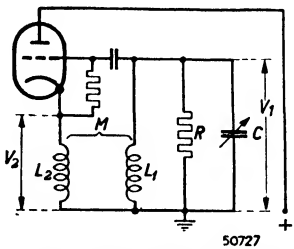

Fig. 114. Hartley circuit with a separate back-coupling coil in place of a tapping on the tuning inductor.

inductor being here replaced by a separate coupling coil; such an arrangement was referred to in section A § 4b, though in that case various positive electrodes performed the function of anode. The slope S_k in this circuit is the slope of the first grid in relation to the total cathode current.

Particularly for simple receivers the circuit of fig. 113 is attractive, as a separate coupling coil is not required.

The condition for oscillation will be derived for the case in which the tuned circuit is damped only by parallel resistance.

When the voltage across the resonant circuit is V_1, that across the cathode coil is:

$$V_2 = V_1 \frac{M}{L_1} \quad \text{(II B 42)}$$

This voltage $-V_2$ is ultimately the active voltage in the anode circuit. From the voltage relation in equation (II B 42) it follows that at resonance the dynamic resistance in the anode circuit is

$$Z = R \left(\frac{M}{L_1}\right)^2 .$$

For the voltage between cathode and grid we find:

$$V_g = (V_1 - V_2) = V_1 \left(1 - \frac{M}{L_1}\right) \quad \text{(II B 43)}$$

The back-coupling ratio is thus:

$$t = \frac{V_g}{-V_2} = -\frac{1 - M/L_1}{M/L_1} \quad \text{(II B 44)}$$

The general condition for oscillation (II B 3) now becomes

$$\frac{1 - M/L_1}{M/L_1} \cdot (M/L_1)^2 \, R \, . \, S_{k\,eff} = 1,$$

or:

$$(M/L_1 - M^2/L_1^2) \, R \, S_{k\,eff} = 1 \quad \text{(II B 45)}$$

The value of the expression within brackets is a maximum when $M/L_1 = \frac{1}{2}$, and in that case equation (II B 45) becomes:

$$\tfrac{1}{4} \, R \, S_{k\,eff} = 1.$$

The same condition for oscillation is found with a tuned-anode circuit used in conjunction with a coupling coil if $t = \frac{1}{4}$. In comparison with such an arrangement the Hartley circuit has the drawback that the amount of feedback obtainable is severely limited. Thus the normal tuned-anode circuits, with which the ratio M/L may be as high as 1, needs an effective slope only one fourth as great.

With a tuned circuit of dynamic resistance $R = 5000$ ohms we can calculate from the equation $t \, . \, S_{k\,eff} \, . \, R = 1$ that when $M/L_1 = \frac{1}{2}$ a slope $S_{k\,eff} = 0.8$ mA/V will be necessary. If we assume that the required oscillator voltage is 4 V and equal to the cut-off voltage of the valve, then we find from fig. 87 (quadratic characteristic) that $S_{eff}/S_o = 0.2$; it therefore follows that S_{ko} must be 4 mA/V. Such a value is rather high; the slope of most valves in current use is only about 3 mA/V.

Moreover the Hartley circuit has the disadvantage that an H.F. voltage is present between cathode and heater, which is likely to introduce difficulties (see also A § 4b).

§ 9. Valve damping and shunt capacitances

So far we have always assumed an anode impedance Z and a back-coupling factor t, and only incidental reference has been made to the fact that Z is determined not merely by L, C and R, but also by the characteristics of the valve. It will at once be apparent that in the case of a tuned-anode circuit the A.C. resistance of the valve affects the parallel damping and that the anode-to-cathode capacitance contributes to the tuning capacitance.

In the case of a tuned grid circuit we must take into account an extra shunt

damping, equal either to the value of the grid damping or to the equivalent resistance of the grid capacitor in series with the grid damping. Further, the equivalent capacitance of this series combination must be added to the tuning capacitance (see I A § 4).

Elements shunting the coupling coil, such as a resistor or the A.C. resistance of the valve, may, in the case of a tuned-grid arrangement, be multiplied by $(L_1/M)^2$, the resulting product being regarded as lying in parallel with the tuned circuit. Any parallel capacitance, such as C_a, is added, after multiplication by $(M/L_1)^2$, to the total capacitance of the tuned circuit.

The back-coupling ratio t may be affected similarly. For instance the grid capacitor C_r and the grid input capacitance C_{g1} form a potential-divider between grid and cathode, with the result that the voltage fed to the grid is multiplied by a factor:

$$t' = \frac{C_r}{C_r + C_{g1}}. \quad \ldots\ldots\ldots\ldots\ldots \quad \text{(II B 46)}$$

Since the permissible value of the grid capacitor C_r is limited by such phenomena as overoscillation and frequency-drift, it is important to make the grid capacitance as small as possible in order to avoid reducing t' unduly. Especially on short waves, too large a voltage-division is likely to cause trouble.

At the lowest frequencies in the long waveband there is also a division of voltage across C_r and the imaginary resistance represented by the grid damping. At 600 kc/s, corresponding to an I.F. of 450 kc/s and a signal frequency of 150 kc/s, the reactance of a grid capacitor of 25 pF amounts to about 10,000 Ω. With input damping of 17,000 Ω (the influence of the grid input capacitance can be neglected at this frequency) the voltage-division becomes:

$$t' = \frac{17{,}000}{\sqrt{17{,}000^2 + 10{,}000^2}} = 0.85$$

It has been assumed hitherto that in the anode circuit a current of fundamental frequency flowed, the magnitude of which was:

$$I_1 = S_{eff}\, V_g \quad \ldots\ldots\ldots\ldots\ldots \quad \text{(II B 4)}$$

This is correct for a case in which the anode load is short-circuited. In calculating the condition for oscillation any external impedance present was assumed to be in parallel with the A.C. resistance of the valve (see page 148); the net impedance may be calculated from the equation $\frac{1}{Z_{tot}} = \frac{1}{Z} + \frac{1}{R_{i\,eff}}$.

The argument employed here is basically the same as that in the case of an

A.F. amplifying triode when, in the same circumstances, the static slope is used and not the dynamic slope. This possibility is based on the following formula for the valve characteristic:

$$i_a = S\, v_g + \frac{v_a}{R_i} \quad \text{(II B 47)}$$

wherein $S\, v_g$ is the short-circuit current, which is reduced by a current v_a/R_i flowing through a parallel path R_i (the sign of v_a is opposed to that of i_a). Similarly we can write:

$$I_1 = S_{eff}\, V_g + \frac{V_a}{R_{i\,eff}} \quad \text{(II B 48)}$$

What value must be inserted for $R_{i\,eff}$, the effective A. C. resistance? The approximate value may be ascertained as follows: for the valve characteristic we may also write:

$$i_a = S\left(v_g + \frac{v_a}{\mu}\right).$$

If for convenience we consider only the alternating voltages we can write for the anode alternating voltage

$$v_a = \frac{v_g}{t}.$$

The instantaneous value of i_a then becomes:

$$i_a = S\left(v_g + \frac{v_g}{\mu t}\right) = S\, v_g \left(1 + \frac{1}{\mu t}\right) \quad \text{(II B 49)}$$

The current variations are thus reduced by the presence of the alternating voltage at the anode, t being regarded as negative.
If we now calculate the fundamental component of the anode current once more, following the earlier method exactly, we find:

$$I_1 = S_{eff} V_g \left(1 + \frac{1}{\mu t}\right),$$

and for the basic form of the condition for oscillation:

$$t\, S\, Z \left(1 + \frac{1}{\mu t}\right) = -1 \quad \text{(II B 50)}$$

In this, however, we neglect the following. In a circuit with short-circuited anode lead, current begins to flow when the grid becomes more positive than the cut-off voltage V_{go}. If now an anode impedance is introduced the instantaneous value of the anode alternating voltage is generally no longer nil at this grid voltage. It follows that the anode current is no longer nil;

in other words the cut-off point is shifted somewhat. Strictly speaking it is therefore not sufficient to bring the factor $(1 + \frac{1}{\mu t})$ into account; in addition a new value of V_{go} must be used when calculating S_{eff}. This last correction becomes rather cumbersome, however, and measurements show that in practice it may be neglected.

To determine $R_{i\,eff}$ we begin from the last equation but one, writing it thus:

$$I_1 = S_{eff} \,.\, V_g + S_{eff} \frac{V_a}{\mu} \,.$$

From the definition of $R_{i\,eff}$ [equation (II B 48)] it follows that:

$$R_{i\,eff} = \frac{\mu}{S_{eff}} = \frac{R_i\, S_o}{S_{eff}} \quad \ldots\ldots\ldots\ldots \quad \text{(II B 51)}$$

The value of the factor S_{eff}/S_o in varying circumstances may be ascertained from the curves of figs 85, 86 and 87. It is apparent that in practice S_{eff}/S_o often has a value of about 0.25, and it is therefore roughly true to say that the effective A.C. resistance of the oscillator valve is four times the static A.C. resistance.

Measurements of Ri_{eff} demonstrate, in fact, that equation (II B 51) remains valid over a considerable range of oscillator voltage. With large amplitude, however, the difficulty arises that the cut-off point is shifted appreciably, and the equation then ceases to hold good. In normal circumstances, and for the oscillator valves considered here, R_{ieff} can be assessed with the aid of equation (II B 51) and no large error will occur. Equation (II B 50) often provides a clearer picture of oscillation than the earlier equations, in which A.C. resistance had to be taken into account separately. It is, for example, at once apparent that it is not possible, by using a very high impedance Z, to arrive at a very weak back-coupling, because at a certain point the quantity between brackets falls to zero. Clearly Z can never be greater than R_{ieff}. It is evident, then, that we can also say that the back-coupling ratio t must be large in relation to $1/\mu$.

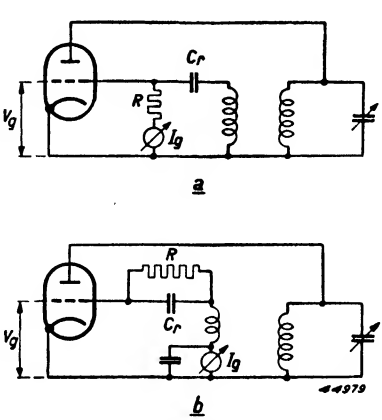

Fig. 115. Two basic oscillator circuits: in *a* the damping effect of grid current is equal to the grid leak R in parallel with the equivalent damping resistance R_{HF} of the grid current; in *b* it is equal to the resistance R_{HF} only.

Another matter of importance in an oscillator circuit is the damping of the tuned circuit by grid current. Between the circuits of figs 115a and b there is no difference as far as grid current is concerned, yet the resultant damping is not the same in the two cases. It is customary to express this damping in terms of an equivalent resistance R_{HF} which causes an identical loading effect.

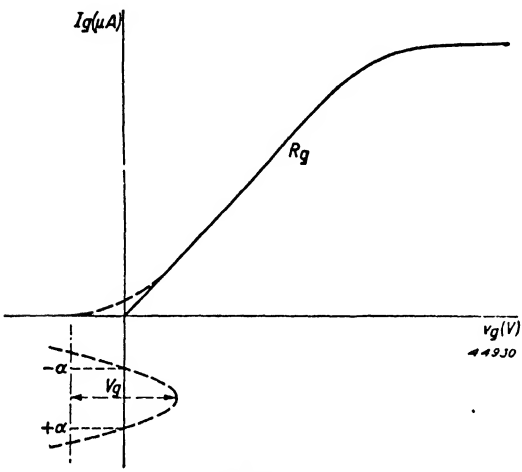

Fig. 116. Grid current characteristic of a triode in which the variation of the oscillator voltage at the grid as a function of time has been plotted.

In the circuit of fig. 115a the damping is equal to the parallel combination of R_{HF} and the grid leak R, but in that of fig. 115b it is equal to R_{HF} alone. Further reference to this subject will be found in Chapter V, under Diode detection. With the normal diode detector, so-called peak rectification occurs *, but this is not the case with oscillators (see II B § 4 regarding the ECH 21 and DK 21).

The grid leak in oscillator circuits must, in view of requirements on short waves, be much smaller than the load resistance of a diode detector. Consequently the grid current will be larger, and the grid-current curve will not, as in Chapter V, be determined by the formula $i_g = A\varepsilon^{\frac{v_a}{V_T}}$ but will be nearly a straight line. (We are thinking all the time of voltages of several volts; voltages below say 2 V can therefore be left out of consideration.) Fig. 116 shows a grid-current characteristic. Both near the origin and around saturation level it is somewhat curved; in the case of battery valves this curvature may be of great importance. With normal oscillator voltages, however, we make no great error in writing the equation of the grid-current characteristic as:

$$i_g = \frac{v_g}{R_g} \quad \ldots\ldots\ldots\ldots\ldots\ldots \quad \text{(II B 52)}$$

where R_g represents the A.C. resistance between grid and cathode. If an

* See for the meaning of this idea Chapter V, Diode-detection.

alternating voltage $V_g \cos \omega t = V_g \cos x$ is fed to the grid via the grid capacitor C_r and the grid leak R, the grid capacitor C_r is charged to a certain steady potential by the pulses of direct current. On the other hand the grid capacitor discharges through the resistor R (both in the circuit of fig. 115a and in that of 115b). A state of equilibrium is reached, at which the current draining away just equals the mean current applied. The relation between the current variations and the DC voltage V_c across the grid capacitor is explained by fig. 117. Current flows during the time between $x = -a$ and $x = +a$. The DC voltage V_c can also be written as $V_g \cos a$. The current drawn off is accordingly:

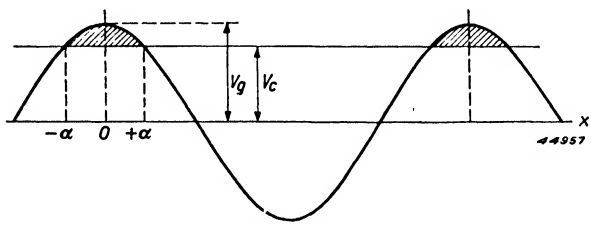

Fig. 117. Relation between current fluctuations and the steady voltage V_c across the grid capacitor; current flows only during the period from $-\alpha$ to $+\alpha$.

$$I_{g\,med} = \frac{V_g \cos a}{R} \quad \text{(II B 53)}$$

The instantaneous value of the voltage at the grid is:

$$v_g = V_g \cos x - V_g \cos a$$

and that of the current, during each pulse:

$$i_g = \frac{V_g \cos x - V_g \cos a}{R_g} \quad \text{(II B 54)}$$

Consequently the mean current applied:

$$I_{g\,med} = \frac{1}{2\pi} \int_{-a}^{+a} i_g \, dx = \frac{V_g}{2\pi R_g} \int_{-a}^{+a} (\cos x - \cos a)\, dx =$$

$$= \frac{V_g}{2\pi R_g} (\sin x - x \cos a) \Big|_{-a}^{+a} = \frac{V_g}{\pi R_g} (\sin a - a \cos a) \quad \text{(II B 55)}$$

From equations (II B 53) and (II B 55) we get:

$$\tan a - a = \pi \frac{R_g}{R} \quad \text{(II B 56)}$$

It follows that the current angle a is independent of the amplitude of the

alternating voltage. For a given ratio Rg/R, a has a fixed value, and $I_{g\ med}$ is thus proportional to the grid A.C. voltage V_g.

Fig. 118 shows the relation between R/R_g and cos a, calculated according to equation (II B 56). If R and R_g are known, cos a may be read directly from fig. 118 and $I_{g\ med}$ can then be calculated from equation (II B 53). As an example, fig. 119 gives the relation between the oscillator voltage V_{osc} and the current $I\,(g_T + g_3)$ through the grid leak for the converter ECH 21. The resistance of the grid leak is 50,000 ohms, and as the oscillator grid/cathode A.C. resistance amounts to 500 ohms we find that $\cos a = 0.90$. We see, in fact, that the relation between $I_{g\ med} = I\,(g_T + g_3)$ and V_g (V_{osc}) may be represented by a straight line. The load imposed by the grid may be replaced by a resistance R_{HF} which draws as much A.C. power as the grid. If I_{g1} is the fundamental of the grid current, then the power absorbed is:

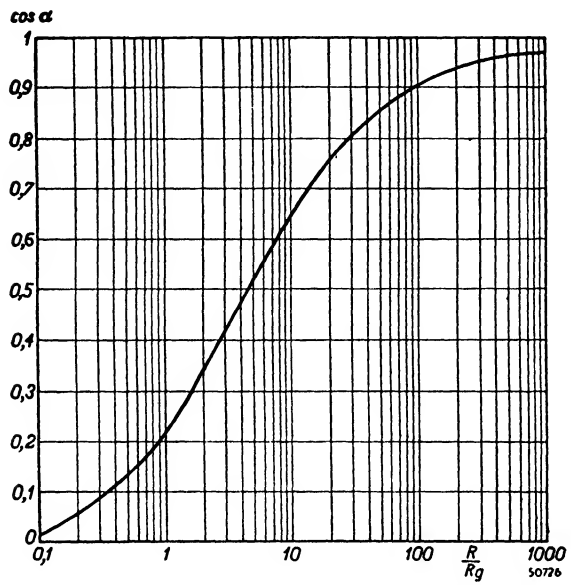

Fig. 118. Cos a as a function of the ratio $\frac{R}{Rg}$, if R is the grid leak and Rg the grid AC resistance of the oscillator triode.

$$P = \frac{I_{g1} \cdot V_g}{2}.$$

The AC power in the equivalent resistance R_{HF} is:

$$P = \frac{V_g^2}{2\,R_{HF}}.$$

Therefore

$$\frac{I_{g1} \cdot V_g}{2} = \frac{V_g^2}{2\,R_{HF}} \text{ and}$$

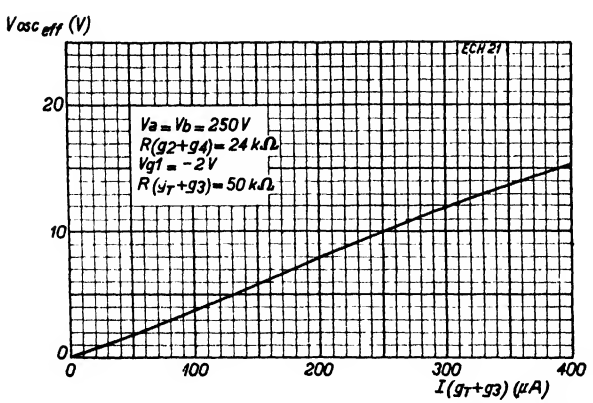

Fig. 119. Oscillator voltage as a function of the oscillator grid current in the triode section of the ECH 21; with this curve cos a = 0.9.

$$R_{HF} = \frac{V_g}{I_{g1}} \quad \text{(II B 57)}$$

I_{g1} may, from Fourier, be written:

$$I_{g1} = \frac{1}{\pi}\int_{-a}^{+a} i_g \cos x \, dx = \frac{V_g}{\pi R_g}\int_{-a}^{+a} (\cos^2 x - \cos x \cos a)\, dx =$$

$$\frac{V_g}{\pi R_g}\left[\frac{x}{2} + \frac{\sin 2x}{4} - \cos a \sin x\right]_{-a}^{+a} = \frac{V_g}{\pi R_g}\left(a - \frac{\sin 2a}{2}\right) \quad \text{(II B 58)}$$

Substituting from equation (II B 58) in (II B 57) we now obtain for the damping resistance R_{HF} in the grid circuit:

$$R_{HF} = \frac{\pi R_g}{a - \frac{\sin 2a}{2}} \quad \text{(II B 59)}$$

Or, making use of equation (II B 54):

$$R_{HF} = \frac{R(\tan a - a)}{a - \frac{\sin 2a}{2}} \quad \text{(II B 60)}$$

We shall now consider this result further for two extreme cases:

a) R/R_g is very large (peak rectification). In the limiting case of equation (II B 60), when $a = 0$, $R_{HF} = 0.5\,R$. This result is also reached in Chapter V, in connection with diode rectification.

b) $R = 0$, the limiting case of small R. In this instance a becomes $\pi/2$, and $R_{HF} = 2\,R_g$; the reason for this result will be evident when it is realised that the circuit is loaded by R_g during every other half-cycle.

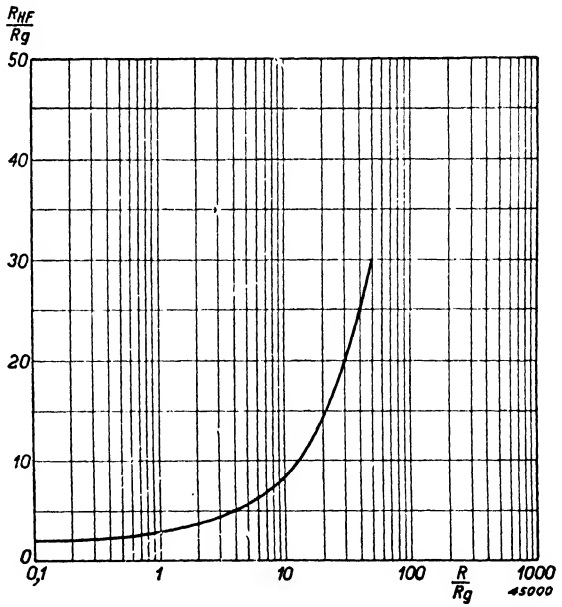

Fig. 120. $\frac{R_{HF}}{R_g}$ as a function of $\frac{R}{R_g}$

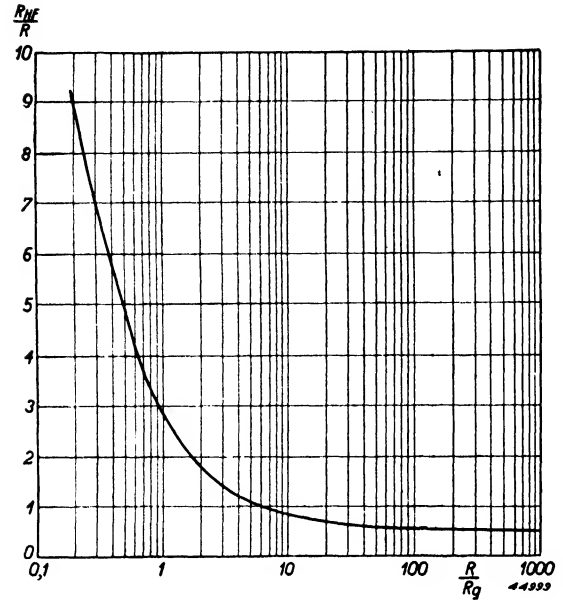

Fig. 121. $\frac{R_{HF}}{R}$ as a function of $\frac{R}{Rg}$

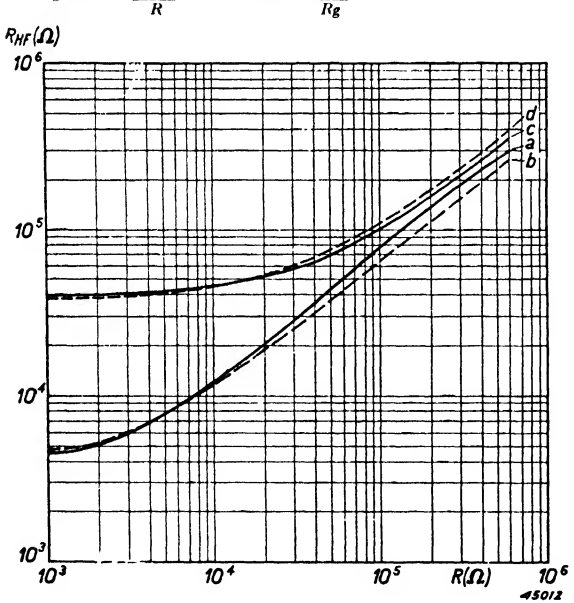

Fig. 122. Grid-current damping R_{HF} as a function of the resistance of the grid leak R, for a particular triode:
a and *b*. Measured and calculated curves respectively for $Rg =$ 2300 ohms.
c and *d*. Measured and calculated curves respectively for $Rg =$ 17,000 ohms.

Equations (II B 59) and (II B 60) are displayed as curves in figs 120 and 121 respectively, *a* being replaced however by R/R_g derived from equation (II B 56).

By way of illustration we shall now calculate the grid damping for two specific cases:

a) The ECH 21 has an oscillator-grid/cathode A.C.-resistance of 500 ohms while the grid leak prescribed is 50,000 ohms; R/R_g is therefore 100. From fig. 121 we find $R_{HF} = 0.6 \times 50{,}000 = 30{,}000$ ohms.

b) For the DK 21 battery octode the values are: $R_g = 5000$ ohms and $R = 35{,}000$ ohms. Therefore $R/R_g = 7$ and $R_{HF} = 0.93 \times 35000 = 32{,}500$ ohms.

As a test of the theoretical figures some measurements were made to establish the grid damping as a function of the resistance of the grid leak. This damping was ascertained by measuring the selectivity of a tuned circuit across which the two valves, with an oscillator-grid/cathode A.C.-resistance Rg of 2300 ohms and 17,000, ohms respectively, were

connected in turn. The results are seen in fig. 122, where *a* is the measured and *b* the calculated curve for $R_g = 2300$ ohms, while *c* en *d* are the measured and calculated curves for $R_g = 17{,}000$ ohms. The agreement between the two curves of each pair is very satisfactory. For all measurements the oscillator voltage was 7 V_{RMS}.

When using the circuit of fig. 115a the grid leak R must still be regarded as being in parallel with R_{HF}, and for the total damping we then get:

$$\frac{1}{R_t} = \frac{1}{R_{HF}} + \frac{1}{R} \quad \text{(II B 61)}$$

§ 10. Influence of the anode-grid capacitance of the oscillator triode

The effect of the anode-grid capacitance of the oscillator triode has not so far been mentioned. Although its value is not usually large, in some circumstances it may be such that the presence of the capacitance can no longer be neglected. A capacitance which influences the circuit in the same way is that which exists between the high-potential ends of the oscillator and coupling coils. These two capacitances will accordingly be considered together. It is clear that their effect is important mainly in the case of tuned-anode circuits. Fig. 123 shows the basic circuit of an oscillator with the inter-electrode capacitance C_{ag} taken into consideration. Were C_{ag} absent, the fraction of the anode voltage indicated by the tapping ratio t_o would be applied to the grid, but allowing for this capacitance it will be seen that a voltage equal to $V_a - t_o V_a$ is present across the series combination of C_{ag} and C_r. (As C_{ag} is usually extremely small, the anode impedance is scarcely affected by this shunt.) Of the above mentioned voltage that part which is developed across the grid capacitor contributes to the voltage controlling the grid.

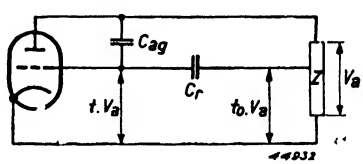

Fig. 123. Basic oscillator circuit, taking into account the effect of C_{ag}. The feedback ratio t is now equal to:
$t = t_o \frac{C_r}{C_r + C_{ag}} + \frac{C_{ag}}{C_r + C_{ag}}$

The voltage across the grid capacitor is:

$$V_c = (V_a - t_o V_a) \frac{C_{ag}}{C_{ag} + C_r},$$

and the voltage at the grid therefore becomes:

$$V_g = t_o V_a + V_c = t_o V_a + V_a (1 - t_o) \frac{C_{ag}}{C_{ag} + C_r}.$$

Throughout we have written $V_g = t\ V_a$. Consequently we get:

$$t = t_o \frac{C_r}{C_r + C_{ag}} + \frac{C_{ag}}{C_r + C_{ag}} \quad \ldots\ldots\ldots \quad \text{(II B 62)}$$

To the original voltage division t_o two corrections must accordingly be made, namely:

1) multiplication by $\frac{Cr}{C_r + C_{ag}}$ to allow for the further potential division across the grid capacitor and the anode-grid capacitance;
2) an additional voltage loss across the grid capacitor.

The value of t_o is increased by a positive amount; as t and t_o are both negative the effect is a reduction of the tapping ratio.

The first correction corresponds exactly to the effect of a grid input capacitance and is usually small. The second correction is more important and becomes percentually greater as the original t_o becomes smaller. As already noted, t_o is bound to be negative, whereas the capacitance ratio can only be positive; the back-coupling is therefore always reduced by this second correction.

The lowest values of t_o occur with a tuned anode circuit, and in particular on the long waveband, for it is then that the circuit impedances tend to be highest. Fairly high values of t_o can however also arise in these circumstances if, for example, the voltage across the padding capacitor is employed to effect the feedback.

We shall now find out how much influence C_{ag} has in the triode section of the ECH 21. It amounts to 1.1 pF. Assuming that the grid capacitor is 50 pF and that t_o for a long-wave coil may be put at 0.1, we then find from the foregoing, for the first correction, that t is reduced by about 3%. The loss on account of the second correction, however, reaches about 22%. With a grid capacitor of 25 pF the reduction might be as much as 50%.

In the example given, the drop in back-coupling brings no serious difficulties in its train. It is a simple matter to off-set the reduction by beginning with a higher ratio t_o. The example was given only to illustrate a phenomenon that might otherwise be overlooked.

Nevertheless, there is an important conclusion to be drawn from the foregoing. On short waves it is of great importance, in view of the risk of frequency drift, to keep the coupling between the oscillator circuit and the valve electrodes as loose as possible.

This may be ensured by making t_o low or by the use of a small grid capacitor. Both measures enhance the influence of C_{ag}; moreover the resultant

looser coupling necessitates a higher slope, and raising the slope usually causes an increase in C_{ag}. Everything thus combines to magnify the effect. Consequently it is of high importance that the other characteristics of the valve should permit the use of a large grid capacitor, in order that the effect of C_{ag} may be kept within reasonable bounds. There can, however, be objections to a large grid capacitor and these are discussed in Section E.

If the leakage inductance in the oscillator-coil assembly makes itself felt (i.e. $L_1 L_2 \neq M^2$), the circuit of fig. 123 must be varied to that of fig. 124. Apart from the voltage drop across C_r there is now a loss of voltage over the leakage inductance $L_2 - M$. This latter voltage is in opposite phase to that across C_r and will therefore compensate for the effect of C_{ag}. With rising frequency this voltage may become greater than the voltage across C_r and in such a case back-coupling is increased. This is a further cause of increased oscillator voltage at the bottom of the short waveband; in certain circumstances the increase is considerable.

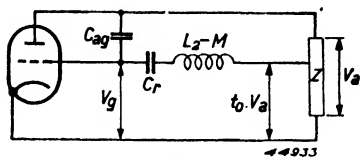

Fig. 124. The circuit of fig. 123 taking into account the stray inductance of the coil set L_2—M. The stray inductance in combination with the capacitance C_{ag} increases the back-coupling, in particular on high frequencies.

The required corrections to the values of t can again be found very simply if it is assumed that the current through the C_{ag} arm is determined only by C_{ag}; in view of the small value of C_{ag} this is practically true.

We can then write:

$$V_g = t_o \cdot V_a + (V_a - t_o \cdot V_a) \frac{\frac{1}{j\omega C_r} + j\omega (L_2 - M)}{\frac{1}{j\omega C_{ag}}},$$

from which we get:

$$t = t_o \left\{ 1 - \frac{C_{ag}}{C_r} + \omega^2 C_{ag} (L_2 - M) \right\} + \frac{C_{ag}}{C_r} - \omega^2 C_{ag} (L_2 - M) \quad . \quad \text{(II B 63)}$$

As already noted, the stray capacitance between the high-potential ends of the coils exercises practically the same influence as C_{ag}. There is however one difference: the current-path no longer contains the grid capacitor but does include the leakage inductance. This stray capacitance thus results only in the oscillator voltage increasing with frequency. The corrected value of t may be found by inserting $C_r = \infty$ in the last equation.

§ 11. Grid current

To determine the oscillator voltage a valve-voltmeter may be used, but indirect measurement by ascertaining the steady current through the grid

eak is easier. As was found in II B § 9, this current is proportional to the oscillator voltage [equation (II B 53)], while the relationship is dependent only in the ratio R/R_g. For a particular valve with a grid A.C.-resistance R_g and the prescribed grid leak R there is thus a fixed relation between grid current and oscillator voltage. With the help of the curve showing this relation (fig. 118) V_g can easily be deduced from $I_{g\ med}$.
A couple of examples will make this clear.

1) The ECH 21 has a grid AC-resistance $R_g = 500$ ohms, and a grid leak of $R = 50{,}000$ ohms is specified; R/R_g is thus 100. It follows from fig. 118 that $\cos a = 0.90$. With an oscillator voltage of 10 V_{RMS} (14 V peak) we find for $I_{g\ med}$ a value of $\frac{14 \times 0{,}90}{50{,}000} \times 10^6 = 252$ μA. The oscillator voltage curve for the ECH 21 (fig. 119) indicates a mean current of 250 μA. The negative bias on the oscillator grid is therefore $250 \times 50{,}000 \times 10^{-6} = 12.5$ V, and consequently the oscillator voltage swings the grid as far as 1.5 V positive.

2) With the battery octode DK 21 the conditions are somewhat different, namely $R_g = 5{,}000$ ohms and $R = 35{,}000$ ohms, so that $R/R_g = 7$ and $\cos a = 0.59$. For $I_{g\ med}$ we now find, at the same oscillator voltage, a value of 235 μA, while the oscillator-voltage curve of the DK 21 gives the figure of 237 μA. The negative grid bias amounts to $237 \times 35{,}000 \times 10^{-6} = 8.3$ V, and the oscillator voltage therefore swings the grid as far as 5.7 V positive.

Although the oscillator-grid current is about the same in both valves, there is a large difference in the extent of the incursion into the positive-grid region.

Finally let us consider two limiting cases, namely:

a) R/R_g is large, i.e. $R_g \approx 0$. It then follows from equation (II B 56) that $\tan a = a$ and $\alpha = 0$. This indicates peak rectification. For this case equation (II B 53) is:

$$I_{g\ med} = \frac{V_g}{R}.$$

b) $R \approx 0$; R_g/R is now very large, so that $\tan a = R_g/R$ or $a = \pi/2$. From equation (II B 55) therefore:

$$I_{g\ med} = \frac{V_g}{\pi R_g}.$$

(V_g/π is the mean value of a half sine wave).

C. Circuits for constant oscillator voltage

For optimum conversion conductance a specific amplitude of heterodyne voltage is necessary (II A § 2). Admittedly this amplitude is not very critical, but with most of the circuits mentioned in Chapter II B the heterodyne voltage varies so much that the conversion conductance cannot but show appreciable deviation. In order to secure constant sensitivity and a good signal-to-noise ratio it is advisable to modify the circuits with a view to getting as constant an oscillator voltage as possible over each waveband. Some possible ways of achieving this end will now be discussed.

§ 1. Parallel-fed tuned-anode circuit

In Chapter II B it was always assumed, for the sake of simplicity, that the steady anode current flowed through the tuned circuit.

Chiefly for practical reasons, however, such as the presence of a padding capacitor in series with the coil, the danger of a DC potential across the variable capacitor, etc., the valve is generally fed through a resistor. The tuned circuit is then joined to the resistor by a capacitor. If this coupling capacitor is large enough the arrangement may be regarded as equivalent to a tuned circuit connected directly in the anode circuit and shunted by the feed resistor. All previous considerations have been based on this supposition.

We shall first of all investigate the effect of using a smaller coupling capacitor. For the purpose of this discussion we shall as far as possible adapt the basic circuit to practical conditions and connect the padding capacitor in series with the coil L_1 (fig. 125). In this diagram C_k is the coupling capacitor and R the feed resistor, while C_a is the anode/cathode capacitance of the valve, including strays. The inevitable resistance of the inductor L_1 is for the moment neglected.

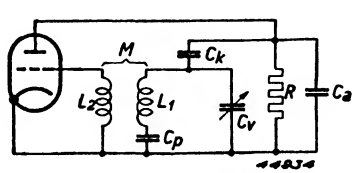

Fig. 125. Basic circuit of a parallel-fed oscillator. C_k is the coupling capacitor, R the feed resistor and C_a the anode/cathode capacitance of the valve including wiring strays.

When C_k has a very large value it may in this circuit be regarded as a short-circuit; the anode circuit then consists of three parallel paths, C_a, R and the combination L_1 C_v C_p. By means of the inductive back-coupling, the

grid is tapped into this last mentioned combination. The ratio of the voltage on the grid to that across the circuit $L_1C_vC_p$ we shall denote by t_o. With C_k short-circuited, t_o is also the feedback ratio which previously was indicated by t. If, however, the coupling capacitor C_k is not large enough to be considered a short-circuit, the overall feedback-ratio is equal to t_o multiplied by the relation between the voltage across the current path $L_1C_vC_p$ and the anode alternating voltage. It is assumed that the small change of oscillator frequency, due to altering C_k, will scarcely affect t_o. Since no resistance is present in the left-hand current path both t and t_o will represent real qualities. From the condition for oscillation (II B 3) it follows that the entire anode load must be purely resistive in character; this means that the reactance of the left-hand current path must be equal and opposite to that of the right-hand path.

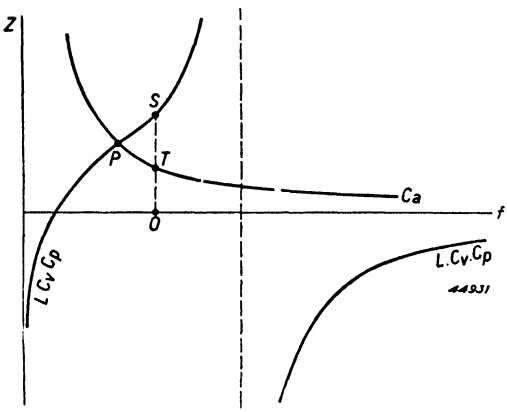

Fig. 126. Reactance of the combination L_1-C_v-C_p in the circuit of fig. 125, as a function of frequency, together with that of C_a in the opposite sense. The intersection of the two lines indicates the frequency at which the current-paths L_1-C_v-C_p and C_a are in equilibrium.
The shape of the L_1-C_v-C_p curve is fixed by the following factors: at very high frequencies the reactance of L_1-C_v-C_p equals that of C_v, and is infinitely great at the resonant frequency of the circuit; at very low frequencies it is practically equal to that of C_p. The intersection with the horizontal axis of the curve so obtained indicates the resonant frequency of the series-combination L_1-C_p.

We shall not on this occasion express the equilibrium in an equation; instead, we shall make use of a graphical method to investigate the problem.

In fig. 126 the reactance of the current path $L_1C_vC_p$ is shown against frequency, in the negative sense with that of C_a. If C_k is very large the state of balance is indicated by P, the point where the curves intersect; at the frequency corresponding thereto the circuit will accordingly oscillate. Since C_a is a capacitance the current path $L_1C_vC_p$ has of necessity an inductive character. Now if C_k is of such a value that the presence of the capacitance is noticeable, the reactance of the left-hand current path diminishes by an amount $1/\omega C_k$. Balance between the two current paths must however be maintained, and this is effected by the oscillator adjusting itself to a higher frequency. The reactance indicated by the point S, reduced by an amount $ST = 1/\omega C_k$, will then equal the reactance of C_a, indicated by the point T. In this way it can be seen that, as C_k is made smaller and therefore as the distance ST increases, the circuit adjusts itself nearer to the natural fre-

quency of the current path $L_1\ C_v\ C_p$, which in fig. 126 is represented by the dotted line. With the aid of this diagram it is also possible to obtain directly the ratio existing between the voltage at the anode and that across the current path $L_1\ C_v\ C_p$; it is equal to the ratio $OT : OS$. It appears now that, as C_k decreases, the voltage across the current path $L_1\ C_v\ C_p$ begins to exceed the voltage at the anode; this means that the back-coupling becomes stronger. Theoretically, therefore, it should be possible to obtain an infinitely tight back-coupling by reducing the value of C_k sufficiently, the resultant oscillator voltage then following the course shown by the dotted curve in fig. 127. Obviously, however, other factors arise to prevent an infinitely tight back-coupling ever being attained in practice. Point S can never, as suggested in fig. 126, lie infinitely far above the horizontal axis, because as soon as the oscillator frequency approaches the natural frequency of the current path $L_1\ C_v\ C_p$ the hitherto disregarded circuit losses prevent the two branches from having a purely reactive character.

In the first place, as the current path $L_1\ C_v\ C_p$ becomes more resistive in character the voltage across it falls in relation to that at the anode. With a pure resistance connected in series with the capacitance C_k this ratio must be less than unity. As the reduction of C_k continues a point is reached where the back-coupling begins to weaken again.

Secondly, the relation between the anode voltage and the voltage across the current path $L_1\ C_v\ C_p$ does not remain real when resistance appears in the left-hand branch of fig. 125. The feedback ratio then also becomes complex and the condition for oscillation involves a complex anode impedance. The condition can be satisfied if the frequency adjusts itself to a value at which the respective reactances of the left-hand and right-hand branches are unbalanced, thus leaving a reactance shunting the two paths. The total impedance is then necessarily smaller than the original value R, and for this reason also the oscillator voltage is bound to be lower.

The result of these two effects is that the curve connecting C_k and oscillator voltage takes the form shown in fig. 127 * for 1000 kc/s. From this it is clear that if C_k is not large the oscillator voltage can diverge considerably from the value calculated according to equation (II B 31).

---

* The quantity $\frac{L_1}{S_{eff}\,MR}$ shown against the vertical axis is derived as follows. As long as C_k is very large the circuit corresponds to that of fig. 97, in which $r_1 = 0$. Consequently:

$$S_{eff} = -\frac{L_1}{MR}\,\frac{C_p}{C_p + C_v},\quad \text{or:}\quad -\frac{L_1}{S_{eff}\,MR} = 1 + \frac{C_v}{C_p}.$$

Since, for a given coil assembly, L_1/MR is practically constant and $1/S_{eff}$ about proportional to the oscillator voltage the factor $\frac{L_1}{S_{eff}\,MR}$ may be taken as a measure of the oscillator voltage. If the value of C_k is such that the capacitance has some influence on the circuit, the value of $\frac{L_1}{S_{eff}\,MR}$ will, when C_v is large (e.g. $f = 580$ kc/s), decrease sharply at low values of C_k; while when C_v is small (e.g. $f = 1000$ kc/s) the oscillator voltage curve shows the typical peak at low values of C_k.

By way of illustration we shall give some measured results. In a normal tuned anode-oscillator circuit with an ECH 21 the grid current was measured, at several frequencies, as a function of the value of the coupling capacitor. For each curve the oscillator frequency was held constant by small adjustments to C_v. The curves, relating to various frequencies corresponding to the long-wave range, are reproduced in fig. 128. As long as C_k exceeds 400 pF the oscillator voltage is practically independent of the value of C_k. In the curves for 1200 and 900 kc/s, which are also given in fig. 128, the effect referred to above is well marked when C_k is less than 400 pF; yet at the lower frequencies the oscillator voltage shows no increase; it decreases with C_k. Clearly the damping of the circuit L_1 C_v C_p at the lower frequencies has an immediate and quite large influence.

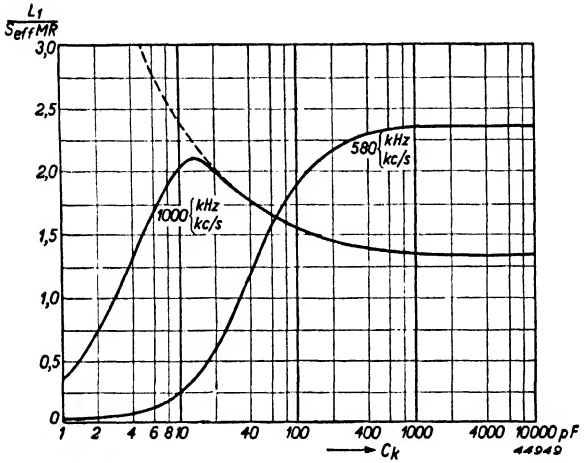

Fig. 127. The factor $\frac{L_1}{S_{eff}\,MR}$, which is proportional to oscillator voltage, as a function of C_k, calculated for two different oscillator frequencies.

In the medium waveband oscillator voltage displays a more or less similar trend, though the various curves do not, as in fig. 128, traverse a point of intersection.

The upshot of these measurements is that for the long waveband a value may be found for C_k (about 100 pF in this case) with which oscillator voltage is nearly independent of wavelength. In the example described, the trend of oscillator voltage on medium waves would however be in accordance with

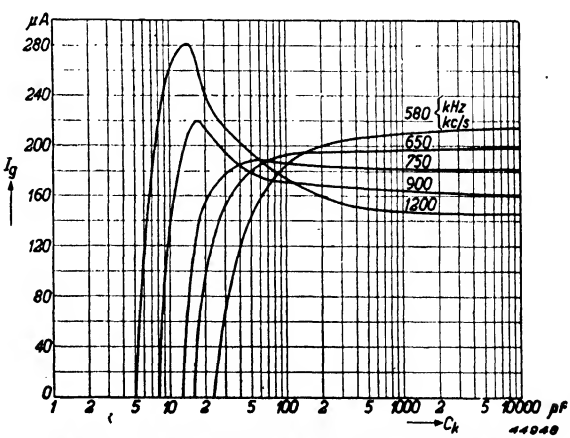

Fig. 128. Oscillator grid current I_g as a function of C_k for various oscillator frequencies.

earlier calculations (B § 5) if the same coupling capacitor were used, for the influence of C_k in that band would still be very small. It follows that by suitable choice of C_k the above mentioned effect may be turned to advantage.

§ 2. Influence on short-wave working of a resistor connected between the grid and the tuned circuit

A resistor in the grid lead also has the aim of keeping oscillator voltage more constant over the short-wave band. Generally, of course, the voltage in this wave range rises rather rapidly with frequency, owing to the marked variation in the impedance of the oscillator circuit. Even heavy artificial damping of the tuned circuit hardly suffices to smooth out the large variation. Furthermore, the C_{ag} effect and the coil dispersion can no longer be neglected at high frequencies. It is therefore desirable to seek means of holding the oscillator voltage whithin narrower limits, without lowering the voltage in the 6-megacycle region, where no great reduction can be tolerated. If a resistor is joined in the oscillator grid lead the tuned circuit is damped additionally to a degree which increases approximately as the square of the frequency. (This will be proved later.) In fig. 129a * r is the resistance introduced and C_g the grid/cathode capacitance (including possible wiring strays). The tuned circuit is thus loaded by r and C_g in series; this arrangement is equivalent to the parallel circuit of fig. 129b. In practice of course the resistance r is made low in relation to the reactance of C_g, and in the equivalent parallel circuit this capacitance will therefcre have about the same value.

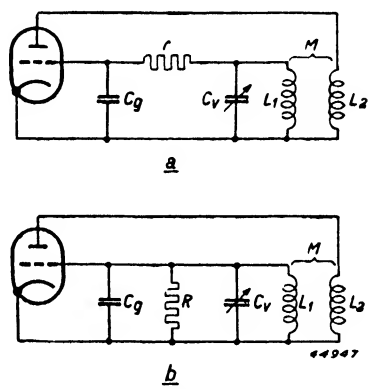

Fig. 129a. Basic oscillator circuit, with a series resistor in the grid lead.
b. Equivalent circuit of 129a. The series combination of r and C_g is replaced by the parallel-combination of R and C_g.

The equivalent resistance R follows from the relationship derived earlier:

$$R = r\left(1 + \frac{1}{r^2\,\omega^2\,C_g^2}\right) \quad \ldots\ldots\ldots\ldots \quad \text{(I A 28)}$$

* In fig. 129 a tuned-grid circuit is shown shunted by the series combination of r and C_g. For the case of a tuned anode circuit the equivalent loading reflected into the anode circuit may be ascertained as described in II B § 9.

In the present case the quantities are such that 1 is negligible by comparison with the fraction, so that we may write:

$$R = \frac{1}{r\,\omega^2\,C_g{}^2} \quad \ldots\ldots\ldots\ldots\ldots\ldots \quad (\text{II C 1})$$

Consequently the circuit is damped by a parallel resistance inversely proportional to ω^2 and the rise in circuit impedance with frequency is more or less countered. Taking, for example, a tuned circuit for the short-wave band whose dynamic resistance varies from 5000 to 15,000 ohms over the wave range, we require additional parallel damping of about 10,000 ohms at the end of the band in order to bring the net dynamic resistance back to 5000 ohms. If we arrange that R is 10,000 ohms at the high-frequency end of the waveband, then at the other end, where the frequency is only one-third, its value will be nine times as great, namely 90,000 ohms. Such a degree of damping scarcely affects the tuned circuit and its dynamic resistance remains at 5000 ohms.

By means of equation (II C 1) it is possible to calculate how large r must be to give the desired effect. At a wavelength of 15 metres ω is of the order of 10^8. The grid-cathode capacitance including wiring strays may be put at about 10 pF. For R to be 10^4 ohms the series resistance required is:

$$r = \frac{1}{R\,\omega^2\,C_g{}^2} = \frac{1}{10^4 \times 10^{16} \times 10^{-22}} = 100 \text{ ohms.}$$

With a resistor of this value inserted in the grid lead the same oscillator voltage may therefore be expected at each end of the waveband. Whether the compensation in the middle of the band will be too much or too little depends on the original trend of the oscillator voltage. Generally the mid-band compensation will not be perfect, but the overall shape of the frequency-voltage curve is in every case considerably improved.

§ 3. A circuit for generating constant oscillator voltage on medium and long waves

It was deduced in II B § 6 that in an oscillator circuit with inductive back-coupling and the padding capacitor in series with the tuning coil the highest slope was needed with the tuning capacitor at maximum [equation (II B 29)]. On the other hand we know that in the Colpitts circuit the highest slope is required when the tuning capacitor is at minimum. Both circuits have the drawback that the oscillator voltage varies considerably across the wave range. The possibility presents itself of combining the circuits, thereby yielding the arrangement shown in fig. 130a. The coupling

coil is no longer connected to the chassis but to the padding capacitor. When C_v is small the feedback is mainly inductive, but at larger values the capacitive coupling predominates. The slope required will thus be fairly constant over the whole waveband and the oscillator voltage will show no great variation. This is evident also from the condition for oscillation, which may be derived quite simply from the equivalent circuit (fig. 130b).

The condition for oscillation is:

$$S_{eff} = -\frac{1}{tZ} \quad \ldots\ldots\ldots \quad \text{(II B 3)}$$

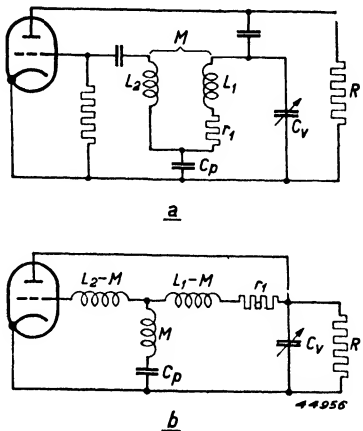

Fig. 130a. Circuit for generating constant oscillator voltage in the medium and long wavebands.
b. Equivalent circuit.

From fig. 130b we have:

$$\frac{1}{t} = \frac{V_a}{V_g} = \frac{j\omega L_1 + r_1 + \frac{1}{j\omega C_p}}{j\omega M + \frac{1}{j\omega C_p}} \quad \ldots\ldots \quad \text{(II C 2)}$$

and

$$\frac{1}{Z} = \frac{\left(j\omega L_1 + r_1 + \frac{1}{j\omega C_p}\right)(1 + R j\omega C_v) + R}{\left(j\omega L_1 + r_1 + \frac{1}{j\omega C_p}\right) R} \quad \text{(II C 3)}$$

Inserting the values of t and Z in equation (II B 3) we then get:

$$S_{eff} = -\frac{\left\{\left(j\omega L_1 + r_1 + \frac{1}{j\omega C_p}\right)\left(\frac{1}{R} + j\omega C_v\right) + 1\right\} j\omega C_p}{1 - \omega^2 M C_p} \quad \ldots \quad \text{(II C 4)}$$

We are assuming that neither the electron transit time nor the grid capacitor/grid leak circuit causes any phase shift; in consequence the required slope is a real quantity. Therefore:

$$S_{eff} = \frac{\omega^2 r_1 C_v C_p}{1 - \omega^2 M C_p} + \frac{\omega^2 L_1 C_p - 1}{1 - \omega^2 M C_p} \times \frac{1}{R} \quad \ldots \quad \text{(II C 5)}$$

The imaginary part must be equal to nil, thus:

$$1 + \frac{r_1}{R} - \omega^2 L_1 C_v + \frac{C_v}{C_p} = 0.$$

Since $\frac{r_1}{R} \ll 1$, $\omega^2 L_1 \frac{C_v C_p}{C_p + C_v} = 1$. Substituting this equation for the angular frequency ω in (II C 5), we finally obtain:

$$S_{eff} = \left\{ \frac{\frac{C_p}{C_v}}{1 - \frac{M}{L_1} - \frac{M}{L_1}\frac{C_p}{C_v}} \right\} \left\{ \frac{1}{R} + \frac{\frac{r_1}{L_1} C_p \left(1 + \frac{C_p}{C_v}\right)}{\left(1 - \frac{M}{L_1} - \frac{M}{L_1}\frac{C_p}{C_v}\right)\left(\frac{C_p}{C_v}\right)} \right\} \quad \ldots \quad \text{(II C 6)}$$

With this equation S_{eff} may be determined immediately in terms of C_p/C_v if the values of r_1/L_1, C_p and R are known. For the purpose of such a calculation the coupling M/L_1 must be regarded as a negative quantity. For the medium-wave band, with $L_1 = 100$ µH and $r_1 = 30$ Ω, $R = 20{,}000$ ohms and $C_p = 600$ pF, the calculated performance is given in fig. 131. Curve I shows the required effective slope for the Colpitts circuit, which employs no coupling coil; the curve makes it clear that the slope needed with $C_v = 40$ pF is about 2.5 times that required when the tuning capacitor has a value of 500 pF. Curve II indicates the slope necessary with a purely inductive coupling, the feedback coil being joined to the chassis instead of to the padding capacitor; the coupling amounts to $M/L_1 = -0.2$. The required slope for this case was calculated from the formula:

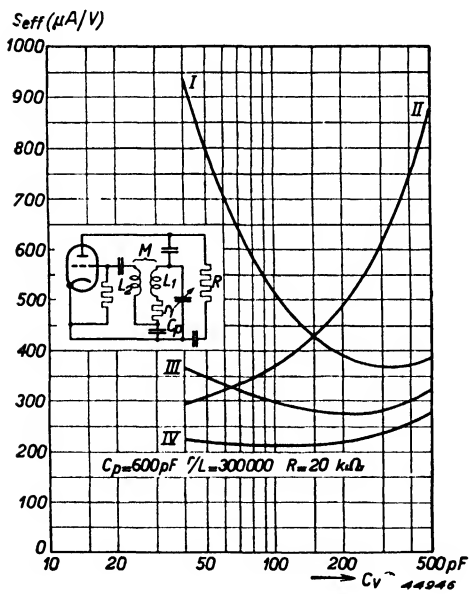

Fig. 131. S_{eff} as a function of C_v, for a parallel-fed oscillator circuit with $r = 30$ Ω, $L = 10^{-4}$ Henry, $R = 20{,}000$ Ω and $C_p = 600$ pF.
Curve I Colpitts circuit
Curve II Inductive back-coupling
Curve III Mixed coupling (loose inductive coupling of $M/L_1 = -0.1$)
Curve IV Mixed coupling (tighter inductive coupling of $M/L_1 = -0.2$)

$$S_{eff} = -\frac{L_1}{M}\left(\frac{r_1}{L_1} C_v + \frac{C_p}{C_p + C_v}\frac{1}{R}\right) \quad \text{(II B 27)}$$

Curves III and IV indicate the

behaviour of mixed couplings. Curve III refers to a weak inductive coupling, namely $M/L_1 = -0.1$; the influence of this coupling is however already considerable. The slope required at $C_v = 40$ pF is only two-fifths of that needed under Curve I conditions. With $C_v = 500$ pF, on the other hand, the capacitive coupling becomes noticeable, the required slope being about one-third of that necessary with an inductive coupling $M/L_1 = -0.2$. Over the whole wave range the slope required is reasonably constant.
With tighter inductive coupling (Curve IV $M/L_1 = -0.2$) the slope needed at small values of the tuning capacitor declines further, whereas at large values there is scarcely any further decrease. If the inductive coupling is made still tighter (e.g. $M/L_1 = -0.3$) the oscillator voltage will rise too sharply at low values of the tuning capacitor, thus becoming even greater than the voltage generated at high values. The overall performance would then be worse, and tight inductive coupling is accordingly not to be recommended. The calculated results quoted above were confirmed by measurements.
This circuit is often useful where a high-slope oscillator valve is replaced by a valve of lower conductance; the oscillator voltage will then fall too much at high values of the tuning capacitor, but the position may be improved by joining the coupling coil to the padding capacitor. In this way the desired voltage is obtained without the need for drastic alteration to the coil.

§ 4. A circuit for generating constant oscillator voltage on short waves

With the usual parallel-fed inductive back-coupling an oscillator voltage is obtained which varies a good deal with wavelength. In D § 10 of this chapter, which gives the results with this circuit, we find that the voltage generated at 15 metres is about twice that at 50 metres. To obtain the correct oscillator voltage at the latter wavelength a fairly tight coupling is needed ($t = -0.5$). As a result thevoltage at 15 metres is considerably larger than is required for good conversion gain.
Furthermore this large oscillator voltage promotes radiation by the receiver, while a tight coupling unfavourably influences the frequency drift of the mixer valve. The danger of frequency drift is in any case greatest around 15 metres when the tuning capacitance is low. Frequency drift due to varying the control bias on the R.F. input grid, or to mains voltage fluctuations, is roughly proportional to the square of the coupling factor. By weakening the coupling from $t = -0.5$ to $t = -0.25$ the drift may be reduced about fourfold (see II H § 1).
For the short-wave band a circuit is desirable which provides tight coupling at 50 metres, where the circuit impedance is small ($Z = 5000\ \Omega$), but loose

coupling at 15 metres, where the circuit impedance is large ($Z = 15{,}000\,\Omega$). Such a circuit is shown in fig. 132a. The inductive coupling between L_1 and L_2 is only half that in the circuits discussed hitherto, i.e. $M/L_1 = -0.25$. By this coupling alone, the oscillator voltage obtained at 50 metres would be much too small. In addition to the normal grid-capacitor and leak, a capacitor C and an inductor L are therefore connected in the grid circuit in the manner indicated, the values of L and C being chosen to cause resonance at 55—60 metres. In consequence, magnification of the voltage induced in L_2 occurs at the longer wavelength and the correct oscillator voltage is obtained in the 50 metres region.

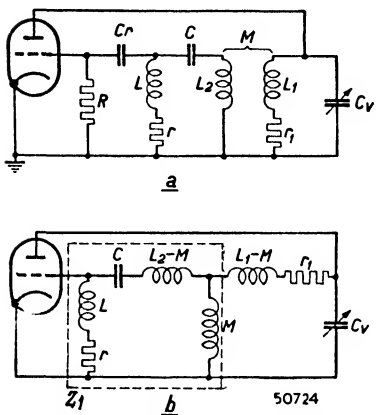

Fig. 132a. Circuit for generating constant oscillator-voltage in the short-wave band. b. Equivalent circuit of 132a.

These qualitative considerations will now be confirmed, making use of the condition for oscillation. The equivalent circuit of the diagram in fig. 132a is given in fig. 132b, and we begin as usual with the formula:

$$S_{eff} = -\frac{1}{t \,.\, Z_{tot}}.$$

In this equation the values of t and Z_{tot} require to be inserted. The value of the feedback ratio follows from:

$$\frac{1}{t} = \frac{V_a}{V_g} = \frac{Z_1 + j\omega\,(L_1 - M) + r_1}{Z_1} \times \frac{j\omega\,(L + L_2 - M) + r + \dfrac{1}{j\omega\,C}}{j\omega\,L + r} \qquad \text{(II C 7)}$$

The impedance between anode and cathode of the oscillator valve amounts to:

$$\frac{1}{Z_{tot}} = \frac{1 + \{\, Z_1 + j\omega\,(L_1 - M) + r_1 \,\} j\omega\, C_v}{Z_1 + j\omega\,(L_1 - M) + r_1}. \qquad \text{(II C 8)}$$

We thus obtain the following figure for the slope required:

$$S_{eff} = -\frac{\left[1 + \{\, Z_1 + j\omega\,(L_1 - M) + r_1 \,\} j\omega\, C_v\right]\left[j\omega\,(L + L_2 - M) + r + \dfrac{1}{j\omega C}\right]}{Z_1\,(j\omega\,L + r)}$$

or:

$$S_{eff} = -\frac{\left\{j\omega\,(L + L_2) + r + \dfrac{1}{j\omega\,C}\right\}\left\{1 - \omega^2\,L_1\,C_v + r_1\,j\omega\,C_v\right\} + j\omega^3\,M^2\,C_v}{(j\omega\,L + r)\,j\omega\,M} \qquad \text{(II C 9)}$$

We are again supposing that no phase shift occurs by reason of the electron transit time in the valve, or on account of the presence of the grid capacitor and leak. The slope is therefore a real quantity and:

$$S_{eff} = -\frac{r_1 C_v}{M}\left\{\left(1+\frac{L_2}{L}\right)-\frac{1}{\omega^2 LC}-\frac{r}{r_1}\left(\frac{1-\omega^2 L_1 C_v}{\omega^2 L C_v}\right)\right\}$$

or approximately:

$$S_{eff} \approx -\frac{r_1}{M}\left\{C_v\left(1+\frac{L_2}{L}\right)-\frac{C_v^2}{C}\frac{L_1}{L}\right\} \quad . \quad . \quad . \quad \text{(II C 10)}$$

This approximation is permissible if $\omega^2 L_1 C_v \approx 1$. It will be seen that the required slope consists of two terms, the first proportional to C_v and the second to C_v^2. The difference between these two terms is more or less constant over a certain range. Fig. 133 shows the measured performance of a circuit of this kind, the resonant frequency of the LC-network lying outside the waveband in curve I and within it in curve II. Bearing in mind the requirements for good tracking, the second case is to be avoided.

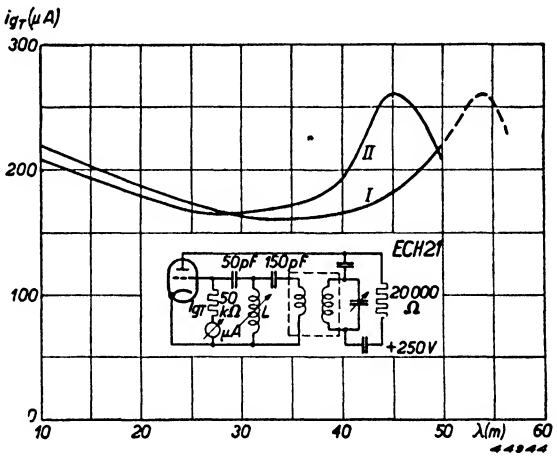

Fig. 133. Oscillator grid current i_{gT} as a function of wavelength, for the circuit of fig. 132a.
Curve I: the resonant frequency lies outside the waveband
Curve II: the resonant frequency lies within the waveband.

It will be observed from the figure that the oscillator voltage does not vary more than 25%. The circuit described is of particular interest for all receivers of which a good short-wave performance is expected.

D. Design of the parallel-fed oscillator circuit

§ 1. Introduction

In the designing of variable-mu mixer valves two requirements decide more or less the optimum oscillator voltage: minimum cross-modulation and low noise. With most valves this voltage is about 8 V_{RMS} with 250 V supply voltage and about 4 V_{RMS} with 100 V.

In order to obtain this voltage the oscillator valve or the oscillator section of the frequency-changer must satisfy certain requirements, and the oscillator circuit must be suitable for the supply voltage. Although the solution of this problem normally falls to the valve-maker, it is also important for the manufacturer of receivers to know what factors need consideration and what difficulties arise when it is sought to generate a specific oscillator voltage. These difficulties come from two sides: from the requirements which the oscillator circuit must meet, for example small frequency drift, and from the lack of control over such things as supply voltages, currents and slopes. In many cases, therefore, we have to content ourselves with a compromise. Although oscillator circuits are very numerous, consideration will here be limited to the most common arrangement, that with a tuned-anode circuit. This circuit has the advantage that variations of inter-electrode capacitances in the mixer section, due to control of the grid bias or to mains voltage fluctuations, affect the tuning less than in the case of the tuned-grid circuit. Such capacitance variations, in the tuned-anode arrangement, are transferred to the tuned circuit only in proportion to the square of the feedback-ratio; as a result frequency drift due to gain control or to mains-voltage fluctuations is much smaller. Keeping the feedback ratio as low as possible is a further precaution against frequency drift.

A disadvantage of the tuned-anode circuit is that the valve oscillates less readily, owing to the greater influence of the A.C.-resistance and of the grid/anode capacitance. The effect of the former is expressed indirectly in equation (II B 50).

$$S_{eff}\, tZ \left(1 + \frac{1}{\mu t}\right) = -1.$$

In the tuned-anode circuit $|t| < 1$. If we assume, for example, $t = -0.25$ and $\mu = 20$, we obtain for the factor $(1 + 1/\mu t)$ a value of 0.80.

If in a tuned-grid arrangement the same tuned circuit is used and the same

coupling coil, then $t = -4$ and the impedance $Z = \frac{Z_{tuned\ circuit}}{16}$. For the factor tZ we find again $tZ = \frac{Z_{tuned\ circuit}}{4}$. The quantity $(1 + \frac{1}{\mu t})$ now amounts, however, to 0.99.

The effect of the grid/anode capacitance is indicated by equation (II B 62). C_{ag} reduces the feedback ratio by $\frac{C_{ag}}{C_{ag} + C_r}$. Assuming $C_r = 50$ pF and $C_{ag} = 2$ pF, we find that the reduction amounts to 0.04. In the tuned-anode case here discussed $t = -0.25$ and the feedback ratio is consequently diminished by 16%. In the tuned-grid arrangement the feedback ratio is $t = -4$ and the reduction represents only 1%.

It might be thought that this drawback of the tuned-grid arrangement, namely the variation of the mixer-section inter-electrode capacitances with supply-voltage changes, could be avoided by taking the heterodyne voltage from the anode of the oscillator. In most cases, however, the voltage will be much too low. In general, the difficulties are so great that the tuned-anode circuit is used, unless special circumstances rule it out. With battery valves, for instance, which have only a small slope in the oscillator section, the tuned-anode arrangement is mostly impossible. Two cases of the tuned-anode circuit are to be distinguished: series-feed and parallel-feed. Normally the voltage from the power section or the battery is too high to be applied directly to the oscillator anode. In order to drop it to the required value a resistor may be joined in series with the tuned circuit; in that case we speak of series-feed, and we distinguish two cases:

a) the feed resistor is connected parallel to the padding capacitor (fig. 134a);
b) the feed resistor is connected in series with the tuning inductor, while the padding capacitor is connected in series with the tuning capacitor (fig. 134b.)

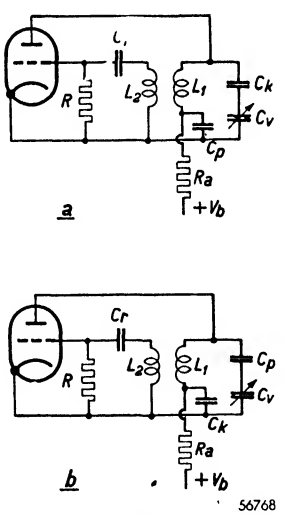

Fig. 134. Series-fed tuned-anode oscillator circuit:
a. with the feed resistor R_a in parallel with the padding capacitor C_p;
b. with the feed resistor Ra in series with the tuning coil.

As we saw in II C § 1, it is also possible to supply the valve through a resistor parallel to the tuned circuit, and in such a case we speak of parallel-feed. This circuit is shown in fig. 135.

In all the cases mentioned above the use of a capacitor C_k is essential: in

the circuits of figs 134a and 135 to avoid applying a steady voltage to the tuning capacitor, and in that of fig. 134b to complete the oscillatory circuit. The circuits shown in figs 134a and b have, compared with the arrangement given in figs 135, these disadvantages:

1. Waveband switching is rather complicated.
2. The switch contacts carry a positive potential in relation to the chassis; this is undesirable from the safety point of view.
3. The trend of oscillator voltage over the waveband is unfavourable; in the short-wave band, for example, a 1 : 5 variation may be expected. At maximum oscillator voltage the mean current is smallest and the anode DC voltage in the triode therefore highest. For this reason the voltage characteristic over the short-wave band is affected very unfavourably.

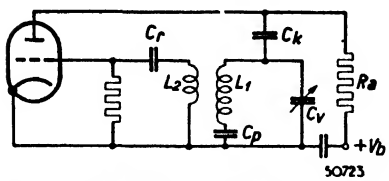

Fig. 135. Parallel-fed tuned anode oscillator circuit.

As we shall see, with parallel feed the tuned circuit receives additional damping from the feed resistor and more uniform oscillator voltage is obtained.

Yet another drawback of the circuit of fig. 134a is that on medium waves, and even more so on long waves, the resistor R_a affects the tracking curve unfavourably (Chapter III B § 3).

On account of these disadvantages parallel feed as shown in fig. 135 is to be preferred with the tuned-anode circuit, and only this arrangement will be considered further.

In dimensioning the tuned-anode circuit we shall first enquire how the required oscillator voltage can be obtained in certain limiting conditions, such as low supply voltage (e.g. with 110 V DC mains) or low permissible anode current.

The voltage across the tuned-anode circuit is in the first place determined by the anode current and the circuit impedance. The anode current depends, moreover, on the anode voltage, amplification factor and slope, while the circuit impedance comprises the tuned circuit itself, the parallel connected feed resistor and the A.C.-resistance of the valve. It will appear that none of these quantities can be fixed arbitrarily. This is quite clear, for instance, in the case of the feed resistor. If this is made too high the oscillator voltage will be too low. On the other hand if the resistor chosen is too low, although a high anode voltage will be obtained the circuit impedance will be damped too heavily.

Similar observations can be made regarding the other quantities.

It is therefore necessary, with the help of what has already been derived, to set up a general equation for the oscillator voltage and then to try and find the optimum values for all the terms which appear.

§ 2. Expression for the oscillator voltage V_g

The basic circuit of a parallel-fed oscillator is shown in fig. 136.

The relation between oscillator voltage V_g and effective slope S_{eff} follows from II B §§ 2 and 3, where S_{eff}/S_o is given as a function of V_g/V_{go} for different cases. If V_g/V_{go} becomes larger S_{eff}/S_o diminishes and over a considerable range it is approximately true that

$$\frac{V_g}{V_{go}} \cdot \frac{S_{eff}}{S_o} = f\,(= \text{constant})$$

This relation can also be written in the following form:

$$V_g = f \frac{S_o}{S_{eff}} V_{go} \quad . \quad . \quad . \quad . \quad \text{(II D 1)}$$

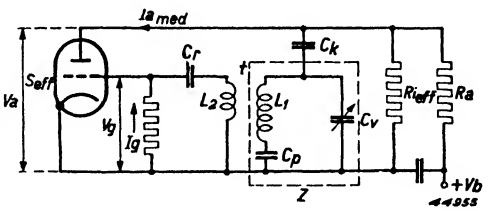

Fig. 136. Basic parallel-fed tuned-anode oscillator circuit, indicating the symbols employed.

From fig. 86, which refers to a pure quadratic characteristic and to the case in which the oscillator voltage carries the grid just to the point at which grid current begins, and from the measured curve for the ECH 21 in fig. 89, we get an average value for f of 0.25.

Starting from the condition for oscillation we can express S_{eff} in terms of the circuit elements and valve characteristics:

$$S_{eff}\, t\, Z_{tot} = -1 \quad . \quad . \quad . \quad . \quad . \quad . \quad . \quad . \quad . \quad . \quad . \quad . \quad \text{(II D 2)}$$

where:

$$\frac{1}{Z_{tot}} = \frac{1}{R_a} + \frac{1}{Z} + \frac{1}{R_{i\,eff}} \quad . \quad . \quad . \quad . \quad . \quad . \quad . \quad . \quad . \quad \text{(II D 3)}$$

We shall, for simplicity, assume that $C_k = \infty$. From II B § 9 [equation (II B 51)] it is evident that:

$$S_{eff}\, R_{i\,eff} = \mu \quad . \quad . \quad . \quad . \quad . \quad . \quad . \quad . \quad . \quad . \quad . \quad . \quad . \quad \text{(II D 4)}$$

Substituting equations (II D 2), (II D 3) and (II D 4) in (II D 1) we then obtain:

$$V_g = -f \frac{S_o\, V_{go}\, (\mu t + 1)}{\left(\frac{1}{Z} + \frac{1}{R_a}\right) \mu} \quad . \quad . \quad . \quad . \quad . \quad . \quad . \quad . \quad . \quad \text{(II D 5)}$$

Here S_o and V_{go} still depend on the steady anode potential V_a, and therefore also on R_a. Therefore we shall express S_o and V_{go} in terms of the valve characteristics and of the resistance R_a and the supply voltage V_b. For this purpose we begin with the supposition that the valve characteristic can be represented by the quadratic equation:

$$i_a = \beta \left(v_g + \frac{v_a}{\mu} \right)^2 \quad \ldots\ldots\ldots\ldots \quad \text{(II D 6)}$$

in which β is an inherent quantity for the valve in question. As we saw earlier, an equation in this form is a good-enough approximation to the characteristic. From the equation we can now deduce:
for the cut-off voltage:

$$V_{go} = \frac{V_a}{\mu} \quad \ldots\ldots\ldots\ldots\ldots\ldots \quad \text{(II D 7)}$$

for the initial slope:

$$S_o = \left(\frac{\partial i_a}{\partial v_g} \right)_{v_g = o} = 2 \beta \frac{V_a}{\mu} \quad \ldots\ldots\ldots \quad \text{(II D 8)}$$

for the anode current at $V_g = V_{g\,med} = 0$ V:

$$I_{ao} = \beta \left(\frac{V_a}{\mu} \right)^2 \quad \ldots\ldots\ldots\ldots\ldots \quad \text{(II D 9)}$$

The magnitude of β in equation (II D 6) is not generally known. For an oscillator valve the slope S_{o-100} (i.e. at $V_g = 0$ and $V_a = 100$ V) is generally quoted. From equation (II D 8) it follows that:

$$\beta = \frac{\mu S_o}{2 V_a} = \frac{\mu S_{o-100}}{200} \quad \ldots\ldots\ldots\ldots \quad \text{(II D 10)}$$

In order to give an idea of the numerical value of β we furnish some figures for the ECH 21. For this valve $\mu = 20$ and $S_{o-100} = 3$ mA/V. Consequently the quantity β is 3.10^{-4} A/V^2.
Substituting equations (II D 7) and (II D 8) in (II D 5) gives:

$$V_g = - \frac{2 \beta f V_a^2 (\mu t + 1)}{\left(\frac{1}{Z} + \frac{1}{R_a} \right) \mu^3} \quad \ldots\ldots\ldots \quad \text{(II D 11)}$$

From this equation V_a needs to be eliminated; in its place we can write:

$$V_a = V_b - I_{a\,med} R_a \quad \ldots\ldots\ldots\ldots \quad \text{(II D 12)}$$

If the oscillator voltage is not too low we can write:

$$\frac{I_{a\,med}}{I_{ao}} = C \quad \ldots\ldots\ldots\ldots\ldots \quad \text{(II D 13)}$$

Fig. 89 clearly shows the constancy of ratio $I_{a\,med}/I_{ao}$ of the ECH 21 (about 0.4).

After substituting equations (II D 9) and (II D 13) in (II D 12) we obtain:

$$V_a = V_b - \frac{R_a C \beta V_a^2}{\mu^2},$$

or:

$$V_a^2 + \frac{\mu^2}{R_a C \beta} V_a - \frac{\mu^2 V_b}{R_a C \beta} = 0 \quad \ldots\ldots \quad \text{(II D 14)}$$

From this it follows that:

$$V_a = -\frac{1}{2}\frac{\mu^2}{R_a C \beta} + \sqrt{\frac{1}{4}\frac{\mu^4}{R_a^2 C^2 \beta^2} + \frac{\mu^2}{R_a C \beta} V_b},$$

and

$$V_a^2 = \frac{\mu^2}{R_a C \beta} V_b \left\{1 + \frac{1}{2}\frac{\mu^2}{R_a C \beta V_b} - \sqrt{\frac{1}{4}\left(\frac{\mu^2}{R_a C \beta V_b}\right)^2 + \frac{\mu^2}{R_a C \beta V_b}}\right\} \quad \text{(II D 15)}$$

Finally, if we substitute equations (II D 15) and (II D 10) in (II D 11) we find:

$$V_g = -\frac{\frac{2f}{C}\frac{(\mu t + 1)}{\mu} V_b \left\{1 + \frac{100\,\mu}{R_a C V_b S_{o\text{-}100}} - \sqrt{\left(\frac{100\,\mu}{R_a C V_b S_{o\text{-}100}}\right)^2 + 2\left(\frac{100\,\mu}{R_a C V_b S_{o\text{-}100}}\right)}\right\}}{1 + \frac{R_a}{Z}} \quad \text{(II D 16)}$$

We can now derive a further equation expressing the relation between the oscillator voltage and the current consumption of the oscillator. If we substitute for β according to the relation:

$$I_{a\,med} = C I_{ao} = C \beta \left(\frac{V_a}{\mu}\right)^2 \quad \ldots\ldots\ldots \quad \text{(II D 17)}$$

in equation (II D 11), we then obtain:

$$V_g = -\frac{2f}{C}\frac{(\mu t + 1)}{\mu} I_{a\,med} \frac{Z R_a}{Z + R_a} \quad \ldots\ldots \quad \text{(II D 18)}$$

In equation (II D 16) μ, $S_{o\,-100}$ and R_a are the quantities of which it is necessary to establish the optimum values. The values of V_b and t are known and depend on a variety of circumstances. The final equation is unfortunately so unconclusive that it is impossible by simple means to observe the effect of every term on V_g. We might therefore try to draw

some conclusions from a set of curves, each using different parameters. It is clear that with so many parameters in equation (II D 16) this is out of the question, but fortunately some of the variables may be combined, so as to leave a manageably small number of curves. It will appear possible to fix the most favourable value for μ, almost independently of the other quantities. Some terms occur in a tight combination. These circumstances serve to limit the total number of possibilities.

§ 3. Determining the optimum value of the amplification factor μ

As it is a fairly simple matter to make valves of different amplification factor, and the influence of the combination of μ and t in equation (II D 16) can be represented easily in the factor $\frac{(\mu t + 1)}{\mu}$, it seems logical to begin by fixing the amplification factor.

Let us write equation (II D 18) in the form:

$$V_g = + \frac{2f}{C} \frac{(-\mu t - 1)}{\mu} Ia_{med} \frac{Z R_a}{Z + R_a}.$$

In this formula there are two terms which are a function of the amplification factor μ and the tapping ratio t, namely:

$$\left(\frac{-\mu t - 1}{\mu} \right) \text{ and } \frac{Z R_a}{Z + R_a} Ia_{med}.$$

The origin of the first term is known; it is the influence of the effective AC-resistance of the valve on the basic equation (II B 3) which is transformed into (II B 50). It is at once clear that this term increases in value as μ becomes greater ($t < 0$).

In the second term we must take into account the voltage drop due to the direct current flowing through the resistance R_a. It is evident that for constant R_a the magnitude of the direct current Ia_{med} is dependent on the μ of the valve; a higher value of μ results in a smaller value of Ia_{med}.

The two terms exert their maximum effect at a certain value of the amplification factor μ, which we find to be dependent on the other parameters t and the combination $R_a C V_b S_{o-100}$.

The variation of the following factor in equation (II D 16)

$$\frac{(+\mu t + 1)}{\mu} \left\{ 1 + \frac{100\mu}{R_a C V_b S_{o\text{-}100}} - \sqrt{\left(\frac{100\,\mu}{R_a C V_b S_{o\text{-}100}} \right)^2 + 2 \left(\frac{100\,\mu}{R_a C V_b S_{o\text{-}100}} \right)} \right\} (= A)$$

may now be shown as a function of μ, with the quantities (R_a C V_b S_{o-100}) and t as parameters.

First we shall consider what values the parameters can have. We know in practice that in normal receivers the feedback ratio in the short-wave band amounts to about 0.4 — 0.5. In view of frequency drift resulting from control of the valve or mains voltage fluctuations this ratio should certainly be smaller, but in the 50-meter region the oscillator voltage would then be too low owing to the low circuit impedance (about 5000 ohms). In the medium-wave and long-wave bands a lower ratio is however practicable, as is evident from equation (II B 31). In this equation the feedback ratio is given for the case in which the padding capacitor is in series with the tuning coil; the ratio is then:

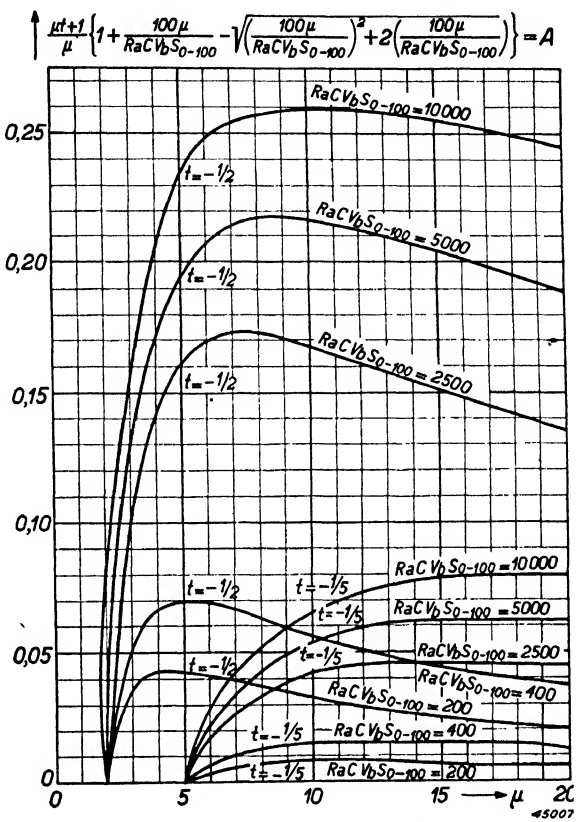

Fig. 137. Factor A from equation (II D 16) as a function of μ for $t = -0.5$ and -0.2, and $(RaCV_bS_{0-100}) = 200$, 400, 2500, 5000 and 10000.

$$t = \frac{(C_p + C_v)}{C_p}\,\frac{M}{L}.$$

Bearing in mind tuning difficulties and the damping caused by the grid leak resistor, we must ensure in every case that t is less than 1 throughout the wavebands. In the long-wave range the padding capacitor is 150 pF and at the largest value of the tuning capacitor ($C_v = 500$ pF) t therefore becomes:

$$t = \frac{650\,M}{150\,L} < 1.$$

Consequently at smaller values of the tuning capacitor ($C_v = 70$ pF) the

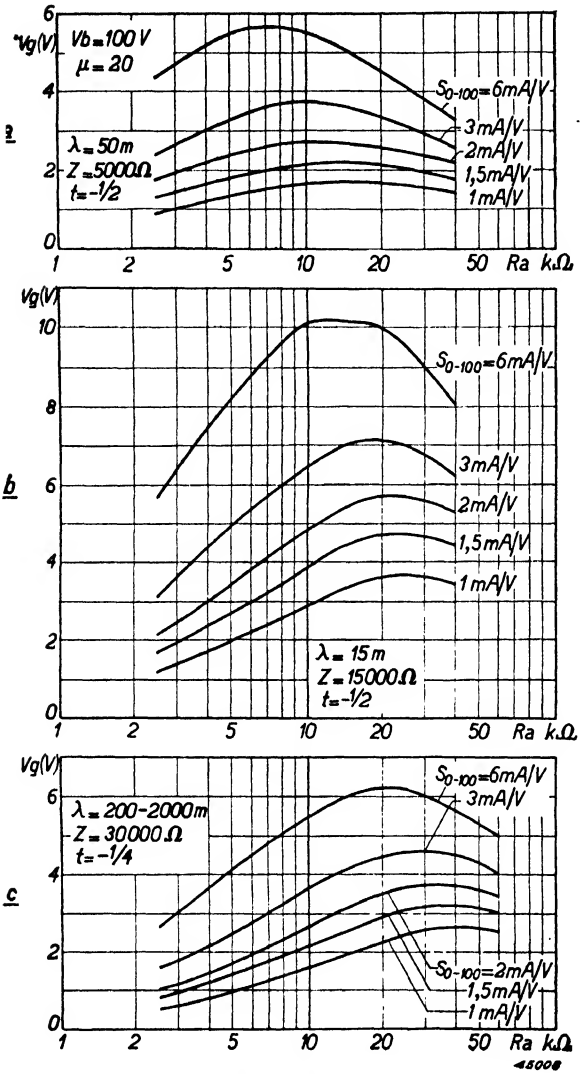

Fig. 138. Oscillator voltage (peak) as a function of the feed resistance R_a, for S_{0-100} = 1, 1.5, 2, 3 and 6 mA/V; calculated for a triode with $\mu = 20$ and for a supply voltage of 100 V.
a λ = 50 metres; Z = 5000 ohms; t = —0.5
b λ = 15 metres; Z = 15,000 ohms; t = —0.5
c λ = 200—2000 metres; Z = 30,000 ohms; t = —0.25.

feedback ratio is much smaller, viz:

$$t = \frac{220\,M}{150\,L}$$

We see, therefore, that on long waves the coupling M/L can be about 0.2 if we take care that t remains less than 1 at all points.

Regarding the factor $(R_a C V_b S_{o-100})$ the following is to be noted. A practical value for R_a is about 20,000 ohms. The supply voltage V_b lies between 100 and 250 V; S_{o-100} varies between 1 and 3 mA/V with normal valves. For C we have already ascertained a value of 0.4 (page 215). Small values of $(R_a\ C\ V_b\ S_{o-100})$ are thus 200—400; average values are 2500—5000, and 10,000 would be a large figure. For these reasons fig. 137 shows the variation of the factor A as a function of μ, for t = —0.5 and t = —0.2, for $(R_a\ C\ V_b\ S_{o-100})$ = 200, 400, 2500, 5000 and 10,000. It is evident from the curves that with t = —0.5 the factor reaches its maximum value when μ = 4—15, while with t = —0.2 the optimum value of the amplification factor is about 15—20.

Taking into consideration that the triode section of some mixer valves, e.g. the ECH 21, must be suitable for use as an A.F. amplifier and must accor-

dingly have a high μ in most cases, we can regard a value of $\mu = 20$ as a satisfactory compromise. A triode section having this compromise value of μ provides adequate A.F. amplification and alternatively makes possible the generation of a sufficient oscillator voltage in all wavebands.

§ 4. Determining the slope S_{o-100}

Once the amplification factor μ is determined, it becomes rather easier to get an idea of the magnitude of the other factors. First we can, for the sake of simplicity, combine two quantities and thereby reduce the number of unknowns. We shall use the same figures as in § 3, viz.: Short-wave band:

$t = -0.5$

Z = about 5000 ohms (at 50 metres)

Z = about 15,000 ohms (about 15 metres)

Medium- and long-wave bands:

$t = -0.25$

Z = about 30,000 ohms (including damping by grid current).

The only supply voltages which need be considered

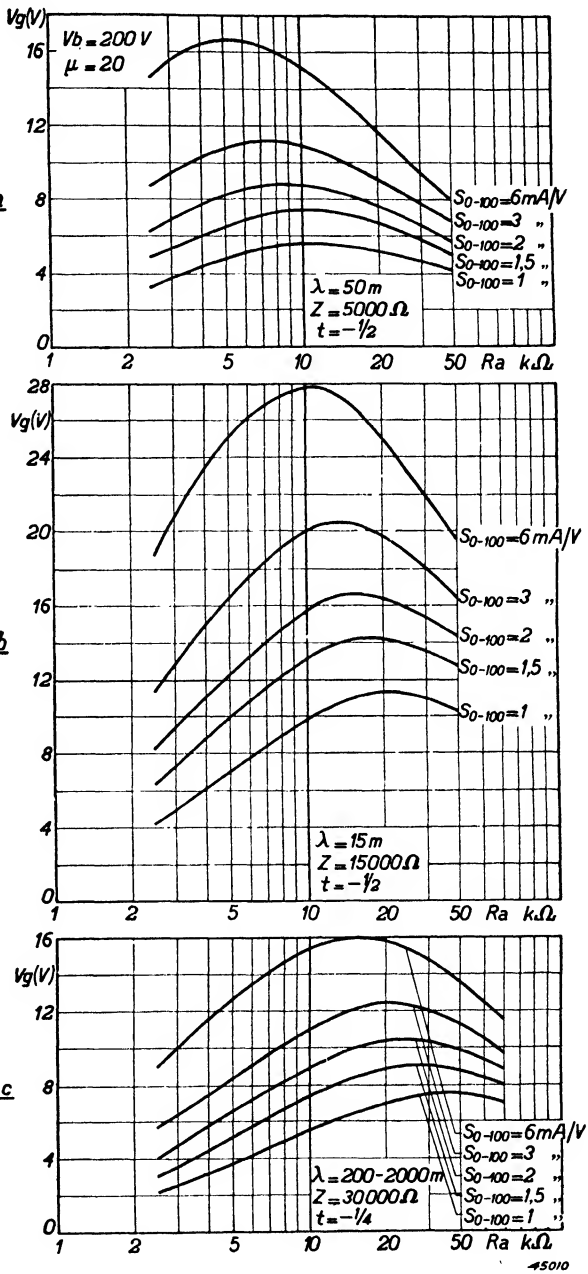

Fig. 139. Oscillator voltage (peak) as a function of the feed resistance R_a for S_{o-100}= 1, 1.5, 2, 3 and 6 mA/V; calculated for a triode with μ = 20 and for a supply voltage of 200 V.
a λ = 50 metres; Z = 5000 ohms; t = —0.5
b λ = 15 metres; Z = 15000 ohms; t = —0.5
c λ = 200—2000 metres, Z = 30000 ohms; t = —.025

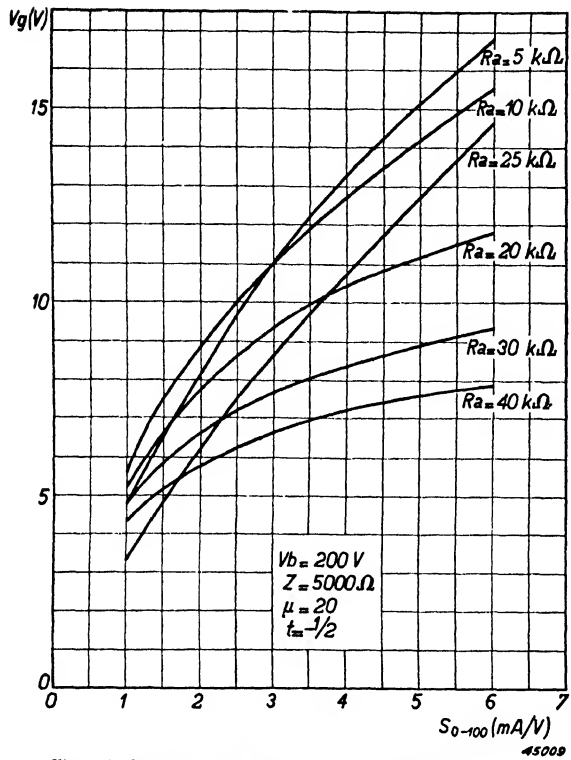

Fig. 140. Oscillator voltage as a function of the slope S_{0-100}, for various values of the feed resistance R_a.

are 100 V and 200—250 V. If we calculate the peak value of the oscillator voltage as a function of the parallel resistance R_a for values of S_{o-100} of 1, 1.5, 2, 3 and 6 mA/V, and if we take the above mentioned values for t and Z and assume $\mu = 20$, we obtain, by substituting in equation (II D 16), the curves of figs 138 and 139. The first thing which follows from these graphs is that the oscillator voltage obtained increases with S_{o-100}, though not proportionately. In order to attain the desired oscillator voltage of $8 V_{RMS}$ (11 Vpeak) in all circumstances, a certain minimum slope is necessary. Now we have not complete freedom in fixing S_{o-100}; raising the slope makes the valve more complicated and also increases the current consumption of the heater. The latter result is of especial importance in battery valves. In present-day battery types S_{o-100} has a value of about 1 mA/V (in the DK 21, 0.8 mA/V). With such valves we can reckon on a high tension supply of no more than 120 V; even with the optimum value of R_a the oscillator voltage obtained is so low that the parallel-fed oscillator circuit must be condemned as impracticable, a tuned-grid arrangement being adopted instead. Under optimum conditions an oscillator voltage of about 2 V is obtainable with a battery valve at a wavelength of 50 metres (fig. 138a) and in the medium- and long-wave bands about 3 V (fig. 138c).

With A.C. and A.C./D.C. valves the circumstances are easier, because considerably higher slope is much more readily attainable.

Fig. 139 shows that with a slope of $S_{o-100} = 3$ mA/V and $V_b = 200$ V the required oscillator voltage of 11 V (peak) can be reached throughout the three wavebands if the parallel resistance R_a is of optimum value in each

case. With a slope of this value we find from fig. 138 that the oscillator voltage of 5 V required at $V_b = 100$ V is not quite reached. It is not worth while to increase S_{o-100} as the improvement in performance is less than proportional, while a much larger heater-dissipation would be necessary. The small extent of the improvement is seen clearly in fig. 140, in which the oscillator voltage V_g is given as a function of S_{o-100} for various values of the parallel resistance R_a.

§ 5. Determining the resistance R_a

In the previous section it was assumed, in determining the slope, that the parallel resistance was of optimum value. For $S_{o-100} = 3$ mA/V and $V_b = 100$ V (fig. 138) this value lies between 10,000 and 30,000 ohms, and for $V_b = 200$ V (fig. 139) between 7000 and 20,000 ohms. It should, however, be possible to use the same value in each case, for the curves display no sharp maxima.

Beginning with the most difficult case, that of fig. 138a, we find that a value of 10,000 Ω is needed. There are reasons, however, against using such a low value:

1. at a wavelength of 15 metres a low value of parallel resistance affects the oscillator voltage unfavourably;
2. the parallel damping is greater, resulting in a noticeable detuning through phase shift in the circuit elements (Section III B § 3);
3. the anode dissipation of the valve becomes excessive;
4. as the valve oscillates very readily in the 15-metre region, the mean anode current is relatively low and consequently the anode voltage will be rather high, which with some valves is inadmissible.

For these reasons we make the parallel resistance 20,000 ohms. The oscillator voltage is then still sufficient in all bands, while phase shift is kept down. Furthermore both the anode dissipation and the anode voltage of the oscillator valve are held within permissible limits.

§ 6. Changing from 100 V to 200 V mains

A comparison of figs 138 and 139 shows that raising the supply voltage results in a more than proportionate increase in the oscillator voltage. (The factor between brackets in equation (II D 16) also increases with a rise in V_b.) When changing from a 100 V supply voltage to one of 200 V the oscillator voltage becomes about three times as great. Now the usual mixer valves fortunately require only a low oscillator voltage at a supply voltage of 100 V, so that changing to a 200 V supply does not generally cause the

oscillator voltage to reach too high a value. If this does happen, however, special safeguards against radiation via the aerial circuit are necessary.

§ 7. Anode dissipation of the valve

Neglecting tuned-circuit losses, we can write for the anode dissipation W_a of the valve:

$$W_a = I_{a\,med}\, V_b - I_a{}^2{}_{med}\, R_a$$

From this equation we see that the anode dissipation would be nil when $I_{a\,med} = 0$ or when $I_{a\,med} = V_b/R_a$. Between these two values of current is another at which the anode dissipation is a maximum, namely when:

$$I_{a\,med} = \frac{V_b}{2\,R_a}.$$

The anode dissipation is then:

$$W_{a\,max} = \frac{V_b{}^2}{4\,R_a}.$$

In order to ascertain whether the dissipation can occur in practice we shall insert this value of $I_{a\,med}$ in equation (II D 18), thereby obtaining:

$$V_g = -\frac{f}{C}\, V_b \cdot \frac{\mu t + 1}{\mu} \frac{1}{1 + \frac{R_a}{Z}}.$$

Filling in now the following practical figures:

$V_b = 250$ V
$\mu = 20$
$t = -0.5$
$R_a = 20{,}000$ ohms
$Z = 5000$ ohms,

we find that the oscillator voltage V_g is about 14 V. Certainly such a voltage can easily occur, and it is therefore necessary to take care that the anode dissipation $W_{a\,max} = V_b{}^2/4R_a$ does not exceed the published maximum. For the triode section of the ECH 21 and UCH 21 mixers the permissible anode dissipation is 0.8 W. Consequently there is a minimum value for the parallel resistance, namely:

$$\text{UCH 21 and } V_b = 200 \text{ V: } R_a = \frac{V_b{}^2}{4 \times 0.8} = 12{,}500 \text{ ohms;}$$

$$\text{ECH 21 and } V_b = 250 \text{ V: } R_a = \frac{V_b{}^2}{4 \times 0.8} = 20{,}000 \text{ ohms.}$$

The value of 20,000 ohms already found does not, therefore, conflict with the maximum anode dissipation.

§ 8. Voltage at the anode of the valve

It remains to be discovered whether this value of resistance is compatible with the permitted anode voltage, which for the UCH 21 and ECH 21 is 175 V. The highest anode voltage will obviously occur with the highest supply voltage, i.e. 250 V. From equations (II D 14) and (II D 10) it follows that

$$\frac{200\ V_b\ \mu}{R_a\ C\ S_{o-100}} - \frac{200 V_a\ \mu}{R_a\ C\ S_{o-100}} < 175^2,$$

or:

$$R_a > \frac{15{,}000 \times 20}{0.4 \times 30{,}000 \times 3 \times 10^{-3}} = 8000 \text{ ohms}$$

The value of resistance calculated in § 5 is thus acceptable in relation to the permitted maximum anode voltage.

§ 9. Steady anode current $I_{a\ med}$ of the oscillator

The current consumption of the oscillator may be deduced directly from equation (II D 18). For the examples given in § 4 and § 5 the calculated figures are as under:

$S_{o-100} = 3$ mA/V		$\mu = 20$		$R_a = 20{,}000$ ohms			
$V_b =$	100 V		200 V		250 V		
t	Z (kΩ)	V_g (V)	$I_{a\ med}$ (mA)	V_g (V)	$I_{a\ med}$ (mA)	V_g (V)	$I_{a\ med}$ (mA)
—0.5	5	3.4	1.6	9.3	5.2	12.8	7.2
—0.5	15	7.2	1.5	20.5	4.1	27.5	5.8
—0.25	30	4.5	1.9	12.4	5.2	17.1	7.2

§ 10. Measurements

The theoretical results obtained in the preceding section were tested by measurements on the triode part of a UCH 21. The initial slope at an anode

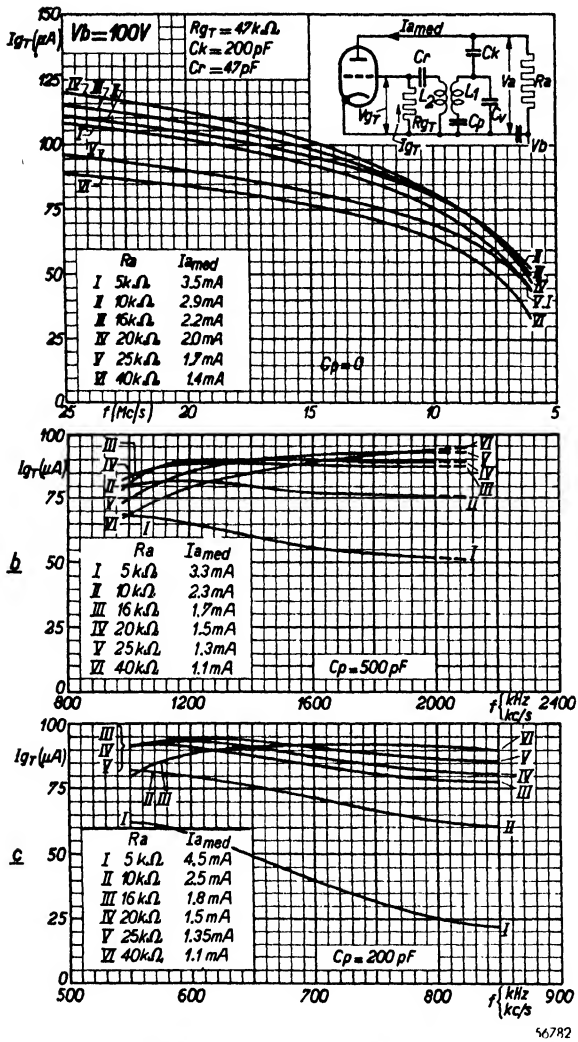

Fig. 141. Oscillator grid current in the triode section of the UCH 21 as a function of frequency, for various values of the feed resistance R_a, with $V_b = 100$ V
a short-wave band
b medium-wave band
c long-wave band.

voltage of 100 V is 3 mA/V. Using a normal coil assembly, the current through the grid leak was measured against frequency for various values of the parallel resistance, and the results are reproduced in figs 141a, b and c for three different wavebands. It will be noted that at 6 Mc/s (50 metres) the greatest oscillator voltage is obtained with a parallel resistance of 10,000 ohms, but that at 20 Mc/s (15 metres) 20,000 ohms yields the highest voltage. At 50 metres a grid current of 50 μA flows with $R_a = 20{,}000$ ohms; this corresponds to an oscillator voltage of 3.2 V (grid leak $R_gT = 47{,}000$ ohms) and is in agreement with the calculated value in fig. 138a. In the medium-wave and long-wave bands we obtain, with $R_a = 20{,}000$ ohms, an oscillator voltage of about 5 V, which is sufficient for good conversion gain. Fig. 141 shows that the optimum value $R_a = 10{,}000$ ohms for the short-wave range differs only slightly from the most favourable value for the other two bands. The variation of oscillator voltage over the short-wave band is 2 : 1. The measured results for a 250 V supply are given in figs 142a, b, and c. Here also the best value for R_a at 6 Mc/s is 10,000 ohms. With $R_a = 20{,}000$ ohms the oscillator voltage is 11 V, which agrees with the calculated figure. In the medium- and long-wave bands the oscillator voltage is about 15 V.

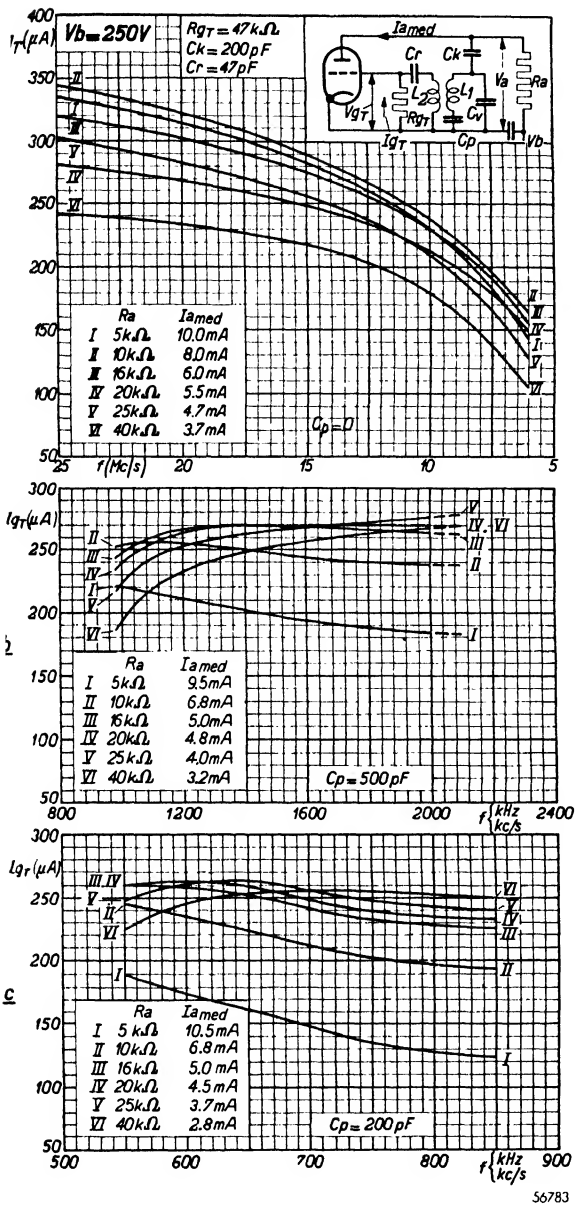

Fig. 142. Oscillator grid current in the triode section of the UCH 21 as a function of frequency, for various values of the feed resistance R_a, with $V_b = 250$ V.
a short-wave band,
b medium-wave band,
c long-wave band.

§ 11. Effect of the coupling capacitor

In our calculations we have taken no account of the size of the coupling capacitor, assuming throughout that its capacitance was high enough to be neglected. It was demonstrated in II C § 1, however, that in the long-wave band the magnitude of the capacitor undeniably has a considerable influence on the trend of the oscillator voltage. Had this capacitor been brought under notice in the preceding section, however, the discussion would have been of less general application. For this reason it has hitherto been ignored, and a correction for the magnitude of C_k must be made subsequently. It was shown in II C § 1 that the influence of C_k consists mainly in the raising of the feedback ratio at high frequencies and in the lowering of the ratio at low frequencies. In the middle of the waveband, therefore, the effect of the coupling capacitor may be neglected. The value of the earlier discussion is unimpaired provided that, when determining the feedback ratio, the presence of C_k is taken into consideration.

§ 12. Conclusions

Summarising, the following points may be stated regarding parallel-fed oscillator circuits:

1. For every case there is an optimum value for the μ of the valve, a good compromise being 20. The valve then functions very well on medium and long waves and, when used as an A.F. amplifier, provides adequate gain. In the short-wave band it still yields a satisfactory oscillator voltage at 50 metres.
2. The slope of the valve must be at least 2 mA/V. Increasing it beyound 3 mA/V gives no proportionate increase in the oscillator voltage. Battery valves have too low an initial slope for use with parallel-fed oscillator circuits. AC valves, which possess an initial slope of 3 mA/V at an anode voltage of 100 V, provide a satisfactory oscillator voltage.
3. The oscillator voltage attainable with a valve of 3 mA/V initial slope amounts to about 3.5 V at 50 metres. In the medium- and long-wave bands it is about 4—5 V with a 100 V supply. The circuit cannot deliver a higher oscillator voltage unless the supply voltage is raised; with 200 V it is about three times as great.
4. There is an optimum value for the parallel resistance. In the short-wave band it is around 10,000 ohms. A compromise value of 20,000 ohms is chosen, however, after taking into consideration damping, detuning due to phase shift, and the permissible anode dissipation of about 0.8 W with normal valves.
5. The current consumption of a valve with an amplification factor $\mu = 20$ and initial slope $S_{o-100} = 3$ mA/V is, on a supply of 100 V, about 1.8 mA, on 200 V 4.8 mA and on 250 V 6—7 mA.

E. Squegging oscillation

§ 1. Introduction

Apart from the effect required, various subsidiary effects occur during the mixing process which must be regarded as parasitic phenomena. Some of them appear also in the R.F. and. IF. stages and are dealt with in Chapter IV of this book and in Chapter XIII of book III. They include, for example, cross-modulation, modulation hum, background noise, hum disturbances and microphony. A parasitic effect not met with in the R.F. and I.F. stages, but which is of especial importance in the mixing operation, is squegging oscillation.

Squegging is prone to occur as a parasitic phenomenon in receivers with reaction and in oscillator circuits with excessively tight back-coupling. It can make itself shown in various ways, for instance by a squeaking sound, or by a succession of whistles distributed over the waveband, or by a strong hiss. If an attempt is made to tune in such a squegging oscillator on a separate receiver a whole series of tuning points is found. In order to gain an insight into squegging oscillation an oscillogram of the voltage across an oscillating circuit was taken. With the circuit in a condition of squegging the trace has the form seen in fig. 143. We see that the amplitude of the oscillation grows rapidly to a certain point, afterwards falling to zero; the whole process is completed in a very short time, for example during 60 R.F. cycles, and is repeated several thousand times a second.

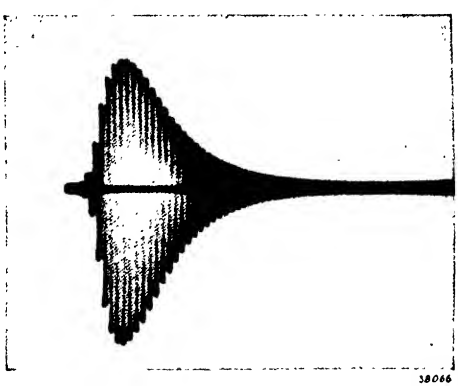

Fig. 143. Oscillogram of the voltage across an overoscillating oscillator circuit, as a function of time.

Clearly in this case the state of stable equilibrium described in B § 1, in which the oscillator voltage and the grid bias become so large that the effective slope is reduced to the exact value required, is not realised. Owing to damping of the circuit, the oscillator voltage and the grid bias adjust

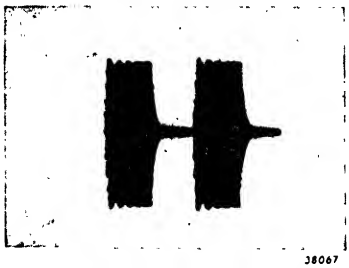

Fig. 144. Oscillogram of the alternating voltage across a normally-oscillating circuit as a function of time, the anode supply being periodically interrupted.

themselves only after some delay. In certain circumstances this stationary balance may temporarily be lacking. Such a condition is seen in the oscillogram of fig. 144, which shows the alternating voltage across a normal oscillator circuit as a function of time. The anode circuit of the valve was interrupted periodically. The oscillatory voltage does not reach its eventual amplitude instantaneously: it first increases rapidly, then wavers about its equilibrium value and finally settles down to the steady state. On the anode supply being broken, the amplitude of oscillation decreases exponentially.

§ 2. Equilibrium adjustments with various values of grid bias

As the grid bias and the oscillator voltage do not at once adjust themselves to their final value, we shall find it worth while to investigate the state of balance at various values of fixed grid bias derived, for instance, from a battery. According to B § 1 the effective slope must equal the required slope if oscillation is to be stable. In fig. 145, for the idealised i_a/v_g characteristic of fig. 84, we have shown both slopes as a function of the oscillator voltage, at various values of negative grid bias. Curve I of fig. 145a indicates effective slope against oscillator voltage for a initial bias $V_{g\ med} = 0$. As long as the oscillator voltage remains less than the cut-off voltage V_{go} the slope S_{eff} equals the initial slope S_o. At larger amplitudes the effective slope gradually declines to the final value of $S_o/2$*.

At I in fig. 145b we have a similar curve for $V_{g\ med} = -{}^1/_2\ V_{go}$. For an oscillator voltage less than $V_{go}/2$ the slope is equal to S_o; at larger voltages it decreases gradually to the limiting value of $S_o/2$. Curve I of fig. 145c shows the variation of slope with $V_{g\ med} = -V_{go}$; in this case the effective slope is always equal to $S_o/2$, because during every half-cycle the whole i_a/v_g characteristic is traversed.

In figs 145d, e, f and g similar curves are given for $V_{g\ med} = -2\ V_{go}$, $-3\ V_{go}$, $-3.3\ V_{go}$ and $-4\ V_{go}$. As long as no anode current flows S_{eff} is zero. Only after anode current begins to flow can we properly speak of an effective slope (its variation is depicted in curve I of figs 145d, e, f and g) and with very large amplitudes it approaches the limiting value $S_o/2$.

* This is the limit necessarily reached, because we can assume that at very large oscillator voltages one half of each cycle traverses a region in which the slope is S_o and the other half a region where the slope is nil.

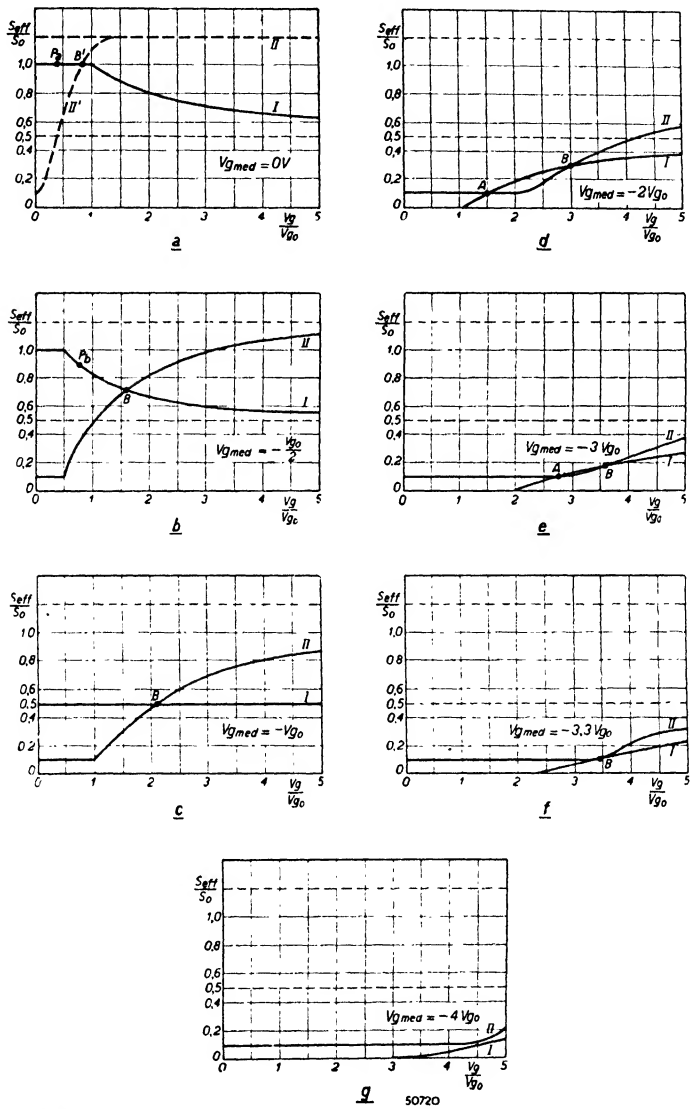

Fig. 145. S_{eff}/S_o as a function of V_g/V_{go} for various values of V_{gmed}. Curves I show the effective slope obtained, as a function of the oscillator voltage, and curves II the required slope for stable oscillation. Stability is secured if the slope obtained is equal to the required slope, i.e. at the intersections A and B of curves I and II. Balance at points B is always stable, but at points A only in certain circumstances. The limiting value of S_{eff}/S_o lies at 0.5.

We shall now assume that the required slope is constant, provided no grid current flows, and that it is determined solely by the damping of the tuned circuit. Curves II in figs 145a–g, which indicate the slope required for steady oscillation, then all begin at the same value. If grid current flows the required slope is higher. The damping due to grid current is given by the equation:

$$R_{HF} = \frac{\pi R_g}{\alpha \frac{sin\, 2\,\alpha}{2}} \quad \ldots\ldots\ldots\ldots \quad \text{(II B 59)}$$

(see section II B § 9). Here R_g is the grid A.C. resistance and $\cos \alpha = V_{g\,med} / V_g$ [equation (II B 53)].

This damping has a certain limiting value, namely 2 R_g, and consequently there is also a limiting value for the required slope. With a normally tapped oscillator coil and a customary value of grid AC-resistance R_g, a limiting value of about 1.2 S_o is found with indirectly-heated types.

In the state of equilibrium the effective slope equals the required slope, and in fig. 145 this condition is therefore represented by the intersection of curves I and II. In figs 145 a, b and c only one intersection, B, occurs, so that in these cases only one state of balance is possible*.

In figs 145d and e we find two points of intersection, A and B. In fig. 145 f curves I and II touch, while in g they have no contact at all. In this last case the required slope is evidently greater than the available slope for every oscillator voltage; in other words the circuit does not oscillate. Fig. 145 f refers to the limiting case of the maximum negative bias at which the circuit will still just oscillate; increasing the bias further causes oscillation to cease. The question now is: to which of the intersection points A and B in figs 145d and e will the oscillator adjust itself when fixed negative grid bias is applied? It is evident that the valve adjusts itself to point B, because the balance at A is unstable. After the onset of oscillation we first arrive at point A. As the oscillator voltage rises the effective slope will increase faster than the required slope, and a further rise in the oscillator voltage will result.

The adjustment at point B is stable in all circumstances. Should the oscillator voltage rise, the required slope increases faster than the effective slope and the oscillator is forced back to the point of equilibrium B.

If the negative grid bais is gradually increased from $V_{g\,med} = 0$ the

* Regarding fig. 145a, the following should be noted. At $V_{g\,med} = 0$ the grid damping is $2R_g$ for every oscillator voltage. In the case of a straight grid-current characteristic curve II would run straight from the initial value to the limiting value. In reality the lower part of the grid-current characteristic is curved, so that the required slope follows the trend indicated by curve II^I The point of intersection B^I corresponds to the state of equilibrium to which the oscillator adjusts itself when $V_{g\,med} = 0$.

amplitude of the oscillator voltage adjusts itself successively to all the points B in figs 145a to f inclusive; eventually oscillation ceases (fig. 145g).

§ 3. Equilibrium adjustment with automatic grid bias

When a grid capacitor and leak are used the situation may be entirely different. If now the oscillator voltage rises, the grid bias increases automatically and the effective slope therefore declines. Should this effect take control of the circuit, an originally unstable condition will be rendered stable. The final state of equilibrium is then determined by one of the points A in fig. 145.

The progress of the oscillation is now as follows. When $V_{g\ med} = 0$ the effective slope is greater than the required slope; the valve therefore goes into oscillation and should adjust itself to point B′ in fig. 145a. It does not reach that point, however, because while the amplitude of oscillation has been rising towards point P_a the grid bias has so increased that the adjustment shifts to that of fig. 145b. If, for example, the amplitude rises to P_b, $V_{g\ med}$ will as a result reach the final value indicated in fig. 145c. and so on. The rate at which the oscillator voltage and the grid bias increase depends on many factors and these will be dealt with in detail.

These factors may be such that from a particular moment of time $V_{g\ med}$ increases faster than V_g. With a grid capacitor and leak of low RC-value $V_{g\ med}$ will reach finality little later than the oscillator voltage; on the other hand with a large RC-value the attainment of a steady bias voltage is much delayed.

It will also be clear that the rate of increase of the oscillator voltage depends on the available surplus of effective slope.

The various stages in figs 145 a to g inclusive can be set out in a series of curves. We show first of all, in fig. 146, the case in which $V_{g\ med}$, following V_g almost instantaneously, adjusts itself to a stable point A. In this diagram curve II represents the required slope. The gradually increasing oscillator voltage (plotted on the horizontal axis) is shown with different values for $V_{g\ med}$.

Curve 1 is valid for the negative grid bias corresponding to the oscillator voltage $V_{g(1)}$ (compare curve I in fig. 145a) and its point of intersection P_1 with the vertical corresponding to $V_{g(1)}$ represents the effective slope obtained.

Since surplus slope, represented by the distance O_1P_1, is still present in this state of balance, the oscillator voltage will increase to a value of say $V_{g(2)}$, at which the grid bias will be greater; the relative slope curve is now curve 2. The distance O_2P_2 represents in this case the excess of effective slope.

Finally, the intersection of the S_{eff}-curve with the perpendicular corresponding to the oscillator voltage $V_{g(3)}$ falls on line II, representing the required slope, at P_3; in this case there is no longer any surplus slope and the amplitude ought therefore to remain constant. The grid bias $V_{g\ med}$ has, however, still not reached its final value, and it consequently rises somewhat, say to the value given by curve 4: the effective slope is then represented by P_4. Now this slope is lower than the value needed, and for this reason the oscillator voltage will drop. As the bias follows the oscillator voltage almost instantaneously, $V_{g\ med}$ will also decrease, and in this way we come say to point P_5. During this short space of time the oscillator voltage will swing above and below a point of equilibrium but will eventually adjust itself to a certain amplitude, P_6 in fig. 146, to which curve 6 corresponds. After the oscillator has adjusted itself to this point no further variation will occur.

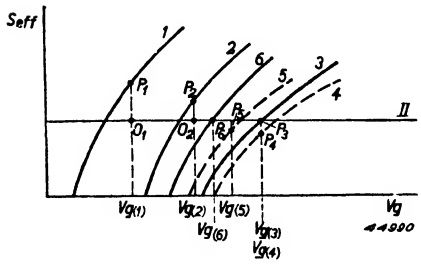

Fig. 146. Variation of effective slope as a function of the oscillator voltage at the grid bias appropriate thereto, if the RC-time is fairly small. The successive values to which the slope adjusts itself are given by the points P. The oscillator voltage finally settles down at P_6.

Similar curves may be drawn for the case in which the grid bias follows the oscillator voltage only after an appreciable interval (see fig. 147). At first the same intersection points P_1 and P_2 are found. At point P_3 the oscillator voltage has reached equilibrium, although the grid voltage has still to make good a certain lag. We first obtain, for example, curve 4 with the intersection P_4: here a much greater lack of effective slope is evident than in the corresponding case in fig. 146, and once more we find that the grid bias has not reached its final value: it is still increasing, while the oscillator voltage is decreasing.

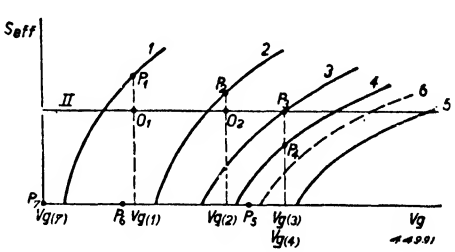

Fig. 147. The same curves as in fig. 146, but for the case in which the negative grid bias lags considerably behind the oscillator voltage; i.e. when the RC-time is large. First the oscillator voltage increases to a particular value, at which the actual effective slope equals the required slope. The negative grid bias however continues to rise, and the effective slope falls so much that oscillation declines and finally ceases.

So we arrive at curve 5, the relative value of the oscillator voltage being represented by P_5 on the horizontal axis. This means that the effective slope is nil, and in consequence the oscillation will rapidly die away. From its value in curve 5 the negative grid bias will recede, and for curve 6 the oscillator voltage may be indicated by,

say, P_6, Finally the oscillator voltage drops to zero (point P_7) and the grid bias diminishes until oscillation begins once more. The whole phenomenon is known as squegging oscillation. The oscillogram in fig. 148, like that in fig. 143, gives a picture of such squegging oscillation and shows the variation of grid voltage as a function of time. From this the grid bias at any instant can be determined: its magnitude is equal to the mean of the instantaneous values of the R.F. voltage and is indicated in the figure by a white line. With the circuit from which the oscillogram was derived it was ascertained, by varying the grid bias, that oscillation began as soon as $V_{g\ med}$ became more positive than —9 V. This point is identified in fig. 148 by the figure 9 (the cut-off voltage of the valve was —10V). After the onset of oscillation the oscillator voltage increases very rapidly to a certain maximum, beyond which it quickly declines. It is clear from the course of the grid bias in this oscillogram that the decline begins at $V_{g\ med}$ = —29 V. If the circuit is allowed to oscillate steadily, with the grid capacitor shorted and bias provided by a potentiometer, it is again found that the oscillation dies away at $V_{g\ med}$ = —29 V. Evidently at this voltage the situation shown in fig. 145 is reached. Owing to lack of slope the oscillation falls to zero. It will also be observed from fig. 148 that while an appreciable grid current is flowing the grid bias increases very rapidly. During this very short period large positive grid voltages occur, and these are clearly to be seen in the oscillogram of fig. 148 as a peak below the horizontal axis. Furthermore it will be noticed that, due to the presence of the RC-combination, the grid bias attains its maximum some cycles later than the oscillator voltage. If the grid bias reaches a value of about —30 V the grid becomes less positive during the peaks of the alternating voltage and at the same time the grid bias increases more slowly.

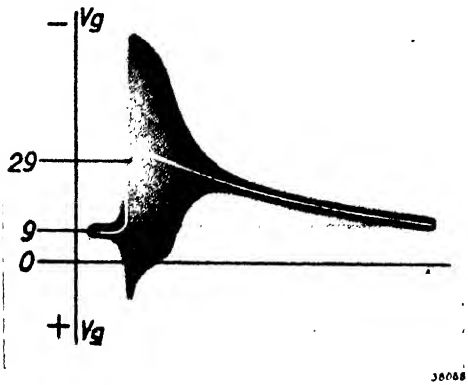

Fig. 148. Oscillogram of the voltage at the grid of an oscillator, as a function of time. In this trace the occurrence of squegging oscillation as explained by the curves of fig. 147 is plainly seen. For clarity the variation of grid bias is indicated also.

Before the grid current falls to nil, the bias is already decreasing again. The grid leak now discharges the grid capacitor faster than it is charged by the grid current. As soon as grid current ceases the bias decreases according to the well-known exponential function until $V_{g\ med}$ = —9 V is again reached.

It follows from the foregoing that squegging oscillation occurs when the equilibrium indicated by point A in fig. 145 is not realised, and the oscillation seeks to adjust itself to point B. The stability of the point A may not be sufficient to prevent squegging; the adjustment may so quickly be passed over that a region of instability is again reached. The danger can be made clear with the following example from mechanics, in which an inherently stable position is passed over so rapidly that instability again results. Fig. 149 shows the contour of a switchback. A is a point of equilibrium for a ball placed there. But a ball rolling down from B may pass this point with such velocity that it reaches C and enters the unstable region CD. In order now to establish the conditions for good stability at point A we should follow the growth of the oscillation step by step to this point. Owing to various unrelated factors, however, this is difficult to do, and we satisfy ourselves with observing that squegging oscillation will certainly occur if the equilibrium points A are unstable.

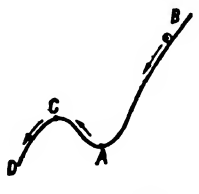

Fig. 149. Mechanical example of a stable point A, which can be unstable if the ball passes it with sufficient velocity to reach point C.

Investigations have demonstrated that *stability of the points A is in every case essential to the avoidance of squegging oscillation.* For this reason it is worth enquiring whether, in a circuit including a grid capacitor and leak, an amplitude differing little from the amplitude at point A tends to approach the adjustment at point A or to move away from it. In the latter case squegging oscillation is bound to occur. We shall see later from several factors that instability at A can be predicated with certainty.

As mentioned above, A is a point of equilibrium and the corresponding amplitude is consequently steady. An amplitude differing from that at A will however vary with time, because not all determining influences are in balance. It is thus possible to state an equation with the amplitude as a function of time; from this equation it will be apparent whether, after some time, the amplitude settles down at point A.

§ 4. Investigating the stability of the equilibrium adjustment

Thorough investigation of stability, or rather of the various transient conditions, necessitates calculating the effect on the amplitude of an excess of slope, and ascertaining how this amplitude influences the negative grid bias and therefore the effective slope and the damping.

In the calculations which follow we shall indentify the values assumed by the various quantities in the contemplated steady condition by using

the index s. During the transient period the quantities will generally deviate from these values by an amount to be denoted by a small letter. It may happen, then, that exceptionally an amplitude will be indicated by a small letter. Before the oscillation reaches a steady value, therefore:

$$S_{eff} = S_{eff_s} + s_{eff},$$
$$V_g = V_{gs} + v_g,$$
$$V_a = V_{a_s} + v_a$$
$$V_{g\ med} = V_{g\ med_s} + v_{g\ med},$$
$$I_{g\ med} = I_{g\ med_s} + i_{g\ med}.$$

The behaviour of the circuit is now known if we can establish the variation of one of these quantities, s_{eff}, v_g, etc. as a function of time. If the quantity eventually approaches nil a steady condition arises and the circuit is therefore stable.

It is possible to state two equations in which only the quantities v_g and $v_{g\ med}$ appear. The first, with v_g, relates to phenomena in the tuned circuit, the second to the variation $v_{g\ med}$ of the grid voltage in the grid capacitor — grid leak — valve combination. But it is first necessary to express s_{eff} and $i_{g\ med}$ in terms of v_g and $v_{g\ med}$.

In fig. 150 we have the basic tuned-anode back-coupled circuit.

When oscillation is present the tuned circuit holds a certain quantity of energy which at the instant of maximum voltage is concentrated entirely in the capacitor. If the amplitude of the voltage is V_a this energy is:

$$P = \tfrac{1}{2}\, C_v\, V_a^2 \quad \text{(II E 1)}$$

During oscillation, however, power is lost in the circuit resistance r, and the circuit energy P therefore decreases with time. On the other hand the alternating anode current is supplying power to the tuned circuit, and the difference between the loss and gain determines whether P increases or decreases. The power lost in the resistance r is:

$$\tfrac{1}{2}\, I_k{}^2 r = \tfrac{1}{2}\, \frac{V_a^2}{\omega^2 L^2}\, r.$$

The anode current I_a supplies:

$$\tfrac{1}{2}\, I_a\, V_a = \tfrac{1}{2}\, S_{eff} \frac{M}{L}\, V_a^2\,{}^*.$$

* In this section the value of M/L is positive.

The circuit energy therefore changes each second by an amount:

$$\frac{dP}{dt} = \tfrac{1}{2}\left(S_{eff}\frac{M}{L} - \frac{r}{\omega^2 L^2}\right) V_a^2 \quad \ldots\ldots \quad \text{(II E 2)}$$

Expressing this change, by differentiating equation (II E 1), as a variation in the amplitude of the voltage (i.e. as a variation in the successive amplitudes) we find:

$$\frac{dP}{dt} = C_v V_a \frac{dV_a}{dt} = \tfrac{1}{2} V_a^2 \left(S_{eff}\frac{M}{L} - \frac{r}{\omega^2 L^2}\right),$$

or:

$$\frac{dV_a}{dt} = \tfrac{1}{2} V_a\left(\frac{S_{eff} M}{L C_v} - \frac{r}{L}\right) \quad \ldots\ldots \quad \text{(II E 3)}$$

Now in the steady state as much power is supplied as is lost in the resistance r. The amplitude V_a then remains constant and:

$$\frac{dV_a}{dt} = 0.$$

In this case the effective slope is S_{eff_s}. Using equation (II E 3) we can write:

$$0 = \frac{S_{eff_s} M}{C_v} - r \quad \ldots\ldots\ldots\ldots \quad \text{(II E 4)}$$

(This agrees entirely with the condition for oscillation (II B 18).) Subtracting this equation from (II E 3) we then get:

$$\frac{dv_a}{dt} = \frac{s_{eff} M V_{a_s}}{2 L C_v} \quad \ldots\ldots\ldots\ldots \quad \text{(II E 5)}$$

and similarly, since V_{g_s} is a specific fraction of V_{a_s}:

$$\frac{dv_g}{dt} = \frac{s_{eff} M V_{g_s}}{2 L C_v} \quad \ldots\ldots\ldots\ldots \quad \text{(II E 6)}$$

This differential equation shows how v_g behaves in relation to time. As already mentioned, it is still necessary to express s_{eff} in terms of v_g and $v_{g\,med}$. S_{eff} is dependent on V_g and $V_{g\,med}$, and in the case of a small deviation s_{eff} can therefore be written as:

$$s_{eff} = \left(\frac{\partial S_{eff}}{\partial V_{g\,med}}\right)_{V_{g_s}} v_{g\,med} + \left(\frac{\partial S_{eff}}{\partial V_g}\right)_{V_{g\,med_s}} v_g.$$

If this value of s_{eff} is substituted in equation (II E 6) we have:

$$\frac{dv_g}{dt} = Av_g - Bv_{g\,med} \quad \text{(II E 7a)}$$

in which:

$$A = \frac{V_{g_s} M}{2 L C_v}\left(\frac{\partial S_{eff}}{\partial V_g}\right)_{V_{g\,med_s}}$$

$$B = -\frac{V_{g_s} M}{2 L C_v}\left(\frac{\partial S_{eff}}{\partial V_{g\,med}}\right)_{V_{g_s}} \quad \text{(II E 7b)}$$

The next stage in the calculation is the stating of an equation for the grid capacitor-grid leak-valve combination.

For the currents at the junction of the grid capacitor and leak in fig. 150 we get:

$$\frac{V_{g\,med}}{R} + C_r \frac{dv_{g\,med}}{dt} = I_{g\,med}.$$

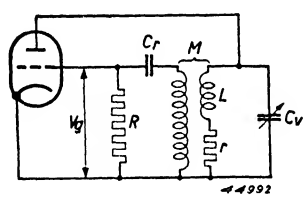

Fig. 150. Basic tuned-anode oscillator circuit.

$V_{g\,med}$ represents the absolute value of the negative grid bias. Since in the steady state

$$\frac{V_{g\,med\,s}}{R} = I_{g\,med_s},$$

we find by subtracting this from the previous equation:

$$\frac{v_{g\,med}}{R} + C_r \frac{dv_{g\,med}}{dt} = i_{g\,med} \quad \text{(II E 8)}$$

This equation expresses the behaviour of $v_{g\,med}$ as a function of time. As $i_{g\,med}$ is also dependent on V_g and $V_{g\,med}$, the variation of $i_{g\,med}$ can be written as:

$$i_{gmed} = \left(\frac{\partial I_{g\,med}}{\partial V_g}\right)_{V_{gmed_s}} v_g + \left(\frac{\partial I_{g\,med}}{\partial V_{g\,med}}\right)_{V_{gs}} v_{g\,med}.$$

If we substitute this value of $i_{g\,med}$ in equation (II E 8) we obtain:

$$\frac{dv_{g\,med}}{dt} = Cv_g - Dv_{g\,med} \quad \text{(II E 9a)}$$

in which:

$$\left.\begin{aligned} C &= \frac{1}{C_r}\left(\frac{\partial I_{g\,med}}{\partial V_g}\right)_{Vg\,med_s} \\ \text{and} \qquad D &= \frac{1}{C_r}\left[\left(-\frac{\partial I_{g\,med}}{\partial V_{g\,med}}\right)_{Vg_s} + \frac{1}{R}\right] \end{aligned}\right\} \quad \ldots \quad \text{(II E 9b)}$$

The differential coefficients C and D will later be worked out further.
From equations (II E 7a) and (II E 9a) the differential equation for v_g, expressed in A, B, C and D, can be derived by eliminating $v_{g\,med}$. Differentiating equation (II E 7a) gives

$$\frac{d^2 v_g}{dt^2} = A\frac{dv_g}{dt} - B\frac{dv_{g\,med}}{dt} \quad \ldots \quad \text{(II E 10)}$$

From equations (II E 7a) and (II E 9a) we find:

$$\frac{dv_{g\,med}}{dt} = Cv_g - \frac{D}{B}Av_g + \frac{D}{B}\frac{dv_g}{dt} \quad \ldots \quad \text{(II E 11)}$$

Substituting (II E 11) in (II E 10) gives:

$$\frac{d^2 v_g}{dt^2} + (D - A)\frac{dv_g}{dt} + (BC - AD)\,v_g = 0 \quad \text{(II E 12)}$$

It is therefore clear that the value of v_g is given by the general equation for oscillation. From this we may draw the conclusion that v_g dies away to nothing if the "damping coefficient", i.e. the coefficient of dv_g/dt in the differential equation, and furthermore the coefficient of v_g, are positive. The condition for a stable balance at point A thus becomes:

$$D > A \quad \ldots \quad \text{(II E 13)}$$

provided $(BC - AD) > 0$. Usually this latter condition is satisfied.
If we now substitute the values of D and A in equation (II E 13) we finally get:

$$\frac{1}{C_r}\left[\left(\frac{1}{R} + \left(-\frac{\partial I_{g\,med}}{\partial V_{g\,med}}\right)_{Vg_s}\right] > \frac{M}{2LC_v}V_{gs}\left(\frac{\partial S_{eff}}{\partial V_g}\right)_{Vg\,med_s} \quad \text{(II E 14)}$$

The way in which the amplitude settles down, like a damped oscillation,

to eventual equilibrium, is clearly seen in the oscillogram of fig. 144 where, by periodic interruption of the anode voltage, the oscillation was continually compelled to readjust itself.

§ 5. Qualitative conclusions from the condition for stability

From the stability equation we can now draw some important conclusions regarding the circuit elements and valve constants in a specific oscillator.

a. Conclusions regarding circuit elements

1. In order to prevent squegging oscillation it is advisable to keep the value of the grid capacitor C_r small. It cannot however be reduced indefinitely, or an unfavourable voltage division across the input capacitance and grid/anode capacitance of the valve will occur (B § 9).
2. The grid leak R must have as low a value as possible.
   These stipulations for the grid capacitor and leak agree with the practical results obtained earlier.
3. It follows from the second term of equation (II E 14) that a large feedback ratio M/L increases the risk of squegging oscillation. Experience with old-time receivers equipped with reaction confirms this statement and also explains why the oscillator section of the mixing valve shows the greatest tendency to squeg on short waves, for in that band the feedback ratio M/L is considerably larger than in the medium-wave and long-wave bands.
4. Finally, squegging oscillation is especially liable to occur when the tuning capacitor C_v has a low value, as it has at the bottom of the waveband.

d. Conclusions regarding the constants of the oscillator valve

1. From the requirement for stability (II E 14) it is evident that $\left(\frac{-\partial I_{g\,med}}{\partial V_{g\,med}}\right)_{V_{gs}}$ must be large at the point of balance A, i.e. a change of $V_{g\,med}$ must result in a large change of grid current $I_{g\,med}$. This means that with a steep grid-current characteristic squegging oscillation occurs less readily. With some valves, for instance the ECH 21 and UCH 21, such a characteristic is achieved by providing the grid with an anode-like extension (fig. 151).

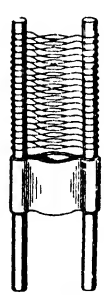

Fig. 151. The grid of the oscillator section in the mixing valve ECH 21; the lowest part is built as a diode.

2. It will further be noticed that squegging is discouraged when $\left(\frac{\partial S_{eff}}{\partial V_g}\right)_{V_{g\,med_s}}$ has a low value. Regarding this we note from the example of fig. 145 (straight i_a/v_g characteristic) the following: In figs 145a and b $\left(\frac{\partial S_{eff}}{\partial V_g}\right)_{V_{g\,med_s}}$ is negative or nil. In such a case the adjustment is always stable. In fig. 145c $\left(\frac{\partial S_{eff}}{\partial V_g}\right)_{V_{g\,med_s}}$ is always equal to zero, i.e. the adjustment is also stable for oscillator voltages less than the cut-off voltage. In figs 145d to g inclusive stability at point A depends (with specific values of circuit elements and a given shape of grid-current characteristic) on the magnitude of V_g and $\left(\frac{\partial S_{eff}}{\partial V_g}\right)_{V_{g\,med_s}}$.

Having derived these conclusions from equation (II E 14), we shall of course endeavour to make quantitative predictions. The values of the various circuit elements are already known accurately enough; the two differential quotients in equation (II E 10), are however, still to be determined. In the last of the conclusions use was made of data from fig. 145, which is based on a straight i_a/v_g characteristic. In general, however, more accurate information is required. The values of the differential quotients may be ascertained by measurements with the valve concerned (E § 6) or by calculation with the help of a suitable approximation of the valve characteristic (E § 7).

§ 6. Measuring the differential quotients $\left(-\frac{\partial I_{g\,med}}{\partial V_{g\,med}}\right)_{V_{g_s}}$ and $V_{gs}\left(\frac{\partial S_{eff}}{\partial V_g}\right)_{V_{g\,med_s}}$

The measurements may be made with the circuit of fig. 152. The impedance Z is tuned to the frequency of the signal-generator G.
The A.C. voltage V_g at the grid is measured with a diode-voltmeter DM_1, the A.C. voltage across the tuned-anode circuit with the diode voltmeter DM_2, and the steady voltage $V_{g\,med}$ on the grid with the voltmeter VM. The grid current through the leak R can be determined with the microammeter AM. The negative bias $V_{g\,med}$ on the grid is controlled by means of the potentiometer P.

a. Measuring $\left(-\frac{\partial I_{g\,med}}{\partial V_{g\,med}}\right)_{V_{g_s}}$

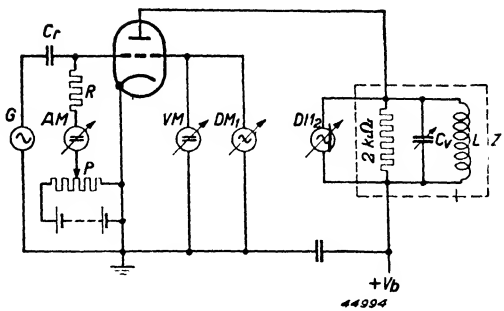

Fig. 152. Circuit for measuring the quantities $\left(\frac{-\partial I_{gmed}}{\partial V_{gmed}}\right)_{V_{g_s}}$ and $V_{g_s}\left(\frac{\partial S_{eff}}{\partial V_g}\right)_{V_{gmed_s}}$

In order to determine this quantity at the point of balance A we proceed as follows:
First the oscillator voltage and the negative bias at the equilibrium point A are ascertained. If we substitute a feedback coil for the signal generator and connect the grid leak R straight to the cathode, the oscillator voltage and the negative bias at the grid can then be read off the diode-voltmeter DM_1 and the voltmeter VM respectively. The measured values correspond to those at point A.

Let us assume, for example, that for an ECH 21 with a grid leak of 50,000 ohms the oscillator voltage in a particular circuit amounts to 8 V_{RMS}, and that for this adjustment the ratio $\left(-\frac{\partial I_{g\,med}}{\partial V_{g\,med}}\right)_{V_{g_s}}$ is to be determined.

The feedback coil is replaced by the signal generator G. The oscillator voltage and the negative bias are then adjusted to mutually appropriate values with the help of the signal generator G and the potentiometer P, the grid leak being again joined direct to the cathode. If the oscillator voltage V_{g_s} is kept constant, the change of $I_{g\,med}$ due to varying $V_{g\,med}$ (observable on meter VM) can be read off the microammeter AM. The value of $\left(-\frac{\partial I_{g\,med}}{\partial V_{g\,med}}\right)_{V_{g_s}}$ is the quotient of these two readings.

For the ECH 21, with an oscillator voltage of 8 V_{RMS}, the quotient has a value of 300 μA/V.

This quantity may of course also be determined for other points of balance which are possible with different degrees of coupling. It is then found that over a large range of oscillator voltage $\left(-\frac{\partial I_{g\,med}}{\partial V_{g\,med}}\right)_{V_{g_s}}$ is almost independent of V_{g_s}.

b. Measuring $V_{g_s}\left(\frac{\partial S_{eff}}{\partial V_g}\right)_{V_{g\,med_s}}$

For this measurement, too, the oscillator voltage V_{g_s} and the negative bias $V_{g\,med_s}$ at the point A concerned are first determined, as in the previous case. Next the signal generator and potentiometer are adjusted to bring the oscillator voltage V_{g_s} and the negative bias $V_{g\,med_s}$ once more to the point of balance A. The voltage V_{a_s} across the tuned-anode circuit is then measured with the diode-voltmeter DM_2. For V_{a_s} we have (since $Z \ll R_i$):

$$V_{a_s} = S_{eff_s}\, V_{g_s}\, Z.$$

The oscillator voltage is now increased by an amount v_g, the potentiometer P being adjusted so that the grid bias remains at $V_{g\,med_s}$. The voltage across the tuned circuit is now $V_{a_s} + v_a$ and we can write:

$$V_{a_s} + v_a = (S_{eff\,s} + s_{eff})\ (V_{g_s} + v_g)\, Z.$$

The term $s_{eff}\, v_g\, Z$ is small in relation to the others and may be neglected. We then get:

$$V_{a_s} + v_a = S_{eff_s}\, V_{g_s}\, Z + s_{eff}\, V_{g_s}\, Z + S_{eff_s}\, v_g\, Z$$

or:

$$v_a = S_{eff_s}\, v_g\, Z + s_{eff}\, V_{g_s}\, Z$$

or:

$$\frac{V_{g_s}\, s_{eff}}{v_g} = V_{g_s}\left(\frac{\partial S_{eff}}{\partial V_g}\right)_{V_{g med_s}} = \left(\frac{v_a}{v_g} - \frac{V_{a_s}}{V_{g_s}}\right)\frac{1}{Z}.$$

The quantities V_{a_s}, V_{g_s}, v_a and v_g are known from the measurements.

The circuit impedance is also known, and amounts to say 2000 ohms. $\frac{V_{g_s}\, s_{eff}}{v_g}$ can thus be computed.

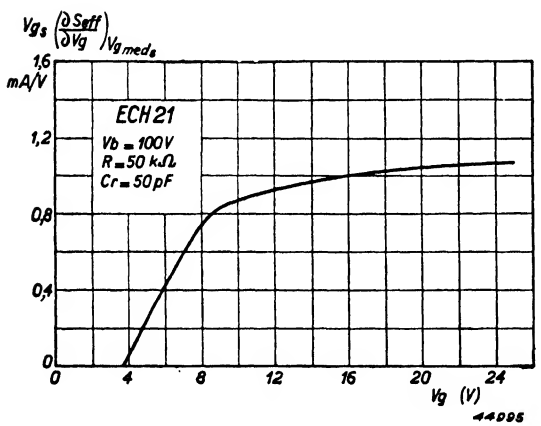

Fig. 153. The quantity $V_{g_s}\left(\frac{\partial S_{eff}}{\partial V_g}\right)_{V_{g med_s}}$ as a function of the oscillator voltage V_g (peak), measured on the triode section of the ECH 21.

These measurements may be repeated for various points A; the results obtained with an ECH 21 are set out in fig. 153.

§ 7. Calculating the differential quotients

$$\left(-\frac{\partial I_{g\,med}}{\partial V_{gmed}}\right)_{V_{g_s}} \quad \text{and} \quad V_{g_s}\left(\frac{\partial S_{eff}}{\partial V_g}\right)_{V_{g\,med_s}}$$

The measurements described above make it possible to judge to some extent the stability of specific valves in an oscillator circuit. In order, however, to be able to choose the optimum operating conditions we may evaluate the foregoing quotients from the characteristics of the valve.

a. Calculating $\left(-\frac{\partial I_{g\,med}}{\partial V_{g\,med}}\right)_{V_{g_s}}$

The grid-current characteristic is assumed to be straight. To calculate the quotient $\left(-\frac{\partial I_{g\,med}}{\partial V_{g\,med}}\right)_{V_{g_s}}$ it is then only necessary to determine the change of grid current with change of grid bias, the A.C.-voltage on the grid being constant. In fig. 154 the voltages at the grid are shown against time. If in this figure the negative grid bias $V_{g\,med_s}$ increases by an amount $v_{g\,med}$, the fall in mean grid current [see also (II B § 9)] is:

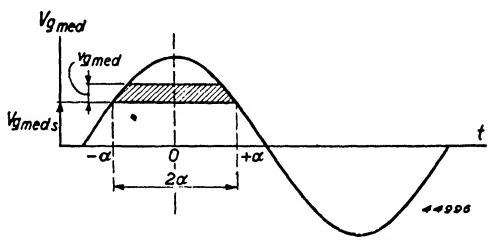

Fig. 154. The voltages V_g and $V_{g\,med}$ at the grid of an oscillator, as a function of time.

$$i_{g\,med} = -\frac{\text{hatched surface}}{2\pi R_g} = -\frac{2\alpha\, v_{g\,med}}{2\pi R_g} = -\frac{\alpha\, v_{g\,med}}{\pi R_g};$$

therefore:

$$\frac{-i_{gmed}}{v_{g\,med}} = \left(-\frac{\partial I_{g\,med}}{\partial V_{gmed}}\right)_{V_{g_s}} = \frac{\alpha}{\pi R_g} \quad . \quad . \quad . \quad . \quad . \text{(II E 15)}$$

Here R_g denotes the grid A.C.-resistance and α the current angle given by:

$$tan\ \alpha - \alpha = \pi\frac{R_g}{R} \quad . \quad . \quad . \quad . \quad . \quad . \quad . \quad . \quad . \quad . \quad . \quad . \quad . \text{(II B 56)}$$

With the aid of these last two equations the quotient $\left(-\frac{\partial I_{g\,med}}{\partial V_{gmed}}\right)_{V_{g_s}}$ can now be expressed in terms of R and R_g. We thus reach the important conclusion that this quotient is independent of the oscillator voltage V_{g_s} and is determined only by R and R_g.

With the ECH 21, if $R = 50{,}000$ ohms and $R_g = 500$ ohms so that $\cos \alpha = 0.9$ (see fig. 118), we obtain a value of 314 μA/V, assuming that the grid-current characteristic is straight. In the test described above a figure of 300 μA/V was found, and the agreement is therefore satisfactory.

As $\cos \alpha = V_{g\,med_s} / V_{g_s}$, the factor $\left[\frac{1}{R} - \left(\frac{\partial I_{g\,med}}{\partial V_{g\,med}}\right)_{V_{g_s}}\right]$ in the stability equation (II E 14) may be written also in the form:

$$\frac{1}{R} - \left(\frac{\partial I_{g\,med}}{\partial V_{g\,med}}\right)_{V_{g_s}} = \frac{1}{R} + \frac{\alpha}{\pi R_g} = \frac{1}{\pi R_g}\left(\frac{\pi R_g}{R} + \alpha\right) =$$

$$= \frac{\tan \alpha}{\pi R_g} = \frac{\sqrt{\left(\frac{V_{g_s}}{V_{g\,med_s}}\right)^2 - 1}}{\pi R_g} \quad \ldots\ldots \text{(II E 16)}$$

b. Calculating $V_{g_s}\left(\frac{\partial S_{eff}}{\partial V_g}\right)_{V_{g\,med_s}}$

For the calculation of this quantity the assumption of a straight characteristic is no longer a sufficiently accurate approximation (this would at once become apparent if, using fig. 145 as a basis for the calculation, we were to compare our findings with the measurements shown in fig. 153). In this case we shall therefore start from the quadratic characteristic $i_a = \frac{S_o}{2\,V_{go}}(V_g + V_{go})^2$, which approaches the actual characteristic much more closely (see fig. 87). Both S_o and V_{go} are proportional to the anode voltage V_a.

The instantaneous grid voltage is:

$$v_g = -V_{g\,med} + V_g \sin x, \text{ when } x = \omega t.$$

The instantaneous anode current therefore is:

$$i_a = \frac{S_o}{2\,V_{go}}\left\{(-V_{g\,med} + V_{go})^2 + 2\,V_g\,(-V_{g\,med} + V_{go}) \sin x + V_g^2 \sin^2 x\right\}$$

The first harmonic of the anode current is given by the equation:

$$I_{a1} = \frac{1}{\pi}\int_{o}^{2\pi} i_a \sin x\, dx = \frac{S_o}{2\pi\, V_{go}}\int_{A}^{B}\{\,(-V_{g\,med} + V_{go})^2 \sin x + 2\,V_g\,(-V_{g\,med} + V_{go})\sin^2 x + V_g^2 \sin^3 x\,\}\,dx;$$

$$I_{a1} = \frac{S_o}{2\pi\, V_{go}}\left\{-(-V_{g\,med} + V_{go})^2 \cos x + 2\,V_g\,(-V_{g\,med} + V_{go}) \times \left(\frac{x}{2} - \frac{\sin 2x}{4}\right) + V_g^2\left(-\cos x + \frac{\cos_3 x}{3}\right)\right\}_A^B.$$

The mean effective slope is therefore:

$$S_{eff} = \frac{I_{a1}}{V_g} = \frac{S_o}{2\pi\, V_g\, V_{go}}\left\{-(-V_{g\,med} + V_{go})^2 \cos x + 2\,V_g(-V_{g\,med} + V_{go}) \times \left(\frac{x}{2} - \frac{\sin 2x}{4}\right) + V_g^2\left(-\cos x + \frac{\cos^3 x}{3}\right)\right\}_A^B.$$

Two cases can occur:

1. $(V_{g\,med} + V_g) < V_{go}$.

The complete cycle of oscillation is accommodated by the characteristic. The equation must be integrated between 0 and 2 π and then becomes:

$$S_{eff} = \frac{S_o}{2\pi\, V_{go}\, V_g}\left\{2\,V_g\,(-V_{g\,med} + V_{go})\,\pi\right\} = \frac{So}{V_{go}}\,(V_{go} - V_{g\,med}).$$

It is clear that S_{eff} is independent of V_g, and therefore:

$$\left(\frac{\partial\, S_{eff}}{\partial\, V_g}\right)_{V_{g\,med_s}} = 0.$$

2. $(V_{gmed} + V_g) > V_{go}$.

Here we distinguish alternative possibilities:

I. $V_{g\,med} < V_{go} < (V_{g\,med} + V_g)$. (This we call Class AB in the case of output valves.)
The limits between which we must integrate are now $-\varphi_o$ and $\pi + \varphi_o$ (see fig. 155a).

II. $V_{g\,med} > V_{go}$ (so-called Class C operation).
The limits between which we must integrate are φ_o and $\pi - \varphi_o$ (see fig. 155b).

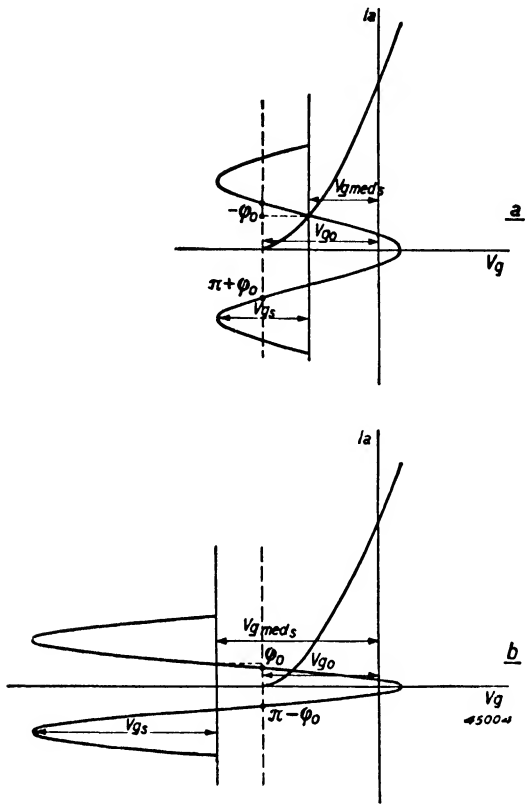

Fig. 155. Quadratic i_a/v_g characteristic of an oscillator valve, with alternating grid voltages
(a) $V_{gmed} < V_{go} < (V_{gmed} + V_g)$
(b) $V_{gmed} > V_{go}$.

φo is determined from:

$$\sin \varphi_o = \frac{V_{g\ med_s} - V_{go}}{V_{g_s}},$$

and:

$$\left(\frac{\partial \varphi_o}{\partial V_g}\right)_{V_{g\ med_s}} = -\frac{V_{g\ med_s} - V_{go}}{V_{gs}^2 \cos \varphi_o}.$$

After substituting the integration limits we obtain for S_{eff} in both cases:

$$S_{eff} = \frac{S_o}{\pi\ V_{go}} (V_{gmed} - V_{go}) \left(\varphi_o - \frac{\pi}{2} + \frac{\cos \varphi_o - \frac{\cos^3 \varphi_o}{3}}{\sin \varphi_o} \right),$$

and consequently:

$$\left(\frac{\partial S_{eff}}{\partial V_g}\right)_{V_{g\,med_s}} = \left(\frac{\partial S_{eff}}{\partial \varphi_o}\right)_{V_{g\,med_s}} \left(\frac{\partial \varphi_o}{\partial V_g}\right)_{V_{g\,med_s}} = -\frac{S_o}{\pi V_{go}} \frac{(V_{g med_s} - V_{go})^2}{V_{g_s}^2 \cos \varphi_o} \times$$

$$\left\{1 + \frac{\sin \varphi_o (-\sin \varphi_o + \sin \varphi_o \cos^2 \varphi_o) - \cos \varphi_o \left(\cos \varphi_o - \frac{\cos^3 \varphi_o}{3}\right)}{\sin^2 \varphi_o}\right\} =$$

$$= \frac{2}{3\pi V_{go}} - S_o \cos^3 \varphi_o.$$

Thus:

$$V_{g_s}\left(\frac{\partial S_{eff}}{\partial V_g}\right)_{V_{g\,med_s}} = \frac{2 V_{g_s} S_o}{3\pi V_{go}} \cos^3 \varphi_o = \frac{2}{3\pi} S_o \frac{V_{g_s}}{V_{go}} \sqrt{1 - \left(\frac{V_{g\,med_s} - V_{go}}{V_{gs}}\right)^2}^3 \qquad \text{(II E 17)}$$

From equation (II E 17) it is evident that

$$V_{g_s}\left(\frac{\partial S_{eff}}{\partial V_g}\right)_{V_{g\,med_s}}$$

is proportional to the initial slope S_o. In fig. 156 the proportionate factor is shown as a function of V_{g_s} / V_{go} for various values of $V_{g\,med_s} / V_{gs}$. The measured curve obtained with the ECH 21 (fig. 153) is also reproduced as a dotted line, on the same scale (namely after being divided by S_o = 3 mA/V. This curve corresponds to that for $V_{g\,med_s} / V_{gs}$ = *cos x* = 0.9 (calculated from R = 50,000 Ω and R_g = 500 Ω, vide B § 8). The agreement of the measured and the calculated curves is evident.

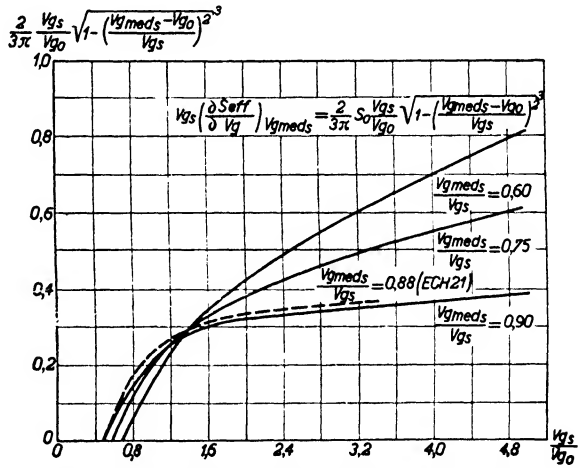

Fig. 156. Factor of S_o from equation (II E 17), as a function of V_{gs}/V_{go} for various values of V_{gmed_s}/V_{g_s}.

§ 8. Quantitative conclusions from the condition for stability

While qualitative conclusions have already been dealt with in § 5, it is also

possible, in view of the good agreement of the measured with the calculated values, to derive the optimum numerical values for the various circuit and valve elements from the condition for stable oscillation. For this purpose we rewrite the stability formula (II E 14) after substituting equations (II E 16) and (II E 17) and obtain:

$$f > \frac{M\,C_r}{L\,C_v} \qquad \text{(II E 18a)}$$

where:

$$f = 3\,\frac{V_{go}}{V_{g_s}}\,\frac{\sqrt{\left(\frac{V_{g_s}}{V_{g\,med_s}}\right)^2 - 1}}{R_g\,S_o\sqrt{1-\left(\frac{V_{g\,med_s} - V_{go}}{V_{g_s}}\right)^{2\,3}}} \qquad \text{(II E 18b)}$$

We see at once from the expression (II E 18a) that a small value of f is unfavourable. The minimum value of f for freedom from squegging is determined by the magnitude of C_r, M/L and C_v. The grid capacitor C_r will not usually be made smaller than 50 pF, in order to avoid a division of voltage across the input and grid/anode capacitances. The smallest value of C_v is found on short waves and is about 40 pF. The highest value of M/L, about 1/3, also occurs in the SW band. Thus the smallest permissible value of f amounts to $40/50 \times 1/3 = 0.3$. To avoid squegging oscillation the factor f must therefore be decidedly more than 0.3.

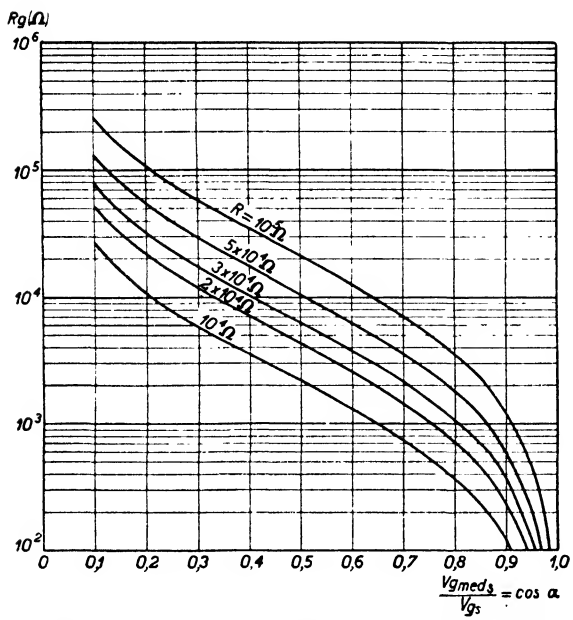

Fig. 157. R_g as a function of V_{gmed_s}/V_{g_s} for grid leak values of 10,000, 20,000, 30,000, 50,000 and 100,000 ohms.

Using equation (II E 18b) we shall now calculate f from the valve constants and for various values of grid leak. In fig. 118 the relation between R_g/R and $V_{gmed_s}/V_{g_s} = \cos\alpha$ was given, and it is a simple matter to deduce therefrom the relation between R_g and $V_{g\,med_s}/V_{g_s}$ for particular values of the

Fig. 158. The factor f in equation (II E 18a) as a function of the grid A.C.-resistance Rg for various values of S_o and of the grid leak.

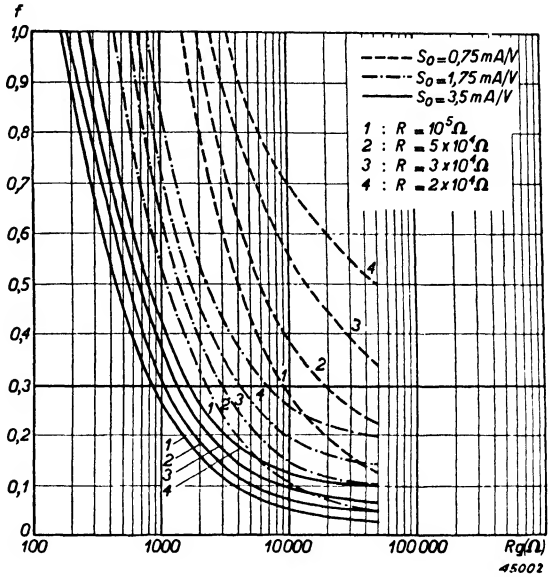

grid leak. This relationship is indicated in fig. 157, which includes curves for grid leaks of 10,000, 20,000, 30,000, 50,000 and 100,000 ohms. We have now calculated f as a function of the grid A.C.-resistance Rg, for various values of S_o and the grid leak R. The slope figures are 3.5, 1.75 and 0.75 mA/V, and the grid leak values 20,000, 30,000, 50,000 and 100,000 ohms.

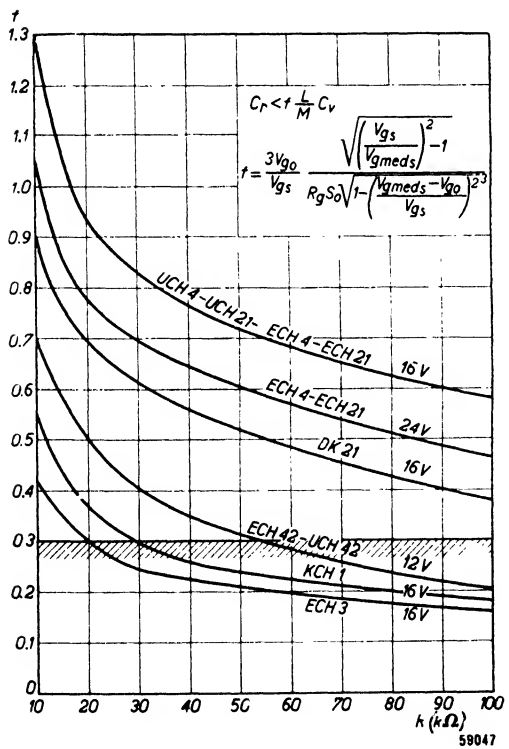

It has been assumed that in the condition most favouring squegging oscillation the oscillator voltage remains less than twice the cut-off voltage of the valve. The result of this calculation is shown in fig. 158. Some conclusions can be drawn from this figure, which are confirmed by practice:

a. With the ECH 4 and ECH 21, $S_o = 3.2$ mA/V and $R_g = 500$ ohms.
For a grid leak of 50,000 ohms we therefore find that $f = 0.55$. There is thus a large reserve against squegging oscillation. This agrees with the experience in practice, that the ECH 4 and

Fig. 159. The factor f in equation (II E 18a) as a function of the grid-leak resistance for various present-day types of mixer valve. After each type number the oscillator voltage (peak) to which the curve refers is indicated.

ECH 21 do not squeg on short waves until the grid capacitor exceeds 100 pF.

b. With the DK 21 $S_o = 0.75$ mA/V and $R_g = 5000$ ohms. Consequently $f = 0.55$ when a grid leak of 50,000 ohms is used. In this case, too, there is a very large margin of safety. The diagram indicates, furthermore, that with a 20,000 ohms grid leak there is practically no risk of squegging with this valve. On the other hand there is the danger that, should it occur, the grid will then be swung so far into the region of grid current ($V_{g\ med}/V_{g_s} = 0.47$) that the cathode becomes damaged.

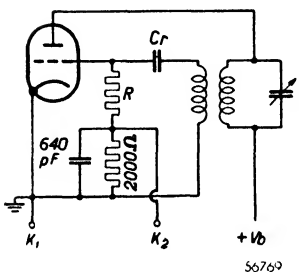

Fig. 160. Circuit for visualizing oscillation on a cathode-ray oscilloscope.

Finally, in fig. 159 the factor f is expressed as a function of the grid-leak resistance for various types of mixer valve.
From this diagram we may readily ascertain the value of grid leak which, from the point of view of avoiding squegging, it is safe to use with a given valve. The conclusions to be drawn from fig. 159 are wholly in agreement with the practical results obtained with these valves.

§ 9. A circuit for observing squegging oscillation

From what has been said in the previous section it will be apparent that squegging oscillation, i.e. the periodic interruption of the train of oscillation as the grid capacitor charges and discharges, is accompanied by a low-frequency variation of the current through the grid leak. This A.C. component may easily be observed with the help of the circuit given in fig. 160.

A resistor of say 2000 ohms is joined in series with the grid leak and the voltage across it is fed to the input of a cathode-ray oscilloscope. The high-frequency voltage is bypassed to earth by a capacitor of about 640 pF shunting the 2000 ohms resistor.
When the oscillator circuit goes into squegging a trace similar to fig. 161 appears on the screen of the cathode-ray tube; with normal oscillation the (horizontal) time-base (line) remains undeflected.

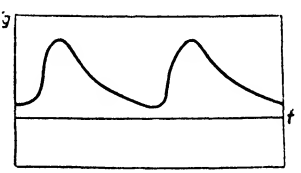

Fig. 161. Trace obtained on the cathode-ray tube from an over-oscillating circuit.

F. Interaction between oscillator and input circuits

§ 1. Introduction

The combining of oscillator and modulator in a single valve has the disadvantage that certain capacitances between the two systems cause undesirable interaction.

These capacitances appear between the respective grid supports, between the leading-out wires and between the contact pins; in addition to these strays there are capacitances and space charges between certain electrodes.

The capacitive influence of such space charges is known as induction effect. Two main types of parasitic effect result from these unwanted couplings. The first is that the rather high voltage across the oscillator tuned circuit causes a voltage of oscillator frequency to appear in the R.F. input circuit; it was this difficulty which originally led to the development of a mixing valve having separate control and modulator grids. The problem is how to minimise the induced voltage. The parasitic voltage not only causes undesirable radiation from the aerial but it can be so large that grid current flows and damps the R.F. circuit. Furthermore, mixing is affected; the signal-frequency voltage and the induced voltage of oscillator frequency, applied together to the control grid, give rise to an I.F. current in the anode circuit which either increases or reduces the normal I.F. current. The conversion conductance is therefore either raised or lowered, according to the phase of the parasitic voltage. Not only does reduction of the conversion conductance impair the sensitivity of the receiver but the signal-noise ratio is also affected. From all angles it is thus desirable to limit the transfer of oscillator voltage to the input circuit, or else to compensate for it.

Another parasitic phenomenon is "pulling" between the input circuit and the oscillator circuit, the influencing of the oscillator frequency by the R.F. circuit being especially disturbing. This phenomenon will be dealt with further in section H, dealing with frequency drift.

§ 2. Stray capacitances

Fig. 162 indicates those inter-electrode capacitances in a mixer valve which carry alternating voltages. Only the significant electrodes are shown; the remainder are capacitively earthed and therefore, as far as alternating

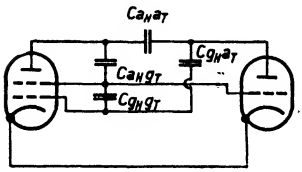

Fig. 162. The inter-electrode capacitances in a mixer valve carrying alternating voltages.

voltages are concerned, can neither affect other electrodes nor be influenced thereby.

The following capacitances have to be considered: C_{aHgT}, C_{aHaT}, C_{g1HaT} and C_{g1HgT}.

The first parasitic effect we shall deal with is the voltage transferred from the oscillator section to the mixer control-grid via the capacitances C_{g1HaT} and C_{g1HgT}. The voltage induced at the anode of the mixer section is unimportant; later, however, we shall consider what influence the mixer anode has on the oscillator section.

That fraction of the parasitic voltage which reaches the mixer control-grid by way of C_{g1HaT} bears a fixed relationship to the fraction carried by C_{g1HgT}. The alternating voltage at the anode of the triode section is $1/t$ times that at the oscillator grid and in opposite phase thereto (therefore $t < 0$). Accordingly the respective voltages induced at the mixer grid are in opposition. The same net voltage would appear if no voltage came from the triode anode and if the feedback capacitance C_{g1HgT} were replaced by a capacitance C_k.

The actual coupling capacitance C_k is given by:

$$C_k = C_{g1HgT} + \frac{1}{t} C_{g1HaT} \quad \ldots\ldots\ldots \quad \text{(II F 1)}$$

In subsequent calculations we can now assume that only the grid of the oscillator is coupled to the hexode control-grid and that the capacitance between these electrodes is C_k; the parasitic voltage V_s passed by this capacitance may be calculated in the same way as in Section II A § 2 for the circuit of figs 74 and 75. For the medium-wave and long-wave bands we get:

$$V_s = \frac{C_k}{C_k + C_i} \frac{1}{\beta} V_h \quad \ldots\ldots\ldots\ldots \quad \text{(II A 26)}$$

and:

$$\beta = \frac{\omega_h}{\omega_i} - \frac{\omega_i}{\omega_h} \approx \frac{2\,(\omega_h - \omega_i)}{\omega_i} \quad \ldots\ldots\ldots \quad \text{(I A 11)}$$

If the oscillator frequency is higher than the signal frequency the input circuit may in practice be regarded as a capacitance. V_s arises therefore from the division of V_h across a capacitive potential-divider and it is therefore in phase with V_h. In equation (II A 26) we can substitute for β from (I A 11). Since, moreover, in any particular waveband the tuning

capacitance $C_k + C_i$ is inversely proportional to ω_i^2 we obtain:

$$V_s \mathrel{\dot{\sim}} C_k \frac{\omega_i^3}{\omega_h - \omega_i} \mathrel{\dot{\sim}} C_k \frac{\omega_i^3}{\omega_0} \quad \text{(II F 2)}$$

The induced voltage is thus inversely proportional to the intermediate frequency, directly proportional to the stray capacitance C_k and, for a given waveband, proportional to the cube of the input frequency. From wave-range to wave-range it varies in proportion to the input frequency, assuming the same tuning capacitance in each case.

In the medium waveband the greatest parasitic voltage therefore occurs at 200 metres and with a low intermediate frequency of say 125 kc/s. If $C_i = 50$ pF and $C_k = 1$ pF:

$$V_s = \frac{1}{51} \times \frac{1500}{2 \times 125} V_h = 0.12\ V_h.$$

With a heterodyne voltage $V_h = 8$ V the parasitic voltage reaches a value of about 1 V. At an intermediate frequency of 475 kc/s we find:

$$V_s = \frac{1}{51} \times \frac{1500}{2 \times 475} = 0.03\ V_h.$$

In the case of the ECH 21 mixer $C_{g_1 HgT} = 0.4$ pF and $C_{g_1 HaT} = 0.02$ pF. On medium waves the feedback ratio t will be about —0.25 with a tuned-anode circuit and —4 with a tuned-grid circuit.

We then get from equation (II F 1):

$C_k = 0.4—0.25 \times 0.02 = 0.395$ pF, resp. $C_k = 0.4—4 \times 0.02 = 0.32$ pF.

The actual voltage induced is thus roughly half that calculated for $C_k = 1$ pF, namely about 0.4 V with an intermediate frequency of 125 kc/s, or 0.012 V with 475 kc/s.

In the short waveband the approximation in equation (II A 26) is no longer permissible. For the attenuation of resonance we must now write:

$$a = \sqrt{1 + Q^2 \beta^2}$$

and we therefore get:

$$V_s = \frac{C_k}{C_i + C_k} Q \times \frac{1}{\sqrt{1 + Q^2 \beta^2}} V_h \quad \text{(II F 3)}$$

At 15 metres Q can have a value of 100, and with an intermediate frequency of 125 kc/s β equals 0.013. With an intermediate frequency of 475 kc/s, $\beta = 0.048$.

With $C_k = 0.4$ pF and for an intermediate frequency of 125 kc/s the absolute value of the voltage V_o is:

$$V_s = \frac{0.4}{50.4} \frac{100}{\sqrt{1 + 1.3^2}} \times 8 = 3.9 \text{ V}$$

and for an intermediate frequency of 475 kc/s:

$$V_s = \frac{0.4}{50.4} \frac{100}{\sqrt{1 + 4.8^2}} \times 8 = 1.28 \text{ V}$$

When the parasitic voltage is excessive it is worth while providing compensation, by suitably increasing $C_{g_1 Ha T}$ or $C_{g_1 Hg T}$; which alternative to adopt must be determined by measurement (see below).

§ 3. Induction effect

If a charge $-Q$ leaves a conductor, for example by emission, there remains in the conductor a charge $+Q$. Fig. 163a represents an interrupted circuit one face of which at the break is emissive; the departing $-Q$ is still quite close to the lower face from which it came. The charge $-Q$ and the remaining charge $+Q$ attract one another and the latter therefore concentrates on the surface. If, however, the charge $-Q$ is brought near to the upper face a charge $+Q$ will appear at that side. During the movement of the negative charge a current will therefore flow in the conductor, transferring an equivalent charge $-Q$ from top to bottom (fig. 163b), so that an equally large positive charge remains. When the charge $-Q$ is moving, and therefore located somewhere between the lower and upper faces (fig. 163c), part of $+Q$, say $+aQ$, still remains at the lower face, the other part being neutralised by the electrons coming from the other face, and accordingly a positive charge Q (1—a) remains at the upper face. This latter charge is the greater the nearer $-Q$ is located to the upper face.

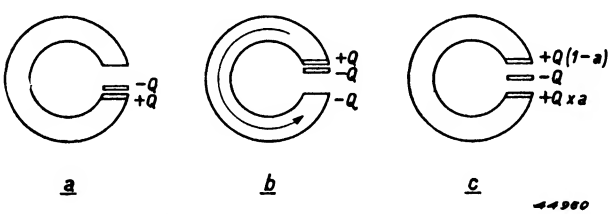

Fig. 163. Fundamental representation of a current circuit.
a. The charge -Q is still quite close to the lower face from which it came.
b. The charge -Q is brought near the upper face.
c. The charge -Q is located somewhere between the lower and upper faces.

In a valve we have to reckon not with a single charge $-Q$ at a defined point between the cathode and another electrode but with the distributed space charge formed by all electrons which have still to reach an electrode. Each

electron causes a positive charge at the electrode concerned, the magnitude of which depends on the location of the electron. The sum of all these charges is the charge induced by the space charge.

The combined result depends on how the density of the space charge is distributed. Generally the density is not constant. Clearly it decreases where the electron beam broadens, and vice versa. The velocity of the electrons is also important. If we imagine a slice cut from an electron beam of thickness x and area O, the charge it contains, for a charge density ϱ, is:

$$Q = \varrho O x \quad \ldots \ldots \ldots \ldots \ldots \quad \text{(II F 4)}$$

If the slice is moving with a velocity v, then v/x such slices will follow every second. The total charge passing per second is the current i and amounts therefore to:

$$i = \frac{v}{x} \varrho O x = v \varrho O \quad \ldots \ldots \ldots \ldots \quad \text{(II F 5)}$$

Conversely the charge density for a given current i is:

$$\varrho = \frac{1}{v} \frac{i}{O} \quad \ldots \ldots \ldots \ldots \ldots \quad \text{(II F 6)}$$

The charge density is thus inversely proportional not only to the section O but also to the velocity. The velocity, however, is not constant throughout the space, because potential differences between the various electrodes result in acceleration and deceleration. For example, in an octode the emitted electrons accelerate towards the third grid but after passing it lose speed owing to the negative potential on the fourth grid. The velocity of many of these electrons will fall to nil on reaching the zone in front of the fourth grid, where the potential is roughly zero in relation to the cathode. They then turn back and are trapped by the third grid. In this turn-round zone, therefore, the charge density is very great, as shown by equation (II F 6), and it may be said that it is the negative charge existing here which induces the positive charge on the fourth grid.

The magnitude of the induced charge thus depends on the location of the turn-round zone and on the current i_{g_3} which returns to the third grid. Now in the octode this current is controlled by the oscillator voltage v_h on the first grid. As a first approximation we can therefore write:

$$i_{g_3} = S_{g_1 g_3} v_h.$$

From this it follows that the charge induced on the third grid is proportional to the instantaneous value of the oscillator voltage on the first grid. Thus:

$$q_{g_4} = C_{ind} v_h \quad \ldots \ldots \ldots \ldots \quad \text{(II F 7)}$$

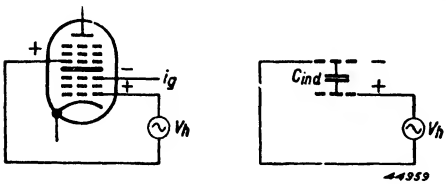

Fig. 164. *a*. The place of the space charge in an octode between the third and fourth grids. As a consequence a positive charge is induced at the fourth grid. *b*. The space charge between the first and fourth grids of the octode could be regarded as an apparent negative and onesided capacitance C_{ind}.

Fig. 164a illustrates how a positive increase of v_h raises the negative space charge, causing in turn an increased positive charge at the fourth grid. Such a variation of q_{g_4} must be accompanied by a transfer of charge over the external circuit between the fourth grid and the cathode. The current which then flows is:

$$i_{g_4} = \frac{d q_{g_4}}{dt} = C_{ind} \frac{d v_h}{dt} \quad \ldots\ldots\ldots\ldots \quad \text{(II F 8)}$$

The appearance of this current in the input circuit connected to the fourth grid is known as induction effect. A similar current would flow if between the first and fourth grids a capacitance of the magnitude of C_{ind} were present, but in that case the phase of the current would be the opposite of that given by equation (II F 8). A positive voltage at the first grid would then cause a negative charge on the fourth grid (fig. 164b). We may therefore regard this induction effect as being caused by an apparent negative, and one-sided, capacitance C_{ind} between the first and fourth grids; it is one-sided because a voltage at the fourth grid does not react on the first grid.

The total coupling between the oscillator and mixer sections is now given by:

$$C_k = C_{g_{1II} g_T} - C_{ind} + \frac{1}{t} C_{g_{1II} a_T} \quad \ldots\ldots \quad \text{(II F 9a)}$$

For the case of an octode this may be written in the following form:

$$C_k = C_{g_4 g_1} - C_{ind} + \frac{1}{t} C_{g_4 g_2}.$$

The space-charge capacitance thus operates to counteract the normal capacitance between the first and fourth grids. With the ordinary type of octode, such as the AK 2 and the EK 2, C_{ind} amounts to about 2 pF and has a much greater influence than the capacitance $C_{g_4 g_1}$. It is for this reason that in the EK 3 the inter-electrode capacitance $C_{g_4 g_1}$ has been purposely increased, in order to minimise C_k. The compensation, however, is correct for only one set of operating conditions, because C_{ind} is dependent on the screen-grid voltage V_{g_3} and the slope $S_{g_1 g_3}$. That C_{ind} varies with

$S_{g_1g_3}$ is at once evident from the derivation of equation (II F 7). The screen-grid voltage affects the location of the centre of gravity of the space charge. As V_{g_3} is raised the turn-round zone is moved nearer to the fourth grid and the induction effect therefore becomes stronger.

$S_{g_1g_3}$ and V_{g_3} are, moreover, both dependent on the grid bias (control voltage) and on the heterodyne voltage V_h. In the EK 3 $C_{g_4g_1}$ is so increased that with normal oscillator voltages and minimum bias full compensation is obtained. If greater bias is applied to the valve the coupling is no longer quite compensated, and C_k then becomes negative; this is not serious, because the voltage induced in the input circuit at high bias is less disturbing than when the bias is low.

In mixing-hexodes and mixing-heptodes the situation differs somewhat from that in an octode. The first grid is here the input grid and the second the screen, while the heterodyne voltage is applied to the third grid. A dense space charge is found on both sides of the screen grid, because some electrons stop in front of the screen, while others pass through its meshes before turning back (fig. 165). The space charge now increases when the instantaneous value of v_h becomes negative, whereas in octodes the reverse is the case. Thus more electrons are turned back by the third grid and the apparent capacitance C_{ind} is accordingly positive. The total coupling capacitance between the triode and heptode sections now becomes:

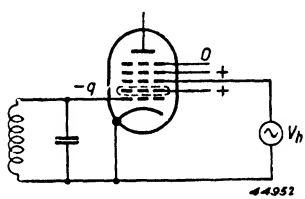

Fig. 165. Place of the space charge (on both sides of the screen grid) in a mixing hexode or heptode.

$$C_k = C_{g_1 IIg_3 + T} + C_{ind} + \frac{1}{t} C_{g_1 IIaT} \quad . \quad . \quad . \quad . \quad . \quad \text{(II F 9b)}$$

In this case, therefore, compensation is possible only if $C_{g_1\,IIaT}$ is increased (t being always negative) until $C_k = 0$. With hexodes and heptodes the capacitance C_{ind} is much smaller than with octodes, being of the order of 0.3 pF.

C_{ind} has been referred to as a "one-sided" capacitance, because the interaction between oscillator and input circuits is not mutual. The space charge, which is modulated by the heterodyne voltage, can admittedly also be affected by the input-grid voltage, but it has no influence on the oscillator grid because the screen grid acts as a shield. Furthermore, the oscillator voltage induced at the input grid modulates the space charge on the cathode side of the screen grid. This heterodyne voltage is indeed smaller than in the case of the octode mentioned above, but on the other hand a much

greater current, namely the total cathode current, is controlled by it; often, therefore, the effect is too large to neglect. A second one-sided capacitance thus exists between the input and oscillator grids, its value generally being different from that of C_{ind} already mentioned.

§ 4. Measuring the oscillator voltage at the signal grid

As is evident from the foregoing, this induced voltage depends on rather uncertain factors, and usually direct measurement is necessary. There are several ways of measuring it. If no R.F. voltage is present, a valve-voltmeter may be connected to indicate the induced oscillator voltage directly.

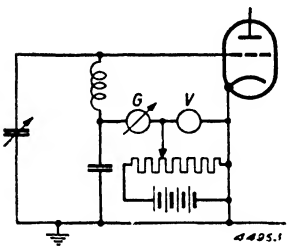

Fig. 166. Circuit for measuring the induced voltage in the case where there is no R.F. input voltage.

The input grid may also itself be employed as a diode voltmeter, as shown in fig. 166. A controllable and accurately known steady voltage is applied to the grid via a microammeter. This bias is adjusted so that grid current just ceases when the input circuit is shorted. On the short circuit being removed the induced voltage causes grid current to flow. The negative bias is then increased until grid current again ceases, and the amount of the increase is then equal to the peak value of the induced voltage. If, however, an R.F. voltage is also present it is simpler to couple the input circuit loosely to a separate receiver, which, when tuned to the oscillator frequency, will pick up only the oscillator voltage. The apparatus is first calibrated with known voltages and the induced oscillator voltage may then be determined by interpolation.

G. Some results of electron transit time

§ 1. Introduction

The inertia of electrons becomes noticeable when the transit time between the various electrodes is comparable with a cycle of the applied voltage, i.e. at high frequencies, and with widely separated electrodes. In general, transit times are unimportant at wavelengths exceeding 10 m. Certain effects attributable to electron inertia are found in the frequency-changers, however, even around 15 metres, for in these valves, owing to the many grids, the transit times are longer than in amplifying valves. Although transit-time phenomena are not confined to mixers, they are considered in this chapter because, at the frequencies used for normal broadcasting, it is only such valves whose function is affected.

The inertia of electrons crossing the inter-electrode spaces is reflected in the behaviour of the currents in the external circuits. When discussing transit-time effects it is thus logical first to refer to the relation between the external currents and the movement of electrons in the valve. The current in such an external circuit may be regarded as comprising three components:

1. The current due to the cold capacitance between the electrodes. When two electrodes are connected to an external circuit in which an alternating voltage is present, a current flows across the inter-electrode capacitance even when the cathode is cold and there is no emission. Such a current also flows when the cathode is emitting, but then it is unaffected by transit times since no electrons traverse the space between the electrodes. There flows a so-called dielectric displacement current.
2. The current set up in the external circuit by space charge between the electrodes concerned. This space charge may, as already mentioned, vary in sympathy with an alternating voltage at a third electrode (the induction effect).

   As variations of the space charge are the direct result of the electron movements, transit-time phenomena will play a part.

   If the space charge is varied by an alternating voltage applied between the two electrodes in question, an additional capacitive current will flow and the hot capacitance will therefore be different from the cold one. This additional capacitive current will also be influenced by transit times (§ 3).

3. The current carried over by the electrons reaching the positive electrodes. This represents the continuation in the external circuit of the so-called convection current in the valve. Considering one simple electron of this convection current, we know (F § 3) that during its transit in the external circuit it gives rise to a current which increases as the electron approaches the positive electrode with growing velocity. At the moment of impact the electron is neutralised by the charge which has meanwhile accumulated, the current dropping suddenly to zero. The passage of each electron is thus attended by a pulse of current, which reaches its maximum value when the electron has almost completed its traject.

If we imagine a sudden increase in the control-grid voltage, resulting in more electrons passing to the anode than before, the rise in the external current does not become noticeable until the electrons have almost completed their flight. Thus between the change of control grid voltage and the consequent anode current variation there is a delay, dependent on the transit time of the electrons.

Moreover there is a delay in the growth of the convection current itself, which further retards the current in the external circuit. It is well known * that the current, being limited by the space charge, is determined by the number of electrons possessing sufficient velocity to pass the so-called Epstein potential minimum. For any given grid voltage there is a corresponding distribution of the space charge round the cathode and consequently also a certain potential minimum which holds back some of the electrons. At another grid voltage the equilibrium changes, and both the space charge and the current are modified. Since, however, the electrons have to move a certain distance before the space charge is redistributed, the new equilibrium is not attained instantaneously. For these reasons too, there is thus a delay between signal voltage changes and the corresponding changing of current.

Of the three current components, the purely capacitive, the current due to space charges and the convection current, only the last two are affected by the transit time of the electrons; the several effects are described in the following paragraphs.

§ 2. The results of transit time on the control grid

When an alternating voltage is applied between the cathode and the negative-biased control grid there flows in the grid circuit an alternating current containing only the first two components mentioned above; no

* See also "Fundamentals of Radio Valve Technique" by J. Deketh, Section IV § 4.

convection current can flow to a negative grid. Apart from the current across the cold cathode/grid capacitance the varying space charge in front of the grid gives rise to a current, in phase with the purely capacitive current, which may be ascribed to an apparent increase of the cold capacitance. At low frequencies, at which transit times are of no consequence, the apparent increase is one-third of this cold capacitance.

The purely capacitive current is also encountered at higher frequencies; the current due to the varying space charge is then no longer in phase but lags behind it. The imaginary extra capacitance is thus not purely reactive, and grid damping results. At 10 metres this may amount to about 0.2 MΩ, which is negligible at such wavelengths.

As the frequency rises still higher the current due to the varying space charge lags more and more until it again becomes in phase with the grid voltage. The valve then has a normal input capacitance once more. With a still greater phase difference the cathode/grid capacitance becomes partly annulled, and finally there is a possibility of the grid presenting a negative resistance. But these cases need not to be considered here.

§ 3. Transit time and induction effect

When the electron stream is modulated by the heterodyne voltage, at the higher frequencies the space-charge variations in front of the control grid lag noticeably behind the oscillator voltage; accordingly the current induced in the input circuit lags behind the current expressed by equation (II F 8). This latter current, which, as already indicated, must in the case of an octode be regarded as a negative capacitive current, is represented by I_1 in the vector diagram of fig. 167. If the angle of lag due to the transit-time effect amounts to φ, then the actual induced current is represented by the vector I_2, which can be compensated by a current I_k; thus the compensating current must lead by less than 90° and should therefore be passed through a capacitor in series or in parallel with a resistor; these components may be included in the chassis wiring or can be mounted inside the valve, as in the case of the EK 3 octode. Clearly the resistance value can be correct only at one frequency, but as the induction effect is marked only at the bottom of the short waveband any deviation at longer wavelengths is of no great consequence.

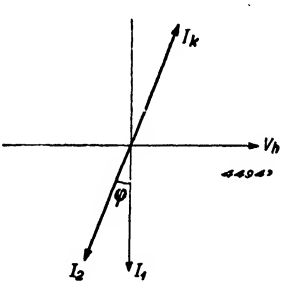

Fig. 167. Vector diagram of the various current components in the input circuit of an octode mixing valve.
I_1 = the current induced in the input circuit without taking into consideration the transit time.
I_2 = the actual induced current in the input circuit the angle of lag due to the transit time amounting to φ.
I_k = the compensating current.

§ 4. Transit time and slope

Only at low frequencies does the electron stream instantaneously adjust itself to the value corresponding to the control-grid voltage v_g. At higher frequencies the space-charge equilibrium needs time to adjust itself after every change of grid voltage, and the anode alternating current thus lags behind the grid voltage. We can also say that the slope becomes complex and takes on an inductive character. The effect is particularly marked at the lower end of the short waveband. At still higher frequencies the absolute value of the slope remains fairly constant but, expressed as an angular displacement, the lag increases, and at very much higher frequencies the slope may even become negative.

The phase angle of the slope is important in the oscillator section of a mixing stage, because in the condition for oscillation it affects the frequency and the back-coupling required. If at a low frequency the effective slope is S_{eff}, we can write for higher frequencies at which a lag of φ occurs:

$$S_{eff}\,(\cos\varphi - j\sin\varphi).$$

The general condition for oscillation then becomes:

$$tZ\,S_{eff}\,(\cos\varphi - j\sin\varphi) = -1. \quad \text{(II G 1)}$$

This equation can be satisfied only if t or Z is complex. As t is practically fixed for the whole of each waveband and is usually real, Z becomes complex; that is to say, the oscillator oscillates off the resonant frequency of the tuned circuit. The impedance of the tuned circuit is then, from equation (I A 9):

$$Z = \frac{Z_o}{1 + j\beta Q}$$

and equation (II G 1) now becomes:

$$\frac{t\,S_{eff}\,Z_o \cos\varphi\,(1 - j\tan\varphi)}{1 + j\beta Q} = -1 \quad \text{(II G 2)}$$

This equation can be satisfied only if:

$$-\beta Q = \tan\varphi \quad \text{(II G 3)}$$

thus if, for given values of φ and Q, a specific degree of detuning occurs. Equation (II G 2) now becomes:

$$-t\,S_{eff}\,Z_o = \frac{+1}{\cos\varphi} \quad \text{(II G 4)}$$

Instead of $+1$ a larger number now appears, for $\cos\varphi$ is less than unity.

Evidently the absolute value of t or S_{eff} must be raised at higher frequencies, as otherwise the valve will oscillate the more weakly as the lag increases.

Especially in those valves in which the electron path is long, the valvue of φ will be great. This is true of the older octodes such as the AK 2 and the EK 2, in which , after passing the first grid, the electrons cannot reach the second grid directly because they are deflected by the support of the first grid. The electrons go first through the positive third grid (the screen grid), and some then turn round in the vicinity of the negative fourth grid, again pass the third grid and finally reach the positive second grid (the oscillator anode). The time needed to cover this distance depends on the velocity of the electrons; in the main their speed is determined by the voltage on the third grid, viz. roughly proportional to the square root of the voltage.

The transit time and, accordingly, the lag φ are thus about inversely proportional to the root of the screen-grid voltage. Fig. 168 shows the relation between the phase angle and the screen-grid voltage at a wavelength of 9 metres, measured with the EK 2. The length of the electron path depends on the voltages at the third and fourth grids. If the fourth grid is considerably negative the electrons will be more inclined to turn round in the neighbourhood of the third grid than if the fourth grid is less negative; the electron path is shortened as the negative bias on the fourth grid i, increased. Measurements confirm, as indicated by the following tables that the phase angle does indeed decrease with increasing negative bias on the fourth grid.

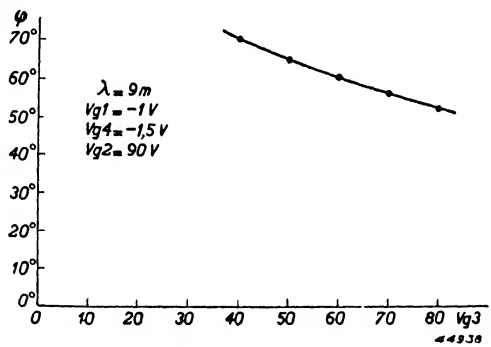

Fig. 168. The phase angle φ due to the transit time at $\lambda = 9$ m as a function of the screen-grid voltage of the octode EK 2.

$\lambda = 9$ m, $V_{g_1} = -1$ V, $V_{g_2} = 90$ V, $V_{(g_3 + g_5)} = 70$ V						
Vg_4	0	—2	—5	—10	—20	V
φ	60.1	59.7	47.5	45.5	42.5	degrees

These results demonstrate that with the EK 2 octode the oscillator voltage increases at very short wavelengths if higher negative bias is applied to the fourth grid.

With the newer octodes special measures are taken to avoid this effect. In the EK 3, for example, the electrons are beamed straight onto the second grid, and as a result the phase angle becomes very small.

H. Frequency drift

§ 1. Introduction

By frequency drift we mean an unwanted change of oscillator frequency while the receiver is working. Here we shall consider only those variations which are caused by the mixing valve, and not those resulting from temperature changes in capacitors, coils and resistors or from mechanical defects.

Oscillator frequency is affected by the mixer mainly in two ways:

1. By changing supply voltages due to mains-voltage fluctuations.
2. By the variation of control-grid bias as a result of A.V.C. Moreover these grid-voltage changes give rise to variations in anode and screen grid current, so that the supply voltages fluctuate even though the mains voltage is constant, While the mains fluctuations are determined by the properties of the particular power circuit, the grid bias varies in sympathy with the strength of the incoming signal. In nearly all modern receivers fading is compensated by automatic control of the amplification (see chapter X). If regulating the mixing valve leads to appreciable drift of frequency, the output voltage will be kept constant by the A.V.C. but the drift will be recognisable by the accompanying detuning. In such a case, therefore, the control voltage should be applied only to the IF stage and to any R.F. amplifier, in which the frequency-changer is not regulated.

It will be evident, then, how important it is that the mixer should be insensitive to changes of mains voltage or grid bias. If such changes occur frequency drift will follow by reason of:

1. Variation of inter-electrode capacitances in parallel with the oscillator tuned circuit.
2. Variation of the phase-angle of the slope of the oscillator valve.
3. Variation of the coupling between the input and oscillator circuits.

In the following pages these effects will be considered in turn, and it will be observed that the various voltage variations often bring about the same result.

§ 2. Variations of inter-electrode capacitances

In parallel with the tuned oscillator-circuit several inter-electrode capaci-

tances are connected directly or indirectly, such as the grid/cathode and anode/cathode capacitances of the oscillator valve and the capacitance of the modulator grid to the surrounding electrodes. All these capacitances consist of two parts: the "cold capacitance", which is constant and may be calculated from the dimensions of the electrodes and their separation; and an additional capacitance due to the presence of space charges between the various electrodes (II G § 2). This extra capacitance is not constant but is affected by the magnitude and distribution of the space charge.

The supply voltages determine electron-velocity and thus also the density of the space charges [equation (II F 6)]. Further, the region of minimum velocity and maximum density is fixed by these voltages. Variations of the supply voltages will therefore influence the "hot" inter-electrode capacitances. The application of a control voltage also affects the intensity of the stream of electrons, and thus the space charge density as well. At high frequencies the transit time of the electrons affects the additional capacitive currents and, since the transit time depends on the voltages, fluctuation of the latter leads to frequency drift.

Seeing that the space charge capacitances are larger or smaller according to whether the cold capacitances are large or small, it is clearly desirable in mixers and oscillator valves that the inter-electrode capacitances should be low; by this means the changes of capacitance are minimised.

From the resonance formula for the oscillator circuit:

$$\omega^2 LC = 1$$

we find by differentiating that for a small change of capacitance the detuning is:

$$d\omega = -\frac{\omega}{2C} dC \quad \ldots\ldots\ldots\ldots\ldots \quad \text{(II H 1)}$$

The frequency drift due to capacitance variations is thus greatest when the tuning capacitance is smallest and the frequency highest, i. e. on short waves. For any particular band we can write:

$$C = \frac{1}{\omega^2 L}$$

Substituting this in equation (II H 1) gives:

$$d\omega = -\frac{1}{2} \omega^3 L\, dC \quad \ldots\ldots\ldots\ldots \quad \text{(II H 2)}$$

In any waveband the drift is thus proportional to the third power of the frequency.

If after a superheterodyne is tuned to a signal the heterodyne alters by $\Delta\omega$, the intermediate frequency is changed by the same amount. The detuning of the signal from the resonant frequency of the I.F. band-pass filter results in reduced gain and in unequal amplification of the two sidebands, accompanied by distortion of the modulation (see section V, C § 2). With normal I.F. band-pass filters it is important that the frequency drift should not exceed 2—3 kc/s. At a wavelength of 15 metres (f_h = 20 Mc/s) and with a tuning capacitance of 30 pF we calculate from equation (II H 1) that the permissible variation of capacitance is:

$$\Delta C = -2C\frac{\Delta f}{f} = -2 \times 30 \times \frac{2}{20{,}000} = 0.006 \text{ pF}.$$

The change of grid/cathode capacitance due to voltage variations can easily be more than this. If, instead, the tuned circuit is connected to the anode, and the feedback coil to the grid, the grid capacitance behaves as a parallel capacitance t^2C_g, where t is the feedback ratio. It is thus an advantage if t is small at the lower end of the waveband (vide C § 4).
The anode/cathode capacitance shunts the tuned circuit directly. The space-charge capacitance of the anode, and certainly its variation, is considerably less than that of the grid, because the electron velocity between the grid and the anode is high, and each electron remains in the region for only a brief period. From the point of view of frequency drift the tuned-anode circuit therefore offers important advantages.

§ 3. The phase angle of the slope

The second effect which has a bearing on frequency drift is the variation of the phase angle of the slope, due to mains-voltage fluctuations. (The absolute value of the slope does not change.) This variation of phase angle is particularly felt on short waves; only there does the slope become complex, and variation of the phase angle become possible. The phenomenon is very disturbing in some octodes, for example the AK 2 and EK 2, if the conversion-conductance is controlled.
It has already been explained in G § 4 how the oscillator frequency is influenced by the phase angle of t and/or of S, and we derived:

$$-\beta Q = \tan\varphi \quad \text{(II G 3)}$$

Thus if there is a phase-angle φ the detuning of the oscillator frequency from the resonant frequency of the tuned circuit is given by β. As in this case the detuning is relatively small, we can write:

$$\beta = \frac{2\Delta\omega}{\omega} \quad \text{(I A 11)}$$

On short waves, where there is usually a lagging slope, a detuning $\Delta\omega$ in relation to $\omega^2 LC = 1$ must be regarded as normal. If now the phase angle φ alters, for instance due to a change in supply voltages, the detuning will be modified by an amount $d\,\Delta\,\omega$; this latter is the frequency drift.
The magnitude of $\Delta\,\omega$ is first calculated from equations (II G 3) and (1 A 11):

$$\left|\Delta\,\omega\right| = \frac{\beta\,\omega}{2} = \frac{1}{2}\,\frac{\omega \tan\varphi}{Q}$$

By differentiation we get:

$$\left|d\,\Delta\,\omega\right| = \frac{1}{2}\,\frac{\omega}{Q}\,\frac{1}{\cos^2\varphi}\,d\varphi \quad \ldots\ldots\ldots \quad \text{(II H 3)}$$

In this case also the frequency drift is greatest at the shortest wavelengths, not only because ω is then large but also because cos φ decreases with wavelength Drift can be limited, however, by keeping the quality factor of the tuned circuit high.
As is apparent from fig. 168, the slope of the EK 2 may be expected to lag by 60° at a wavelength of 9 metres; ω is then 2.10^8, and $Q = 100$. Frequency drift of about 10 kc/s per degree therefore occurs. [In equation (II H 3) φ is expressed in radians.]
If, at a wavelength of 9 metres, the bias on the fourth grid of the EK 2 is varied from —2 to —20 V, the phase angle φ changes from about 60° to 42° (section II G § 4) and the drift thus amounts to 200 kc/s. Obviously at these wavelengths it is out of the question to regulate the bias on the EK 2; the use of a separate triode to generate the heterodyne voltage is then preferable.

§ 4. Coupling between the oscillator and input circuits

A third source of frequency drift is the coupling between the mixer and oscillator sections of the valve, and the changes which occur therein when the conversion-conductance is regulated. Fig. 169 indicates the coupling in a triode-heptode. In the first place there is capacitive coupling between the mixer control grid and the triode, through the capacitances $C_{g_1 HaT}$ and $C_{g_1 HgT}$ (see F § 2).
These capacitances can be

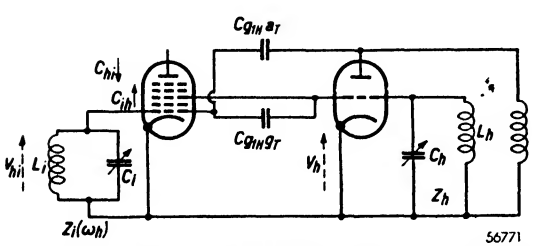

Fig. 169. Fundamental representation of the coupling between the oscillator and mixer sections of a triode heptode, which is one of the sources of frequency drift.

substituted by a single capacitance C_k between the mixer control grid and the oscillator grid:

$$C_k = C_{g_1 H g T} + \frac{C_{g_1 H a T}}{t} \quad \ldots\ldots\ldots \quad \text{(II F 1)}$$

Apart from this capacitive coupling there are two electronic couplings between the input grid and the modulator grid which is joined to the triode grid. Firstly, there is the electronic coupling between the modulator grid and the input grid, described in detail in II F § 3, which may be regarded approximately as an apparent one-side capacitance C_{hi} between these grids. In consequence an additional current $V_h\, j\omega_h\, C_{hi}$ flows through the R.F. circuit, and across it there is a voltage V_{hi} of oscillator frequency.

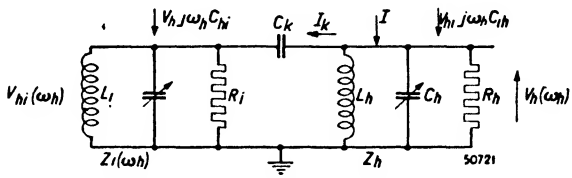

Fig. 170. Equivalent circuit of the arrangement of fig. 169.

Secondly, there is the effect on the modulator grid of the voltage V_{hi} in the R.F, input circuit. This may be regarded as an apparent one-sided capacitance C_{ih} between the input grid and the modulator grid, resulting in an additional current $V_{hi}\, j\omega_h\, C_{ih}$ in the oscillator circuit. This effect was referred to at the end of F § 4.

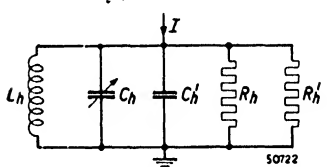

Fig. 171. Transformation of the equivalent circuit of fig. 170, containing an extra damping Rh' and an additional capacitance Ch' in parallel with the oscillator circuit. The coupling between the oscillator and mixer sections is represented by the current I.

Fig. 170 shows the equivalent circuit of the arrangement of fig. 169, which can evidently be transformed into a circuit containing an extra damping R_h' and an additional capacitance C_h' in parallel with the oscillator circuit (see fig. 171). The back-coupling is now expressed by the current I. The value of C_h' can be calculated with the aid of figs 169 and 170, and we get *

$$I = \frac{V_h}{Z_h} + I_k - V_{hi}\, j\omega_h\, C_{ih} = V_h \left(\frac{1}{Z_h} + \frac{1}{R_h'} + j\omega_h\, C_h' \right) \quad \ldots \quad \text{(II H 4)}$$

Dividing both sides of equation (II H 4) by $j\omega_h$, C_h' becomes equal to the real part.

* In equations (II H 4) and (II H 6) the capacitances C_{ih} and C_{hi} are included in Z_h and Z_i respectively.

Thus:

$$C_h' = \text{Real} \left\{ \frac{I_k}{V_h} \frac{V_{hi}}{V_h} j\omega_h C_{ih} \right\} \frac{1}{j\omega_h} = \text{Real} \left\{ \frac{I_k}{j\omega_h v_h} - \frac{V_{hi}}{V_h} C_{ih} \right\} \quad \text{(II H 5)}$$

Furthermore:

$$I_k + V_h j\omega_h C_{hi} = \frac{V_{hi}}{Z_{i(\omega h)}} \quad \text{(II H 6)}$$

in which $Z_i(\omega_h)$ denotes the impedance of the R.F. circuit to the oscillator frequency.

$$I_k = (V_h - V_{hi}) j\omega_h C_k \quad \text{(II H 7)}$$

From this it follows that:

$$V_h j\omega_h (C_k + C_{hi}) = V_{hi} \left\{ \frac{1}{Z_i(\omega_h)} + j\omega_h C_k \right\}$$

and

$$V_{hi} = V_h \frac{j\omega_h (C_k + C_{hi})}{j\omega_h C_k + \frac{1}{Z_i(\omega_h)}} \quad \text{(II H 8)}$$

or

$$V_{hi} = V_h \frac{j\omega_h (C_k + C_{hi})}{1 + j\beta Q_i} R_i \quad \text{(II H 9)}$$

because

$$\frac{1}{Z_{i(\omega h)}} + j\omega_h C_k = j\omega_h (C_k + C_i) + \frac{1}{j\omega_h L_i} + \frac{1}{R_i} =$$

$$= j\omega_h (C_k + C_i) \left\{ 1 - \frac{1}{\omega_h^2 L_i (C_k + C_i)} \right\} + \frac{1}{R_i} = \frac{1 + j\beta Q_i}{R_i} \quad \text{(II H 10)}$$

in which

$$\beta = \left(1 - \frac{\omega_i^2}{\omega_h^2} \right) \frac{\omega_h}{\omega_i}$$

and

$$Q_i = R_i \omega_i (C_k + C_i).$$

Substituting the values of V_{hi} and I_k from equations (II H 9) and (II H 7) respectively in equation (II H 5) we get:

$$C_h' = \text{real} \left(\frac{V_h - V_{hi}}{V_h} C_k - \frac{V_{hi}}{V_h} C_{ih} \right).$$

$$C_h' = \text{real} \left(C_k - \frac{V_{hi}}{V_h}(C_k + C_{ih}) \right) = \text{real} \left(C_k - \frac{j\omega_h (C_k + C_{hi})(C_k + C_{ih})}{1 + j\beta Q_i} R_i \right)$$

or:

$$C_h' = \text{real} \left(C_k - \frac{jQ_i (C_k + C_{ih})(C_k + C_{hi})}{(C_i + C_k)(1 + \beta^2 Q_i^2)} (1 - j\beta Qi) \right)$$

or:

$$C_h' = C_k - \frac{(C_k + C_{ih})(C_k + C_{hi})\, \beta Q_i^2}{(C_k + C_i)(1 + \beta^2 Q_i^2)} \quad \ldots \quad \text{(II H 11)}$$

The extra capacitance thus consists of a constant term C_k and a capacitance which varies with grid bias. This variable capacitance includes three quantities which change with control of the mixer slope, namely C_{ih}, C_{hi} and the tuning capacitance C_i of the input circuit. The last-named capacitance must be regarded as including the varying space-charge capacitance of the mixer section.

Further it is clear from equation (II H 11) that the capacitance variation is greatest when the tuning capacitance is small and the quality factor is high. The factor $\frac{\beta Q_i}{1 + \beta Q_i^2}$ has a maximum value of 0.5 when $\beta Q_i = 1$. If at a wavelength of 15 metres $Q_i = 100$ this maximum value is reached if $\beta = 2\,\Delta\omega/\omega = 0.01$. But $\Delta\omega$ is here equal to the difference of the oscillator and R.F. frequencies — hence the I.F. frequency.

Thus $\Delta\omega = \omega_h - \omega_i = 2\pi \times \frac{0.01 \times 2 \times 10^7}{2} = 2\pi \times 10^5$.

This means that a receiver using a low intermediate frequency, for instance 125 kc/s, suffers much greater frequency drift due to capacitance variations than one operating at a high intermediate frequency, say 475 kc/s.

Several phenomena can now be explained from the foregoing equation. The most important conclusions are:

1. The frequency drift with the input circuit short-circuited is usually much smaller than when the input circuit is not short-circuited.

2. For given operating conditions of the valve it should be possible to make the sum $(C_k + C_{ih})$ or $(C_k + C_{hi})$ in equation (II H 11) equal to nil by varying the capacitance C_k with a trimmer [for C_k see equation (II F 9)]. In the ECH 3, for example, C_{hi} amounts to about + 0.15 pF; if C_k be made equal to —0.15 pF the variable capacitance C_h' should then equal C_k.
   If the control bias becomes sufficiently negative to cut off the space current, the electron capacitances C_{ih} and C_{hi} disappear. With an intermediate frequency of 500 kc/s βQ_i is about 5 at a wavelength of 15 metres, so that with a tuning capacitance of 40 pF we find from equation (II H 11):

$$C_h' = \frac{0.15^2 \times 5}{0.01 \times 40 \times 26} = 0.011 \text{ pF}$$

   With a tuned-grid circuit such a capacitance change means a frequency drift of about 3 kc/s at 15 metres, and with a tuned-anode circuit a drift of about 1 kc/s.
   With the ECH 21 the situation is rather less favourable; the electron capacitance C_{hi} in this case is 0.3 — 0.4 pF, and the frequency drift when a control voltage is applied to the first grid is therefore twice as great.
3. When the bias on a mixing valve is varied the input capacitance also changes and detuning of the signal-frequency circuit results. This means that in equation (II H 11) β alters and the change can be considerable. Apart from possible changes of C_{ih} and C_{hi}, a capacitance variation therefore occurs in the oscillator circuit whenever a capacitance C_k is present.
   When increased bias is applied to the valve the input capacitance diminishes and the resonant frequency of the input circuit therefore increases. If ω_h is higher than ω_i, β decreases and the effect described in paragraph 2 above can therefore be more or less compensated.
   Generally speaking, however, the variation of the frequency is not easy to predict.
4. The most logical method of reducing frequency drift is to decouple the mixer and oscillator sections, by employing a tuned-anode oscillator circuit, and minimum back-coupling. To ensure adequate feedback at the low-frequency end of the band a special circuit may be used (C § 4).
5. Suitable design of the valve also helps to reduce drift. If in equation (II H 11) the factor $(C_k + C_{hi})$ always remains nil, no drift occurs. It is possible to reduce C_{hi} considerably if care is taken, by means of appro-

priate deflection, that no electrons from the modulator grid reach the neighbourhood of the input grid. It then remains to compensate the net stray capacitance C_k. As is apparent from equation (II F 9), the coupling between the input grid and the triode-anode and triode-grid respectively must be in exactly the right relation. The required values can be ascertained as described in F § 3.

§ 5. Frequency drift due to warming-up of the valve

On short waves drift due to the change of temperature in the oscillator valve becomes very important. The main cause is the gradual heating of the whole valve after switching on, and the consequent change in the di-electric constant of the glass. Some improvement can be obtained by using glass having a fairly stable di-electric constant.

Apart from capacitance variations in the valve, changes in capacitors, inductors and other components are to be expected as a result of temperature fluctuations. And the shorter the wavelength the greater the drift of frequency.

In modern receivers employing bandspread, drift is especially irritating, for it spoils the intended greater accuracy of the tuning scale. But by the use of capacitors having a di-electric constant with a negative temperature co-efficient over the range of temperature concerned, drift due to warming-up can be largely compensated.

SURVEY OF LITERATURE CHAPTER II

1. *Alway, E. J.*, An improved short-wave frequency-changer; Wireless World. March 1st, 1935, p. 213.
2. *Armstrong, E. H.* A new system of short-wave amplification, Proc. I.R.E., Febr. 1921, p. 3.
3. *Armstrong, E. H.* The superheterodyne, its origin, development and some recent improvements; Proc. I.R.E. Oct. 1924, p. 539.
4. *Bell, D. A.* The diode as rectifier and frequency-changer; Wireless Engineer, Oct. 1941, p. 395.
5. *Cocking, W. T.* Single-valve frequency-changers; Wireless World, July 29th (p. 74), Aug. 5th (p. 110) 1932.
6. *Cocking, W. T.* Short-wave oscillator problems; Wireless World, Febr. 9th, 1939, p. 127.
7. *Colebrook, F. M.* Valve oscillators of stable frequency; H. M. Stationery Office, Special Report No. 13, 1933.
8. *Corbeiller, P. le.* The non-linear theory of the maintenance of oscillations; Journal I.E.E., Sept. 1936, p. 361.
9. *Edgeworth, K. E.*, Frequency variations in thermionic generators; Journal I.E.E., Vol. 64, 1926, p. 349.
10. *Eller, K. B.*, On the variation of generated frequency of a triode oscillator; Proc. I.R.E., Dec. 1928. p. 1706.
11. *Haantjes, J. en Tellegen, B. D. H.*, De diode als mengbuis en als detector, Tijdschr. Ned. Radio Genootschap 10, 1943, p. 237. (The diode as frequency converter and detector.)

12. *Harris, W. A.* The application of superheterodyne frequency-conversion systems to multirange receivers; Proc. I.R.E. April 1935, p. 279.
13. *Herold, E. W., Harris, W. A., Henry T. J.*, A new converter tube for all-wave reception, R.C.A. Review, July 1938, pp. 67.
14. *Jonker, J. L. H. and Overbeek, A. J. W. M. van*, A new converter valve; Wireless Engineer, Aug. 1938. p. 423.
15. *Klipsch, P. W.*, Suppression of interlocking in first detector circuits; Proc. I.R.E., June 1934, p. 699.
16. *König, H.* Selbsterregung von Triodenschaltungen im Ultrakurzwellengebiet; Wiss. Veröff. Siemens-Werke, Vol. 20 (1941) pp. 10-27.
17. *Llewellyn, F. B.* Constant frequency oscillators; Proc. I.R.E. Dec. 1931, p. 2063.
18. *Pol, B. van der.* The non-linear theory of electric oscillations; Proc. I.R.E. Sept. 1934, p. 1051.
19. *Richter, H.* Elektrische Kippschwingungen; 154 p. Leipzig, Hirzel 1940.
20. *Schottky, W.* On the origin of the superheterodyne method; Proc. I.R.E., Oct. 1926, p. 265.
21. *Slooten, J. v.* The functioning of triode oscillators with grid condenser and grid resistance; Philips Techn. Review, Vol. 7 (1942) p. 40.
22. *Slooten, J. v.* Stability and instability in triode oscillators; Philips Techn. Review, Vol. 7 (1942) p. 171.
23. *Slooten, J. v.* The stability of a triode oscillator with grid-condenser and leak; Wireless Eng. Vol. 16 (1939) pp. 16-19.
24. *Stewart, J.* The operation of superheterodyne first detector valves; Journal I.E.E. Febr. 1935, p. 227.
25. *Strutt, M. J. O.* Moderne Mehrgitter-Elektronenröhren; Text-book, Springer, Berlin 1940.
26. *Strutt, M. J. O.* On conversion detectors; Proc. I.R.E. Aug. 1934, p. 981.
27. *Strutt, M. J. O.* Mixing valves; Wireless Eng. Febr. 1935, p. 59.
28. *Strutt, M. J. O.* Frequency changers in all-wave receivers; Wireless Eng., April 1937. p. 184.
29. *Strutt, M. J. O.* Electron transit-time effects in multigrid valves; Wireless Eng. June 1938, p. 315.
30. *Strutt, M. J. O.* On conversion detectors; Proc. I.R.E. Aug. 1934 p. 981.
31. *Strutt, M. J. O.* Diode frequency changers; Wireless Eng. Febr. 1936 p. 73.
32. *Strutt, M. J. O. and Ziel, A. van der*, The diode as a frequency-changing valve especially with decimetre waves; Philips Techn. Review, Vol. 6 (1941) p. 285.
33. *Strutt, M. J. O.* Moderne Kurzwellen-Empfangstechnik, 245 S., Springer, Berlin, 1939.
34. *Szabadi, J. A.* Why the triode-hexode? Wireless World. May 7th (p. 446) and May 14th (p. 472), 1937.
35. *Thomas, H. A.* Theory and design of valve oscillators; Messrs. Chapman and Hall. Text-book.
36. *Vilbig, F.* Untersuchung der Vorgänge beim Uberlagerungsempfang; Telegr. u. Fernspr. Techn. Vol. 19 (1930) pp. 109-120 and 140-145.
37. *Wheeler, H. A.* The hexode tube; Radio Engineering, March (p. 19) and April (p. 12) 1933.

III. DETERMINING THE TRACKING CURVE

A. Calculating the circuit constants

§ 1. Introduction

As already mentioned in the preceding chapter, the difference between the frequencies to which the oscillator circuit and the input circuit are tuned must be equal to the intermediate frequency. It is in principle immaterial whether the oscillator frequency is higher or lower than that of the received signal, but generally it is higher. If the signal frequency is lower than the intermediate frequency, as is the case when a long-wave station is received on a set employing a higher intermediate frequency, there is indeed no other possibility. But even when receiving signals of higher frequency than the intermediate frequency, the choice of a higher oscillator frequency is advantageous, for then the widest possible waveband can be covered.

The fact that, for convenience of manufacture, the same type of tuning capacitor is used in the R.F. and the oscillator circuits means that the same maximum ratio of highest frequency to lowest frequency is imposed on both circuits; if now the oscillator frequency is made lower than the signal frequency, it is evident that the range of frequency covered by the input circuit will be curtailed.

In the alternative case, where the oscillator frequency is the higher, the R.F. circuit determines the frequency band that can be covered. The frequency coverage of the oscillator circuit is then appropriately reduced, by means which will be discussed later.

When, as is the usual practice, the two tuning capacitors are ganged, the problem arises of tracking the circuits, that is to say of maintaining a constant frequency difference (the intermediate frequency) over the whole band. The problem can be solved by providing specially shaped plates in the oscillator tuning capacitor, so that the variation capacitances conform to requirements. Such a solution is satisfactory for a single wave band. It is evident, however, that for a second wave band the plate shape required would be different, and since nearly all receivers include more than one wave range this solution is usually impracticable.

The customary method then is to use identical tuning capacitors in the two circuits and to correct the variation of frequency of the oscillator circuit by means of fixed capacitors. However, this solution is not entirely satisfactory, and in the following pages we shall consider how the oscillator circuit should be designed in order to reach the best compromise.

When the oscillator frequency is higher than the signal frequency, the frequency range covered by the oscillator circuit is smaller than that of the input circuit; in consequence the ratio of the variable capacitance to the fixed capacitance (C_v/C_o) in the oscillator circuit must be reduced.

One method is to reduce the variable part C_v by inserting a fixed capacitor (called a padder) in series with the variable capacitor; another method is to increase C_o by connecting additional fixed capacitance across the tuned circuit; or both measures may be applied together. The best approach to the required tracking is attained with a certain combination of the two methods, that is to say for a given input circuit, with closely determined values of the padder C_p, the zero capacitance C_o and the inductance I.

As there is an infinite number of combinations of these three quantities, it is possible accurately to obtain the required oscillator frequency at any three points in the waveband. If these three points are chosen first, it is a fairly simple algebraic problem to calculate the values of C_p, C_o and L needed. Such a calculation is made in paragraph 4. Many variations on this theme are to be found in radio literature which, by introducing substitute quantities, simplify the numerical work to some degree. In general, however, the calculation is a rather laborious process; especially is this so when many cases have to be computed successively.

The tediousness of this calculating has given rise to a desire for a quicker method, even if it is of necessity somewhat less accurate. A solution by a graphical method is described in par. 5—11. The choice of method is ruled by the degree of accuracy required, and by personal taste. Before tackling the calculation it is necessary to settle at which point in the wave band a greater error can be conceded in favour of greater accuracy elsewhere; this is generaly decided by local conditions.

§ 2. Choice of the ganging points

For our considerations we shall begin with the basic circuit of fig. 172, which shows the most common type of oscillator circuit: C_v is the tuning capacitor, C_p the padder and C_o the stray capacitance of the tuned circuit. The padder will in practice often be joined in series with the coil instead of in series with the variable capacitor: we shall return to this matter in § 7.

The problem is thus as follows:

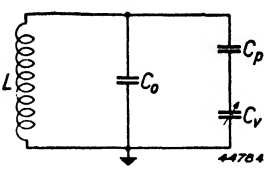

Fig. 172. Basic tuned circuit of an oscillator.

We are given the mixer valve input circuit, consisting of inductance, stray capacitance and a variable capacitance C_v. By means of a similar capacitance C_v, a circuit like fig. 172 must now be composed, whose natural frequency will, at any position of C_v, exceed that of the input circuit by the amount of the intermediate frequency. As this requirement cannot be met exactly, we must accept that solution with which the frequency difference always approaches the intermediate frequency as nearly as possible. The deviations which occur may be displayed as a function of the frequency of the input circuit, a so-called tracking curve being thereby obtained of the characteristic form seen in fig. 173. A positive value of Δf here means that the frequency difference between the input and the oscillator circuits exceeds the intermediate frequency. By correct choice of L, C_o and C_p, we endeavour, within the specific band delineated by f_a and f_b in fig. 173, to minimise the unavoidable deviation.

We are at once bound to ask ourselves what we regard as a sufficient limitation of Δf, and whether a certain value of Δf is equally important throughout the tuning range. We can, for example, try to make the area enclosed by the wave range or we can limit Δf over a given part of the wave range as small as possible at the cost of larger errors in less used parts of the band. Thus there are many possibilities, which could be endlessly argued. For the present general discussion, however, we shall assume that the deviation Δf is equally important over the whole frequency band and consequently we shall try to make the greatest error occurring anywhere as small as possible. In fig. 173 the largest deviations Δf arise at the limits of wave band f_A and f_B, and at the peaks lying in between.

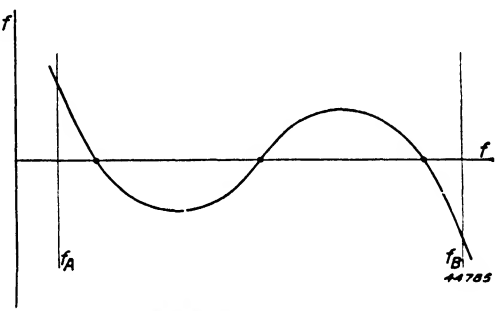

Fig. 173. Example of a tracking curve. Δf is the difference between the actual and the correct oscillator frequency within the range f_A to f_B.

The four maxima may be given any values by varying L, C_p and C_o. But a precise calculation is very hard to make. The curve in fig. 173, however, much resembles a third power the equation of which is:

$$y = x^3 + ax^2 + bx + c \quad \ldots\ldots\ldots\ldots \quad \text{(III A 1)}$$

Tchebycheff has deduced that with such a curve, if the postulated requirement of minimum deviations is achieved by suitable choice of a, b and c, the four maxima are equal. When by correct choice of L, C_p and C_o, a tracking curve is obtained in which the four largest deviations Δf from the nominal intermediate frequency are equal, we may possibly reduce one of the maxima by small changes of L, C_p or C_o. But the result must be an increase of one of the two of the other maxima. This phenomenon is well known in practice and we may conclude that adjustment with which the four greatest divergences are equal is in general to be preferred to any other.

The problem may now be defined in another way: the aim is no longer to find the smallest maxima, but to achieve the tracking curve in which the greatest deviations from the nominal frequency are all equal. This condition may be expressed directly in simple equations. We shall for the moment take L, C_p and C_o as the unknowns and express the largest deviations Δf_1, Δf_2, Δf_3, and Δf_4 in terms of these quantities. The requirement postulated becomes:

$$\left.\begin{aligned} \Delta f_1 &= \Delta f_2 \\ \Delta f_1 &= \Delta f_3 \\ \Delta f_1 &= \Delta f_4 \end{aligned}\right\} \quad \text{(Equations with } L, C_p \text{ and } C_o\text{)}$$

Three equations are thus obtained, with L, C_p and C_o as the unknown quantities; it should be possible, though it will be very difficult, to solve the unknowns from the equations. In order to simplify the calculation we shall assume that the tracking curve can be approximated by equation (III A 1). Starting from that and considering only the region limited by $x = +1$ and $x = -1$ * we can then calculate that

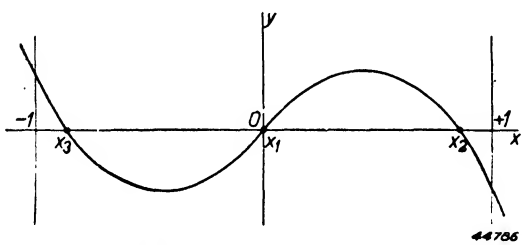

Fig. 174. Third-power curve in which the four greatest deviations are equal.

we get four equal extreme values of y if:

$$a = 0, b = -3/4 \text{ and } c = 0 \quad \text{(III A 2)}$$

(see fig. 174)

As the computation with this third power curve evidently leads to simple

* The choice of the region lying between +1 and —1 does not limit the general application of the argument: it is merely a question of the scale of the X-axis.

results we shall go a step further and calculate where the intersections with the horizontal axis lie. In radio technique these are the so-called ganging points at which the tuning of the input circuit and the oscillator circuit differ by precisely the intermediate frequency. Substituting from equation (III A 2) in (III A 1) we get:

$$y = x^3 - {}^3/_4\, x \quad \text{(III A 3)}$$

For $y = 0$ it therefore follows that

$$x_1 = 0;\ x_2 = +\,{}^1/_2\sqrt{3} \text{ and } x_3 = -{}^1/_2\sqrt{3} \quad \text{(III A 4)}$$

From this we can draw the following conclusion:

If a tracking curve corresponds to a third-power curve, which in fact is roughly the case, the adjustment points are best fixed in the frequency range so that x_1, x_2 and x_3 fall between $+1$ and -1. Consequently one adjustment point lies midway between f_A and f_B and the other two symmetrically about the first, at a distance therefrom of $\frac{f_B - f_A}{4}\sqrt{3}$.

§ 3. Practical effect of the chosen adjustment points

In order to provide an insight into the practical effect of this conclusion, a curve A following equation (III A 3) is given in fig. 175, the input frequency being measured along the X-axis. The frequency range under consideration runs from 536 to 1500 kc/s. Curve B is the actual tracking curve calculated for a circuit like fig. 172 if L, C_p and C_o are so chosen that the adjustment points obtained are the same as those on curve A. It will be seen that there is some difference between the two curves, though it is very slight. Furthermore it is clear that when the adjustment points are ascertained by Tchebycheff's approximate method

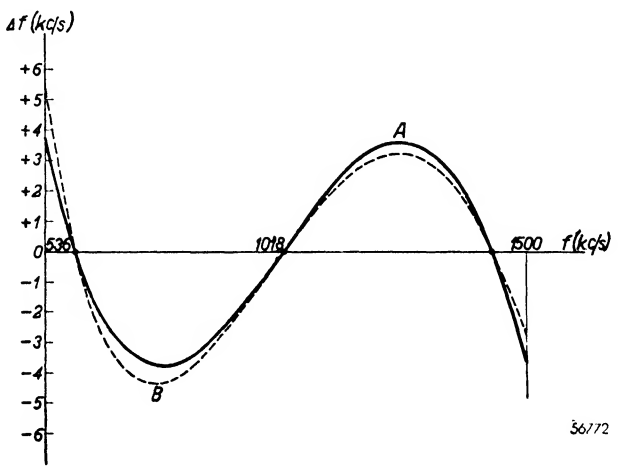

Fig. 175. Two tracking curves for the band from 536 to 1500 kc/s. A is a third-power curve given by the equation $y = x^3 - 3/4\ x$. B is an actual tracking curve for which L, C_p and C_o (see fig. 172) were so chosen that the same adjustment points were obtained as in curve A

the error at the high frequency end (1500 kc/s) is smaller than at the low frequency end (536 kc/s).

The goal of equal deviations is not quite reached. The question now is whether the result is better or worse. We must grant that, looked at as a whole, it is worse, for usually the selectivity of the pre-selector circuit is rather poorer at high frequencies than at low, and therefore it is at the high-frequency end, where the input tuned circuit has a flatter resonance curve, that a greater deviation could be allowed.

For this reason, then, these symmetrically placed adjustment points will be regarded only as landmarks from which a more favourable result may be found experimentally. If, for example, only a small error is acceptable at the low-frequency end of the band, a better performance can be expected if the first two adjustment points, to the left of fig. 175, are put a little lower than was originally calculated. If, however, special importance is attached to the reception of particular stations elsewhere in the band the adjustment points must be shifted accordingly.

§ 4. Calculating L, Cp and Co

Using equation (III A 1) as a basis, we must try to find a third-power curve approximating to Δf. Instead of the co-efficients a, b and c in equation (III A 1), we require formulae containing L, C_p and C_o, and to these equation (III A 2) could be applied. This leads again, however, to difficult and tedious calculation, and it is much simpler to start from the known adjustment points. The frequencies corresponding to these points are known, and therefore also the respective values of C_v in the input circuit; moreover we know the oscillator frequency at these points, since the error is nil. Thus we know the resonant frequency of the oscillator circuit at three positions of C_v (which are the same as those of C_v in the pre-selector circuit). Therefore we have three equations again containing L, C_p and C_o, which can be solved fairly easily *.

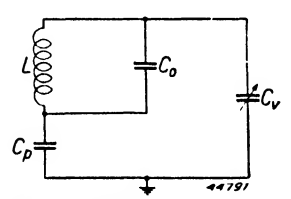

Fig. 176. Oscillator tuned circuit with the padder in series and the trimmer in parallel with the coil.

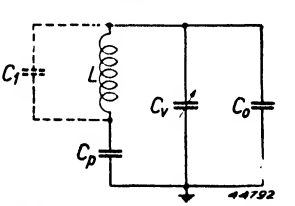

Fig. 177. Oscillator tuned circuit with the padder in series with the coil and the trimmer parallel to the tuning capacitor.

The basic oscillator tuned circuit was given in fig. 172. This arrangement is not often used: usually the padding capacitor C_p is joined in series with the oscillator coil. In such a case there are two

* See, for instance, Soweby, "Wireless Engineer", October 1932 — Landon and Sveen "Electronics", August 1932 — Couppez, "L'onde Electrique", Dec. 1936.

ways of connecting the parallel capacitance C_o: first, across the coil (fig. 176) and, secondly, in parallel with the variable capacitor (fig. 177). A drawback of the latter method of connection is that the self-capacitance C_1 of the coil must be considered separately, whereas in the circuit of fig. 176 it is reckoned with the capacitance C_o.

The resonance formula for the circuit of fig. 172 and fig. 176 is:

$$\omega^2 L \left(C_o + \frac{C_v C_p}{C_p + C_v}\right) = 1 \quad \text{(III A 5a)}$$

The resonance formula for the circuit of fig. 177 is:

$$\omega^2 L \frac{C_p (C_v + C_o)}{C_p + C_v + C_o} = 1 \quad \text{(III A 5b)}$$

The respective values of the tuning capacitor at the adjustment points we shall call C_I, C_{II} and C_{III} and the corresponding oscillator frequencies ω_1, ω_2 and ω_3. If we further define $\delta = 1/\omega_1^2$, $\varepsilon = 1/\omega_2^2$, $\eta = 1/\omega_3^2$, we then find the following quantities in the oscillator circuit to which equation (III A 5a) refers:

$$C_p = \frac{(\varepsilon-\eta)\, C_{II}\, C_{III} + (\eta-\delta)\, C_I\, C_{III} + (\delta-\varepsilon)\, C_I\, C_{II}}{(\varepsilon-\eta)\, C_I + (\eta-\delta)\, C_{II} + (\delta-\varepsilon)\, C_{III}} \quad \text{(III A 6a)}$$

$$C_o = \frac{\{(\varepsilon-\eta)\, C_{II}\, C_{III} + (\eta-\delta)\, C_I\, C_{III} + (\delta-\varepsilon)\, C_I\, C_{II}\}}{(\delta-\varepsilon)\,(\varepsilon-\eta)\,(\eta-\delta)} \times$$

$$\times \frac{\{\delta(\varepsilon-\eta)\, C_{II}\, C_{III} + \varepsilon(\eta-\delta)\, C_I\, C_{III} + \eta(\delta-\varepsilon)\, C_I\, C_{II}\}}{(C_I-C_{II})\,(C_{II}-C_{III})\,(C_{III}-C_I)} \quad \text{(III A 7a)}$$

$$L = \frac{(\delta-\varepsilon)\,(\varepsilon-\eta)\,(\eta-\delta)\,(C_I-C_{II})\,(C_{II}-C_{III})\,(C_{III}-C_I)}{\{(\varepsilon-\eta)\, C_{II}\, C_{III} + (\eta-\delta)\, C_I\, C_{III} + (\delta-\varepsilon)\, C_I\, C_{II}\}^2} \quad \text{(III A 8a)}$$

For the circuit of fig. 177, to which equation (II A 5b) refers, we obtain:

$$C_p = \frac{(\delta-\varepsilon)\,(\varepsilon-\eta)\,(\eta-\delta)}{\{(\varepsilon-\eta)\, C_I + (\eta-\delta)\, C_{II} + (\delta-\varepsilon)\, C_{III}\}} \times$$

$$\times \frac{(C_I-C_{II})\,(C_{II}-C_{III})\,(C_{III}-C_I)}{\{\delta(\varepsilon-\eta)\, C_I + \varepsilon(\eta-\delta)\, C_{II} + \eta(\delta-\varepsilon)\, C_{III}\}} \quad \text{(III A 6b)}$$

$$Co = \frac{\delta(\varepsilon-\eta)\, C_{II}\, C_{III} + \varepsilon(\eta-\delta)\, C_I\, C_{III} + \eta(\delta-\varepsilon)\, C_I\, C_{II}}{\delta(\varepsilon-\eta)\, C_I + \varepsilon(\eta-\delta)\, C_{II} + \eta(\delta-\varepsilon)\, C_{III}} \quad \text{(III A 7b)}$$

$$L = \frac{\{\delta(\varepsilon-\eta)\, C_I + \varepsilon(\eta-\delta)\, C_{II} + \eta(\delta-\varepsilon)\, C_{III}\}^2}{(\delta-\varepsilon)\,(\varepsilon-\eta)\,(\eta-\delta)\,(C_I-C_{II})\,(C_{II}-C_{III})\,(C_{III}-C_I)} \quad \text{(III A 8b)}$$

In practice the calculation of the oscillator-circuit constants from these

formulae is often too cumbersome and the simpler, though less accurate, graphical method is then preferred.

§ 5. Graphic determination of L, Cp and Co

For the graphic determination of L, C_p and C_o we use as a basis a paper by McNamee in Electronics of May 1932. The method given therein we apply in a rather different way, however, and certain advantages accrue. In the article mentioned, instead of three previously fixed adjustment points, a larger number of arbitrary points are used with which approximately correct alignment of the circuits is obtained.

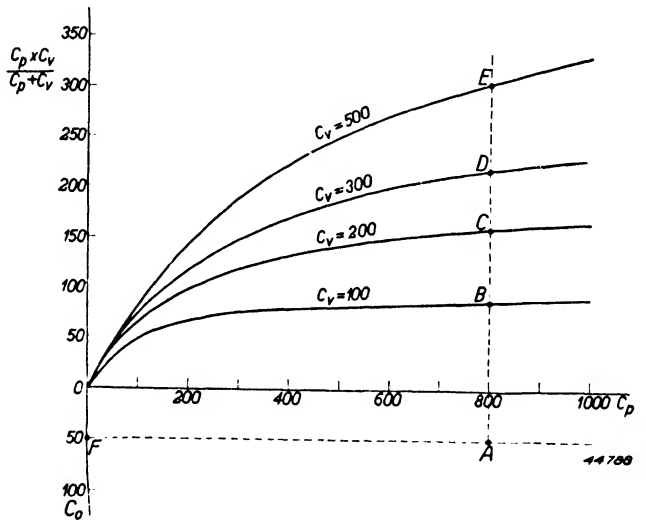

Fig. 178. Graphic method of determining the total capacitance in the oscillator circuit of fig. 172 for various values of C_v, C_p and C_o. The capacitance of C_v and C_p in series can be read off the vertical axis directly; and since C_o is measured along the same axis, below zero, the total capacitance follows from: $C_{tot} = \frac{C_p \times C_v}{C_p + C_v} + C_o$.

We shall first calculate, with an arbitrarily chosen value of C_v as parameter, the net capacitance of C_v and C_p in series for various values of C_p. The curves given in fig. 178 are thereby obtained. In this diagram the vertical axis is also scaled for the value of C_o. The following information may now be extracted from the curves:

Assuming $C_p = 800$ pF, the points B C, D and E indicate the capacitance of C_p and C_v in series when C_v has values of 100, 200, 300 and 500 pF respectively. And if we further assume that the zero capacitance C_o is 50 pF the distances AB, AC, AD and AE represent the total capacitance of the tuned circuit at the values of C_v mentioned. In this way we quickly and easily get an insight into all available possibilities. Now the oscillator frequencies required at these several positions of C_v are known, but L at the moment is not, and consequently the total capacitances are still unknown. However we know that they are inversely proportional to the squares of the required frequencies.

Thus:

$$AB : AC : AD : AE = \frac{1}{f_1^2} : \frac{1}{f_2^2} : \frac{1}{f_3^2} : \frac{1}{f_4^2}$$

It is already known that this requirement can be satisfied for no more than three positions of C_v. By shifting the lines AE and AF, however, we can make AB, AC, etc., agree more closely with the required ratios. A convenient method is to use a sheet of transparent paper ruled with a series of parallel lines spaced according to the desired ratios (any straight line drawn across a set of parallel lines is intersected in the same ratio). The ruled sheet

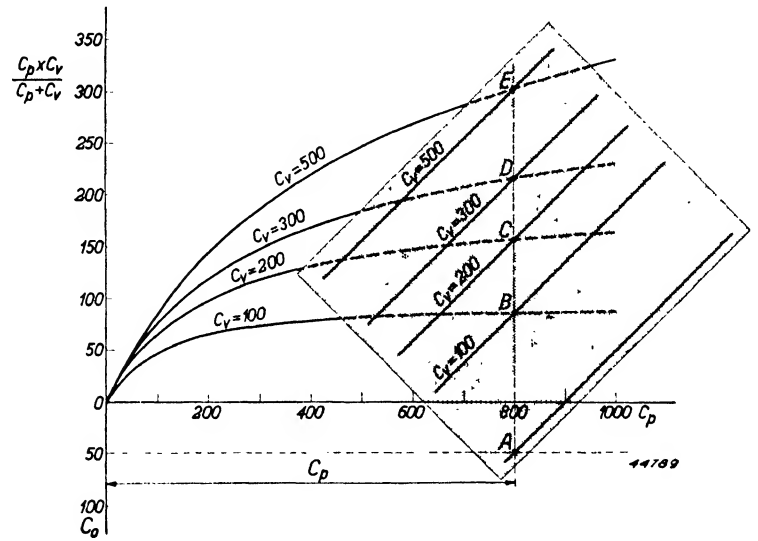

Fig. 179. For ascertaining the optimum values of C_p and C_o, a transparent sheet ruled with parallel lines may be used, the separation of the parallels being inversely proportional to the differences between the squares of the required frequencies. The sheet is placed on fig. 178 in such a way that a perpendicular (in this figure AE) is intersected as nearly as possible at the same point by the curves as by the parallels.

is now placed on fig. 178 and moved about until a vertical line is found (in our example AB) which is divided off by the curves as nearly as possible in correspondence with the intervals between the parallel lines (fig. 179). The needed values of C_p and C_o are then immediately ascertainable. By this method it is possible to work quite quickly once a diagram like fig. 178 has been drawn. But there are some disadvantages. Inevitably small errors occur in drawing the point-to-point curves of fig. 178 and since even small percentage frequency differences must be avoided the result is often unreliable.

Secondly, the intervals between the parallel lines must coincide as nearly

as possible with the intersections of the vertical line with the curves. Discrepancies are bound to exist, but how large these may be and where they are most important is not immediately apparent.

Following on the reasoning at the beginning of this chapter, the foregoing method will now be modified, fig. 178 being redrawn for the three values of C_v which correspond to the most desirable adjustment points mentioned in § 2. At the same time the oscillator frequencies appropriate thereto will be determined and a set of parallel lines drawn conforming to these frequencies, i.e. the intervals between the parallels will be inversely proportionate to the squares of the frequencies. It will now be possible to find a position for AE and AF at which the ratios $AB : AC : AD$ coincide with intervals between the parallel lines. The advantage of this method over the first one is that we do not have to choose from an infinite number of compromises, but have only to find the one correct and definite position. A practical drawback of the method is that a fresh set of curves must be drawn for every case, because with varying types of receiver different values of C_v are generally found at the most suitable adjustment points. What we need is a diagram in which not only C_p but also C_v is shown continuously variable. Such a diagram, reproduced in fig. 180, has two vertical scales for C_v and C_p respectively, separated by an arbitrary distance $a + b$. If now we choose any values C_{v1} and C_{p1} on the C_v- and C_p-axes and draw diagonals as in fig. 180 we derive the following for the perpendicular x:

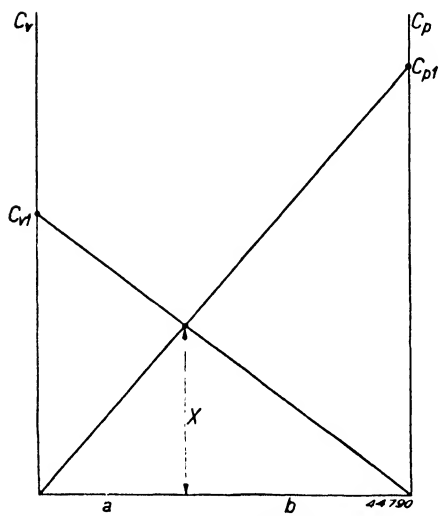

Fig. 180. Abac with two vertical axes C_v and C_p. The distance X of the intersection of the two diagonals from the horizontal is a measure of the capacitance of C_{v1} and C_{p1} in series.

$$\frac{b}{x} = \frac{a+b}{C_{v1}}$$

$$\frac{a}{x} = \frac{a+b}{C_{p1}}$$

$$\frac{a+b}{x} = (a+b)\left(\frac{1}{C_{v1}} + \frac{1}{C_{p1}}\right)$$

or:

$$\frac{1}{x} = \frac{1}{C_{v1}} + \frac{1}{C_{p1}} \quad \ldots\ldots\ldots\ldots\ldots \quad \text{(III A 9)}$$

It follows therefore that the length x indicates the capacitance of Cv_1 and C_{p1} in series. Using this principle it is very simple to draw a diagram from which the total circuit capacitance at various adjustment points may be read directly. The values of C_v at the chosen adjustment points are again calculated and the diagonals drawn (fig. 181). If now a specific value of C_p is taken and a diagonal drawn from the C_p axis, the perpendiculars X_1, X_2 and X_3 are obtained, which indicate the resultant capacitances of C_{p1} with C_{v1}, C_{v2} and C_{v3}. If we also show the stray capacitance C_o below the horizontal axis we can, for any given value of C_o, ascertain the total circuit capacitance immediately from A_1B, A_2C and A_3D. This diagram is thus entirely equivalent to fig. 178 but it consists only of straight lines, and it is a simple matter to introduce other values of C_v.

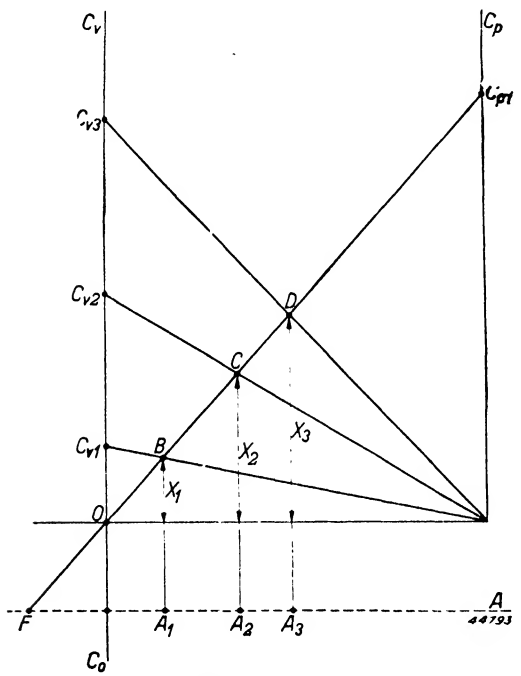

Fig. 181. The abac of fig. 180 modified by the addition to the C_v axis of C_o below the zero. The total capacitance is now always equal to the distance between the intersection of the diagonals and the new horizontal axis AF.

To determine the correct value of C_p and C_o, the oscillator frequencies f_1, f_2, f_3 corresponding to C_{v1}, C_{v2} and C_{v3} are again calculated and the lines AF and $C_{p1}F$ then shifted until the required relation is obtained, namely:

$$A_1B : A_2C : A_3D = \frac{1}{f_1^2} : \frac{1}{f_2^2} : \frac{1}{f_3^2}$$

This requirement can be satisfied exactly, but the task is made more difficult by the fact that the distances A_1B, A_2C and A_3D are not all measured along the same line. However, the distances FB, FC and FD are in

the same ratio and we can take advantage of this circumstance. In order to ascertain the ratios we now draw radii on transparent paper, as in fig. 182.

The quantities $\frac{1}{f_1^2}, \frac{1}{f_2^2}, \frac{1}{f_3^2}$ are measured out on some convenient scale along the vertical axis, and from any suitable point radiating lines are drawn. All the intersected vertical lines on the graph paper are now divided in like ratio. The sheet can now be placed on fig. 181 and moved about, always keeping the perpendicular ruling parallel to OC_{p1} until a position is found in which the three intersections on a vertical line coincide with points B, C and D. Point F, the remaining intersection of OC_{p1} with the base line, is thereby fixed. Failure with a given value of C_p to get the two sets of points to coincide means that that value is wrong. Further attempts with other values must then be made until coincidence is secured; the correct value of C_p may then be read directly from the diagram, while the position of F fixes the value of C_o. The value of A_3D, for example, may also be measured and, as the frequency f_3 relating to this circuit capacitance is known, the required value of L can be calculated. With this method the line OC_{p1} can best be represented by the base line of the transparent graph paper, which must pass through point O exactly.

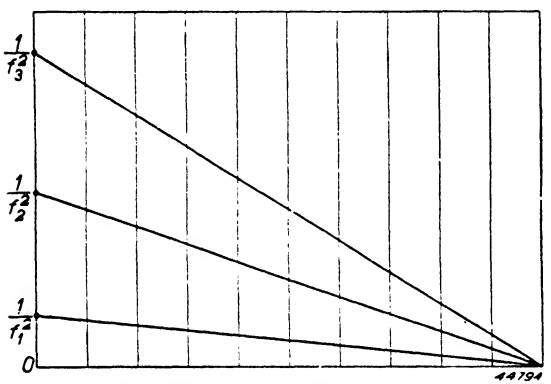

Fig. 182. Fanshaped raster for the determination of the values of C_p and C_o in the diagram of fig. 181. Distances indirectly porportional to the squares of the desired adjust frequencies are plotted on the ordinates; the lines are drawn from an arbitrary point from the fanshaped raster.

§ 6. Practical example

We shall now illustrate the foregoing with an example, and the receicer considered in § 3, which covered the band from 536 to 1500 kc/s, will serve our purpose. First the adjustment points are determined by Tchebycheff's approximate method. One point falls in the middle of the band, at 1018 kc/s. On each side lies a range of 482 kc/s. The two other points are therefore separated from the middle by:

$$1/2\ \sqrt{3} \times 482 = 417 \text{ kc/s}$$

and lie at 601 and 1435 kc/s respectively. By adding the intermediate frequency, 470 kc/s, to these three figures we arrive at the oscillator frequencies corresponding thereto, namely:

$$f_1 = 1905 \text{ kc/s}, f_2 = 1488 \text{ kc/s}, f_3 = 1071 \text{ k/cs}.$$

The capacitance of C_v at these points must now be calculated. We assume an R.F. tuned circuit with $L = 160$ μH, $C_o = 50$ pF and $C_v = 20$—500 pF. At the upper end of the wave band the circuit tunes to 536 kc/s with a total capacitance of 550 pF. At the first adjustment point the total capacitance is therefore:

$$C = 550 \left(\frac{536}{1435}\right)^2 = 77 \text{ pF}$$

Thus:

$$C_{v1} = 77 - 50 = 27 \text{ pF}.$$

Similarly for the other adjustment points we find:

$$C_{v2} = 102 \text{ pF and } C_{v3} = 388 \text{ pF}$$

The values of C_v are the same in the oscillator circuit.
The first three columns of the following table summarise the figures so far ascertained:

Signal frequency (kc/s)	C_v (pF)	Oscillator frequency (kc/s)	$\frac{10^6}{f_{osc}^2}$	Distance along axis (mm)
1500	20	—	—	—
1435	27	1905	0.276	82.8
1018	102	1488	0.452	135.6
601	388	1071	0.872	261.6
536	500	—	—	—

On not too small a scale a diagram similar to fig. 181 is now prepared, with diagonals drawn to points C_{v1}, C_{v2} and C_{v3}, situated respectively 27, 102 and 388 mm from the base line; for safety a space 100 mm deep is left under the latter for C_o.
A drawing on the lines of fig. 182 is next made on a sheet of transparent millimetre squared paper, distances proportional to $1/f_{osc}^2$ being measured out along one of the axes. The values are given in the fourth column of the

table above, and in the diagram they may be represented, for example, by distances of 82.8, 135.6 and 261.6 mm respectively. To the three points thus determined radiating lines are drawn from any suitable point. It is to be noted that the present construction embodying radiating lines is better than the set of parallel lines used in fig. 179, since it permits a very large

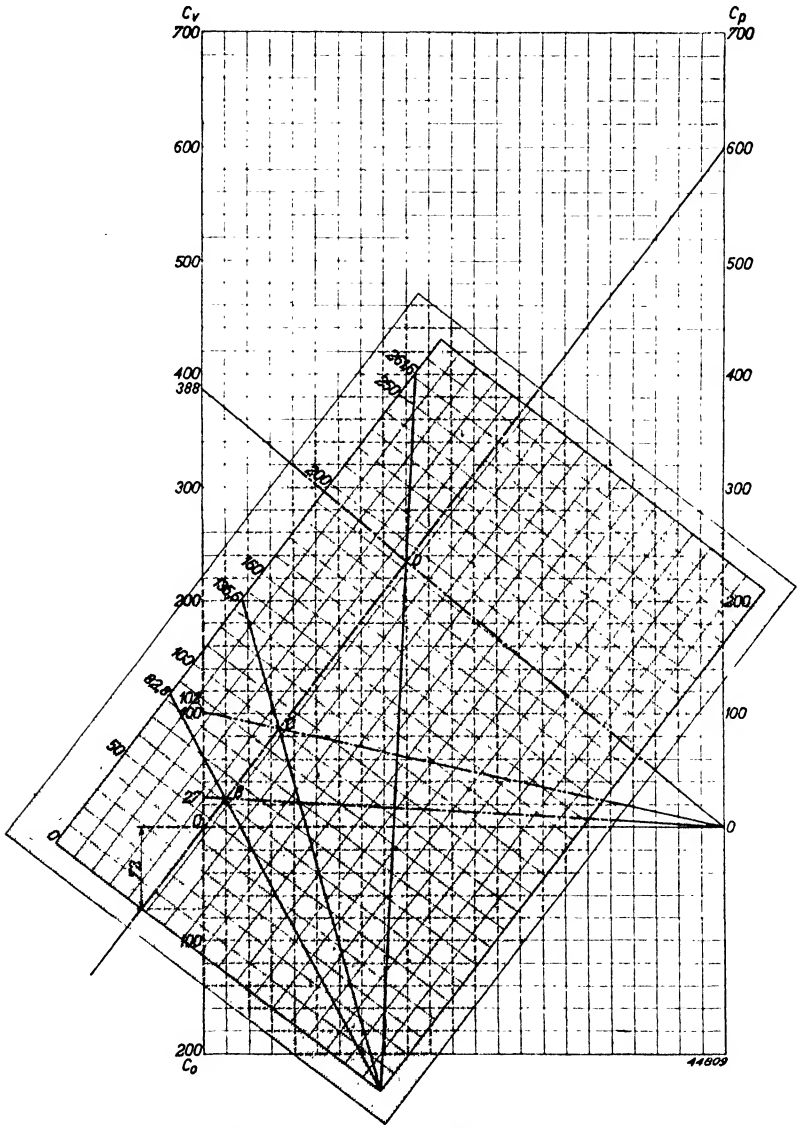

Fig. 183. Example of the graphic method of determining the constants of an oscillator circuit for the 536 — 1500 kc/s band.

scale (in this case the largest dimension is 261.6 mm) and therefore greater accuracy.

The parallel-line diagram, on the other hand, cannot be indefinitely enlarged, or it would fail to fit the intercepts of line OC_{p1}; thus the accuracy is limited. Fig. 183 shows the diagram drawn for the present example, with the transparent squared paper laid in the position found correct. It is evident that this position is reached with a padding capacitor of 600 pF. The location of point F indicates that C_o should be 72 pF.

The inductance of the oscillator tuned circuit has still to be determined. It follows from fig. 183 that when $C_v = 388$ pF the capacitance of C_v and C_p in series is 236 pF, and the total circuit capacitance is consequently $236 + 72 = 308$ pF. At this position of C_v the table shows that the oscillator frequency is 1071 kc/s. The inductance now follows from:

$$f = \frac{10^6}{2\pi\sqrt{LC}} = \frac{159155}{\sqrt{LC}}$$

where f is expressed in kc/s, L in μH and C in pF. Thus:

$$L = \frac{159155^2}{1071^2 \times 308} = 71.7 \ \mu H$$

§ 7. The possibilities of the graphic method

It is apparent from the foregoing that the determination of the constants of an oscillator circuit by graphic means can be a fairly simple task. The accuracy is naturally not so high as with calculation from the formulae, for which a calculating machine or logarithm tables may be employed. On the other hand the effect of possible errors in drawing may be easily examined, because in the diagram the frequencies arising if C_p is made a certain amount too high or too low can be measured. This possibility is especially valuable when, in designing a receiver, it is necessary to compare alternatives quickly.

The method just described may also be employed for an oscillator circuit in which the padding capacitor is connected in series with the coil L (fig. 184).

At first sight there is no striking difference between this circuit and that of fig. 172 but it will be realised that a capacitance is also present between the top of the coil and earth, i.e. parallel to C_v. To investigate its influence we shall rearrange this circuit of fig. 184a as far as possible on the lines of fig. 172; thus we obtain fig. 184b, in which the total zero capacitance is divided between C_1 and C_2. In precise calculations we may not, without

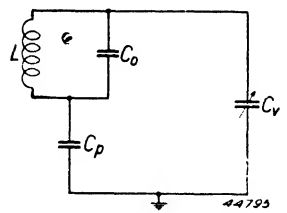

Fig. 184 a. Basic form of a commonly used oscillator circuit. The padder is in series and the trimmer in parallel with the coil L.

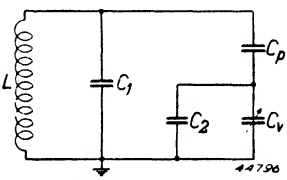

Fig. 184 b. The same circuit as fig. 184a, but with the stray capacitance divided between C_1 and C_2. C_1 is the trimmer, and C_2 a capacitance the value of which must be estimated in the light of experience.

question, regard C_1 and C_2 as being in parallel. However, the formulae do not become more complicated if for C_2 we substitute an amount estimated in the light of experience and then reckon how large C_1 must be. The constants of this circuit can now be determined graphically by modifying fig. 181 somewhat. The diagram must now be used to find the capacitance of C_p in series with $C_v + C_2$, and accordingly on the C_v scale a fixed amount, previously estimated, is added to C_v. By drawing diagonals to C_{v1}, C_{v2} and C_{v3} the additional C_2 could be taken into account directly. For another value of C_2 new diagonals would then, however, have to be drawn; to avoid this, the quantity C_2 is added under point O. If now we draw a new base line, as in fig. 185, and draw diagonals from the new vertices of the base line, the capacitance of the series circuit $C_p - (C_v + C_2)$ is indicated by X. To this the zero capacitance C_1 has still to be added. A convenient method is to draw a line parallel to the new base at a distance of C_1, the total capacitance being then measured from this new line, e.g. A_2B. The intersection of the C_{p1} diagonal with the base A is once more indicated by F, and the distances FB, FC, etc. are again proportional to the circuit capacitances A_2B, A_1C_1, etc. The graphic method described above may similarly be employed for determining C_1. Having found the correct position of the frame of lines on the C_p - diagonal, note that a line (FA) parallel to the new base line must be drawn through F in order to obtain the correct value for C_1.

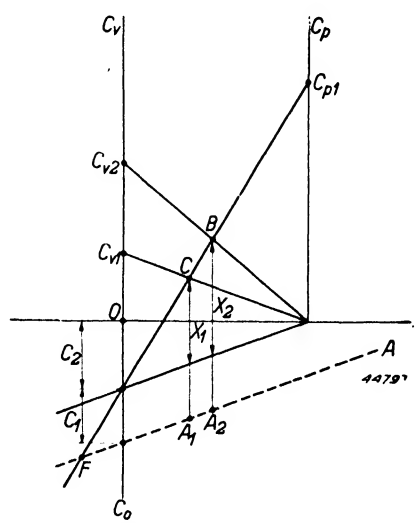

Fig. 185. Abac for determining C_p and C_1 in the circuit of fig. 184b. As C_2 is now set out below the zero on the C_p-axis, the base line is no longer horizontal.

§ 8. Accuracy of the graphic method

As already mentioned, calculation of the circuit constants from the appropriate formulae is undoubtedly more accurate than the graphic method described above. It will be observed that, when using the

graphic method over a small range of the C_p scale an equally good result is obtained anywhere. In theory there is of course only one correct value of C_p, but it seems that over this particular range a variation of C_p hardly affects the fitting of the ruled sheet to the diagram.

The inaccuracy of the graphic method however is no great drawback when the object is to find a starting point for the experimental determination of the circuit constants.

In order to investigate the order of magnitude of the errors which may occur with the graphic method, we shall assume that in fig. 183 the value taken for C_p is not correct. This means that the three radiating lines on the transparent sheet do not in fact pass through points B, C and D. Taking now the most unfavourable case (smallest distance and highest frequency), we assume that the line on the transparent sheet misses point B and passes half a millimetre wide (measured along FC_p). Such an error is just perceptible when good drawing materials are used.

In the original drawing, reproduced in fig. 183, FB is 60 mm long. An error of 0.5 mm thus represents 0.8%, and in the total circuit capacitance the error will amount to the same percentage. The frequency is inversely proportional to the square root of the capacitance, and the error will thus be 0.4%. As the oscillator frequency must be 1905 kc/s with the variable capacitor in the position corresponding to point B, the discrepancy will amount to $0.4 \times 19 =$ about 8 kc/s.

In practice, however, there is some compensation. Owing to the faulty drawing C_p and L are wrongly determined; C_o is fixed in conformity, and at the first adjustment point there would consequently be an error of 8 kc/s. In fact, however, when setting up the receiver the tuning capacitor is given such a value that the correct oscillator frequency is obtained. The zero capacitance is not equal to the calculated value, and as a result wrong frequencies are obtained at the other adjustment points. Point F is displaced 0.5 mm along FC_p. In the distance FC which measures 100 mm an error of 0.5% is therefore made, and at the frequency corresponding to C, namely 1488 kc/s, there is an error of 0.25%, i.e. of 3.6 kc/s. At the third adjustment point a small error also occurs, but if the padder is adjustable this error will be reduced when the receiver is trimmed, thus somewhat diminishing also the previous error.

It is now possible to estimate how the shape of the tracking curve seen in fig. 175 will be affected by the inaccuracies described above. At the frequency originally chosen for the middle adjustment point a deviation of the order of 3 kc/s occurs, as shown in fig. 186. Clearly, it is essential in preparing the drawings to work to the highest possible accurary. The effect

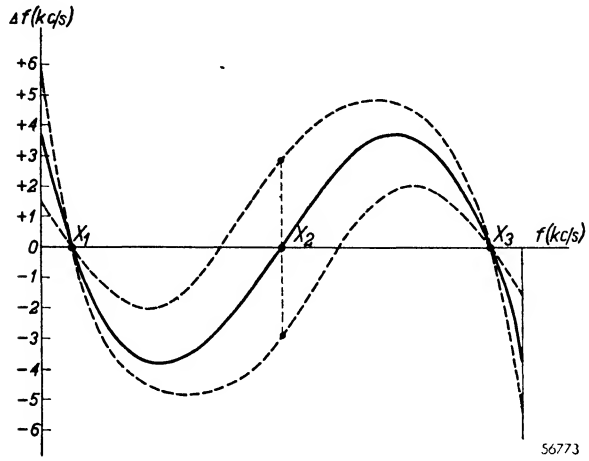

Fig. 186. Two tracking curves (dotted lines), each showing an error of 3 kc/s at the mid-adjustment point, due to an inaccuracy of about 0.8% in the drawing.

of an error can of course be limited by making the scale of the diagram very large. In our example the scale was 1 mm to 2 pF.

A weakness of the graphic method described is that the highest oscillator frequencies correspond to the shortest distances along the line FC_p. Thus at these high frequencies there is a risk of a large percentage error, and therefore of a large absolute error in terms of kilocycles. Since it is the error in kilocycles which is important, it would be better to use a layout in which a higher frequency was represented by a greater distance in the diagram; such a method is described in the following section.

§ 9. The inverse method

The foregoing graphic method of determining circuit constants made use of an abac which gave us the total value of C composed of C_v, C_p and C_o. As the scale employed was proportional to the capacitance C the distances were necessarily proportional to $1/f^2$. It would be much better to use a scale proportional to $1/C$ and this is not difficult to do.

For the series connection of the capacitances C_p and C_v we have:

$$\frac{1}{C} = \frac{1}{C_p} + \frac{1}{C_v}$$

Working with reciprocal values is logical in the present case. Thus if the scales for C_v^{-1} and C_p^{-1} are laid end to end, the total value C^{-1} is always to be found by adding the values of C_v^{-1} and C_p^{-1} concerned. When reciprocal values are used for series connected capacitances the same sort of formula is required as with parallel-connected capacitances. The converse is also true. For two parallel capacitances, e.g. C_v and C_o, $C = C_o + C_v$. Or we can write:

$$\frac{1}{C} = \frac{1}{C_o + C_v}$$

If both numerator and denominator on the right hand side are divided by $C_o . C_v$, we get

$$\frac{1}{C} = \frac{\frac{1}{C_o} \times \frac{1}{C_v}}{\frac{1}{C_o} + \frac{1}{C_v}}.$$

By using reciprocal values it becomes possible to employ an abac like that in fig. 180 for capacitances in parallel. Fig. 187 shows such an abac for the circuit of fig. 172. Along the left-hand scale C_v^{-1} is measured above O and C_p^{-1} below. If, for example, a particular value of C_p^{-1} corresponds to FO, the reciprocal value of C_{v1} and C_p is given by the distance FC_{v1}^{-1}. The connection of C_o in parallel with this combination is dealt with by the same method, but the base line now runs obliquely to F, which is not otherwise of importance. The total reciprocal capacitance values are represented by the distances A_1B, A_2C and A_3D, and again these are proportional to the intercepts FB, FC, and FD. The last named are however related:

$FB : FC : FD = f_1^2 : f_2^2 : f_3^2$

In order to locate these ratios, radii are drawn on ruled transparent paper in such a way that the parallel ruling is intersected in proportion to the values of f_1^2, f_2^2 and f_3^2. It is clear that when the sheet is laid on the abac the line with this frequency division does not pass through point O as in the first method but through a point F, to be found by trial.

Once a suitably intersected line FC_o^{-1} is found the required values of C_p and C_o follow from the reciprocal values, which may be read from either

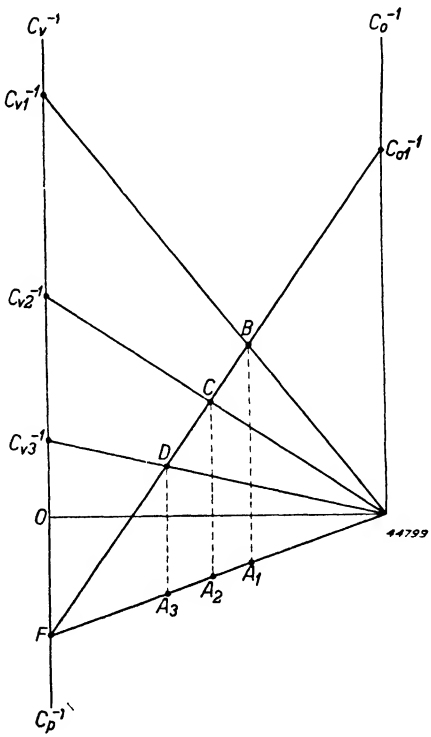

Fig. 187. Abac with two vertical axes C_v^{-1} and C_o^{-1} above the zero point and C_p^{-1} below. The total capacitance in the circuit of fig. 172, e.g. for the values C_{v1}^{-1}, C_{o1}^{-1}, and FO (C_p^{-1}) is proportional to the distance A_1B.

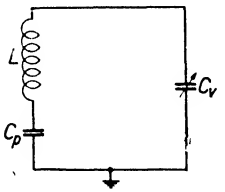

Fig. 188a. Basic oscillator circuit, with the padding capacitor connected between the chassis and the coil.

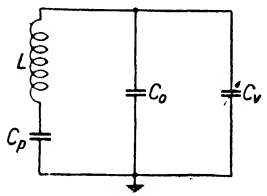

Fig. 188b. The same circuit with the difference, compared with fig. 188a, that there is an appreciable capacitance between the chassis and the high-potential side of the tuned circuit.

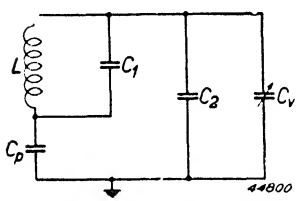

Fig. 188c. The coil has also a certain self-capacitance. The total stray capacitance is thus divided between C_2 and C_1, C_1 being the trimmer and C_2 an estimated quantity.

the left-hand or the right-hand scale. Further, the inductance may be ascertained from any of the vertical distances, e.g. from A_1B and the corresponding frequency.

A minor drawback of this method, compared with the earlier one, is that owing to the reciprocal scale division the value of C cannot be read off directly. The calculation is of course very simple and can be made very quickly with a slide-rule, but the whole method thereby becomes rather more cumbersome. This difficulty is particularly apparent when a reciprocal scale is used in connection with a circuit like that shown in fig. 188.

Fig. 188a represents the basic oscillator circuit in which the padding capacitor is joined between the chassis and the coil. Two variations are possible, figs. 188b and 188c. In the former it is assumed that the inductor has little self-capacitance but that there is an appreciable capacitance between the top of the tuned circuit and earth, i.e. the chassis. If now the trimming capacitor is also connected between the top of the circuit and the chassis, C_o must be in parallel with C_v. The abac of fig. 187 must accordingly be modified, as in fig. 189; in this case the reciprocal value of the parallel circuit C_vC_o is first determined and then that of C_p is added. Point F falls outside the left-hand vertical axis. No fresh difficulties arise.

It is a different matter, however, if the constants of the much used circuit in fig. 188c are to be determined: here a certain amount of self-capacitance C_1 in the coil is taken into account. To compute the total capacitance of this circuit it is first necessary to use the construction of fig. 189 for the combination C_v, C_2 and C_p, the coil capacitance C_1 in parallel being reckoned afterwards. Unfortunately it is not possible simply to add an estimated amount C_1; the nomogram constructions with diagonals must again be applied. With this circuit, therefore, there is no chance of arriving quickly at the best combination of circuit constants by trial and error. But it is possible, however, to estimate C_2 and then to find the optimum value for

C_1 (the trimmer being connected across the coil). In this case the method given in fig. 187 can be employed. By using the left-hand vertical for C_v^{-1} the parallel capacitance C_2 is first brought into account; on this axis we thus have distances corresponding to $(C_{v1} + C_2)^{-1}$, $(C_{v2} + C_2)^{-1}$ and so on. The construction brings no insuperable difficulties in its train but does make the inverse method less attractive when dealing with this very commonly used circuit.

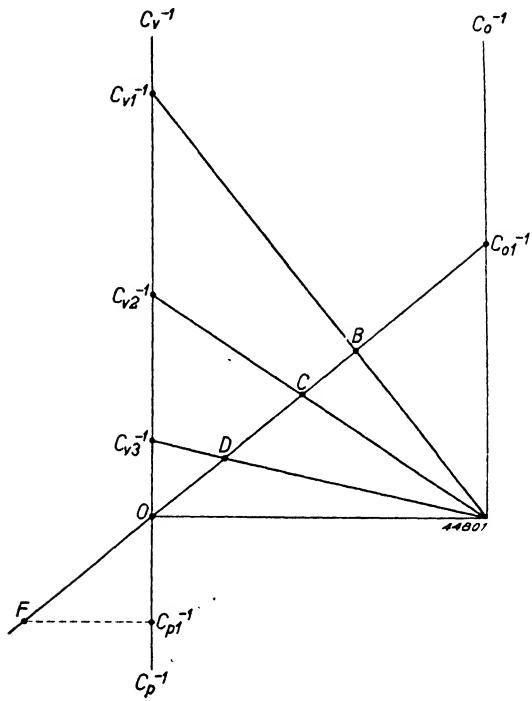

Fig. 189. Nomogram for the determination of the total capacitance in the circuit of fig. 188b.

§ 10. Practical example

As an example we shall now determine by the inverse method the constants for the circuit of fig. 188c, using the values assumed in § 6. Again we shall first compile a table showing the known values, the input frequency f_{HF} in kc/s, and the corresponding values of C_v and $(C_v + C_2)$. C_2 is the stray capacitance between the high-potential side of the circuit and the chassis and will be put at 20 pF.

f_{HF} (kc/s)	C_v (pF)	$(C_v + C_2)$ (pF)	$\frac{10^4}{C_v + C_2}$ ($\times$ 2 *mm*)	f_{osc} (kc/s)	$\frac{7 \times f_{osc}^2}{10^5}$ (mm)
1500	20	—	—	—	—
1435	27	47	426	1905	254
1018	102	122	164	1488	155
601	388	408	49	1071	80
536	500	—	—	—	—

In the fourth column of the foregoing table the reciprocal values of $(C_v + C_2)$,

multiplied by 2×10^4, are indicated and these are set out (see fig. 190) along the vertical on a scale of 2 mm per unit. The value $\frac{10^4}{C_v + C_2} = 213$, corresponding to a capacitance $C_v = 27$ pF, is represented by a distance of

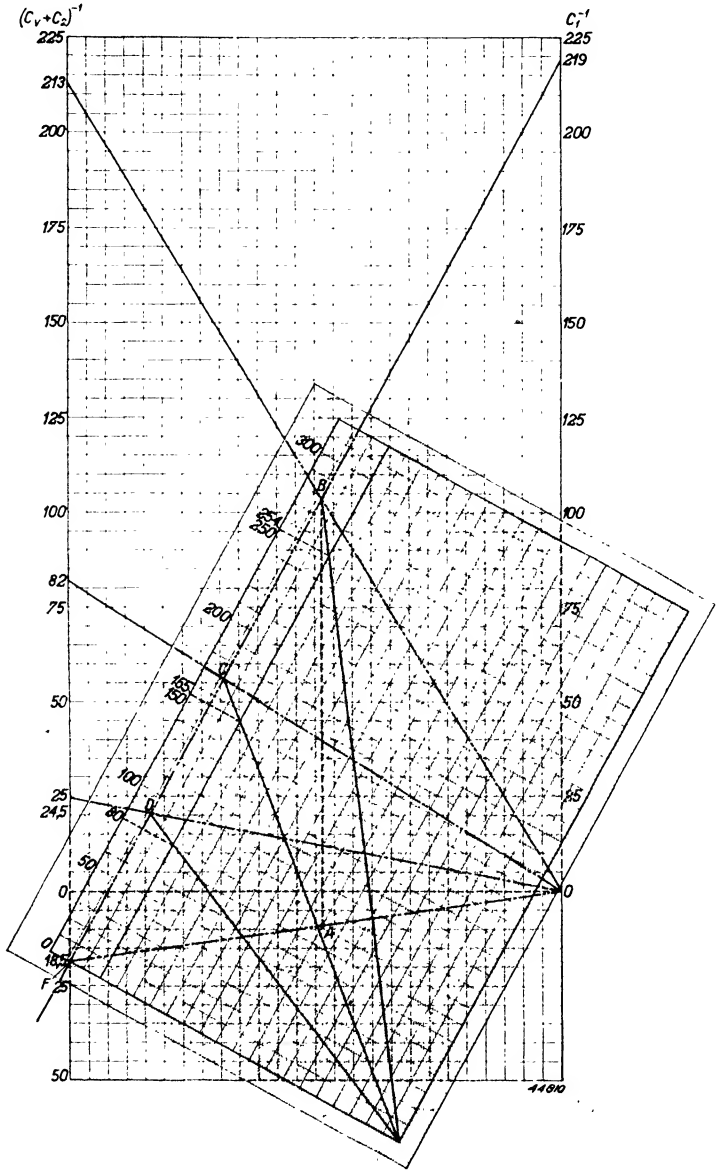

Fig. 190. Example of the graphic method of determining the constants for the oscillator circuit of fig. 188c, for frequency band of 536 to 1500 kc/s.

426 mm. The other two points are similarly inserted and the diagonals drawn. The vertical ruling on the transparent sheet must now be divided proportionally to f_{osc}^2. In the last column of the table the various values of f_{osc}^2, multiplied by 7×10^{-5}, are given; it is these which are used for setting out the radial lines on the transparent sheet *.

When the transparent sheet is correctly placed the intersection with the left-hand vertical indicating the value of C_p^{-1} falls at 37 mm below the horizontal axis; as the scale is 2 mm per unit, C_p^{-1} amounts to 18.5 and therefore:

$$C_p = \frac{10^4}{18.5} = 540 \text{ pF}.$$

The intersection with the right-hand vertical indicating C_1^{-1} lies 438 mm above the horizontal axis, equivalent to 219 units. Thus:

$$C_1 = \frac{10^4}{219} = 46 \text{ pF}.$$

It follows from these values for C_p and C_1 that the circuit differs from that of the example in § 6; C_p was 600 pF in the earlier example, compared with 540 pF in the present case, and C_o was 72 pF instead of 46 + 20 = 66 pF. These divergences are not large. They show that the accuracy of the graphic method is high enough to make the difference between the two circuits quite plain. Finally it is necessary to ascertain the required inductance; this follows from *fosc* and the total capacitance at a given position of C_v. At intersection B, corresponding to an oscillator frequency of 1905 kc/s, the total capacitance is given by AB. This distance amounts in the drawing to 225 mm, or 112.5 units, and consequently:

$$C_{tot} = \frac{10^4}{112.5} = 89 \text{ pF}.$$

The inductance follows from:

$$L = \frac{159155^2}{1905^2 \times 89} = 78 \ \mu\text{H}.$$

The value found in the earlier example was 71.7 μH.

§ 11. Accuracy of the inverse method

In order to gain a better idea of the accuracy of the inverse method we

* It is apparent from fig. 190 that the values are really too small, with the result that the intersections with the diagonals fall outside the ruling of a normal-sized sheet. In fig. 190 a larger sheet is shown, so as to include these.

use fig. 183, which was drawn on the same scale as fig. 190. $(C_{v1} + C_2)^{-1} = 47^{-1}$ was represented by a distance of 426 mm.

The length of the diagonal FB, corresponding to an oscillator frequency of 1905 kc/s, is 278 mm. On this distance an error of 0.5 mm amounts to 0.18 % of f^2 and therefore to 0.09 % of the frequency f; the frequency error is thus $0.09 \times 1905 = 1.7$ kc/s.

This is certainly small, especially when it is remembered that in practice the trimming of the circuits results in the error at the other adjustment points in the frequency band being still smaller. An error of 0.5 mm on FD (89 mm) means a frequency error of 0.28 %: since point D corresponds to a frequency of 1071 kc/s, the divergence here is $0.28 \times 10.71 = 3$ kc/s. It is clear, therefore, that the error is generally less with the inverse method than with the method described in § 6. On the other hand this greater accuracy is achieved at the expense of less straightforward procedure and rather more difficulty in finding the diagonal FC_1^{-1}.

B. Corrections to the calculated tracking curve

§ 1. Introduction

It is a known fact that the measured tracking curve only rarely agrees with the calculated curve. That certain errors are to be expected when graphic methods are employed to determine the constants was mentioned in §§ A 8 and 11. Further, deviations are likely to occur owing to tolerances in the values of inductors and capacitors.

Certain fundamental divergences arise, however, on account of the use of a simplified basic circuit (fig. 176 or 177) with the methods described. It was thereby possible to calculate the oscillator frequency from the classic formula $\omega^2 L\, C_{tot} = 1$. The frequency generated in simple circuits has already been touched on in Chapter II B § 5, and it was noted that if a circuit like that of fig. 176 or 177 was completed by inserting the series resistance of the coil, the frequency still conformed to the classic equation, whereas when parallel damping was also added a rather different frequency was obtained.

A further step towards a better approximation to reality is the bringing into account of the effect of the grid capacitor and leak. With the circuit of fig. 191, for example, it was assumed in the first instance that the voltage applied to the grid was the same as that across L_2, i.e. that the feed-back ratio was equal to the ratio between the tuned-circuit voltage and the voltage across L_2. The elements C_r and R, however, modify the voltage slightly: in the main their effect is to introduce phase-shift, and the feedback ratio therefore has a rather more complicated form.

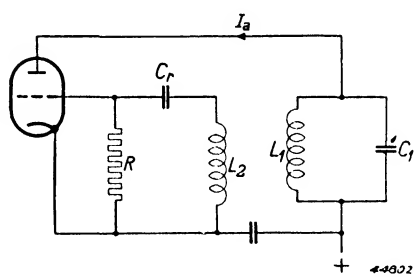

Fig. 191. Example of a simple back-coupled circuit.

Naturally this correction also affects the frequency of the oscillation. With some circuits there are doubtless still other effects to be tracked down, but we shall not discuss all these cases here. It will suffice to illustrate the reasoning by reference to the two matters just mentioned, which in fact are the main causes of divergence in the tracking curve.

§ 2. Detuning due to the distribution of damping

For the reason for deviation in the tracking curve, section II B § 5 may be referred to. There it was found that the oscillator frequency of a tuned circuit like that in fig. 94 was given by:

$$\omega^2 LC = 1 + \frac{r}{R} \quad \text{(II B 15)}$$

where C is the capacitance of the tuning and padding capacitors in series, r the series resistance of the coil and R the resistance parallel to the tuned circuit. The equation may also be written:

$$\omega^2 \frac{L}{1 + \frac{r}{R}} . C = 1 \quad \text{(III B 1)}$$

From this it is clear that the effect of the distributed damping may be regarded as an apparent reduction of the inductance. It seems it ought therefore to be possible to compensate for the phenomenon by increasing the actual inductance if r and R remain constant over the wave band. In general, however, that is not so.

In order to discover whether this reduction factor is much below 1, we shall take the following values for the elements in the anode circuit:

$$\frac{\omega L}{r} = 50,$$
$$R = 15{,}000\ \Omega,$$
$$\omega = 10^7$$
$$L = 75.10^{-6}\ \text{H}.$$

We then get:

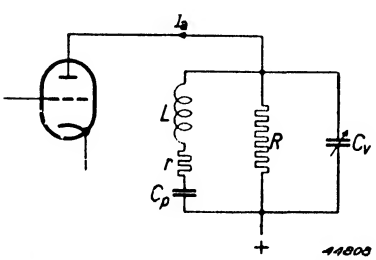

Fig. 192. Customary form of tuned-anode circuit with series and parallel damping.

$$\frac{r}{R} = \frac{\omega L}{50 R} = \frac{10^7 \times 75 \times 10^{-6}}{50 \times 15000} = 0.001.$$

A variation of 0.1 % in the effective inductance causes a change of frequency of 0.05 %; at the frequency in question, about 1600 kc/s, it is thus 0.8 kc/s.

This error cannot be called large, but with abnormal values of r or R, i.e. with heavy additional damping, considerable detuning may be expected.

With a normal circuit like fig. 192 the oscillator frequency differs little from the calculated figure according to (II B 5); the actual result (see II B 5) is given by:

$$\omega_0^2 L\, C_{tot} = 1 + \frac{r}{R} \cdot \frac{C_p}{C_p + C_v} \quad \text{(II B 25)}$$

The factor $\frac{C_p}{C_p + C_v}$ is always less than 1; when C_v is small it is nearly equal to 1. Consequently the detuning at the bottom of the wave band may be expected to be as great as in the preceding case. Compensation is impossible here, even with a constant value of r. The conclusion to be drawn for this example is that the detuning caused by the various dampings is normally fairly small. In general, parallel damping and, therefore, detuning are the same whether the tuned circuit is connected in the anode or in the grid circuit. If for any reason extra damping is introduced it is advisable to apply it in either one form or the other, i.e. if parallel damping is introduced the series resistance should be kept at aminimum. If parallel damping is applied in order to keep oscillator voltage constant, the limiting of series damping is desirable for other reasons already mentioned.

§ 3. Detuning through phase shift in the combination CrR

In II B § 5 the product tZ was considered as an entity. It will now be advantageous to examine separately some of the factors arising in the sequence grid voltage, anode current, circuit voltage, back-coupling. Starting with the circuit without grid capacitor and leak, we can then calculate the effect on frequency of phase shift occurring in the C_rR combination. In II B § 5 the frequency was determined from the negative and real value of the product tZ. This means that we regard the alternating voltage applied to the control grid as causing a back-coupled voltage exactly in phase.

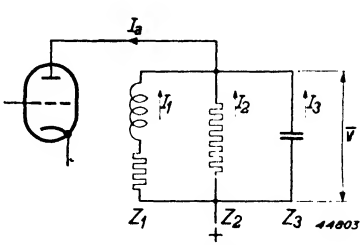

Fig. 193. Simplified form of fig. 192.

In the simplified case, in which the tuned circuit of fig. 193 is coupled by a feedback coil to the grid without the interposition of C_r and R, the voltage across the coupling coil must be exactly in phase with the anode current I_a, i.e. the current I_1 through the tuning coil must be precisely 90° out of phase with I_a. From this condition the frequency can be calculated.

If, however, through the introduction of C_r and R further phase shift of the feed-back voltage occurs, then I_1 must be shifted in relation to 90° by the same amount but in the opposite sense. From this condition the corrected frequency may be calculated; the latter we shall again consider as a detuning in relation to the resonant frequency of the tuned circuit alone. We shall first calculate, for the basic circuit of fig. 193, the relation between the additional phase shift of I_1 and the detuning. For this purpose the ratio I_a/I_1 must be ascertained.

In fig. 193:

$$I_1 = \frac{V_a}{Z_1}, \quad I_2 = \frac{V_a}{Z_2} \text{ and } I_3 = \frac{V_a}{Z_3}$$

Therefore:

$$I_a = I_1 + I_2 + I_3 = V_a \left(\frac{1}{Z_1} + \frac{1}{Z_2} + \frac{1}{Z_3}\right),$$

$$\frac{I_a}{I_1} = \frac{Z_1}{Z_1} + \frac{Z_1}{Z_2} + \frac{Z_1}{Z_3} = 1 + \frac{Z_1}{Z_2} + \frac{Z_1}{Z_3} \quad . \quad . \quad . \quad . \quad \text{(III B 2)}$$

If this ratio is purely imaginary the phase shift between I_1 and I_a is 90°. If it includes a real element, however, the ratio between this real element and the imaginary element is equal to the tangent of the additional phase shift.

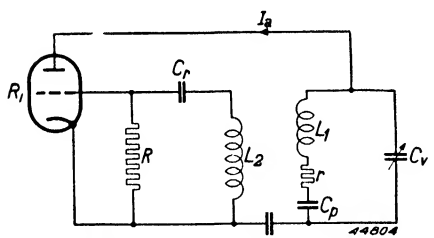

Fig. 194. Oscillator circuit in which only series resistance is taken into account.

In equation (III B 2) the impedances Z_1, Z_2 and Z_3 may be written in less general terms. For example, in a tuned circuit without parallel damping $Z_2 = \infty$,

$$Z_1 = j\omega L_1 + r + \frac{1}{j\omega C_p} \text{ and } Z_3 = \frac{1}{j\omega C_v},$$

and the equation then takes the following form:

$$\frac{I_a}{I_1} = 1 + \left(j\omega L_1 + r + \frac{1}{j\omega C_p}\right) j\omega C_v$$

$$\frac{I_a}{I_1} = 1 - \omega^2 L_1 C_v + jr\omega C_v + \frac{C_v}{C_p} \quad . \quad . \quad . \quad . \quad . \quad \text{(III B 3)}$$

This form becomes purely imaginary if

$$1 - \omega^2 L_1 C_v + \frac{C_v}{C_p} = 0$$

$$\text{or } \omega^2 L_1 \frac{C_v C_p}{C_v + C_p} = 1$$

As might be expected, there is in fact a 90° phase difference between I_1 and I_a when oscillation at the resonant frequency is present. Off this frequency extra phase shift occurs, thus:

$$tan\ \varphi = \frac{1 + \frac{C_v}{C_p} - \omega^2 L_1 C_v}{r\omega C_v} \quad \ldots\ldots\ldots \quad \text{(III B 4)}$$

or:

$$tan\ \varphi = \frac{1 - \omega^2 L_1 C_{tot}}{r\omega C_{tot}} \quad \ldots\ldots\ldots\ldots \quad \text{(III B 5)}$$

in which

$$C_{tot} = \frac{C_p C_v}{C_p + C_v}.$$

If we denote the resonant frequency by ω_0, multiplying the numerator and denominator in equation (III B 5) by ω_0/ω gives us:

$$\tan \varphi = \frac{1 - \omega^2/{\omega_0}^2}{r\ \omega\ C_{tot}} = \frac{\omega_0/\omega - \omega/\omega_0}{r\ \omega_0\ C_{tot}} = \beta \frac{\omega_0 L_1}{r} = \beta Q \quad \ldots\ldots \quad \text{(III B 6)}$$

Here β is again the relative detuning mentioned earlier and it may be written with some approximation as

$$\beta = \frac{2\,\Delta\,\omega}{\omega_0}.$$

Equation (III B 6) thus provides a simple statement connecting the additional phase shift between I_1 and I_a and the detuning $\triangle\omega$ of the oscillator frequency from the resonant frequency. We shall now apply this result to a practical case.

The greatest phase shift may be expected to occur in the C_rR combination at the lowest frequency. With a high intermediate frequency this lowest oscillator frequency will be about 150 + 450 = 600 kc/s. If we say that $C_r = 50$ pF and $R = 17{,}000\ \Omega$ (total grid damping with a grid leak of 50,000 Ω) then:

$$tan\ \varphi = \frac{1}{R\omega C_r} = \frac{10^{12}}{17{,}000 \times 2\,\pi \times 600{,}000 \times 50} = 0.3.$$

This degree of shift can therefore be compensated by detuning the oscillator circuit:

$$\beta = \tan\varphi \frac{r}{\omega_0 L_1} = \frac{tan\ \varphi}{Q} \quad \ldots\ldots\ldots \quad \text{(III B 7)}$$

Taking, for a normal circuit: $Q = \frac{\omega_0 L_1}{r} = 50$, we find:

$$\beta = 0.3 \times \frac{1}{50} = 0.006 = \frac{2\,\Delta f}{f}.$$

The relative detuning required to compensate for the phase shift is therefore 0.3%. At the assumed frequency of 600 kc/s this is 1.8 kc/s, not a particularly large amount. But there is a clear indication here that bigger errors in the tracking curve will arise if normal values are departed from. If for instance $C_r = 25$ pF and $R = 3300$ ohms (grid leak of 10,000 ohms), tan φ becomes ten times greater and the frequency change is then 18 kc/s. It follows from equation (III B 7) that the detuning may be reduced by improving the coil quality Q; practical considerations soon impose a limit, however.

On the other hand the series resistance of the coil is not the only damping present: in practice there is always some parallel damping. In the first place there is the A.C. resistance of the oscillator valve; in many cases there is also damping due to a resistance for parallel feeding or for keeping the oscillator voltage constant (see chapter II C). In order to get an idea of the effect of these sources of parallel damping upon the detuning caused by the $C_r R$ combination we shall take as a final example the tuned circuit given in fig. 195. In the general equation (III B 2) we must now write for the various impedances

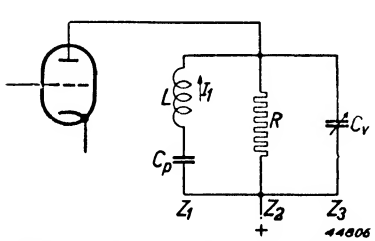

Fig. 195. The circuit of fig. 192, but taking only parallel resistance into account.

$$Z_1 = j\omega L_1 + \frac{1}{j\omega C_p}. \quad Z_2 = R \text{ and } Z_3 = \frac{1}{j\omega C_v}.$$

Therefore:

$$\frac{I_a}{I_1} = 1 + \frac{j\omega L_1 + \dfrac{1}{j\omega C_p}}{R} + \left(j\omega L_1 + \frac{1}{j\omega C_p}\right) j\omega C_v;$$

$$\frac{I_a}{I_1} = 1 + \frac{C_v}{C_p} - \omega^2 L_1 C_v + \frac{j\omega L_1}{R} + \frac{1}{j\omega R C_p}. \quad \text{(III B 8)}$$

If the real part of the equation is put equal to nil, corresponding to a phase difference of 90° between I_1 and I_a, we again find that the oscillator frequency without C_r and R is the resonant frequency. With a grid capacitor and leak in circuit a new frequency arises, the additional phase shift being:

$$\tan\varphi = \frac{1 + \dfrac{C_v}{C_p} - \omega^2 L_1 C_v}{\dfrac{\omega L_1}{R} - \dfrac{1}{\omega R C_p}},$$

$$\tan\varphi = \frac{C_p + C_v}{C_p} \cdot \frac{(1 - \omega^2 L_1 C_{tot})\, R}{\omega L_1 - \dfrac{1}{\omega C_p}} \quad \text{(III B 9)}$$

Since, in general the actual frequency does not differ greatly from the resonant frequency, it is permissible to approximate the denominator of the second fraction as follows

$$\omega L_1 - \frac{1}{\omega C_p} = \frac{1}{\omega C_v}.$$

Equation (III B 9) then becomes:

$$\tan\varphi = \frac{C_p + C_v}{C_p} (1 - \omega^2 L_1 C_{tot})\, R\, \omega C_v =$$

$$= (1 - \omega^2 L_1 C_{tot}) \frac{C_p + C_v}{C_p \cdot C_v} R\omega C_v^2$$

or:

$$\tan\varphi = \beta \frac{\omega}{\omega_0} \cdot \frac{1}{C_{tot}} \cdot \omega R C_v^2 \quad \text{(III B 10)}$$

and if the ratio ω/ω_0 is approximated to 1:

$$\beta = \tan\varphi \frac{C_{tot}}{\omega R C_v^2} \quad \text{(III B 11)}$$

As illustration we may take some practical figures. If the parallel-feed resistance is 25,000 Ω and the A.C. resistance of the valve 50,000 Ω, R, the resultant of the two, is about 17,000 Ω. At the upper end of the long wave band $C_v = 500 + 80 = 580$ pF and $C_p = 200$ pF; C_{tot} is therefore 150 pF. In the previous example we found that tan φ was 0.3, so that the detuning is now:

$$\beta = 0.3 \times \frac{150.10^{-12}}{2\pi \times 600{,}000 \times 17{,}000 \times 580^2 \times 10^{-24}} = 0.002.$$

The relative detuning thus amounts only to 0.1 % or 0.6 kc/s in this instance. With a grid capacitor of 25 pF and leak of 10,000 Ω, however, the detuning would be 6 kc/s.

Whereas in equation (III B 7) the ratio $r/\omega_0 L$ is fairly constant over the wave band, this is not the case with the corresponding fraction in (III B 11). It is therefore worth enquiring what detuning occurs at the lower end of the wave band. The frequency is then $400 + 450 = 850$ kc/s and the phase shift with normal values of C_r and R is tan φ = 0.21. In order to evaluate the fraction we take $C_v = 20 + 80 = 100$ pF and C_{tot} = about 70 pF. Therefore:

$$\beta = 0.21 \times \frac{70 \times 10^{-12}}{2\pi \times 850{,}000 \times 17{,}000 \times 100^2 \times 10^{-24}} = 0.016.$$

The relative detuning is again half this amount, or 0.8 %, representing a deviation from the tracking curve of 6.8 kc/s at the assumed frequency of 850 kc/s. This is a rather large amount in normal circumstances.

This last example shows very clearly the danger of parallel damping in the oscillator circuit; the oscillator becomes sensitive to phase shift. In the circuit of fig. 194 the parallel damping present lies directly across the tuned circuit. In tuned grid circuits R_a is not used, while the A.C. resistance of the valve shunts the coupling coil and therefore has less effect on the tunedcircuit. The resistance R_a is replaced by the grid damping, which is of the same order of magnitude.

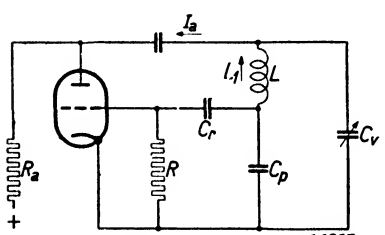

Fig. 196. Oscillator circuit with back-coupling across the padding capacitor.

Cases occur in which the parallel damping is higher, for instance when an endeavour is made to maintain constant oscillator voltage over the wave band by suitable choice of parallel resistance; this commonly adopted method for achieving constant voltage is thus not without its disadvantages.

Another case in which additional phase shift occurs is the Colpitts circuit (fig. 196) described in chapter II B § 7. We can say in principle that $I_1 = 90°$ out of phase with I_a and that in consequence the voltage across C_p is in phase with I_a, which is what is required. The valve ought therefore to oscillate at the resonant frequency. We are forgetting, however, that the grid damping R is in parallel with C_p and that the latter is therefore no longer a pure reactance. A small deviation from 90° occurs in C_p, quite apart from the phase shift in the C_rR combination, and this must also be compensated by detuning from the resonance frequency.

In order to get an idea of the magnitude of this detuning we shall assume that $R = 17{,}000$ Ohms (the grid damping with a grid leak of 50,000 Ohms), that $C_p = 200$ pF and that the frequency is 850 kc/s. The phase shift in relation to 90° in the combination C_pR then becomes:

$$\tan \varphi = \frac{1}{R\omega C_p} = \frac{10^{12}}{17{,}000 \times 2\pi \times 850{,}000 \times 200} = 0.055.$$

This additional phase shift is thus comparable with that already found for the C_rR combination. Here the tuned circuit is damped to a similar degree. Thus it will be seen that in all the examples dealt with detuning occurs in the same order of magnitude as the deviations in normal tracking curves; in consequence a measured tracking curve rarely agrees exactly with the calculated curve.

SURVEY OF LITERATURE CHAPTER III

1. *Couppez.* Les superhétérodynes à commande unique, L'onde Electrique, Déc. 1936.
2. *Landon, V. D.* and *Sveen, E. A.* A solution of the superheterodyne tracking problem; Electronics, Vol. 5 (1932) pp. 250-251.
3. *Meisinger, O.* Die Berechnung des Oszillatorkreises im Überlagerungsempfänger; Funktechn. Mh. 1940 Heft 11, pp. 161-164.
4. *McNamee, B. F.* The padding condenser; Electronics, May 1932, p. 160.
5. *Prytz. Kj.* The padding condenser: Ingeniörvidenskabelige Skrifter. København, Nr. 3 (1941) p. 55
6. *Roder, H.* Oscillator padding; Radio Engineering, March 1935, p. 7.
7. *Singer, C. P.* Ganging a superhet; Wireless Engineer, June 1936, p. 307.
8. *Sowerby, A. L. M.* Ganging the tuning controls of a superheterodyne receiver; Wireless Engineer, Febr. 1932, p. 70.
9. *Wald, M.* Ganging Superheterodyne Receivers; Wireless Engineer, March 1940, p. 105, and April 1941. p. 146.

IV. PARASITIC EFFECTS AND DISTORTION DUE TO CURVATURE OF VALVE CHARACTERISTICS

Introduction

For distortion-free working a valve requires to have a straight anode-current/grid-voltage characteristic, or, in a push-pull circuit, either a straight or a quadratic characteristic. In a valve of conventional design, however, the equation of the curve approximates to the well-known 3/2-power law. A further cause of curvature of the characteristics is the so-called island effect, as a result of which those areas of the cathode lying directly under the grid wires emit less strongly than the rest of the cathode surface or do not emit at all. The extent of these areas varies with the grid voltage and in consequence there is departure from the 3/2 power relationship. Finally the characteristic may be distorted intentionally, by the use of special kinds of grid, to permit control of the working slope.

Distortion and other unwanted effects therefore arise, which the setmaker must take into consideration when developing new receivers. These parasitic effects are:

a. modulation hum;

b. increase of modulation depth and modulation distortion;

c. cross-modulation;

d. superheterodyne whistles;

e. distortion by addition of second and third harmonics.

Effects a, b and c occur in R.F. and I.F. amplifiers as well as in frequency changers; effect d arises only in the mixer valves. Second and third harmonics are mainly generated by A.F. amplifiers and output valves; such distortion will be dealt with in the sections of Book II relating to A.F. amplification and power stages.

After an explanation and mathematical treatment of these parasitic phenomena, practical examples will be given, and the counter-measures to be adopted when designing a receiver will also be indicated.

A. R.F. and I.F. amplifying valves

§ 1. Modulation hum

For a straight i_a/v_g characteristic as in fig. 197a the curve connecting slope and negative grid bias is a horizontal line (fig. 197b). Although a valve with such a characteristic might at first glance seem desirable, as an R.F. amplifier it would have the drawback that the gain could not be controlled by varying the bias. for the slope in this imaginary case is either zero or constant, depending on the grid voltage. In nearly every R.F and I.F. valve the amplification is controlled by an A.V.C. system and the i_a/v_g characteristic of fig 197a is therefore unsuitable.

When the i_a/v_g characteristic is a purely quadratic curve (fig. 198a) the slope characteristic is an oblique straight line (fig. 198b), for the first derivation of a quadratic curve is represented by a straight line. In this case the slope is not constant and the amplification of the valve can accordingly be regulated by means of the grid bias. Any valve which has a characteristic of

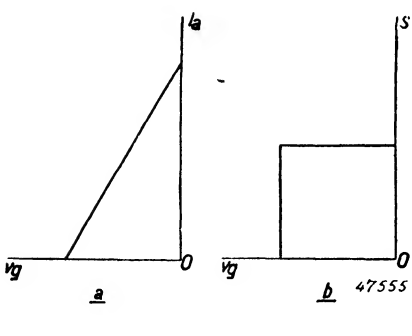

Fig. 197. a. Straight i_a/v_g characteristic. b. The corresponding S/v_g characteristic runs horizontally.

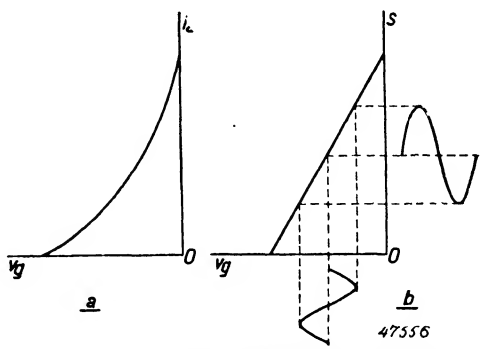

Fig. 198. a. Pure quadratic i_a/v_g characteristic. b. The corresponding S/v_g characteristic is an oblique straight line.

inconstant slope also has the property that alternating voltages applied simultaneously to the grid become mixed, i.e. an R.F. voltage is modulated if an A.F. or another R.F. voltage is present. This can easily be explained. When, apart from the wanted R.F. signal of a frequency ω, a second signal of a frequency p is fed to the control grid, the latter voltage will vary the working slope of the valve at a rate determined by p (see fig. 198b). The gain (slope $\times$ anode load) will thus also fluctuate at a frequency p. In conse-

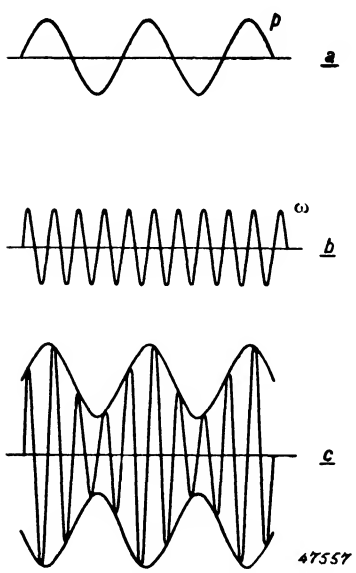

Fig. 199. a. Sinusoidal alternating voltage of frequency p;
b. Sinusoidal alternating voltage of high frequency ω.
c. Application of the foregoing voltages to the grid of a valve with a curved i_a/v_g characteristic results in an anode current of frequency ω, the amplitude of which varies at frequency p.

quence the R.F. signal of frequency ω will be modulated at the frequency p, as illustrated in fig. 199, and a current of this form will appear in the anode circuit.

The superimposing of one frequency on another by a curved characteristic is made use of, for example, in superheterodyne receivers; the R.F. input ω_1 is mixed with the heterodyne voltage ω_2 to produce an I.F. voltage $\omega_3 = \omega_2 - \omega_1$.

Modulation of the wanted signal results in the appearance in the anode circuit of, among others, alternating currents with the sum and difference frequencies of the two oscillations ω_1 and ω_2 (see section II on mixer valves). If the frequency of the second oscillation p is very low, namely an audible frequency such as might be introduced into the anode circuit or into the grid circuit due to inadequate smoothing, so-called modulation hum occurs: the wanted high frequency ω is then modulated at mains frequency. Fig. 200 shows a circuit in which the modulation hum is liable to appear: an AC/DC receiver with the aerial coupled by bottom-capacitance to the tuned circuit. If the receiver is connected to the mains in such a way that the chassis potential is, say, 220 V above earth, the mains voltage is divided across the coupling capacitance C_k and the aerial capacitance C_a. For $C_k = 1500$ pF and $C_a = 125$ pF the voltage appearing across C_k is:

$$\frac{220}{1+\frac{C_k}{C_a}} = \frac{220}{13} = 17 \text{ V}.$$

This hum voltage is at the same time wholly applied to C_v; thereafter, however, the combination $C_r R_g$ may introduce some smoothing, thus if $C_r = 100$ pF and $R_g = 0.8$ MΩ the

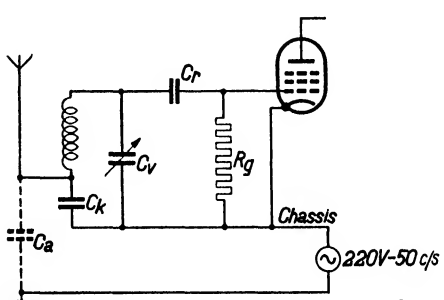

Fig. 200. Basic aerial circuit with bottom-capacitance coupling, in an AC/DC receiver. The voltage division across Ck and Ca can lead to an intolerably high hum-voltage at the grid of the R.F. valve.

hum voltage will reduced in the ratio $\frac{1}{R_g \omega C_r}$, i.e. by forty times.

A 50-cycle voltage of $\frac{17}{40} = 0.425$ V therefore reaches the grid of the R.F. valve and modulates the signal; after amplification and rectification it gives rise to an audible hum in the loudspeaker.

To get a better insight into this problem we shall now consider it mathematically, and we begin with the power series for the valve characteristic

$$i_a = I_{ao} + \alpha v_g + \beta v_g^2 + \gamma v_g^3, \text{ etc.} \quad \text{(IV A 1)}$$

in which v_g is a change of grid voltage in relation to the standing bias V_{go}. The co-efficients α, β, etc. refer therefore to this operating point V_{go}. Alternatively we can write:

$$i_a = I_{ao} + S_1 v_g + \tfrac{1}{2} S_2 v_g^2 + \tfrac{1}{6} S_3 v_g^3 \text{ etc.} \quad \text{(IV A 2)}$$

where i_a = instantaneous value of the total anode current,
I_{ao} = DC component of the anode current,
v_g = grid voltage variation,
$S_1 = \alpha$ = slope of the i_a/v_g characteristic,
$S_2 = 2\beta$ = slope of the S_1/v_g characteristic,
$S_3 = 6\gamma$ = slope of the S_2/v_g characteristic.

In the case of modulation hum we have at the grid of the valve concerned the wanted signal $V_1 \cos \omega t$ and the parasitic alternating voltage $V_2 \cos pt$. In equation (IV A 1) we accordingly substitute as follows:

$$v_g = V_1 \cos \omega t + V_2 \cos pt \quad \text{(IV A 3)}$$

Neglecting I_{ao}, which is constant, and also v_g^3 and higher terms, we get:

$$i_a = \alpha V_1 \cos \omega t + \alpha V_2 \cos pt + \beta V_1^2 \cos^2 \omega t + \beta V_2^2 \cos^2 pt + 2\beta V_1 V_2 \cos \omega t \cos pt \quad \text{(IV A 4)}$$

Here p is the angular frequency of the A.F. alternating voltage. Since in the anode circuit of the valve there is a tuned circuit resonant at the angular frequency ω, only those terms containing $\cos \omega t$ are of importance, so that:

$$i_{a1} = \alpha \left(1 + \frac{2\beta}{\alpha} V_2 \cos pt\right) V_1 \cos \omega t \quad \text{(IV A 5)}$$

From this equation it is apparent that the wanted signal of frequency ω is modulated by the interference to a depth of $\frac{2\beta}{\alpha} V_2 = \frac{S_2}{S_1} V_2$. Thus the modulation hum, expressed as a percentage of the R.F. voltage, amounts to:

$$m_b = \frac{2\beta}{\alpha} V_2 = \frac{S_2}{S_1} V_2 \times 100\% \quad \text{(IV A 6)}$$

We may therefore conclude that:

1. the modulation depth of the hum is, roughly speaking, independent of the amplitude of the required signal;
2. the modulation depth of the hum is directly proportional to the amplitude of the hum voltage and to the slope of the S/v_g characteristic.

From equation (IV A 6) it is now possible to deduce the percentage of modulation hum with a given valve from its i_a/v_g characteristic; it is, however, much easier to ascertain it by measurement, and it is therefore the practice to publish a characteristic for every valve concerned, showing as a function of S the permissible hum voltage at the grid for a hum modulation depth of 1%. Fig. 201 shows such a characteristic for the R.F. pentode UF 21.

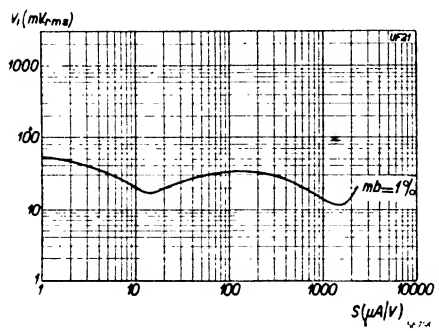

Fig. 201. Uum voltage at the grid of the UF 21 R.F. valve for 1% modulation hum, as a function of the slope.

The hum modulation depth being directly proportional to the hum voltage, we can calculate m_b from this characteristic for other values of hum voltage. For instance, if the slope of the UF 21 is adjusted to 1 mA/V, a hum voltage of 15 mV_{RMS} on the grid will cause 1% modulation hum and, at the same slope, 10 mV_{RMS} will result in 2/3%. As a standard for comparison, it may be said that, for a frequency of 500 c/s, $^1/_2$‰ is the maximum permissible depth of modulation (see also section XIII of volume III). As the published modulation hum characteristic refers to a modulation depth of 1%, the permissible hum voltage is only 1/20 of the value given by the curve. At other frequencies the relative sensitivity of the ear must be taken into account (fig 202). The human ear is much less sensitive to frequencies of 50—100 c/s than to those of 500 c/s; in fact between 500 and 100 c/s its sensitivity falls 30 dB, and consequently at 100 c/s a parasitic voltage 32 times higher than at 500 c/s can be tolerated. In other words

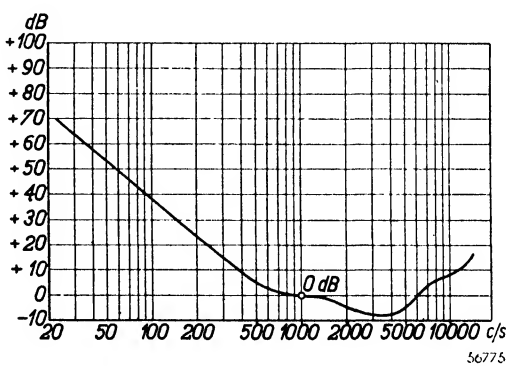

Fig. 202. Aural sensitivity curve, related to a frequency of 1000 c/s.

the permissible hum voltage is about 1.5 times the level indicated by the characteristic for 1% modulation hum. At 50 c/s aural sensitivity is about 40 dB lower than at 500 c/s; this represents a hundredfold decrease, and a hum voltage five times as great as the curve indicates can therefore be tolerated.

In the example on page 311 we found that the 50-cycle voltage on the grid of the UF 21 amounted to 0.425 V. Fig. 201 shows that when the UF 21 is used as an R.F. amplifier an average of $5 \times 0.03 = 0.15$ V at hum frequency is permissible; 0.425 V is clearly intolerable.

In the circuit of fig. 200 an improvement may be effected by inserting a small capacitance in the aerial lead, or by increasing C_k, but both these solutions reduce the magnification of the aerial circuit. A better solution in this case is to connect an inductance, large by comparison with the tuning coil, in parallel with the coupling capacitance C_k. Such an inductance is almost a short-circuit to the hum voltage, while the R.F. current continues to pass through C_k. In AC/DC receivers it is evident that inductive aerial-coupling is preferable to bottom-capacitance coupling.

§ 2. Increase of modulation depth and modulation distortion

If a modulated R.F. oscillation is applied to the grid of a valve having a straight characteristic, i.e. a constant slope, the amplification is independent of the instantaneous amplitude and the modulation envelope is faithfully reproduced.

This is also true in the case of a purely quadratic characteristic, in spite of the fact that the differential slope is no longer constant. We can confirm this easily by omitting the A.F. voltage V_2 in equation (IV A 5), when we find that the anode alternating current I_a is directly proportional to the input V_1, and that as slope we get the constant factor α, which is the differential slope at the operating point.

If now, for a given negative bias, we set out the anode alternating current I_a as a function of the alternating voltage V_g at the grid, we obtain a straight line (fig. 203) *. The distance Oa in this diagram indicates the carrier voltage at the grid; as a result of modulation its value varies from Ob to Oc, and the anode current fluctuates between Ob_1 and Oc_1.

Repeating the figure for a normal i_a/v_g characteristic, diverging from the purely quadratic, we find that the gain depends on the input, as indicated in fig. 203b. In fig. 203a the ratio a_1c_1/Oa_1 equals ac/Oa; in 203b (for a curved S/v_g characteristic) a_1c_1/Oa_1 is, however, larger than ac/Oa and a_1b_1/Oa_1

* I_a and V_g here denote the amplitudes of the alternating current and voltage.

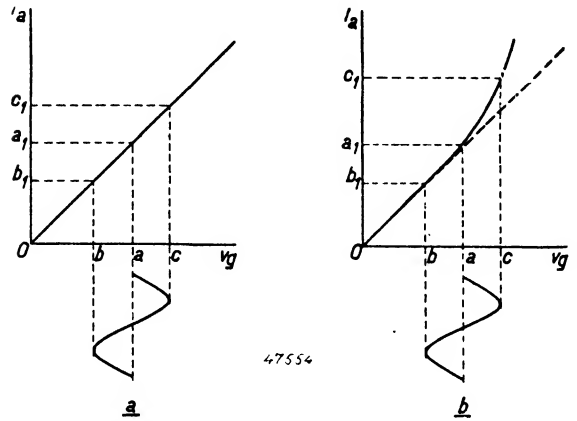

Fig. 203. Amplitude of the alternating anode current as a function of the input to the grid: (a) for a purely quadratic i_a/v_g characteristic; (b) for an i_a/v_g characteristic which diverges from the quadratic. In the latter case the alternating anode current rises faster than the input voltage to the grid, and increase of modulation depth and modulation distortion result.

is larger than ab/Oa. In the second case, therefore, the curvature of the characteristic has increased the depth of modulation. If we denote the original modulation depth of the signal by m_1 and the modulation depth after amplification in the R.F. valve by m_2, the increase is given by:

$$M = \frac{m_2 - m_1}{m_1} . 100\% \qquad \text{(IV A 7)}$$

It is at the same time apparent from fig. 203b that the modulation has been distorted, because in this figure a_1c_1 is greater than a_1b_1. An originally sinusoidal modulation will now therefore contain harmonics, and the distortion may be expressed as:

$$D_{2\ (\text{or } 3)} = \frac{\text{amplitude of the modulation with frequency } 2p \text{ (or } 3p)}{\text{amplitude of the modulation with frequency } p} \qquad \text{(IV A 8)}$$

For a closer investigation into these distortion phenomena we return to the progression of equation (IV A 1) and substitute therein for v_g the alternating voltage $V_1 \cos \omega t$. We assume that the anode circuit is tuned to the frequency ω, and in consequence only terms containing ωt are of importance.

If we neglect the terms V_1^4 and above, the power series becomes:

$$i_{a1} = \alpha V_1 \left(1 + \frac{3}{4} \frac{\gamma}{\alpha} V_1^2\right) \cos \omega t \qquad \text{(IV A 9)}$$

It is evident that the amplification is dependent on the input voltage, unless owing to the curvature of the characteristic the term with γ may be neglected. If the R.F. signal is modulated V_1 must be replaced in equation (IV A 9) by $V_1 (1 + m_1 \cos pt)$, in which expression m_1 stands for the original modulation depth and p the modulation frequency. The result of this substitution is:

$$i_{a1} = \alpha V_1 \left[1 + \frac{3}{4}\frac{\gamma}{\alpha} V_1^2 \left(1 + \frac{3}{2} m_1^2\right) + \left\{1 + \frac{9}{4}\frac{\gamma}{\alpha} V_1^2 \left(1 + \frac{1}{4} m_1^2\right)\right\} \times \right.$$

$$\left. \times m_1 \cos pt + \frac{9}{8}\frac{\gamma}{\alpha} V_1^2 m_1^2 \cos 2pt + \frac{3}{16}\frac{\gamma}{\alpha} V_1^2 m_1^3 \cos 3pt \right] \cos \omega t$$

. . . . (IV A 10)

From this we find for the new modulation depth:

$$m_2 = \frac{1 + \frac{9}{4}\frac{\gamma}{\alpha} V_1^2 \left(1 + \frac{1}{4} m_1^2\right)}{1 + \frac{3}{4}\frac{\gamma}{\alpha} V_1^2 \left(1 + \frac{3}{2} m_1^2\right)} m_1. \quad \ldots\ldots \quad \text{(IV A 11)}$$

so that the increase of modulation depth is:

$$M = \frac{m_2 - m_1}{m_1} = \frac{\frac{3}{2}\frac{\gamma}{\alpha} V_1^2 \left(1 - \frac{3}{8} m_1^2\right)}{1 + \frac{3}{4}\frac{\gamma}{\alpha} V_1^2 \left(1 + \frac{3}{2} m_1^2\right)} \quad \text{(IV A 12)}$$

For a sufficiently small input equation (IV A 12) can be simplified to:

$$M = \frac{3}{2}\frac{\gamma}{\alpha} V_1^2 \left(1 - \frac{3}{8} m_1^2\right),$$

and for shallow modulation to:

$$M = \frac{3}{2}\frac{\gamma}{\alpha} V_1^2 = \frac{1}{4}\frac{S_3}{S_1} V_1^2 \quad \ldots\ldots\ldots \quad \text{(IV A 13)}$$

From equations (IV A 8) and (IV A 10) we derive for modulation distortion by second harmonics:

$$D_2 = \frac{9}{8}\frac{\gamma}{\alpha} m V_1^2 = \frac{3}{16}\frac{S_3}{S_1} m V_1^2 \quad \ldots\ldots \quad \text{(IV A 14)}$$

The distortion by introduction of third and higher harmonics is so much less that it may be ignored.

From equations (IV A 13) and (IV A 14) we conclude that the increase of modulation depth and the modulation distortion are both proportional to the square of the R.F. input of the grid, while the distortion is also in direct proportion to the depth of modulation.

Taking the case of a carrier originally 30% modulated with a sinusoidal frequency of 500 c/s, a modulation distortion D_2 of 1% means that the

output voltage of the valve contains a modulation frequency of 1000 c/s, of which the amplitude is 1% of that of the original 500 c/s. The modulation depth of the second harmonic is thus 0.3%.

In order to assist the set designer it is the practice to publish for R.F. amplifier valves a characteristic indicating the magnitude of the modulation distortion for a particular input to the grid (the modulation rise is less important). Fig. 204 gives such a characteristic for the heptode section of the ECH 21. It shows, as a function of slope, the grid voltage which produces 3/8 m% modulation distortion. Since for every amplifier valve a grid-voltage/mutual-conductance characteristic is also published, it is readily possible from the two curves to ascertain, for any operating condition of the valve, at what input the modulation distortion will amount to 3/8 m%. (Why such a value is chosen is explained below.)

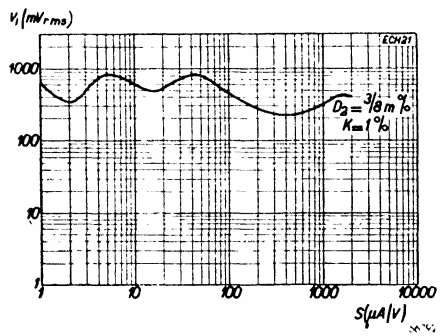

Fig. 204. Input to the grid of an ECH 21 used as I.F. amplifier, for 3/8m% modulation distortion, as a function of slope; this curve corresponds to that for cross-modulation of 1%.

To illustrate the problem we shall compute the distortion which occurs in the I.F. section of a receiver containing two ECH 21 and one EBL 21 valves (fig. 205). The overall gain in this set is divided over the several stages as

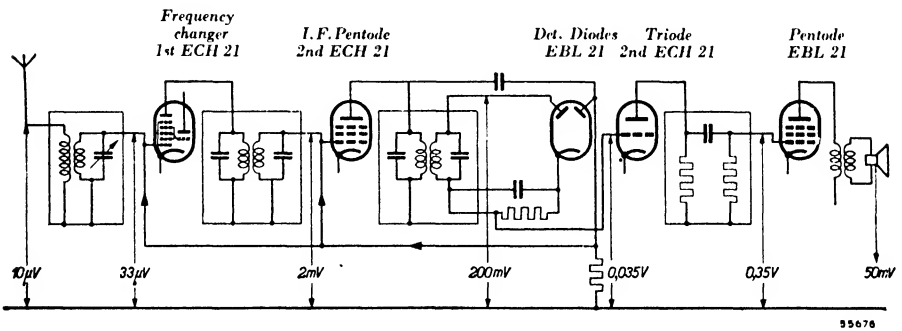

Fig. 205. Diagram of a receiver equipped with ECH 21 - ECH 21 - EBL 21 valves, showing the sensitivity at each stage.

follows. The grid sensitivity of the EBL 21 is 0.35 V for standard output of 50 mW. The triode section of the second ECH 21 gives tenfold amplification and hence requires an input of 0.035 V. This corresponds to an I.F. signal of 200 mV (30% modulated) at the detector diode. The I.F. gain in the heptode section of the second ECH 21 is about 100 times, while the

ECH 21 frequency-changer amplifies roughly 60 times. Consequently the sensitivity at the grid of the mixer is about 33 μV and, assuming that the input tuned circuit provides threefold magnification, the aerial sensitivity is approximately 10 μV.

For standard output of 50 mW there is thus a signal of 2 mV at the grid of the I.F. valve. Assuming that the AVC intervenes only when the input reaches five times this amplitude, the signal at the grid of the I.F. valve would then be 0.01 V and the slope still 2200 μA/V. From fig. 204 we see that with this input and in this operating condition the distortion is negligible. If we now assume that AVC is applied to both ECH 21's and that when the aerial signal increases 2000 times there is a roughly eightfold increase in the voltage across the loudspeaker, the overall gain must clearly have been reduced 2000/8 = 250 times. If the same control bias is applied to each ECH 21 the gain per valve must thus have fallen $\sqrt{250} = 15.8$ times and the slope from 2200 to 140 μA/V. How much distortion occurs with the I.F. valve in this condition?

The I.F. signal has to be 0.01 V before the AVC operates. For an increase in the loudspeaker voltage of eight times, a maximum signal of 8 × 0.01V = 0.08 V at the grid of the I.F. valve might be expected. But as the gain of the I.F. valve is reduced 15.8 times the grid signal must actually be 15.8 × 0.08 = 1.3 V.

Fig. 204 shows that, at a slope of 140 μA/V, modulation distortion of 3.8 m% occurs when the signal is about 0.3 V. As this distortion is proportional to the square of the AC-voltage at the grid, in our example we may expect it to be $(1.3/0.3)^2 \,.\, {}^3/_8\, m\%$. With modulation of 30% the distortion due to second harmonic will thus equal $(1.3/0.3)^2 \,.\, {}^3/_8 \,.\, 0.3\% = 2.3\%$.

§ 3. Cross-modulation

If two alternating voltages of different frequency are applied to the grid of an R.F. valve the curvature of the i_a/v_g characteristic may cause cross-modulation. By this we mean that during reception of a mostly weak signal the modulation of a powerful transmission on another wavelength is heard, this interference disappearing, or being greatly reduced, when the wanted carrier is switched off.

Cross-modulation arises in this way. If there are present at the grid of an R.F. valve with a curved i_a/v_g characteristic the wanted signal V_1 and an interfering signal of amplitude V_2, for example from a local station, the amplification α_1 of the desired signal V_1 can be expressed as a function of the unwanted carrier voltage V_2. As has already been shown in § 2, gain is independent of the AC voltage at the grid where the i_a/v_g characteristic is

quadratic. In such a case, therefore, α_1 does not vary with the amplitude of the interfering signal V_2 and we have the condition represented in fig. 206a. But if the i_a/v_g characteristic deviates from the quadratic form the amplification α_1 will depend on the magnitude of V_2, as indicated in fig. 206b. If we draw a varying V_2 in the two diagrams we see that in fig. a the

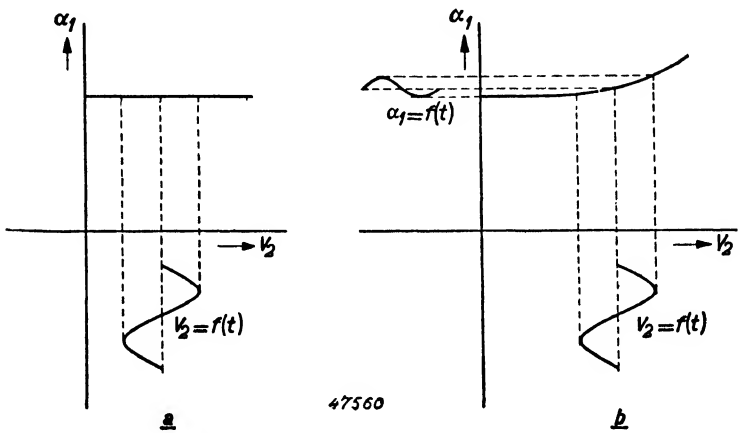

Fig. 206. Amplification α_1 of the wanted signal as a function of the carrier-voltage V_2 of an interfering signal: (a) for a valve with a quadratic i_a/v_g characteristic; (b) for a valve with an i_a/v_g characteristic diverging from the quadratic. In the latter case the amplification of the wanted signal fluctuates in sympathy with the modulation of the interfering carrier (cross-modulation).

amplification remains unaffected, whereas in fig. b it changes with the modulation of V_2.

To gain a closer insight into this phenomenon we return to the power series of equation (IV A 1). In addition to the desired signal $V_1 \cos \omega_1 t$ there is at the grid an interfering signal $V_2 \cos \omega_2 t$, so that for v_g in equation (IV A 1) we must substitute:

$$v_g = V_1 \cos \omega_1 t + V_2 \cos \omega_2 t.$$

Since the anode circuit of the valve in question contains a tuned circuit resonant at the frequency ω_1, only terms with $\cos \omega_1 t$ are important. If we omit v_g^4 and higher terms the foregoing substitution gives us:

$$i_{a1} = \alpha V_1 \cos \omega_1 t \left(1 + \frac{3}{4} \frac{\gamma}{\alpha} V_1^2 + \frac{3}{2} \frac{\gamma}{\alpha} V_2^2\right) . . \quad \text{(IV A 15)}$$

Cross-modulation mostly occurs when a weak transmission is being received, i.e when V_1 is small compared with V_2; equation (IV A 15) may therefore be simplified to:

$$i_{a1} = \alpha V_1 \cos \omega_1 t \left(1 + \frac{3}{2} \frac{\gamma}{\alpha} V_2^2\right) \quad . . . . . \quad \text{(IV A 16)}$$

This formula confirms the fact, already mentioned, that the amplification of the wanted signal is dependent on the amplitude of the interference, unless the γ-term in the progression can be neglected.

If the interfering signal is modulated V_2 in equation (IV A 16) must be replaced by $V_2 (1 + m_2 \cos pt)$, and we then get:

$$i_{a1} = \alpha V_1 \cos \omega_1 t \left\{ 1 + \frac{3}{2} \frac{\gamma}{\alpha} (1 + {}^1/_2 m_2^2) + 3 \frac{\gamma}{\alpha} V_2^2 m_2 \cos pt \right\}.$$

The depth of modulation imposed on the carrier of the required signal by the interfering transmission is thus:

$$m_k = \frac{3 \frac{\gamma}{\alpha} V_2^2}{1 + \frac{3}{2} \frac{\gamma}{\alpha} V_2^2 (1 + {}^1/_2 m_2^2)} m_2.$$

For a small enough value of V_2 this formula can be reduced to:

$$m_k = 3 \frac{\gamma}{\alpha} V_2^2 m_2 = K m_2 \quad \ldots\ldots\ldots \quad \text{(IV A 17)}$$

In this equation we thus have the interference which is transferred to the wanted signal expressed as a fraction K of the modulation m_2 of the unwanted transmission. K is termed the cross-modulation factor, and it is evident that, like the modulation hum factor m_b, it is dependent on the amplitude V_2 of the interfering signal.

K may alternatively be defined as the ratio of the transferred modulation m_k to the modulation m_1 of the wanted carrier.

If we assume for the moment that the wanted and unwanted transmissions are modulated to the same depth, namely $m_1 = m_2$, the above-mentioned ratio becomes:

$$\frac{m_k}{m_1} = \frac{m_k}{m_2} = K.$$

The cross-modulation factor K is thus also the ratio of the interfering modulation to the required modulation in cases where the two transmitters modulate to the same depth.

With the aid of equation (IV A 2) K may be written:

$$K = 3 \frac{\gamma}{\alpha} V_2^2 = {}^1/_4 \frac{S_3}{S_1} V_2^2 \quad \ldots\ldots\ldots \quad \text{(IV A 18)}$$

It is apparent from this equation that, as a rough approximation, the cross-

modulation factor is independent of the magnitude of the wanted signal, and directly proportional to the square of the interfering signal. From the fact that the interference occurs as a modulation of the required signal we deduce that, once cross-modulation is present, no amount of selectivity after the cross-modulating valve can remove the interference: *it must be suppressed by adequately selective circuits before the valve.*

A comparison of (IV A 14) and (IV A 17) reveals that both the modulation distortion D_2 and the cross-modulation factor K are determined by the factor γ/α, which connotes the curvature of the valve characteristic, and further that both phenomena are proportional to the square of the grid signal. Their mutual relationship is:

$$\frac{D_2}{V_1^2} : \frac{K}{V_2^2} = 9/8 \frac{\gamma}{\alpha} m : 3 \frac{\gamma}{\alpha} = 3/8\, m : 1$$

The curve expressing AC-voltage input as a function of slope for 3/8 m% modulation distortion is thus also valid for 1% cross-modulation, but with one difference: that in the case of modulation distortion V_1 refers to the wanted signal, and in the case of cross-modulation to the interfering signal (see fig. 204). In practice a cross-modulation factor of 1% is generally found satisfactory, and the characteristic published is therefore for this percentage.

A basic difference between the two effects described above needs to be mentioned. In connection with modulation distortion (and increase of modulation depth) it is desirable that when working at low slope the valve should be able to handle a large input. At small values of bias only limited amplitudes are applied to the grid, so that the permissible maximum alternating grid voltage for the avoidance of undue modulation distortion need not be large. Regarding cross-modulation the situation is less favourable; the valve must also be able to handle a considerable interference-voltage when adjusted to high slope for reception of a weak signal.

As far as cross-modulation is concerned there is often also a difference between the R.F. valve and the frequency-changer.

At the R.F. valve the strength of the interfering signal V_2 does not depend on that of the wanted transmission, but only on the pre-selection. At the grid of the frequency-changer, when preceded by a controlled R.F. stage, V_2 is strongest when V_1 is weak. If V_1 is also fairly strong AVC intervenes and V_2 is reduced. Interference is, therefore, more severe when the wanted signal is weak. (The I.F. valve need hardly to be considered, as there is adequate pre-selection.) Speaking very generally, for minimum cross-modulation the permissible interference voltage at the grid needs to be large at every point of the characteristic.

To illustrate the concept of cross-modulation we shall consider a practical case. Let us assume that the receiver is tuned to a station radiating on 1000 kc/s and modulated 30% with music. The signal induced in the aerial is 100 μV. In addition a local transmitter on 1020 kc/s, modulated 100% with speech, produces a 1 V signal in the aerial. In the R.F.-valve anode circuit the wanted signal will be modulated with music to a depth of 30%, as well as with speech from the other transmitter to a depth of K%. The question for decision is whether K% of interference is large enough, in relation to the 30% music modulation, to be disturbing.

If the interfering transmission were also modulated to a depth of 30% the interference modulation transferred to the wanted carrier would be proportionately smaller, namely 0.3 K %. When two signals have the same modulation depth K represents the percentage ratio of the interference to the wanted modulation [see equation (IV A 17)].

Let us suppose that the EF 22 R.F. valve is preceded by one tuned circuit (Q = 125) providing, at resonance, a magnification of the aerial coupling of 6. The interfering signal, of course, is not magnified six times, since it is 20 kc/s off tune. The attenuation depends on the factor βQ, which we can ascertain from fig. 20 on page 48 : for Δf = 20,000 c/s, βQ = 5. From fig. 17 on page 36 we then find that the interfering signal is magnified only one-fifth as much as the wanted transmission, and the interference reaching the grid of the R.F. valve is therefore 6/5 × 1 = 1.2 V.

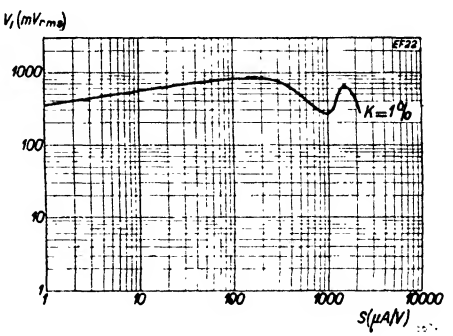

Fig. 207. Interference voltage at the grid of an EF 22 RF amplifier, for 1% cross-modulation, as a function of slope.

With a signal of 100 μV it is probable that the automatic volume control just fails to operate, and the EF 22 is consequently working at its initial slope of about 2.2 mA/V. The characteristic in fig. 207 shows that, in this condition, 1% cross-modulation occurs with an input of 0.24 V; the interfering signal of 1.2 V will therefore cause cross-modulation of $(1.2/0.24)^2$ = 25%, and the modulation of the unwanted transmission will be as much as 80% of that of the wanted signal. This is of course an extreme case. If interference-free reception of a weak transmission is required in the neighbourhood of a powerful station differing only 20 kc/s in frequency and employing 100% modulation, two tuned circuits should precede the R.F. valve. A second circuit of the same characteristics, critically coupled to the first, would attenuate the unwanted

carrier a further five times and thus reduce the cross-modulation by 25 times. The factor K would then be 1 % instead of 25 %, a much more satisfactory result.

Outside those cases in which the interference is of the order of 1 V, cross-modulation is usually unimportant. Nearly everywhere the field strength of a large number of transmitters is high enough to ensure that AVC is operative, and we see from fig. 207 that over a considerable section of the characteristic a signal of 0.5 V or more can be handled without the cross-modulation exceeding 1 %. Assuming, in place of 1 V, an input of 0.25 V, which is still a very strong signal, the interference voltage on the grid with one tuned circuit will be $1.2 \times 0.25 = 0.3$ V and the cross-modulation factor is then $(0.3/0.5)^2 \times 1\% = 0.36\%$.

§ 4. The logarithmic slope characteristic

Starting from the power series:

$$i_a = I_{ao} + \alpha v_g + \beta v_g^2 + \gamma v_g^3 + \ldots$$

(v_g being considered from the working point) we can write for the slope in the immediate vicinity of the operating point V_{go}:

$$S = \frac{d\,i_a}{d\,v_g} = \alpha + 2\,\beta v_g + 3\,\gamma v_g^2 + \ldots \ldots \quad \text{(IV A 19)}$$

For the plotting of the logarithmic slope characteristic we thus have as ordinate:

$$\log S = \log (\alpha + 2\,\beta\,v_g + 3\,\gamma\,v_g^2 + \ldots) = f(v_g) \ldots \ldots \ldots \quad \text{(IV A 20)}$$

Since $\log x = 0.434 \ln x$, we can also write:

$$\log S = f(v_g) = 0.434 \ln (\alpha + 2\,\beta\,v_g + 3\,\gamma\,v_g^2 + \ldots).$$

The slope of this characteristic at the working point is equal to:

$$f'(v_g)_{v_g = 0} = \left| \frac{d\,(\log S)}{d\,v_g} \right|_{v_g = 0} = 0.434 \frac{1}{S} \left(\frac{dS}{dv_g}\right)_{v_g = 0} =$$

$$= 0.434 \left(\frac{2\,\beta + 6\,\gamma\,v_g + \ldots}{\alpha + 2\,\beta\,v_g + 3\,\gamma\,v_g^2 + \ldots}\right)_{v_g = 0} = 0.434 \frac{2\,\beta}{\alpha} \ldots \quad \text{(IV A 21)}$$

For modulation hum we derived the formula:

$$m_b = 2\,\frac{\beta}{\alpha}\,V_2 \ldots \ldots \ldots \ldots \quad \text{(IV A 6)}$$

From equation (IV A 6) and (IV A 21) then follows:

$$\left.\begin{aligned} m_b &= \frac{f'(v_g)}{0.434} V_2, \\ \text{and:} \qquad V_2 &= 0.434\, m_b \frac{1}{f'(v_g)} \end{aligned}\right\} \quad \ldots\ldots\ldots\ldots \quad \text{(IV A 22)}$$

This equation indicates that the permissible voltage for a given percentage of modulation hum increases as $f'(v_g)$ becomes smaller, i.e. as the slope of the logarithmic slope characteristic decreases. Although the permissible hum voltage at a specified slope for 1% modulation hum may be read from the published characteristic, equation (IV A22) enables us to calculate it roughly from the S/v_g characteristic of the valve concerned. As an example we may take the S/v_g characteristic (fig. 208) of the UF 21, for $V_b = 200$ V and $R_{g2} = 60{,}000\ \Omega$ (sliding screen-grid voltage).

At the point on the characteristic for which we require to determine the hum voltage permissible for $m_b = 1\%$ we draw a tangent; in fig. 208 this is at point A, corresponding to $S = 200\ \mu A/V$. To ascertain $d \log S$ we choose, for the sake of simplicity, the two points on this line corresponding to $100\ \mu A/V$ and $1000\ \mu A/V$ respectively. We now find, for $d(\log S) = \log S_2 - \log S_1 =$

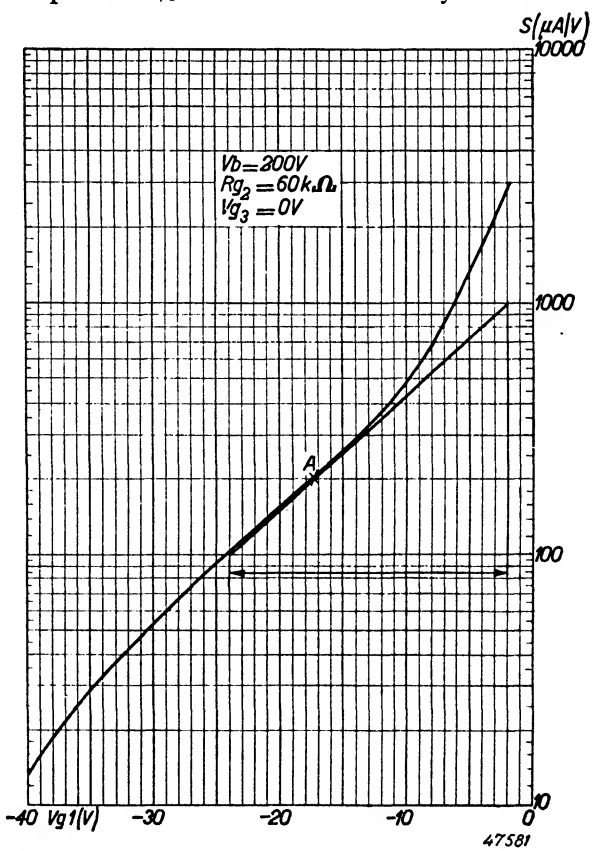

Fig. 208. Logarithmic slope characteristic of the UF 21 R.F. pentode. The tangent indicates the slope of the curve at the point where $S = 200\ \mu A/V$, and is a measure of the modulation hum and cross-modulation in that working point.

$\log S_2/S_1 = \log 10$. The distance between the two points represents a dv_g of 22 V.

Thus:

$$f'(v_g) = \frac{d(\log S)}{dv_g} = \frac{\log 10}{22} = 1/22 = 0.0455.$$

The permissible hum voltage (*RMS*) at this operating point is therefore:

$$V_2 = \frac{0.434 \times 0.01}{0.0455 \times \sqrt{2}} = 0.0665 \text{ V} = 66.5 \text{ mV}.$$

In this way we can of course estimate the permissible hum voltage at other working points as well.

Certain conclusions regarding the cross-modulation factor K may also be drawn from the slope of the logarithmic S/v_g characteristic. Differentiating equation (IV A 21) again with respect to v_g, we obtain:

$$f''(v_g) = \frac{d^2 f(v_g)}{d v_g^2} = 0.0434 \frac{1}{S} \frac{d^2 S}{d v_g^2} - 0.434 \frac{1}{S^2} \left(\frac{d S}{d v_g}\right)^2,$$

or:

$$\frac{d^2 f(v_g)}{d v_g^2} = 0.434 \left(\frac{6\gamma}{\alpha + 2\beta v_g + 3\gamma v_g^2}\right) - 0.434 \left(\frac{2\beta + 6\gamma v_g}{\alpha + 2\beta v_g + 3\gamma v_g^2}\right)^2.$$

For the working point this becomes:

$$\left\{\frac{d^2 f(v_g)}{d v_g^2}\right\}_{v_g = 0} = 0.434 \frac{6\gamma}{\alpha} - 0.434 \left(\frac{2\beta}{\alpha}\right)^2 \quad \text{(IV A 23)}$$

from which it follows that:

$$\frac{3\gamma}{\alpha} = {}^1/_2 \left(\frac{2\beta}{\alpha}\right)^2 + \frac{1}{0.868} \frac{d^2 f(v_g)}{d v_g^2} \quad \text{(IV A 24)}$$

Now $\dfrac{d^2 f(v_g)}{d v_g^2}$ is a measure of the curvature of the line $f(v_g)$ at the point V_{go}.

For any sections of the logarithmic slope characteristic which are fairly straight, i.e. whose curvature is slight, the second term in equation (IV A 24) is negligible compared with the first. If, for simplicity, we limit ourselves to such sections of the characteristic we get:

$$\frac{3\gamma}{\alpha} = {}^1/_2 \left(\frac{2\beta}{\alpha}\right)^2 = {}^1/_2 \left|\frac{f'(v_g)}{0.434}\right|^2 = 2.65 \{f'(v_g)\}^2. \quad \text{(IV A 25)}$$

For the cross-modulation factor we had:

$$K = \frac{3\gamma}{\alpha} V_2^2 \quad \text{(IV A 18)}$$

From equations (IV A 18) and (IV A 25) it follows that:

$$V_2^2 = \frac{K}{2.65\{(f'(v_g)\}^2},$$

or:

$$V_2 = \frac{1}{f'(v_g)}\sqrt{\frac{K}{2.65}} \quad \ldots\ldots\ldots\ldots \quad \text{(IV A 26)}$$

For a given percentage of cross-modulation, therefore, the permissible value of the interference voltage increases as the slope of the logarithmic S/v_g characteristic diminishes. For a cross-modulation factor $K = 1\%$ equation (IV A 26) becomes:

$$V_2 = \frac{1}{f'(v_g)}\sqrt{\frac{0.01}{2.65}} = \frac{0.0615}{f'(v_g)}.$$

Combining equations (IV A 22) and (IV A 26) for $m_b = K = 1\%$ we find:

$$\frac{V_K}{V_{mb}} = \frac{0.0615}{f'(v_g)} : \frac{0.00434}{f'(v_g)} = 14.2,$$

i.e., in the straight parts of the logarithmic S/v_g characteristic the permissible interference voltage for 1 % cross-modulation is 14.2 times the permissible hum voltage for 1 % modulation hum. In the example on page 323 the permissible voltage for $K = 1\%$ will accordingly be:

$$V_{2eff} = 14.2 \times 0.0665 = \text{about } 0.95 \text{ V}.$$

For the curved parts of the logarithmic S/v_g characteristic the last term in equation (IV A 24) must also be taken into account. According to this equation $\frac{3\gamma}{\alpha}$ is increased if $\frac{d^2 f(v_g)}{d\, v_g^2}$ is positive and diminished if it is negative. As we already know, a positive value of this term indicates that the logarithmic S/v_g characteristic is concave (seen from above), while a negative value means that the curve is convex.

To determine the correction for $3\,\gamma/\alpha$ we make use of the radius of curvature of the logarithmic S/v_g characteristic. This radius is given by:

$$\varrho = \frac{\{1 + f'(v_g)^2\}^{3/2}}{f''(v_g)} \quad \ldots\ldots\ldots\ldots \quad \text{(IV A 27)}$$

Since ϱ is measured in centimetres we introduce:

a = the logarithmic unit on the ordinate in centimetres;

b = the number of centimetres corresponding to 1 V on the abscissa.

Working out equation (IV A 27) with the help of (IV A 21) and (IV A 23) we get:

$$\varrho = \frac{\left\{1 + \frac{a^2}{b^2} 0.434^2 \left(\frac{2\beta}{\alpha}\right)^2\right\}^{3/2}}{\frac{a}{b^2} 0.434 \left\{\frac{6\gamma}{\alpha} - \left(\frac{2\beta}{\alpha}\right)^2\right\}} \text{cm},$$

thus:

$$\frac{3\gamma}{\alpha} = {}^1/_2 \left(\frac{2\beta}{\alpha}\right)^2 + \frac{\left\{1 + \frac{a^2}{b^2} 0.434 \left(\frac{2\beta}{\alpha}\right)^2\right\}^{3/2}}{2 \frac{a}{b^2} 0.434 \varrho},$$

or:

$$\frac{3\gamma}{\alpha} = {}^1/_2 \left(\frac{2\beta}{\alpha}\right)^2 + p \quad \ldots\ldots\ldots\ldots \quad \text{(IV A 28)}$$

where:

$$p = \frac{\left\{1 + \frac{a^2}{b^2} 0.434 \left(\frac{2\beta}{\alpha}\right)^2\right\}^{3/2}}{0.868 \frac{a}{b^2} \varrho} \quad \ldots\ldots\ldots \quad \text{(IV A 29)}$$

In the "curved" parts of the logarithmic S/v_g characteristic we can now roughly ascertain ϱ in centimetres by drawing a circle of such radius that its circumference coincides with the characteristic at the working point. This radius, measured in centimetres, then gives us the required value of ϱ. If this quantity is inserted in equation (IV A 29) p can be calculated and then we are in a position also to determine, with the aid of equation (IV A 28), the value of $3\,\gamma/\alpha$ for the "curved" sections of the S/v_g characteristic.

§ 5. Sliding screen-grid voltage

The foregoing has shown us that, to be satisfactory from the point of view of modulation hum, cross-modulation and modulation distortion, a valve should have a flat, straight log S-characteristic, such as *a-b-c-d* in fig. 209. It is not difficult to design such a valve, but it would have certain disadvantages.

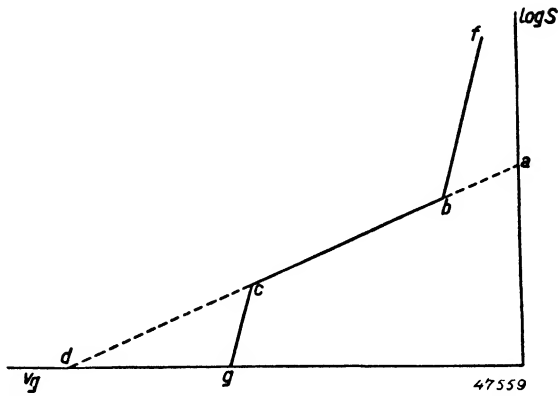

Fig. 209. Basic form of the logarithmic slope characteristic of a variable-gain amplifying valve. A characteristic *a-b-c-d* would give the greatest freedom from cross-modulation and modulation distortion, but practical considerations require a characteristic of the form *f-b-c-g*.

At minimum bias (point *a*) a certain slope is necessary to achieve a given sensitivity, the usual value being about 2 mA/V.

If, in order to minimise distortion, etc., we make the slope decline only slowly with increasing negative bias, a large control voltage will be required for a given reduction in amplification. In other words, the improvement is obtained to the detriment of the control characteristic. To reduce the gain sufficiently without an excessive control voltage, it is necessary to make the slope decrease more rapidly after a certain point, *c*. Adopting this course, however, means more cross-modulation, etc. when the valve is working on the tail of the characteristic.

We thus obtain a characteristic in which, over a comparatively large range *c-a*, the slope is only a little less than at *a*. If we plot the i_a/v_g characteristic for such a case we find that at point *a* the anode current reaches a considerable figure. And not only is this uneconomical, but it also affects the noise in the anode circuit unfavourably.

A solution is to remove the flat part of the characteristic to a lower level, i.e. below the usual 2 mA/V. The log *S*-characteristic must then, however, rise more steeply beyond point *b* if the required maximum slope is to be reached, and as a result the behaviour of the valve in regard to cross-modulation, etc. will be impaired.

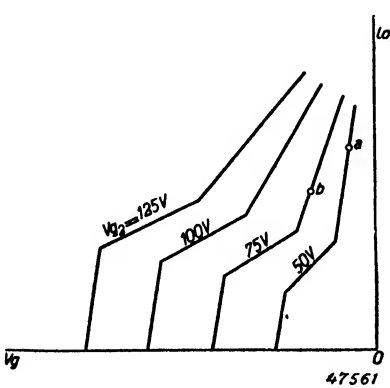

Fig. 210. Family of logarithmic S/v_g characteristics. The points *a*, *b* indicate the successive working points of the valve as its gain is regulated.

In the log *S*-characteristic of variable-gain valves the three parts discussed above are nearly always recognisable. Such curves are a compromise between three requirements: good control characteristics, minimum cross-modulation, etc., and low anode current.

The aim, of course, is always to find the most satisfactory compromise. A good solution is more easily found if we examine a series of log S-characteristics relating the different screen-grid voltages. A family of such characteristics, reduced to essentials, is given in fig. 210. For $V_{g_2} = 50$ V the characteristic is such that at point a the required maximum mutual conductance is obtained without the curve being too steep. As long as the valve operates at a, the gradient of the remainder of the characteristic is unimportant.

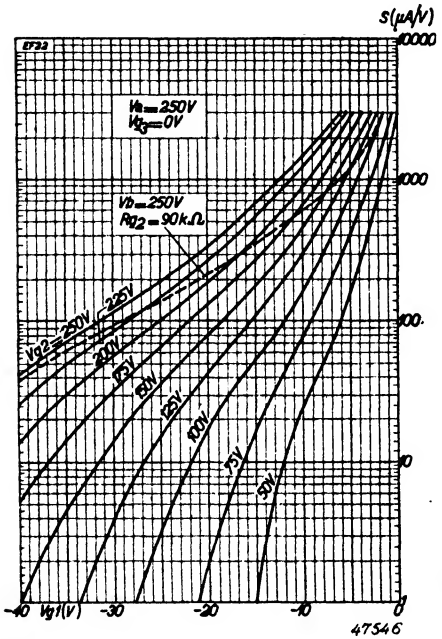

Fig. 211. Logarithmic S/V_g characteristics of the EF 22 R.F. pentode for various values of screen-grid voltage. The dotted line shows the movement of the working point with control of the negative grid bias, when the screen grid is fed through a series resistance (i.e. sliding screen-grid voltage).

If lower slope is required it is better to use a higher screen-grid voltage and work at, say, point b, where the characteristic is rather flatter than in the previous example. That the anode current for $V_{g_1} = 0$ is now excessive does not matter, for the valve is never operated at zero bias. For still lower slope it would be advantageous to make the screen-grid voltage higher, say 100 V, and so on. In this way the valve is worked under the most favourable conditions, whatever the slope, and the disadvantage of a high initial anode current is avoided.

A screen-grid voltage which rises as grid bias increases can be obtained automatically by feeding the screen grid through a fairly high series resistance: as the negative bias is increased both the anode and the screen grid draw less current, and the screen-grid voltage therefore rises. The variation of slope in a valve with sliding screen grid voltage is usually indicated in the published characteristics by a dotted line. An example, for the EF 22 pentode, is given in fig. 211.

B. Distortion in mixing valves

§ 1. Introduction

We have already seen in A § 1 that when two signals of different frequency are applied to the grid, curvature of the i_a/v_g characteristic causes currents of sum- and difference-frequencies, among others, to appear in the anode circuit. This property finds application in superheterodynes, where $V_i \cos \omega_i t$ is the R.F. signal and $V_h \cos \omega_h t$ the oscillator voltage. In the anode circuit, therefore, a voltage of frequency $\omega_o = \omega_h - \omega_i$ is present.

In developing the equations relating to distortion and other parasitic phenomena, we shall find it convenient to divide mixer valves into two classes:

a. those in which the R.F. signal and the heterodyne voltage are fed to the same grid;
b. those in which the R.F. signal and the heterodyne voltage are fed to different grids.

Although in current practice frequency-changing is mostly effected by the second method, we shall, for simplicity, first derive the formulae for mixers of type (a). As in the earlier discussion on R.F. amplification, we begin with the progression containing terms up to v_g^6:

$$i_a = I_{ao} + \alpha v_g + \beta v_g^2 + \gamma v_g^3 + \delta v_g^4 + \varepsilon v_g^5 + \zeta v_g^6 \ldots \quad \text{(IV B 1)}$$

The voltage v_g at the control grid consists in every case of:

$$v_g = V_i + V_h \cos \omega_h t,$$

in which V_i represents the wanted signal + any interference and V_h the oscillator voltage. Substituting this value of v_g in equation (IV B 1) and re-arranging, we get:

$$i_a = A_o + \alpha_o V_i + \beta_o V_i^2 + \gamma_o V_i^3 + \ldots.$$
$$+ (A_1 + \alpha_1 V_i + \beta_1 V_i^2 + \gamma_1 V_i^3 + \ldots.) V_h \cos \omega_h t +$$
$$+ (A_2 + \alpha_2 V_i + \beta_2 V_i^2 + \gamma_2 V_i^3 + \ldots.) V_h^2 \cos 2\omega_h t + \ldots \text{etc.,} \quad \text{(IV B 2)}$$

in which:

$$A_o = I_{ao} + \frac{1}{2}\beta V_h^2 + \frac{3}{8}\delta V_h^4 + \frac{5}{16}\zeta V_h^6 + \ldots.$$

$$\alpha_o = \alpha + \frac{3}{2}\gamma V_h^2 + \frac{15}{8}\varepsilon V_h^4 + \ldots.$$

$$\beta_0 = \beta + 3\,\delta\,V_h^2 + \frac{15}{8}\,\zeta\,V_h^4 + \ldots\ldots$$

$$\gamma_0 = \gamma + 5\,\varepsilon\,V_h^2 + \ldots\ldots \text{etc.}$$

$$A_1 = \alpha + \frac{3}{4}\gamma\,V_h^2 + \frac{5}{8}\,\varepsilon\,V_h^4 + \ldots\ldots$$

$$\alpha_1 = 2\,\beta + 3\,\delta\,V_h^2 + \frac{15}{4}\,\zeta\,V_h^4 + \ldots\ldots$$

$$\beta_1 = 3\,\gamma + \frac{15}{2}\,\varepsilon\,V_h^2 + \ldots\ldots$$

$$\gamma_1 = 4\,\delta + 15\,\zeta\,V_h^2 + \ldots\ldots \text{etc.}$$

As the anode circuit is tuned to the frequency $(\omega_h - \omega_i) = \omega_o$, only those terms containing $V_h \cos \omega_h t$ are of importance; only in special circumstances will the other terms produce the frequency ω_o. Thus we need interest ourselves only in the following part of equation (IV B 2):

$$i_a = (A_1 + \alpha_1\,V_i + \beta_1\,V_i^2 + \gamma_1\,V_i^3 \ldots.)\;V_h \cos \omega_h t \quad \ldots\ldots \quad \text{(IB V 3)}$$

This formula can be further simplified by first assuming that the heterodyne voltage is very small. For the expressions A_1, α_1, β_1, etc. we can then write:

$$A_1 = \alpha,$$

$$\alpha_1 = 2\,\beta,$$

$$\beta_1 = 3\,\gamma,$$

$$\gamma_1 = 4\,\delta,$$

and equation (IV B 3) reduces to:

$$i_a = (\alpha + 2\,\beta\,V_i + 3\gamma\,V_i^2 + 4\,\delta\,V_i^3 + \ldots\ldots)\,V_h \cos \omega_h t. \quad \ldots \quad \text{(IV B 4)}$$

Substituting $V_i = V_i \cos \omega_i t$, we obtain:

$$i_a = \left[\alpha + \frac{3}{2}\,\gamma V_i^2 + 2\beta\,V_i\left(1 + \frac{3}{2}\frac{\delta}{\beta}\,V_i^2\right)\cos \omega_i t + \frac{3}{2}\,\gamma V_i^2 \cos 2\,\omega_i t + \right.$$

$$\left. + 3\delta\,V_i^3 \cos 3\,\omega_i t + \ldots\ldots\right] V_h \cos \omega_h t.$$

Replacing $\omega_h - \omega_i$ by ω_o, omitting unimportant terms and rearranging, we then get:

$$i_a\,(\omega_0) = \beta\, V_i\, V_h \left(1 + \frac{3}{2}\frac{\delta}{\beta}\, V_i^2 + \ldots\right) \cos\,\omega_0 t \quad \ldots\ldots \quad \text{(IV B 5)}$$

Here $i_a\,(\omega_0)$ denotes the I.F. current *.

§ 2. Modulation hum

If, in addition to the wanted signal $V_i \cos\,\omega_i t$, a hum voltage $V_2 \cos\,pt$ is present at the grid we must substitute $V_1 \cos\,\omega_1 t + V_2 \cos\,pt$ for V_i in equation (IV B 4). Leaving out of consideration the harmonics of the modulation hum, we find that the element of the anode current comprising terms with $\cos\,\omega_0 t$ and $\cos\,pt$ is as follows (the harmonics of the modulation hum not being considered):

$$i_a\,(\omega_0) = \beta\, V_1\, V_h \left[\left(1 + \frac{3}{2}\frac{\delta}{\beta}\, V_1^2 + 3\frac{\delta}{\beta}\, V_2^2 + \ldots\right) + 3\frac{\gamma}{\beta}\, V_2 \left\{1 + \frac{5}{3}\frac{\varepsilon}{\gamma}\,(V_1^2 + V_2^2) + \ldots\right\} \cos\,pt\right] \cos\,\omega_0 t \quad \ldots \quad \text{(IV B 6)}$$

This corresponds to the case of an I.F. signal modulated by a voltage V_2 of frequency p to a depth:

$$m_b = \frac{1 + \frac{5}{3}\frac{\varepsilon}{\gamma}\,(V_1^2 + V_2^2) + \ldots}{1 + \frac{3}{2}\frac{\delta}{\beta}\, V_1^2 + 3\frac{\delta}{\beta}\, V_2^2 + \ldots}\, 3\frac{\gamma}{\beta}\, V_2 \quad \text{(IV B 7)}$$

For small values of V_1 and V_2 the equation can be simplified to:

$$m_b = 3\frac{\gamma}{\beta}\, V_2 \quad \ldots\ldots\ldots\ldots\ldots \quad \text{(IV B 8)}$$

The first conclusion to be drawn from this is that modulation hum is, roughly speaking, directly proportional to the amplitude of the hum voltage,

---

* Following from the definition of conversion conductance, $i_a\,(\omega_0) = S_c V_i$, and therefore:

$$S_c = \beta V_h \left(1 + \frac{3}{2}\frac{\delta}{\beta}\, V_i^2 + \ldots\right).$$

For small values of V_i this becomes:

$$S_c = \beta V_h.$$

As $\frac{\delta^2 i_a}{\delta v_g^2} = \frac{\delta S}{\delta v_g} = 2\beta$, the slope of the S/v_g characteristic is a measure of the conversion conductance. Furthermore it is apparent from the foregoing that S_c is proportional to the heterodyne voltage V_h. This relationship has already been mentioned in A § 1 of chapter II.

and independent of the strength of the R.F. signal. Compared with the corresponding case with R.F. amplifying valves the only difference is that here the factor γ/β instead of β/α is determinable for the modulation hum.

§ 3. Increase of modulation depth and modulation distortion

In order to derive a formula for the increase of modulation depth and the modulation distortion occurring in a frequency-changer, we first arrange (IV B 5) in the same form as the equation relating to R.F. and I.F. valves, namely (IV A 9):

$$i_a = (\beta V_h)\, V_i \left[1 + \frac{3}{4}\left(\frac{2\delta V_h}{\beta V_h}\right) V_i^2 + \ldots .\right] \cos \omega_o t \quad . \quad . \quad . \quad . \quad . \quad . \quad \text{(IV B 9)}$$

In place of α in equation (IV A 9) we now have βV_h, and instead of γ we now obtain $2\delta V_h$. Equation (IV A 13) thus becomes

$$M = \frac{3}{2} \times \frac{2\delta V_h}{\beta V_h} V_i^2 \left(1 - \frac{3}{8} m_1^2\right) = 3\frac{\delta}{\beta}\left(1 - \frac{3}{8} m_1^2\right) V_i^2 \ldots . \quad \text{(IV B 10)},$$

and for shallow modulation:

$$M = 3\frac{\delta}{\beta} V_i^2 \quad . \quad . \quad . \quad . \quad . \quad . \quad . \quad . \quad . \quad . \quad . \quad . \quad \text{(IV B 11)}$$

Similarly, for the distortion due to the presence of second harmonic we find:

$$D_2 = \frac{9}{4}\frac{\delta}{\beta} m V_1^2 \quad . \quad . \quad . \quad . \quad . \quad . \quad . \quad . \quad . \quad . \quad . \quad . \quad \text{(IV B 12)}$$

From these equations it is thus clear that both the modulation rise and the modulation distortion are, as in the case of R.F. and I.F. valves, directly proportional to the square of the R.F. input voltage, while the modulation distortion is also proportional to the depth of modulation. With frequency-changers δ/β is the determining factor, whereas with R.F. valves it was γ/α. Thus we can say that, in principle, the same formulae apply to mixers as to R.F. amplifiers, though they are of a higher order. As in the case of R.F. and I.F. valves, characteristics are published also for mixing valves, showing the modulation distortion for any given conditions of operation.

§ 4. Cross-modulation

We can, as in the preceding section, rewrite equation (IV A 18) in the form:

$$K = 3\frac{2\delta V_h}{\beta V_h} V_2^2 = 6\frac{\delta}{\beta} V_2^2 . \quad . \quad . \quad . \quad . \quad . \quad . \quad . \quad . \quad \text{(IV B 13)}$$

Regarding all three parasitic effects we may then conclude that frequency-changers behave in fundamentally the same way as R.F. amplifiers, but in the case of mixing valves it is necessary to employ a progression extending one term higher when calculating the magnitude of the effects. This is true also for the amplification of these valves. In the case of R.F. amplifiers we base our calculation on the mutual conductance S, or by approximation, on α; for the mixer we take as basis the conversion conductance S_c, or, with some approximation, β.

The expressions derived for modulation hum, modulation distortion and cross-modulation hold good, however, only when the various applied voltages are small. As far as wanted and interfering R.F. signals are concerned, the condition is nearly always satisfied. The conversion conductance, however, is, as we saw in chapter II, roughly proportional to the heterodyne voltage V_h, and consequently this voltage is generally made as large as possible. For practical use, therefore, the derived expressions need to be amended.

§ 5. Calculations for an arbitrary oscillator voltage

To obtain results of more general usefulness it is necessary in equation (IV B 3) to work out accurately those quantities, namely A_1, α_1, β_1 and γ_1, which affect the magnitude of the heterodyne voltage V_h. If now in this equation we substitute $V_1 \cos \omega_1 t + V_2 \cos pt$ for V_i (modulation hum) we get, after re-arranging, omitting unimportant terms and replacing $\omega_h - \omega_i$ by ω_o:

$$i_{a(\omega_o)} = \frac{1}{2} \alpha_1 V_1 V_h \cos \omega_o t \left(1 + 2 \frac{\beta_1}{\alpha_1} V_2 \cos pt\right), \quad \text{(IV B 14)}$$

which roughly corresponds to a modulation by the interfering frequency p to a depth of:

$$m_b = 2 \frac{\beta_1}{\alpha_1} V_2.$$

Replacing α_1 and β_1 by the equations given on page 330, we once more obtain, after dropping terms of higher order, the value already found:

$$m_b = \frac{3\gamma}{\beta} V_2.$$

In the same way we can derive the expressions for the other forms of interference, finding for:

increase of modulation depth:

$$M = \frac{3\gamma_1}{2\alpha_1} V_i^2;$$

modulation distortion

$$D_2 = \frac{9\gamma_1}{8\alpha_1} m V_i^2;$$

cross-modulation factor:

$$K = 3\frac{\gamma_1}{\alpha_1} V_2^2.$$

After substituting for α_1 and γ_1, and neglecting the terms of higher order, as is to be expected, we find that these expressions for M, D_2 and K assume the forms already derived for a small value of the oscillator voltage. But the advantage of these new equations is that they are applicable to any value of the heterodyne voltage V_h. The magnitude of V_h affects the terms α_1, β_1 and γ_1, but no difficulty arises because the oscillator voltage normally has a specific value, determined in advance. The same restriction applies here as with straight R.F. amplification, namely that the amplitudes of V_1 and V_2 must be small, i.e. $\gamma_1/\alpha_1 V^2 <$ about 0.02.

§ 6. Mixer valves in which the R.F. signal and the oscillator voltage are applied to different grids

In this case we have at our disposal two control grids, *a* and *b*, and the anode current is influenced by the voltages at both.
The general formula is therefore:

$$i_a = \alpha_a V_a + \alpha_b V_b + \beta_{2a} V_a^2 + \beta_{ab} V_a V_b + \beta_{2b} V_b^2 + \\ + \gamma_{3a} V_a^3 + \gamma_{2ab} V_a^2 V_b + \gamma_{a2b} V_a V_b^2 + \gamma_{3b} V_b^3 + \text{etc.}$$

Assuming the heterodyne voltage to be applied to grid *a* and the R.F. signal plus any interference to grid *b*, the following expressions are to be inserted in the foregoing equation:

$$V_a = V_h \cos \omega_h t$$

and:

$$V_b = V_i$$

Developing the progression gives us:

$$i_a = A_o + \alpha_o V_i + \beta_o V_i^2 + \gamma_o V_i^3 + \ldots (A_1 + \alpha_1 V_i + \beta_1 V_i^2 + \gamma_1 V_i^3 + ..) \times \\ V_h \cos \omega_h t + (A_2 + \alpha_2 V_i + \beta_2 V_i^2 + \gamma_2 V_i^3 \ldots) V_h^2 \cos 2\omega_h t, \text{ etc.,}$$

in which:

$$A_o = I_{ao} + \frac{1}{2}\beta_{2a} V_h^2 + \ldots,$$

$$\alpha_o = \alpha_b + \frac{1}{2}\gamma_{2ab} V_h^2 + \ldots,$$

$$\beta_o = \beta_{2b} + \frac{1}{2}\delta_{2ab} V_h^2 + \text{etc.}$$

$$A_1 = \alpha_a + \frac{3}{4}\gamma_{3a} V_h^2 + \ldots,$$

$$\alpha_1 = \beta_{ab} + \frac{3}{4}\delta_{3ab} V_h^2 + \ldots,$$

$$\beta_1 = \gamma_{a2b} + \ldots \text{etc.}$$

As the anode circuit is tuned to the frequency $\omega_o = \omega_h - \omega_i$, only terms containing $V_h \cos \omega_h t$ are of importance and it is sufficient to write:

$$i_a = (A_1 + \alpha_1 V_i + \beta_1 V_i^2 + \gamma_1 V_i^3 \ldots\ldots) V_h \cos \omega_h t.$$

This formula agrees exactly with equation (IV B 3), so that the expressions for the various phenomena can be ascertained by reference to the foregoing reasoning.

§ 7. The logarithmic slope characteristic

In the foregoing paragraphs the similarity between the properties of R.F. valves and those of frequency-changers has become clear. We noted that with both types of valves the expressions for S, K, m_b, etc. are determined by the factors of a power series, the only difference being that in the case of mixers the co-efficients are shifted one place to the right. It is evident, then, that with mixing valves the relationship between the factors K and m_b and the logarithmic S_c/v_g characteristic is identical with the corresponding relationship for R.F. amplifiers (see A § 4); in consequence the theoretical discussion can be omitted.

C. Measurement of the parasitic phenomena

§ 1. Theoretical considerations

If we have an audio voltage $V_1 \cos pt$ at the grid of an amplifying valve the anode current will contain harmonics of the original frequency, due to the curvature of the characteristic. This is seen at once if we again begin with the progression:

$$i_a = I_{ao} + \alpha v_g + \beta v_g^2 + \gamma v_g^3 \ . \ . \text{ etc.}$$

Substituting $V_1 \cos pt$ for v_g gives us:

$$i_a = I_{ao} + \frac{1}{2}\beta\, V_1^2 + \alpha V_1 \cos pt \left(1 + \frac{3}{4}\frac{\gamma}{\alpha} V_1^2\right) +$$

$$+ \frac{1}{2}\beta\, V_1^2 \cos 2pt + \frac{1}{4}\gamma\, V_1^3 \cos 3pt \ . \ . \ . \ . \ . \quad \text{(IV C 1)}$$

The percentage of second harmonic to fundamental is equal to:

$$d_2 = \frac{\frac{1}{2}\beta\, V_1}{\alpha\left(1 + \frac{3}{4}\frac{\gamma}{\alpha} V_1^2\right)} \ . \ . \ . \ . \ . \ . \ . \ . \ . \ . \quad \text{(IV C 2)}$$

For a small alternating voltage on the grid equation (IV C 2) can be simplified to:

$$d_2 = \frac{1}{2}\frac{\beta}{\alpha} V_1 \,.\, 100\,\% \ . \ . \ . \ . \ . \ . \ . \ . \ . \ . \quad \text{(IV C 3)}$$

Similarly, for the percentage of third harmonic we may write:

$$d_3 = \frac{1}{4}\frac{\gamma}{\alpha} V_1^2 \,.\, 100\,\% \ . \ . \ . \ . \ . \ . \ . \ . \ . \ . \quad \text{(IV C 4)}$$

(In chapter VI on A.F. amplification this matter will be found dealt with in more detail.) Comparison of these formulae with those for modulation hum (IV A 6), increase of modulation depth (IV A 13), modulation distortion (IV A 14) and cross-modulation (IV A 17) reveals an inter-relationship, which we may express as follows:

modulation hum	m_b	$= 4\, d_2$
modulation rise	M	$= 6\, d_3$
modulation distortion	D_2	$= 4^1/_2\, m d_3$
cross-modulation	K	$= 12\, d_3$

The grid input voltage at which, for example, 1% modulation hum occurs may thus be ascertained by measuring the input for which $d_2 = {}^1/_4\,\%$. However, in arriving at the foregoing formulae certain approximations were introduced, and consequently their use does not lead to the most accurate results. It is better to make direct measurements of each effect, and a method of doing this will now be briefly described.

§ 2. Increase of modulation depth and modulation distortion

A sinusoidal R.F. voltage of frequency ω is applied to the grid of the valve under examination via an amplifier, and the amplitude is modulated by a sinusoidal A.F. voltage of frequency p. The modulation depth is adjusted, for example, to $m_1 = 30\,\%$. See fig. 212.

After passing through the valve under examination the signal is more deeply modulated than before owing to curvature of the characteristic.

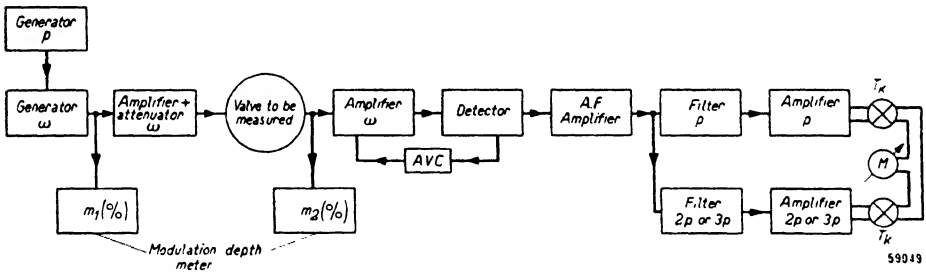

Fig. 212. Set-up for measuring modulation rise and modulation distortion; ω = carrier-frequency, p = modulation-frequency.

Immediately after the valve the new modulation depth of the signal, m_2, is measured and we then get for the percentage increase of modulation depth:

$$M = \frac{m_2 - m_1}{m_1}\ \%.$$

The valve is followed by an amplifier tuned to the frequency ω which has such a high degree of feedback that its gain is almost independent of the characteristics of the valves contained in it. This amplifier is in turn followed by a detector which supplies a modulated DC-voltage. After smoothing,

this rectified voltage is applied to the R.F. amplifier as a control voltage, and a very constant carrier amplitude to the detector is thereby ensured. The unsmoothed detector output is also applied to an A.F. amplifier feeding two filters, each of which is followed by a further amplifier. One filter passes only the fundamental frequency p, the other the frequency $2p$ or $3p$. The gain of the amplifier following the latter filter is adjustable. Two thermocouples T_k are connected to the respective amplifier outputs, with their secondaries in opposition. By adjusting the harmonic amplifier until the meter M indicates zero we can determine the ratio of harmonic to fundamental from the relative gain of the two amplifiers. From equation (IV A 8) the distortion due to second harmonic is:

$$D_2 = \frac{\text{amplitude second harmonics}}{\text{amplitude fundamental}}$$

§ 3. Modulation hum

To the grid of the valve under examination the amplified sinusoidal R.F. voltage ω and an A.F. voltage of frequency $p = 500$ c/s are applied (see fig. 213). Due to curvature of the valve characteristic the R.F. voltage becomes modulated by the 500-cycle voltage. The test can have either of two objects: the determination of the modulation depth for a given amplitude of interference; or the determination of the interference voltage required to produce a given depth of modulation, say 1%. In both cases the modulated voltage is first amplified and then rectified. The amplifier used includes strong feedback and its output is kept as constant as possible by applying an amplified control voltage derived from the detector. A

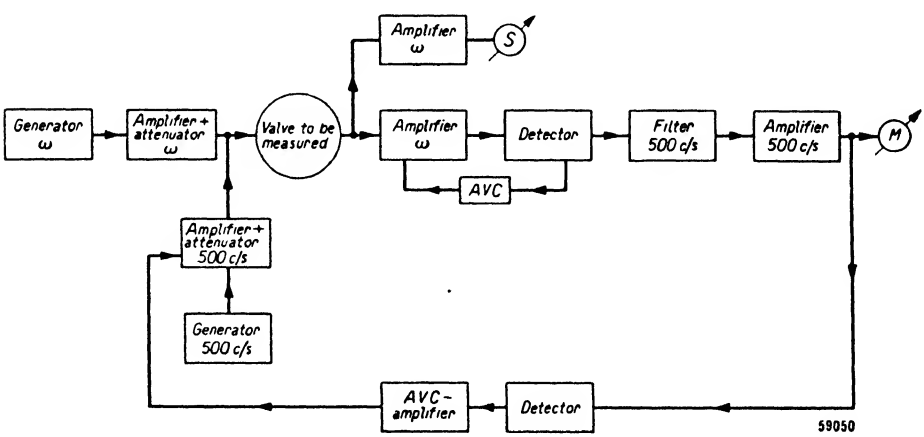

Fig. 213. Set-up for measuring the permissible hum voltage at the grid of the valve under examination, for given modulation hum.

filter tuned to 500 c/s follows the detector and this in turn is followed by an A.F. amplifier. The output voltage from this amplifier is a measure of the modulation depth of the hum.

If it is desired to plot a curve like that in fig. 201 the A.F. amplifier should be followed by another detector to which a specific bias is applied. The rectified voltage is then fed to a DC amplifier the output of which is applied as a control voltage to the amplifier following the 500-cycle generator. As a result of this very rigid control the A.F. output voltage remains constant at a level just exceeding the standing bias on the detector and corresponding to a modulation depth of say 1%. The output voltage from the amplifier fed by the 500-cycle generator is thus the required hum voltage, which in fig. 201 is shown on the vertical axis. A second amplifier, tuned to ω, is also connected after the valve and its output voltage serves to indicate the slope.

§ 4. Cross-modulation

The object of the test is to determine the depth of the interference modulation p which is impressed on the wanted carrier of frequency ω_1. To the grid of the valve under investigation two voltages are therefore applied, as shown in fig. 214:

1. a sinusoidal R.F. voltage of frequency ω_1;
2. an R.F. voltage of frequency ω_2, 30% modulated at a frequency p.

In passing through the valve the wanted carrier ω_1 becomes modulated by the modulation of the unwanted carrier. The valve is followed by the same set-up as was used in measuring modulation hum. In this case too the installation may be arranged so that the voltage necessary for 1% cross-modulation is measured at the output of the amplifier ω_2. The curve of fig. 204 was obtained in this way.

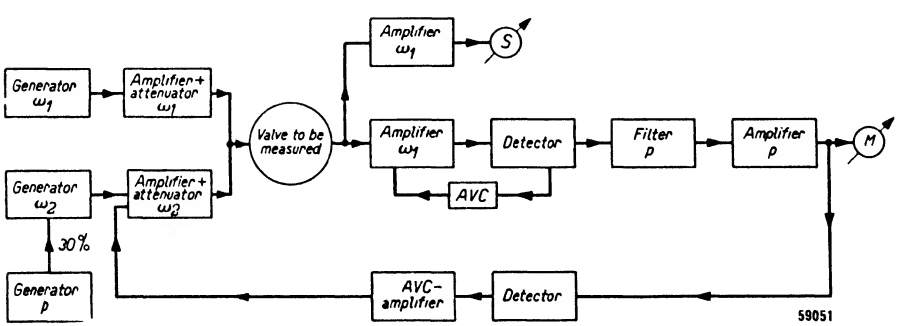

Fig. 214. Set-up for measuring the permissible interference voltage at the grid of the valve under examination, for given cross-modulation; ω_1 = wanted carrier, ω_2 = unwanted carrier, p = modulation of unwanted carrier

D. Whistles

§ 1. Introduction

Although heterodyne whistles can occur in straight receivers, it is in the superhet that they are most evident. If, in addition to the desired signal, a second frequency is present at the detector, curvature of its characteristic will give rise to the appearance, among others, of sum- and difference-frequencies. If the difference-frequency is below about 8000 c/s it will be amplified in the A.F. section and will be heard as a whistle from the loudspeaker. This will occur whether the receiver is a straight set or a superheterodyne; the difference between the two types in this respect is that with the superhet there is more chance of an interfering signal, differing little in frequency from the wanted signal, reaching the detector. In the straight set a whistle can appear only as the result of interference between carrier frequencies which differ by an audible amount. In superhets, however, the oscillator is an additional cause of whistles

When designing a superheterodyne it is necessary to bear in mind that whistles are bound to occur; in the following paragraphs, therefore, we shall deal with their various causes. The frequencies we have to consider are:

f_i = wanted signal frequency
f_h = oscillator frequency
f_o = intermediate frequency
f_s = interfering frequency

It will be evident from what follows that completely whistle-free reception over an entire waveband is unattainable. Nevertheless, by careful choice of the intermediate frequency in relation to the frequencies of local transmitters, the number of whistles can be kept low, while matters may be so arranged that such whistles as do occur interfere only with stations of minor interest in the country concerned.

We know already that if voltages with the frequencies f_i, f_s and f_h interact in the mixing valve its anode circuit will contain all kinds of combination frequencies of the form:

$$\pm m f_i \pm n f_s \pm q f_h,$$

in which m, n and q may be whole numbers or nil. Generally speaking, any combinations with higher values of m, n and q are of small amplitude. These combination frequencies may interfere with the normal intermediate frequency ($m = -1, n = 0, q = +1$) and with one another. The possibilities of interference are thus manifold, and in the following paragraphs we shall deal with the more important of them.

§ 2. $f_s = f_o$ ($m = 0, n = 1, q = 0$)

When an unwanted station transmits on a frequency differing little from the receiver's intermediate frequency a whistle will be heard if the interfering signal is sufficiently strong at the grid of the mixer. In section II A § 1 we have seen that in the anode circuit of the frequency-changer the original frequency is present, as well as the sum- and difference-frequencies. As far as the interference is concerned, therefore, the mixer functions like an ordinary R.F. amplifier. If there were no tuned circuit before the mixing valve then the interfering transmission beating with the intermediate frequency would give rise to a whistle on every station received. When the mixer is preceded by one or more signal-frequency tuned circuits the risk of this type of interference is greatest in the waveband lying closest to the intermediate frequency; the latter must therefore always be outside the broadcast bands. The generation of whistles can be minimised by providing, in addition to good pre-selection, an I.F. rejector in the aerial circuit. This may be in the form of either a series or a parallel tuned circuit, resonating at the intermediate frequency.

§ 3. $f_s = \frac{1}{2} f_o$ and $f_s = \frac{1}{3} f_o$ ($m = 0, n = 2$ or $3, q = 0$)

Transmitters using a frequency equal to about a half or a third of the intermediate frequency may also cause whistles if their second or third harmonic is strongly received, as is the case with a local station. A beat-note between the harmonic and the intermediate frequency then occurs, in the same way as was described in the preceding paragraph. Furthermore, there is the possibility that whistles will be caused by a transmission of frequency $\frac{1}{2} f_o$ or $\frac{1}{3} f_o$, through curvature of the valve characterstic introducing a harmonic close to the intermediate frequency.

§ 4. $f_s = f_i + 2 f_o$ (image frequency) ($m = 0, n = 1, q = -1$)

In Section III A § 1 we saw that the oscillator frequency is usually made higher than the signal frequency. If there were no pre-selection the required intermediate frequency could as well be provided by a signal $f_h + f_o$ as by one $f_h - f_o$. As $f_i = f_h - f_o$ is the wanted signal, we call $f_s = f_h + f_o$

the image frequency, since in relation to the oscillator frequency it is, as it were, the reflection of the desired signal frequency. If now, apart from the wanted transmission, a signal on a frequency in the neighbourhood of the image frequency reaches the grid of the mixer, a whistle will result. Clearly, such interference can be reduced by good pre-selection. The required attenuation at the image frequency is determined by the quality of the tuned circuit used, by the frequency-separation and by the relative strength of the wanted and the interfering signals. This attenuation, i.e. the relative strength, at the control grid of the mixing valve, of the wanted and the interfering signals (assuming their carrier amplitude to be the same at the aerial) is known as the image ratio of the receiver. As the image frequency differs from the wanted frequency by twice the intermediate frequency, the image ratio will improve as the intermediate frequency is increased. In practice it is found that a ratio of at least 5000 is needed to prevent second-channel interference by strong transmissions. With a low intermediate frequency (say 125 kc/s) and a coil quality Q of 50 at least two signal frequency circuits are required, and even then special measures, such as the use of an image filter, have often to be taken. Circuits of better quality naturally result in a higher image ratio, but the exigencies of tracking prevent our going very far in that direction.

As the image frequency is higher than that of the wanted transmission it is very undesirable that the resonance curve of the signal-frequency section should show a "tail" on the higher frequency side, as in the case of top-capacitive coupling (see section I D § 9). Image frequency interference is not, however, equally severe in all wavebands. If we consider only the medium and long waves we find the following situation for low (e.g. 125 kc/s) and high (e.g. 475 kc/s) intermediate frequencies.

	f_o = 125 kc/s	f_o = 475 kc/s
	interference band	interference band
medium waves: (500—1500 kc/s)	750—1750 kc/s	1450—2450 kc/s
long waves: (150—300 kc/s)	400—550 kc/s	1100—1250 kc/s

When the intermediate frequency is low it is evident that the medium-wave band is particularly subject to second-channel interference; all stations in this band on frequencies above 750 kc/s can give rise to it. There is less risk on long waves, for very few transmitters operate between 400 and

500 kc/s. The situation is more favourable with the higher intermediate frequency; there is scarcely any risk of image interference on medium waves, but on the long-wave band reception may be marred by interference from powerful transmissions between 1100 and 1250 kc/s.
It is evident in this connection that the most exacting demands are made for the signal-frequency part of the receiver when a low intermediate frequency is used. Other factors, such as cross-modulation (see A § 3 of this chapter), also have a bearing on the degree of pre-selection required.

§ 5. $\pm n f_s \mp q f_h = f_o$ ($m = 0, n \neq 0, q \neq 0$)

An interfering transmitter and the oscillator may produce harmonics which differ by about the intermediate frequency. If we denote the harmonics of the interfering signal by n and those of the oscillator voltage by q, we get the general formula:

$$\pm n f_s \mp q f_h = f_o \quad \text{(IV D 1)}$$

Therefore the frequency of the interfering transmission is:

$$\pm f_s = \frac{f_o}{n} \pm \frac{q}{n} f_h \quad \text{(IV D 2)}$$

Substituting $f_h = f_i + f_o$ we obtain:

$$\pm f_s = \frac{f_o}{n} \pm \frac{q}{n} (f_i + f_o) \quad \text{(IV D 3)}$$

or:

$$\pm \frac{f_s}{f_o} = \frac{1}{n} \pm \frac{q}{n} \left(\frac{f_i}{f_o} + 1 \right) \quad \text{(IV D 4)}$$

For any given intermediate frequency a diagram may be drawn with the aid of equation (IV D 3), from which we may at once ascertain the carrier frequencies apt to cause whistles; an example, relating to an intermediate frequency of 470 kc/s, is given in fig. 215, where along the horizontal axis we have the frequency f_i of the wanted transmission and along the vertical axis that of the interference, f_s. The numbered lines indicate whistles due to the causes tabulated on the next page.

Many of the listed whistles result from harmonics of an unwanted carrier; in practice, however, they are troublesome only when the interfering transmission is fairly strong.
To ascertain whether a particular station will cause whistles we draw a horizontal line in fig. 215 corresponding to its frequency. The intersections

Line no.	Cause of whistle	Line no.	Cause of whistle
1	$f_s = f_o$	10	$3f_s - f_h = f_o$
2	$f_s - f_h = f_o$	11	$3f_s - 2f_h = f_o$
3	$2f_s - f_h = f_o$	12	$3f_s - 3f_h = f_o$
4	$2f_s - 2f_h = f_o$	13	$f_h - 3f_s = f_o$
5	$f_h - 2f_s = f_o$	14	$2f_h - 3f_s = f_o$
6	$2f_h - f_s = f_o$	15	$3f_h - 2f_s = f_o$
7	$2f_h - 2f_s = f_o$	16	$3f_h - 3f_s = f_o$
8	$f_s - f_i = f_o$	17	$3f_s - 4f_h = f_o$
9	$f_i - f_s = f_o$	18	$4f_h - 3f_s = f_o$

of this line with the various oblique lines indicate the frequencies at which a whistle will be heard. Taking Hilversum on 995 kc/s as an example, we find that reception of the following stations will be marred by a whistle especially in the neighbourhood of the Hilversum transmitter.

a. Warsaw — 758 kc/s.

The intersection with line 7 indicates that when the receiver is tuned to 760 kc/s the intermediate frequency is produced by the second harmonics of the oscillator and of the Hilversum carrier. When Warsaw (758 kc/s) is tuned in, the frequency difference between the harmonics becomes:

$$2\,(758 + 470) - 2 \times 995 = 466 \text{ kc/s}.$$

A whistle of about 4000 c/s will therefore be heard.

b. Leipzig — 785 kc/s.

The intersection with line 11 falls at 790 kc/s (third harmonic of Hilversum and second harmonic of oscillator). On tuning in Leipzig (785 kc/s) the frequency difference becomes:

$$3 \times 995 - 2\,(785 + 470) = 475 \text{ kc/s}.$$

A whistle of about 5000 c/s will therefore be heard.

c. Northern Ireland — 1050 kc/s.

The intersection with line 3 occurs at 1050 kc/s. The second harmonic of Hilversum beats with the oscillator frequency to produce the intermediate frequency of 470 kc/s. Any small change in the oscillator frequency will accordingly give rise to a whistle.

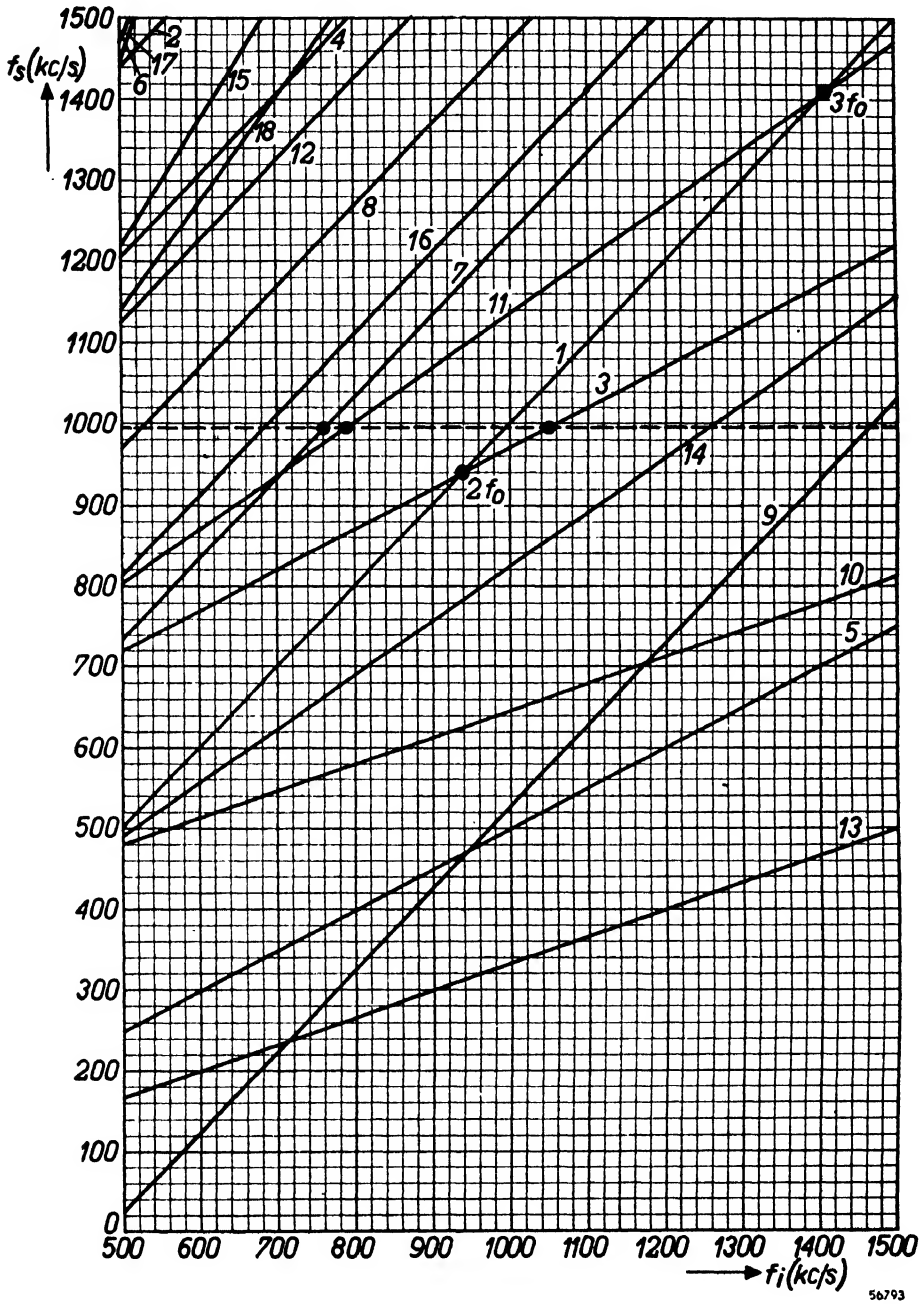

Fig. 215. Whistle diagram for an intermediate frequency of 470 kc/s. The frequency of the wanted transmission is set out along the horizontal axis and that of the interfering transmission along the vertical axis. A horizontal line corresponding to the frequency of an interfering carrier intersects the diagonals at the frequencies at which whistles are liable to be heard.

§ 6. $f_s - f_i = f_o$ ($m = -1$, $n = 1$, $q = 0$)

Normally the intermediate frequency is produced in the frequency-changer by mixing the wanted signal with the oscillator voltage, but it is clear that an interfering carrier of suitable frequency is also capable of producing the intermediate frequency if mixed with the wanted signal. In Chapter II it was shown that a fairly large heterodyne voltage was necessary for frequency-changing; only if f_s comes from a powerful local transmitter is a whistle therefore to be expected. This type of interference is indicated by line 8 in fig. 215.

§ 7. $f_s = n f_o$ or $f_i = n f_o$

These cases are rather different from those considered above. Harmonics of the intermediate frequency appear at the detector owing to curvature of the diode characteristic and can be quite strong at high inputs. By various routes, such as heater and HT leads and the AVC circuit, these harmonics reach the signal-frequency part of the receiver and give rise to whistles. As an example, if the intermediate frequency is 125 kc/s the fifth harmonic is 625 kc/s; when the receiver is tuned to Brussels (620 kc/s) the oscillator will be working at 620 + 125 = 745 kc/s, and should the fifth harmonic of the intermediate frequency reach the control grid of the mixer it will combine with the heterodyne voltage to produce a difference-frequency of 745 — 625 = 120 kc/s. A whistle of 125 — 120 kc/s = 5000 c/s will consequently be heard. For $f_i = nf_o$ these whistles can be very tiresome, sinc they appear on both sides of each station. When the receiver is accurately tuned, however, the whistle disappears, because the harmonic feedback is then of the same frequency as the original signal. Whistles due to this cause are thus readily distinguishable from other kinds.

SURVEY OF LITERATURE CHAPTER IV

1. *Ballantine, S.* and *H. A. Snow.* Reduction of distortion and cross talk in radio receivers by means of variable mu-tetrodes. Proc. I.R.E., Vol. 18 (1930) p. 2102.
2. *Beljers, H. G.* Toelaatbare niet-lineaire vervormingen bij de geluidsweergave. Tijdschr. Ned. Rad. Genootschap, No. 6 (1934).
3. *Braunmühl, H. J. von.* Neue Untersuchungen über nicht-lineare Verzerrungen. Z. techn. Physik, Vol. 15 (1934) p. 617.
4. *Bull, C. S.* Non-linear valve characteristics, a brief discussion on their use. Wirel. Engr. Vol. 10 (1933) p. 83.
5. *Carter, R. O.* Distortion in screen-grid valves with special reference to the variable conductance type. Wirel. Engr. Vol. 9 (1932) p. 123.
6. *Carter, R. O.* The theory of distortion in screen-grid valves, Wirel. Eng. Vol. 9 (1932) p. 429.
7. *Faulhaber, H.* Messungen über nicht-lineare Verzerrungen. Elektr. Nachr. Techn. Vol. 11 (1934) p. 351.
8. *Ferris, W. R.* Graphical harmonic analysis for determining modulation distortion in amplifier tubes. Proc. I.R.E. Vol. 23 (1935) p. 510.
9. *Floyd, W. F.* A note on interference tones in superheterodyne recievers. Proc. Phys. Soc. July 1933, p. 610.
10. *Heins v. d. Ven, A. J.* Modulatiebrom, modulatieverdieping, vervorming der modulatie en kruismodulatie. Radionieuws Vol. 17 (1934) p. 29.
11. *Howe G. O. W.* Second channel and harmonic reception in superheterodynes, Wireless Eng. Sept. 1934, p. 461.
12. *Kinross, R. I.* Second channel suppression, Wireless World, June 1933 p. 416.
13. *Kleen, W.* Zum Problem der linearen Kennlinie, Telefunkenröhre 10 (1938) p. 147.
14. *Kleen, W. and H. Rothe.* Verstärkungseigenschaften der H. F. Penthode, Telefunkenröhre 7 (1936) p. 109.
15. *Kleen, W.* and *K. Wilhelm.* Über Regelkennlinien, Telefunkenröhre 12 (1938) p. 1.
16. *Kniepkamp, H.* Die Abweichungen der Verstärkerröhrenkennlinien vom $e^{3/2}$-Gesetz, Telegr. u. Fernspr. Technik. Vol. 20 (1931) p. 71.
17. *Kober, C. L.* Die Berechnung von nichtlinearen Verzerrungen, Elektr. Nachr. Techn. Vol. 13 (1936) p. 336.
18. *Langley, R. H.* Undesired responses in superheterodynes, Electronics May 1931, p. 618.
19. *Lucas, G. S. C.* Distortion in valve characteristics, Wireless Eng. Vol. 8 (1931), p. 595 and 660.
20. *Morgan, H. K.* Interfering responses in superheterodynes. Proc. I.R.E. Vol. 23 (1935), p. 1164.
21. *Scroggie, M. G.* Superheterodyne whistles, Wireless World, Sept. 1936 p. 302.
22. *Strutt, M. J. O.* Whistling notes in superheterodyne receivers, Wireless Eng. Vol. 12 (1935), p. 194.
23. *Strutt, M. J. O.* Verzerrungseffekte bei Mischröhren, Zeitschr.f. H. F. Technik, Vol. 49 (1937) p. 20.
24. *Wheeler, H. A.* Image suppression in superheterodyne receivers, Proc. I.R.E. June 1935, p. 569.
25. *Wilhelm, K.* Die Röhre im Rundfunkempfänger. III. Die Mehrdeutigkeiten in der Mischröhre. Telefunkenröhre 6 (1936) p. 58.

V. DETECTION

A. Detector circuits

§ 1. Introduction

In order to separate the modulation from the carrier, the R.F. or I.F. voltage must be rectified and smoothed; a current or voltage is thereby obtained which fluctuates with the original modulation. Speaking very generally, rectification is achieved by the use of a circuit element having a curved characteristic, and when an alternating voltage is applied to such an element an increase in the mean current occurs. If the characteristic is represented by a power series of v.

$$i = I_o + \alpha v + \beta v^2 + \ldots = I_o + \alpha V \sin \omega t + \beta V^2 \sin^2 \omega t + \ldots \ldots$$
$$= I_o + \alpha V \sin \omega t - \tfrac{1}{2} \beta V^2 \cos 2\omega t + \tfrac{1}{2} \beta V^2 + \ldots$$

then we see at once that the direct current I_o increases by an amount $\frac{1}{2} \beta V^2$. Several kinds of non-linear elements are available: metal rectifiers, diodes, triodes and multigrid valves. Of these alternatives the diode is most used in radio receivers, and it will be dealt with separately in V B.

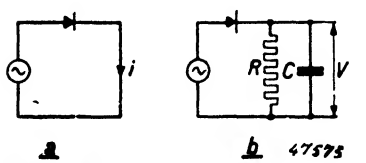

Fig. 216a. Basic rectifier circuit.
b. Fig. a with the addition of an RC-load, from which the rectified voltage may be taken.

Fig. 216a illustrates the most primitive rectifier circuit. As the relation between the mean current and the applied alternating voltage is in this case not linear, but roughly quadratic, the rectification is commonly called square-law detection, though, strictly speaking, this expression is correct only when the rectifier has a pure quadratic characteristic. Usually the equation for the rectified current includes terms higher than the square.

In practice the circuit of fig. 216a is meaningless, because a voltage, not a current, is needed if the modulation is to be amplified.

In fig. 216b the original circuit is modified by the addition of a resistance R, the voltage across which can be amplified. The resistance is bridged by a capacitance C, which smooths the remaining R.F. ripple and improves

efficiency. In the rectification circuit the DC output voltage appears in series with the applied alternating voltage; this circumstance has in the case of most rectifiers the favourable result that the relation between the DC and the AC voltages approximates to a direct proportion, the more so as the input voltage is increased. We then speak of "linear detection". Such detection may be described roughly as follows. As the signal increases, the traversed part of the characteristic of a diode, and also that of a metal rectifier, approaches more and more the characteristic of an ideal rectifier, that is to say, an element which for one direction of current has a certain resistance R and for the other direction acts as an insulator. With indirectly heated diodes the AC resistance R_i in the cathode-to-anode direction quickly falls to a small fraction of the external resistance R. For that reason the capacitance C becomes loaded almost to the peak voltage during the first cycle, and thereafter the charge, which is continuously draining away through R, is replenished at the peak of the successive cycle. For alternating voltages above a certain minimum, the DC voltage across C thus remains equal to the input amplitude and the relation is linear.

In the foregoing case we speak of "peak detection". That the voltage across C should equal the peak input is not, however, essential for linear rectification. There are detectors, including some directly-heated diodes, in which R_i falls with an increasing signal but only to a certain limit. An equilibrium between the charging through R_i and the discharging through R is then reached, at which the voltage across C remains below the input amplitude. Nevertheless there is still a linear relation between the AC and DC voltages over a large range. But we can no longer speak of peak detection. When the arrangements of figs 216a and 216b are employed with simple two-electrode rectifiers, the alternating voltage gives rise to a current in the rectifier circuit, and the R.F. or I.F. voltage-source is loaded. It is possible, however, to use a valve as a non-linear element, the alternating voltage being fed to a control electrode in such a way that no current is drawn from the source. We then get fig. 217a, in which of, course, the triode may be replaced by a tetrode or pentode. This circuit is entirely comparable with fig. 216a, but in this case the rectified voltage may be taken from a resistance in the anode circuit, without affecting the working point on the detection characteristic. In general, therefore, this so-called anode-bend detection is not linear. There is, however, no fundamental reason why anode

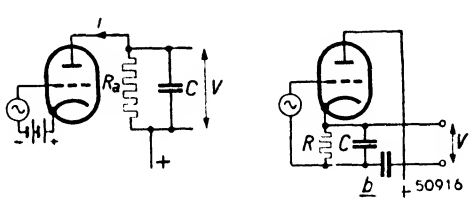

Fig. 217a. Non-linear anode detector.
b. Anode detector with automatic bias giving practically linear detection.

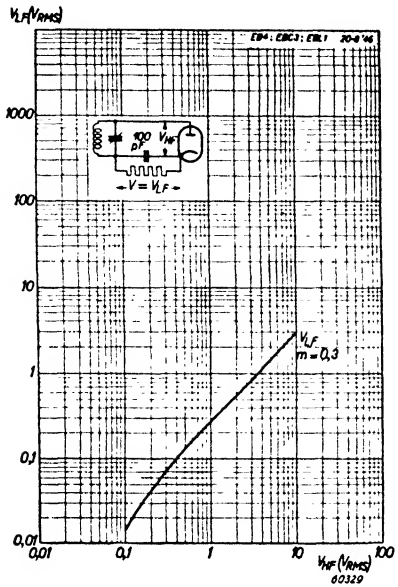

Fig. 218. Detection characteristic of a diode (L.F. RMS voltage against the 30%-modulated R.F. input).

rectification should be non-linear; the circuit may be rearranged on the lines of fig. 216b, and we then get fig. 217b. If the cathode resistance R is high enough the resultant automatic bias reduces anode current virtually to nil in the absence of a signal. When a signal is present even the small rise in current appreciably raises the bias on the control grid, and consequently anode current flows only at the positive peak of the cycle. The mean voltage across C keeps in step with the input and the relation is constant; as in the case of the circuit given in fig. 216b, we may therefore speak of linear detection.

§ 2. Diode detection

Although diode detection will be dealt with exhaustively in V B, we shall briefly refer to its salient properties here in order to facilitate comparison with other methods of rectification. As already mentioned, detection is linear with a sufficiently large signal, the minimum being about 0.5—1 V. Above this level linearity is not impaired until the diode becomes saturated, but input should not be permitted to reach this level.

Since the rectified voltage is almost equal, over the whole range, to the amplitude of the alternating voltage, it is simple to calculate the "gain" of the detector stage, or more properly its transmission; by this expression we mean the ratio of the RMS value of the A.F. voltage to the RMS value of the R.F. or I.F. voltage, for a signal modulated to a depth of 30%. In the circumstances mentioned the gain would be about 0.3, as may readily be confirmed from published curves (see for example fig. 218). The diode may be used in two different ways, illustrated in fig. 219. With the circuit of 219a the A.F. voltage has only a very small I.F. or R.F. ripple superimposed if the smoothing

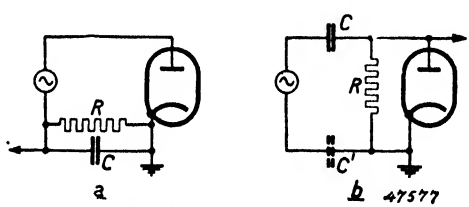

Fig. 219. Diode detector: a. with series load resistance; b. with parallel load resistance.

capacitance is sufficiently large, and this is of course a great advantage. Moreover, the damping of the preceding tuned circuit is less than with the circuit of 219b, which also suffers from the drawback that the full R.F. or I.F. voltage is present with the A.F. voltage and must be filtered off. The arrangement of fig. 219b is employed, for example, when the preceding tuned circuit is earthed at one side, either directly or through the HT supply; this is the case with most straight receivers. The circuit is used also where it is essential that there should be no direct connection between the A.F. amplifier and the R.F. or I.F. circuit, or if the latter is connected directly to the anode of the previous amplifying valve and thus to the HT source. A blocking capacitor C' may then be included; if this is large in relation to C, these two form a potential divider and prevent any A.F. voltage appearing across the tuned circuit.

This circuit imposes more damping than that of fig. 219a; the preceding circuit has to supply not only the current pulses through the diode but also an alternating current through R. Whereas for large signals the equivalent resistance in fig. 219a is equal to $\frac{1}{2}R$, in the circuit of fig. 219b the damping is:

$$R_{HF} = \tfrac{1}{2}R // R = \frac{1}{3}R \quad \ldots\ldots\ldots\ldots \quad \text{(V A 1)}$$

In modern superheterodynes the detector is usually preceded by an I.F. bandpass filter, the secondary of which is isolated from the primary; the circuit of fig. 219a is then normally used. In the earlier straight receivers the detector stage often followed a tuned-anode circuit connected directly to the anode of the R.F. amplifier, and the circuit of fig. 219b was therefore employed unless separation of the two stages was provided by a special secondary winding

For the method of detection described here it is not essential to use a diode. A metal rectifier will serve, but the properties of the metal rectifiers so far available are not equal to those of a normal diode. The characteristic does not so closely approach that of the ideal rectifier, and transmission is poor; furthermore, metal rectifiers have a rather high, and sometimes varying, input capacitance and a lower damping resistance.

The applications of these rectifiers are consequently limited and they will not be considered further; the same is true of crystal detectors.

§ 3. Grid detection

The grid detector circuit is a combination of a diode rectifier and an A.F. amplifier in one valve, and follows from fig. 219b if the control grid and the cathode of an amplifying valve are used as a diode. Since the A.F. voltage also appears at the grid, amplification is at once possible. We thus have the

circuit of fig. 220; here the anode load, across which the A.F. voltage is developed, is bridged by a capacitance in order to suppress the R.F. and I.F. component still present. In many receivers advantage is taken of the presence of this high-frequency component in the anode current to feed energy back to the preceding tuned circuit and thereby reduce damping. Such an arrangement, grid detector with reaction, is commonly employed in small local-station receivers.

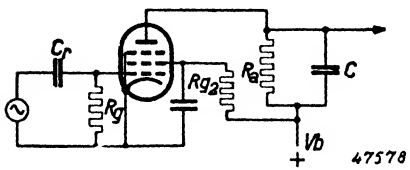

Fig. 220. Pentode as grid detector.

If a pentode is used in the circuit of fig. 220, fairly high A.F. gain, say 100 to 200 times, may be obtained. For an A.F. output of several volts, sufficient fully to load a high-slope output valve, only a quite small R.F. input to the grid is necessary and rectification at such a level is quadratic. It is therefore not possible to specify the gain given by the circuit, though we may quote the R.F. voltages needed for various levels of A.F. output. The table below provides some figures for the EF 6, a valve commonly used as a grid detector. The anode load is 0.2 MΩ while the screen-grid resistance is made 0.6 MΩ in order that the screen-grid voltage shall not exceed the anode voltage. The A.F. voltages shown are those necessary for standard output (50 mW) from the EL 3, EL 5 and EL 2 pentodes respectively, and a modulation depth of 30% is assumed.

Output valve	EL 3	EL 5	EL 2	max.
V_i (R.F. or I.F.)	0.035 V	0.043 V	0.063 V	appr. 1.5
V_o (A.F.)	0.35 V	0.5 V	0.9 V	19

It is clear from the first three columns that the output increases faster than the input voltage, indicating that at these low signal levels the rectification is still roughly quadratic. The fourth column shows the maximum obtainable A.F. output. Thus, as the R.F. input rises a point is reached at which detection is linear, and beyond that the A.F. voltage increases less than proportionately; 19 V is the limiting output (fig. 221). With increasing R.F. input the grid acquires a larger negative bias as a result of rectification of the carrier, and the working point of the valve is shifted towards the bottom bend of the i_a/v_g characteristic. In consequence, A.F. amplification falls off and, furthermore, anode rectification supervenes.

In its effect, anode-bend detection is the opposite of grid rectification: the first causes mean anode current to rise, the second reduces it. With an increasing signal the A.F. voltage becomes the resultant of the two effects, anode rectification finally gaining the upper hand and causing the curve in fig. 221 to pass its peak. This limitation, present in all grid detectors, led to the use of valves with a large cut-off voltage, in which anode rectification occurred only with a high R.F. input; these were referred to as "power-grid detectors". This solution was soon abandoned, however, in favour of complete separation of the functions of detector and A.F. amplifier. Multiple valves combining a diode and an amplifier were introduced in diverse types, all of which operate in a circuit like that of fig. 219.

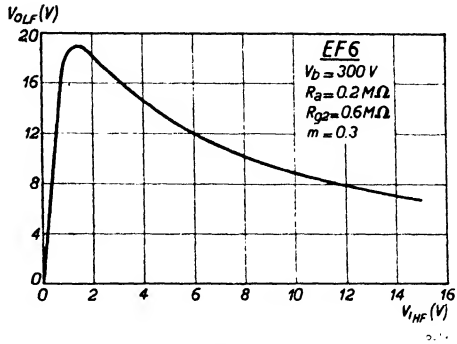

Fig. 221. A.F. output voltage as a function of R.F. input modulated 30%, for an EF 6 in the circuit of fig. 220.

For very simple receivers, however, the grid detector remains an attractive solution despite its lack of linearity.

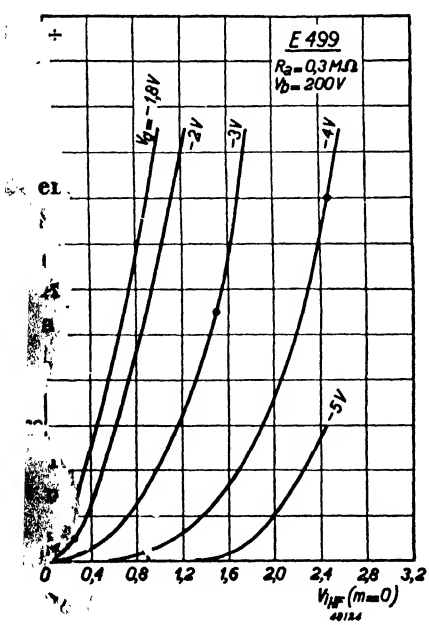

Fig. 222. Change of anode voltage ΔV_a as a function of the unmodulated R.F. input voltage, for various values of grid bias, for the Philips diode E 499 connected as an anode-bend detector.

§ 4. Anode detection

The anode-bend detector is used in straight receivers when high selectivity is required, for it imposes only light damping on the tuned circuit, but this advantage is gained at the cost of non-linear rectification. The best result is obtained by employing a valve with a marked bend in its i_a/v_g characteristic, the co-efficient of the quadratic term being then high, and in particular by adjusting the bias so that the valve works at the point of greatest curvature.

Moreover the AC resistance of the valve should be high, in order that the A.F. current variations in the anode circuit shall produce large voltage variations. A valve formerly used for this application

was the Philips E 499, a triode with $\mu = 100$; the operating conditions for a supply voltage of 200 V were: $R_a = 0.3$ MΩ and $V_{gmed} = -1.8$ V. Fig. 222 reproduces curves for various values of grid bias, relating unmodulated input voltage and change of anode voltage. It will be noticed that all curves show a practically quadratic trend. By taking a specific carrier amplitude and imagining a 30% variation, we can calculate from these curves the amplification yielded by the detector with the given input. If the signal voltage is so large as to exceed the negative bias, grid current flows and the advantage of this form of detection is lost. The anode rectifier can thus, like the grid detector, accept only a limited input. If the grid is directly connected to the tuned circuit, grid current imposes on the latter a discontinuous, heavy load which will strongly distort the A.F. voltage. On the other hand, if the grid is joined to the tuned circuit through a capacitor and leak, grid rectification will occur in opposition to the anode rectification, and a detector characteristic of the form seen in fig. 221 will result.

Grid current may be prevented by substituting automatic for fixed bias, a resistor shunted by a large capacitor being inserted in the cathode lead; bias then increases with signal strength. The detector adjusts itself continuously to new working points as input becomes greater, and with a bias resistor of 16 000 Ω these are as indicated in fig. 222 on the curves for —2, —3 and —4 V. It is evident that at large inputs detection is less effective with automatic than with fixed bias, and also that there is a risk of grid current occurring. With a signal of 2.4 V and 30% modulation, for example, voltage peaks of $2.4\sqrt{2} \times 1.3 = 4.3$ V appear at the grid, while the bias is only —4 V.

On the whole we may conclude that in broadcast receivers anode detection has more drawbacks than advantages; in consequence, present-day valve types are not recommended for this application.

§ 5. Linear anode detection

From the data already given for the anode detector it is evident that this form of rectifier is scarcely to be considered for radio receivers; in measuring instruments, however, it has its uses.

The circuit given in fig. 217b is actually an anode rectifier with the coupling resistor transferred to the cathode lead. It differs from the anode detector with automatic bias in having a cathode resistor of much higher value and a smaller parallel capacitor. The charge on the capacitor must be able to follow the modulation. If the cathode resistor R is sufficiently large the anode current is almost nil in the absence of a signal, and such a working point (A in fig. 223) is fairly favourable for anode rectification. On an alter-

nating voltage being applied to the grid, anode current rises. The voltage across R increases at the same time and the valve therefore receives a higher negative bias (point B). This increase of bias can never exceed the amplitude of the signal, for no rise in anode current could then occur. A state of balance is therefore reached in which the negative bias, having increased from A to B, is just maintained by the passage through R of the positive current pulses. The greater R is, the smaller the pulses needed to maintain the bias, and the more nearly the rise of voltage across R approaches the maximum, namely the amplitude of the signal.

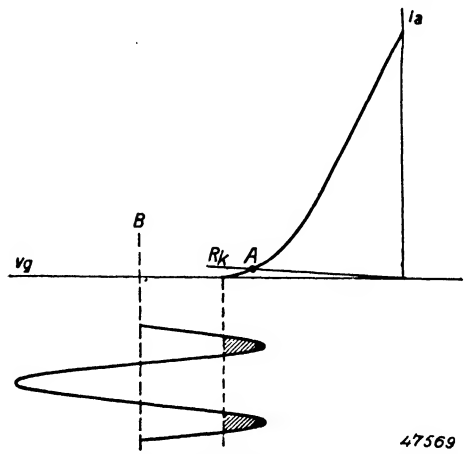

Fig. 223. i_a/v_g characteristic with load-line for the cathode resistance R_k. The pulses of current which flow in correspondence with the positive voltage peaks produce the required negative bias across the resistance R_k.

Detection at point A is never perfect and with a small input is poor. The rectifier becomes linear only when a certain amplitude is exceeded. With very high inputs, however, the voltage pulses to the right of point A become so large (though always small in relation to the amplitude) that grid current flows. If it is to be linear, and also to impose no damping, this kind of detector must therefore be operated only over a certain range of amplitude. Freedom from damping is not secured at very high frequencies, for other factors then supervene.

Some measurements were made on an EBC 3 connected as an infinite impedance detector. With a cathode load of $R = 0.1$ MΩ grid current began to flow when the amplitude of a carrier modulated 90% reached 40 V_{RMS}; for a load of 0.5 MΩ the limiting input was 50 V_{RMS}. In both cases the sinusoidal modulation was distorted less than 1%.

The departure from linear rectification is clearly seen in the following table, which shows the A.F. output as a function of the grid signal for various conditions; the figures refer to a cathode load of 0.5 MΩ.

A serious practical disadvantage of this circuit is the very high resistance in the cathode lead. In measuring apparatus the resultant difficulties are perhaps less troublesome than in receiving equipment, and special measures may be taken to overcome them.

Carrier V_{RMS}	$m = 0.9$		$m = 0.3$	
	A.F. voltage V_{RMS}	Distortion %	A.F. voltage V_{RMS}	Distortion %
1.5	0.9	14	—	—
2	1.3	10	0.44	2.5
3	2.2	7	0.7	1.1
4	3.0	5.6	1.0	1
7	5.5	2.7	1.8	1
10	7.5	2.0	2 5	1
15	13.4	1.4	4.4	1
20	17	1.1	5.6	1

B. Diode detection

§ 1. Basic equations for diode rectification

We have seen that of the detectors available the diode is the most satisfactory for broadcast receivers.

With the circuit of fig. 224, in which the resistance R may be in parallel with either the capacitance C or the diode, we find that, on rectification of an unmodulated signal $v = V_{HF} \cos \omega t$, a steady voltage $V=$ appears across R. The diode is subjected to both voltages simultaneously. For the moment the origin of the steady voltage $V=$ will be left out of consideration, its presence being taken for granted.

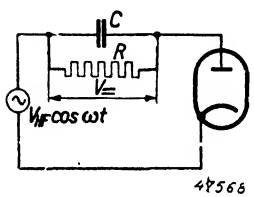

Fig. 224. Diode detector circuit; the R.F. carrier $V_{HF} \cos \omega t$ is rectified, giving rise to a steady voltage $V=$ across the resistance R.

For the small currents usually met with in diode detection the following relation between diode current and voltage holds good:

$$i = A\, \varepsilon^{\frac{v_a}{V_T}} \quad \ldots\ldots\ldots \quad \text{(V B 1)}$$

in which:

i = the diode current for an anode voltage v_a;

A = the diode current for an anode voltage of 0 V;

V_T = a constant, the so-called temperature voltage, which for most diodes is about 0.1 V;

ε = the base of the natural logarithm = 2.72.

This relation holds for most diodes if the anode current does not exceed about 100 μA; a measured curve is given in fig. 225. A in equation (V B 1) is a fictitious value, namely the current which would flow if the equation held good at $v_a = 0$ V. In the case of fig. 225 A is therefore 3.7 mA,

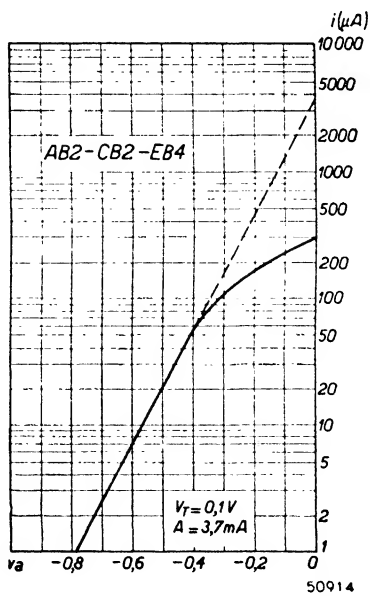

Fig. 225. Diode current as a function of the applied voltage.

and not 0.3 mA, the actual current at zero volts. As the voltage at the anode is composed of a steady voltage $V=$ and an alternating voltage $V_{HF} \cos \omega t$, we can write for equation (V B I):

$$i = A\varepsilon^{\frac{V_{HF}}{V_T}\cos \omega t + \frac{V=}{V_T}} \quad \ldots\ldots\ldots\ldots \quad \text{(V B 2)}$$

The mean current through the diode may be found by integrating i over a whole cycle, and we get:

$$I_{med} = \frac{1}{2\pi}\int_0^{2\pi} i \, d\omega t = \frac{A\varepsilon^{\frac{V=}{V_T}}}{2\pi}\int_0^{2\pi} \varepsilon^{\frac{V_{HF}}{V_T}\cos \omega t} \, d\omega t \quad \ldots\ldots\ldots \quad \text{(V B 3)}$$

If we call the expression $\frac{1}{2\pi}\int_0^{2\pi} \varepsilon^{\frac{V_{HF}}{V_T}\cos \omega t} \, d\omega t$,

which cannot be further simplified, B_0, the mean diode current then becomes:

$$I_{med} = A\varepsilon^{\frac{V=}{V_T}} B_0 \quad \ldots\ldots\ldots\ldots \quad \text{(V B 4)}$$

The value of B_0 for various values of V_{HF}/V_T is indicated in the following table *:

$\frac{V_{HT}}{V_T}$	B_0	$\frac{V_{HF}}{V_T}$	B_0	$\frac{V_{HF}}{V_T}$	B_0
0	1.0	1.4	1.55	6	67
0.1	1.0025	2.0	2.28	7	168
0.2	1.01	2.5	3.29	8	427
0.3	1.02	3.0	4.88	9	1094
0.5	1.06	3.5	7.4	10	2816
0.7	1.13	4.0	11.0		
1.0	1.27	5.0	27.0		

For values of $V_{HF}/V_T < 1$ we can write as an approximation

$$B_0 = 1 + \left(\tfrac{1}{2}\frac{V_{HF}}{V_T}\right)^2 \quad \ldots\ldots\ldots\ldots \quad \text{(V B 5)}$$

* B_0 is a Bessel function of zero order; its value can be found in function tables as e.g. those of Jahnke and Emde).

When $V_{HF}/V_T = 1$ the error due to this approximation is about 1.3%. For values of $V_{HF}/V_T \gg 1$ the following approximation may be made:

$$B_o = \frac{1}{\sqrt{2\pi \frac{V_{HF}}{V_T}}} \varepsilon^{\frac{V_{HF}}{V_T}} \quad \ldots\ldots\ldots \quad \text{(V B 6)}$$

The error in this case is about 5% when $V_{HF}/V_T = 3$ and less than 1% when $V_{HF}/V_T > 5$.

In fig. 226 I_{med} is given as a function of $V =$ for various values of V_{HF}. These measured curves agree with the calculated curves for $V_T = 0.1$ V and $A = 3.7$ mA. It is still necessary to confirm that the assumed steady voltage is in fact provided by the voltage drop across the leak R, in order

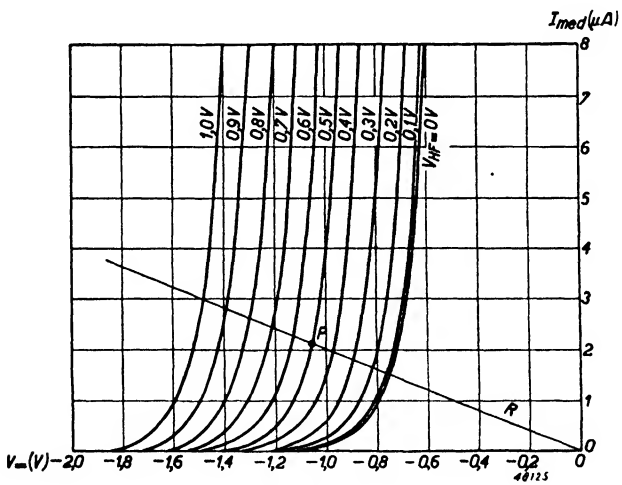

Fig. 226. Mean diode current I_{med} as a function of the negative voltage $V=$, for small values of the R.F. voltage V_{HF}.

that the current I_{med} shall satisfy not only equation (V B 4) but also:

$$V_{=} = I_{med} R \quad \ldots\ldots\ldots\ldots\ldots \quad \text{(V B 7)}$$

In fig. 226 this relation for $R = 0.5$ MΩ is represented by the straight line OP, and the point P indicates the value of I_{med} for a leak of 0.5 MΩ and an R.F. input of 0.5 V. From equations (V B 4) and (V B 7) we then get:

$$V_{=} = -A R \varepsilon^{\frac{V_{=}}{V_T}} B_o \quad \ldots\ldots\ldots \quad \text{(V B 8)}$$

If we write for $V_{\overline{}}$:

$$V_{\overline{}} = V_r + \Delta V,$$

V_r being the voltage drop in the resistance R in the absence of a signal and ΔV the rise of voltage due to rectification, equation (V B 8) then becomes:

$$V_{\overline{}} = V_r + \Delta V = -AR\,\varepsilon^{\frac{V_r + \Delta V}{V_T}} B_o \quad \text{(V B 9)}$$

When $V_{HF} = 0$, $B_o = 1$ and then:

$$V_r = -AR\,\varepsilon^{\frac{V_r}{V_T}}$$

Equation (V B 9) may accordingly be written:

$$V_r + \Delta V = V_r\,\varepsilon^{\frac{\Delta V}{V_T}} B_o \quad \text{(V B 10)}$$

or:

$$1 + \frac{\Delta V}{V_r} = \varepsilon^{\frac{\Delta V}{V_T}} B_o \quad \text{(V B 11)}$$

From this expression ΔV can be calculated. We shall make the calculation for two extreme cases, for a very small signal ($V_{HF} < 0.03$ V) and for a very large one ($V_{HF} > 1$ V).

§ 2. Rectification of a very weak signal

For the case that $V_{HF} \ll V_T$ (for instance $V_{HF} < 0.03$ V) equation (V B 5) holds good, and consequently equation (V B 11) becomes:

$$1 + \frac{\Delta V}{V_r} = \varepsilon^{\frac{\Delta V}{V_T}} \left(1 + \frac{V_{HF}^2}{4 V_T^2}\right) \quad \text{(V B 12)}$$

If V_{HF} is small, ΔV will also be small in relation to V_T, and approximately:

$$\varepsilon^{\frac{\Delta V}{V_T}} = 1 + \frac{\Delta V}{V_T}.$$

Equation (V B 12) then becomes:

$$1 + \frac{\Delta V}{V_r} = \left(1 + \frac{\Delta V}{V_T}\right)\left(1 + \frac{V_{HF}^2}{4 V_T^2}\right)$$

or, approximately:

$$\frac{\Delta V}{V_r} = \frac{\Delta V}{V_T} + \frac{V_{HF}^2}{4 V_T^2}$$

from which we obtain:

$$\Delta V = -\frac{1}{4}\frac{V_{HF}^2}{V_T}\frac{1}{1-\frac{V_T}{V_r}} \quad \text{(V B 13)}$$

From this equation we may conclude that when the signal is very small ($V_{HF} \ll V_T$) the change of DC voltage across the resistance due to rectification is proportional to the square of the amplitude of the signal. We can therefore write, more shortly:

$$\Delta V = k V_{HF}^2,$$

where:

$$k = -\frac{1}{4}\frac{1}{V_T}\frac{1}{1-\frac{V_T}{V_r}}.$$

We reach the same conclusion if we begin from the characteristic for $V_{HF} = 0$ V in fig. 240 page 378. The position of the working point is given by the intersection of the various curves with the load line.
The increase of V_- for an R.F. signal of 0.2 V (intersection point S) is about four times as great as that for an input of 0.1 V (point P), and ΔV is thus proportional to V_{HF}^2.

§ 3. Rectification of a strong R.F. signal

When $V_{HF} > 1$ V equation (V B 6) is approximately true. Substituting it in equation (V B 11) gives us:

$$1 + \frac{\Delta V}{V_r} = \frac{1}{\sqrt{2\pi\frac{V_{HF}}{V_T}}}\varepsilon^{\frac{\Delta V}{V_T}+\frac{V_{HF}}{V_T}} \quad \text{(V B 14)}$$

or, using natural logarithm:

$$ln\left(1+\frac{\Delta V}{V_r}\right) = \frac{V_{HF}}{V_T} + \frac{\Delta V}{V_T} - \tfrac{1}{2}\, ln\, 2\pi\frac{V_{HF}}{V_T} \quad \text{(V B 15)}$$

For high values of V_{HF}/V_T (> 10), V_{HF}/V_T and $\Delta V/V_T$ are large in relation to both logarithmic terms, so that equation (V B 15) becomes:

$$0 = \frac{V_{HF}}{V_T} + \frac{\Delta V}{V_T}$$

or:

$$\Delta V = -V_{HF}. \quad \text{(V B 16)}$$

The change of DC voltage across the load resistance is equal to the amplitude of the R.F. voltage, and detection is therefore linear. The same conclusion is reached if we regard the action of the diode in the following way. Owing to the strong signal the anode receives a large negative bias from the charged capacitor, and in consequence the diode is practically non-conducting for the greater part of the cycle. As the resistance of the leak is so high that only a negligible fraction of the charge drains away during this non-conducting phase, the capacitor becomes charged to the peak value of the R.F. voltage.

§ 4. Practical example of detection curve

For an R.F. signal of amplitude between 0.03 and 1 V, which are limits commonly found in practice, the equation derived in B § 2, (V B 11), would have to be used. It would be necessary, however, to ascertain B_o from a table for every separate case. A more convenient method is to prepare curves relating to normal conditions and showing $V_{=}$ and ΔV as functions of V_{HF}. Those given in fig. 227 refer to a load of 0.5 MΩ, a common value. As the valves concerned all have indirectly heated cathodes of the same type, and therefore have a similar temperature-voltage V_T, the curves of fig. 227 are applicable to many diodes, the AB 1 for example, as well as the EB 4, EBC 33, UAF 42, etc.

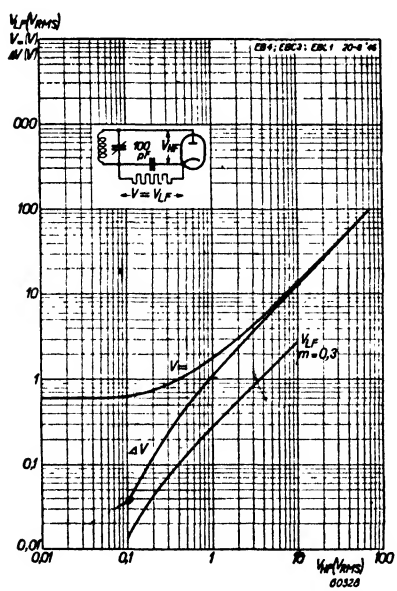

Fig. 227. Standing voltage $V_{=}$, and increase thereof ΔV, across the load resistance R (= 0.5 megohm) of an indirectly-heated diode, as a function of the unmodulated R.F. voltage V_{HF}. Also the A.F. output V_{LF} as a function of the 30%-modulated R.F. voltage.

To ascertain the A.F. voltage yielded by the circuit of fig. 227 when the carrier V_{HF} is modulated we can use the curve for ΔV. As V_{HF} varies between the limits set by the modulation depth, we observe the corresponding variation of ΔV. The standard modulation for receiver measurements and calculations is 30%, and it is on this percentage that the curve in fig. 227 connecting A.F. output with R.F. input V_{HF} is based. Actually is it not quite correct to use this V_{LF} curve. In nearly all circuits the grid leak of the following valve is connected, via a coupling capacitor, in parallel with the diode

load. In consequence the diode circuit is not loaded to the same degree for A.F. voltages as for the steady voltage, i.e. $R_w \neq R_g$. The magnitude of the A.F. voltage in such a case may be determined from the characteristics given in fig. 226 and is found to be rather lower than the curve of fig. 227 would indicate; it depends, in fact, on the value of R_w.

The extent of the divergence may be ascertained from fig. 228, which repro-

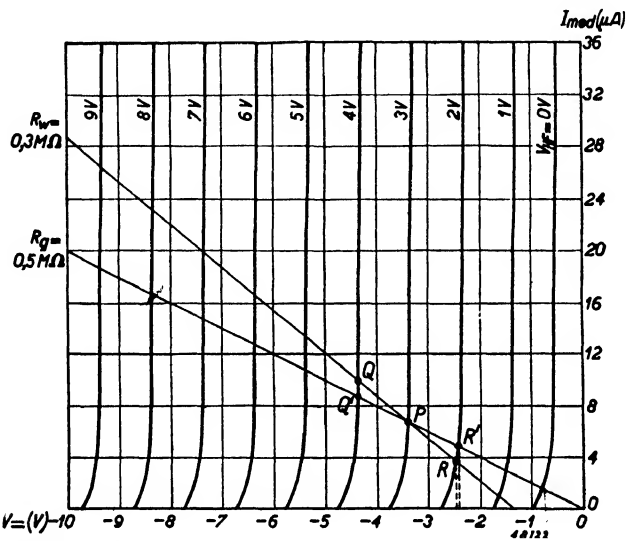

Fig. 228. Mean diode current I_{med} as a function of the standing negative voltage $V_{=}$, for various values of the R.F. voltage V_{HF}.

duces curves similar to those of fig. 226, but for large inputs. The magnitude of the voltage $V_{=}$, obtained with a given carrier (say 3 V) and a load $R_g = 0.5$ MΩ, is indicated, as already mentioned, by the intersection of the load line R_g with the curve for $V_{HF} = 3$ V. If I_{med} now varies, as a result of modulation, the corresponding variation of $V_{=}$ is determined no longer by the line $R_g = 0.5$ MΩ but by a line $R_w = 0.3$ MΩ, R_w being the resultant of $R_g = 0.5$ MΩ and the grid leak of the following valve, for example 0.7 MΩ. The line R_w is now drawn through the static working point at such an angle that a rise in I_{med} of 1 μA corresponds to an increase ΔV of 0.3 V.

When V_{HF} fluctuates due to modulation, the variations of $V_{=}$ and I_{med} are determined both by the curve for the value of V_{HF} in question and by the newly found load line R_w; from their intersections the variations may be ascertained.

For a carrier $V_{HF} = 3$ V the value of $V_{=}$ is given by the intersection of the line R_g and the curve for 3 V. If V_{HF}, being modulated 33.3 %, now

varies from 2 V to 4 V, the limiting values of $V_{\underline{\underline{\ }}}$ are found from the intersections of R_w with the curves concerned.

Fig. 228 shows that owing to the steep slope of the V_{HF} curves the variation of $V_{\underline{\underline{\ }}}$ is extremely small when the AC load R_w differs only a little from the DC load R_g; the difference may normally be ignored.

§ 5. Effect on diode detection of the reservoir capacitance and load resistance

In B §§ 3 and 4 the conditions were idealised and no account was taken of the values of the resistance R or of the capacitance C in fig. 224; in practice, however, they have a marked influence.

When R is comparatively low, instantaneous values of i occur which no longer conform to the exponential diode characteristic of equation (V B 1) seen in fig. 225, but approximate to a characteristic of the form:

$$i = \frac{v_a}{R_i} \quad \ldots\ldots\ldots\ldots\ldots\ldots \quad \text{(V B 17)}$$

The exponential part of the curve lying to the left of the vertical axis is now of less importance, the influence of the current, roughly indicated by equation (V B 17), which flows when the diode anode becomes positive, now being predominant. (That positive voltages appear is evident from fig. 228.)

This type of rectification is also met with in mains rectifiers and in oscillator circuits (see Chapter II). Here it will suffice to observe that the rectified voltage is proportional to the alternating input voltage but is of smaller amplitude than V_{HF}; the ratio $\Delta V / V_{HF}$ now has a fixed relationship with the ratio R_g/R_i, and the smaller the latter the smaller ΔV is in relation to V_{HF}. The relationship is clearly illustrated in the right half of fig. 229, when we find various ratios $\Delta V / V_{HF}$ depending on the parameter R_g/R_i. The influence of R_g becomes important in directly-heated battery diodes, with which the deviation from the exponential characteristic begins sooner than with indirectly-heated types.

The effect of the capacitance C received little notice in B §§ 3 and 4, because it was supposed that only a steady voltage ΔV appeared across the combination RC and that C was large enough to suppress R.F. ripple.

There are special cases, however, the rectification of the AVC voltage for instance, in which C is for particular reasons made fairly small. The ripple voltage across C, which can then no longer be neglected, must be denoted by a third term in the ε-power of equation (V B 2); in this term i again appears.

The calculation of the steady voltage $V_{\underline{\underline{\ }}}$ now becomes so complicated, how-

ever, that it is better to use data derived from measurements. At low values of C the RC impedance of the rectifier circuit rises and both the mean current I_{med} and the voltage $V_{=}$ therefore fall. The reactance $1/\omega C$ must, however, be considered in relation to R_g, and the quantity $R_g\,\omega C$ is thus a measure of the voltage drop (see also Chapter IX). Experiment confirms this. It is accordingly useful to plot the relation $\frac{\Delta V}{V_{HF}}$ of fig. 229 not only for different values of R_g/R_i but as a function of $R_g\omega C$ as well.

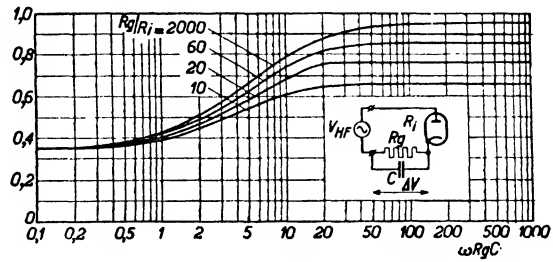

Fig. 229. $\Delta V/V_{HF}$ as a function of ωRgC for various values of Rg/Ri, with series-connected load resistance.

The curves thus obtained all approach the value $1/\pi$ at low values of C or of ω, the mean voltage across R_g unshunted by capacitance being $\frac{V_{HF}}{\pi}$ when R_i is small compared with R_g. It is also apparent from these curves that in normal circumstances this voltage decrease is negligible. For example, in a detector circuit with $R_g = 0.5$ MΩ and $C = 100$ pF, at a frequency of 125 kc/s $\omega = 10^6$ and ωCR_g is accordingly equal to 50.

But in the AVC diode circuit C may be only a tenth of the foregoing value, and therefore $\omega CR_g = 5$; a considerable reduction in the DC voltage is noticeable in such a case. If the circuit of fig. 219b is used rectification may be impossible if C has a very low value; a family of measured curves for this circuit is reproduced in fig. 230.

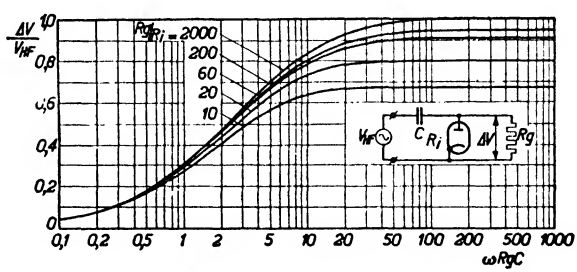

Fig. 230. $\Delta V/V_{HF}$ as a function of ωRgC for various values of Rg/Ri, with parallel-connected load resistance.

When the carrier to be rectified is modulated an undesirable effect may occur if C is too large; if the envelope of the carrier includes very sharp falls in amplitude the rectified voltage across C may be unable to drain away fast enough through the load resistance R and will therefore lag behind the modulation and lead to appreciable distortion. Put in another way, distortion arises if the RC-time constant is large in relation to one cycle of the modulation; it therefore varies with

modulation frequency, becoming most evident for the highest frequencies. This phenomenon may also be regarded as a case of the A.F. load of the detector being less than the DC load. The AC load consisting of R and C in parallel is here complex. In B § 11 we shall deal with the case of the two loads being different but real quantities, a condition what better lends itself to detailed analysis. The argument in § 11 may serve, however, to explain the result of an excessive value of C; the conclusion is reached that the distortion introduced depends on the relation between $1/pC$ (where p is the angular frequency of the modulation) and R, or, what comes to the same thing, on the relation between CR and $1/p$. It was this conclusion that we reached above.

In practice the following values are commonly found: $C = 100$ pF, $R = 0.5$ MΩ and $p = 2\pi \times 5000$. For $1/pC$ we then get $\frac{10^{12}}{100 \times 30{,}000} = 1/3$ MΩ, and the A.F. load is thus much lower than the DC load of 0.5 MΩ. Nevertheless, marked distortion does not occur, because the depth of modulation at frequencies around 5000 c/s is mostly slight, and the amplitude of the carrier does not decline so steeply as with 100% modulation. That this distortion is affected by modulation depth is demonstrated on other grounds in § 11.

Finally, there is reduction of the DC voltage by reason of the anode/cathode capacitance of the diode. An additional current therefore flows through the diode, whether the circuit used is that of fig. 219a or of 219b, causing a potential drop in C. If the reactance of C is small compared with R_g, and thus ωCR_g is large in relation to unity, this reduction of the DC voltage corresponds to an apparent fall in the alternating input voltage, which becomes:

$$V_{HF}' = V_{HF}\frac{C}{C + C_d} \quad \ldots\ldots\ldots\ldots \quad \text{(V B 18)}$$

In most cases, however, C_d is so small compared with C that its effect on the DC voltage may be disregarded.

§ 6. Damping of the preceding tuned circuit by the diode

In fig. 224 the diode was imagined as connected directly to a voltage source. Usually this source is a tuned circuit and it is therefore important to know what load the diode imposes. The damping, which may be regarded as being in parallel with the tuned circuit, we shall denote by R_{HF} (see fig. 231).

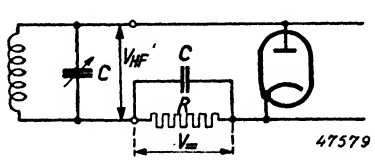

Fig. 231. Diode following a tuned circuit.

If the amplitude of the R.F. current through the diode, I_{HF}, is calculated, the value of R_{HF} follows from equation (V B 19):

$$R_{HF} = \frac{V_{HF}}{I_{HF}} \quad \ldots\ldots\ldots\ldots \quad \text{(V B 19)}$$

I_{HF} is the amplitude of the fundamental in the diode current i, which is given by equation (V B 2); in normal selective circuits it is only the damping at the fundamental frequency which is of importance.
Now according to the Fourier series expansion:

$$I_{HF} = \frac{1}{\pi} \int_0^{2\pi} i \cos \omega t \, d\omega t \quad \ldots\ldots\ldots \quad \text{(V B 20)}$$

Combining this with equation (V B 2) we therefore find:

$$I_{HF} = \frac{A}{\pi} \int_0^{2\pi} \varepsilon \frac{V_{HF}}{V_T} \cos \omega t + \frac{V_=}{V_T} \cos \omega t \, d\omega t,$$

or:

$$I_{HF} = 2 A \varepsilon \frac{V_=}{V_T} \frac{1}{2\pi} \int_0^{2\pi} \varepsilon \frac{V_{HF}}{V_T} \cos\omega t \cos \omega t \, d\omega t \quad \ldots\ldots\ldots \quad \text{(V B 21)}$$

If the expression:

$$\frac{1}{2\pi} \int_0^{2\pi} \varepsilon \frac{V_{HF}}{V_T} \cos\omega t \cos \omega t \, d\omega t \quad \ldots\ldots\ldots \quad \text{(V B 22)}$$

is denoted by B_1, equation (V B 21) * then becomes:

$$I_{HF} = 2 A \varepsilon \frac{V_=}{V_T} B_1 \quad \ldots\ldots\ldots\ldots \quad \text{(V B 23)}$$

When $\frac{V_{HF}}{V_T} < 1$ it is approximately true that:

$$B_1 = \tfrac{1}{2} \frac{V_{HF}}{V_T} \left(1 + \frac{1}{8} \frac{V_{HF}^2}{V_T^2}\right) \quad \ldots\ldots\ldots \quad \text{(V B 24)}$$

* B_1 is a Bessel function of the first order, which, like Bo, can be obtained from tables.

If $\frac{V_{HF}}{V_T} \gg 1$ we get:

$$B_1 = B_o = \frac{1}{\sqrt{2\pi \frac{V_{HF}}{V_T}}} \varepsilon^{\frac{V_{HF}}{V_T}} \quad \ldots\ldots \text{(V B 25)}$$

Using (V B 4) we can rewrite equation (V B 23) thus:

$$I_{HF} = 2\, I_{med}\, Q \quad \ldots\ldots\ldots\ldots \text{(V B 26)}$$

where:

$$Q = \frac{B_1}{B_o} \quad \ldots\ldots\ldots\ldots\ldots\ldots \text{(V B 27)}$$

In the following table Q is given for various values of V_{HF}/V_T.

$\frac{V_{HF}}{V_T}$	Q	$\frac{V_{HF}}{V_T}$	Q	$\frac{V_{HF}}{V_T}$	Q
0	0	1.4	0.57	6	0.91
0.1	0.05	2	0.7	7	0.92
0.2	0.1	2.5	0.76	8	0.93
0.3	0.15	3	0.81	9	0.94
0.5	0.24	3.5	0.84	10	0.94
0.7	0.33	4	0.86	11	0.95
1.0	0.45	5	0.89		

It follows from equations (V B 5) and (V B 24) that when $V_{HF}/V_T < 1$ it is approximately true, as the table indicates, that:

$$Q = \tfrac{1}{2}\, \frac{V_{HF}}{V_T} \quad \ldots\ldots\ldots\ldots\ldots \text{(V B 28)}$$

and from equations (V B 6) and (V B 25), when $V_{HF}/V_T \gg 1$, that:

$$Q = 1 \quad \ldots\ldots\ldots\ldots\ldots\ldots \text{(V B 29)}$$

The damping of the preceding tuned circuit is thus, according to equations (V B 19) and (V B 26):

$$R_{HF} = \frac{V_{HF}}{I_{HF}} = \frac{V_{HF}}{2\, I_{med}\, Q} \quad \ldots\ldots\ldots \text{(V B 30)}$$

As $I_{med} = \frac{V_{=}}{R}$, we find:

$$R_{HF} = \frac{1}{2} R \frac{V_{HF}}{V_{=}} \frac{1}{Q} \quad \ldots\ldots\ldots\ldots \quad \text{(V B 31)}$$

The ratio $V_{HF}/V_{=}$ depends not only on the signal V_{HF}, but also on the temperature voltage V_T, which is rarely known; instead, the DC voltage across R in the absence of a signal may be employed as a basis.
In fig. 232 the measured value of R_{HF} as a function of V_{HF} is given for three values of the no-signal DC voltage V_r.

§ 7. Damping by the diode when the R.F. input is small

Although fig. 232 shows the damping for almost all likely cases where a diode load of 0.5 MΩ is used, it is worth while also to examine the general formula (V B 31) for two extreme cases, for then we can draw some fairly simple conclusions which will enable us in many cases to fix tentatively the value of the damping R_{HF}. First let us consider the case in which V_{HF} is less than 0.1 V. The value of Q from (V B 28) can then be inserted in equation (V B 30) and we get:

$$R_{HF} = \frac{V_T}{I_{med}} \quad \ldots\ldots \quad \text{(V B 32)}$$

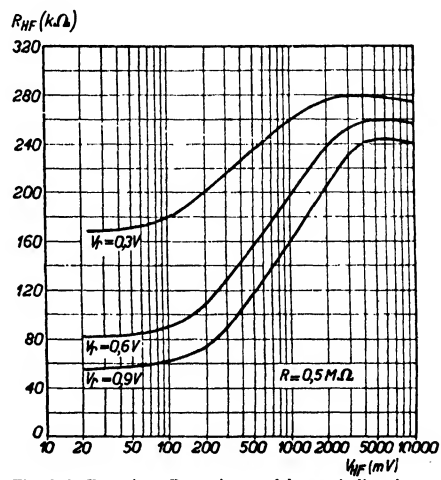

Fig. 232. Damping, R_{HF}, imposed by an indirectly-heated diode, as a function of the carrier amplitude V_{HF} for three values of the no-signal voltage V_r and with a load resistance of 0.5 megohm.

If V_T is known, the damping can then be ascertained merely by measuring the direct current. The value of I_{med} in this case is nearly the same as the direct current I_r in the absence of a signal, the superposition of the small alternating current on I_r having little effect on the mean value, and we may therefore also write:

$$R_{HF} = \frac{V_T}{I_r}.$$

From this we conclude that the damping resistance is equal to the differential resistance $\partial v_a/\partial i$ of the diode at the current I_r. Differentiating (V B 1) we obtain:

$$\frac{\partial v_a}{\partial i} = \frac{1}{V_T} A \varepsilon^{\frac{v_a}{V_T}} = \frac{i}{V_T} \quad \ldots\ldots\ldots \quad \text{(V B 33)}$$

This result is readily understandable: with very small signals detection is so ineffective that the steady voltage developed across the resistance R is small compared with V_{HF}. Little power is therefore lost in R. Thus nearly all the power supplied by the tuned circuit is absorbed by the diode, which may accordingly be regarded as a resistance parallel to the circuit; the value of this resistance to the superimposed alternating current is the differential resistance.

In conclusion we can consider a numerical example. Many present-day diodes which have a temperature voltage of about 0.1 V pass an initial current of 1 μA with a load of 0.5 MΩ (corresponding to $V_{=} = 0.5$ V). The differential resistance is thus 100,000 Ω and, for inputs below 100 mV, this is in agreement with fig. 232.

§ 8. Damping by the diode when the R.F. input is large

When $V_{HF} > 1$ V (corresponding to $V_{HF}/V_T > 10$) we find from the table that the value of Q approaches 1. Thus:

$$R_{HF} = \tfrac{1}{2} R \frac{V_{HF}}{V_{=}} \quad \ldots\ldots\ldots\ldots \quad \text{(V B 34)}$$

For very large signals of, say, $V_{HF} = 10$ V, the value of $V_{HF}/V_{=}$ also approaches unity, and we therefore find:

$$R_{HF} = \tfrac{1}{2} R \quad \ldots\ldots\ldots\ldots\ldots\ldots \quad \text{(V B 35)}$$

We observe in fig. 232 that for signals over 2 V the R.F. resistance is in fact of the order of 250,000 Ω, i.e. $\frac{1}{2} R$.

Over a certain range of signals damping higher than $\frac{1}{2} R$ is encountered, despite the computed values, thus showing that the conditions were approximated in the calculation. With large inputs the instantaneous diode current may exceed 100 μA, so that equation (V B 1), from which we started, is no longer valid. The following simple proof demonstrates, however, that at high signal levels the damping always approximates to the value given by equation (V B 35), whatever the shape of the diode characteristic.

If the equivalent resistance of the diode circuit is R_{HF} a signal of amplitude V_{HF} develops a power of:

$$W_d = \frac{V_{HF}^2}{2 R_{HF}} \quad \ldots\ldots\ldots\ldots\ldots \quad \text{(V B 36)}$$

This power is dissipated partly in the resistance R and partly in the diode. In the resistance, across which the measured steady voltage is nearly equal to V_{HF}, the power lost is:

$$W_R = \frac{V_{HF}^2}{R} \quad \ldots\ldots\ldots\ldots\ldots \quad \text{(V B 37)}$$

In the diode it seems that the loss is very small, for during the passage of current there is a negligible voltage across the diode; indeed, almost the whole of V_{HF} is found to be across R. No great error is therefore committed if we put the power in the last two equations equal to one another:

$$\frac{V_{HF}^2}{2\,R_{HF}} = \frac{V_{HF}^2}{R},$$

or:

$$R_{HF} = {}^1/_2\,R \quad \ldots\ldots\ldots\ldots\ldots \quad \text{(V B 35)}$$

This is the value of the diode damping when the load is in parallel with the capacitor. If on the other hand R is parallel to the diode, the tuned circuit supplies AC power to the load resistance in addition to the power W_d absorbed by the diode circuit, and the equivalent circuit is as given in fig. 233.

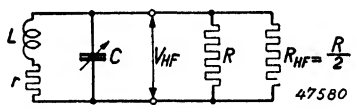

Fig. 233. Equivalent circuit of diode with parallel load, to illustrate the damping imposed on the source of R.F. voltage.

We then find for the total damping:

$$R_{HF} = \frac{1}{3}R \quad \ldots\ldots\ldots\ldots\ldots \quad \text{(V A 1)}$$

§ 9. Practical example of the effect of diode damping on gain

The calculations in the preceding pages having led to quite simple results, we may now conveniently make use of them for preliminary estimations. When test measurements are made, however, divergences from calculated conditions are found, and it is desirable to ascertain the magnitude of such differences.

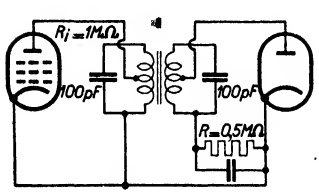

Fig. 234. Final I.F. stage and diode detector. To reduce damping, both valves are joined to tappings ($t = 0.7$) on the coils.

Diode damping affects the gain and the selectivity of the immediately preceding amplifier stage. As an example we can take a normal I.F. stage, as depicted in fig. 234. The coils of the I.F. transformer have an r/L ratio of 20,000 and

are tapped on 7/10 from the low-potential ends; the tuning capacitance across each winding is 100 pF. The dynamic resistance of each I.F. circuit, ignoring external damping, is $Z = L/rC = 500{,}000\ \Omega$, while the preceding pentode has an AC resistance of 1 MΩ.

With a strong I.F. signal, say 10 V, the damping of the secondary circuit may be put at $R_{HF} = 0.5\ R = 0.25$ MΩ; but as R_{HF} is connected to the 7/10 tap the damping of the whole circuit is only about 0.5 MΩ. The dynamic resistance of the primary is 0.5 MΩ shunted by $(10/7)^2 \times 1$ MΩ, thus 0.4 MΩ. That of the secondary circuit is 0.5 MΩ shunted by 0.5 MΩ, or 0.25 MΩ. The mean load, which determines the gain, would for a large signal therefore be:

$$Z = \sqrt{Z_1 Z_2} = 317{,}000\ \Omega.$$

With a much smaller signal, for example 200 mV, the damping with an average indirectly-heated diode having $V_r = 0.6$ V is 110,000 Ω (see fig. 232). The dynamic resistance of the secondary is then 153,000 Ω (i.e. 500,000 Ω shunted by 220,000 Ω), so that the band-pass filter presents a load of:

$$Z = \sqrt{Z_1 Z_2} = 248{,}000\ \Omega.$$

Comparing this with the earlier result we note an error of about 25 %, due to using an approximated figure of 0.5 MΩ for the damping instead of the complete formula.

But even when the damping is accurately calculated there is still the possibility that the diode used is not an average specimen but has V_r of, say, 0.3 V or 0.9 V. In these cases the actual damping is respectively 200,000 Ω and 75,000 Ω, and the dynamic resistance values become:

$$V_r = 0.3\ \text{V};\ Z_2 = 222{,}000\ \Omega \text{ and } Z = 298{,}000\ \Omega$$
$$V_r = 0.9\ \text{V};\ Z_2 = 115{,}000\ \Omega \text{ and } Z = 214{,}000\ \Omega$$

Measurement would therefore show divergencies from the calculated I.F. amplification of 20 % and 14 % respectively. Had the diode been joined across the whole secondary instead of to the tapping, still greater variations would have been found.

Similarly, divergencies from the calculated selectivity of the I.F. transformer will occur; they are of the same order as those just found in connection with dynamic resistance.

Apart from the dynamic resistance of the I.F. band-pass filter, the amplifi-

cation depends also on the coupling between the two circuits. The voltage across the secondary is:

$$V_2 = I_a \frac{K\,Q}{1 + K^2\,Q^2} Z \quad \ldots\ldots\ldots\ldots \quad \text{(I B 16)}$$

where Z is the mean dynamic resistance already calculated and $K\,Q$ the relative coupling. The variation of $\frac{K\,Q}{1 + K^2\,Q^2}$ with $K\,Q$ was indicated in fig. 13.

When $K\,Q = 1$ (critical coupling) the gain is a maximum and varies to only a small extent with changes in Q. For the sake of selectivity, however, $K\,Q$ is often made less than unity, and the effect of damping on amplification is then more evident.

The mean quality factor is:

$$Q = \sqrt{Q_1\,Q_2} = \sqrt{\frac{\omega\,L_1}{r_1}\,\frac{\omega\,L_2}{r_2}}.$$

For the Q of each individual circuit we may write:

$$Q_1 = \frac{\omega L_1}{r_1} = \frac{L_1}{r_1\,C_1} \times \omega\,C_1 = Z_1\,\omega\,C_1.$$

It follows that the mean quality factor is directly proportional to the mean dynamic resistance of the band-pass filter, and a given percentage change in the mean dynamic resistance thus produces the same percentage variation in the relative coupling.

We shall now return to the case in which the diode damping was assessed at $^1/_2$ R and the I.F. transformer was so constructed that the coupling with such damping was critical. The desired degree of coupling may be attained, for example, by adjusting the transformer by means of a frequency-modulator and a cathode-ray oscillograph. When the input is reduced to 200 mV the mean dynamic resistance Z is found to fall 25%, and consequently the coupling decreases in the same proportion. From fig. 13 it follows that the factor $\frac{K\,Q}{1 + K^2 Q^2}$ reduces the amplification by 6%, apart altogether from the decrease due to the smaller dynamic resistance Z. The reduction in gain is even larger when the relative coupling with a strong signal is say 0.5; in such a case a 25% change in the coupling causes amplification to decline by about 20%.

The variations described above can also occur as a result of the differences between diodes of the same nominal characteristics, or between indirectly-heated and battery diodes.

If the coupling is originally overcritical the factor in fig. 13 increases with heavier damping and in consequence the reduction in gain due to the smaller mean dynamic resistance is to some extent compensated.

§ 10. Directly heated diodes

The foregoing calculations were based on the equation for the so-called initial current.

$$i = A\varepsilon^{\frac{v_a}{V_T}} \quad \ldots\ldots\ldots\ldots\ldots\ldots \quad \text{(V B 1)}$$

It has already been noted however, in B §§ 1 and 5, that this relation holds good only for currents below a certain level. Above that the curve passes through a transitional stage and reaches the positive grid-voltage region, where, due to the increasing influence of the space charge, we find:

$$i = kV_a^{3/2}.$$

In some circumstances the transition area, possibly extending into the space-charge region, is of greater importance than the so-called exponential part. This was the case, for example, in B § 5. The majority of directly-heated diodes provide a further example. With these valves the transition region begins at fairly low values of current, because the space-charge affects the very thin cathode earlier than it would the thicker cathode of an indirectly-heated valve. The result is less effective rectification. With signals of certain magnitudes a part of the diode characteristic is traversed which may best be represented by the equation:

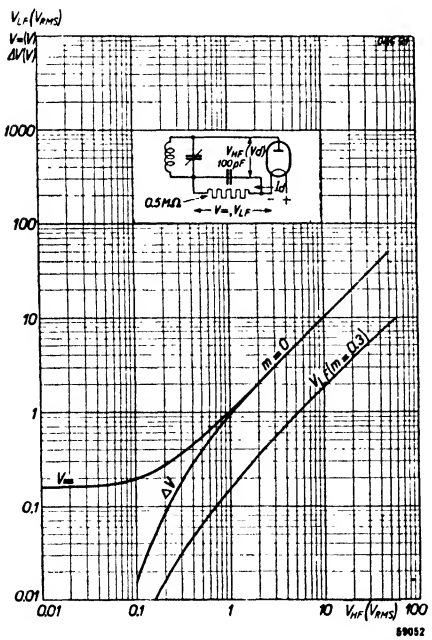

Fig. 235 Standing voltage $V=$, and increase thereof $\Delta V=$, across the load resistance R of a directly-heated battery diode, as a function of the unmodulated R.F. voltage V_{HF}. Also the A.F. output V_{LF} as a function of the 30% modulated R.F.-voltage.

$$i = \frac{v_a}{R_i} \quad \ldots\ldots \quad \text{(V B 17)}$$

Starting with this characteristic we can calculate ΔV as a function of V_{HF} (see II B § 9). We find a relation between them, depending on R_i/R, which in normal circumstances is less

than $\sqrt{2}$, the value valid for peak detection calculated from (V B 1). For battery valves the published curve (fig. 235) shows a ratio $\Delta V/V_{HF}$ of 1.0. In the region in which equation (V B 1) holds good for the initial current, differences between battery and indirectly heated diodes can arise due to differences in the constants A and V_T. The quantity A depends on the saturation current and the contact potential, and on both these grounds

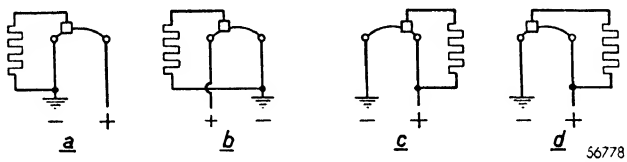

Fig. 236. Four methods of connecting the filament of a directly-heated battery diode; arrangement *a* is the most favourable for detection.

it is smaller with battery than with indirectly-heated diodes. The practical results of a lower value of A are a smaller no-signal bias V_r, and with small inputs less effective rectification and less damping. The temperature voltage V_T is about the same for both types of diode, and the cathode temperature is similar.

The similarity of V_T becomes evident at once if the current-characteristic of the diode is drawn on a logarithmic scale; the initial part is then straight, and its slope is a measure of V_T. In both types of diode the slope of the straight part is indeed the same.

A possible cause of variation is the potential drop along a directly heated cathode, but in modern diodes the possibility may be excluded, for the anode encloses only a comparatively short section of the filament, along which the voltage drop is unimportant. There are, however, several methods of connecting the filament of a directly heated diode (fig. 236 a-d) and these deserve some consideration. The usual and recommended circuit is shown in fig. 236a. It yields the highest A.F. voltage and permits a second anode at the other end of the filament to be used for AVC purposes; on this second anode there is then a delay equal to the voltage across the filament.

In fig. 236b the other extremity of the filament is joined to earth and LT negative. In consequence a negative bias equal to the filament voltage is applied to the anode. This circuit has no advantages and yields a lower A.F. voltage.

In fig. 236c the anode has a small positive bias, equal to the potential drop along the filament between the section enclosed by the anode and the LT positive end. Detection now occurs at a more curved part of the characteristic, and for small signals it is therefore more effective, but owing to the

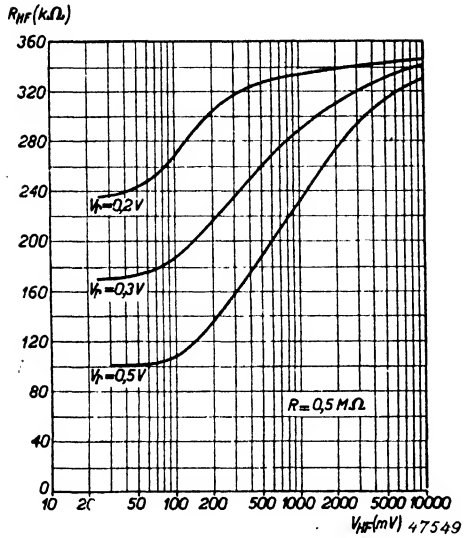

Fig. 237. Damping, R_{HF}, imposed by a directly-heated battery diode, as a function of the carrier amplitude V_{HF}, for three values of the no-signal voltage Vr and with a load resistance of 0.5 megohm.

larger space current the damping is heavier and the net result is not so good as in fig. 236a.

The performance given by fig. 236d is worse than that of fig. 236c, as the damping is increased to an even greater degree.

The A.F. voltage yielded by the four circuits was measured in a normal receiver, a constant I.F. signal being supplied; the following results were obtained:

a) 35.4 mV
b) 19.0 mV
c) 21.5 mV
d) 15.0 mV

For comparison with figs 227 and 232 relating to indirectly-heated diodes, corresponding curves for battery diodes are reproduced in figs 235 and 237.

§ 11. Distortion in diode detection

The leak resistance acts as an A.F. load of the detector. In the circuits of figs 219a and 219b the A.F. load is almost equal to the DC resistance R_g (= R). In practice, however, the A.F. load differs from R_g, because to AC the load resistance is reduced by the parallel connections of the grid leak R_2 of the following valve, and possibly also by the smoothing resistance R_3 of the AVC circuit (see fig. 238).

Finally, as was observed in B § 5. the by-pass capacitance forms part of the A.F. load.

Divergence between the AC and DC loads in the diode circuit can lead to distortion. Consider fig.239 which corresponds to fig. 228. If the R.F. input is say 5 V, the working point is at P with a DC load R_g of 0.5 MΩ. If the load at audio frequencies is formed only

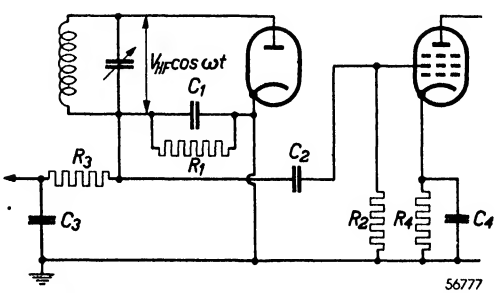

Fig. 238. Diode and succeeding A.F. stage. Due to the parallel connection of the grid leak R_2 (and possibly of a smoothing resistance R_3) the AC load R_w of the diode is reduced, and distortion may occur with deep modulation.

by the leak $R_1 = R_g$, 80 % modulation will cause the operating point to move back and forth along the line R_g between S and Q. Since, for constant V_{HF}, the lines between these points are uniformly separated, the alternating voltage which appears across the leak will, with sinusoidal modulation, also be of sine form. But if the AC load is not equal to R_g the relation between ΔV and I_{med} is given by a line R_w passing through P (see also B § 4). On the onset of modulation the working point now moves to and fro along the line R_w.

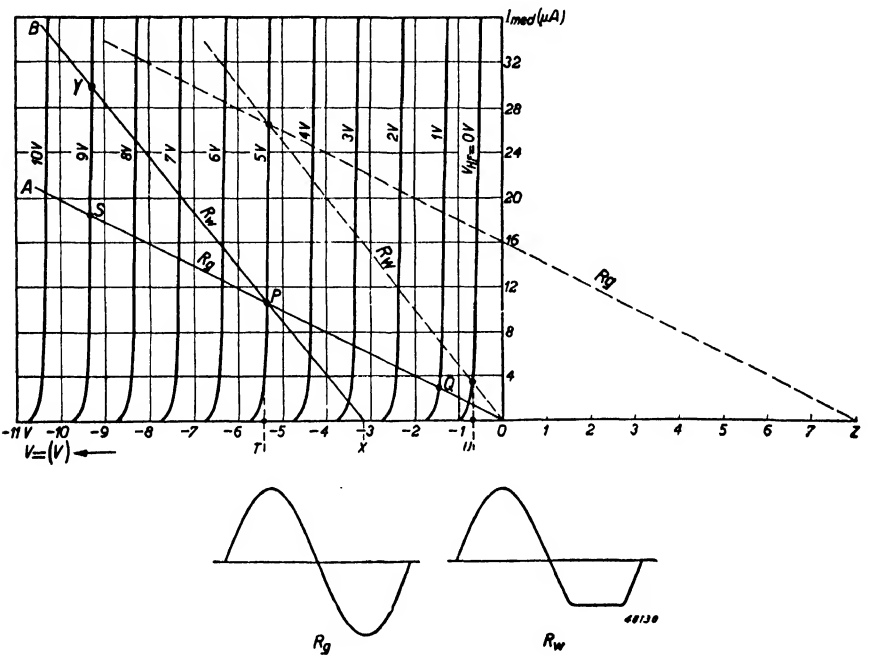

Fig. 239. Mean diode current *Imed* as a function of the standing voltage $V=$, with the amplitude V_{HF} of the R.F. voltage as parameter. The line Rg represents the diode load resistance, i.e. the DC load, and the line R_w the AC load. As soon as the A.F. amplitude exceeds PX serious distortion results from the clipping of the modulation peaks.

At a certain depth of modulation the working point will reach X; with any deeper modulation it is clear that distortion will occur, and the peaks of A.F. voltage will be cut off.

Neglecting the curvature at the bottom of the characteristics, we find that the maximum modulation depth which avoids the distortion referred to above is:

$$m_{max} = \frac{(XT)}{(UT)}.$$

For simplicity we put the requirement rather higher and say:

$$m_{max} = \frac{(XT)}{(OT)}.$$

It is approximately true that:

$$(XT) = (PT)\, R_w \text{ and } (OT) = (PT)\, R_g;$$

therefore:

$$m_{max} = \frac{R_w}{R_g} \quad \ldots\ldots\ldots\ldots\ldots \quad \text{(V B 38)}$$

In reality m_{max} is rather greater, for the characteristics do not run parallel to the current co-ordinate, and O does not coincide with U.

For small signals the permissible modulation depth is considerably greater and may be equal to 100%. This is seen most plainly if the diagram is redrawn on another scale (fig. 240). With low inputs the peaks will not be

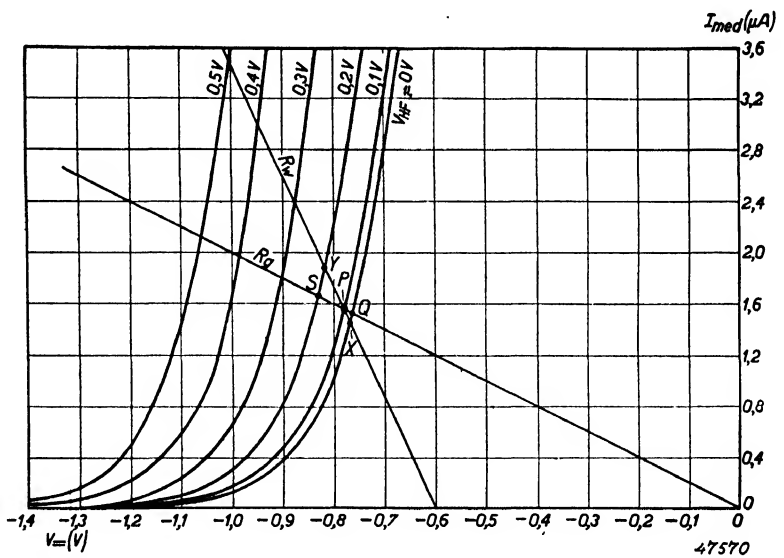

Fig. 240. Mean diode current *Imed* as a function of the standing voltage $V=$, with low amplitudes of V_{HF} as parameter. With such small signals detection is quadratic; with deep modulation, however, the peaks of modulation are not cut off.

cut off. But it is clear that $PY \neq PX$ and $PS \neq PQ$, so that, apart from the R_w/R_g ratio, distortion in fact occurs; on small signals detection is quadratic.

It followed from equation (V B 13) that for small inputs:

$$\Delta V = k V_{HF}^2.$$

For a modulated signal V_{HF} has to be substituted by $V_{HF}(1 + m \cos pt)$, so that:

$$\Delta V = k V_{HF}^2 (1 + m \cos pt)^2,$$

or:

$$\Delta V = k V_{HF}^2 (1 + \tfrac{1}{2} m^2 + 2 m \cos pt + \tfrac{1}{2} m^2 \cos 2 pt). \quad . \; . \; . \quad \text{(V B 39)}$$

Thus the A.F. voltage contains, in addition to the frequency p, a frequency $2p$. The distortion is given by:

$$d_2 = \frac{\frac{1}{2} m^2}{2m} = \tfrac{1}{4} m \quad . \; . \; . \; . \; . \; . \; . \; . \; . \; . \; . \; . \; . \quad \text{(V B 40)}$$

In other words, at a modulation depth of 80% there is already 20% of second harmonic present.

We may therefore conclude from the foregoing that detection is distortionless only when the diode works into a load of which the value to AC differs little from that to DC (i.e. R_g).

If R_w differs appreciably from R_g the cutting of the peaks of modulation can be avoided by joining the leak to a point positive with respect to the cathode; this is demonstrated by the dotted lines in fig. 239.

The damping of the preceding tuned circuit is then much increased, as indicated by equation (V B 30):

$$R_{HF} = \tfrac{1}{2} \frac{V_{HF}}{I_{med}} \frac{1}{Q}.$$

Owing to the positive bias I_{med} increases and the value of R_{HF} therefore falls.

It follows from equation (V B 38) that for linear detection the diode load must not be too high nor the grid leak of the following valve too low. There is, however, a limit to the value of the latter resistance, especially when fixed grid bias is employed. Preferably, therefore, the valve following the diode should have automatic bias. On the other hand the diode load cannot be made too small as otherwise the preceding tuned circuit will be unduly damped, and a compromise is thus necessary. Assuming the diode load to be 0.5 MΩ and the grid leak of the succeeding valve 1.0 MΩ, $R_w = \frac{0.5 \times 1.0}{0.5 + 1.0}$ $= 0.33$ MΩ and $R_w/R_g = 0.33/0.5 = 0.66$. In this case the maximum depth of modulation is thus 66%. If the diode load is made 0.3 MΩ the permissible modulation depth improves to 77%; if also the grid leak of the A.F. amplifier

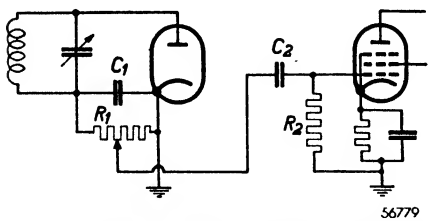

Fig. 241. Diode and succeeding A.F. stage, with the diode load resistance serving as volume control.

is raised to 1.5 MΩ 83 % modulation can then be handled. These are conservative figures if the diode load serves also as the volume control, as in fig. 241. This method of connection is to be preferred to the alternative circuit, fig. 242, in which the volume control is in the grid circuit of the following valve. In fig. 241 the resistance of that sector of the potentiometer R_1 between the slider and earth is equal to pR_1, and the impedance at audio frequencies of the detector circuit is:

$$R_w = (1 - p)\, R_1 + \frac{pR_1\, R_2}{pR_1 + R_2} \quad \ldots\ldots \quad \text{(V B 41)}$$

The DC load R_g is equal to R_1 and the maximum permissible depth of modulation is accordingly:

$$\frac{R_w}{R_g} = (1 - p) + \frac{pR_2}{pR_1 + R_2} \quad \ldots\ldots\ldots \quad \text{(V B 42)}$$

If $p = 1$ (maximum volume) R_w/R_g becomes $\dfrac{R_2}{R_1 + R_2}$, and as p decreases R_w/R_g rapidly approaches unity.
In the circuit of fig. 242, on the other hand, R_w/R_g is always equal to $\dfrac{R_2}{R_1 + R_2}$ whatever the position of the volume control.

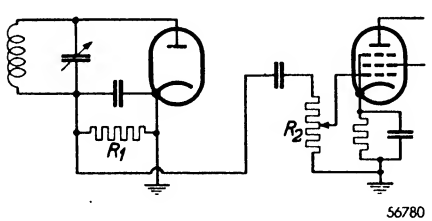

Fig. 242. Diode and succeeding A.F. amplifier; here the grid leak of the A.F. valve forms the potentiometer for controlling volume; this arrangement gives a less favourable R_w/R_g ratio than the circuit of fig. 241.

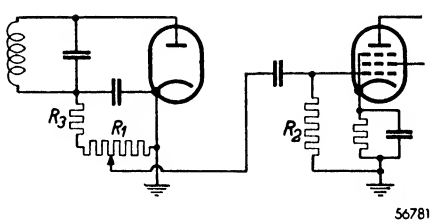

Fig. 243. The circuit of fig. 241 with the addition of a fixed resistance R_3 in series with the potentiometer R_1; the R_w/R_g ratio is thereby improved.

Thus in the first case the permissible modulation depth increases as volume is reduced. This is a favourable circumstance, for it is only at small modulation depths that maximum gain is needed.
In order to prevent the whole of the diode load in the circuit of fig. 241

being shunted by the volume control and the permissible depth of modulation thereby unduly reduced, the arrangement of fig. 243 is often adopted. Here a resistance R_3 of say 0.1 MΩ is joined in series with the potentiometer. Clearly the maximum A.F. voltage obtainable at the grid of the following valve is then less, but with $R_1 = 0.5$ MΩ the drop is only about 16%.
The resistance R_3 serves two other purposes. Firstly, it reduces the influence of the stray capacitances in the last I.F. transformer (see chapter X), and secondly it prevents excessive damping by the diode when a pick-up is connected to the volume control R_1.
If the diode is followed immediately by the output valve it is necessary to make the diode load smaller, because of the comparatively low values of grid leak which are permissible for output valves; this limiting of the diode load resistance is especially important in view of the heavily modulated transmission of the present day.
No consideration has yet been given to the smoothing resistance in the AVC circuit. To avoid the control having too long a time constant the value of this resistance cannot be too high, and it will therefore affect the permissible modulation depth if it is connected to the detector circuit; its effect is readily calculable. The use of a separate diode for AVC is, however, an advantage; the detector circuit is then unaffected, and moreover it becomes possible to apply a delay voltage to the anode of the AVC diode.

§ 12. Interaction between the tuned circuit and the A.F. load

In the foregoing we started from a specified alternating voltage, either modulated or unmodulated, the magnitudes of which were not influenced by conditions in the detector stage. Neither the amplitude of the carrier nor the modulation depth was affected by the characteristics of the diode or by the A.F. load.
This situation is encountered, for instance, when the alternating voltage is derived from a calibrated oscillator whose internal impedance is very low compared with the equivalent resistance of the diode circuit. The number of parameters involved in such a case was therefore not great.
In a radio receiver the input to the diode is derived from a tuned circuit or a band-pass filter to which a current is fed. A new parameter is thus introduced: the dynamic resistance of this tuned circuit. The question now is what influence this parameter has on the conclusions already drawn. It will appear that it is not enough to calculate the carrier voltage V_{HF} across the tuned circuit and then to apply the formulae arrived at in the preceding pages, because in fact the A.F. load does have a considerable effect. The magnitude of this effect depends on the dynamic resistance of the tuned

circuit; in other words, as "seen" by the A.F. load the circuit possesses a certain internal resistance, which is dependent on its dynamic resistance. Furthermore the damping of the tuned circuit by the diode is important, and here it is necessary to distinguish between damping of the carrier and damping of the sidebands; these dampings are different and depend on the

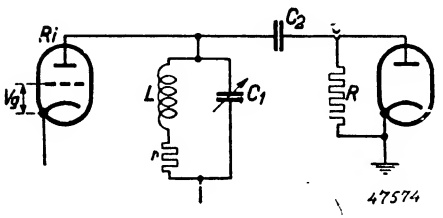

Fig. 244. Diode and preceding R.F. stage.

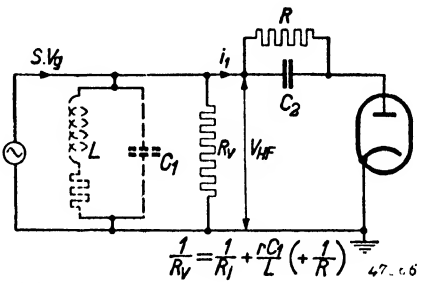

Fig. 245a. Equivalent circuit of fig. 244, the R.F. stage being replaced by a current source SV_g.

A.F. load; that is to say, the final tuned circuit or band-pass filter, being a voltage source, is loaded by the A.F. impedance via the diode. Due to the presence of the intermediary diode circuit the actual load applied to the tuned circuit is not equal to the A.F. load, though it is closely related thereto. We shall give closer consideration to this question in the following pages.

§ 13. Detection characteristics after a tuned circuit

Fig. 244 shows a simple circuit of a diode preceded by an amplifier stage with a single tuned circuit. For the amplifying valve we can substitute a current source SV_g, assuming that the AC resistance of the valve is included in the circuit impedance. We may represent the total of the AC resistance R_i, the dynamic resistance of the tuned circuit and any damping due to the diode load resistance, by a single resistance R_v in parallel with the no-loss circuit $L\ C_1$ (fig. 245a). In this equivalent resistance R_v the damping R_{HF} due to the diode current is not included. The total damping of the circuit is now therefore divided into two parts: the equivalent resistance R_v, the magnitude of which is independent of amplitude, and the damping R_{HF}, which does depend on the amplitude of the circuit voltage (fig. 245b).

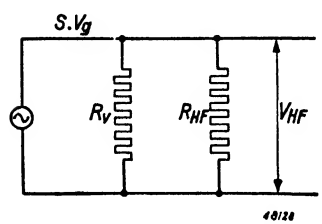

Fig. 245b. Equivalent circuit of fig. a, in which everything is reduced to a current source SV_g, with parallel resistances R_v, the load as seen by the diode, and R_{HF}, the damping imposed on the R.F. circuit by the diode.

The alternating voltage across the tuned circuit,

and therefore applied to the diode, is now:

$$V_{HF} = S\, V_g \frac{R_v\, R_{HF}}{R_v + R_{HF}} \quad \ldots\ldots\ldots \quad \text{(V B 43)}$$

With the help of this formula it would be a simple matter to calculate the detection factor as a function of $S\, V_g$ instead of V_{HF} were it not that R_{HF} depends on V_{HF}. R_{HF} should therefore be eliminated.
By definition:

$$R_{HF} = \frac{V_{HF}}{I_{HF}} \quad \ldots\ldots\ldots\ldots\ldots \quad \text{(V B 44)}$$

For signals greater than 1 V, from equation (V B 26) I_{HF} is equal to $2\, I_{med}$ $(Q = 1)$.
Substituting (V B 44) in (V B 43) we then get:

$$V_{HF} = R_v\,(S\, V_g - 2\, I_{med}) \quad \ldots\ldots\ldots \quad \text{(V B 45)}$$

If on the other hand we base our calculations on equation (V B 4), inserting

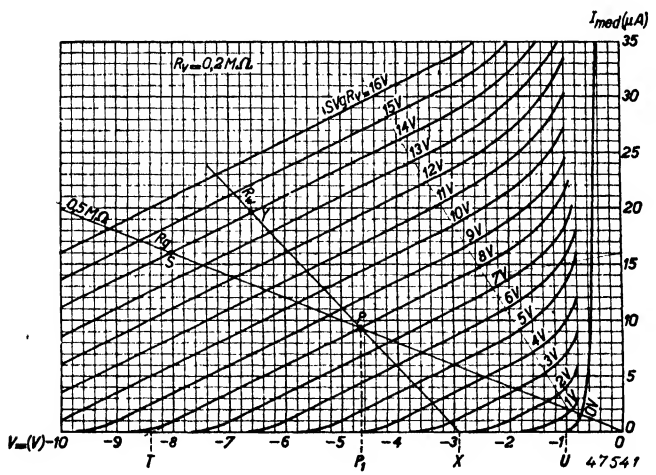

Fig. 246. Family of curves showing the relation between the mean diode current *Imed*, the standing voltage $V_=$ across the load resistance, and the R.F. voltage $S V_g R_v$ supplied by the previous valve ($R_v = 0.2$ megohm).

therein the value for B_o given by (V B 6) for the case of a strong signal, we obtain:

$$I_{med} = \frac{A}{\sqrt{2\,\pi \frac{V_{HF}}{V_T}}}\, \varepsilon^{\frac{V_{HF}}{V_T} + \frac{V_=}{V_T}} \quad \ldots\ldots \quad \text{(V B 46)}$$

Substitution from equation (V B 45) gives:

$$I_{med} = \frac{A}{\sqrt{2\pi \frac{(SV_g - 2I_{med})R_v}{V_T}}} \varepsilon^{\frac{(SV_g - 2I_{med})R_v}{V_T} + \frac{V_=}{V_T}} \quad \ldots \quad \text{(V B 47)}$$

Instead of a relation between V_{HF}, I_{med} and $V_=$, as given in figs 226 and 228, we now have a relationship connecting SV_g, I_{med} and $V_=$ or, by analogy of V_{HF}, connecting SV_gR_v, I_{med} and $V_=$. In the last case the voltage which would appear across the tuned circuit if there were no diode damping has taken the place of V_{HF}. Fig. 246 shows curves calculated from equation (V B 47), based on a total loss resistance R_v of 200,000 Ω and using the quantity $SV_g R_v$ as parameter; with the circuit of fig. 247 such curves could also be obtained by measurement.

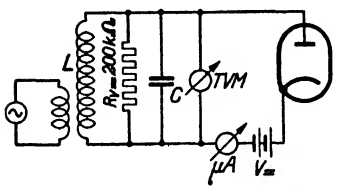

Fig. 247. Basic circuit for measuring the curves of fig. 246.

In B § 3 it was deduced that for large signals ($V_{HF} > 1$ V) the rectified voltage was $\Delta V = -V_{HF}$, and similarly we now find for the rectified voltage:

$$\Delta V \approx V_= = -(S V_g - 2 I_{med}) R_v \quad \ldots \quad \text{(V B 48)}$$

Since $I_{med} = \frac{V_=}{R}$, equation (V B 48) becomes:

$$V_= = -\frac{S V_g R_v}{1 + 2\frac{R_v}{R}},$$

or:

$$V_= = -S V_g R_v \frac{R}{R + 2R_v} \quad \ldots \ldots \quad \text{(V B 49).}$$

This last relation is also arrived at if we insert $\frac{1}{2}R$ for R_{HF} in equation (V B 43). The previous derivation of formulae is however necessary for constructing the curves in fig. 246.

Where a diode follows a band-pass filter, for equation (V B 43) we must write:

$$V_{HF} = f S V_g \sqrt{R_v \frac{R_v R_{HF}}{R_v + R_{HF}}} \quad \ldots \ldots \quad \text{(V B 50)}$$

It is assumed here that the total dynamic resistance of each circuit is equal to R_v. Usually f is of the order of $\frac{1}{2}$ (see section I B § 2).
Again putting for R_{HF}:

$$R_{HF} = \frac{V_{HF}}{I_{HF}} = \frac{V_{HF}}{2\,I_{med}},$$

we get a quadratic equation for V_{HF} which reduces * approximately to:

$$V_{HF} = R_v\,(f\,S\,V_g - I_{med}) \quad \ldots\ldots\ldots \quad \text{(V B 51)}$$

This corresponds to equation (V B 45) for a single circuit and leads on to a further equation entirely comparable to (V B 47), in which however $S\,V_g$ is replaced by $f\,S\,V_g$ and $2\,I_{med}$ by I_{med}. In this way we obtain a family of curves for a diode following a band-pass filter similar to those of fig. 246 but about twice as steep and with $f\,S\,V_g\,R_v$ as parameter.
Finally we get in place of equation (V B 49):

$$V_{=} = -f\,S\,V_g\,R_v\,\frac{R}{R + R_v} \quad \ldots\ldots\ldots \quad \text{(V B 52)}$$

As $f\,S\,V_g\,R_v$ denotes the voltage induced in the tuned circuit when it is undamped by the diode (for a single circuit $f = 1$) it follows from equations (V B 49) and (V B 52) that the rectified voltage depends on the value of the load resistance, whether the AC resistance of the diode circuit is equal to $2\,R_v$ in the case of a simple circuit or to R_v in the case of a band-pass filter.
If the applied alternating voltage is modulated allowance must be made for any difference between the AC load and the DC load R_g imposed by the rectifier circuit. Thus in fig. 246 a new load line XY corresponding to the AC load R_w must be drawn through the working point P. Comparing this diagram with figs 228 and 239 we observe that the value of R_w has a far greater influence on the A.F. output voltage, owing to the characteristics being much less steep.

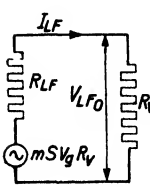

A diode preceded by either a single circuit or band-pass filter may thus be regarded as an A.F. voltage source with an internal resistance R_{LF} (fig. 248).
Although the A.F. voltage in a given case can be ascertained

Fig. 248. Equivalent circuit of fig. 245a from the point of view of the A.F. voltage. The diode and the preceding R.F. stage are regarded as an A.F. generator yielding a voltage $mS\,V_g R_v$ and having an internal resistance R_{LF}.

* The approximation makes use of the fact that $I_{med} \ll f\,S\,V_g$.

graphically from a family of curves (fig. 246), it is generally sufficient to know R_{LF}, the internal resistance of the circuit to audio frequencies. The A.F. output voltage may then be calculated from:

$$V_{LF_o} = V_{LF_i} \frac{R_w}{R_w + R_{LF}} \quad \ldots\ldots\ldots \quad \text{(V B 53)}$$

Here V_{LF_i} is the internal A.F. voltage which would appear across the circuit if it were loaded with an infinite resistance. Since with R_g infinitely high a DC voltage equal to $S\ V_g\ R_v$ or $f\,S\ V_g\ R_v$ occurs, the alternating voltage in those conditions would be $m\,S\,V_g\,R_v$ or $m\,f\,S\ V_g\ R_v$ respectively. Thus:

$$\left.\begin{aligned} V_{LF_o} &= m\ S\ V_g\ R_v \frac{R_w}{R_{LF} + R_w} \\ \text{and:} \qquad V_{LF_o} &= mfS\ V_g\ R_v \frac{R_w}{R_{LF} + R_w} \end{aligned}\right\} \quad \ldots\ldots \quad \text{(V B 54)}$$

It is clear from the equivalent circuit (fig. 248) that the internal resistance R_{LF} can also be defined as:

$$R_{LF} = -\frac{\partial\, V_{LF_o}}{\partial\, I_{LF}} \quad \ldots\ldots\ldots\ldots \quad \text{(V B 55)}$$

for a constant voltage $m\ S\ V_g\ R_v$.

Indeed, when the current through the circuit increases due to a change of R_w a proportionately greater voltage drop occurs across R_{LF}, and V_{LF_o} therefore decreases.

We may consider this further with the aid of fig. 246; we take the load R_g, while the modulation corresponds to PS along the load line R_g. If now we alter the load to R_w the modulation extends to point Y. The change of amplitude $-\partial\ V_{LF_o}$ is then equal to the horizontal distance separating S and Y, an amount which we may call $\partial\ V_{=}$. Simultaneously the amplitude of the alternating voltage increases by an amount equal to the vertical distance separating S and Y, namely $\partial\ I_{med}$.

In place of equation (V B 55) we can therefore write:

$$R_{LF} = \frac{\partial\ V_{=}}{\partial\ I_{med}} \quad \ldots\ldots\ldots\ldots \quad \text{(V B 56)}$$

This differential quotient may be calculated either from equation (V B 47) for the curves of a single circuit, or from the equation relating to the curves of the bandpass filter.

Differentiating from the logarithm of equation (V B 47) we obtain:

$$R_{LF} = \frac{\partial V_=}{\partial I_{med}} = \frac{V_T}{I_{med}} + 2 R_v \left\{ 1 - \frac{V_T}{2 (S V_g - 2 I_{med}) R_v} \right\} \quad \text{(V B 57)}$$

For values of $S V_g R_v$ greater than 1 V this may be approximated to:

$$R_{LF} = \frac{V_T}{I_{med}} + 2 R_v \quad \text{(V B 58)}$$

In most cases the dynamic resistance of the tuned circuit will be large in relation to V_T/I_{med}, so that:

$$R_{LF} = 2 R_v \quad \text{(V B 59)}$$

which expression could actually have been predicated from equation (V B 49). Similarly, for a diode following a band-pass filter we get from equations (V B 47) and (V B 52):

$$R_{LF} = \frac{\partial V_=}{\partial I_{med}} = \frac{V_T}{I_{med}} + R_v \left\{ 1 - \frac{V_T}{2 (S f V_g - I_{med}) R_v} \right\} \quad \text{(V B 60)}$$

or approximately:

$$R_{LF} = R_v \quad \text{(V B 61)}$$

We have thus reached the following conclusion. The damping imposed by the detector on the carrier voltage across the preceding tuned circuit is chiefly determined by the DC load of the diode circuit, while the internal resistance of the diode circuit at modulation frequencies is fixed mainly by the dynamic resistance of the preceding tuned circuit or band-pass filter.

As $R_{LF} = \frac{\partial V_=}{\partial I_{med}}$ was calculated for constant V_g, the internal resistance of the diode circuit at modulation frequency is also determined by the slope of the curves in fig. 246.

§ 14. Distortion of the modulation if $R_W \neq R_g$ (after a tuned circuit)

It was deduced in § 11 that the maximum depth of modulation (i.e. the modulation depth at which the peaks of A.F. voltage are just not clipped) is given by:

$$m_{max} = \frac{R_w}{R_g} \quad \text{(V B 38)}$$

It is however necessary here to consider the depth of modulation at the grid of the previous valve. Neglecting curvature of the characteristic, we

find from fig. 246:

$$m_{max} = \frac{(XT)}{(UT)}.$$

For simplicity we set the requirement rather higher, at:

$$m_{max} = \frac{(XT)}{(OT)}.$$

Now:

$$(XP_1) = (PP_1)\, R_w,$$
$$(OP_1) = (PP_1)\, R_g,$$
$$(TP_1) = (PP_1)\, R_{LF}.$$

Therefore:

$$m_{max} = \frac{R_{LF} + R_w}{R_{LF} + R_g}, \quad \ldots\ldots\ldots\ldots \quad \text{(V B 62)}$$

a condition usually satisfied more easily than the equation derived earlier (V B 38). It is shown below that a diode circuit in which $R_w < R_g$ causes reduction of the modulation-depth at the detector.

§ 15. Diode damping if $R_w \neq R_g$ (after a tuned circuit)

In § 13 we calculated the unmodulated alternating voltage present across a tuned circuit, and also the consequent rectified voltage across R_g. Moreover it appeared possible to go further and we calculated the characteristics, so that the A.F. voltage resulting from modulation might be ascertained. But, going back to the beginning, we find we can calculate directly the damping due to the modulated carrier, and therefore deduce the amplitude of the carrier voltage across the tuned circuit and the depth of modulation. For the damping imposed by the diode on the preceding tuned circuit where the R.F. input exceeds 1 V we found:

$$R_{HF} = \tfrac{1}{2}\, R\, \frac{V_{HF}}{V_{=}} \quad \ldots\ldots\ldots\ldots \quad \text{(V B 34)}$$

If the carrier is unmodulated the parallel connection of R_2 via the coupling capacitance C_2 has no effect (fig. 238); consequently the carrier is damped to the same degree as in the simple circuit where $R_w = R_g$. But when the carrier is modulated energy is lost in R_2 which must be supplied by the idebands. With modulation of a carrier of sufficient amplitude (i.e. $_{HF}/\, V_T \gg 1$) a voltage $V_{=} + m\, V_{HF} \cos pt$ appears across the load resis-

tance, and the current through the diode is accordingly:

$$I_{med} = \frac{V_{=}}{R_g} + \frac{m\, V_{HF} \cos pt}{R_w}, \quad \ldots\ldots \quad \text{(V B 63)}$$

where p denotes the modulation frequency.

The power supplied to the rectifier during one R.F. cycle is:

$$w = \tfrac{1}{2}\, I_{HF}\, V_{HF}\,(1 + m \cos pt). \quad \ldots\ldots \quad \text{(V B 64)}$$

or, substituting from equation (V B 26):

$$w = I_{med}\, V_{HF}\,(1 + m \cos pt) \quad \ldots\ldots \quad \text{(V B 65)}$$

Eliminating I_{med} [equation (V B 63)], this becomes:

$$w = \frac{V_{=}\, V_{HF}\,(1 + m \cos pt)}{R_g} + \frac{m\, V_{HF}^2 \cos pt}{R_w} + \frac{m^2\, V_{HF}^2 \cos^2 pt}{R_w} \quad \ldots\ldots \quad \text{(V B 66)}$$

The energy during a whole A.F. cycle is thus:

$$W = \frac{1}{2\pi} \int_0^{2\pi} w\, dpt,$$

$$W = \frac{V_{=}\, V_{HF}}{R_g} + \tfrac{1}{2}\, \frac{m^2\, V_{HF}^2}{R_w}, \text{ or}$$

$$W = \frac{V_{HF}^2}{2} \left\{ \frac{1}{\tfrac{1}{2} R_g \dfrac{V_{HF}}{V_{=}}} + \tfrac{1}{2}\, m^2 \frac{1}{\tfrac{1}{2} R_w} \right\} \quad \text{(V B 67)}$$

From this it follows that for the carrier the load is:

$$\tfrac{1}{2}\, R_g \frac{V_{HF}}{V_{=}} \quad \ldots\ldots \quad \text{(V B 68)}$$

and for the sidebands:

$$\tfrac{1}{2}\, R_w \quad \ldots\ldots \quad \text{(V B 69)}$$

A diode for which $R_w < R_g$ thus leads to a reduced modulation depth in the anode circuit of the preceding amplifier valve; the original depth of modulation is altered in the ratio of the dynamic resistance of the tuned circuit for the sidebands to its dynamic resistance for the carrier.

$$m' = m \frac{(R_v /\!/ \tfrac{1}{2}\, R_w)}{(R_v /\!/ \tfrac{1}{2}\, R_g)} = m \frac{R_w\,(2\, R_v + R_g)}{R_g\,(2\, R_v + R_w)} \quad \text{(V B 70)}$$

If to this new modulation depth we apply the limitation expressed in equation (V B 38), we obtain for the maximum original depth of modulation, as in § 13:

$$m_{max} = \frac{2R_v + R_w}{2R_v + R_g} = \frac{R_{LF} + R_w}{R_{LF} + R_g} \quad \ldots \quad \text{(V B 62)}$$

For the case of a band-pass filter the effect of the various dampings is found from equation (V B 50). The original modulation depth is altered in the ratio:

$$m' = m \sqrt{\frac{\frac{\frac{1}{2} R_w}{R_v + \frac{1}{2} R_w}}{\frac{\frac{1}{2} R_g}{R_v + \frac{1}{2} R_g}}} = m \sqrt{\frac{1 + \frac{2 R_v}{R_g}}{1 + \frac{2 R_v}{R_w}}}.$$

Since R_w and R_g are usually large compared with R_v, it is approximately correct to write:

$$m' = m \frac{1 + R_v/R_g}{1 + R_v/R_w} = m \frac{R_w}{R_g} \frac{R_v + R_g}{R_v + R_w} \quad \ldots \quad \text{(V B 71)}$$

As was the case in equation (V B 52), here too we observe that R_v appears in place of $2R_v$ for a single circuit.

From §§ 13—15 we may now draw the following conclusions regarding the effects on the preceding tuned circuit or band-pass filter:

1. The gain of the previous stage is apparently reduced. Normally this figure is ascertained by measuring the respective alternating voltages at the diode and at the grid of the preceding amplifier valve, but when measuring the voltage at the diode the low internal impedance of the signal generator results in there being no reduction in the depth of modulation, and accordingly the stage gain thus measured is less than the true figure by the amount of the reduction in modulation depth.
2. A further result of the reduction in the depth of modulation is that signals more deeply modulated than R_w/R_g can still be handled without distortion, and a modulation depth of R_w/R_g at the diode corresponds to deeper modulation at the grid of the preceding valve.
3. At high modulation frequencies the dynamic resistance of the inter-valve R.F. circuit is less than R_v and, moreover, contains a reactive component. The damping of the sidebands, which is equal to $\frac{1}{2} R_w$, is thus of less effect at high modulation frequencies than at low ones; in consequence the loss of high audio frequencies due to the selectivity of the tuned circuit is partly compensated.

In conclusion it may be observed that with small signals equations (V B 70) and (V B 71) do not hold good. Indeed for signals of less than 1 V a small rise in modulation occurs, equal to about 10% of the original modulation depth. The depth of modulation of signals around 1 V remains unchanged.

§ 16. Numerical example

To illustrate the results found above we shall now work out the following example.

Given: an I.F. band-pass filter of dynamic resistance $R_v = 400{,}000\ \Omega$ (including the AC resistance of the preceding valve); DC load of the detector $R_g = 0.5\ \text{M}\Omega$ and AC-load $R_w = 0.33\ \text{M}\Omega$; slope of the previous valve $S = 1.8$ mA/V; amplitude of the unmodulated carrier at the grid of the amplifier $V_g = 50$ mV.

Required:

1. the steady voltage $V_{=}$ across the diode load resistance;
2. the amplitude of the audio voltage output V_{LF} for a modulation depth of 30%;
3. the maximum depth of modulation of V_g which can be handled without clipping the voltage peaks.

(1) Supposing that the band-pass filter is critically coupled, we can write for equation (V B 52):

$$V_{=} = \tfrac{1}{2} \times 0.0018 \times 0.05 \times 400{,}000 \times \frac{0.5}{0.5 + 0.4} = 10\text{V}.$$

If it is possible to make use of published characteristics the alternating voltage applied to the diode circuit may first be calculated. The voltage being in this case high, the damping is $R_d = \frac{1}{2} \times 500{,}000 = 250{,}000\ \Omega$. The secondary circuit of the band-pass filter has therefore a dynamic resistance of:

$$400{,}000\ //\ 250{,}000 = 154{,}000\ \Omega$$

and the amplitude of the voltage induced in this circuit is:

$$V_{HF} = 0.05 \times 0.0018 \times \tfrac{1}{2} \sqrt{400{,}000 \times 154{,}000} = 11.1\ \text{V (peak)} = 8\ \text{V}_{\text{RMS}}.$$

Fig. 227 shows that with such an input an indirectly-heated diode gives a DC output of about 11 V and a battery diode about 8 V (fig. 235).

It appears that in view of the approximations employed very high accuracy must not be expected from this calculation.

(2) The amplitude of the A.F. voltage at a modulation depth of 30% is, from

fig. 248 and equation (V B 54):

$$V_{LF} = m f S V_g R_v \frac{R_w}{R_v + R_w} =$$

$$0.3 \times 0.5 \times 0.0018 \times 0.05 \times 400{,}000 \times \frac{0.33}{0.33 + 0.4} = 2.45 \text{ V}.$$

It should also be possible to calculate the reduced modulation depth of the carrier at the diode and then make use of the diode characteristic (fig. 227). From equation (V B 71):

$$m' = 0.3 \frac{0.33}{0.5} \times \frac{0.4 + 0.5}{0.4 + 0.33} = 0.243.$$

Fig. 227 shows an A.F. voltage of 2.3 V_{RMS} for $m = 0.3$ and $V_{HF} = 8\ V_{RMS}$. For $m = 0.243$ the A.F. amplitude is therefore:

$$V_{LF} = 2{,}3 \sqrt{2} \times \frac{0.243}{0.3} = 2.6 \text{ V}.$$

(3) The maximum permissible depth of modulation at the grid of the preceding amplifier valve is ascertained from equations (V B 61) and (V B 62):

$$m_{max} = \frac{0.4 + 0.33}{0.4 + 0.5} = 0.81 = 81\%.$$

§ 17. Measurements on the detector stage

In the foregoing we have dealt with the main points to be considered in designing a detector stage, and it will be apparent that when carrying out measurements on a detector, or preferably on a detector with its preceding I.F. tuned circuit, special precautions must be taken.

The classic method of measuring the gain of a particular stage in a receiver is to apply a modulated signal from a calibrated oscillator to the output terminals of the stage concerned and ascertain the magnitude of the output voltage, and afterwards to transfer the oscillator to the input terminals and adjust it so that the output voltage from the stage is the same as before. The ratio of the two applied signals indicates the amplification.

Taking measurements with constant output ensures that the detector is operating each time under the same conditions; this precaution is necessary, as signal strength affects the working of the detector. Nevertheless, by itself this precaution does not prevent errors, as will be evident from the following:

a. If the signal at the detector is of such strength that change of the modulation depth occurs (see § 13), the variation is observed only when the signal is fed to the I.F. amplifier and not when it is applied directly to the diode. When the signal is applied to the I.F. valve not only is amplification obtained but there is also a simultaneous reduction or increase of modulation depth, depending on whether the signal is large or small. Thus with large signals the measured I.F. gain is an understatement, and with small signals an overstatement. For practical reasons, therefore, the actual gain obtained during reception should be measured with a constant input to the detector. The resulting gain factor is, however, still untrustworthy for checking the constants of the I.F. circuit, as an error of as much as 10% may occur. It is therefore more accurate to measure the I.F. gain in such a way that modulation depth can play no part, namely with an unmodulated signal. The A.F. output can then of course no longer be used as an indicator, but instead the direct current through the diode load resistance must be measured. Generally, however, the rise compared with the no-signal current is so small that inaccuracy results. A considerable improvement is obtained if another receiver of the same type is brought into use and its second I.F. stage employed as measuring amplifier. The diode current of this auxiliary receiver is measured, the grid of the I.F. valve being coupled through a capacitance of 1 pF to the diode anode in the set under test. This coupling is preferably variable, in order that overloading of the I.F. valve in the auxiliary receiver may be avoided.

Measuring the I.F. gain in this way, with a constant carrier voltage at the diode, it is a simple matter to determine at the same time the variation of modulation depth. It is merely necessary to modulate the test signal and, keeping the carrier at the same amplitude, measure the A.F. output voltage from the diode. This latter voltage will generally change if the test signal is transferred from the diode to the I.F. valve, and the ratio of the respective A.F. voltages indicates the change of modulation depth. The same set-up is very suitable for experimental determination of diode damping by a substitution method. With a constant test signal to the I.F. valve the diode is replaced by a resistor of such value that the measured direct current in the detector of the auxiliary receiver remains unchanged. It is of course necessary to check that the tuning of the I.F. transformer secondary in the receiver under test is not disturbed when the resistor is substituted for the diode *.

* When, as will usually be necessary, the I.F. tuned circuit is retrimmed, a new danger arises. In modern I.F. transformers trimming is often effected by turning the iron core. This alters not only the resonant frequency but also the quality factor Q of the coil, and there is in consequence a change in the amplification, which is admittedly not large but cannot be neglected when the damping resistance being ascertained is high. For example, in a specific coil, turning the core through its range of adjustment altered Q from 168 to 138.

b. Due to the self-capacitance of the diode an error arises which is not easily avoided. It was shown in B § 5 that the applied voltage is reduced by voltage drop over the capacitance bridging the load resistance. When the test signal is transferred from the I.F. valve to the diode this reduction disappears (see fig. 249). While it would be logical to apply the test signal between points 1 and 2, to which usually the secondary of the I.F. transformer is also joined, it is not possible to do so because one side of the test oscillator is almost always earthed. Consequently there is now no longer a division of voltage across C_1 and C_2, but across C_k (the coupling capacitance to the signal generator) and C_2 ,which is in parallel with the very high impedance presented by the I.F. tuned circuit.

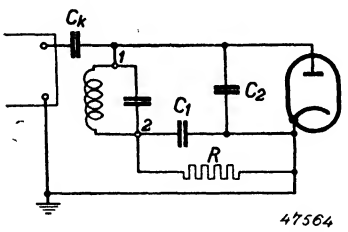

Fig. 249. Circuit for measuring the sensitivity of the detector stage.

Now C_k is generally much larger than C_1, so that the reduction of the applied voltage can be neglected. It might be supposed that the solution would be to make the coupling capacitance C_k smaller, so that when taking a measurement directly on the diode the same reduction of voltage occurred. This course, however, introduces a great deal of uncertainty into the measurements, because already any slight detuning of the I.F. circuit, due for instance to the lead to C_k, considerably alters the magnitude of the total capacitance C_2. It is therefore better to keep C_k large. It is, however, possible to short-circuit points 1 and 2, so that a division of voltage across C_k and $(C_1 + C_2)$ occurs; being determined by larger capacitances, this division is more certain. C_k can now be so fixed in relation to $C_1 + C_2$ that the same reduction appears as when measuring via the I.F. valve.

The reduction of voltage can be ascertained by taking a measurement via an I.F. valve while temporarily giving C_1 a fairly high value; but not too high, as otherwise the A.F. load of the diode will be appreciably altered (a suitable value for C_1 is 200 pF). The reduction of voltage then disappears; it is equal to the increase of sensitivity caused by raising the value of C_1.

c. When measuring directly on the diode a blocking capacitor C_k (fig. 249) is necessary; otherwise the load R would be shorted through the I.F. transformer and the generator. While it was recommended under *b* not to make C_k too small, this capacitance must not on the other hand be too large, for, being in parallel with R, it affects the A.F. load on the diode. It was observed in B § 4 that the A.F. signal is diminished when R_w

becomes smaller than R_g. With indirectly-heated diodes the effect is slight but can be appreciable with battery diodes. As the modulation frequency used in measurements is generally 400—500 c/s, difficulties may be avoided by ensuring that C_k has a high reactance in relation to 0.3 MΩ, the customary value of R_w. If we make C_k 200 pF, its reactance at 500 c/s is:

$$\frac{1}{\omega C_k} = 1.6 \text{ MΩ},$$

which in practice is high enough.

d. Under *a* the measurement of diode damping by the substitution method was described. Sometimes, however, it is preferable to ascertain the damping by measurements on the I.F. circuit. With this method we note by how much the signal generator must be detuned from resonance to reduce amplification in the ratio $1 : 1/\sqrt{2}$. Accuracy depends on keeping the signal constant at the diode, since the damping varies with signal strength; accordingly it is necessary instead to increase the output of the signal generator by $\sqrt{2}$ and then to detune it until the rectified signal from the diode falls to its original level.
Fig. 232 shows that if, for example, diode damping be measured by detuning the generator until the original rectified signal of 0.3 V is reduced to $0.3/\sqrt{2}$ = approximately 0.2 V, a figure of 110,000 Ω would be obtained, whereas the correct figure is 130,000 Ω.

e. Occasionally it is necessary to measure the rectified output voltage from a diode. When the I.F. signal is small, the rectified voltage is so low in relation to the no-signal voltage that accurate determination is impossible. In such cases it is possible to balance out the no-signal voltage, thus permitting the use of a more sensitive instrument to measure the change of voltage. A suitable circuit is given in fig. 250.

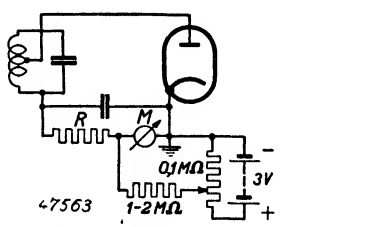

Fig. 250. Compensated circuit for measuring the increase of voltage, ΔV, across the diode load.

The meter M, with a full-scale deflection of 1 or 2 μA, is then adjusted to 0 by means of the potentiometer, the signal input to the diode being zero. The quantity ΔV for any signal is then ascertained by multiplying the meter reading by the known value of R.

C. Diode detection under different circumstances

§ 1. Introduction

In the foregoing pages we have considered first the detection of an unmodulated carrier and afterwards that of an amplitude-modulated carrier. In passing through the selective amplifier preceding the detector, a modulated carrier may suffer deformation of a kind which will affect the rectified signal. Such deformation consists in the unequal amplification of the three components comprising the modulated wave: the carrier and its two sidebands.

If the sidebands are passed at the same level, differing however from that of the carrier, change of modulation depth occurs, but if the two sidebands are passed at different levels distortion of the modulation envelope and thus also of the post-detector signal will result. Although this distortion actually occurs before the detector, it can best be dealt with under detection. By regarding the modulated wave as the sum of several components of different frequency we can derive expressions which will also be applicable to the case of two signals, one wanted and the other unwanted, applied simultaneously to a detector. In such a case, assuming linear rectification, it will be found that the stronger signal demodulates the weaker one.

§ 2. The carrier with unequal sidebands

Suppression of the sidebands in relation to the carrier occurs in any selective system. It has already been observed in Chapter I that in order to limit this suppression selective devices are sought which have a flat-topped resonance curve.

Asymmetrical sidebands may occur intentionally or unintentionally. Sometimes one sideband is completely suppressed at the transmitter, in order to reduce the bandwidth. The same course is adopted, for example, in the R.F. or I.F. section of a television receiver where, other things being equal, the gain of the tuned circuits depends on the width of the frequency band to be passed; if the bandwidth can be halved the amplification is considerably increased.

Partial suppression of one sideband occurs involuntarily in superheterodyne receivers when, owing to frequency drift in the oscillator, the I.F. signal no longer corresponds to the resonant frequency of the I.F. amplifier; one

sideband may then fall at the peak of the response curve and the other at its foot. The same sort of thing happens if a receiver is slightly detuned in order to reduce interference from a transmission on an adjacent channel.

We shall first consider, by way of illustration, the nature of a carrier with asymmetrical sidebands, and afterwards examine an approximate method of calculating the effects which arise.

A pure sinusoidal amplitude-modulated wave is represented by the formula:

$$v = V\{\, 1 + m \cos (pt + \varphi) \,\} \cos \omega t \quad . \quad . \quad . \quad . \quad . \quad \text{(V C 1)}$$

in which ω is the frequency of the carrier and p that of the modulation. (In this formula cosines are often used instead of sines, as only plus signs then occur in the calculations and there is less risk of mistakes.)

The equation may be written in the following form:

$$v = V \cos \omega t + \tfrac{1}{2} m V \cos\{ (\omega + p) t + \varphi \} + \tfrac{1}{2} m V \cos\{ (\omega - p) t - \varphi \} \quad . \quad . \quad . \quad \text{(V C 2)}$$

and we now easily recognise the carrier of frequency ω and the two sidebands of frequency $\omega + p$ and $\omega - p$ respectively.

It follows from equation (V C 1) that v is nil when $\cos \omega t = 0$, i.e. the nodes of the modulated R.F. oscillation coincide with the nodes of the carrier, so that the frequency ω can easily be traced in the modulated carrier. This

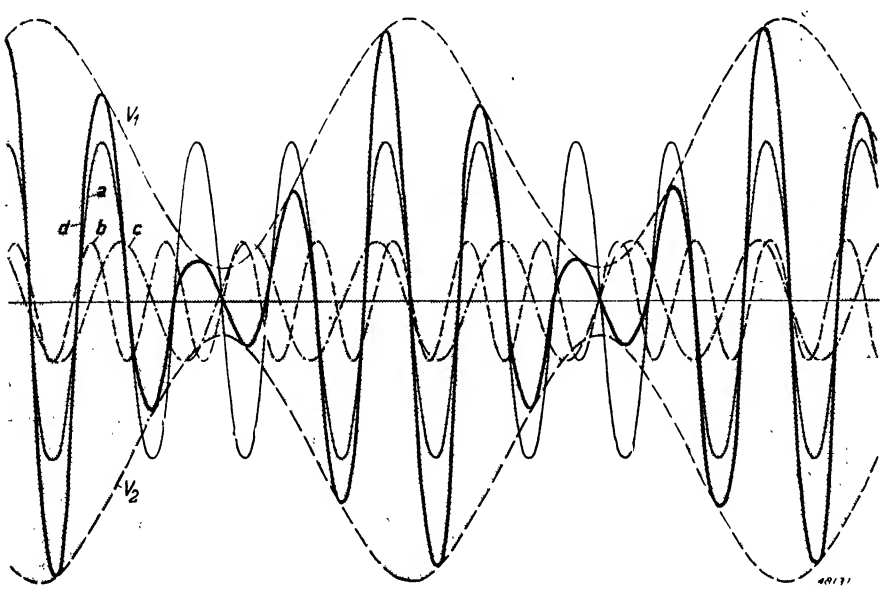

Fig. 251. Modulated R.F. oscillation, composed of a carrier *a* and sidebands *b* and *c*. The resultant wave is indicated by the heavy line *d*.

means, in equation (V C 2), that at the nodes of the carrier the amplitudes of the sideband components are equal and opposite. The significance of the angle φ is best seen by considering the situation at the instant when $t = 0$. From equation (V C 2) it follows that the carrier then has its maximum value V, while the sideband components are equal and opposite and have a magnitude of $\frac{1}{2}\, m V \cos \varphi$.

On the other hand we see from equation (V C 1) that, at the moment when $t = 0$ the modulation term has a value $1 + m \cos \varphi$. Furthermore, we note that whenever the carrier attains its peak value the amplitudes of the sideband components are equal in magnitude and phase.

Fig. 251 depicts a modulated oscillation, the result of combining a carrier and sideband components. Curve *a* represents the carrier of frequency ω and amplitude V; curve *b* is a sideband of frequency $\omega + p$ and amplitude $\frac{1}{2}\, m V$, and curve *c* the other sideband of frequency $\omega - p$ and the same amplitude.

In our example $m = 0.8$ and, for clarity, p has been made $\frac{1}{4}\, \omega$. The durations of the cycles *c*, *a* and *b* are related:

$$T_c : T_a : T_b = \frac{1}{\omega - p} : \frac{1}{\omega} : \frac{1}{\omega + p} = \frac{1}{3/4\,\omega} : \frac{1}{\omega} : \frac{1}{5/4\,\omega} = 20 : 15 : 12.$$

In practice ω will of course be very much greater than p; this we shall refer to later. The angle φ is taken as 30° in the present example. The resultant *d* of the carrier *a* and the sidebands *b* and *c* is arrived at by adding the corresponding vertical distances of *a*, *b* and *c* from the axis; how an amplitude-modulated sine-wave is composed of the several frequencies is now clearly seen in the diagram; the same applies for the various properties mentioned above.

After rectification of the R.F. signal we obtain the A.F. voltage. As has already been observed, diode detection is mostly employed, in which rectification occurs through the charging of a capacitance to the peak value of the resultant, *d*. These peaks lie along curve V_1 and, if they follow one another in quick succession, as they usually do ($\omega \gg p$), the voltage across the capacitance will correspond to this curve. The envelope is sinusoidal, as indicated in equation (V C 1) by the term $\{1 + m \cos (pt + \varphi)\}$. It is further to be noted that the mean DC voltage after rectification is equal to the amplitude of the carrier *a*.

We may now enquire what happens when, in fig. 251, one sideband is omitted entirely. The R.F. voltage in such a case is given by:

$$v = V \cos \omega t + \alpha\, V \cos \{(\omega + p)\, t + \varphi\}. \quad . \quad . \quad \text{(V C 3)}$$

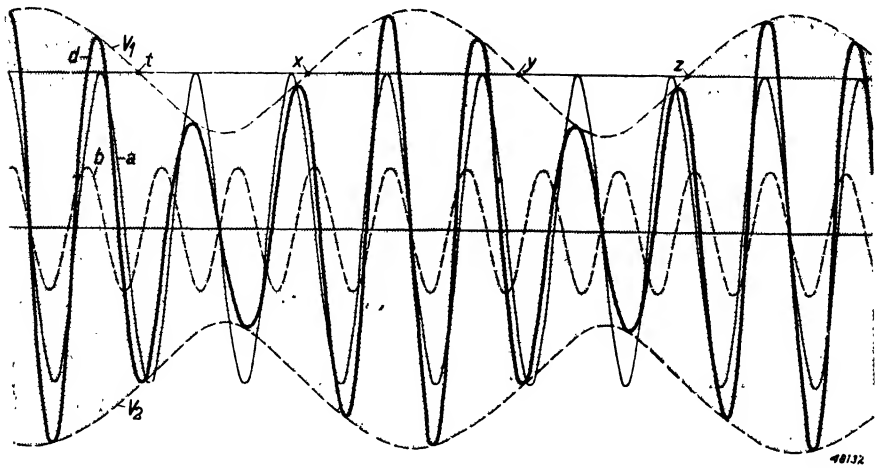

Fig. 252. Modulated R.F. oscillation, consisting of a carrier a and only one sideband b; the resultant wave is indicated by the heavy line d.

The quantity α represents the ratio of the amplitude of one sideband to that of the carrier and replaces the quantity $\frac{1}{2}\ m$ in equation (V C 2). Fig. 252 shows equation (V C 3) in graphic form; a is again the carrier of frequency ω and amplitude V, while b is the sideband of frequency $\omega + p$ and amplitude $\alpha\ V$.

The other sideband component is thus omitted. In this example $\alpha = 0.4$ and, for clarity, $p = \frac{1}{4}\ \omega$.

The angle φ is 30°; the resultant d is obtained by adding the vertical distances of a and b from the axis. From equation (V C 3) we see that when $cos\ \omega t = 0$ the amplitude of the R.F. oscillation is usually not zero; in this case, therefore, the nodes of d do not coincide with those of the carrier a.

This is also made plain in fig. 252, where we find that the nodes of d are no longer uniformly spaced: frequency-modulation is thus occurring. With suppression of one sideband this cannot be avoided.

After detection the A.F. voltage appears. Assuming once more that ω is large compared with p, we know that the A.F. output will follow the envelope of the voltage peaks. By making use of the calculation given below the contours V_1 and V_2 in fig. 252 were constructed.

In fig. 253 the distorted envelope is redrawn in such a way that the areas enclosed are equal on each side of the axis. In addition a pure sine wave f is shown, the amplitude of which, for sake of comparison, has been made about the same as that of V_1.

We now see that V_1 does not reach the same amplitude on the two sides

of the axis; the distortion thus consists mainly of second harmonics. If one sideband of a normally modulated carrier is suppressed the amplitude of the A.F. voltage is about halved, owing to the absence of the periodic

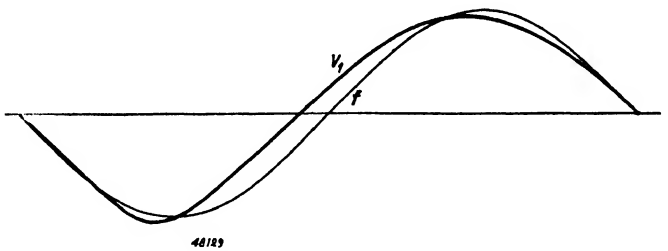

Fig. 253. One cycle of the distorted envelope V_1 in fig. 252, compared with a pure sine wave f.

additive effect of the second sideband; this shallower modulation is clearly shown in fig. 252.

Assuming a carrier with one sideband of equal amplitude ($\alpha = 1$), we obtain the result illustrated in fig. 254 and given by:

$$v = V \cos \omega t + V \cos (\omega + p)\, t = 2V \cos \frac{pt}{2} \cos (\omega + \frac{p}{2})\, t \quad . \quad . \quad \text{(V C 4)}$$

The phase angle φ is again zero.

After detection the A.F. voltage is found to have a positive value of $\cos pt/2$. The individual pulses of audio voltage are half-sines of frequency $p/2$, and the minima fall on the axis. The A.F. voltage is thus much distorted, containing about 15% of second and 3% of third harmonics. Such a result will be obtained if one sideband of a normally modulated carrier is suppressed and at the same time the carrier is attenuated in relation to the other sideband. In commercial radio-telephony practice sometimes only one sideband is transmitted, the carrier being completely suppressed. In such a case the carrier is restored at the receiver, in order to prevent excessive distortion appearing in the rectified A.F. voltage.

For the case of a carrier with a single sideband we reach the following conclusions:

1. the resulting R.F. wave is frequency-modulated;
2. the amplitude of the A.F. signal after detection is about half that derived from a carrier with two sidebands;
3. the rectified voltage is of sine form with some distortion, mainly second harmonic.

A carrier with unequal sidebands can be considered on similar lines to the

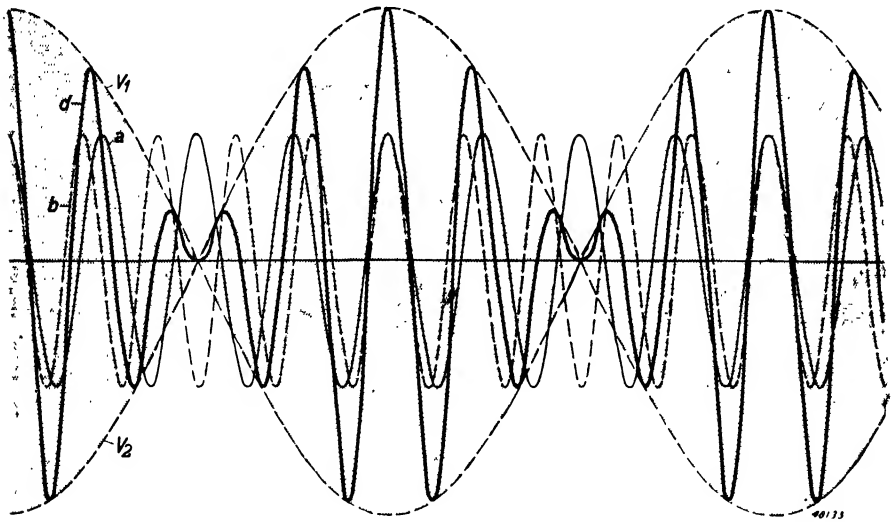

Fig. 254. Modulated R.F. oscillation, composed of a carrier a and one sideband b of the same amplitude; the heavy line d shows the resultant.

foregoing. For the respective amplitude ratios of the sidebands to the carrier we may put α and β, thus:

$$v = V \cos \omega t + \alpha V \cos\{(\omega + p)\, t + \varphi\} + \beta\, V \cos\{(\omega - p)\, t - \varphi\} \quad \text{(V C 5)}$$

It should be noted that in the following discussion no account is taken of possible variation of the angle φ for the frequencies $\omega + p$ and $\omega - p$, which may for various reasons occur during the passage of the carrier and its sidebands through the amplifier. In consequence φ will not be considered further, and for simplicity only the special case of $\varphi = 0$ will be dealt with, since it is always possible to find a starting point at which the three components are in phase. The question now is what does equation (V C 5) indicate regarding the A.F. signal.

In order to simplify the mathematics we shall suppose that the detector is linear, and therefore that the A.F. voltage is always equal to the instantaneous peak voltage of the R.F. signal. Since distortion is then at a minimum, this is the condition normally sought. The instantaneous peak voltages may now be calculated as follows.

The similarity of figs 252 and 254 suggests that equation (V C 3) might be rewritten in a form representing a carrier multiplied by a periodically varying factor, namely a modulation term.

We have already seen in fig. 254 that this modulation term is no longer of pure sine form.

Equation (V C 5) can now be written:

$$v = V\,[\,cos\ \omega t\,\{\,1 + (\alpha + \beta)\ cos\ pt\,\} + sin\ \omega t\,\{\,(\beta - \alpha)\ sin\ pt\,\}\,]. \quad \text{(V C 6)}$$

In this equation v consists of two components, with a frequency ω and a phase difference of 90°; vectorial addition of the components gives us the total voltage. The amplitude then follows from:

$$v_{max} = V\sqrt{\{\,1 + (\alpha + \beta)\ cos\ pt\,\}^2 + \{\,(\beta - \alpha)\ sin\ pt\,\}^2} \quad \ldots \quad \text{(V C 7)}$$

This equation may be rearranged to:

$$v_{max} = V\sqrt{1 + (\alpha - \beta)^2 + 2\,(\alpha + \beta)\ cos\ pt + 4\ \alpha\ \beta\ cos^2\ pt} \quad \ldots \quad \text{(V C 8)}$$

In these two formulae, (V C 7) and (V C 8), we thus have the rectified voltage expressed as a function of time. By substituting $\alpha = \beta = \frac{1}{2}\ am$, we can at once derive from (V C 7) the normal A.F. voltage obtained with equal sidebands; the equation then becomes:

$$v_{max} = V(1 + am\ cos\ pt).$$

The derived A.F. voltage can be determined from equation (V C 8) in the form of a Fourier series with the frequencies p, $2p$, $3p$, etc., but this method leads to a solution containing elliptical integrals. We shall accordingly adopt the simpler method, which nevertheless is accurate enough, of developing the expression (V C 8) into a power series of *cos pt*. If from this series we separate the components which produce the frequencies p, $2p$, $3p$, etc., we finally obtain the required distortion percentage. We shall compute the distortion up to and including the fourth harmonic, i.e. the series is developed only as far as the term *cos* $4pt$.

We shall first show how the harmonics *cos pt*, *cos* 2 *pt*, etc. can very easily be picked out of a power series of *cos pt*.

The development of the power series for (V C 8) can be represented by:

$$v_{max} = V\{f_0 + f_1\ cos\ pt + f_2\ cos^2 pt + f_3\ cos^3 pt + f_4\ cos^4 pt + \ldots\} \quad \text{(V C 9)}$$

and the harmonics *cos pt*, *cos* 2 *pt*, etc. are then to be derived. If we consider (V C 9) in the following form:

$$v_{max} = V\{g_0 + g_1\ cos\ pt + g_2\ cos\ 2\ pt + g_3\ cos\ 3\ pt + g_4\ cos\ 4\ pt + \ldots\} \quad \text{(V C 10)}$$

the problem is then to express g_0, g_1, etc. in terms of f_0, f_1, etc.

We know the following relations:

$$\left.\begin{aligned} \cos pt &= \cos pt \\ \cos^2 pt &= \frac{1}{2} + \frac{1}{2}\cos 2pt \\ \cos^3 pt &= \frac{3}{4}\cos pt + \frac{1}{4}\cos 3pt \\ \cos^4 pt &= \frac{5}{8} + \frac{1}{2}\cos 2pt + \frac{1}{8}\cos 4pt \end{aligned}\right\} \quad \ldots \quad \text{(V C 11)}$$

Substituting the values of equations (V C 11) in equation (V C 9) gives the series of (V C 8) the form of (V C 10). Admittedly some error then occurs, because, for example, a term such as $\cos^6 pt$ also includes terms with $\cos 4\,pt$ and $\cos 2\,pt$, but the last-named are small compared with the same terms in the lower powers. For (V C 10) we can therefore write:

$$\begin{aligned} v_{max} = V \Big\{ &\left(f_o + \frac{1}{2}f_2 + \frac{5}{8}f_4 + \ldots\right) + \left(f_1 + \frac{3}{4}f_3 + \ldots\right)\cos pt + \\ &+ \left(\frac{1}{2}f_2 + \frac{1}{2}f_4 + \ldots\right)\cos 2\,pt + \left(\frac{1}{4}f_3 + \ldots\right)\cos 3\,pt + \\ &+ \left(\frac{1}{8}f_4 + \ldots\right)\cos 4\,pt + \ldots \Big\} \quad \ldots \quad \text{(V C 12)} \end{aligned}$$

From this it follows that:

$$\left.\begin{aligned} g_o &= f_o + \frac{1}{2}f_2 + \frac{5}{8}f_4 \\ g_1 &= f_1 + \frac{3}{4}f_3 \\ g_2 &= \frac{1}{2}f_2 + \frac{1}{2}f_4 \\ g_3 &= \frac{1}{4}f_3 \\ g_4 &= \frac{1}{8}f_4 \end{aligned}\right\} \quad \ldots \quad \text{(V C 13)}$$

We shall first deal with the case of a completely suppressed sideband. In equation (V C 8) we then have $\beta = 0$, or, what amounts to the same thing, $\alpha = 0$. Consequently:

$$v_{max} = V\sqrt{1 + \alpha^2 + 2\alpha \cos pt} =$$

$$= V\sqrt{(1 + \alpha^2)}\left(1 + \frac{2\alpha}{1 + \alpha^2}\cos pt\right)^{\frac{1}{2}} \quad \ldots \quad \text{(V C 14)}$$

We now make use of the following well-known series development (applicable where $x < 1$):

$$(1 + x)^n = 1 + \frac{n}{1}x + \frac{n(n-1)}{1.2}x^2 + \frac{n(n-1)\ (n-2)}{1.2.3.}x^3 + \ldots$$

$$+ \frac{n}{1}x^{n-1} + x^n,$$

in which

$$x = \frac{2\alpha}{1 + \alpha^2}\cos pt$$

is substituted. It is true that the condition $x < 1$ is not satisfied if $\alpha = 1$ and $\cos pt = 1$, but in practice the difficulty may be avoided by ignoring the case of $\alpha = 1$. A close approach thereto does not invalidate the calculation.

For $n = \frac{1}{2}$ the progression becomes:

$$(1 + x)^{1/2} = 1 + \tfrac{1}{2}x - \frac{1}{8}x^2 + \frac{1}{16}x^3 - \frac{5}{128}x^4 \ldots\ldots$$

The series is not continued beyond $\cos 4\ pt$, as the higher harmonics are of no concern to us. If we apply this series development for (V C 14) we get:

$$v_{max} = V\left\{(1 + \alpha^2)^{1/2} + \frac{\alpha}{(1 + \alpha^2)^{1/2}}\cos pt - \tfrac{1}{2}\frac{\alpha^2}{(1 + \alpha^2)^{3/2}}\cos^2 pt + \right.$$

$$\left. + \tfrac{1}{2}\frac{\alpha^3}{(1 + \alpha^2)^{5/2}}\cos^3 pt - \frac{5}{8}\frac{\alpha^4}{(1 + \alpha^2)^{7/2}}\cos^4 pt \ldots\right\} \ldots\ldots \quad \text{(V C 15)}$$

From equations (V C 15) and (V C 13) it now follows, if α is fairly small in relation to unity, that:

$$\left.\begin{aligned}
g_4 &= \frac{1}{8} f_4 = -\frac{5}{64}\frac{\alpha^4}{(1+\alpha^2)^{7/2}} \approx \frac{5}{64}\alpha^4; \\
g_3 &= \frac{1}{4} f_3 = \frac{1}{8}\frac{\alpha^3}{(1+\alpha^2)^{5/2}} \approx \frac{1}{8}\alpha^3; \\
g_2 &= \frac{1}{2} f_2 + \frac{1}{2} f_4 = -\frac{1}{4}\frac{\alpha^2}{(1+\alpha^2)^{3/2}} - \frac{5}{16}\frac{\alpha^4}{(1+\alpha^2)^{7/2}} \approx -\frac{1}{4}\alpha^2; \\
g_1 &= f_1 + \frac{3}{4} f_3 = \frac{\alpha}{(1+\alpha^2)^{1/2}} + \frac{3}{8}\frac{\alpha^3}{(1+\alpha^2)^{5/2}} \approx \alpha; \\
g_0 &= f_0 + \frac{1}{2} f_2 + \frac{5}{8} f_4 = (1+\alpha^2)^{1/2} - \frac{1}{4}\frac{\alpha^2}{(1+\alpha^2)^{1/2}} \approx (1+\alpha^2)^{1/2}
\end{aligned}\right\} \quad \text{(V C 16)}$$

For the distortion we find:

$$\left.\begin{aligned}
&\text{Second harmonic:} \quad d_2 = \frac{|g_2|}{|g_1|} = \frac{1}{4}\alpha \\
&\text{Third harmonic:} \quad d_3 = \frac{|g_3|}{|g_1|} = \frac{1}{8}\alpha^2 \\
&\text{Fourth harmonic:} \quad d_4 = \frac{|g_4|}{|g_1|} = \frac{5}{64}\alpha_3
\end{aligned}\right\} \quad \ldots \quad \text{(V C 17)}$$

If $\alpha = 0.15$ we thus get:

$$d_2 = 3.75\%; \; d_3 = 0.3\%; \; d_4 = \text{extremely small}$$

and for $\alpha = 0.4$:

$$d_2 = 10\%; \; d_3 = 2\%; \; d_4 = 0.5\%.$$

In the case of $\alpha = 1$, i.e. when the amplitudes of the carrier and of the sidebands are equalised by artificial means, it is not permissible to employ this approximate method of computing the distortion. The values of d_2, d_3 and d_4 must then be calculated from the full equations for g_2, g_3 and g_4, and we get:

$$d_2 = 15\%; \; d_3 = 3\%; \; d_4 = 1\%.$$

In fig. 255 the distortion due to second and third harmonics is shown as a function of α.

We can of course also calculate the distortion present when the two sidebands are asymmetrical, but as the process is rather tedious it will suffice here to give the results:

$$\left.\begin{aligned} &\text{Second harmonic:} \quad d_2 = \frac{1}{2}\,\frac{(\alpha-\beta)^2}{(\alpha+\beta)}\,; \\ &\text{Third harmonic:} \quad d_3 = \frac{1}{8}\,(\alpha-\beta)^2\,; \\ &\text{Fourth harmonic:} \quad d_4 = \frac{1}{64}\,\frac{(\alpha-\beta)^2(5\alpha^2+6\alpha\beta+5\beta^2)}{(\alpha+\beta)} \end{aligned}\right\} \quad . \; . \quad \text{(V C 18)}$$

From these we then get:

For $\alpha = 0.15$ and $\beta = 0.05$: $d_2 = 1.25\,\%$;
$d_3 = 0.1\,\%$;
$d_4 =$ extremely small.

For $\alpha = 0.4$ and $\beta = 0.1$: $d_2 = 4.5\,\%$;
$d_3 = 1.1\,\%$;
$d_4 = 0.3\,\%$.

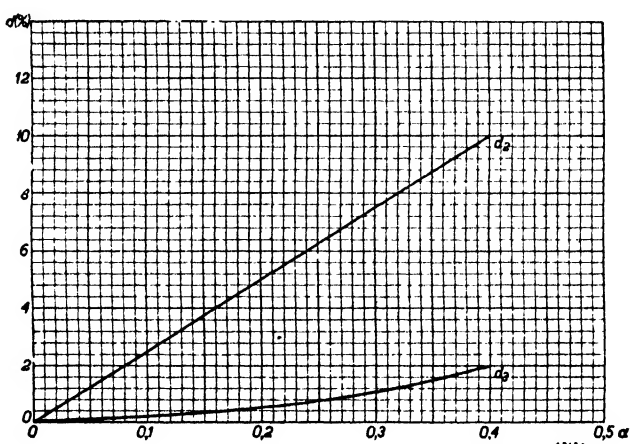

Fig. 255. Distortion due to second and third harmonics as a function of the factor α, the ratio of the sideband amplitude to that of the carrier.

These results lead to the following conclusions:

1. the distortion consists mainly of second harmonic;
2. when the second sideband is not completely suppressed the distortion diminishes rapidly.

In fig. 252 we had the wave-form resulting from the combination of a carrier with a single sideband ($\alpha = 0.4$ and $\varphi = 30°$). The envelopes V_1 and V_2 in this figure, which were drawn by using the calculations given, clearly indicate, as has already been remarked, that the A.F. voltage derived from such a modulated carrier is only about half that obtained from a carrier with two sidebands.

The occurrence of frequency-modulation (as evidenced in fig. 252 by the unequal spacing of the nodes of the modulated wave) has already been mentioned, but it also becomes apparent from calculation.

From equation (V C 6), in which the R.F. voltage was analysed into a sine component and a cosine component, it follows that for the phase angle of the resultant RF wave-form:

$$\tan \varphi = \frac{(\beta - \alpha) \sin pt}{\{1 + (\beta + \alpha) \cos pt\}} \quad \ldots\ldots\ldots \quad \text{(V C 19)}$$

We see then that the phase of the R.F. wave depends on the modulation, and strictly we ought to speak of phase-modulation. This variation of phase is naturally accompanied by shifting of the nodes.

Finally, it can be shown mathematically that, with asymmetrical sidebands as in other cases, combination tones appear in addition to the harmonics if the modulation is made up of various frequencies p, q, etc.

§ 3. Demodulation effect

If two signals V_1 and V_2 are fed to a detector simultaneously, their sum can be represented by equation (V C 5), in which $V = V_1$, $\alpha V = V_2$ and $\beta = 0$. The frequencies of the two signals are then ω and $\omega + p$ respectively. The results already derived above may thus be used in relation to the detection of these simultaneous signals.

We shall now use $V_2 = \alpha V$ to denote a comparatively weak interfering transmission, and V_1 the wanted and much stronger signal. Both carriers are for the moment unmodulated, but V_2 would nevertheless show itself by causing a heterodyne of frequency p; unless that frequency were outside the audible spectrum, as it could very well be, in which case V_2 would cause no disturbance. It is clear, however, that as soon as the unwanted carrier is modulated, after rectification the modulation will become audible and cause a disturbance. How strong an A.F. signal can the modulation of V_2

be expected to produce? When only the interfering transmission V_2 is present, and its depth of modulation is m, the A.F. signal will be equal to mV_2 if detection is linear. But when the wanted transmission V_1 is also being received it is found that the interfering signal is considerably reduced; this fortunate phenomenon thus confers a degree of selection on a receiver in addition to the selectivity provided by its tuned circuits. With square-law detection the effect does not occur.

In § 2 it was shown that a sum of voltages, as in equation (V C 5), can also be written as a voltage of one frequency but with varying phase and modulated as in (V C 8). In the case now being considered we should get:

$$V_{max} = V_1 \sqrt{1 + \alpha^2 + 2\,\alpha \cos pt} \quad \ldots\ldots \quad \text{(V C 20)}$$

or, rearranged as in equation (V C 10):

$$V_{max} = V_1 (g_o + g_1 \cos pt + g_2 \cos 2pt + \ldots) \quad \text{(V C 21)}$$

The values of g_o, g_1, g_2, etc. can be ascertained for a known value of α and $\beta = 0$ from the data in C § 2 [equation (V C 16)].

In equation (V C 21) we thus have a wanted and an interfering signal combined as a wave-form the envelope of which varies according to the progression within brackets.

With linear detection the A.F. voltage across the diode load is equal to V_{max}, and equation (V C 21) tells us that this voltage includes components of frequency p, $2p$, $3p$, etc. As, however, it was postulated that p was inaudible, these frequencies do not further interest us. There remains the rectified voltage $V_1 g_0$. As long as V_2 is unmodulated, i.e. constant, this steady voltage is harmless, but as soon as V_2 is modulated α varies and consequently g_o too. $V_1 g_o$ then becomes a varying quantity, which passes into the audio amplifier as interference.

For the effect of variation of V_2 on $V_1 g_o$ we can write with some approximation:

$$\Delta V_{max} = V_1 \frac{dg_o}{dV_2} \Delta V_2 \quad \ldots\ldots\ldots \quad \text{(V C 22)}$$

Although it might be expected that when V_2 changes by ΔV_2 an A.F. voltage equal to the latter quantity would appear, in fact ΔV_{max} occurs, and this will apparently be a smaller amount. The demodulation factor may therefore be defined as the ratio:

$$D = \frac{\Delta V_{max}}{\Delta V_2} = V_1 \frac{dg_o}{dV_2} \quad \ldots\ldots\ldots \quad \text{(V C 23)}$$

In order to calculate this demodulation factor we must first ascertain the value of g_o from equation (V C 16):

$$g_o \approx (1 + \alpha^2)^{1/2} - \frac{1}{4} \frac{\alpha^2}{(1 + \alpha^2)^{1/2}} \quad \ldots\ldots \quad \text{(V C 16)}$$

Therefore:

$$D = V_1 \frac{dg_o}{dV_2} = V_1 \frac{dg_o}{d\alpha} \frac{d\alpha}{dV_2} \quad \ldots\ldots\ldots \quad \text{(V C 24)}$$

and, since $\alpha = \frac{V_2}{V_1}$:

$$D = \frac{dg_o}{d\alpha} \quad \ldots\ldots\ldots\ldots\ldots \quad \text{(V C 25)}$$

By differentiating the value of g_o given above we find:

$$D = \frac{1}{2} \frac{\alpha}{\sqrt{1 + \alpha^2}} + \frac{1}{4} \frac{\alpha^3}{\sqrt{(1 + \alpha^2)^3}} \quad \ldots\ldots\ldots \quad \text{(V C 26)}$$

The relation between the demodulation factor D and the ratio of the two carrier waves, α, is shown in fig. 256. With small values of α, i.e. when the interfering signal is weak, the factor is roughly equal to half the ratio of the carriers. This is evident also in equation (V C 26): when α is small, the second term diminishes compared with the first, and the root may be taken as equal to 1.

It is wrong to jump to the conclusion that when α is large the demodulation factor is 3/4, for the approximation used for g_o is then no longer valid. It is more likely that with large values of α (interference much stronger than the required signal) demodulation of the interference no longer occurs, namely $D = 1$. Precise calculation proves this to be the case; at $\alpha = 0.8$ the curve in fig. 256 begins to diverge appreciably from reality.

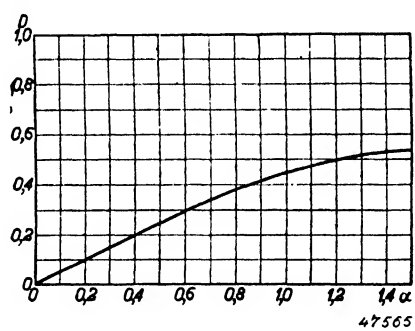

Fig. 256. Demodulation factor D as a function of the factor α, representing the ratio of the carriers of the wanted and of the interfering transmitters.

Fig. 256 shows that, if the interfering transmission is already reduced by the selectivity of the tuned circuits to 1/10 of the strength of the wanted signal, the demodulation effect will result in a further 20 : 1 reduction of

the interference. The apparent selectivity is thus materially enhanced. That this demodulation does not occur with square-law detection is immediately evident. In such conditions the rectified voltage is:

$$V = k V_{max}^2.$$

Substituting for V_{max} from equation (V C 20) we then get:

$$V = k V_1^2 (1 + \alpha^2 + 2 \alpha \cos pt),$$

or:

$$V = k (V_1^2 + V_2^2 + 2 V_1 V_2 \cos pt) \quad . \quad . \quad . \quad . \quad \text{(V C 27)}$$

Neglecting the beat-frequency $2 k V_1 V_2 \cos pt$, there remains

$$V = k V_1^2 + k V_2^2$$

whereas, if the wanted signal V_1 had not been present we should have had:

$$V = k V_2^2.$$

Thus in these two cases the variations of V_2 due to modulation have precisely the same influence on V: there is no demodulation effect.
Between the two types of detection there is an intermediate condition, moderately strong signals giving rise to a limited degree of demodulation, less than that found where the signal strength is sufficient to ensure linear rectification.

SURVEY OF LITERATURE CHAPTER V

1. *Chaffee, E. L.* and *G. H. Browning*, A theoretical and experimental investigation of detection for small signals, Proc. I.R.E. Febr. 1927, page 113.
2. *Colebrook, F. M.* The apparent demodulation of a weak station by a stronger one, Wireless Eng. 1931, p. 409.
3. *Court, W. P. N.* Diode operating conditions, Wireless Eng. 1939, p. 548.
4. *David, P.* Quelques remarques sur les détecteurs, L'onde électrique 1934, page 403.
5. *Nelson, J. R.* Some notes on grid circuit and diode rectification, Proc. I.R.E. 1932, p. 989.
6. *Roder, H.* Ueber die Wechselwirkung zwischen Diode und H.F.-Spannungsquelle bei der Gleichrichtung modulierter Hochfrequenz, Telefunken-Röhre, Dec. 1942.
7. *Weeden, W. N.* New detector circuit, Wireless World 1937, p. 6.
8. *Wheeler, H. A.* Design formulas for diode detectors, Proc. I.R.E. 1938, p. 745.
9. *Wilhelm, K.* Die Röhre im Rundfunkempfänger — Diode-Gleichrichtung, Telefunken Röhre 1936, p. 196.
10. *Williams, F. C.* The modulation response and selectivity curves of a resonant circuit, loaded by a diode rectifier, Wireless Eng. 1938, p. 189.
11. Mutual demodulation and allied problems, Wireless Eng. 1931, p. 405.

INTRODUCTION TO BOOKS V AND VI

A summary is given of the subject matter to be dealt with in Books V and VI following upon that dealt with in this book.

The A.F. oscillations obtained after detection are transmitted to the output stage via the various coupling elements, which do not as a rule allow all frequencies to pass through in the same degree. This results in linear distortion of the A.F. signal, as manifested in the reproduction curve of the receiver. This and the various coupling possibilities with their properties are dealt with in Chapter VI. The third duty of the receiver is to raise the energy level. This takes place in the output stage, in the power amplifying valve with the loudspeaker connected to it. Since, however, the actual acoustic energy is difficult to measure, it is usually the output of the final-stage valve that is taken as criterion.

The final stage of the receiver consumes most energy and therefore in many cases measures are taken to keep this consumption as low as possible, for instance by employing special circuits like the class A/B and class B push-pull circuits. All problems relating to this are dealt with in chapter VII.

Distortion also takes place in the output stage, especially through the curvature of the characteristic. Both the linear and this non-linear distortion of the A.F. signal can in many cases be reduced by applying negative feedback. Part of the output voltage or current is fed back in counterphase to the input circuit of the A.F. stage. The larger the part of the voltage fed back, the more the total amplification is reduced, but the less is this amplification influenced by the coupling elements and the curvature of the valve characteristic. This back-coupling is dealt with at length in chapter VIII.

The power required for the receiver can be derived from a battery or from the lighting mains, in the latter case either AC or DC. When batteries are used there are not many problems encountered. In the case of mains receivers, and particularly those that have to be made suitable both for AC and for DC supply (possibly also for battery supply) several interesting problems arise, which are dealt with in chapter IX, the last chapter in book V.

In a modern receiver one finds several refinements in the circuiting; controls originally manipulated by hand are now automatic. It is now neces-

sary, for instance, for the sensitivity and thus the amplification of the receiver to be adapted to the voltage induced by the transmitter in the aerial; this voltage may be between 1 μV and 1 V. For this purpose amplifying valves are employed which have a decidedly curved characteristic, the slope of which can be regulated with the negative grid bias. Although this introduces distortion (see chapter IV), it makes a simple automatic control of amplification possible. The grid bias is then obtained by rectification of the amplified carrier-wave voltage. This principle is known under the name of automatic volume control, or automatic fading compensation. Owing to the automatic volume control the amplification round about the tuning point is more or less smoothed, so that it is more difficult for the listener to find the right tuning. This is the reason why a system of visible tuning indication is now so often applied together with automatic volume control. In addition to this automatic volume control the receiver has a hand-manipulated volume control for adjusting differences in the depth of modulation or, where the modulation is constant, the desired level of volume.

Another automatic control applied in the top class of superheterodyne receivers is automatic frequency adjustment. This corrects small deviations in the oscillator frequency as may arise through various causes. However, the wiring is rather complicated and the effect of these small deviations is not by any means so troublesome as fading, and therefore this automatic adjustment is not so commonly applied. Instead, it is preferred to avoid variations in the oscillator frequency. This adjustment is, however, described in detail because of the interesting problems connected with it which may be of importance for other cases.

There is a third adjustment aiming at the automatic correction of an inevitable fault in the transmitter: compression of the contrasts in music and speech. The contrasts of the A.F. signal conducted to the output stage are smaller than those of the original music, and although this is not so immediately noticeable a correction naturally improves the quality of reproduction. This correction is called contrast expansion and it can only be done automatically.

There are some cases where just the reverse, thus contrast compression, is applied in receivers and amplifiers, when it is desired to get the highest possible output without having to provide for an extra reserve in the final stage for the often extremely short voltage pulses. The strong contrasts then have to be suppressed in order to avoid overmodulation and the accompanying strong distortion; naturally this amounts, in effect, to a certain amount of distortion, but this is less troublesome than overmodulation of the output stage.

The aforementioned three adjustments come under the heading of "Adjustment technique" and as such are dealt with in the first chapter of Book VI (chapter X).

The fundamental fact in all these adjustments is that a voltage or current is fed back to another part of the circuit, thus purposely bringing about a coupling between these parts of the circuit. As is known, it depends upon the phase of the fed-back voltage or current whether the circuit tends to oscillate, that is to say whether the adjustment of the respective circuit is stable or unstable. The manner in which this can be controlled and previously calculated is dealt with in chapter XI.

In various places in the receiver, however, back-couplings and reactances occur which are of a parasitic nature. The main cause of this lies in the anode-grid capacitance of the electronic valve. In chapter XII the effects of these reactances are described and it is shown how they can be dealt with.

Finally, various secondary phenomena occur in receivers which may prove to be more or less troublesome. They give rise to irregular current fluctuations in the resistors, and in the electronic valves voltages which make rustling noises in the loudspeaker. Other causes of interference are for instance hum, microphonic effect and residual signal, interferences which must and can be taken into account in the designing of receivers. All these more or less disturbing secondary phenomena are dealt with in chapter XIII.

At the end of Book VI (chapter XIV) detailed calculations are given for several designs of receivers and amplifiers in which the principles dealt with in the preceding chapters are applied.

INDEX

	Students/Spl/'C'		Teachers—'A'
Duration of Loan	Text Books	— 3 days	One month
	Technical Books	— 7 days	
	General Books	— 14 days	

FROM THE DATE OF ISSUE